Title
Selective Silylation of Aromatic and Aliphatic C–H Bonds

Author
Karmel, Caleb

Publication Date
2020

Peer reviewed|Thesis/dissertation

Selective Silylation of Aromatic and Aliphatic C–H Bonds

By

Caleb Karmel

A dissertation submitted in partial satisfaction of the

requirements for the degree of

Doctor of Philosophy

in

Chemistry

in the

Graduate Division

of the

University of California, Berkeley

Committee in charge:

Professor John F. Hartwig, Chair
Professor F. Dean Toste
Professor Thomas J. Maimone
Professor Alexis T. Bell

Spring 2020

Abstract

Selective Silylation of Aromatic and Aliphatic C–H Bonds

By

Caleb Karmel

Doctor of Philosophy in Chemistry

University of California, Berkeley

Professor John F. Hartwig, Chair

The following dissertation discusses the development of silylations of C–H bonds that occur with high selectivity and investigations of the mechanisms by which they occur. The work includes intramolecular silylations of aliphatic C–H bonds, catalyzed by Rh complexes, and intermolecular silylations of aromatic C–H bonds, catalyzed by Ir complexes.

Chapter 1 provides a review of catalysts, reagents, and conditions for the undirected functionalization of C–H bonds with high selectivity. This review focuses on catalysts that alter or improve the selectivity of borylation and silylation reactions.

Chapter 2 discusses the development of a rhodium complex containing the Xantphos ligand which catalyzes the intramolecular silylation of alkyl C–H bonds with unusual selectivity for the C–H bonds located δ to the oxygen atom of a silyl ether over typically more reactive C–H bonds more proximal to the same oxygen atom. This chapter describes experimental studies on the mechanism of the silylation and DFT studies on the origin of the selectivity with which it occurs.

Chapter 3 describes the discovery of new catalysts for the silylation of aromatic C–H bonds. Analysis of initial rates uncovered the high reactivity of iridium catalysts containing a hindered phenanthroline ligand but accompanying rapid inhibition by hydrogen gas. With this catalyst, under a flow of nitrogen to remove hydrogen, electron-rich arenes, including those containing sensitive functional groups, undergo silylation in high yield for the first time.

Chapter 4 presents a detailed mechanistic analysis of the iridium-catalyzed silylation of aromatic C–H bonds. Until this study, no experimental data on the identity of complexes related to the mechanism of this process or the mechanisms by which they react to functionalize C–H bonds had been reported. In this chapter, we identify the resting state of the catalyst as an iridium disilyl hydride complex. Studies on the kinetics of the reaction revealed that the rate-limiting step varies with the electronic properties of the arene.

Chapter 5 describes the discovery of new catalysts for the silylation of heteroaromatic C–H bonds with high sterically derived selectivity. A novel pyridyl-imidazoline ligand is shown to improve the selectivity of the reaction for silylation of the least hindered C–H bond. The origin of selectivity was investigated and we determined that the rates of formation of the C–Si bond from isomeric heteroaryliridiuim complexes influences the selectivity of the silylation reaction more than the rates of the cleavage of C–H bonds to form these complexes.

Table of Contents

Acknowledgements

Arriving at Berkeley, I was woefully ill-prepared for a PhD in chemistry. Like many other students, I found the quantities and range of knowledge and techniques I was expected to quickly master dizzying. As I finish my PhD, I feel that the knowledge that Berkeley instilled in me is that chemistry is a vast field of research and that the pleasure of working within it comes from constant learning and not total mastery.

Over these years, I have been lucky to have the mentorship of amazing scientists in the Hartwig lab, especially John himself. I am grateful to John for teaching me how to analyze problems in chemistry and how to think and present rigorously. Most important, from John I've learned to maintain a passion for chemistry that comes from a belief in our ability as chemists to make an impact on the world, while maintaining humility with respect to our work thus far.

Although John has taught me much, I have only seen him in the lab for a few minutes over the five years of my PhD. I owe great thanks to my mentor and lab mate, Dr Ala Bunescu. Ala taught me how to overcome the hundreds of small problems I faced every day in the lab. Without her help, advice, and support, I would not have made it far. She has been a great friend to me and will remain my main source of chemistry guidance for a long time to come.

Throughout my years at Berkeley, almost every person I crossed paths with in the Hartwig group has been a source of advice, inspiration, and mirth. Great friends from within my group, Dr Raphael Oeschger, Dr Noam Saper, Dr Justin Wang, Dr Mike Mormino, and without, Chris Anderson, Marco Lobba, transformed my experience in graduate school. I will miss the coffee breaks that defined my PhD as much as anything else.

Finally, I reach the end of my formal education. This path is one my parents and grandparents have always supported me on. My mother and father instilled the value of education in me and supported me in my decision to pursue a PhD. Although their research in literature and art history has not been a source of practical advice, our shared love of learning will always bring us closer together. My family and friends outside of chemistry have been incredibly supportive and loving throughout these long years, and patient with my being late to everything because of one last experiment.

Over the last five years, my research has often felt like an all-consuming endeavor. For this reason, I am filled with gratitude towards those who opened my mind to the pleasures of the world outside of chemistry, especially my wife. My wife, Bela Karmel, has always been there to support me, give me a sense of perspective, and fill my life with warmth and joy. The work described in this thesis would surely not exist if not for her years of patience and support. I am so grateful to be loved by someone so brilliant and hardworking and who always inspires me to do better.

Chapter 1

Recent Advances in Selective Functionalization of C–H Bonds Without a Directing Group

1.1 Classic Strategies for the Undirected Functionalization of C–H Bonds

The functionalization of C–H bonds has the potential to transform simple, abundant feedstocks into complex, high-value chemicals.[1] Organic molecules contain many C–H bonds possessing distinct steric and electronic properties. A wide array of reagents will react with organic molecules to functionalize C–H bonds with a selectivity that is determined by the properties of the substrates and reagents (Figure 1.1).[2] A wide array of catalyzed and uncatalyzed reactions can be directed by the functional groups native to the substrate.[3] In each class of reaction, the selectivity is determined by the properties of the substrate, but used in concert, these reactions can be used to functionalize a molecule at many different positions. Indeed, such classic reactions have enabled innumerable chemical syntheses of complex molecules and chemical feedstocks.[4]

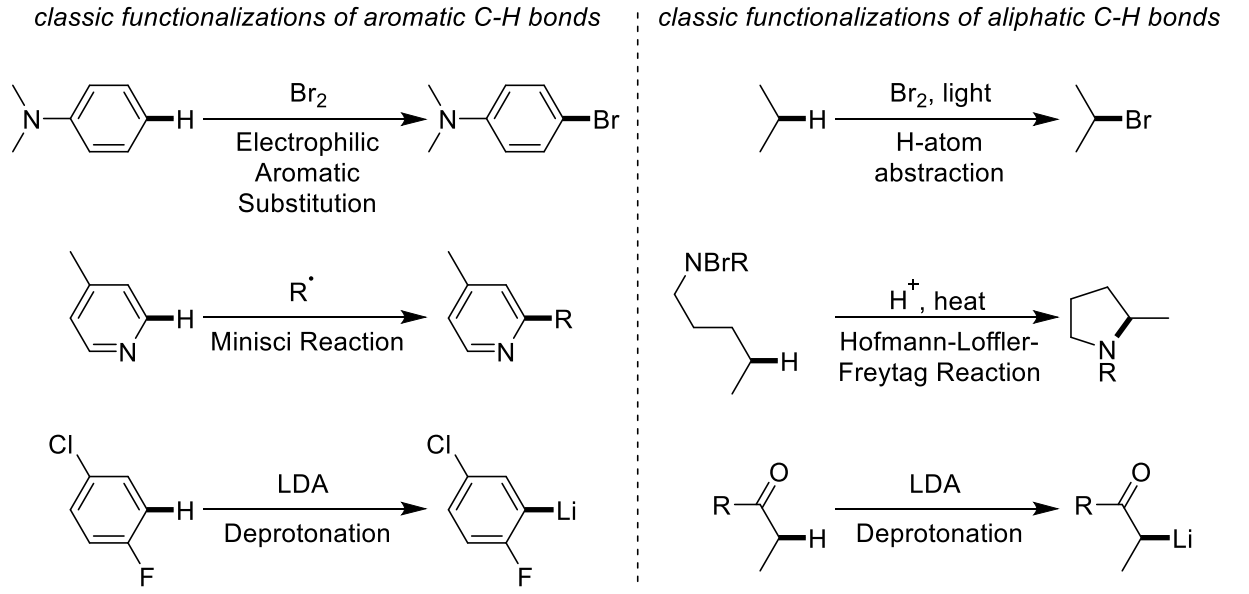

Figure 1.1 Classic Methods for the Functionalization of C–H Bonds

Yet, there are many C–H bonds that would be challenging to functionalize with classic approaches. The selectivity between aromatic C–H bonds of similar electronic character but differing steric environments in electrophilic aromatic substitution and Minisci-type reactions is low.[5] The selective deprotonation of molecules containing multiple acidic sites is challenging. It is also challenging to cleave C–H bonds of similar bond dissociation energies but differing steric properties selectively. Within each class of reaction, there may be some types of functional groups that can be installed with good selectivity on an organic molecule of interest, but the introduction of related functional groups may occur with poor selectivity. Thus, the development of new synthetic methods that alter or improve the selectivity of C–H bond functionalization would greatly increase the utility of C–H bond functionalization in synthetic chemistry.

1.2 Functionalization of C–H Bonds with Selectivity Determined by Properties of Reagents

The selectivity of reactions that functionalize C–H bonds can be altered by careful choice of reagents and conditions. In this section, we will focus on noteworthy advances in C–H bond functionalization in which catalyst are not involved in the C–H bond cleavage step.

1.2.1 Functionalization of Arenes

A classic example C–H functionalization in which modification of the reagent improves the selectivity of the reaction is the bromination of arenes. Elemental bromine is suitable for the bromination of aromatic C–H bonds but is highly corrosive, may react with other functional groups and may functionalize benzylic C–H bonds through radical pathways. For these reasons, *N*-bromo amides and succinimides have become useful reagents in place of elemental bromine for generating aryl bromides under mild conditions.[6] Recent years have seen many groups report new reagents that enable the functionalization of aromatic and aliphatic C–H bonds with heightened selectivity.

The Ritter group reported the S-arylation of thianthrene derivatives and *N*-arylation of selectfluor.[7] The products of the thianthrenation reaction are especially usefully because they undergo a wide range of reactions to install carbon-carbon and carbon-heteroatoms bonds. These reactions are proposed to proceed by reaction of thianthrene or trialkyl ammonium di-cations or radical cations with arenes, followed by loss of proton to generate functionalized product. This mechanism is analogous to that of the classic electrophilic aromatic substitution reaction, but the thianthrenation reaction occurs with exquisite sterically and electronically derived selectivity. The thianthrenation of ethylbenzene occurs with greater than 500:1 selectivity for positions *para* to ethyl over those *ortho* to ethyl (figure 1.2). In comparison, the bromination of benzene leads to formation of significant amounts of products from functionalization at the electron-rich positions *ortho* to the ethyl group. The thianthrenation reaction occurs with high functional group tolerance and selectivity across a wide range of substrates, including natural products and drugs.

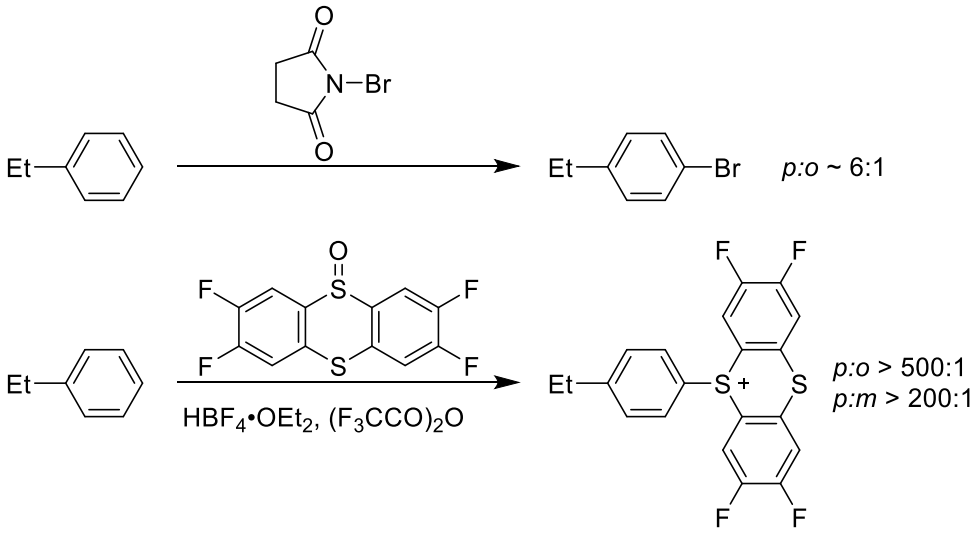

Figure 1.2 Classic and Modern Electrophilic Aromatic Substitution Reactions

To predict the selectivity for the functionalization of different positions of pyridyl substrates, the Blackmond and Baran groups studied the effects of solvent, acidic additives, and radical on the selectivity of Minisci-reactions.[8] Among various results, they found that, for 2-cyano-6-Me-pyridine, additions of nucleophilic radicals occur primarily at the 4-position in chloroform/water mixtures with acid additives but that additions occurred primarily at the 5-position in DMSO and without acidic additives (figure 1.3). The guidelines they articulate aid the identification of conditions for Minisci reactions that form products with good selectivity.

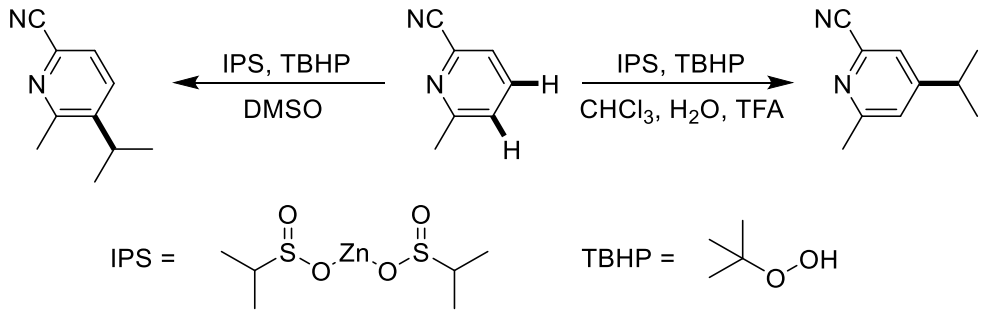

Figure 1.3 Radical Regio-divergent Functionalization of Heteroarenes

1.2.2 Hydrogen Atom Transfer

Classic intramolecular C–H bond functionalization reactions, such as Hoffman-Loffler-Freytag reactions, occur through 1,5 hydrogen atom transfer (HAT). The transition state for 1,5-HAT is a six-membered ring and six-membered rings are usually less strained than analogous five or seven-membered rings. Classic Hoffman-Loffler-Freytag and Barton reactions are often highly selective for 1,5-HAT and generate products functionalized δ to the nitrogen of amines and δ to the oxygen of a nitrate ester.[2c] Recently, the Roizen and Nagib groups reported new strategies to vary the distance between the original functional group and the position at which functionalization occurs. The Nagib lab showed that alcohols react with electron-poor nitriles to form imidates. Imidates undergo a version of the Hoffman-Loffler-Freytag reaction to introduce a range of functional groups that are δ to the nitrogen atom but β to the oxygen atom. On hydrolysis, these reactions yield β amino alcohols (figure 1.4).[9] The Roizen group showed that *N*-chloro sulfamic acids and sulfamides that are derived from alcohols and amines undergo 1,6-HAT processes instead of the more commonly observed 1,5-HAT.[10] These reactions yield products that are functionalized γ to the oxygen or nitrogen of the parent alcohols or amines. These new strategies, in concert with classic Hoffman-Loffler-Freytag and Barton reactions, demonstrate how selective functionalization β, γ, or δ to a heteroatom can be obtained.

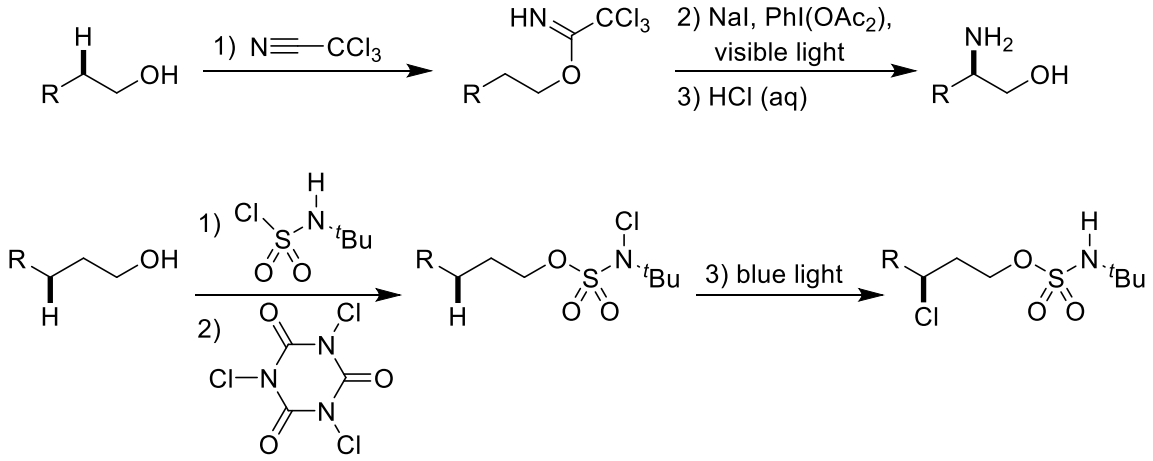

Figure 1.4 New Radical Chaperones for Intramolecular Hydrogen Atom Transfer (HAT)

The Hartwig and Alexanian groups have reported complementary methods for the undirected radical functionalization of aliphatic C–H bonds with high selectivity. In such reactions, obtaining high selectivity between secondary and tertiary C–H bonds of similar bond strength is challenging. Recently, the Alexanian group has reported that *tert*-butyl *N*-haloamides halogenate secondary C–H bonds with high selectivity (figure 1.5). These reactions occurred at the most electron-rich and sterically accessible C–H bond.[11]

The Hartwig group reported the azidation of aliphatic C–H bonds with Zhdankin's reagent and an iron catalyst containing a bisoxazoline ligand.[12] Although the mechanism of this reaction is not understood in detail, a possible mechanism is that Zhdankin's reagent undergoes homolytic cleavage to generate an iodine centered radical that abstracts the hydrogen atom of aliphatic C–H bonds. This C–H bond cleavage occurs with high selectivity for electron-rich tertiary C–H bonds or secondary benzylic C–H bonds. The Hartwig group demonstrated the selective azidation of complex natural products containing many secondary and tertiary C–H bonds. In most of the reported cases, a single major product was observed. The azidation reaction is especially useful because the products can be transformed in primary amines, triazoles, tetrazoles and amides.

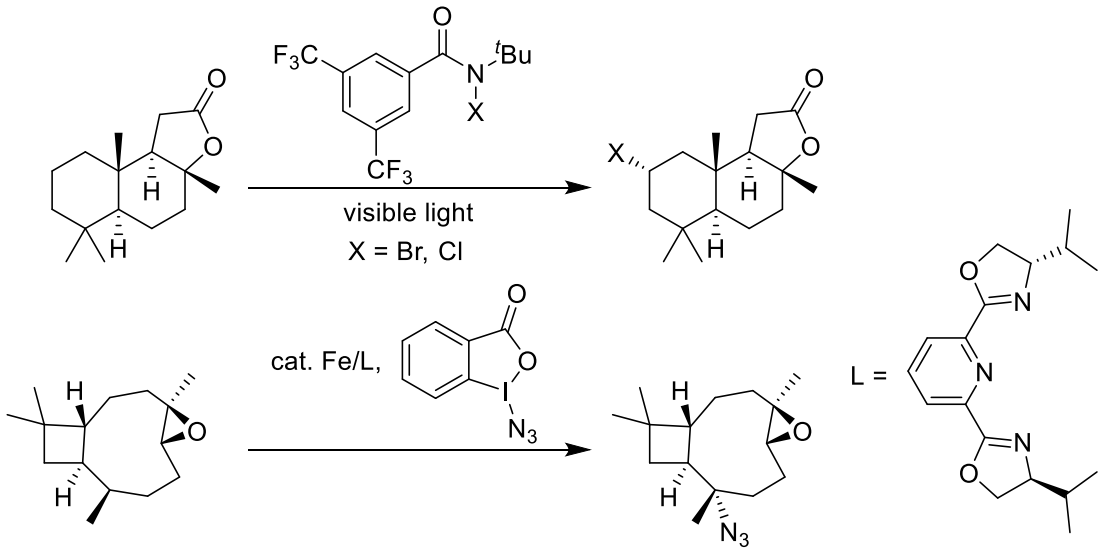

Figure 1.5 Applications of Novel HAT reagents for the Functionalization of Natural Products

1.2.3 Summary of Reagent Based Approaches

The results in these examples show that advances in controlling the selectivity of C–H functionalization reactions can be achieved by the introduction of novel reagents. Manipulation of the steric and electronic properties of the reagents used in these processes has led to reactions that occur with a selectivity that is different from what would be obtained under classical conditions based on the steric and electronic properties of the substrate.

Yet, such advances in controlling the selectivity of C–H functionalization reactions are not without drawbacks. The reagents that lead to greater selectivity in C–H functionalization reactions are generally more complex, more expensive, and produced on smaller scales than the reagents used in the classical versions of the reaction classes. A more attractive approach would be the catalytic functionalization of C–H bonds with selectivity that is determined by the property of the catalyst.

1.3 Intermolecular Functionalization of Aliphatic C–H Bonds with Selectivity Determined by Properties of Catalysts

1.3.1 Overview

Transition metal catalysts can alter or increase the selectivity of classical reactions that functionalize C–H bonds. The effect of a transition metal complex on the selectivity of a C–H functionalization reaction depends on C–H bond cleavage occurring within the inner sphere of the metal complex. Typical mechanisms for C–H bond cleavage mediated by a transition-metal complex are depicted in Figure 1.6. Many of these processes are not classified as C–H bond activation. Shilov described C–H activation as the reaction of a metal with a C–H bond to form a complex with a sigma bond between the metal and the carbon.[13] In such reactions, the selectivity of the overall functionalization reaction will be determined by the properties of metal alkyl or aryl intermediate and of the transition states leading to and from it. However, the following sections will show that transition-metal complexes can control the selectivity of C-H bond functionalization reactions, even when no bond between the metal and the carbon is formed.

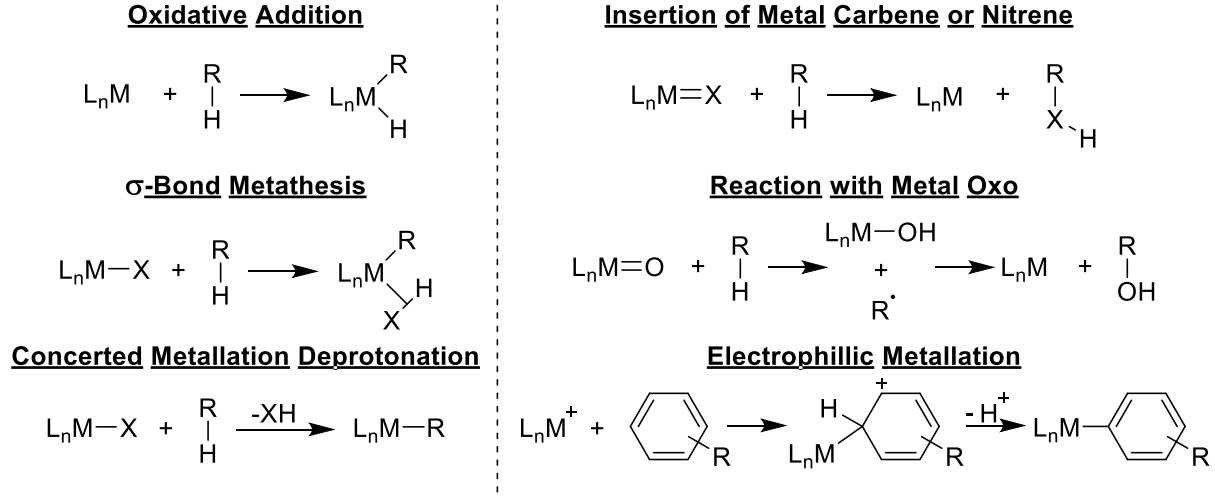

Figure 1.6 Typical Mechanisms for Transition Metal Catalyzed C–H Bond Functionalization

1.3.2 Oxidation of C–H Bonds

The earliest report of undirected C–H functionalization of alkanes with a homogeneous transition-metal catalyst is Shilov's system for the oxidation of alkanes.[14] In this reaction, a platinum catalyst cleaves a C–H bond with selectivity for the stronger primary C–H bonds over weaker secondary C–H bonds. Oxidation of the platinum alkyl complex and reaction of the high valent platinum alkyl with hydroxide or halide nucleophiles furnishes the functionalized product. However, the selectivity of the classic Shilov system for primary over secondary C–H bonds is only modest. More recently, the Sanford group demonstrated the classic Shilov system is applicable to protonated aliphatic amines (Figure 1.7). For these substrates, the selectivity for reaction at the primary C–H bonds is high. The origin of this selectivity is likely due to the combined influence of the positive charge of the ammonium group on the electron density of proximal C–H bonds and the inherent preference of the platinum catalyst for the cleavage of primary C–H bonds.

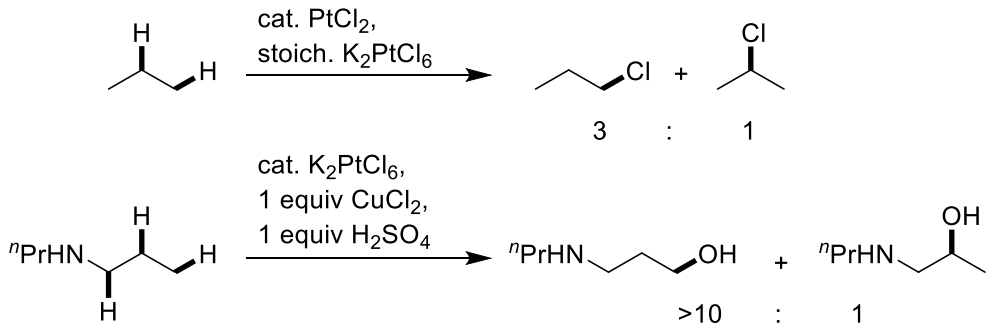

Figure 1.7 Shilov System for the Oxidation of Aliphatic C–H Bonds

1.3.3 Intermolecular Borylation of Aliphatic and Benzylic C–H Bonds

The transition-metal catalyzed borylations of C–H bonds are among the most selective methods for the undirected functionalization of aliphatic C–H bonds. Stoichiometric reactions of tungsten complexes with alkanes to form alkyl boronate esters in the presence of UV light were reported by Hartwig and Waltz in 1997.[15] Subsequently, catalytic borylation reactions with complexes of Rh, Ir, and Ru and many other metals were developed that occurred under thermal conditions.[16] The Hartwig group reported that an Ir complex, widely used for the borylation of arenes, catalyzes the borylation of alkanes with high selectivity for primary C–H bonds.[16a, 17] These catalysts are Ir(III) trisboryl complexes of bipyridine or phenanthroline ligands.[18] Such catalysts functionalize C–H bonds with a high selectivity that is derived from the steric properties of the substrate. Reactions occurred at primary C–H bonds over secondary C–H bonds but occurred readily at secondary C–H bonds in saturated heterocycles lacking unhindered primary C–H bonds. In aliphatic ethers and amines, reactions occurred β to the heteroatom, if the steric properties of the C-H bonds are otherwise equal. Such borylation reactions are generally conducted with solvent quantities of substrate. However, recent reports from the Schley and Hartwig groups showed that some aliphatic substrates undergo borylation with only a 5-fold excess of alkane or limiting alkane, relative to boron, in the presence of an iridium catalysts containing novel bipyridine ligands (Figure 1.8).[19] In addition, the Hartwig group has demonstrated that the C–H bonds of cyclopropanes undergo borylation with either limiting amounts or a small excess of cyclopropane.[20] By replacing the typical, unhindered phenanthroline ligand with the hindered ligand 2,9-dimethylphenanthroline, high trans-selectivity was obtained in the borylation of the C–H bonds of cyclopropane. These results demonstrate that the high-sterically derived selectivity of the iridium-catalyzed borylation can be further improved by increasing the steric encumbrance of the ligand.

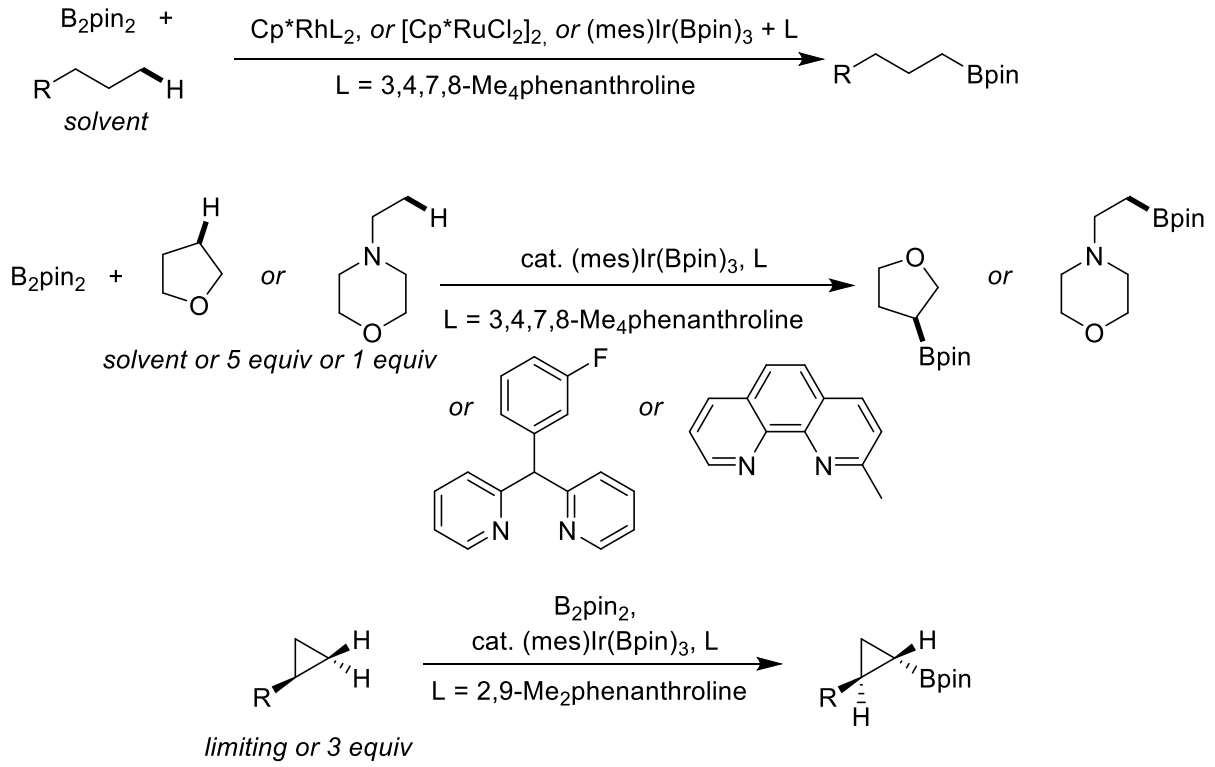

Figure 1.8 Boryations of Aliphatic C–H Bonds

Primary benzylic C–H bonds are more reactive toward borylation than alkyl C-H bonds. With careful choice of catalyst and reagent, primary benzylic C–H bonds are borylated with methylarene as limiting reagent and with high selectivity for the borylation of the benzylic position over the borylation of sterically accessible aromatic C–H bonds (Figure 1.9).[21] Moderately electron-poor phenanthroline ligands were shown to decrease the rate at which aromatic C–H bonds are borylated while having little effect on the rate of benzylic C–H borylation. The selectivity for the borylation of the benzylic positions was improved by substituting $Et_3SiBpin$ for B_2pin_2. The new reagent changes the resting state of the catalyst to an Ir(III) complex with a silyl group in the axial position instead of a boryl group. Silyl ligands are less donating than boryl ligands, and this substitution decreases the electron density at Ir.[22]

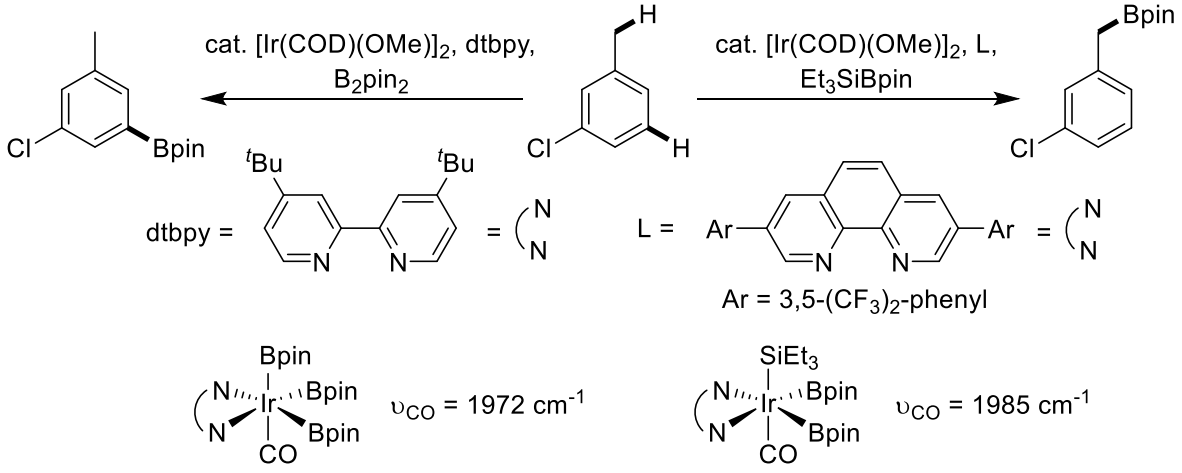

Figure 1.9 Borylation of Benzylic C–H bonds in the Presence of Sterically Accessible Aromatic C–H Bonds

The mechanism of the iridium catalyzed borylation of aliphatic C–H bonds has been studied in much less detail than the borylation of aromatic C–H bonds. The mechanism of the borylation of arenes has been well established and occurs as depicted in Figure 1.10.[18] There are conflicting experimental and data reported on the mechanism of the borylation of aliphatic C–H bonds. Studies on the rates of the borylation of THF and THF-d_8 showed a primary kinetic isotope effect of 2.4. The conclusion drawn from this result was that the oxidative addition of the C–H bond is the rate- and selectivity-determining step in the borylation of THF. However, the Sakaki group proposed that the difference in rates between reactions of THF and THF-d_8 can be explained as an equilibrium isotope effect that is not indicative of rate-limiting C-H bond cleavage. Computational studies from the Sakaki group indicate that reductive elimination of the carbon-boron bond is rate-determining and that this step controls the selectivity of the overall reaction.[23] It remains unclear whether the high selectivity observed for the borylation of aliphatic C–H bonds is due to selective oxidative addition to C–H bonds or reversible oxidative addition, followed by a more selective carbon-boron bond forming reductive elimination.

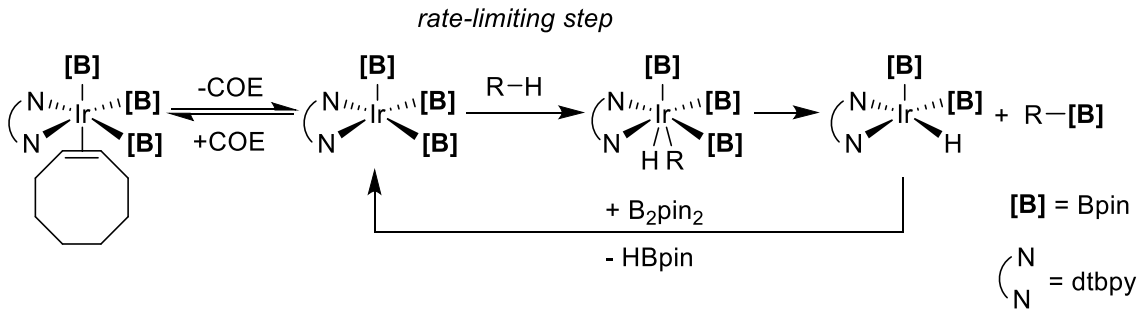

Figure 1.10 Mechanism of the Iridium-Catalyzed Borylation of C–H Bonds

1.3.4 Reactions that Occur Through the Generation of Metal-Carbene, Metal-Nitrene or Metal-Oxo Species

Transition-metal catalysts are also useful for the functionalization of secondary and tertiary C–H bonds. Typically, such reactions do not occur through generation of discreet metal alkyl complexes but rather through reactions of C–H bonds with metal-carbene, -nitrene or -oxos.

The White group has reported iron complexes that catalyze the oxidation of aliphatic C–H bonds with good selectivity.[24] These iron complexes of tetradentate nitrogen-based ligands react with peroxides to form iron oxo complexes. The oxo unit reacts with aliphatic C–H bonds to abstract a hydrogen atom. For iron, rebound to deliver a hydroxyl group is fast and the hydroxylation occurs with retention of configuration at carbon. Overall, these complexes selectively cleave weak C–H bonds over stronger C–H bonds, which is typical for reactions which form carbon radicals. However, by modifying the ligand on the iron catalyst, the White group has shown that they can oxidize stronger but more electron-rich C–H bonds in the presence of weaker but more electron-poor C–H bonds and can oxidize stronger but less sterically hindered C–H bonds in the presence of weaker but more hindered C–H bonds. The White group was also able to demonstrate that methylene groups are oxidized to ketones in the presence of sensitive aromatic

functionality in the presence of a related Mn catalyst.[25] This catalyst is selective for the functionalization of secondary C–H bonds over primary, tertiary, and aromatic C–H bonds. The high functional group tolerance with which the oxidation reaction occurred also allowed them to functionalize methylene positions of complex natural products (Figure 1.11). In most cases, a single product was formed without the oxidation of any sensitive functional groups.

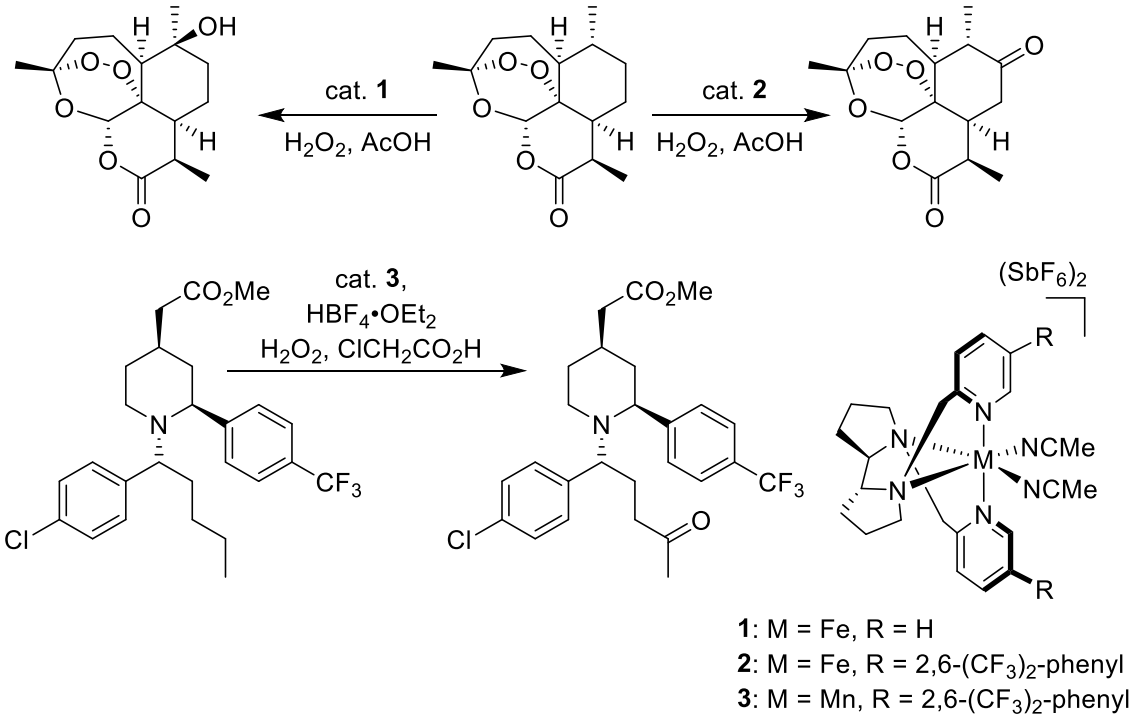

Figure 1.11 Iron and Manganese-Catalyzed Oxidations of Complex Structures

Carbenes insert into C–H bonds without a catalyst. Generally, weaker C–H bonds are functionalized over stronger ones, but the selectivity also arises from steric effects.[26] Many transition-metals will react with carbene and nitrene precursors to form metal carbenes. Dirhodium tetracarboxylate complexes form rhodium-carbenes that, in many cases, react with aliphatic C–H bonds with excellent selectivity. The Davies group has developed chiral carboxylate ligands for dirhodium catalysts that control the site and enantio-selectivity of the insertion of Rh-carbene into C–H bonds.[27] These catalysts are selective for secondary C–H bonds because they are more electron-rich than primary C–H bonds but less hindered than tertiary C–H bonds. However, careful design of ligand has enabled the Davies group to construct catalysts that are selective for tertiary or primary C–H bonds (Figure 1.12).[28]

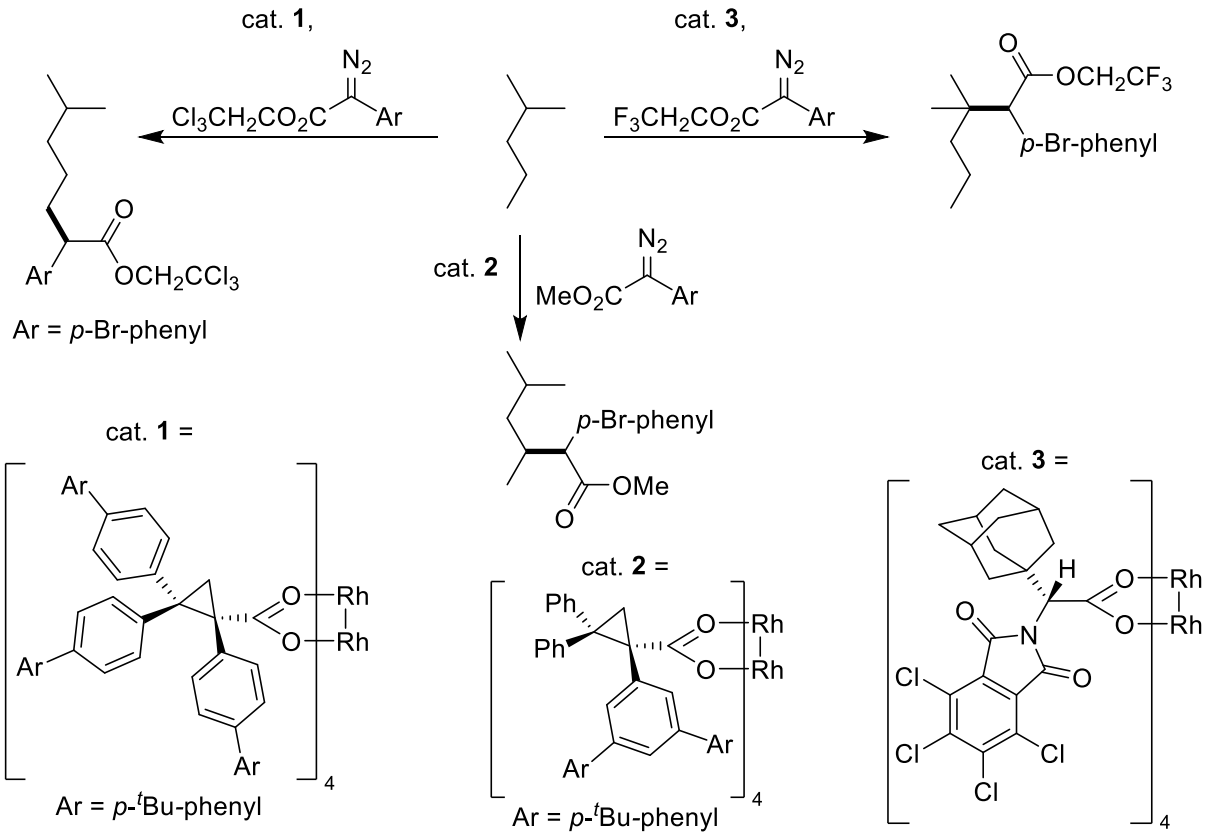

Figure 1.12 Selective Insertions of Carbenes into Primary, Secondary, or Tertiary C–H Bonds catalyzed by Dirhodium Complexes

The undirected intermolecular reaction of metal-nitrenes with aliphatic C–H bonds is less well developed; most reported reactions of this type are intramolecular. However, the Daubin and Dodd groups have reported intermolecular diastereoselective insertions of nitrenes into activated benzylic and allylic C–H bonds catalyzed by chiral dirhodium complexes with chiral sulfonimidamide reagents.[29] Unactivated aliphatic C–H bonds were functionalized with the same system with selectivity for the secondary C–H bonds.[30] Later, the DuBois group demonstrated that amination of a complex structure with a sulphamate and oxidant catalyzed by a dirhodium complex was selective for the most electron rich tertiary C–H bond.[31]

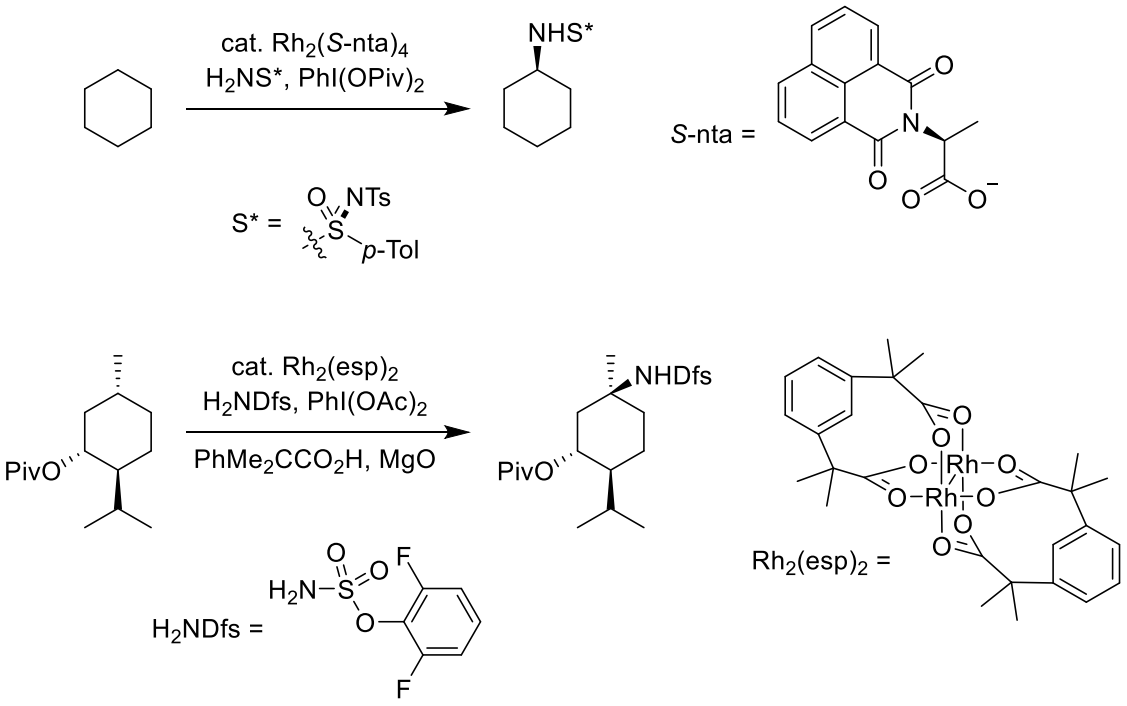

Figure 1.13 Selective Insertions of Nitrenes into C–H Bonds

1.3.5 Conclusion

In summary, many useful transition-metal catalyzed reactions of aliphatic C–H bonds have been developed that occur with high selectivity for benzylic, tertiary, secondary or primary C–H bonds. Many of these reactions have been used to derivatize the C–H bonds of complex natural products with high selectivity. Yet, there remain few reactions of primary C–H bonds, and those that do occur most often require a large excess of C–H bond containing substrate, limiting reactions to substrates of lower value. More reactive catalysts and new approaches for the selective functionalization of primary C–H bonds would be useful.

1.4 Intermolecular Functionalization of Aromatic C–H Bonds with Catalyst Controlled Selectivity

The rates with which transition metal complexes cleave and functionalize aromatic C–H bonds are generally higher than the rates with which aliphatic C–H bonds are functionalized.[32] The higher activity of catalysts with aromatic C–H bonds makes it feasible to use the substrate with the C–H bond as limiting reagent. Thus, the functionalization of aromatic C–H bonds can be used for compounds of high value or complexity that would not be suitable for reactions requiring solvent quantities of organic substrate. Amongst undirected C–H functionalization reactions that occur with limiting arene, the borylation, silylation, direct arylation, and olefination reactions have been reported to occur with the broadest scope.

1.4.1 Borylation of Aromatic C–H bonds

Perhaps the most widely practiced transition metal-catalyzed functionalization of C–H bonds is the borylation of arenes. Ir and bisphosphine or bipyridine ligands form complexes that

are highly active catalysts for the borylation of arenes, even with arene as limiting reagent.[33] The iridium complexes of nitrogen-based ligands borylated the C–H bonds of arenes under milder conditions than the iridium complexes of phosphorous based ligands. Iridium-catalyzed C–H borylation occurs with a broad functional group tolerance. The iridium-catalyzed borylation of aromatic C–H bonds has become a widely used because the products of the reaction undergo further transformations to install a wide range of functional groups and the reaction occurs with high site-selectivity.[34] In recent years, this reaction has been applied at the multi kg scale in the synthesis of active pharmaceutical ingredients (API) for clinical trials of the drugs Doraverine,[35] an FDA approved HIV treatment, and AZD4635,[36] an anti-cancer drug-candidate (Figure 1.14).

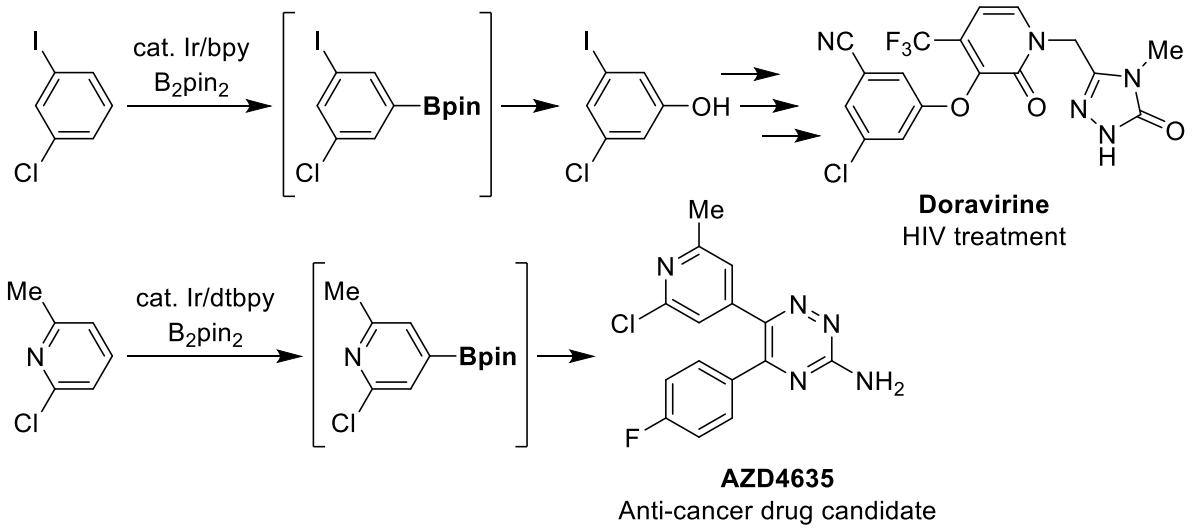

Figure 1.14 Applications of iridium-catalyzed arene borylation to synthesis of APIs

Iridium catalyzed C–H borylation reactions occur with a high sterically derived selectivity, no borylated product is formed from functionalization of positions ortho to medium-sized or large substituents. However, borylated products are observed from functionalization at positions ortho to substituents such as fluoro, cyano, and methoxy. The ρ value of a Hammett plot constructed from competition experiments on the borylations of arenes with varying electronic properties was 3.3, which indicates that the borylation reaction is selective for the functionalization of electron-poor C–H bonds over electron-rich C–H bonds.[21] The selectivity of the borylation of heteroarenes is complex, but empirical rules have been developed to predict the outcome of borylation reactions on different classes of heteroarenes.[37]

Although the selectivity with which the borylation reaction occurs is generally high, several groups have developed new catalysts and conditions to improve or alter the selectivity of undirected iridium-catalyzed borylation reactions. These advances have led to useful new methods for the preparation of diverse aryl boronate esters from mono-substituted arenes, phenols, pyridines, and fluoroarenes. Borylation of mono-substituted arenes occurs with poor selectivity between the *meta* and *para* positions with typical catalysts. In borylations of mono-substituted arenes, the *meta* and *para* positions have similar steric properties, and typical catalysts form products from borylation of these positions in statistical mixtures. The Segawa and Itami groups discovered that iridium catalysts containing bulky bisphosphine ligands improved the selectivity of the borylation reaction for the *para* position.[38] They found that the borylation of TMS-benzene with the typical catalyst formed from iridium and ditertbutylbipyridine occurred with selectivity

for *meta* position over the *para* positions of only 3 to 1. However, by replacing the bipyridine ligand with bulky bisphosphines, especially Segphos and BIPHEP ligands with *m*-xylyl groups on phosphorous, the selectivity of the borylation reaction increased to almost 9 to 1 in favor of the para position (Figure 1.15). The selectivity for the *para* positions was only high with a limited range of substrates containing either silyl or a tertiary alkyl substituents on the arene.

The Nakao group reported a complementary approach to the *para* selective borylation of mono-substituted arenes and pyridines. The selectivity of the iridium catalyzed borylation of Lewis-basic heteroarenes is toward positions distal to existing substituents and away from the Lewis-basic nitrogen. Thus, the borylation of 3-substituted pyridines occurs with high selectivity for the borylation of the 5-position and the borylations of 2,6-substituted pyridines occurs with high selectivity for the borylation of the 4-position. However, 2-substituted pyridines form mixtures of products from borylation at both the 4 and 5-positions. Nakao's group found that when a bulky Lewis-acidic aluminum co-catalyst is added to the borylation reaction, the 4-positions of unsubstituted or 2-substituted pyridines are borylated with high selectivity.[39] Nakao hypothesizes that the aluminum binds to the nitrogen of the pyridine, which activates the aromatic C-H bonds for borylation. The substituents on the aluminum complex shield the 3 and 5-positions from borylation. Likewise, the borylation of benzamide derivatives, including those with substituents in the 2-position, occurred with high selectivity for borylation at the *para* position when the aluminum co-catalyst was present (Figure 1.15).

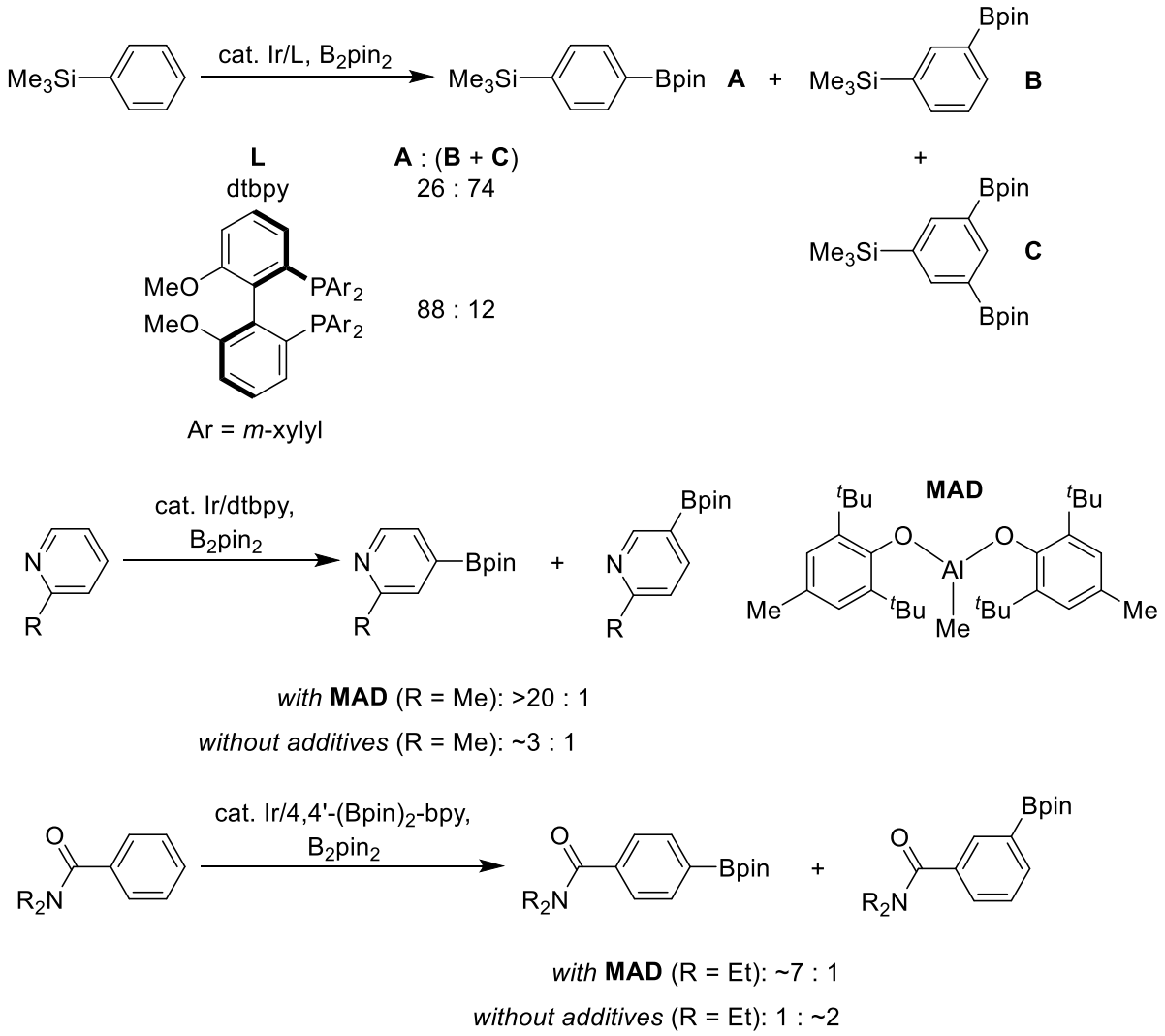

Figure 1.15 Selective borylations of mono-substituted (hetero)arenes

The iridium-catalyzed borylations of 1,3 disubstituted or 1,2,3 trisubstituted arenes usually occur with high selectivity for borylation at the 5-position. However, significant amounts of products from borylation *ortho* to small substituents such as fluorine or cyano are observed with typical iridium catalysts. In addition, products from borylation at the 2-position are observed in 3-substituted 5-member heteroarenes because the more acute bond angles in those heteroarenes place the substituents further apart and make steric effects less pronounced. To functionalize the C–H bonds of fluoroarenes, benzonitriles, and 5-member ring heteroarenes with high sterically derived selectivity, the groups of Smith and Maleczka developed a new iridium catalyst for the borylation of these structures with high sterically derived selectivity and the groups of Cui and Driess synthesized a cobalt complex that also catalyzed the borylation of fluoroarenes with high sterically derived selectivity (Figure 1.16).[40] The iridium catalyst developed by Smith and Maleczka contained a dipyridylmethane (DPM) ligand. This ligand binds iridium to form a 6-membered metallacycle, whereas the typical bipyridine ligands bind to form a 5-membered metallaycle. Smith and Maleczka hypothesized that the DPM ligand makes a catalyst that is more selective for the least sterically encumbered C–H bond because it binds with a wider bite angle.

The catalyst synthesized by the Cui and Driess groups is based on a cobalt complex with a tridentate ligand with two silylene donors and one pyridine donor.[40b] The cobalt complex they developed catalyzed the borylation of electron-poor arenes and heteroarenes with B_2pin_2 and cyclohexene as an acceptor for the HBpin byproduct. This catalyst displayed the typical selectivity for the borylation of the least sterically hindered C–H bonds of aromatic and heteroaromatic substrates. Despite the small size and strong electron withdrawing effect of fluorine, the selectivity for the borylation of positions *meta* to fluorine substituents over positions *ortho* to fluorine was greater than 10 to 1 for a range of fluoroarenes.

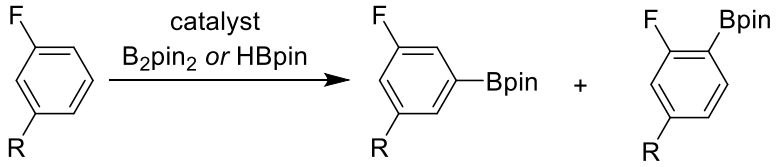

Catalyst	R	Selectivity (*meta* : *ortho*)
Ir/dtbpy	Cl	1.8 : 1
Ir/dtbpy	Me	1.2 : 1
Ir/DPM	Cl	5 : 1
Co-**1**	Me	7 : 1

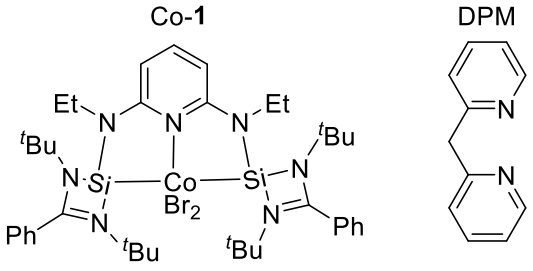

Figure 1.16 Borylations of fluorinated arenes with steric-selectivity

In some cases, it would be useful to decrease the sterically derived selectivity with which the borylation occurs so that selectivity for more acidic C–H bonds exerts greater control over the selectivity of the borylation process. The groups of Smith, Maleczka, and Singleton reported studies on the iridium catalyzed borylations of phenols.[41] In the first step of the reaction sequence, the phenol is treated with a borane to form a phenyl borate derivative. In the subsequent step, that intermediate is treated with an iridium catalyst that borylates the C–H bonds of the protected phenol. The selectivity of the borylation for positions *ortho* and *meta* to the hydroxy group depends on both the boronate ester protecting group and the properties of the catalyst. If Bpin is used to protect the OH group and B_2pin_2 is used as borylating reagent, most of the product from borylation of a 1,3-disubstituted phenol is from borylation of the position *meta* to OH. However, if HBeg (eg = ethylene glycol) is used as the protecting reagent and B_2eg_2 as the reagent in the borylation reaction, then the C–H borylation occurred with high selectivity for the position *ortho* to the phenol (Figure 1.17). This reversal of the selectivity is due in part to the smaller steric bulk and greater inductive withdrawing effect of an OBeg group compared to an OBpin group. However, the change of reagent also changes the properties of the catalyst. The active catalyst species is an iridium complex with three boryl ligands. If the boryl groups contain smaller ethylene glycol units, the catalyst is less sterically hindered. The steric effects on selectivity using this catalyst are diminished, relative to the catalyst containing bulkier pinacol groups.

The Chirik group has reported a series of cobalt complexes that catalyze the borylation of aromatic and heteroaromatic C–H bonds.[42] These complexes contain P,N,P ligands, and extensive mechanistic studies from the Chirik group have shown that the species that cleaves the C–H bond is a Co(I) complex with a boryl ligand.[43] In general, these catalysts borylate the C–H bonds of

arenes with a selectivity that is like that observed for the iridium-catalyzed borylation reaction. However, the borylation of 1,3 disubstituted fluoroarenes with the iridium catalyst occurs with a roughly statistical selectivity for borylation of positions *ortho* and *meta* to fluorine. In contrast, Chirik's cobalt complexes catalyze the borylation of fluoroarenes with high selectivity for the position *ortho* to fluorine.[44] Mechanistic studies on the borylation of these arenes showed that reversible C–H activation occurred at both positions and that the selectivity for the borylation at the position *ortho* to fluorine was due the greater stability of the Co-aryl complex resulting from C–H activation at that position.[45]

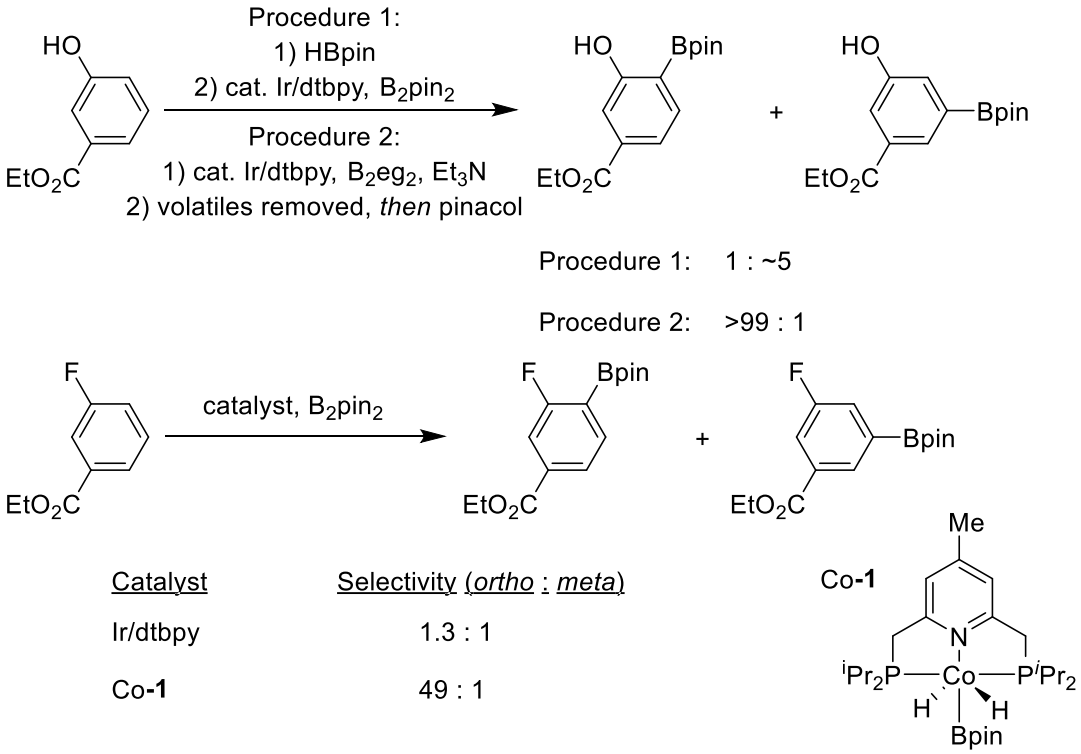

Figure 1.17 Borylations of phenols and fluorinated arenes with electronic-selectivity

1.4.2 Silylation of Aromatic C–H bonds

The silylation of aromatic C–H bonds is a useful reaction because, like aryl boronate esters, aryl silanes undergo a wide array of cross-coupling reactions and can be transformed into the corresponding aryl halides, phenols and amines.[46] The silylation of aromatic C–H bonds is catalyzed by iridium complexes of bipyridine ligands that are like those that catalyze the borylation of aromatic C–H bonds.[47] A wide range of silanes and disilanes have been reported to undergo dehydrogenative coupling with arenes in the presence of iridium catalysts containing phenanthroline or bipyridine ligands.[48] However, most of these systems require a large excess of arene due to the low rates with which the reactions occur. The most active systems for the silylation of arenes use the 1,1,1,3,5,5,5-heptamethyltrisiloxane (HMTS) as the silane reagent. The silylation of 3-tolunitrile with HMTS catalyzed by the combination of $[Ir(cod)(OMe)]_2$ and 2-Me-phenanthroline occurred with greater than 20 to 1 selectivity for the silylation of the position *meta* to the cyano group over the position *ortho* to the cyano group.[49] This selectivity is much higher than the selectivity of the iridium-catalyzed borylation of benzonitriles. However, the rates of the iridium catalyzed silylation of arenes are much lower than the rates of the iridium-catalyzed

borylation. Silylations with this catalyst system require 2-3 days at elevated temperatures of 100 °C to reach high conversions for electron-neutral substrates (Figure1.18). Nevertheless, the iridium catalyst is useful because it tolerates a broad array of functional groups and silylates the C–H bonds of many heterocycles in high yields.

The first undirected silylation of aromatic C–H bonds with limiting arene was reported with a rhodium catalyst.[50] The combination of Rh(I) precatalysts and bisphosphine ligands was shown to catalyze the silylation of arenes with HMTS in high yield under mild conditions. The catalyst formed with BIPHEP ligands catalyze the silylation of arenes with much higher site-selectivity than the iridium-catalyzed borylation reaction. Detailed studies on the mechanism of the silylation reaction showed that the resting state of the catalyst is a Rh(III) silyl complex and that Rh(I) hydride and silyl complexes are intermediates in the reaction.[51] Rhodium silyl or hydride complexes of many bisphosphine ligands are intermediates in the hydrosilylation of carbonyl containing compounds.[52] Indeed, reduction of ketones, esters, nitriles, and heavy halides was observed in the rhodium catalyzed C–H silylation.

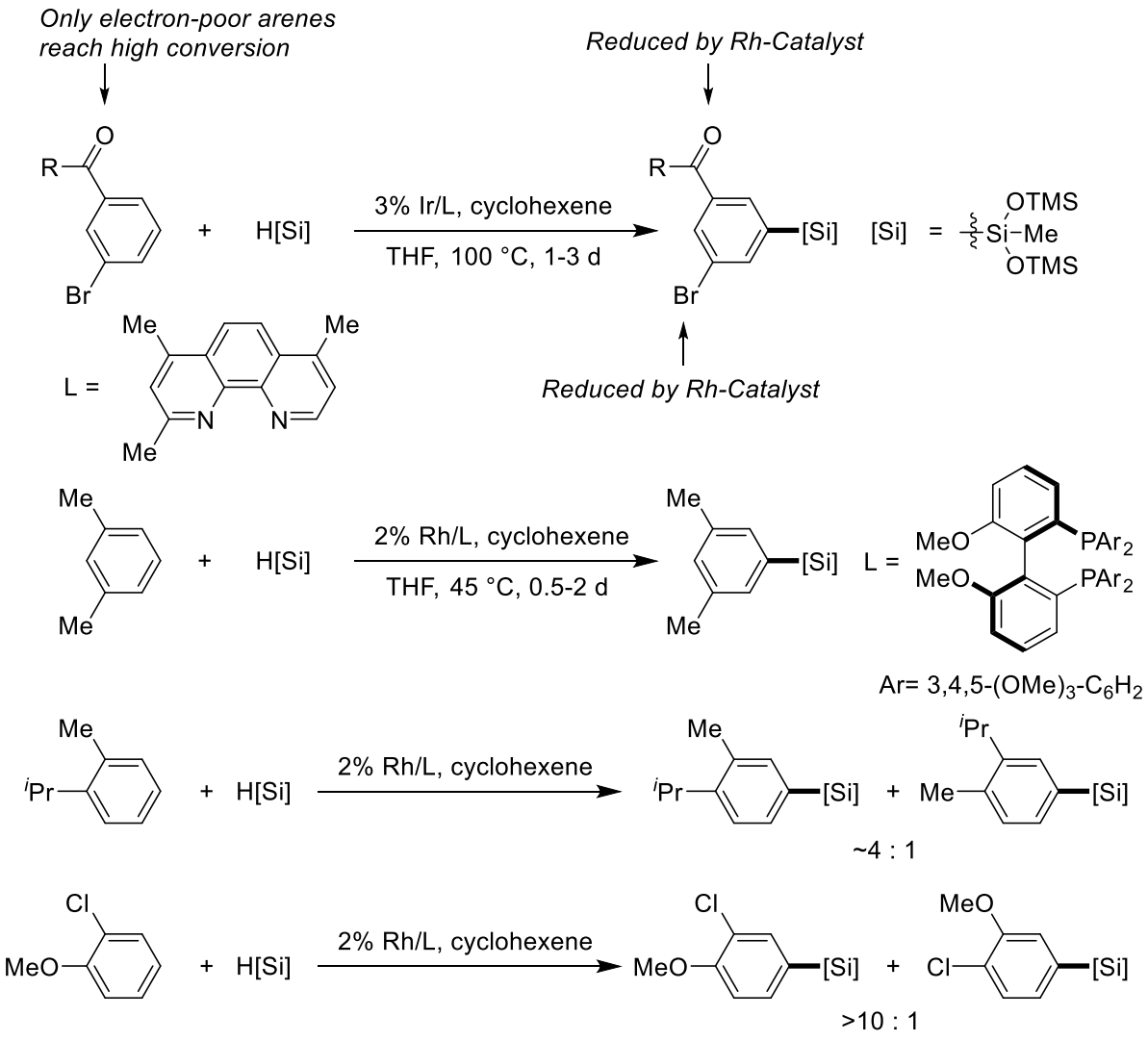

Figure 1.18 Silylations of arenes with limiting arene

Despite the limitations in substrate scope, the rhodium catalyzed silylation of aromatic C–H bonds is useful because it occurs with extraordinary site selectivity. The iridium-catalyzed borylation of C–H bonds occurs with little selectivity between 4 and 5-positions of 1,2-disubstituted arenes, even if the two substituents have very different steric and electronic properties. In contrast, the rhodium catalyzed silylation of 2-methylcumene occurred with high sterically derived selectivity. The selectivity for the silylation of the 4-position over the 5-position is greater than 4 to 1. No selectivity between the 4 and 5 positions was observed from the borylation of 2-methylcumene (Figure 1.18). Similarly, the selectivity for the rhodium-catalyzed silylation of two positions of varying electronic character was also very high. The silylation of 2-chloroanisole occurred with greater than 10 to 1 selectivity for the electron-rich 4-position, whereas the borylation reaction occurred with a slight preference for the electron poor 5-position. Overall, the hallmark of the iridium catalyzed silylation and borylation reactions and the rhodium catalyzed silylation reaction is a high selectivity for functionalization of less hindered aromatic C-H bonds over aromatic C-H bonds that are *ortho* to existing substituents.

1.4.3 Arene-Limited C–H Bond Functionalization to Form C–C Bonds

The undirected silylation and borylation of aromatic C–H bonds occur with limiting arene across a broad range of aromatic and heteroaromatic structures. By contrast, most other transition-metal catalyzed C–H functionalization reactions of arenes either require a large excess of arene, occur with poor selectivity, or have a narrow scope.[32] For example, Lloyd-Jones and Russell groups reported the oxidative coupling of arenes with aryl silanes catalyzed by an Au(I) phosphine complex.[53] Although this reaction occurred with good selectivity for the least hindered electron-rich C–H bond, the scope is limited alkoxyarenes and alkylarenes (Figure 1.19). The Yu group reported the first undirected arene-limited palladium-catalyzed Fujiwara-Moritani reaction.[54] In such reactions, the C–H bond is cleaved in a concerted metallation deprotonation pathway. In such a reaction, a ligand on Pd deprotonates a sigma bound C–H bond. The Yu group showed that the rate of the C–H functionalization reaction was much higher with a catalyst containing a pyridone ligand instead of the typical acetate ligands. The reaction occurred with both electron-poor and electron-rich arenes. For reactions of mono-substituted arenes, mixtures of products were obtained from olefination at the *meta* and *para* positions. However, the reaction of *o*-xylene gave a single product from functionalization at the positions distal to the methyl groups.

Cross-coupling reactions to form biaryls are amongst the most practiced reactions in organic synthesis.[55] Therefore, the undirected arylation of the C–H bonds of arenes would be useful if valuable or complex aromatic structures were suitable substrates. Although most undirected arylations occur with a large excess of arene,[56] arylations of heteroaromatic C–H bonds often occur with limiting-arene or only a small excess of arene. The greater acidity of the C–H bonds of heteroarenes makes the formation of the metal-aryl intermediates more favorable. The Fagnou group reported reactions of aryl bromides with thiophenes, N-protected pyrroles, furans, and a broad array of azole structures catalyzed by Pd complexes with the heteroarene as limiting reagent. In each case, the most acidic C–H bond of the heteroarene reacted.[57]

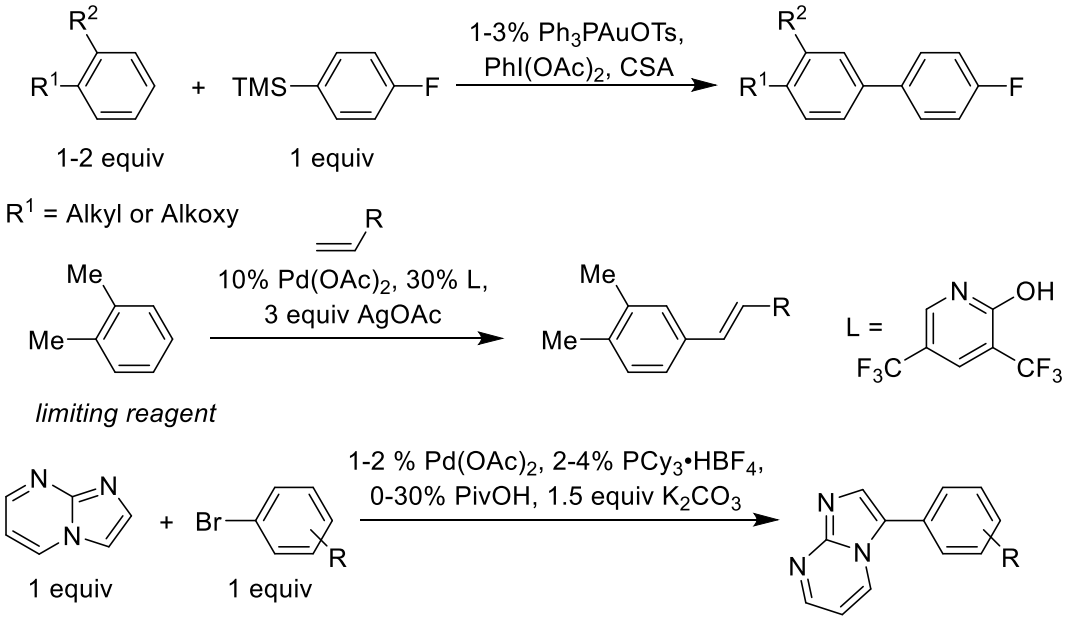

Figure 1.19 Catalytic olefination and arylation of arenes with limiting arene

1.4.4 Conclusion

Catalytic methods for the functionalization of aromatic C–H bonds occur with much higher rates than analogous reactions of aliphatic C–H bonds and can be used to synthesize or derivatize complex molecules. Among these reactions, only the borylation of aromatic C-H bonds occurs in truly broad scope, with other transformations limited by low selectivity or low reactivity for most arenes. Although significant advances have been made toward improving the selectivity with which the borylation reaction occurs, the most active catalysts for the borylation reaction functionalize many arenes with modest selectivity. The analogous silylation reactions occur with high selectivity but suffer from poor functional group tolerance or low reactivity. Catalysts for forming bonds other than C–B bonds with high activity would also be useful. In later chapters, more active catalysts for the silylation of aromatic C–H bonds are presented.

1.5 Intramolecular Silylation of C–H Bonds with Selectivity Determined by Properties of Catalysts

The selectivity of intramolecular or directed C–H bond functionalization reactions are controlled primarily by the shape and functional groups of the substrate and not by the properties of the catalyst.[2a] However, the silylation of aliphatic C–H bonds occurs with high selectivity for the functionalization of primary C–H bonds, including those of complex structures.[58] Alkyl silanes can be oxidized to form alcohols, which makes C–H silylations a method for introducing hydroxy groups at specific positions of molecules. The silyl group can be introduced to the substrate by dehydrogenative silylation of an O–H bond to form a silyl ether. C–H silylation with silyl ethers is especially useful because the O–Si bonds is labile, and the silyl group is removed during oxidation of the C–Si bond. The development of the intramolecular silylation of silyl ethers has enabled a reaction sequence in which the sequence of alcohol silylation, C–H silylation, and C-Si

oxidation enables selective hydroxylation directed by hydroxy groups that are native to many substrates.

Early reports of intramolecular silylations of C–H bonds occurred with simple alkyl silanes and under harsh conditions. For example, in 2005, the Hartwig group reported that tributyl silane undergoes intramolecular C–H silylation for form a 5-membered ring product in the presence of a platinum complex (Figure 1.20).[48d] The same complex also catalyzed the cyclization of silanes with pendant phenyl groups in which the aromatic C–H bond was silylated. The reactions required high temperatures (200 °C) and 2-3 days to reach high conversion. However, this initial discovery prompted the investigation of more active catalysts that are useful for the functionalization of substrates of greater complexity.

The Hartwig group later reported much milder silylations of aromatic C–H bonds proximal to hydrido silyl ethers, generated *in situ* from alcohols. Iridium complexes of phenanthroline ligands, related to those used in intermolecular borylation reactions, are highly active for the intramolecular silylation of aromatic C–H bonds in hydrido silyl ethers derived from benzylic alcohols or aromatic ketones. Reactions with substrates containing two geometrically accessible aromatic C–H bonds occurred at the less sterically hindered one.[59]

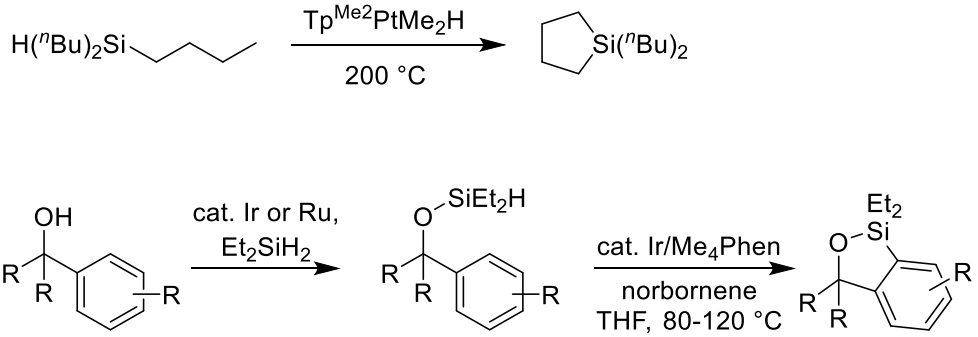

Figure 1.20 Early reports of high yielding intramolecular C-H silylation

In 2012, the Hartwig groups extended the iridium catalyzed intramolecular silylation reaction of silyl ethers to aliphatic C–H bonds.[60] The reactions form 5-membered cyclic silyl ethers, presumably via a 6-membered metallacycle. The reaction is highly selective for the silylation of primary C–H bonds over secondary or tertiary aliphatic C–H bonds (Figure 1.21). Later, the Hartwig group reported that, if no primary C–H bond were present that would lead to formation of a 5-membered ring product, secondary C–H bonds were silylated. The silylation of secondary C–H bonds occurred at higher temperatures than that of primary C–H bonds, but under otherwise identical conditions. In the following chapter, I report catalysts and conditions for the silylation of primary C–H bonds to form 6-membered cyclic silyl ethers with high selectivity over the silylation of secondary C–H bonds to form 5-membered cyclic silyl ethers.

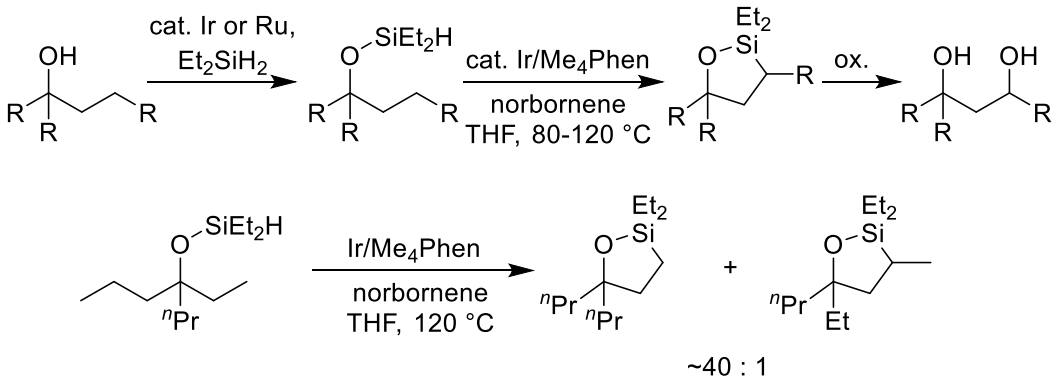

Figure 1.21 Selective intramolecular C-H silylation of silyl ethers derived from alcohols

1.6 Conclusion

In conclusion, this chapter presents an overview of general concepts and recent advances in the functionalization of aliphatic and aromatic C–H bonds without a directing group. In the absence of a directing group, gaining control over the selectivity of the site of reaction is vital to making C–H functionalization a useful class of reactions. Many advances have been made in the selective functionalization of C–H bonds, yet the activity with which aliphatic C–H bonds are functionalized and the selectivity with which transition-metal catalysts react with aromatic C–H bonds remain low. The iridium-catalyzed borylation of primary C–H bonds is among the most promising methods for the functionalization of more complex structures. Yet, the development of more active catalysts for this reaction is hindered by limited mechanistic data about of how Ir-boryl complexes react with C–H bonds and the narrow range of ligands that catalyze these reactions in high yields.

The intramolecular silylation of primary C–H bonds is also a promising class of reaction. Yet, the utility of the silylation reaction is limited by the fact that the alkyl silane products can be used to introduce hydroxyl groups but no other functional groups. Methods for introducing C–B bonds from the same substrates that currently undergo the intramolecular silylation reaction would be of high synthetic utility.

Catalytic functionalization at aromatic C–H bonds been used most frequently by the practicing synthetic chemists because complex structures containing aromatic C–H bonds can be employed routinely as limiting reagent in such transformations. In recent years, many new catalysts and reagents have been developed that improve the selectivity of C–H functionalization reactions at aromatic C–H bonds. Although many advances have been made, further catalyst design could enable more selective borylation and silylation reactions. Detailed data revealing how the mechanism of the iridium-catalyzed silylation differs from that of the borylation reaction could reveal how greater selectivity and activity may be achieved in silylation reactions and is reported in later chapters.

Since early examples of C–H functionalization were reported, chemists have developed catalysts that react with C–H bonds with higher and higher rates. Such advances make it possible for C–H functionalization to be useful for solving synthetic problems in which the selectivity required matches that of the catalyst. Now, chemists have begun to create libraries of catalysts and

ligands that enable the functionalization of C–H bonds at an array of positions in each substrate with high selectivity.

1.7 References

1. Hartwig, J. F. Catalyst-Controlled Site-Selective Bond Activation. *Acc. Chem. Res.* **2017**, *50*, 549.
2. (a) Hartwig, J. F.; Larsen, M. A. Undirected, Homogeneous C–H Bond Functionalization: Challenges and Opportunities. *ACS Cent. Sci.* **2016**, *2*, 281. (b) Corey, E. J.; Hertler, W. R. A Study of the Formation of Haloamines and Cyclic Amines by the Free Radical Chain Decomposition of N-Haloammonium Ions (Hofmann-Löffler Reaction)1. *J. Am. Chem. Soc.* **1960**, *82*, 1657. (c) Majetich, G.; Wheless, K. Remote intramolecular free radical functionalizations: An update. *Tetrahedron* **1995**, *51*, 7095.
3. Engle, K. M.; Mei, T.-S.; Wasa, M.; Yu, J.-Q. Weak Coordination as a Powerful Means for Developing Broadly Useful C–H Functionalization Reactions. *Acc. Chem. Res.* **2012**, *45*, 788.
4. (a) Abrams, D. J.; Provencher, P. A.; Sorensen, E. J. Recent applications of C–H functionalization in complex natural product synthesis. *Chem. Soc. Rev.* **2018**, *47*, 8925. (b) Cernak, T.; Dykstra, K. D.; Tyagarajan, S.; Vachal, P.; Krska, S. W. The medicinal chemist's toolbox for late stage functionalization of drug-like molecules. *Chem. Soc. Rev.* **2016**, *45*, 546. (c) Davies, H. M. L.; Du Bois, J.; Yu, J. Q. C-H Functionalization in organic synthesis. *Chem. Soc. Rev.* **2011**, *40*, 1855.
5. (a) Proctor, R. S. J.; Phipps, R. J. Recent Advances in Minisci-Type Reactions. *Angew. Chem. Int. Ed.* **2019**, *58*, 13666. (b) Olah, G. A.; Kobayashi, S. Aromatic substitution. XXIX. Friedel-Crafts acylation of benzene and toluene with substituted acyl halides. Effect of substituents and positional selectivity. *J. Am. Chem. Soc.* **1971**, *93*, 6964.
6. Voskressensky, L. G.; Golantsov, N. E.; Maharramov, A. M. Recent Advances in Bromination of Aromatic and Heteroaromatic Compounds. *Synthesis* **2016**, *48*, 615.
7. (a) Berger, F.; Plutschack, M. B.; Riegger, J.; Yu, W.; Speicher, S.; Ho, M.; Frank, N.; Ritter, T. Site-selective and versatile aromatic C−H functionalization by thianthrenation. *Nature* **2019**, *567*, 223. (b) Boursalian, G. B.; Ham, W. S.; Mazzotti, A. R.; Ritter, T. Charge-transfer-directed radical substitution enables para-selective C–H functionalization. *Nat Chem* **2016**, *8*, 810.
8. O'Hara, F.; Blackmond, D. G.; Baran, P. S. Radical-Based Regioselective C–H Functionalization of Electron-Deficient Heteroarenes: Scope, Tunability, and Predictability. *J. Am. Chem. Soc.* **2013**, *135*, 12122.
9. Wappes, E. A.; Nakafuku, K. M.; Nagib, D. A. Directed β C–H Amination of Alcohols via Radical Relay Chaperones. *J. Am. Chem. Soc.* **2017**, *139*, 10204.
10. Short, M. A.; Shehata, M. F.; Sanders, M. A.; Roizen, J. L. Sulfamides direct radical-mediated chlorination of aliphatic C–H bonds. *Chem. Sci.* **2020**, *11*, 217.
11. (a) Schmidt, V. A.; Quinn, R. K.; Brusoe, A. T.; Alexanian, E. J. Site-Selective Aliphatic C–H Bromination Using N-Bromoamides and Visible Light. *J. Am. Chem. Soc.* **2014**, *136*, 14389. (b) Quinn, R. K.; Könst, Z. A.; Michalak, S. E.; Schmidt, Y.; Szklarski, A. R.; Flores, A. R.; Nam, S.; Horne, D. A.; Vanderwal, C. D.; Alexanian, E. J. Site-Selective Aliphatic C–H Chlorination Using N-Chloroamides Enables a Synthesis of Chlorolissoclimide. *J. Am. Chem. Soc.* **2016**, *138*, 696.

12. (a) Karimov, R. R.; Sharma, A.; Hartwig, J. F. Late Stage Azidation of Complex Molecules. *ACS Cent. Sci.* **2016**, *2*, 715. (b) Sharma, A.; Hartwig, J. F. Metal-catalysed azidation of tertiary C-H bonds suitable for late-stage functionalization. *Nature* **2015**, *517*, 600.
13. Shilov, A. E.; Shul'pin, G. B. Activation of C-H bonds by metal complexes. *Chem. Rev.* **1997**, *97*, p 2879.
14. Shilov, A. E.; Shteinman, A. A. Activation of Saturated Hydrocarbon by Metal Complexes in Solution. *Coord. Chem. Rev.* **1977**, *24*, p 97.
15. Waltz, K. M.; Hartwig, J. F. Selective Alkane Functionalization by Transition Metal Boryl Complexes. *Science* **1997**, *277*, 211.
16. (a) Li, Q.; Liskey, C. W.; Hartwig, J. F. Regioselective Borylation of the C–H Bonds in Alkylamines and Alkyl Ethers. Observation and Origin of High Reactivity of Primary C–H Bonds Beta to Nitrogen and Oxygen. *J. Am. Chem. Soc.* **2014**, *136*, 8755. (b) Murphy, J. M.; Lawrence, J. D.; Kawamura, K.; Incarvito, C.; Hartwig, J. F. Ruthenium-Catalyzed Regiospecific Borylation of Methyl C-H Bonds. *J. Am. Chem. Soc.* **2006**, *128*, p 13684. (c) Chen, H.; Schlecht, S.; Semple, T. C.; Hartwig, J. F. Thermal, Catalytic, Regiospecific Functionalization of Alkanes. *Science* **2000**, *287*, 1995. (d) Mkhalid, I. A. I.; Barnard, J. H.; Marder, T. B.; Murphy, J. M.; Hartwig, J. F. C-H Activation for the Construction of C-B Bonds. *Chem. Rev.* **2010**, *110*, 890.
17. Hartwig, J. F. Regioselectivity of the borylation of alkanes and arenes. *Chem. Soc. Rev.* **2011**, *40*, 1992.
18. Boller, T. M.; Murphy, J. M.; Hapke, M.; Ishiyama, T.; Miyaura, N.; Hartwig, J. F. Mechanism of the Mild Functionalization of Arenes by Diboron Reagents Catalyzed by Iridium Complexes. Intermediacy and Chemistry of Bipyridine-Ligated Iridium Tris Boryl Complexes. *J. Am. Chem. Soc.* **2005**, *127*, 14263.
19. (a) Jones, M. R.; Fast, C. D.; Schley, N. D. Iridium-Catalyzed sp3 C–H Borylation in Hydrocarbon Solvent Enabled by 2,2′-Dipyridylarylmethane Ligands. *J. Am. Chem. Soc.* **2020**, *142*, 6488. (b) Oeschger, R.; Su, B.; Yu, I.; Ehinger, C.; Romero, E.; He, S.; Hartwig, J. Diverse functionalization of strong alkyl C–H bonds by undirected borylation. *Science* **2020**, *368*, 736.
20. Liskey, C. W.; Hartwig, J. F. Iridium-Catalyzed C-H Borylation of Cyclopropanes. *J. Am. Chem. Soc.* **2013**, *135*, 3375.
21. Larsen, M. A.; Wilson, C. V.; Hartwig, J. F. Iridium-Catalyzed Borylation of Primary Benzylic C-H Bonds without a Directing Group: Scope, Mechanism, and Origins of Selectivity. *J. Am. Chem. Soc.* **2015**, *137*, 8633.
22. Zhu, J.; Lin, Z.; Marder, T. B. Trans Influence of Boryl Ligands and Comparison with C, Si, and Sn Ligands. *Inorg. Chem.* **2005**, *44*, 9384.
23. Zhong, R.-L.; Sakaki, S. sp3 C–H Borylation Catalyzed by Iridium(III) Triboryl Complex: Comprehensive Theoretical Study of Reactivity, Regioselectivity, and Prediction of Excellent Ligand. *J. Am. Chem. Soc.* **2019**, *141*, 9854.
24. (a) White, M. C.; Zhao, J. Aliphatic C–H Oxidations for Late-Stage Functionalization. *J. Am. Chem. Soc.* **2018**, *140*, 13988. (b) Newhouse, T.; Baran, P. S. If C–H Bonds Could Talk: Selective C–H Bond Oxidation. *Angew. Chem. Int. Ed.* **2011**, *50*, 3362.
25. Zhao, J.; Nanjo, T.; de Lucca, E. C.; White, M. C. Chemoselective methylene oxidation in aromatic molecules. *Nat. Chem.* **2019**, *11*, 213.
26. Doyle, M. P.; Duffy, R.; Ratnikov, M.; Zhou, L. Catalytic Carbene Insertion into C-H Bonds. *Chem. Rev.* **2010**, *110*, 704.
27. Davies, H. M. L.; Liao, K. Dirhodium tetracarboxylates as catalysts for selective intermolecular C–H functionalization. *Nat. Rev. Chem.* **2019**, *3*, 347.

28. (a) Liao, K.; Yang, Y.-F.; Li, Y.; Sanders, J. N.; Houk, K. N.; Musaev, D. G.; Davies, H. M. L. Design of catalysts for site-selective and enantioselective functionalization of non-activated primary C–H bonds. *Nat. Chem.* **2018**, *10*, 1048. (b) Liao, K.; Pickel, T. C.; Boyarskikh, V.; Bacsa, J.; Musaev, D. G.; Davies, H. M. L. Site-selective and stereoselective functionalization of non-activated tertiary C–H bonds. *Nature* **2017**, *551*, 609.
29. (a) Collet, F.; Dodd, R. H.; Dauban, P. Catalytic C-H amination: recent progress and future directions. *Chem. Commun.* **2009**, 5061. (b) Liang, C. G.; Robert-Pedlard, F.; Fruit, C.; Muller, P.; Dodd, R. H.; Dauban, P. Efficient diastereoselective intermolecular rhodium-catalyzed C-H amination. *Angew. Chem. Int. Ed.* **2006**, *45*, 4641.
30. Liang, C. G.; Collet, F.; Robert-Peillard, F.; Muller, P.; Dodd, R. H.; Dauban, P. Toward a synthetically useful stereoselective C-H amination of hydrocarbons. *J. Am. Chem. Soc.* **2008**, *130*, 343.
31. Roizen, J. L.; Zalatan, D. N.; Du Bois, J. Selective Intermolecular Amination of C□H Bonds at Tertiary Carbon Centers. *Angew. Chem. Int. Ed.* **2013**, *52*, 11343.
32. Wedi, P.; van Gemmeren, M. Arene-Limited Nondirected C−H Activation of Arenes. *Angew. Chem. Int. Ed.* **2018**, *57*, 13016.
33. (a) Cho, J. Y.; Tse, M. K.; Holmes, D.; Maleczka, R. E.; Smith, M. R. I. Remarkably selective iridium catalysts for the elaboration of aromatic C–H bonds. *Science* **2002**, *295*, 305. (b) Ishiyama, T.; Nobuta, Y.; Hartwig, J. F.; Miyaura, N. Room temperature borylation of arenes and heteroarenes using stoichiometric amounts of pinacolborane catalyzed by iridium complexes in an inert solvent. *Chem. Commun.* **2003**, 2924. (c) Ishiyama, T.; Takagi, J.; Yonekawa, Y.; Hartwig, J. F.; Miyaura, N. Iridium-catalyzed direct borylation of five-membered heteroarenes by bis(pinacolato)diboron: Regioselective, stoichiometric, and room temperature reactions. *Adv. Synth. Catal.* **2003**, *345*, 1103. (d) Takagi, J.; Sato, K.; Hartwig, J. F.; Ishiyama, T.; Miyaura, N. Iridium-catalyzed C-H coupling reaction of heteroaromatic compounds with bis(pinacolato)diboron: regioselective synthesis of heteroarylboronates. *Tetrahedron Lett.* **2002**, *43*, 5649. (e) Ishiyama, T.; Takagi, J.; Ishida, K.; Miyaura, N.; Anastasi, N. R.; Hartwig, J. F. Mild Iridium-Catalyzed Borylation of Arenes. High Turnover Numbers, Room Temperature Reactions, and Isolation of a Potential Intermediate. *J. Am. Chem. Soc.* **2002**, *124*, 390. (f) Ishiyama, T.; Takagi, J.; Hartwig, J. F.; Miyaura, N. A Stoichiometric Aromatic C-H Borylation Catalyzed by Iridium(I)/2,2'-Bipyridine Complexes at Room Temperature. *Angew. Chem. Int. Ed.* **2002**, *41*, p 3056.
34. Hartwig, J. F. Borylation and Silylation of C–H Bonds: A Platform for Diverse C–H Bond Functionalizations. *Acc. Chem. Res.* **2012**, *45*, 864.
35. Campeau, L.-C.; Chen, Q.; Gauvreau, D.; Girardin, M.; Belyk, K.; Maligres, P.; Zhou, G.; Gu, C.; Zhang, W.; Tan, L.; O'Shea, P. D. A Robust Kilo-Scale Synthesis of Doravirine. *Org. Process Res. Dev.* **2016**, *20*, 1476.
36. Douglas, J. J.; Adams, B. W. V.; Benson, H.; Broberg, K.; Gillespie, P. M.; Hoult, O.; Ibraheem, A. K.; Janbon, S.; Janin, G.; Parsons, C. D.; Sigerson, R. C.; Klauber, D. J. Multikilogram-Scale Preparation of AZD4635 via C–H Borylation and Bromination: The Corrosion of Tantalum by a Bromine/Methanol Mixture. *Org. Process Res. Dev.* **2019**, *23*, 62.
37. Larsen, M. A.; Hartwig, J. F. Iridium-Catalyzed C-H Borylation of Heteroarenes: Scope, Regioselectivity, Application to Late-Stage Functionalization, and Mechanism. *J. Am. Chem. Soc.* **2014**, *136*, 4287.
38. Saito, Y.; Segawa, Y.; Itami, K. para-C–H Borylation of Benzene Derivatives by a Bulky Iridium Catalyst. *J. Am. Chem. Soc.* **2015**, *137*, 5193.

39. Yang, L.; Semba, K.; Nakao, Y. para-Selective C−H Borylation of (Hetero)Arenes by Cooperative Iridium/Aluminum Catalysis. *Angew. Chem. Int. Ed.* **2017**, *56*, 4853.
40. (a) Miller, S. L.; Chotana, G. A.; Fritz, J. A.; Chattopadhyay, B.; Maleczka, R. E.; Smith, M. R. C–H Borylation Catalysts that Distinguish Between Similarly Sized Substituents Like Fluorine and Hydrogen. *Org. Lett.* **2019**, *21*, 6388. (b) Ren, H.; Zhou, Y.-P.; Bai, Y.; Cui, C.; Driess, M. Cobalt-Catalyzed Regioselective Borylation of Arenes: N-Heterocyclic Silylene as an Electron Donor in the Metal-Mediated Activation of C−H Bonds. *Chem. Eur. J.* **2017**, *23*, 5663.
41. Chattopadhyay, B.; Dannatt, J. E.; Andujar-De Sanctis, I. L.; Gore, K. A.; Maleczka, R. E.; Singleton, D. A.; Smith, M. R. Ir-Catalyzed ortho-Borylation of Phenols Directed by Substrate-Ligand Electrostatic Interactions: A Combined Experimental/in Silico Strategy for Optimizing Weak Interactions. *J. Am. Chem. Soc.* **2017**, *139*, 7864.
42. (a) Obligacion, J. V.; Semproni, S. P.; Pappas, I.; Chirik, P. J. Cobalt-Catalyzed C(sp(2))-H Borylation: Mechanistic Insights Inspire Catalyst Design. *J. Am. Chem. Soc.* **2016**, *138*, 10645. (b) Obligacion, J. V.; Semproni, S. P.; Chirik, P. J. Cobalt-Catalyzed C–H Borylation. *J. Am. Chem. Soc.* **2014**, *136*, 4133.
43. Obligacion, J. V.; Chirik, P. J. Mechanistic Studies of Cobalt-Catalyzed C(sp2)-H Borylation of Five-Membered Heteroarenes with Pinacolborane. *ACS Catal.* **2017**.
44. Obligacion, J. V.; Bezdek, M. J.; Chirik, P. J. C(sp(2))-H Borylation of Fluorinated Arenes Using an Air-Stable Cobalt Precatalyst: Electronically Enhanced Site Selectivity Enables Synthetic Opportunities. *J. Am. Chem. Soc.* **2017**, *139*, 2825.
45. Pabst, T. P.; Obligacion, J. V.; Rochette, É.; Pappas, I.; Chirik, P. J. Cobalt-Catalyzed Borylation of Fluorinated Arenes: Thermodynamic Control of C(sp2)-H Oxidative Addition Results in ortho-to-Fluorine Selectivity. *J. Am. Chem. Soc.* **2019**, *141*, 15378.
46. (a) Denmark, S. E.; Ambrosi, A. Why You Really Should Consider Using Palladium-Catalyzed Cross-Coupling of Silanols and Silanolates. *Org. Process Res. Dev.* **2015**, *19*, 982. (b) Nakao, Y.; Hiyama, T. Silicon-based cross-coupling reaction: an environmentally benign version. *Chem. Soc. Rev.* **2011**, *40*, 4893. (c) Rayment, E. J.; Mekareeya, A.; Summerhill, N.; Anderson, E. A. Mechanistic Study of Arylsilane Oxidation through ^{19}F NMR Spectroscopy. *J. Am. Chem. Soc.* **2017**, *139*, 6138. (d) Rayment, E. J.; Summerhill, N.; Anderson, E. A. Synthesis of Phenols via Fluoride-free Oxidation of Arylsilanes and Arylmethoxysilanes. *J. Org. Chem.* **2012**, *77*, 7052. (e) Bracegirdle, S.; Anderson, E. A. Arylsilane oxidation—new routes to hydroxylated aromatics. *Chem. Commun.* **2010**, *46*, 3454. (f) Morstein, J.; Kalkman, E. D.; Bold, C.; Cheng, C.; Hartwig, J. F. Copper-Mediated C–N Coupling of Arylsilanes with Nitrogen Nucleophiles. *Org. Lett.* **2016**, *18*, 5244.
47. Cheng, C.; Hartwig, J. F. Catalytic Silylation of Unactivated C–H Bonds. *Chem. Rev.* **2015**, *115*, 8946.
48. (a) Ishiyama, T.; Sato, K.; Nishio, Y.; Miyaura, N. Direct Synthesis of Aryl Halosilanes through Iridium(I)-Catalyzed Aromatic C–H Silylation by Disilanes. *Angew. Chem. Int. Ed.* **2003**, *42*, 5346. (b) Saiki, T.; Nishio, Y.; Ishiyama, T.; Miyaura, N. Improvements of Efficiency and Regioselectivity in the Iridium(I)-Catalyzed Aromatic C-H Silylation of Arenes with Fluorodisilanes. *Organometallics* **2006**, *25*, 6068. (c) Ishiyama, T.; Saiki, T.; Kishida, E.; Sasaki, I.; Ito, H.; Miyaura, N. Aromatic C–H silylation of arenes with 1-hydrosilatrane catalyzed by an iridium(i)/2,9-dimethylphenanthroline (dmphen) complex. *Org. Biomol. Chem.* **2013**, *11*, 8162. (d) Tsukada, N.; Hartwig, J. F. Intermolecular and Intramolecular, Platinum-Catalyzed, Acceptorless Dehydrogenative Coupling of Hydrosilanes with Aryl and Aliphatic Methyl C-H Bonds. *J. Am. Chem. Soc.* **2005**, *127*, 5022. (e) Murata, M.; Fukuyama, N.; Wada, J.-i.;

Watanabe, S.; Masuda, Y. Platinum-catalyzed Aromatic C-H Silylation of Arenes with 1,1,1,3,5,5,5-Heptamethyltrisiloxane. *Chem. Lett.* **2007**, *36*, 910. (f) Ezbiansky, K.; Djurovich, P. I.; Laforest, M.; Sinning, D. J.; Zayes, R.; Berry, D. H. Catalytic C-H Bond Functionalization - Synthesis of Arylsilanes By Dehydrogenative Transfer Coupling of Arenes and Triethylsilane. *Organometallics* **1998**, *17*, 1455.
49. Cheng, C.; Hartwig, J. F. Iridium-Catalyzed Silylation of Aryl C–H Bonds. *J. Am. Chem. Soc.* **2015**, *137*, 592.
50. Cheng, C.; Hartwig, J. F. Rhodium-Catalyzed Intermolecular C-H Silylation of Arenes with High Steric Regiocontrol. *Science* **2014**, *343*, 853.
51. Cheng, C.; Hartwig, J. F. Mechanism of the Rhodium-Catalyzed Silylation of Arene C–H Bonds. *J. Am. Chem. Soc.* **2014**, *136*, 12064.
52. Riener, K.; Högerl, M. P.; Gigler, P.; Kühn, F. E. Rhodium-Catalyzed Hydrosilylation of Ketones: Catalyst Development and Mechanistic Insights. *ACS Catal.* **2012**, *2*, 613.
53. Ball, L. T.; Lloyd-Jones, G. C.; Russell, C. A. Gold-Catalyzed Direct Arylation. *Science* **2012**, *337*, 1644.
54. Wang, P.; Verma, P.; Xia, G.; Shi, J.; Qiao, J. X.; Tao, S.; Cheng, P. T. W.; Poss, M. A.; Farmer, M. E.; Yeung, K.-S.; Yu, J.-Q. Ligand-accelerated non-directed C–H functionalization of arenes. *Nature* **2017**, *551*, 489.
55. Brown, D. G.; Boström, J. Analysis of Past and Present Synthetic Methodologies on Medicinal Chemistry: Where Have All the New Reactions Gone? *J. Med. Chem.* **2016**, *59*, 4443.
56. Alberico, D.; Scott, M. E.; Lautens, M. Aryl-Aryl Bond Formation by Transition-Metal-Catalyzed Direct Arylation. *Chem. Rev.* **2007**, *107*, 174.
57. Liégault, B.; Lapointe, D.; Caron, L.; Vlassova, A.; Fagnou, K. Establishment of Broadly Applicable Reaction Conditions for the Palladium-Catalyzed Direct Arylation of Heteroatom-Containing Aromatic Compounds. *J. Org. Chem.* **2009**, *74*, 1826.
58. Hartwig, J. F.; Romero, E. A. Iridium-catalyzed silylation of unactivated C–H bonds. *Tetrahedron* **2019**, *75*, 4059.
59. Simmons, E. M.; Hartwig, J. F. Iridium-Catalyzed Arene Ortho-Silylation by Formal Hydroxyl-Directed C–H Activation. *J. Am. Chem. Soc.* **2010**, *132*, 17092.
60. Simmons, E. M.; Hartwig, J. F. Catalytic functionalization of unactivated primary C-H bonds directed by an alcohol. *Nature* **2012**, *483*, 70.

Chapter 2

Rhodium-Catalyzed Regioselective Silylation of Alkyl C-H Bonds for the Synthesis of 1,4-Diols

2.1 Introduction

Catalytic functionalization of C-H bonds with main group reagents, such as boranes and silanes, has become a practical synthetic methodology because it occurs with high regioselectivity and generates intermediates that can be transformed into a variety of products.[1,2] Catalytic silylations of C-H bonds occurs both intramolecularly and intermolecularly, but catalytic intramolecular silylation occurs with high regioselectivity, due to the formation of cyclic silane products.[3-7] We first reported the iridium-catalyzed intramolecular silylation of primary C-H bonds of silyl ethers, that had been generated from silanes and either alcohols or ketones, to form 5-membered oxasilolanes.[8] We and others have expanded the scope of this process and applied it to the derivatization of carbohydrates and additional terpene natural products.[8,9] Oxidation of the oxasilolanes in one pot generates 1,3-diols (Scheme 2.1a).

C-H silylation to form a 6-membered cyclic product is also desirable because it would generate 1,4-functionalized products, instead of 1,3-functionalized products. However, formation of a 6-membered cyclic silane is less favorable because it requires the generation of a medium-sized, 7-membered metalacyclic intermediate. The few examples of C-H silylation to generate 6-membered cyclic silanes are limited to the functionalization of activated benzylic C-H bonds.[10] Catalytic silylation of unactivated C-H bonds directed by a common functional group to form a 6-membered cyclic silane is unknown. Radical methods for the oxygenation of alkyl C-H bonds δ to an oxygen are known, but in most cases a cyclic ether is formed.[11a] A nitrate ester has been installed in certain cases at the δ position when the Barton reaction was conducted in the presence of oxygen,[11b,c] but this process is a stoichiometric, photochemical reaction.

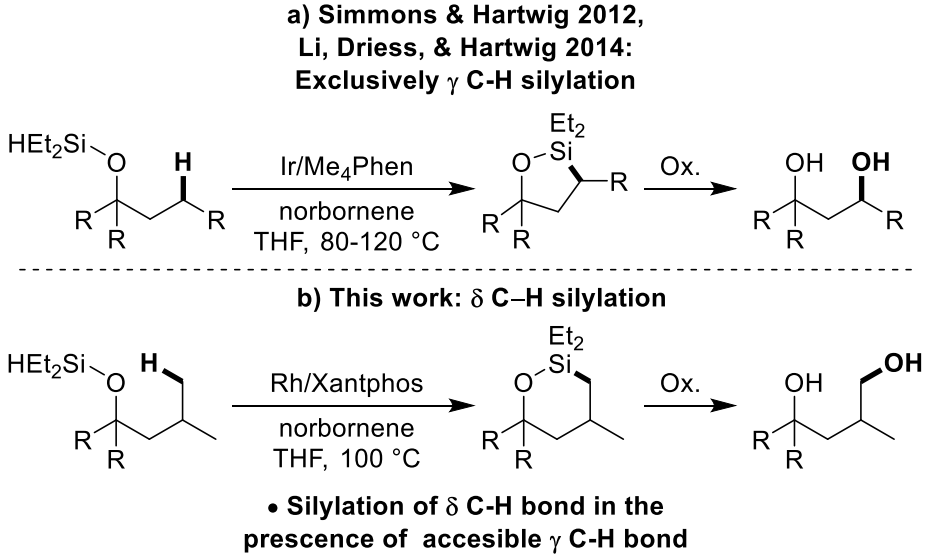

Scheme 2.1 Intramolecular C-H Silylation Forming Cyclic Silyl Ethers and Subsequent Oxidation to Diols

The mechanism of rhodium-catalyzed silylations of C-H bonds has been investigated previously by our group.[12] The resting state of the catalyst in the intermolecular silylation of arenes catalyzed by the combination of Rh and Segphos with cyclohexene as hydrogen acceptor was (Segphos)Rh(III)(SiR_3)$(H)_2$, and the rate-limiting step was found to be the reductive elimination of cyclohexane. The resting state of the catalyst in a subsequent enantioselective intramolecular silylation of aryl C-H bonds revealed a similar Rh(III) resting state, as well as a complex with the

hydrogen acceptor, and the rate-determining step was a related reductive elimination of the reduced hydrogen acceptor.[12b] It is unclear whether the same type of resting state would be present in the reactions with catalysts that form larger metalacyclic intermediates, whether the rate-determining step would be the same, and, most significant for the current study, how the identity and reactivity of these intermediates would influence the regioselectivity.

We report highly selective, silylations of unactivated, primary C-H bonds located δ to hydroxyl groups (Scheme 2.1b) catalyzed by a rhodium complex of Xantphos (Xantphos, 4,5-bis(diphenylphosphino)-9,9-dimethylxanthene). Oxidation of the resulting oxasilolanes generates 1,4-diols. The catalyst for this process is unusual for C-H bond functionalization; complexes of Xantphos have not been shown to catalyze the silylation of alkyl C-H bonds, and ligands like Xantphos with a wide bite-angle have rarely been used for any type of metal-catalyzed functionalization of alkyl C-H bonds.[13,14] Mechanistic studies show that the rhodium-catalyzed silylation of alkyl C-H bonds occurs with a resting state and relative rates of elementary steps that are significantly different from those for the rhodium-catalyzed silylation of aryl C-H bonds and that the unusual regioselectivity results from a high barrier to reductive elimination of secondary alkyl groups from rhodium complexes ligated by Xantphos.

2.2 Results & Discussion

2.2.1 Reaction Development.

To evaluate potential silylations of alkyl C-H bonds located δ to an alcohol, we studied the reaction of silyl ether **2a** in Table 2.1. Ether **2a** is derived from the corresponding tertiary alcohol **1a** by a dehydrogenative coupling with diethylsilane catalyzed by 0.1 mol % $[Ir(OMe)(COD)]_2$. Ether **2a** contains primary, secondary, and tertiary C-H bonds that could undergo silylation. Primary C-H bonds are typically more reactive than secondary and tertiary C-H bonds toward iridium-catalyzed silylation. However, the primary C-H bond in **2a** is located at the position δ to the oxygen atom of the ether, rather than the position γ to oxygen that has undergone silylation in previous work.[8a] Secondary C-H bonds located γ to oxygen have been shown recently to undergo silylation;[8b] therefore, it was unclear whether the reaction would occur at the secondary C-H bond located γ to the oxygen atom or the primary C-H bond located δ to the oxygen atom.

The combination of an iridium pre-catalyst and 3,4,7,8-tetramethyl-1,10-phenanthroline (Me_4Phen) as ligand catalyzed the reaction of **2a** to form products from C-H bond silylation in high yield. However, the reaction occurred at both secondary and primary C-H bonds to give a mixture of the five-membered and six-membered oxasilolanes (Entry 1, Table 2.1). The reaction favored silylation at the secondary C-H bond by a factor of about 5, indicating that the ring size, rather than the degree of substitution at the C-H bond controlled the site selectivity. Silylation at the tertiary C-H bond was not observed.

To identify a catalyst that reacted with distinct selectivity to form the six-membered oxasilolane product selectively, we explored the combination of iridium and rhodium catalyst precursors with a range of bisphosphine ligands in place of bipyridine-type ligands. In the presence of $[Ir(OMe)(COD)]_2$ as the source of iridium and BINAP as the ligand, the silylation of C-H bonds was not observed (Entry 2). In contrast, the reactions conducted with a rhodium precursor and BINAP, Segphos or DTBM-segphos as ligand occurred to form the products of silylation of an

alkyl C-H bond (Entries 3-5), albeit in low to moderate yields. As observed for silylation catalyzed by the complex generated from iridium and Me_4Phen, the silylation of the secondary C-H bond at the position γ to oxygen was favored over silylation of the primary C-H bond at the position δ to oxygen. However, the silylation reaction catalyzed by the combination of $[RhCl(COD)]_2$ and Xantphos occurred at the C-H bond located δ to oxygen to give the six-membered oxasilolane exclusively (Entry 6). The yield of the reaction was a high 96% when conducted with the preformed complex RhCl(Xantphos) as catalyst (Entry 11).[15]

Reactions with a series of Xantphos derivatives showed that the electronic and steric properties of the ligand had a strong influence on the yield of the silylation process. Aromatic Xantphos derivatives generate the most active catalysts. The yields of reactions catalyzed by rhodium complexes of methoxy-substituted or trifluoromethyl-substituted Xantphos were lower than those of reactions conducted with the unsubstituted Xantphos (Entries 7-8). The reactions catalyzed by the combination of $[RhCl(COD)]_2$ and amino-Xantphos analog **L7** or the hindered *t*-butyl-Xantphos analog **L8** did not give any products from silylation of C-H bonds (Entries 9-10).

Table 2.1 Catalytic Silylation of Primary C-H Bonds

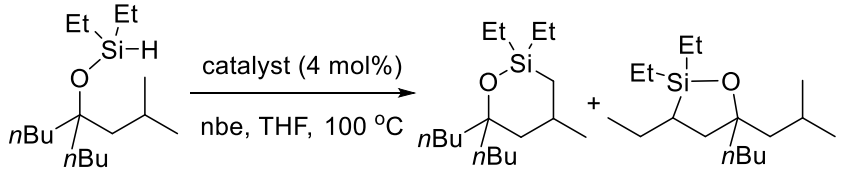

2a **3a** **3b**

entry	catalyst	Yield% (**3a**: **3b**)
1	$[Ir(OMe)(COD)]_2$/Me_4Phen	94 (0.18 : 1)
2	$[Ir(OMe)(COD)]_2$/BINAP (**L1**)	<5 (ND)
3	$[RhCl(COD)]_2$/BINAP (**L1**)	10 (0.48 : 1)
4	$[RhCl(COD)]_2$/Segphos (**L2**)	15 (0.50 : 1)
5	$[RhCl(COD)]_2$/DTBM-Segphos (**L3**)	48 (0.50 : 1)
6	$[RhCl(COD)]_2$/Xantphos (**L4**)	80 (> 20 : 1)
7	$[RhCl(COD)]_2$/MeO-Xantphos (**L5**)	68 (> 20 : 1)
8	$[RhCl(COD)]_2$/CF_3-Xantphos (**L6**)	71 (> 20 : 1)
9	$[RhCl(COD)]_2$/Xantphos-NEt_2 (**L7**)	<5 (ND)
10	$[RhCl(COD)]_2$/Xantphos-*t*Bu (**L8**)	<5 (ND)
11	RhCl(Xantphos)	96 (>20 : 1)

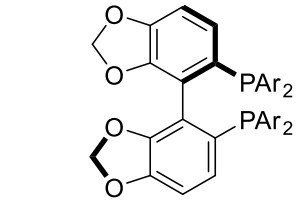

L2, Ar = C_6H_5

L3, Ar = 3,5-(*t*Bu)$_2$-4-OMe-C_6H_2

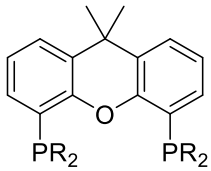

L4, R = C_6H_5

L5, R = 4-$MeOC_6H_4$

L6, R = 4-$CF_3C_6H_4$

L7, R = NEt_2

L8. R = *t*Bu

[a] Conditions: **2a** (1.0 equiv.), catalyst (4 mol% monomer), nbe (1.2 equiv.), THF, 100 °C, 16 h. Yields were determined by GC using *n*-dodecane as an internal standard. ND, not determined.

2.2.2 Scope of Rh-Catalyzed Silylation of C-H Bonds.

Examples of the Rh-catalyzed silylation of primary C-H bonds located δ to the oxygen of tertiary alcohols are summarized in Table 2.2. The yields shown correspond to the 1,4-diols formed

by oxidation of the six-membered oxasilolanes. The reactions occurred in good yields with a variety of tertiary alcohols bearing primary C-H bonds δ to oxygen. Branching at the alkyl chain was important for the silylation to occur; reactions of tertiary alcohols containing an *iso*-butyl group occurred selectively to give the products of silylation at the primary C-H bond (**4a**, **4b**). In the presence of primary C-H bonds at carbons located γ and δ to oxygen in the same substrate, the silylation process occurs at the γ C-H over the δ C-H bond.

In addition to acyclic alcohols, cyclic tertiary alcohols underwent silylation at a primary C-H bond δ to the hydroxyl group (**4c**, **4d**). The reaction occurred at this primary C-H bond over the secondary C-H bond of the ring and at a primary C-H bond δ to the OH group when a primary C-H bond was present at both the δ and ε positions (e.g. to form **4a** or **4e**). The catalyst is not highly sensitive to steric hindrance γ to the reacting C-H bond; hydroxylation occurred in 66-72% yield at the hindered methyl C-H bonds in the neopentyl groups of **4f** and **4g**. In addition to tertiary alcohols with branching γ to the hydroxyl group, alcohols with branching β to the hydroxyl group underwent silylation selectively at the primary C-H bond (**4h**). The reaction did not occur to give substantial amounts of product when the alkyl chain lacked branching altogether, as shown by the low yield of the reaction to form product **4i.**

Table 2.2 Scope of Rh-Catalyzed C-H Silylation[a]

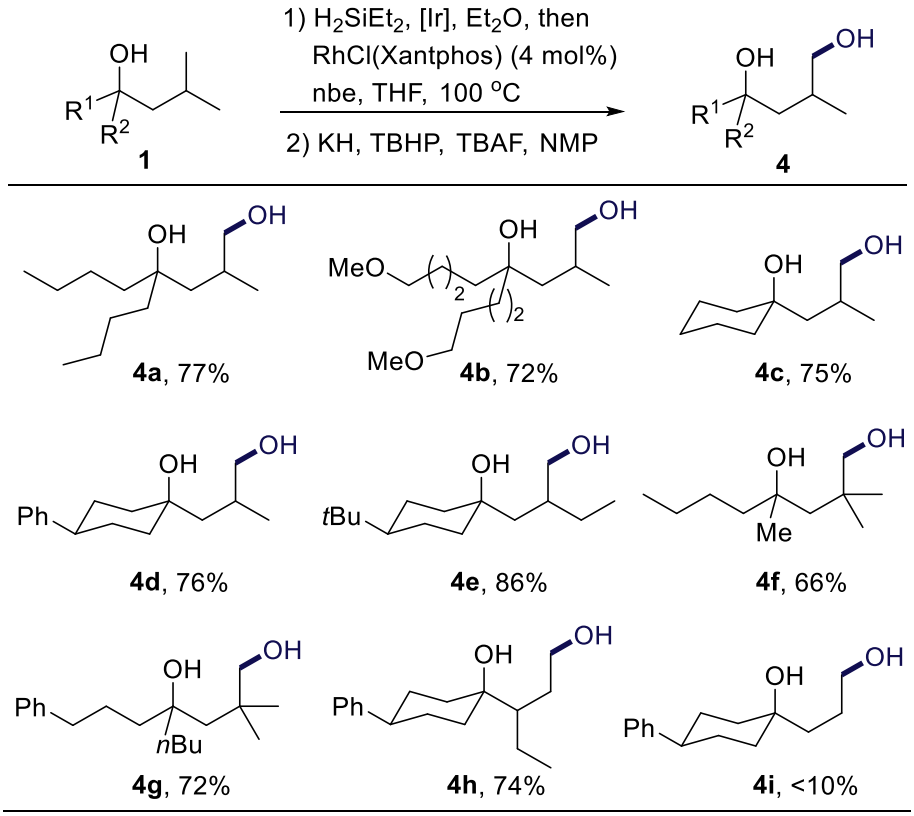

[a] Conditions: **1** (1.0 equiv.), Et_2SiH_2 (1.5 equiv.), $[Ir(cod)OMe]_2$ (0.10-0.20 mol %), Et_2O, room temperature (rt); removal of volatiles, then RhCl(Xantphos) (4 mol%), nbe (1.2 equiv.), THF, 100 °C. Isolated yields are reported.

The functional group tolerance of the process leading to hydroxylation of the C-H bond located δ to the existing hydroxyl group is illustrated by the examples in Table 2.3. Aryl halides, an aryl trifluoromethyl group, and a tri-substituted alkene were compatible with the reaction conditions (**4j**-**4m**). A phenol and an alcohol protected as methyl, benzyl and TBS ethers were also tolerated (**4n**-**4p**). The TBS group in the silylation product cleaved during oxidation, producing a triol (**4p**).

Table 2.3 Functional Group Tolerance of C-H Silylation[a]

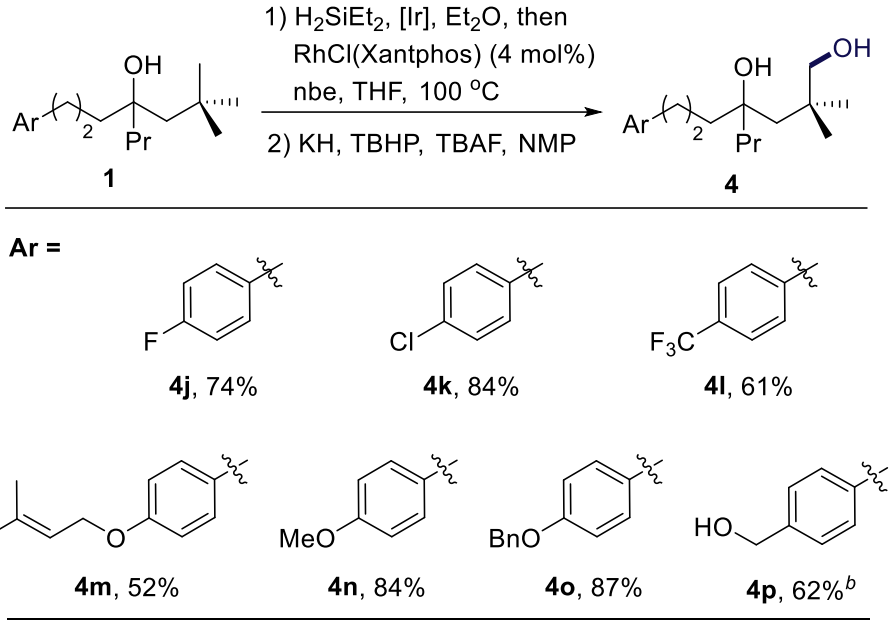

[a] Conditions: **1** (1.0 equiv.), Et_2SiH_2 (1.5 equiv.), $[Ir(cod)OMe]_2$ (0.2 mol %), Et_2O, room temperature (rt); removal of volatiles, then RhCl(Xantphos) (4 mol%), nbe (1.2 equiv.), THF, 100 °C. Isolated yields are reported. [b] Starting from a *tert*-butyldimethylsilyl ether.

The compatibility of the reaction conditions with carbonyl groups was further investigated. In the presence of $RuCl_2(PPh_3)_3$ as a catalyst, the reactions of diethylsilane with tertiary alcohols containing ester and carbamate groups cleanly formed the diethyl(hydrido)silyl ether precursor to the C-H bond functionalization process. The Rh-catalyzed silylation of C-H bonds then formed the six-membered oxasilolanes, demonstrating compatibility of the catalytic chemistry with the carbonyl groups in these silyl ethers. However, this functionality in products **3q**-**3s** (eq 2.1) was not tolerated by the highly basic conditions required for the oxidation of the resulting oxasilolanes under Fleming-Tamao conditions. Thus, reactions at the ester and carbamate must be conducted prior to the Fleming-Tamao oxidation. Perhaps most striking, the silylation of an alkyl C-H bond under these conditions is more tolerant of functional groups than common oxidation of a C-Si bond.

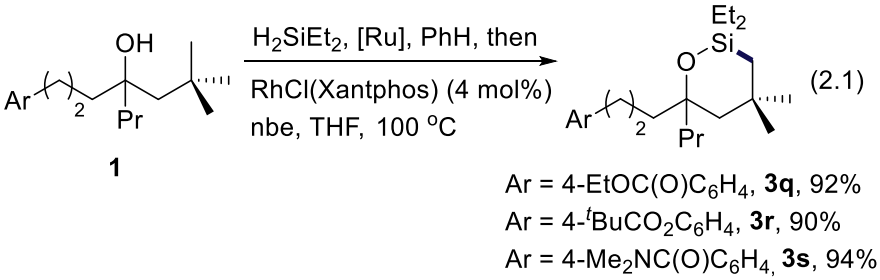

This silylation of an unactivated C-H bond also enables the functionalization of two primary C-H bonds in an *iso*-butyl group sequentially. Starting from alcohol **1d** shown in Scheme 2.2, the first C-H silylation and oxidation occurred in good yield to give the hydroxylation product **4d**. After protection of the primary alcohol as a silyl ether (**5d**), a second C-H bond was silylated. Oxidation of the resulting oxasilolane and *in-situ* deprotection of the silyl ether under the conditions of Fleming-Tamao oxidation provided the triol product **6d**.

Scheme 2.2 Rh-Catalyzed Sequential C-H Silylation

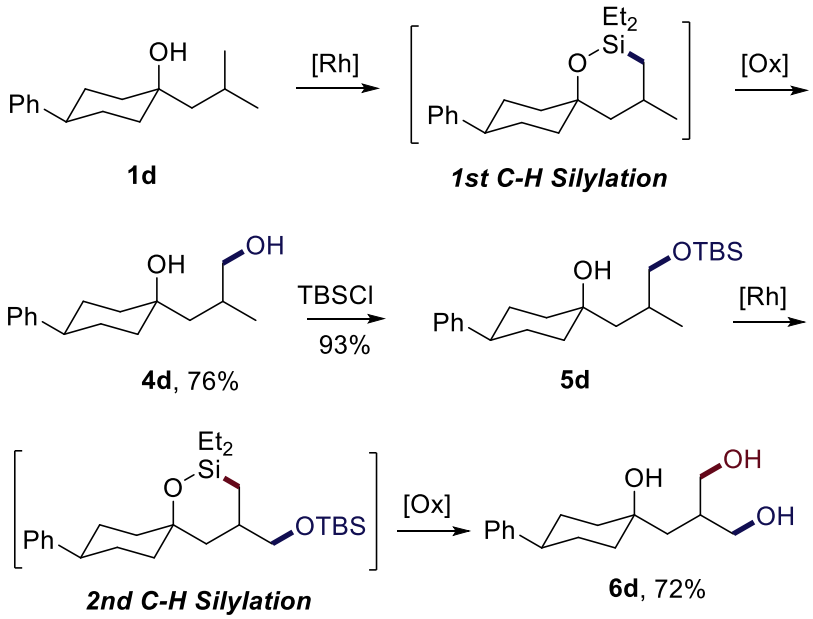

Because the Rh-catalyzed silylation is highly selective and tolerant of functional groups, this process could be applied to the direct functionalization of natural products and their derivatives bearing tertiary alcohols. In an initial example, the reaction of the silyl ether derived from 1-methylneomenthol, synthesized from menthone and MeMgBr, led to the site-selective functionalization of the primary C-H bond to give the corresponding 1,4-diol **4t**. This silylation produced a single diastereomer with the relative configuration confirmed by X-ray crystallography.

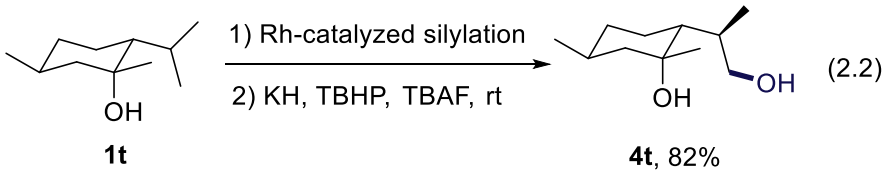

Many more complex, naturally occurring compounds contain multiple hydroxyl groups. To determine the feasibility of conducting site-selective silylation directed by one of the hydroxyl groups in more complex structures, we studied the alcohol-directed oxygenation of 20(*S*)-hydroxycholesterol, a naturally occurring oxysterol. Oxysterols function as signaling molecules that modulate a range of physiological phenomena including transportation of lipids and control over cellular states.[16] Oxidation of the C-H bonds in these molecules changes their physical properties.[17]

To enable functionalization directed by the tertiary alcohol in 20(S)-hydroxycholesterol, the secondary alcohol was selectively protected to form the corresponding silyl ether. Under the conditions we developed for alcohol-directed, site-selective silylation of C-H bonds δ to alcohols, the mono-protected diol **1u'** was functionalized at the C18 position. Subsequent Fleming-Tamao oxidation with concomitant deprotection provided triol **4u**. These results show that the oxygenation of C-H bonds δ to alcohols, in addition to the previously reported oxygenation of C-H bonds γ to alcohols should allow functionalization of a range of terpenoids.

Scheme 2.3 Rh-Catalyzed Silylation of Oxysterol

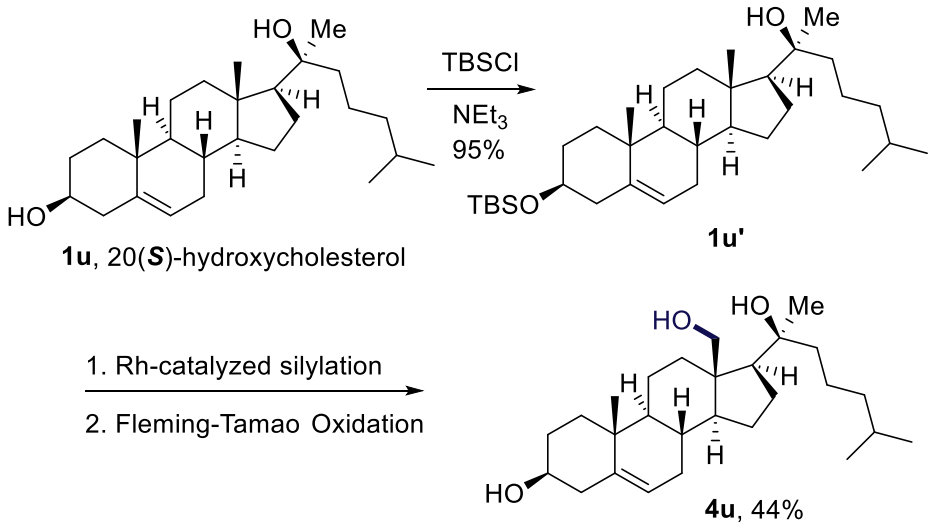

2.2.3 Experimental Mechanistic Studies.

To understand the origin of the regioselectivity of this silylation reaction and the origin of the effect of the ligand on this selectivity, we conducted detailed studies of the mechanism by a combination of experiment and computation. To determine the rate limiting step of this reaction, the resting state of the catalyst was characterized, the reaction orders for each reagent were determined, and the rate of silylation of C-H and C-D bonds was measured. In addition, several rhodium complexes were synthesized that elucidate the path by which the pre-catalyst enters the catalytic cycle. Finally, to gain information on the energetics that control selectivity, computations

were conducted on the Segphos-ligated catalyst, which generates products from silylation of secondary C-H bonds γ to the original hydroxyl group, and on the Xantphos ligated catalyst, which generates products from silylation of primary C-H bonds δ to the original hydroxyl group.

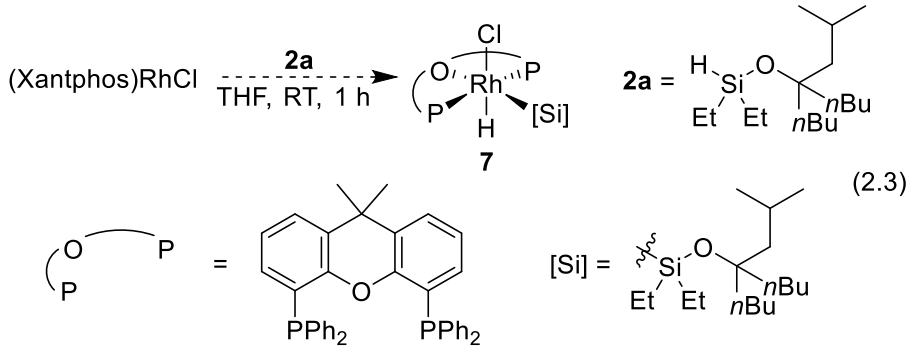

2.2.3.1 Generation and Identification of the Resting State.

To elucidate the pathway by which the pre-catalyst enters the catalytic reaction and the structure of the resting state of the catalyst, the reaction of (Xantphos)Rh(Cl) with silyl ether **2a** and norbornene was conducted. Although (Xantphos)Rh(Cl) is insoluble, the reaction occurred quickly (< 10 m) at room temperature to form a clear homogeneous solution containing complex **7** shown in eq 3. The ^{31}P NMR spectrum of the solution consisted of a doublet (due to coupling to ^{103}Rh) at 36.6 ppm, indicating two equivalent phosphines, and the ^{1}H NMR spectrum contained a doublet of triplets at -14.1 ppm, indicating that the Rh complex contains a metal hydride coupled to rhodium and two equivalent phosphorus atoms. The same species formed from (Xantphos)Rh(Cl) and the silyl ether **2a** in the absence of norbornene, but it was not formed from (Xantphos)Rh(Cl) and norbornene in the absence of the silyl ether.

Heating of the catalytic silylation reaction at 100 °C for 1 h led to a loss of the ^{31}P NMR signal at 36.6. The major resonance observed in the ^{31}P NMR spectrum after heating was a doublet at 22.6 ppm with a ^{31}P-^{103}Rh coupling constant of 142 Hz. No signal in the hydride region of the ^{1}H NMR spectra was observed. Based on these data, we hypothesized that the resting state of the Rh catalyst is a Xantphos-ligated Rh(I) silyl complex.

We were unable to isolate complex **7** formed from (Xantphos)Rh(Cl) and the silyl ether **2a** in pure form, due to its high solubility in organic solvents, but we isolated an analogous complex containing the 1-adamantyl silyl ether **2v**.[18] The reaction of **2v** with (Xantphos)Rh(Cl) formed silyl hydride complex **8** (Figure 2.1). The solution-phase NMR spectral data of complex **8** were analogous to those of the rhodium complex formed in the catalytic system before heating. A single doublet was observed in the ^{31}P NMR spectrum at 35.7 ppm, and a similar doublet of triplets at -14.0 ppm for a hydride ligand was observed in the ^{1}H NMR spectrum. These data are consistent with the formula (Xantphos)Rh(Cl)(H)(SiEt$_2$OAd), resulting from oxidative addition of the Si-H bond of the silane to (Xantphos)Rh(Cl).

Figure 2.1 Synthesis and Solid-State Structure of (Xantphos)Rh(H)(Cl)(SiEt$_2$OAd) (8)

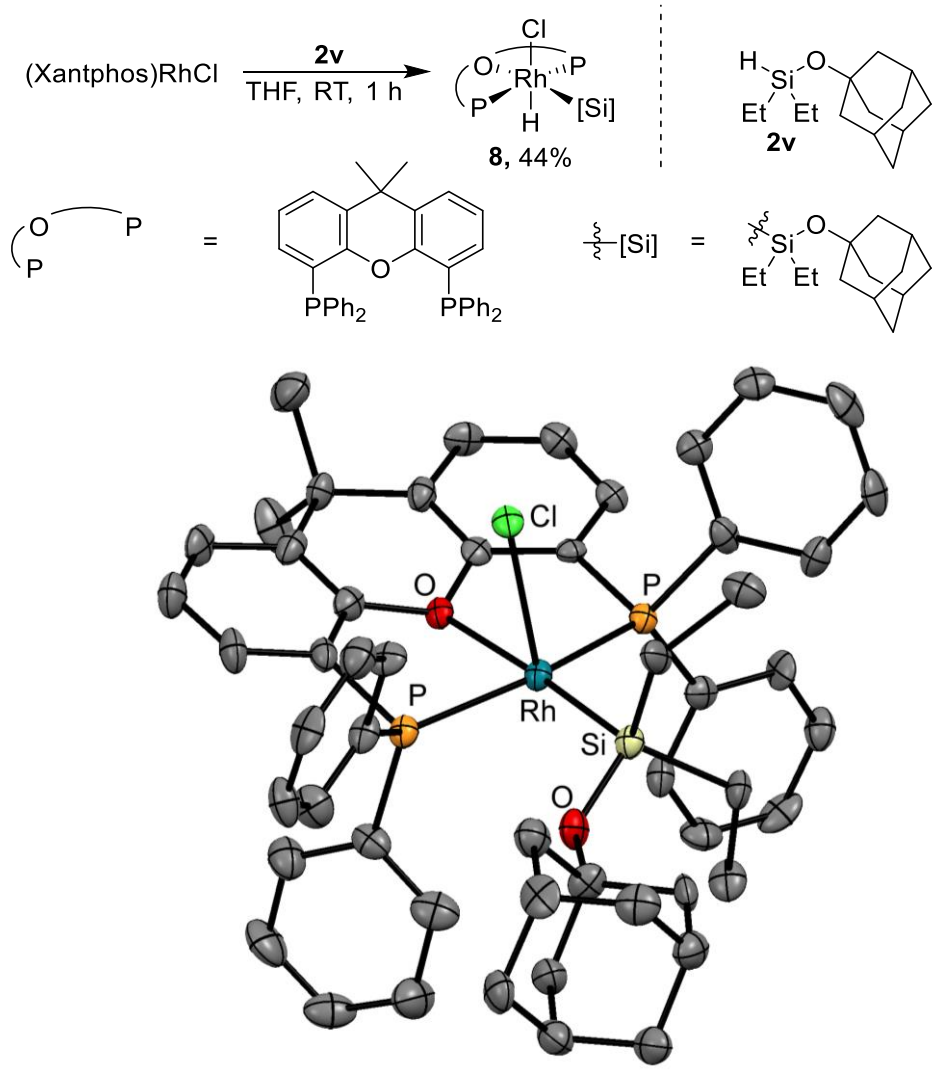

The identity of Rh complex **8** was confirmed by single-crystal x-ray diffraction. The solid-state molecular structure of Rh silyl hydride **8** consists of an octahedral Rh(III) center containing a meridional, tridentate Xantphos ligand. The silyl group is oriented trans to the Xantphos oxygen, and the chloride occupies a position axial to the plane of the Xantphos ligand and the silyl group. The hydride ligand, shown by ^{1}H NMR spectroscopy to be present, would be located at the site trans to the chloride.

Figure 2.2 Synthesis and Solid-State Structure of $(Xantphos)_2Rh(H)$ (9)

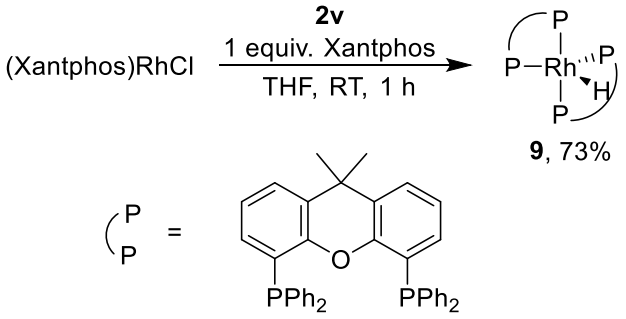

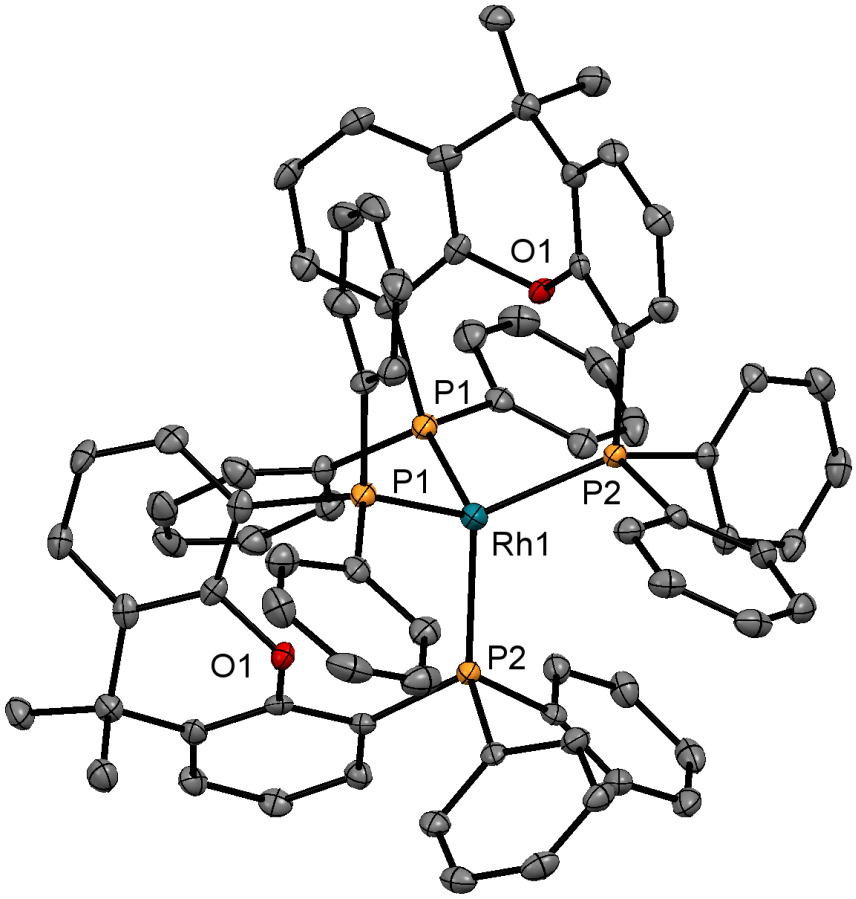

Selected bond lengths (Å) and angles (deg): Rh−P1, 2.35; Rh−P2, 2.34; P1-Rh−P2 (same ligand), 106.4; P1-Rh−P2 (between ligands), 109.8; P1-Rh−P1, 105.9; P2-Rh−P2, 118.0

The reaction of (Xantphos)Rh(Cl) with silane in the presence of additional Xantphos produced a complex that was different from that formed by the reaction of (Xantphos)Rh(Cl) with silane in the absence of added Xanphos. The resulting complex (**9**) is not soluble in common laboratory solvents but was analyzed in the solid state by single-crystal x-ray crystallography. The structure, shown in Figure 2.2, is a rhodium(I) hydride complex containing two Xantphos ligands with phosphorus atoms in a nearly tetrahedral array. The P-Rh-P bite angle for each ligand is 106°. The hydride was not located by X-ray diffraction, but the infrared spectrum contains a stretching

frequency at 2156 cm^{-1}, which is consistent with the presence of a rhodium hydride. The mild conditions under which the complex forms imply that the barrier to reductive elimination of the silyl chloride from complex **8** is low. We propose that complex **8** forms initially in the catalytic reaction, and that it undergoes reductive elimination of the silyl chloride, producing a Rh(I) hydride complex, which enters the catalytic cycle. In the presence of excess Xantphos, this hydride complex forms the crystalline, insoluble **9**.

The catalytic competencies of complexes **8** and **9** were determined. The rate of the reaction conducted with isolated **8** as catalyst was the same as that for the reaction initiated with (Xantphos)Rh(Cl) as catalyst (see experimental section for details). Thus, complex **8** is catalytically competent to be an intermediate in the silylation of C-H bonds located δ to a silyl ether. In contrast, no product was observed when the reaction was conducted with complex **9** as catalyst. Thus, complex **9** is not competent to be part of the catalytic cycle, likely due to the insolubility of this species in THF at 100 °C.

Figure 2.3 Synthesis and Solid-State Structure of (Xantphos)Rh(H)(nbe)($SiEt_2OAd$) (10)

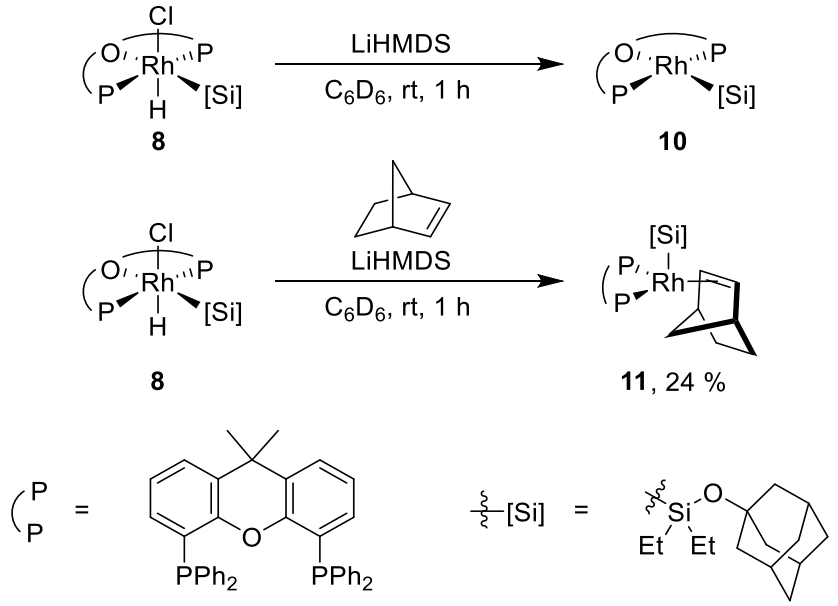

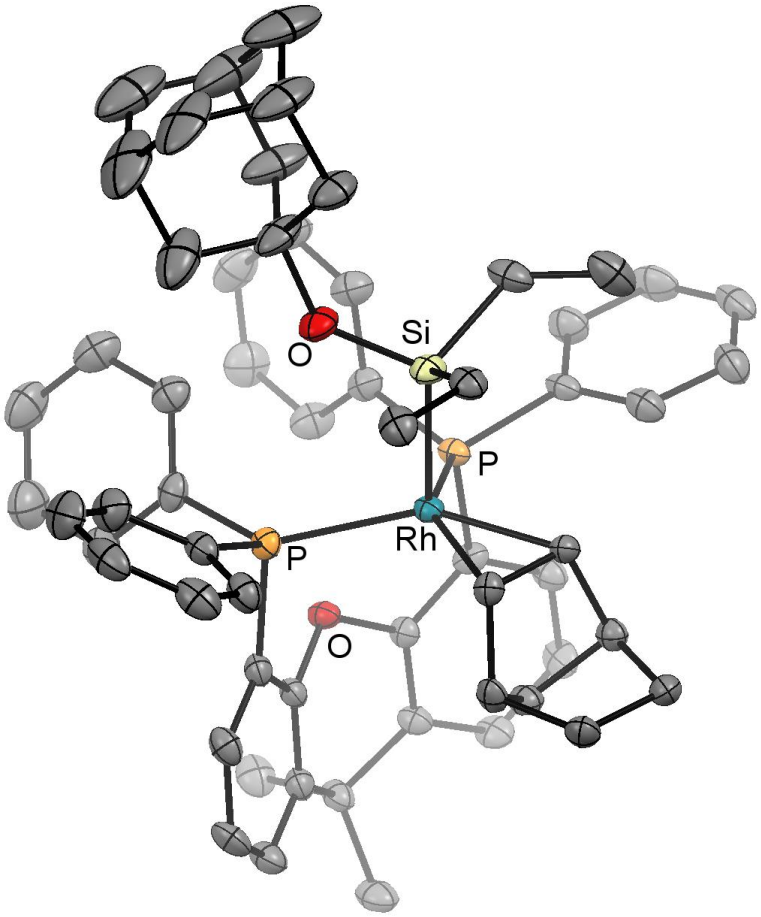

We also sought to identify the resting state of the Rh complex in the catalytic silylation of C-H bonds. We hypothesized that this species was a Xantphos-ligated Rh(I) silyl complex because no signal was observed in the hydride region of the ^{1}H NMR spectra of the reaction obtained after heating. To test this hypothesis, we independently prepared Rh(I) silyl complex **10** (Figure 2.3) from the reaction of Rh hydride complex **8** with LiHMDS (Figure 2.3a).[19] The Rh(I) silyl complex [Rh(Xantphos)($SiEt_2OAd$)] (**10**) was characterized by ^{1}H, and ^{31}P NMR spectroscopy of the crude reaction mixture. The ^{1}H and ^{31}P NMR spectra of the complex are consistent with a Rh(I) silyl complex; The ^{31}P NMR spectra contains a resonance at 32.6 ppm with a strong ^{103}Rh coupling of 193 Hz, indicating that Xantphos remained bound to the metal. Resonances corresponding to the adamantyl group were also observed, showing that the silyl group is still connected to rhodium. NMR spectroscopy does not reveal whether the oxygen of Xantphos is bound to Rh in complex **10**. Silyl complex **10** formed in this manner decomposed during attempts to isolate the complex in pure form.

However, a norbornene adduct of Rh(I) silyl complex **10** was isolated and fully characterized. The deprotonation of Rh-silyl complex **8** containing hydride and chloride ligands in the presence of norbornene formed the isolable norbornene silyl Rh(I) species **11** (Figure 2.3b). The ^{31}P NMR spectrum of this complex contains a single resonance, which is a doublet at 21.4 PPM with a ^{31}P-^{103}Rh coupling of 140 Hz. The ^{1}H NMR spectrum of isolated **11** contains alkyl resonances for the silyl unit and a resonance at 2.6 ppm for the coordinated alkene unit.

The composition of complex **11**, deduced in solution, was confirmed by x-ray crystallography (Figure 2.3). The structure consists of a Rh(III) center in which the two phosphorus atoms, but not the oxygen atom, of Xantphos are bound to rhodium, along with one silyl group, one hydride, and one alkene unit. The geometry at rhodium is trigonal pyramidal or square pyramidal, depending on how one considers the bonding of the alkene. The C-C double bond bound to rhodium is significantly longer (1.45 Å) than that of the free alkene 1.34 Å, suggesting that the alkene is bound in a metallacyclopropane structure and the overall geometry is a square pyramid. The two norbornene carbons bonded to rhodium, the two phosphorus atoms, and the rhodium center lie in a plane; the axial position of the square pyramidal structure is occupied by the silyl group. This 16-electron complex could undergo oxidative addition of a C-H bond. However, the large size of the bound norbornene would hinder the approach of a C-H bond to the metal center.

The full characterization of **11** allows clear assignment of the resting state of the rhodium in the catalytic reaction. As noted earlier in this paper, the ^{31}P NMR signal for the resting state is a doublet at 22.6 ppm with a coupling constant of 142 Hz. Likewise, the ^{31}P NMR signal for complex **11** is a doublet at 21.4 ppm with a coupling constant of 140 Hz. For comparison, the ^{31}P NMR signal for complex **10** lacking norbornene is a doublet at 32.6 ppm with a coupling constant of 193 Hz. Therefore, the resting state of the catalyst is a Rh complex ligated by one Xantphos, one norbornene and one alkoxy diethylsilyl ligand.

2.2.3.2 Kinetic Analysis of the Catalytic Process.

The dependence of reaction rate on the concentration of each reagent was measured to reveal the rate-determining step of the catalytic process. The reaction orders in silane, catalyst, and hydrogen acceptor were determined by measuring initial rates of the silylation at 100-120° C with varied concentrations of each reagent. The reactions were conducted with chloride complex **7** as the pre-catalyst. Reactions with concentrations of catalyst ranging from 2 mM to 16 mM showed that the reaction is first order in catalyst. Reactions with concentrations of silane varying from 0.04 M to 0.3 M showed that the reaction is zero order in silane. Finally, reactions conducted with concentrations of norbornene varying from 0.4 M to 3 M showed that the reaction is inverse first order in norbornene. With the resting state shown to be a silyl norbornene complex, the zero-order behavior in silane indicates that the silane bound to the resting state undergoes C-H bond functionalization, and the inverse reaction order in norbornene indicates that norbornene dissociates reversibly from this resting state to form a 14-electron compound prior to the functionalization process.

Scheme 2.4 Kinetic Isotope Effect

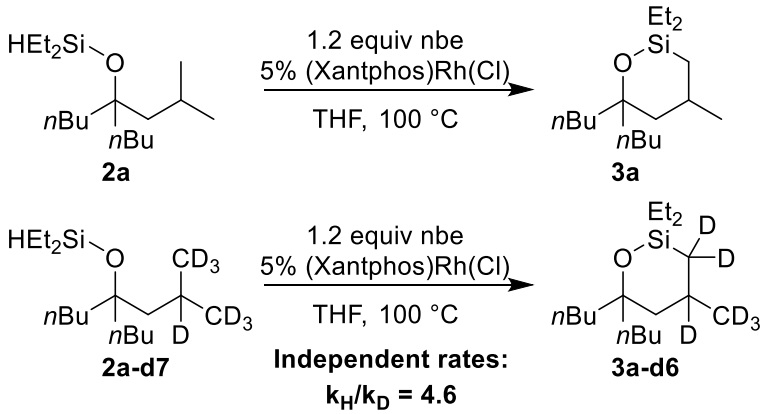

The kinetic isotope effect on the catalytic process was measured to determine the potential reversibility of the C-H bond cleavage process. The rates of the reaction of the protio substrate (**2a**) and deuterio substrate (**2a-*d*$_7$**) containing deuterium at the position δ to the alcohol were measured separately. A kinetic isotope effect of 4.6 was obtained from these rates (5.7 and 1.2 x 10^{-5} M/s), indicating that C-H bond cleavage is irreversible and rate limiting. This result is consistent with the reaction orders and the observed resting state and also implies that the reversible dissociation of norbornene occurs before irreversible cleavage of the C-H bond.

Based on the orders in substrate, hydrogen acceptor and catalyst, kinetic isotope effect, and isolated model of the resting state, we conclude that the reaction occurs by the catalytic cycle in Scheme 2.5. The active catalyst is generated by oxidative addition of a silyl hydride to the RhCl precatalyst to form complex **A**. Complex **A** forms the Rh(I) hydride compound **B**, which lies on the catalytic cycle. Norbornene undergoes migratory insertion into the Rh-H bond to form norbornyl complex **C**, which undergoes oxidative addition of a silyl hydride and reductive elimination of norbornane to produce the 14-electron Rh(I) silyl complex **D**. Complex **D** binds norbornene reversibly to form the resting-state **E**, which lies off the catalytic cycle. Intramolecular oxidative addition of the δ C-H bond to the rhodium center in **D** forms the seven-membered rhodacycle **F**. Reductive elimination from **F** to form the C-Si bond produces a six-membered cyclic silyl ether and regenerates Rh(I) hydride complex **B**.

Scheme 2.5 Proposed Catalytic Cycle for the Silylation of the C-H Bond δ to a Silyl Ether.

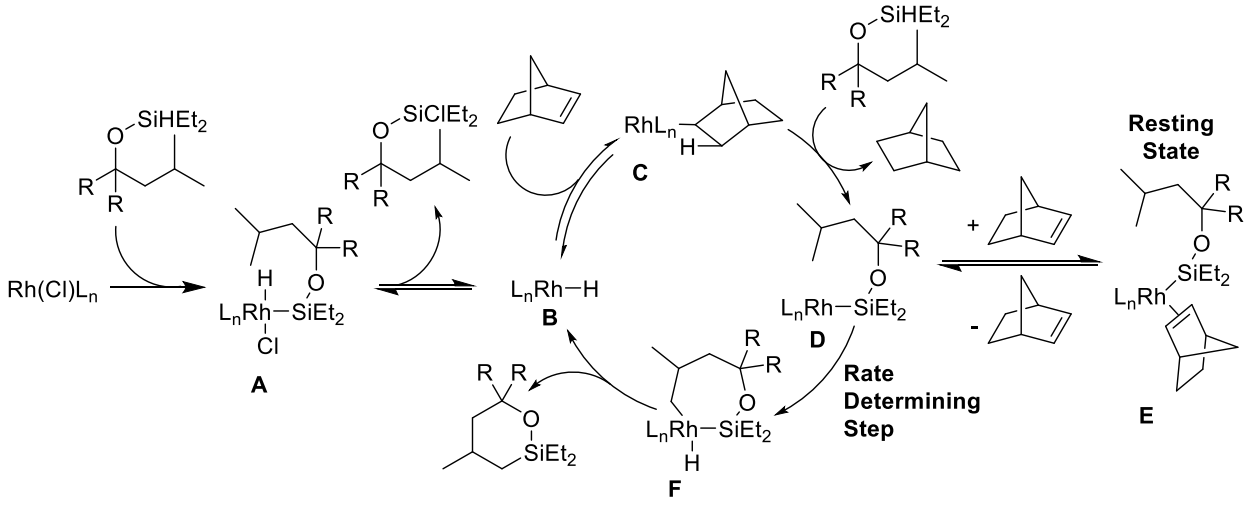

2.2.3.3 Computational Study and Origin of Selectivity.

DFT computations were performed to gain insight into the origin of the selectivity of the Xantphos catalyst for formation of the six-membered oxasilolane product. To do so, we computed the energies and geometries of Rh(I) silyl complexes that are potential catalytic intermediates, transition states for intramolecular cleavage of C-H bonds in those complexes, rhodacycles that result from C-H cleavage, and transition states for reductive eliminations to form C-Si bonds. Geometry optimizations were conducted with the Gaussian 09 software package, B3LYP functional (with gd3 dispersion correction), and LANL2DZ basis set for Rh and 6-31g(d,p) basis set for all other atoms. Single-point energy calculations were conducted with the M06 functional and LANL2TZ basis set for Rh and the 6-31++g** basis set for all other atoms, along with the SMD THF solvent correction. Thermal corrections were applied to the optimized geometries to provide Gibbs free energies. Each Rh(I) hydride complex, Rh(I) silyl complex, transition state, and Rh(III) metallacycle was computed with Segphos (experimental selectivity for silylation of C-H bonds located γ to a silyl ether) and Xantphos (experimental selectivity for silylation of C-H bonds located δ to a silyl ether) as the ligand to reveal the origin of selectivity. To reduce the computational requirements, the calculations were conducted on a model substrate containing methyl groups, instead of ethyl groups, on silicon.

The minimization of the energy of octahedral Rh-Xantphos complexes that result from oxidative addition of a C-H bond showed that many reasonable isomeric products can form. Xantphos can coordinate in a facial or meridonal manner. Any of the three X-type ligands could be trans to the weakly coordinating oxygen of the Xantphos ligand in either coordination mode. The length of the alkyl chain of the substrate is too short to form a complex with the alkyl ligand and the silyl ligand trans to each other. The five 6-coordinate isomers in which the alkyl and silyl ligands are cis to each other were modeled. The square pyramidal complex lacking coordination by the oxygen atom in Xantphos and containing the silyl group in the axial position was also computed. The isomer with the silyl group in this position was computed because the two methyl substituents on silicon in this isomer lie over the backbone of Xantphos, whereas these two methyl substituents clash with the phenyl substituents on phosphorus in the isomer containing the silyl group in an equatorial position.

Figure 2.4 Modeling of Rhodacycles in Various Geometries and Coordination Modes

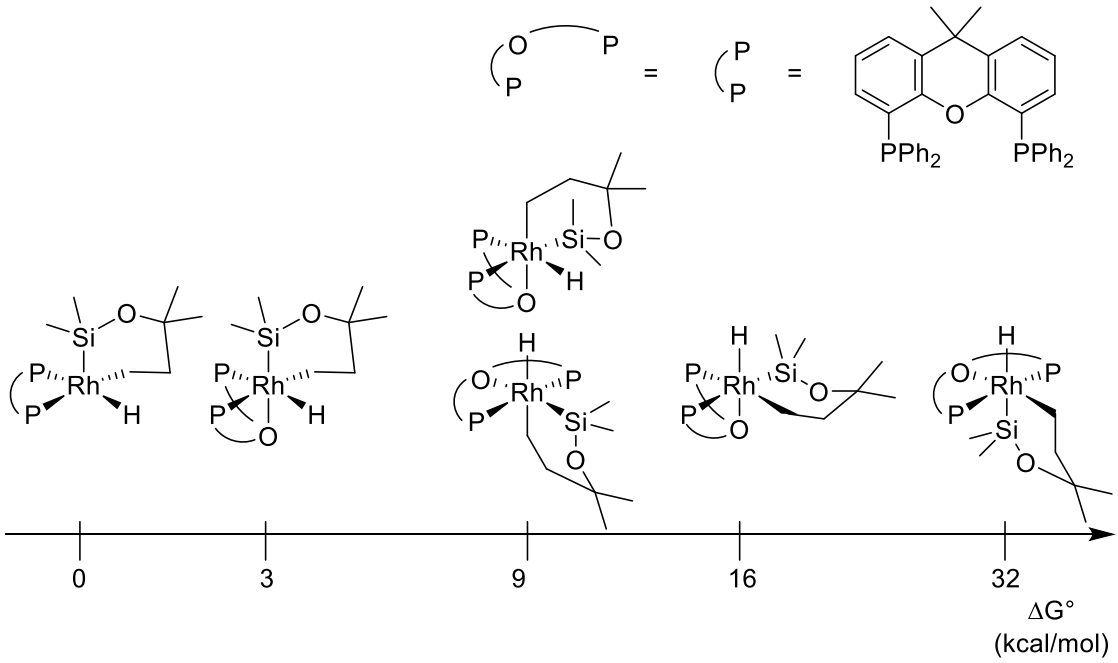

Although the energy of six-coordinate, 18-electron structures in which the oxygen atom in Xantphos binds to rhodium might be expected to be lower than that of square pyramidal 16-electron complexes lacking coordination of the oxygen atom, our calculations showed that the energy of the square pyramidal complex in which this oxygen does not interact with rhodium is lower than that of the complexes in which this oxygen does interact with rhodium. The isolated resting state, complex **11**, also lacked a bonding interaction between the oxygen atom of Xantphos and the rhodium center in the solid-state structure. These two results suggest that the ability of Xantphos to bind as a tridentate ligand does not account for the difference in selectivity between the catalysts containing Xantphos and Segphos as ligand.

Figure 2.5 Computed Energies for Silylation of C-H Bonds δ to a Silyl Ether (red) and γ to a Silyl Ether (Blue). Silylation with the Rh-Xantphos Catalyst (Left). Silylation with the Rh-Segphos Catalyst (Right).

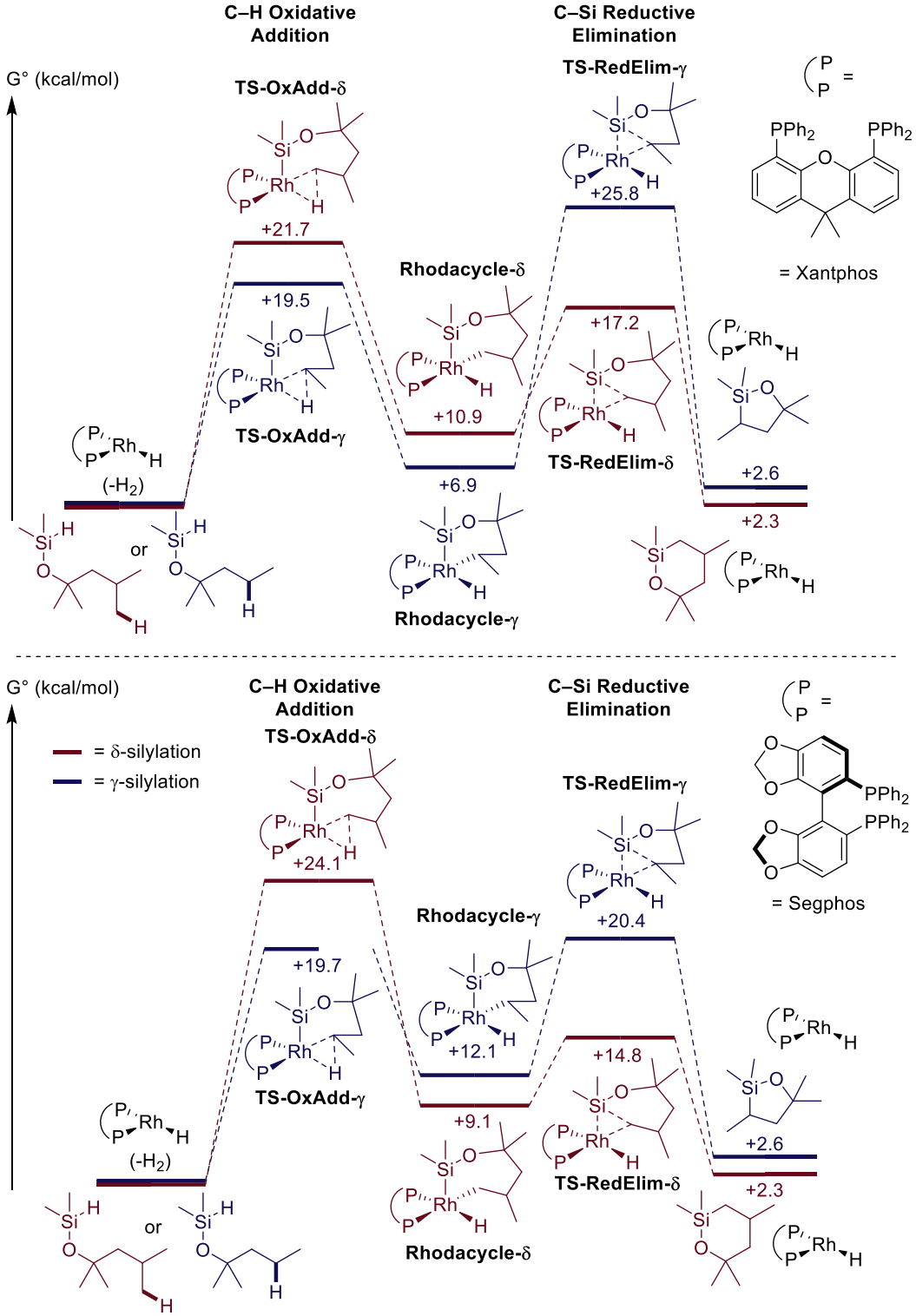

2.2.3.4 Computation of the pathways for silylation of C-H bonds δ and γ to a hydroxyl group.

The computed rate-determining step of the Rh-catalyzed silylation of primary C-H bonds δ to a silyl ether unit is different from the that for the competing silylation of secondary C-H bonds γ to a silyl ether. The highest calculated transition-state energy for functionalization of the δ C-H bond by the rhodium complexes ligated by both Xantphos (21.7 kcal/mol, shown in red in the left energy diagram) and Segphos (24.1 kcal/mol, shown in red in the right energy diagram) is that for oxidative addition of the C-H bond. The highest calculated transition-state energy for functionalization of the γ C-H bond by complexes of both ligands, shown in blue in both diagrams, is that for reductive elimination to form the C-Si bond. The barrier to reductive elimination from the secondary alkylrhodium complex to functionalize the γ C-H bond with the Xantphos-ligated system is almost 19 kcal/mol, and the transition-state free energy is 25.8 kcal/mol higher than that of the catalyst and reactants, whereas the analogous barrier for the complex ligated by Segphos is only 8.3 kcal/mol and the transition state free energy is 20.4 kcal/mol higher than that of the catalyst and reactants.

Figure 2.6 Computed Energies for Oxidative Addition of C-H Bonds δ to a Silyl Ether (red) and Reductive Elimination of C-Si bond γ to a Silyl Ether (Blue). Silylation with Rh/Segphos as Catalyst (Top). Silylation with Rh/Xantphos as Catalyst (Bottom).

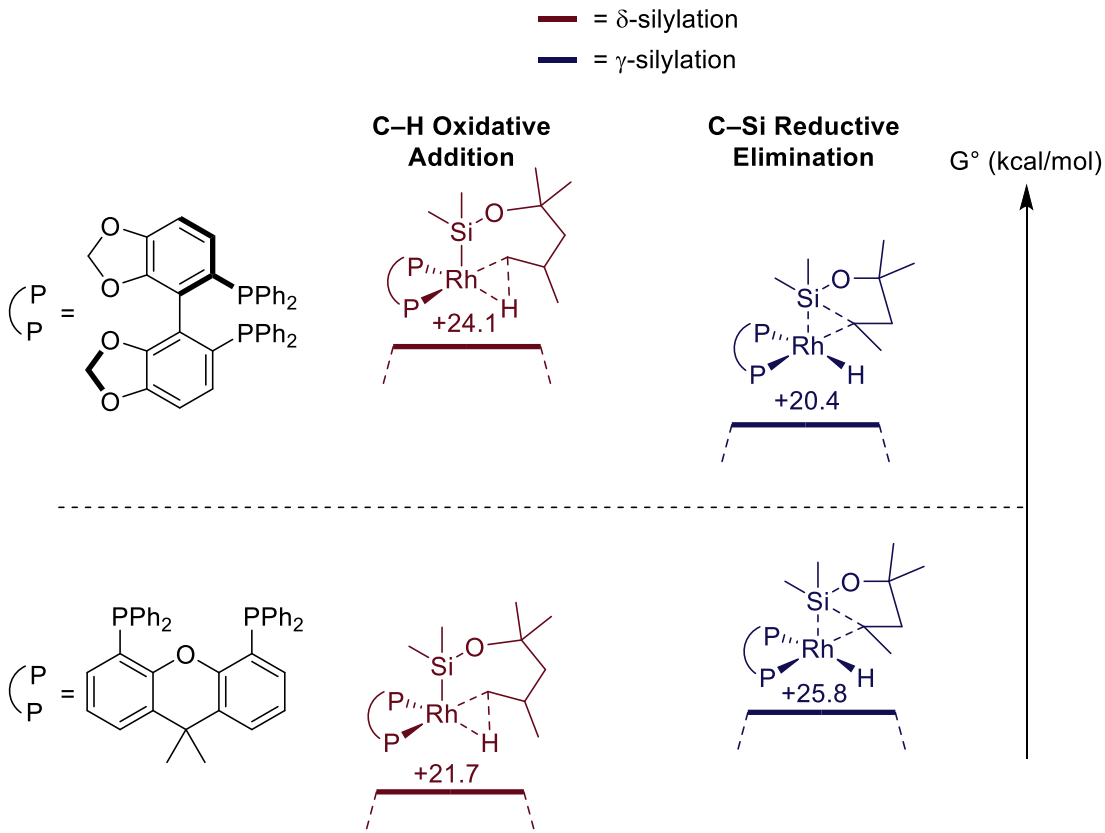

These calculations show that the unusual selectivity for formation of the six-membered oxasilolane with the Rh-Xantphos catalyst results from a high barrier for reductive elimination from a 6-membered metallacycle containing a secondary alkyl and a transition-state energy that is

higher than that for oxidative addition of a δ C-H bond to the same Rh-Xantphos catalyst to form a seven-membered metallacycle. The selectivity for formation of the more common 5-membered oxasilolane with the Rh-Segphos catalysts results from a transition-state energy for oxidative addition of the δ C-H bond to form the seven-membered metallacycle that is higher than that for reductive elimination from a 6-membered metallacycle containing a secondary alkyl.

2.2.3.5 Computational Model of the silylation of primary C-H bonds γ to the silyl ether.

The calculations just discussed show that the rate-determining steps for functionalization of C-H bonds δ to a silyl ether by both catalysts is different from that for functionalization of C-H bonds γ to a silyl ether, but they do not reveal why the oxidative addition of a primary C-H bond δ to the silyl ether is slower than the oxidative addition of a secondary C-H bond γ to the silyl ether for complexes of both ligands. Oxidative addition of a primary C-H bond is usually faster than oxidative addition of a secondary C-H bond. Thus, the relative rates for reactions of primary and secondary C-H bonds are, most likely, influenced by the size of the ring formed in the intramolecular processes. Further, these calculations do not reveal the extent to which formation of a five-membered cyclic silyl ether by reductive elimination from a secondary alkyl intermediate is slow because of the size of the ring that is formed or to what extent it is slow because reductive elimination from a secondary alkyl complex to form an Si-C bond is slower than reductive elimination to form a Si-C bond from a primary alkyl complex.

To address these questions, we computed the reaction coordinate for the silylation of a primary C-H bond γ to a silyl ether by the two catalysts and compared the energies in these reaction coordinates to those discussed in the prior section on the silylation of the substrate containing primary C-H bonds δ to a silyl ether and the substrate containing secondary C-H bonds γ to a silyl ether.

The reaction coordinates for silylations of primary C-H bonds γ to a silyl ether in the model compound catalyzed by the two rhodium-ligand combinations are shown in green color in Figure 2.7, along with the reaction coordinate (in blue color) presented earlier for the silylation of a secondary C-H bond γ to a silyl ether catalyzed by the same two systems. The left side shows the computed reaction coordinates for the silylation of primary and secondary C-H bonds γ to a silyl ether catalyzed by Xantphos-ligated system and the right side shows the computed reaction coordinate for the silylation of the same silyl ethers catalyzed by the Segphos-ligated system. For silylation of a primary C-H bond γ to the oxygen catalyzed by complexes of either ligand, the rate-determining step was computed to be oxidative addition of the C-H bond because reductive elimination from the primary alkyl intermediate has a low barrier. In contrast, for silylation of the secondary C-H bond γ to the silyl ether catalyzed by complexes of either ligand, the rate-determining step was computed to be reductive elimination to form the C-Si bond (vide supra). Thus, the rate-determining step for reaction at the primary C-H bond is computed to be different from that for reaction at a secondary C-H bond located the same distance from the ether oxygen as the primary C-H bond.

2.2.3.6 Conclusion on the Origin of Selectivity for Five vs Six-Membered Cyclic Silyl Ethers with Segphos and Xantphos as ligand.

Insight into the origin of the selectivity for the formation of the various-sized cyclic silyl ethers can be gained by comparing the transition-state energies for the oxidative addition of the primary C-H bond γ to a silyl ether to that for oxidative addition of the primary C-H bond δ to a silyl ether. The comparison of the computed transition-state energies for oxidative addition to form six-membered rhodacycles with primary alkyl groups to that to form the seven-membered rhodacycles with primary alkyls ligated by Xantphos or Segphos shows that oxidative additions that form seven-membered metallacycles are slower than those forming six-membered metallacycles for complexes of both ligands. The difference in computed free energies between the two transition states for reaction of the Xantphos-ligated catalyst is smaller (2.6 kcal/mol) than that for reaction of the Segphos-ligated catalyst (8 kcal/mol). However, this comparison of the transition-state energies for oxidative addition of primary C-H bonds to form six or seven-membered rhodacycles shows that formation of the six-membered rhodacycle is faster for complexes of both ligands. These data show quantitatively the extent to which formation of seven-membered metallacycles is slower than formation of six-membered metallacycles.

Figure 2.7 Computational Model of Silylation of a Primary and Secondary C-H bonds γ to a Silyl Ether with Rh/Segphos and Rh/Xantphos

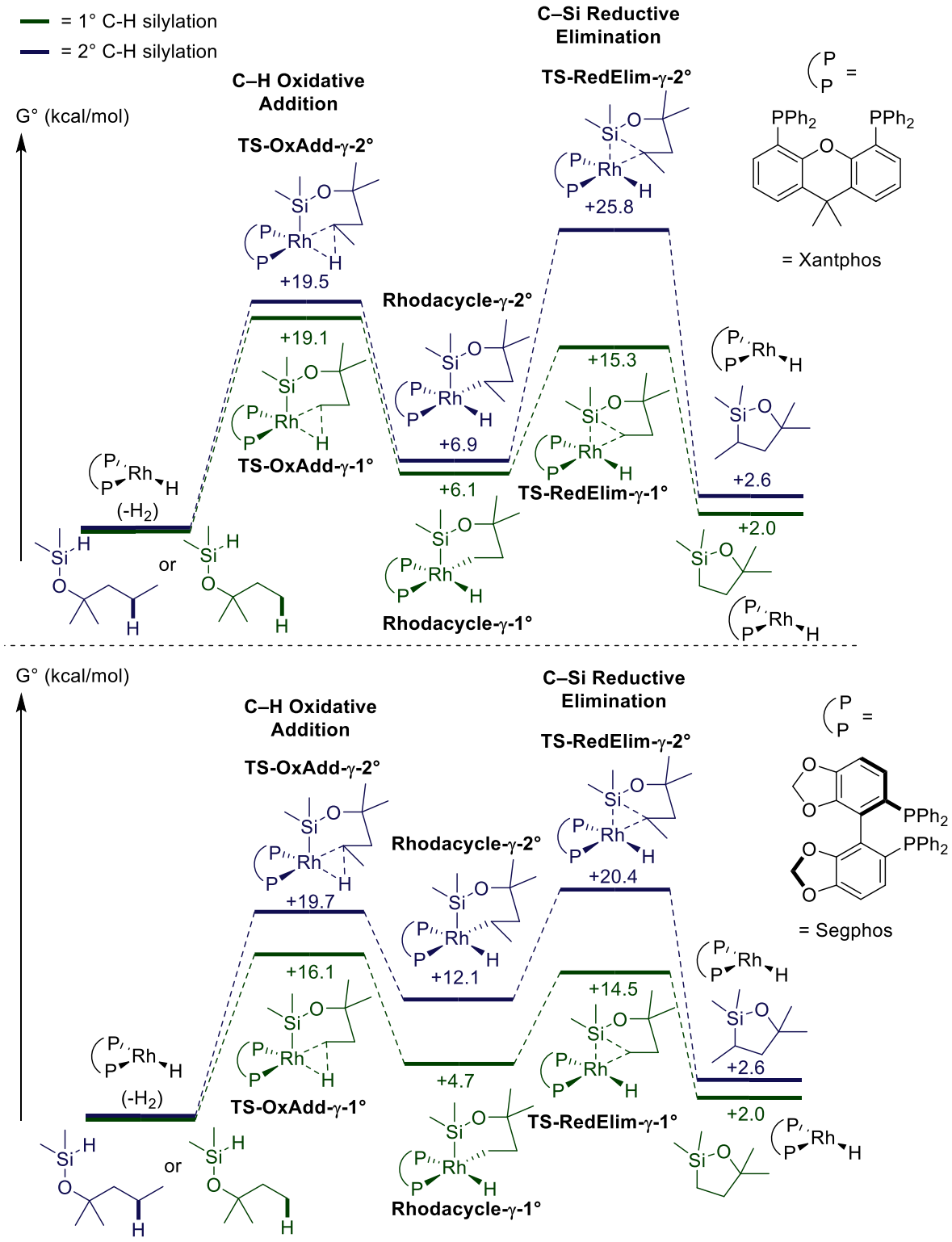

The comparison of the computed barriers to reductive elimination that form five-membered cyclic silyl ethers from primary alkyl complexes to those that form the same size ring from secondary alkyl complexes ligated by Xantphos or Segphos shows that reductive eliminations to form C-Si bonds involving secondary alkyl groups are much slower than those involving primary alkyl groups for complexes of both ligands. However, the *difference* between the transition-state energies of reductive elimination from the primary and secondary alkyl groups to form the C-Si bond in 5-membered rings is much greater for the catalyst containing the Xantphos ligand (10.5 kcal/mol) than it is for the catalyst containing the Segphos ligand (4.9 kcal/mol), and it is the difference in rates for reductive elimination from primary and secondary alkyl groups that lead to the unusual selectivity observed for the silylation of alkyl C-H bonds located δ to the silyl ether over C-H bonds located γ to the silyl ether.

This effect of the two ligands on these relative rates can be ascribed to the greater steric demand of Xantphos ligand. During the reductive elimination of secondary alkyl groups, the substituents on that carbon bound to rhodium tilt away from the silicon, causing these substituents to be closer to the phenyl groups of the ligand in the transition state than in the ground state. The catalyst formed from the Segphos ligand is more able to accommodate this increased steric demand than that formed from the Xantphos ligand possessing a wider bite angle. Thus, the difference in rates of reductive elimination from the primary or secondary alkyl complex containing Segphos as ligand is smaller than the differences in rates of reductive elimination from the analogous complexes containing Xantphos as ligand.

2.3 Conclusion

In summary, we have developed a rhodium-catalyzed site-selective silylation of primary C-H bonds to form six-membered oxasilolanes in the presence of [Rh(Xantphos)Cl] and conducted studies that reveal the origin of the new regioselectivity. After oxidation of the silylation products, 1,4-diols are obtained. This C-H oxidation tolerates many functional groups and has the potential for applications in the synthesis and functionalization of complex molecules.

The mechanism of this process is distinct from that for silylation of arenes. In contrast to the rate-determining reductive elimination to form the C-H bond of the reduced hydrogen acceptor that occurs during the silylation of arenes, the rate-limiting step of the rhodium-catalyzed silylation of alkyl C-H bonds δ to a silyl ether is cleavage of the C-H bond undergoing functionalization. The resting state of the catalyst for this process catalyzed by Xantphos-ligated rhodium is (Xantphos)Rh($SiEt_2OR$)(nbe). Consistent with this structure, the reaction is zero-order in substrate and inverse first-order in norbornene because norbornene dissociates prior to rate-determining intramolecular cleavage of the

alkyl C-H bond. The resting states of prior Rh-catalyzed C-H silylation reactions underwent reductive elimination of dihydrogen or reduction of the hydrogen acceptor before C-H bond cleavage.

Computational studies have revealed the origins of the so-far unique selectivity for silylation of a δ C-H bond over a γ C-H bond with the Rh-Xantphos catalyst. This selectivity results from a higher barrier to reductive elimination from the secondary alkyl intermediate with Xantphos as ligand than with Segphos (and presumably related phosphines) as ligand. This high barrier results from increased steric repulsion between the ligand and the substrate during reductive elimination to form a secondary C-Si bond. These mechanistic insights lay the groundwork for the development of new regioselective C-H silylation methodologies and provide a framework to predict the site of C-H silylation in complex molecules with multiple accessible C-H bonds.

2.4 Experimental

Materials and Methods

All silylation reactions were assembled in an N_2-filled glovebox using oven-dried glassware and were stirred with Teflon-coated magnetic stirring bars. $[Ir(cod)OMe]_2$ was obtained as a gift from Johnson Matthey and was used as received. 3,4,7,8-Tetramethyl-1,10-phenanthroline (Me_4phen) was purchased from Aldrich and was used as received. Diethylsilane (Et_2SiH_2) was purchased from Alfa Aesar and was used as received. Ethyl, *n*-propyl, *n*-butyl and cyclohexyl magnesium chloride were purchased from Acros and were used as received. Other Grignard reagents were prepared from the corresponding alkyl bromides with magnesium turnings. Norbornene (nbe), Xantphos, *tert*-butyl hydroperoxide (5-6 M in decane, stored over molecular sieves), tetra-*n*-butylammonium fluoride (TBAF) and anhydrous dimethylformamide (DMF) were purchased from Aldrich and were used as received. RhCl(Xantphos) was synthesized by literature procedures.[20] Diethyl ether and tetrahydrofuran (THF) were degassed by purging with nitrogen and then dried with a solvent purification system containing activated alumina. All other solvents and reagents were used as received. Reaction temperatures above 23 °C refer to temperatures of an aluminum heating block, which were either controlled by an electronic temperature modulator or controlled manually and monitored using a standard alcohol thermometer. NMR spectra were recorded on Bruker AVQ-400, AVB-400, AV-500, DRX-500 and AV-600 instruments. Chemical shifts (δ) are reported in ppm relative to the residual solvent signal. Data for ^{1}H NMR spectra are reported as follows: chemical shift (multiplicity, coupling constants, number of hydrogens). Abbreviations are as follows: s (singlet), d (doublet), t (triplet), q (quartet), m (multiplet), br (broad). GC-MS data were obtained on an Agilent 6890-N GC system containing an Alltech EC-1 capillary column

and an Agilent 5973 mass selective detector. High-resolution mass spectral data were obtained from the University of California, Berkeley Mass Spectrometry Laboratory. Elemental analysis was conducted at the Micro Analytical Facility in the College of Chemistry. IR spectra were recorded with a Bruker Vertex 80 FTIR spectrometer, the spectra were reported in cm^{-1}.

General procedure for the synthesis of substrates

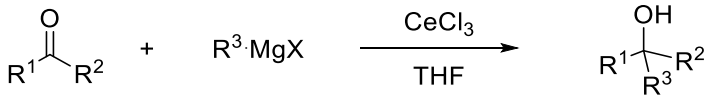

A suspension of $CeCl_3$ (6.0 mmol) in 15 mL of anhydrous THF was stirred at room temperature for 3 h. The suspension was cooled to 0 °C, and a Grignard reagent (5.0 mmol) was added. The resulting mixture was stirred at 0 °C for 1 h before a solution of ketone (5.0 mmol) in 3.0 mL of THF was added. After 30 min at 0 °C, the reaction was quenched by adding 1 mL of water. The mixture was filtered through Celite, dried over Na_2SO_4 and concentrated. The crude product was further purified by column chromatography on silica gel with EtOAc/hexanes mixture as eluent.

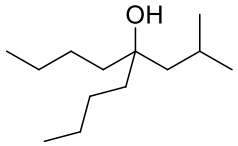

Alcohol 1a: Following the general procedure, 5-nonanone (5.0 mmol) was allowed to react with *iso*-butyl magnesium bromide. The crude product was purified by column chromatography on silica gel to give 792 mg (79% yield) of alcohol **1a** as a colorless oil. ^{1}H NMR (500 MHz, $CDCl_3$) δ 1.76 (hept, *J* = 6.6 Hz, 1H), 1.42 (t, *J* = 3.9 Hz, 4H), 1.37 – 1.18 (m, 11H), 0.95 (d, *J* = 6.6 Hz, 6H), 0.90 (t, *J* = 7.0 Hz, 6H). ^{13}C NMR (126 MHz, $CDCl_3$) δ 75.22, 48.11, 39.54, 25.99, 24.97, 23.91, 23.47, 14.28. HRMS(EI) calcd for $C_{12}H_{24}O$ (M^+) 200.2140, found 200.2136.

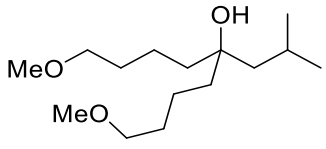

Alcohol 1b: To a cooled solution of ethyl isovalerate (5.0 mmol) in 10 mL of THF at 0 °C was added dropwise 4-methoxybutyl magnesium bromide (12.0 mmol). The resulting mixture was stirred at 0 °C for 1 h. Water (2 mL) was added, and the mixture was filtered through Celite. The filtrate was dried and concentrated. The crude product was purified by column chromatography on silica gel to give 936 mg (72% yield) of alcohol **1b** as a colorless oil. ^{1}H NMR (500 MHz, $CDCl_3$) δ 3.36 (t, *J* = 6.5 Hz, 4H), 3.31 (s, 6H), 1.74 (hept, *J* = 6.6 Hz, 1H), 1.58 – 1.47 (m, 5H), 1.47 – 1.40 (m, 4H), 1.37 – 1.28 (m, 6H), 0.93 (d, *J* = 6.6 Hz, 7H). ^{13}C NMR (126 MHz, $CDCl_3$) δ 75.07, 72.83, 58.66, 47.94, 39.52, 30.23, 24.91, 23.89, 20.40. HRMS(EI) calcd for $C_{15}H_{32}O_3$ (M^+) 260.2351, found 260.2348.

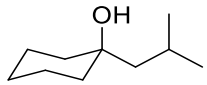

Alcohol 1c: Following the general procedure, cyclohexanone (5.0 mmol) was allowed to react with *iso*-butyl magnesium bromide. The crude product was purified by column chromatography on silica gel to give 604 mg (78% yield) of alcohol **1c** as a colorless oil. ^{1}H NMR (500 MHz, $CDCl_3$) δ 1.82 (hept, *J* = 6.4 Hz, 1H), 1.63 – 1.19 (m, 13H), 0.95 (d, *J* = 6.6 Hz, 6H). ^{13}C NMR (126 MHz, $CDCl_3$) δ 72.25, 51.15, 38.11, 25.96, 25.14, 23.53, 22.42. HRMS(EI) calcd for $C_{10}H_{20}O$ (M^+) 156.1514, found 156.1510.

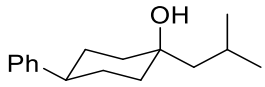

Alcohol 1d: Following the general procedure, 4-phenyl cyclohexanone (5.0 mmol) was allowed to react with *iso*-butyl magnesium bromide. The crude product was purified by column chromatography on silica gel to give 928 mg (80% yield) of alcohol **1d** as a colorless oil. ^{1}H NMR (500 MHz, $CDCl_3$) δ 7.35 – 7.21 (m, 5H), 2.58 – 2.41 (m, 1H), 1.99 – 1.69 (m, 7H), 1.53 (td, *J* = 13.3, 3.6 Hz, 2H), 1.45 (d, *J* = 5.8 Hz, 2H), 1.33 (s, 1H), 1.03 (d, *J* = 6.6 Hz, 6H). ^{13}C NMR (126 MHz, $CDCl_3$) δ 147.42, 128.45, 126.98, 126.06, 71.27, 53.30, 44.18, 37.85, 29.41, 25.21, 23.69. HRMS(EI) calcd for $C_{16}H_{24}O$ (M^+) 232.1827, found 232.1823.

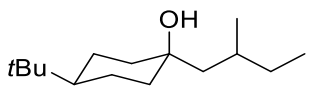

Alcohol 1e: Following the general procedure, 4-tert-butyl cyclohexanone (5.0 mmol) was allowed to react with 2-methylbutyl magnesium bromide. The crude product was purified by column chromatography on silica gel to give 847 mg (75% yield) of alcohol **1e** as a colorless oil. ^{1}H NMR (500 MHz, $CDCl_3$) δ 1.74 – 1.62 (m, 2H), 1.62 – 1.50 (m, 3H), 1.47 – 1.11 (m, 10H), 0.94 (d, *J* = 6.6 Hz, 3H), 0.89 – 0.82 (m, 12H). ^{13}C NMR (126 MHz, $CDCl_3$) δ 71.51, 51.04, 48.04, 38.33, 37.82, 32.53, 31.68, 29.97, 27.71, 22.61, 22.58, 21.99, 11.62. HRMS(EI) calcd for $C_{15}H_{30}O$ (M^+) 226.2297, found 226.2293.

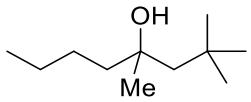

Alcohol 1f: Following the general procedure, 2-hexanone (5.0 mmol) was allowed to react with 2,2-dimethylpropyl magnesium bromide. The crude product was purified by column chromatography on silica gel to give 645 mg (74% yield) of alcohol **1f** as a colorless oil. ^{1}H NMR (600 MHz, $CDCl_3$) δ 1.50 – 1.42 (m, 4H), 1.34 – 1.26 (m, 5H), 1.23 (s, 3H), 1.02 (s, 9H), 0.91 (t, *J* = 6.5 Hz, 3H). ^{13}C NMR (151 MHz, $CDCl_3$) δ 74.46, 53.84, 44.84, 31.75, 31.50, 28.47, 26.46, 23.44, 14.25. HRMS(EI) calcd for $C_{11}H_{24}O$ (M^+) 172.1827, found 172.1823.

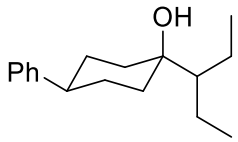

Alcohol 1h: Following the general procedure, 4-phenyl cyclohexanone (5.0 mmol) was allowed to react with 3-pentyl magnesium bromide. The crude product was purified by column chromatography on silica gel to give 1.01 g (82% yield) of alcohol **1h** as a colorless oil. ^{1}H NMR (500 MHz, $CDCl_3$) δ 7.34 (t, *J* = 7.4 Hz, 2H), 7.29 (d, *J* = 7.3 Hz, 2H), 7.23 (t, *J* = 7.1 Hz, 1H), 2.50 (tt, *J* = 14.5, 5.0 Hz, 1H), 1.91 (ddd, *J* = 16.1, 13.2, 3.4 Hz, 2H), 1.84 – 1.71 (m, 5H), 1.70 – 1.54 (m, 4H), 1.28 (tt, *J* = 14.5, 7.3 Hz, 2H), 1.12 – 1.07 (m, 1H), 1.04 (t, *J* = 7.4 Hz, 6H). ^{13}C NMR (126 MHz, $CDCl_3$) δ 147.42, 128.38, 126.92, 125.99, 73.92, 53.53, 44.18, 34.58, 29.39, 22.36, 14.13. HRMS(EI) calcd for $C_{17}H_{26}O$ (M^+) 246.1984, found 246.1981.

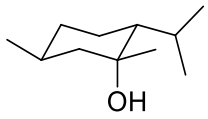

Alcohol 1t: Following the general procedure, (-)-methone (5.0 mmol) was allowed to react with methyl magnesium bromide. The crude product was purified by column chromatography on silica gel to give 697 mg (82% yield) of alcohol **1t** as a colorless oil. ^{1}H NMR (500 MHz, $CDCl_3$) δ 2.18 – 2.08 (m, 1H), 1.80 – 1.72 (m, 1H), 1.70 – 1.61 (m, 1H), 1.57 (d, *J* = 13.5 Hz, 1H), 1.50 (dd, *J* = 13.3, 3.2 Hz, 1H), 1.41 – 1.24 (m, 3H), 1.22 (s, 3H), 1.08 – 0.95 (m, 2H), 0.92 – 0.82 (m, 9H). ^{13}C NMR (126 MHz, $CDCl_3$) δ 73.26, 50.85, 50.61, 35.35, 29.01, 28.35, 26.24, 23.96, 22.46, 21.04, 18.38. HRMS(EI) calcd for $C_{11}H_{22}O$ (M^+) 170.1671, found 170.1667.

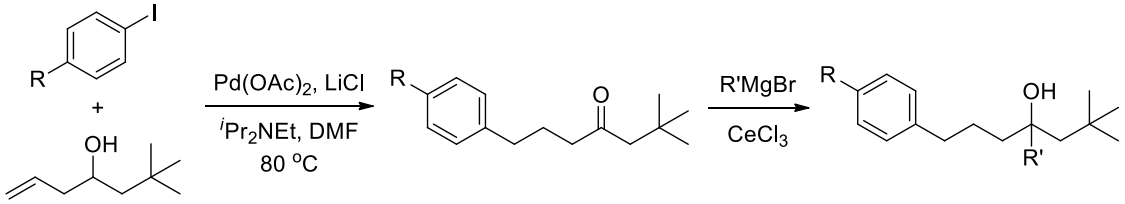

The literature procedure[21] was used with slight modifications. Into a 20 mL screw-capped vial was placed $Pd(OAc)_2$ (0.15 mmol, 0.030 equiv), LiCl (15 mmol. 3.0 equiv) and dried DMF (5.0 mL). The solution was magnetically stirred to afford a yellow suspension. Diisopropylethylamine (7.5 mmol. 1.5 equiv), the homoallylic alcohol (6.0 mmol, 1.2 equiv) and the aryl iodide (5.0 mmol, 1.0 equiv) were added successively. The vial was capped with a Teflon-lined screw cap and placed in a preheated aluminum block at 80 °C. After 18 h, the reaction mixture was poured into 50 mL of H_2O and extracted with ether (20 mL x 3). The combined ether extracts were washed successively with aq. HCl (30 mL, 1N), H_2O (30 mL), saturated brine (30 mL) and H_2O (30 mL). The solution was dried over $MgSO_4$, filtered and evaporated to give the crude ketone product. The crude product was used without further purification. Reaction of the ketone product with a Grignard reagent according to the general procedure for the Grignard reaction provided the tertiary alcohol.

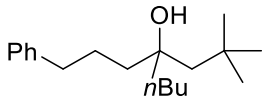

Alcohol **1g**: Following the general procedure, iodobenzene (716 mg, 3.00 mmol) was coupled with 6,6-dimethyl-1-hepten-4-ol. The Grignard reaction of the resulting ketone with *n*-butylmagnesium bromide provided 530 mg (64%) of alcohol **1g** as a colorless oil. ^{1}H NMR (500 MHz, $CDCl_3$) δ 7.33 – 7.18 (m, 5H), 2.63 (t, *J* = 7.2 Hz, 2H), 1.72 – 1.48 (m, 6H), 1.47 (s, 2H), 1.37 – 1.19 (m, 5H), 1.05 (s, 9H), 0.93 (t, *J* = 6.9 Hz, 3H). ^{13}C NMR

(126 MHz, $CDCl_3$) δ 142.62, 128.54, 128.42, 125.87, 76.27, 51.30, 40.46, 40.36, 36.55, 31.83, 31.57, 26.12, 26.07, 23.39, 14.28. HRMS(EI) calcd for $C_{19}H_{32}O$ (M^+) 276.2453, found 276.2448.

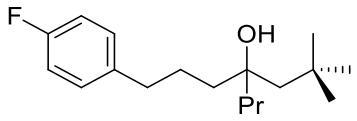

Alcohol **1j**: Following the general procedure, 4-fluoroiodobenzene (1.11 g, 5.00 mmol) was coupled with 6,6-dimethyl-1-hepten-4-ol. The Grignard reaction of the resulting ketone with *n*-propylmagnesium bromide provided 882 mg (63%) of alcohol **1j** as a colorless oil. ^{1}H NMR (500 MHz, $CDCl_3$) δ 7.13 (t, *J* = 8.6 Hz, 2H), 6.96 (t, *J* = 8.6 Hz, 2H), 2.56 (t, *J* = 7.3 Hz, 2H), 1.67 – 1.40 (m, 8H), 1.35 – 1.19 (m, 3H), 1.01 (s, 9H), 0.89 (t, *J* = 7.2 Hz, 3H). ^{13}C NMR (126 MHz, $CDCl_3$) δ 161.31 (d, *J* = 244.4 Hz), 138.16 (d, *J* = 2.5 Hz), 129.81 (d, *J* = 7.5 Hz), 115.09 (d, *J* = 21.4 Hz), 76.22, 51.30, 43.04, 40.25, 35.69, 31.80, 31.54, 26.10, 17.19, 14.71. HRMS(EI) calcd for $C_{18}H_{29}FO$ (M^+) 280.2202, found 280.2198.

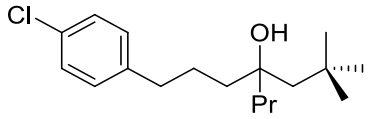

Alcohol **1k**: Following the general procedure, 4-chloroiodobenzene (1.19 g, 5.00 mmol) was coupled with 6,6-dimethyl-1-hepten-4-ol. The Grignard reaction of the resulting ketone with *n*-propylmagnesium bromide provided 1.07 g (72%) of alcohol **1k** as a colorless oil. ^{1}H NMR (500 MHz, $CDCl_3$) δ 7.27 (d, *J* = 7.3 Hz, 2H), 7.13 (d, *J* = 7.3 Hz, 2H), 2.59 (t, *J* = 6.9 Hz, 2H), 1.68 – 1.43 (m, 8H), 1.35 – 1.21 (m, 3H) (s, 3H), 1.04 (d, *J* = 1.2 Hz, 9H), 0.92 (t, *J* = 6.6 Hz, 3H). ^{13}C NMR (126 MHz, $CDCl_3$) δ 141.00, 131.53, 129.87, 128.48, 76.21, 51.30, 43.02, 40.29, 35.86, 31.81, 31.55, 25.86, 17.22, 14.72. HRMS(EI) calcd for $C_{18}H_{29}ClO$ (M^+) 296.1907, found 296.1903.

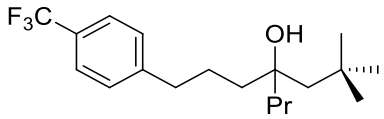

Alcohol **1l**: Following the general procedure, 4-trifluoromethyliodobenzene (1.36 g, 5.00 mmol) was coupled with 6,6-dimethyl-1-hepten-4-ol. The Grignard reaction of the resulting ketone with *n*-propylmagnesium bromide provided 957 mg (58%) of alcohol **1l**

as a colorless oil. ^{1}H NMR (500 MHz, $CDCl_3$) δ 7.53 (d, *J* = 7.5 Hz, 2H), 7.29 (td *J* = 7.5 Hz, 2H), 2.65 (t, *J* = 7.3 Hz, 2H), 1.70 – 1.39 (m, 8H), 1.26 (s, 3H), 1.01 (s, 9H), 0.89 (t, *J* = 7.0 Hz, 3H). ^{13}C NMR (126 MHz, $CDCl_3$) δ 146.72, 128.83, 128.15 (q, *J* = 32.6 Hz), 125.24 (q, *J* = 3.6 Hz), 124.41(q, *J* = 272.4 Hz), 76.20, 51.30, 43.02, 40.31, 36.37, 31.79, 31.55, 25.71, 17.25, 14.70. HRMS(EI) calcd for $C_{19}H_{29}F_3O$ (M^+) 330.2171, found 330.2168.

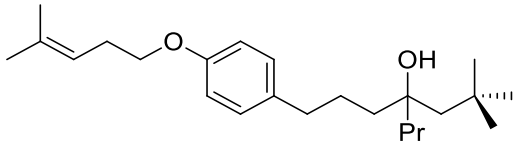

Alcohol **1m**: Following the general procedure, 1-iodo-4-((4-methylpent-3-en-1-yl)oxy)benzene (906 mg, 3.00 mmol) was coupled with 6,6-dimethyl-1-hepten-4-ol. The Grignard reaction of the resulting ketone with *n*-propylmagnesium bromide provided 561 mg (52%) of alcohol **1m** as a colorless oil. ^{1}H NMR (500 MHz, $CDCl_3$) δ 7.09 (d, *J* = 8.1 Hz, 2H), 6.82 (d, *J* = 8.2 Hz, 2H), 5.22 (s, 1H), 3.91 (t, *J* = 7.0 Hz, 2H), 2.63 – 2.40 (m, 4H), 1.73 (s, 3H), 1.65 (s, 3H), 1.61 – 1.34 (m, 8H), 1.35 – 1.21 (m, 2H), 1.20 – 1.09 (br, 1H), 1.02 (s, 9H), 0.89 (t, *J* = 7.1 Hz, 3H). ^{13}C NMR (126 MHz, $CDCl_3$) δ 157.22, 134.59, 134.45, 129.34, 119.77, 114.47, 76.27, 67.76, 51.29, 43.04, 40.39, 35.64, 31.81, 31.54, 28.43, 26.28, 25.90, 18.00, 17.18, 14.73. HRMS(EI) calcd for $C_{24}H_{40}O2$ (M^+) 360.3028, found 360.3024.

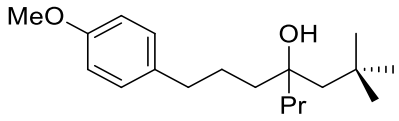

Alcohol **1n**: Following the general procedure, 4-methoxyiodobenzene (1.17 g, 5.00 mmol) was coupled with 6,6-dimethyl-1-hepten-4-ol. The Grignard reaction of the resulting ketone with *n*-propylmagnesium bromide provided 978 mg (67%) of alcohol **1n** as a colorless oil. ^{1}H NMR (500 MHz, $CDCl_3$) δ 7.11 (d, *J* = 8.4 Hz, 2H), 6.83 (d, *J* = 8.5 Hz, 2H), 3.79 (s, 3H), 2.54 (t, *J* = 7.2 Hz, 2H), 1.69 – 1.37 (m, 8H), 1.34 – 1.20 (m, 3H), 1.02 (s, 9H), 0.90 (t, *J* = 7.2 Hz, 3H). ^{13}C NMR (126 MHz, $CDCl_3$) δ 157.78, 134.70, 129.37, 113.79, 76.25, 55.35, 51.28, 43.03, 40.37, 35.62, 31.80, 31.53, 26.28, 17.17, 14.72. HRMS(EI) calcd for $C_{19}H_{32}O_2$ (M^+) 292.2402, found 292.2398.

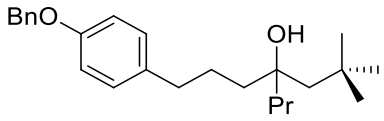

Alcohol **1o**: Following the general procedure, 4-benzyloxyiodobenzene (1.55 g, 5.00 mmol) was coupled with 6,6-dimethyl-1-hepten-4-ol. The Grignard reaction of the resulting ketone with *n*-propylmagnesium bromide provided 1.20 g (65%) of alcohol **1o** as a colorless oil. ^{1}H NMR (500 MHz, $CDCl_3$) δ 7.45 (d, *J* = 7.3 Hz, 2H), 7.40 (t, *J* = 7.4 Hz, 2H), 7.34 (t, *J* = 7.1 Hz, 1H), 7.12 (d, *J* = 8.4 Hz, 2H), 6.92 (d, *J* = 8.5 Hz, 2H), 5.06 (s, 2H), 2.56 (t, *J* = 7.0 Hz, 2H), 1.69 – 1.38 (m, 8H), 1.34 – 1.20 (m, 3H), 1.04 (s, 9H), 0.91 (t, *J* = 7.2 Hz, 3H). ^{13}C NMR (126 MHz, $CDCl_3$) δ 157.04, 137.32, 135.00, 129.40, 128.66, 127.99, 127.58, 114.78, 76.26, 70.13, 51.28, 43.04, 40.38, 35.65, 31.81, 31.54, 26.26, 17.17, 14.73. HRMS(EI) calcd for $C_{25}H_{36}O_2$ (M^+) 368.2715, found 368.2711.

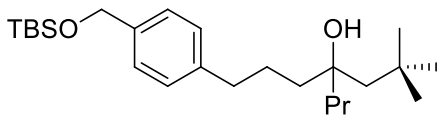

Alcohol **1p**: Following the general procedure, *tert*-butyl((4-iodobenzyl)oxy)dimethylsilane (1.39 g, 4.00 mmol) was coupled with 6,6-dimethyl-1-hepten-4-ol. The Grignard reaction of the resulting ketone with *n*-propylmagnesium bromide provided 1.10 g (68%) of alcohol **1p** as a colorless oil. ^{1}H NMR (500 MHz, $CDCl_3$) δ 7.27 (d, *J* = 7.5 Hz, 2H), 7.18 (d, *J* = 7.6 Hz, 2H), 4.75 (s, 2H), 2.61 (t, *J* = 7.2 Hz, 2H), 1.77 – 1.40 (m, 8H), 1.38 – 1.22 (m, 3H), 1.03 (s, 9H), 0.98 (s, 9H), 0.92 (t, *J* = 7.2 Hz, 3H), 0.13 (s, 6H). ^{13}C NMR (126 MHz, $CDCl_3$) δ 141.22, 138.93, 128.36, 126.25, 76.27, 65.00, 51.30, 43.05, 40.43, 36.24, 31.82, 31.55, 26.11, 18.56, 17.19, 14.74, -5.08. HRMS(EI) calcd for $C_{25}H_{44}OSi$ ($[M-H_2O]^+$) 388.3161, found 388.3157.

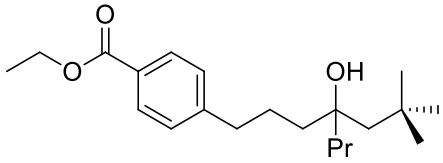

Alcohol **1q**: Following the general procedure, 4-ethyloxycarbonyliodobenzene (828 mg, 3.00 mmol) was coupled with 6,6-dimethyl-1-hepten-4-ol. The Grignard reaction of the resulting ketone with *n*-propylmagnesium bromide at 0 °C provided 521 mg (52%) of alcohol **1q** as a colorless oil. ^{1}H NMR (500 MHz, $CDCl_3$) δ 7.98 (d, *J* = 8.0 Hz, 2H), 7.26 (d, *J* = 8.0 Hz, 2H), 4.38 (q, *J* = 7.1 Hz, 2H), 2.67 (t, *J* = 7.5 Hz, 2H), 1.71 – 1.21 (m, 13H), 1.02 (s, 9H), 0.90 (t, *J* = 7.3 Hz, 3H). ^{13}C NMR (126 MHz, $CDCl_3$) δ 166.82, 148.02,

129.75, 128.52, 128.19, 76.17, 60.90, 51.28, 42.99, 40.31, 36.53, 31.79, 31.53, 25.59, 17.21, 14.70, 14.47. HRMS(EI) calcd for $C_{21}H_{34}O_3$ (M^+) 334.2508, found 334.2504.

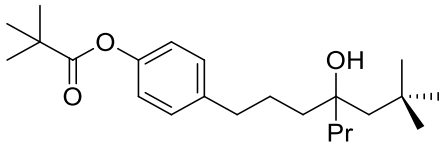

Alcohol **1r**: Following the general procedure, 4-pivolyliodobenzene (912 mg, 3.00 mmol) was coupled with 6,6-dimethyl-1-hepten-4-ol. The Grignard reaction of the resulting ketone with *n*-propylmagnesium bromide at 0 °C provided 586 mg (54%) of alcohol **1r** as a colorless oil. ^{1}H NMR (500 MHz, $CDCl_3$) δ 7.17 (d, *J* = 7.6 Hz, 2H), 6.96 (d, *J* = 7.5 Hz, 2H), 2.58 (t, *J* = 7.0 Hz, 2H), 1.67 – 1.40 (m, 8H), 1.37 – 1.22 (m, 12H), 1.02 (s, 9H), 0.89 (t, *J* = 7.0 Hz, 3H). ^{13}C NMR (126 MHz, $CDCl_3$) δ 177.37, 149.20, 139.89, 129.31, 121.30, 76.23, 51.28, 43.00, 40.41, 39.14, 35.92, 31.80, 31.54, 27.27, 26.00, 17.21, 14.72. HRMS(EI) calcd for $C_{23}H_{36}O_2$ ($[M-H_2O]^+$) 344.2715, found 344.2711.

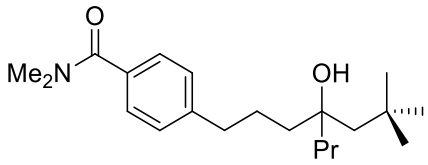

Alcohol **1s**: Following the general procedure, 4-dimethylaminocarbonyliodobenzene (825 mg, 3.00 mmol) was coupled with 6,6-dimethyl-1-hepten-4-ol. The Grignard reaction of the resulting ketone with *n*-propylmagnesium bromide at 0 °C provided 539 mg (54%) of alcohol **1s** as a colorless oil. ^{1}H NMR (500 MHz, $CDCl_3$) δ 7.15 (d, *J* = 8.2 Hz, 2H), 7.00 (d, *J* = 8.3 Hz, 2H), 3.05 (s, 3H), 3.00 (s, 3H), 2.56 (t, *J* = 7.1 Hz, 2H), 1.66 – 1.34 (m, 9 H), 1.31 – 1.18 (m, 2H), 1.01 (s, 9H), 0.88 (t, *J* = 7.2 Hz, 3H). ^{13}C NMR (126 MHz, $CDCl_3$) δ 155.21, 149.59, 139.42, 129.16, 121.58, 76.20, 51.24, 42.96, 40.41, 36.77, 36.51, 35.89, 31.78, 31.51, 26.00, 17.18, 14.69. HRMS(EI) calcd for $C_{21}H_{35}NO_2$ (M^+) 333.2668, found 333.2664.

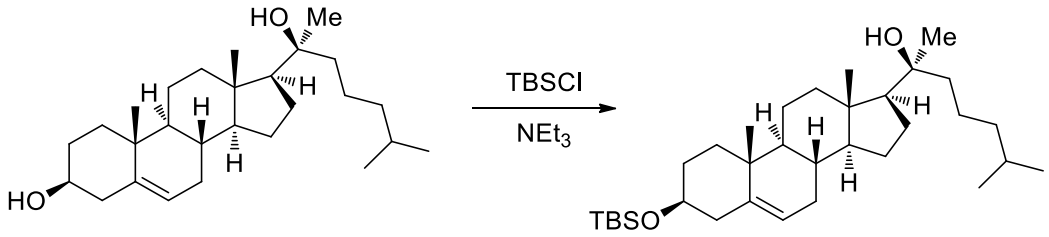

Alcohol **1u'**: To a solution of diol (804 mg, 2.00 mmol) in 10 mL of anhydrous dichloromethane and triethylamine (404 mg, 4.00 mmol) was added dropwise a solution of TBSCl (360 mg, 2.40 mmol) in 5 mL of dichloromethane. The solution was stirred at room temperature for 2 hours. The reaction mixture was concentrated and purified by silica gel chromatography to afford 972 mg of mono-protected diol **1u'** (94% yield) as a white solid. ^{1}H NMR (500 MHz, $CDCl_3$) δ 5.31 (m, 1H), 3.56 – 3.45 (m, 1H), 2.34 – 2.23 (m, 1H), 2.19 (dd, *J* = 13.1, 2.7 Hz, 1H), 2.12 (t, *J* = 12.2 Hz, 1H), 1.99 (d, *J* = 14.6 Hz, 1H), 1.86 – 1.63 (m, 6H), 1.58 – 1.39 (m, 9H), 1.34 – 1.25 (m, 6H), 1.20 – 1.13 (m, 4H), 1.02 (s, 3H), 0.95 – 0.86 (m, 20H), 0.08 (s, 6H). ^{13}C NMR (126 MHz, $CDCl_3$) δ 141.59, 121.10, 75.28, 72.63, 57.67, 56.93, 50.13, 44.20, 42.81, 42.67, 40.15, 39.64, 37.39, 36.61, 32.09, 31.84, 31.35, 27.96, 26.46, 25.97, 23.81, 22.77, 22.61, 22.39, 22.05, 20.93, 19.46, 18.30, 13.63, -4.56. HRMS(EI) calcd for $C_{33}H_{60}O_2Si$ (M^+) 516.4363, found 516.4358.

General procedure for Ir-catalyzed silylation of alcohols:

In an N_2-filled glovebox, 0.50 mmol of the alcohol was weighed into a one-dram screw-capped vial. A stir bar was added, and the substrate was dissolved in Et_2O (1.0 mL). The resulting solution was treated first with $[Ir(cod)OMe]_2$ (0.50 μmol, 0.10 mol %, unless otherwise specified) and then neat Et_2SiH_2 (0.75 mmol). The vial was capped with a Teflon-lined screw cap, and the resulting solution was stirred in the glovebox at room temperature until complete conversion to the corresponding diethyl(hydrido)silyl ether was observed, as determined by GC (generally 1-2 h) (CAUTION: H_2 evolution!).

General procedure for Ru-catalyzed silylation of alcohols:

In an N_2-filled glovebox, 0.50 mmol of the alcohol was weighed into a one-dram screw-capped vial. A stir bar was added, and the substrate was dissolved in PhH (1.0 mL). The resulting solution was treated first with $RuCl_2(PPh_3)_3$ (2.5 μmol, 0.50 mol %, unless otherwise specified) and then neat Et_2SiH_2 (0.75 mmol). The vial was capped with a Teflon-lined screw cap, and the resulting solution was stirred at 50 °C until complete conversion to the corresponding diethyl(hydrido)silyl ether was observed, as determined by GC (generally 3-5 h) (CAUTION: H_2 evolution!).

General procedure for Rh-catalyzed intramolecular aliphatic silylation:

In an N_2-filled glovebox, the crude reaction mixture containing the diethyl(hydrido)silyl ether (ca. 0.50 mmol) and solvent was placed under high-vacuum for 0.5 h (the stir bar was temporarily removed during this operation to prevent bumping). The stir bar was replaced, and the concentrated diethyl(hydrido)silyl ether was then sequentially treated with norbornene (0.60 mmol, 1.2 equiv), RhCl(Xantphos) (0.020 mmol, 4.0 mol %) and THF (1.0 mL). The Teflon-lined screw cap was replaced, and the vial was then removed from the glovebox, placed in a pre-heated aluminum block at 100 °C for 16 h.

General procedure for Tamao-Fleming oxidation of oxasilolanes:

To an ice-cooled (0 °C) stirred solution of KH (120 mg, 3.0 mmol, 6.0 equiv) in 5.0 mL of NMP was added *tert*-butyl hydroperoxide (0.55 mL, 5.0 ~ 6.0 M in decane stored over molecular sieves) dropwise. The mixture was allowed to warm to RT and kept for 10 min. The crude reaction mixture containing the silolane (ca. 0.5 mmol) in 1.0 mL of THF was then added. After stirring at RT for 10 min, 2.5 mL of TBAF solution (2.5 mmol, 1.0 M solution in THF) was added. The resulting mixture was stirred for 14 h at RT. The reaction was carefully quenched with aq. Na_2SO_3 (saturated, 5 mL), and the resulting mixture was extracted with EtOAc (30 mL, then 2 x 15 mL). The combined organic layers were washed (30 mL of saturated Na_2SO_3, 30 mL of brine, 30 mL of 0.1 N HCl, then 30 mL of brine), dried over $MgSO_4$, filtered through Celite, and concentrated by rotary evaporation. The crude diol was further purified by column chromatography on silica gel with EtOAc/hexanes mixture as eluent.

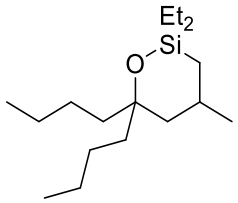

Oxasilolane 3a: In an N_2-filled glovebox, 5-*iso*butylnonan-5-ol (200 mg, 1.00 mmol) and Et_2SiH_2 (132 mg, 1.50 mmol) were weighed in a 20 mL screw-capped vial. A stir bar was added, followed by THF (1.0 mL). The resulting solution was treated with $[Ir(cod)OMe]_2$ (0.6 mg, 1.0 μmol, 0.1 mol %). The vial was capped with a Teflon-lined screw cap, and the resulting solution was stirred in the glovebox at room temperature for 15 h, at which point GC analysis indicated full conversion to diethyl(hydrido)silyl ether. The volatile materials were removed by placing the reaction mixture directly under high vacuum for 0.5 h (the

stir bar was temporarily removed during this operation to prevent bumping). The stir bar was replaced, and the concentrated diethyl(hydrido)silyl ether was then sequentially treated with norbornene (113 mg, 1.20 mmol), RhCl(Xantphos) (29 mg, 0.040 mmol, 4.0 mol %) and THF (3.0 mL). The Teflon-lined screw cap was replaced, and the resulting solution was stirred in a pre-heated aluminum block at 100 °C for 16 h. The reaction mixture was then cooled to room temperature, and the solvent was removed by rotary evaporation. The resulting residue was purified by Kugelrohr distillation (25 mTorr, 75 °C) to give 267 mg (94%) of oxasilolane **3a** as colorless oil. ^{1}H NMR (600 MHz, $CDCl_3$) δ 1.97 – 1.78 (m, 1H), 1.54 (dd, *J* = 18.5, 7.4 Hz, 1H), 1.46 – 1.37 (m, 4H), 1.36 – 1.21 (m, 8H), 1.16 (dd, *J* = 14.7, 8.7 Hz, 1H), 1.10 – 1.03 (m, 1H), 0.97 (d, *J* = 6.3 Hz, 3H), 0.96 – 0.88 (m, 12H), 0.66 (d, *J* = 14.3 Hz, 1H), 0.61 – 0.52 (m, 3H), 0.52 – 0.42 (m, 1H), 0.18 (t, *J* = 13.5 Hz, 1H). ^{13}C NMR (151 MHz, $CDCl_3$) δ 76.79, 45.65, 41.79, 38.90, 27.48, 26.37, 25.71, 24.11, 23.40, 23.34, 18.26, 14.17, 14.13, 8.03, 7.04, 6.84, 6.50. HRMS(EI) calcd for $C_{17}H_{36}OSi$ (M^+) 284.2535, found 284.2531.

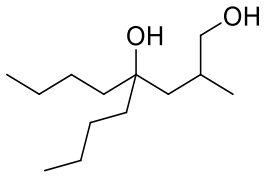

Diol 4a: Following the general procedure, 5-*iso*butylnonan-5-ol (200 mg, 1.00 mmol) was converted to the corresponding diethyl(hydrido)silyl ether with $[Ir(cod)OMe]_2$ (0.10 mol %) as catalyst at room temperature for 14 h. The subsequent cyclization was conducted with RhCl(Xantphos) at 100 °C for 15 h to provide the intermediate oxasilolane. Tamao-Fleming oxidation and purification by silica gel chromatography gave 166 mg (77% overall yield) of **4a** as a colorless oil. ^{1}H NMR (500 MHz, $CDCl_3$) δ 3.78 (s, 1H), 3.58 (dd, *J* = 10.5, 3.4 Hz, 1H), 3.34 – 3.21 (dd, *J* = 10.5, 3.4 Hz, 1H), 1.94 (d, *J* = 3.4 Hz, 1H), 1.63 – 1.38 (m, 6H), 1.32 (dd, *J* = 14.6, 7.0 Hz, 6H), 1.25 – 1.08 (m, 2H), 0.92 (t, *J* = 7.5 Hz, 6H), 0.89 (d, *J* = 6.9 Hz, 3H). ^{13}C NMR (126 MHz, $CDCl_3$) δ 74.43, 69.27, 46.08, 40.65, 37.70, 31.19, 26.43, 25.59, 23.32, 23.31, 19.71, 14.16, 14.14. ESI-HR calcd for $C_{13}H_{28}O_2Na$ ($[M+Na]^+$) 239.1982, found 239.1978.

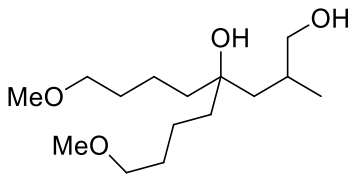

Diol 4b: Following the general procedure, 5-isobutyl-1,9-dimethoxynonan-5-ol (130 mg, 0.500 mmol) was converted to the corresponding diethyl(hydrido)silyl ether with $[Ir(cod)OMe]_2$ (0.20 mol %) as catalyst at room temperature for 14 h. The subsequent cyclization was conducted with RhCl(Xantphos) at 100 °C for 15 h to provide the intermediate oxasilolane. Tamao-Fleming oxidation and purification by silica gel chromatography gave 99 mg (72% overall yield) of **4b** as a colorless oil. ^{1}H NMR (500 MHz, $CDCl_3$) δ 3.59 (d, *J* = 10.4 Hz, 1H), 3.40 (dd, *J* = 8.2, 4.1 Hz, 4H), 3.34 (s, 6H), 3.29 (d, *J* = 8.6 Hz, 1H), 1.94 (br, 2H), 1.64 -1.54 (m, 5H), 1.52 - 1.44 (m, 3H), 1.42 – 1.36 (m, 1H), 1.34 – 1.18 (m, 2H), 0.89 (d, *J* = 6.9 Hz, 3H). ^{13}C NMR (126 MHz, $CDCl_3$) δ 74.26, 72.77, 72.61, 69.29, 58.57, 45.91, 45.89, 40.51, 37.94, 31.26, 30.07, 30.05, 20.78, 20.12, 19.69. ESI-HR calcd for $C_{15}H_{32}O_4Na$ ($[M+Na]^+$) 299.2193, found 299.2189.

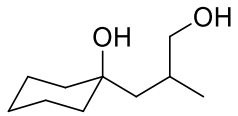

Diol 4c: Following the general procedure, 1-isobutyl-1-cyclohexanol (78 mg, 0.50 mmol) was converted to the corresponding diethyl(hydrido)silyl ether with $[Ir(cod)OMe]_2$ (0.10 mol %) as catalyst at room temperature for 14 h. The subsequent cyclization was conducted with RhCl(Xantphos) at 100 °C for 15 h to provide the intermediate oxasilolane. Tamao-Fleming oxidation and purification by silica gel chromatography gave 65 mg (75% overall yield) of **4c** as a colorless oil. ^{1}H NMR (500 MHz, $CDCl_3$) δ 3.80 (br, 2H), 3.58 (dd, *J* = 10.5, 3.5 Hz, 1H), 3.31 (t, *J* = 9.6 Hz, 1H), 1.94 (t, *J* = 24.7 Hz, 1H), 1.67 (s, 1H), 1.64 – 1.38 (m, 10H), 1.34 – 1.26 (m, 1H), 0.90 (d, *J* = 6.9 Hz, 3H). ^{13}C NMR (126 MHz, $CDCl_3$) δ 71.40, 69.22, 48.18, 40.05, 35.98, 30.85, 25.84, 22.58, 22.23, 19.73. ESI-HR calcd for $C_{10}H_{20}O_2Na$ ($[M+Na]^+$) 195.1356, found 195.1352.

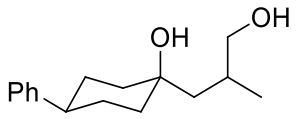

Diol 4d: Following the general procedure, 1-isobutyl-4-phenylcyclohexanol (116 mg, 0.500 mmol) was converted to the corresponding diethyl(hydrido)silyl ether with $[Ir(cod)OMe]_2$ (0.25 mol %) as catalyst at room temperature for 14 h. The subsequent cyclization was conducted with RhCl(Xantphos) at 100 °C for 15 h to provide the intermediate oxasilolane. Tamao-Fleming oxidation and purification by silica gel chromatography gave 94 mg (76% overall yield) of **4d** as a white solid. ^{1}H NMR (500 MHz, $CDCl_3$) δ 7.36 – 7.24 (m, 4H), 7.21 (t, *J* = 6.7 Hz, 1H), 3.81 (s, 2H), 3.65 (dd, *J* =

10.2, 3.2 Hz, 1H), 3.38 (t, *J* = 9.6 Hz, 1H), 2.56 – 2.43 (m, 1H), 2.17 – 1.97 (m, 2H), 1.94 – 1.70 (m, 5H), 1.64 (dd, *J* = 14.6, 8.7 Hz, 1H), 1.59 – 1.48 (m, 2H), 1.42 (td, *J* = 13.4, 3.7 Hz, 1H), 0.94 (d, *J* = 6.8 Hz, 3H). ^{13}C NMR (126 MHz, $CDCl_3$) δ 147.35, 128.43, 126.97, 126.05, 70.24, 69.36, 50.99, 44.21, 39.84, 35.87, 31.06, 29.48, 29.26, 19.80. ESI-HR calcd for $C_{16}H_{24}O_2Na$ ($[M+Na]^+$) 271.1669, found 271.1667.

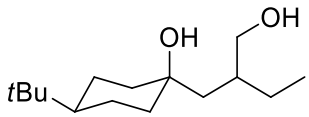

Diol 4e: Following the general procedure, 4-(tert-butyl)-1-(2-methylbutyl)cyclohexanol (113 mg, 0.500 mmol) was converted to the corresponding diethyl(hydrido)silyl ether with $[Ir(cod)OMe]_2$ (0.25 mol %) as catalyst at room temperature for 14 h. The subsequent cyclization was conducted with RhCl(Xantphos) at 100 °C for 15 h to provide the intermediate oxasilolane. Tamao-Fleming oxidation and purification by silica gel chromatography gave 104 mg (86% overall yield) of **4e** as a white solid. ^{1}H NMR (500 MHz, $CDCl_3$) δ 3.68 (dd, *J* = 10.5, 3.3 Hz, 1H), 3.58 (br, 2H), 3.36 (d, *J* = 10.0 Hz, 1H), 1.95 (dd, *J* = 13.0, 2.6 Hz, 1H), 1.76 (s, 1H), 1.70 (d, *J* = 10.4 Hz, 1H), 1.62 (s, 2H), 1.56 – 1.45 (m, 2H), 1.41 – 1.23 (m, 4H), 1.23 – 1.13 (m, 2H), 0.97 (dd, *J* = 19.6, 7.9 Hz, 1H), 0.91 (t, *J* = 7.5 Hz, 3H), 0.88 (s, 9H). ^{13}C NMR (126 MHz, $CDCl_3$) δ 70.49, 67.73, 48.18, 47.96, 40.24, 37.66, 35.93, 32.43, 27.59, 26.54, 22.63, 22.38, 11.72. ESI-HR calcd for $C_{15}H_{30}O_2Na$ ($[M+Na]^+$) 265.2138, found 265.21384.

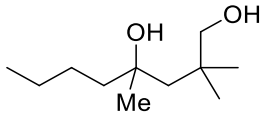

Diol 4f: Following the general procedure, 2,2,4-trimethyloctan-4-ol (86 mg, 0.50 mmol) was converted to the corresponding diethyl(hydrido)silyl ether with $[Ir(cod)OMe]_2$ (0.10 mol %) as catalyst at room temperature for 14 h. The subsequent cyclization was conducted with RhCl(Xantphos) at 100 °C for 15 h to provide the intermediate oxasilolane. Tamao-Fleming oxidation and purification by silica gel chromatography gave 62 mg (66% overall yield) of **4f** as a colorless oil. ^{1}H NMR (500 MHz, $CDCl_3$) δ 4.01 (br, 2H), 3.46 (d, *J* = 11.1 Hz, 1H), 3.37 (d, *J* = 11.0 Hz, 1H), 1.57 (d, *J* = 15.1 Hz, 1H), 1.55 – 1.47 (m, 2H), 1.44 (d, *J* = 15.1 Hz, 1H), 1.35 – 1.28 (m, 4H), 1.27 (s, 3H), 1.00 (s, 3H), 0.95 (s, 3H), 0.91 (t, *J* = 6.6 Hz, 3H). ^{13}C NMR (126 MHz, $CDCl_3$) δ 73.98, 71.04, 50.65, 44.90, 36.43, 28.55, 28.20, 27.03, 26.60, 23.28, 14.14. ESI-HR calcd for $C_{11}H_{24}O_2Na$ ($[M+Na]^+$) 211.1669, found 211.1665.

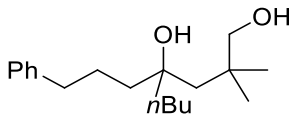

Diol 4g: Following the general procedure, 2,2-dimethyl-4-(3-phenylpropyl)octan-4-ol (138 mg, 0.500 mmol) was converted to the corresponding diethyl(hydrido)silyl ether with $[Ir(cod)OMe]_2$ (0.20 mol %) as catalyst at room temperature for 14 h. The subsequent cyclization was conducted with RhCl(Xantphos) at 100 °C for 15 h to provide the intermediate oxasilolane. Tamao-Fleming oxidation and purification by silica gel chromatography gave 105 mg (72% overall yield) of **4g** as a colorless oil. ^{1}H NMR (500 MHz, $CDCl_3$) δ 7.31 (t, *J* = 7.5 Hz, 2H), 7.22 (t, *J* = 6.2 Hz, 3H), 3.55 (br, 2H), 3.42 (s, 2H), 2.62 (t, *J* = 6.7 Hz, 2H), 1.67 – 1.58 (m, 3H), 1.59 – 1.44 (m, 5H), 1.35 – 1.25 (m, 2H), 1.25 – 1.15 (m, 2H), 0.96 (s, 6H), 0.92 (t, *J* = 7.2 Hz, 3H). ^{13}C NMR (126 MHz, $CDCl_3$) δ 142.36, 128.44, 128.37, 125.86, 75.98, 71.15, 48.52, 40.15, 40.00, 36.45, 36.36, 27.89, 27.87, 26.10, 26.09, 23.23, 14.17. ESI-HR calcd for $C_{19}H_{32}O_2Na$ ($[M+Na]^+$) 315.2295, found 315.2291.

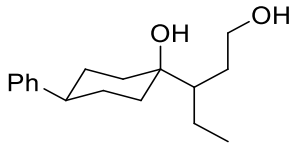

Diol 4h: Following the general procedure, 1-(pentan-3-yl)-4-phenylcyclohexanol (123 mg, 0.500 mmol) was converted to the corresponding diethyl(hydrido)silyl ether with $[Ir(cod)OMe]_2$ (0.10 mol %) as catalyst at room temperature for 14 h. The subsequent cyclization was conducted with RhCl(Xantphos) at 100 °C for 15 h to provide the intermediate oxasilolane. Tamao-Fleming oxidation and purification by silica gel chromatography gave 91 mg (74% overall yield) of **4h** as a colorless oil. ^{1}H NMR (500 MHz, $CDCl_3$) δ 7.42 – 7.10 (m, 5H), 3.83 (dt, *J* = 6.3, 5.7 Hz, 1H), 3.73 – 3.18 (br, 2H), 3.68 – 3.59 (m, 1H), 2.48 (dd, *J* = 16.2, 7.7 Hz, 1H), 2.00 – 1.59 (m, 10H), 1.45 (dt, *J* = 14.1, 4.0 Hz, 1H), 1.40 – 1.31 (m, 1H), 1.31 – 1.19 (m, 1H), 0.98 (t, *J* = 7.3 Hz, 3H). ^{13}C NMR (126 MHz, $CDCl_3$) δ 147.38, 128.40, 126.94, 126.02, 72.75, 61.71, 49.96, 44.14, 36.15, 33.22, 31.03, 29.48, 29.32, 22.79, 13.38. ESI-HR calcd for $C_{17}H_{26}O_2Na$ ($[M+Na]^+$) 285.1825, found 285.1821.

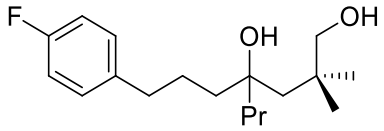

Diol 4j: Following the general procedure, 1-(4-fluorophenyl)-6,6-dimethyl-4-propylheptan-4-ol (140 mg, 0.500 mmol) was converted to the corresponding diethyl(hydrido)silyl ether with $[Ir(cod)OMe]_2$ (0.20 mol %) as catalyst at room temperature for 14 h. The subsequent cyclization was conducted with RhCl(Xantphos) at 100 °C for 15 h to provide the intermediate oxasilolane. Tamao-Fleming oxidation and purification by silica gel chromatography gave 110 mg (74% overall yield) of **4j** as a colorless oil. ^{1}H NMR (500 MHz, $CDCl_3$) δ 7.14 (dd, *J* = 8.1, 5.6 Hz, 2H), 6.98 (t, *J* = 8.6 Hz, 2H), 3.82 (br, 2H), 3.40 (q, *J* = 11.1 Hz, 2H), 2.58 (t, *J* = 6.8 Hz, 2H), 1.64 – 1.42 (m, 8H), 1.25 (td, *J* = 14.8, 7.1 Hz, 2H), 0.97 (s, 3H), 0.96 (s, 3H), 0.91 (t, *J* = 7.2 Hz, 3H). ^{13}C NMR (126 MHz, $CDCl_3$) δ 161.24 (d, *J* = 244 Hz), 137.94 (d, *J* = 2.5 Hz), 129.71 (d, *J* = 7.5 Hz), 115.04 (d, *J* = 21.4 Hz), 75.81, 71.10, 48.59, 42.71, 39.95, 36.41, 35.53, 27.89, 27.77, 26.12, 17.21, 14.58. ESI-HR calcd for $C_{18}H_{29}FO_2Na$ ($[M+Na]^+$) 319.2044, found 319.2040.

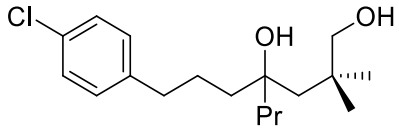

Diol 4k: Following the general procedure, 1-(4-chlorophenyl)-6,6-dimethyl-4-propylheptan-4-ol (148 mg, 0.500 mmol) was converted to the corresponding diethyl(hydrido)silyl ether with $[Ir(cod)OMe]_2$ (0.20 mol %) as catalyst at room temperature for 14 h. The subsequent cyclization was conducted with RhCl(Xantphos) at 100 °C for 15 h to provide the intermediate oxasilolane. Tamao-Fleming oxidation and purification by silica gel chromatography gave 131 mg (84% overall yield) of **4k** as a colorless oil. ^{1}H NMR (500 MHz, $CDCl_3$) δ 7.26 (d, *J* = 8.3 Hz, 2H), 7.12 (d, *J* = 8.2 Hz, 2H), 3.83 (br, 2H), 3.40 (q, *J* = 11.0 Hz, 2H), 2.57 (t, *J* = 6.7 Hz, 2H), 1.62 – 1.42 (m, 8H), 1.24 (dt, *J* = 15.0, 7.0 Hz, 2H), 0.97 (s, 3H), 0.96 (s, 3H), 0.91 (t, *J* = 7.2 Hz, 3H). ^{13}C NMR (126 MHz, $CDCl_3$) δ 140.78, 131.48, 129.77, 128.42, 75.76, 71.10, 48.60, 42.69, 39.98, 36.41, 35.70, 27.93, 27.74, 25.88, 17.25, 14.59. ESI-HR calcd for $C_{18}H_{29}ClO_2Na$ ($[M+Na]^+$) 335.1748, found 335.1744.

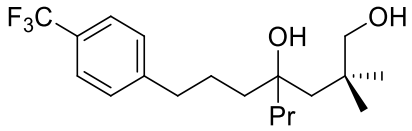

Diol 4l: Following the general procedure, 1-(4-trifluoromethylphenyl)-6,6-dimethyl-4-propylheptan-4-ol (165 mg, 0.500 mmol) was converted to the corresponding diethyl(hydrido)silyl ether with $[Ir(cod)OMe]_2$ (0.20 mol %) as catalyst at room temperature for 14 h. The subsequent cyclization was conducted with RhCl(Xantphos) at 100 °C for 15 h to provide the intermediate oxasilolane. Tamao-Fleming oxidation and purification by silica gel chromatography gave 106 mg (61% overall yield) of **4l** as a colorless oil. ^{1}H NMR (500 MHz, $CDCl_3$) δ 7.55 (d, *J* = 7.9 Hz, 2H), 7.30 (d, *J* = 7.8 Hz, 2H), 3.75 (br, 2H), 3.41 (q, *J* = 11.0 Hz, 2H), 2.66 (t, *J* = 6.9 Hz, 2H), 1.66 – 1.46 (m, 8H), 1.23 (dt, *J* = 34.4, 17.1 Hz, 2H), 0.98 (s, 3H), 0.97 (s, 3H), 0.91 (t, *J* = 7.2 Hz, 3H). ^{13}C NMR (126 MHz, $CDCl_3$) δ 146.49, 128.71, 128.18 (q, *J* = 32.8 Hz), 124.38 (q, *J* = 273 Hz), 125.26 (q, *J* = 273 Hz), 75.73, 71.11, 48.61, 42.67, 40.01, 36.39, 36.19, 27.92, 27.68, 25.71, 17.26, 14.55. ESI-HR calcd for $C_{19}H_{29}F_3O_2Na$ ($[M+Na]^+$) 369.2012, found 369.2008.

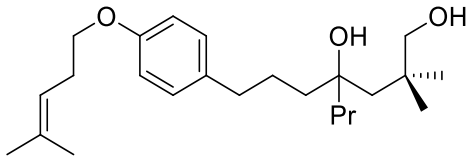

Diol 4m: Following the general procedure, 6,6-dimethyl-1-(4-((4-methylpent-3-en-1-yl)oxy)phenyl)-4-propylheptan-4-ol (108 mg, 0.300 mmol) was converted to the corresponding diethyl(hydrido)silyl ether with $[Ir(cod)OMe]_2$ (0.20 mol %) as catalyst at room temperature for 14 h. The subsequent cyclization was conducted with RhCl(Xantphos) at 100 °C for 15 h to provide the intermediate oxasilolane. Tamao-Fleming oxidation and purification by silica gel chromatography gave 69 mg (61% overall yield) of **4m** as a colorless oil. This compound contained ~15% inseparable impurities. ^{1}H NMR (500 MHz, $CDCl_3$) δ 7.10 (d, *J* = 8.3 Hz, 2H), 6.84 (d, *J* = 8.4 Hz, 2H), 5.28 – 5.16 (m, 1H), 3.94 (t, *J* = 15.3 Hz, 2H), 3.42 (d, *J* = 2.4 Hz, 2H), 3.18 (s, 2H), 2.55 (s, 2H), 2.49 (dd, *J* = 13.6, 6.7 Hz, 2H), 1.75 (s, 3H), 1.68 (s, 3H), 1.58 – 1.50 (m, 7H), 1.29 – 1.23 (m, 3H), 0.98 (s, 3H), 0.97 (s, 3H), 0.91 (t, *J* = 7.1 Hz, 3H). ^{13}C NMR (126 MHz, $CDCl_3$) δ 157.18, 134.39, 134.29, 129.25, 119.66, 114.42, 76.08, 71.15, 67.69, 48.41, 42.73, 40.07, 36.44, 35.45, 28.33, 27.93, 27.80, 26.29, 25.81, 17.91, 17.19, 14.59. ESI-HR calcd for $C_{24}H_{38}O_2Na$ ($[M+Na]^+$) 399.2870, found 399.2866.

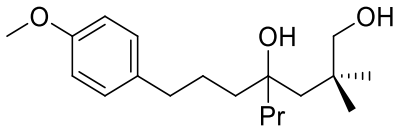

Diol 4n: Following the general procedure, 1-(4-methoxyphenyl)-6,6-dimethyl-4-propylheptan-4-ol (146 mg, 0.500 mmol) was converted to the corresponding diethyl(hydrido)silyl ether with $[Ir(cod)OMe]_2$ (0.20 mol %) as catalyst at room temperature for 14 h. The subsequent cyclization was conducted with RhCl(Xantphos) at 100 °C for 15 h to provide the intermediate oxasilolane. Tamao-Fleming oxidation and purification by silica gel chromatography gave 129 mg (84% overall yield) of **4n** as a colorless oil. ^{1}H NMR (500 MHz, $CDCl_3$) δ 7.12 (d, *J* = 8.3 Hz, 2H), 6.85 (d, *J* = 8.4 Hz, 2H), 3.81 (s, 3H), 3.65 (br, 2H), 3.45 – 3.35 (m, 2H), 2.55 (s, 2H), 1.65 – 1.44 (m, 8H), 1.31 – 1.18 (m, 2H), 0.98 (d, *J* = 1.8 Hz, 3H), 0.96 (s, 3H), 0.91 (t, *J* = 7.2 Hz, 3H). ^{13}C NMR (126 MHz, $CDCl_3$) δ 157.74, 134.47, 129.29, 113.76, 75.95, 71.12, 55.29, 48.51, 42.72, 40.06, 36.43, 35.46, 27.92, 27.80, 26.32, 17.20, 14.60. ESI-HR calcd for $C_{19}H_{32}O_3Na$ ($[M+Na]^+$) 331.2244, found 331.2240.

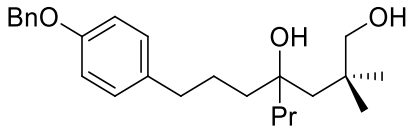

Diol 4o: Following the general procedure, 1-(4-benzyloxyphenyl)-6,6-dimethyl-4-propylheptan-4-ol (184 mg, 0.500 mmol) was converted to the corresponding diethyl(hydrido)silyl ether with $[Ir(cod)OMe]_2$ (0.20 mol %) as catalyst at room temperature for 14 h. The subsequent cyclization was conducted with RhCl(Xantphos) at 100 °C for 15 h to provide the intermediate oxasilolane. Tamao-Fleming oxidation and purification by silica gel chromatography gave 167 mg (87% overall yield) of **4o** as a colorless oil. ^{1}H NMR (500 MHz, $CDCl_3$) δ 7.47 (d, *J* = 7.2 Hz, 2H), 7.42 (t, *J* = 7.4 Hz, 2H), 7.36 (t, *J* = 7.1 Hz, 1H), 7.14 (d, *J* = 8.3 Hz, 2H), 6.94 (d, *J* = 8.4 Hz, 2H), 5.08 (s, 2H), 3.72 (br, 2H), 3.48 – 3.38 (m, 2H), 2.57 (s, 2H), 1.64 – 1.46 (m, 8H), 1.33 – 1.22 (m, 2H), 1.00 (s, 3H), 0.99 (s, 3H), 0.93 (t, *J* = 7.1 Hz, 3H).

^{13}C NMR (126 MHz, $CDCl_3$) δ 157.02, 137.24, 134.80, 129.34, 128.62, 127.96, 127.53, 114.76, 75.97, 71.14, 70.08, 48.54, 42.74, 40.08, 36.45, 35.51, 27.95, 27.83, 26.31, 17.22, 14.63. ESI-HR calcd for $C_{25}H_{36}O_3Na$ ($[M+Na]^+$) 407.2557, found 407.2553.

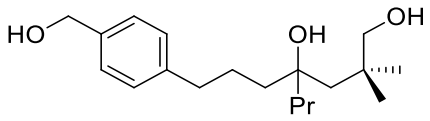

Diol 4p: Following the general procedure, 1-(4-(((tert-butyldimethylsilyl)oxy)methyl)phenyl)-6,6-dimethyl-4-propylheptan-4-ol (102 mg, 0.250 mmol) was converted to the corresponding diethyl(hydrido)silyl ether with $[Ir(cod)OMe]_2$ (0.20 mol %) as catalyst at room temperature for 14 h. The subsequent cyclization was conducted with RhCl(Xantphos) at 100 °C for 15 h to provide the intermediate oxasilolane. Tamao-Fleming oxidation and purification by silica gel chromatography gave 48 mg (62% overall yield) of **4p** as a colorless oil. ^{1}H NMR (500 MHz, $CDCl_3$) δ 7.28 (d, *J* = 7.9 Hz, 2H), 7.17 (d, *J* = 7.8 Hz, 2H), 4.62 (s, 2H), 3.50 (br, 2H), 3.37 (q, *J* = 11.0 Hz, 2H), 2.59 (t, *J* = 6.7 Hz, 2H), 1.65 – 1.41 (m, 8H), 1.30 – 1.18 (m, 2H), 0.95 (s, 3H), 0.95 (s, 3H), 0.90 (t, *J* = 7.2 Hz, 3H). ^{13}C NMR (126 MHz, $CDCl_3$) δ 141.72, 138.52, 128.56, 127.20, 75.82, 71.07, 64.95, 48.64, 42.66, 39.98, 36.39, 36.04, 27.91, 27.75, 26.00, 17.24, 14.61. ESI-HR calcd for $C_{19}H_{30}O_2Na$ ($[M+Na]^+$) 331.2244, found 331.2240.

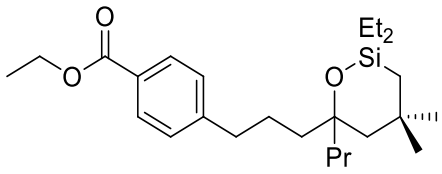

Oxasilolane 4q: Following the general procedure, ethyl 4-(4-hydroxy-6,6-dimethyl-4-propylheptyl)benzoate (84 mg, 0.25 mmol) was converted to the corresponding diethyl(hydrido)silyl ether with $RuCl_2(PPh_3)_3$ (0.50 mol %) as catalyst at 50 °C for 14 h. The subsequent cyclization was conducted with RhCl(Xantphos) at 100 °C for 15 h to provide the intermediate oxasilolane. Purification by preparative TLC gave 96 mg (92% overall yield) of **4q** as a colorless oil. ^{1}H NMR (500 MHz, $CDCl_3$) δ 7.95 (d, *J* = 7.9 Hz, 2H), 7.24 (d, *J* = 7.8 Hz, 2H), 4.36 (q, *J* = 7.0 Hz, 2H), 2.61 (d, *J* = 7.1 Hz, 2H), 1.70 – 1.16 (m, 13H), 1.04 (s, 3H), 1.00 (s, 3H), 0.93 – 0.82 (m, 9H), 0.62 – 0.43 (m, 6H). ^{13}C NMR (126 MHz, $CDCl_3$) δ 166.88, 148.36, 129.69, 128.54, 128.08, 76.86, 60.88, 48.64, 44.58, 41.68, 36.62, 34.32, 34.28, 31.41, 25.62, 23.17, 17.40, 14.85, 14.49, 8.54, 8.50, 6.86, 6.82. ESI-HR calcd for $C_{25}H_{42}O_3Si$ (M^+) 418.2903, found 418.2900.

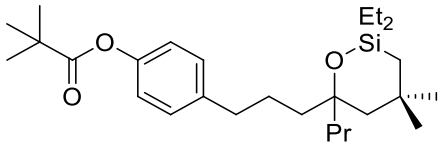

Oxasilolane 4r: Following the general procedure, ethyl 4-(4-hydroxy-6,6-dimethyl-4-propylheptyl)phenyl pivalate (91 mg, 0.25 mmol) was converted to the corresponding diethyl(hydrido)silyl ether with $RuCl_2(PPh_3)_3$ (0.50 mol %) as catalyst at 50 °C for 14 h. The subsequent cyclization was conducted with RhCl(Xantphos) at 100 °C for 15 h to provide the intermediate oxasilolane. Purification by preparative TLC gave 100 mg (90% overall yield) of **4r** as a colorless oil. ^{1}H NMR (500 MHz, $CDCl_3$) δ 7.17 (d, *J* = 8.0 Hz, 2H), 6.95 (d, *J* = 8.0 Hz, 2H), 2.56 (t, *J* = 6.6 Hz, 2H), 1.73 – 1.13 (m, 23H), 1.04 (s, 3H), 1.01 (s, 3H), 0.96 – 0.90 (m, 4H), 0.87 (t, *J* = 7.1 Hz, 3H), 0.64 – 0.43 (m, 6H). ^{13}C NMR (126 MHz, $CDCl_3$) δ 177.38, 149.14, 140.22, 129.32, 121.22, 48.63, 44.63, 41.84, 39.16, 36.03, 34.39, 34.29, 31.43, 27.29, 26.02, 23.20, 17.39, 14.87, 8.56, 8.53, 6.87, 6.84. ESI-HR calcd for $C_{27}H_{46}O_3Si$ (M^+) 446.3216, found 446.3212.

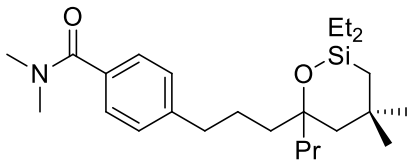

Oxasilolane 4s: Following the general procedure, 4-(4-hydroxy-6,6-dimethyl-4-propylheptyl)-N,N-dimethylbenzamide (83 mg, 0.25 mmol) was converted to the corresponding diethyl(hydrido)silyl ether with $RuCl_2(PPh_3)_3$ (0.50 mol %) as catalyst at 50 °C for 14 h. The subsequent cyclization was conducted with RhCl(Xantphos) at 100 °C for 15 h to provide the intermediate oxasilolane. Purification by preparative TLC gave 98 mg (94% overall yield) of **4s** as a colorless oil. ^{1}H NMR (500 MHz, $CDCl_3$) δ 7.18 (d, *J* = 7.9 Hz, 2H), 7.03 (d, *J* = 8.2 Hz, 2H), 3.12 (s, 3H), 3.03 (s, 3H), 2.55 (t, *J* = 6.2 Hz, 2H), 1.75 – 1.17 (m, 11H), 1.07 (s, 2H), 1.05 (s, 3H), 0.98 – 0.90 (m, 6H), 0.88 (t, *J* = 7.1 Hz, 3H), 0.65 – 0.44 (m, 6H).

^{13}C NMR (126 MHz, $CDCl_3$) δ 155.18, 149.46, 139.67, 129.09, 121.43, 76.86, 48.51, 44.53, 41.80, 36.70, 36.45, 35.93, 34.30, 34.18, 31.32, 25.95, 23.10, 17.28, 14.78, 8.45, 8.42, 6.78, 6.74. ESI-HR calcd for $C_{25}H_{43}NO_2Si$ (M^+) 417.3063, found 417.3060.

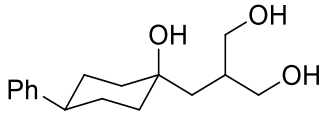

Triol 6d: Following the general procedure, compound **5d** (72 mg, 0.20 mmol) was converted to the corresponding diethyl(hydrido)silyl ether with $[Ir(cod)OMe]_2$ (0.50 mol %) as catalyst at room temperature for 14 h. The subsequent cyclization was conducted with RhCl(Xantphos) at 100 °C for 15 h to provide the intermediate oxasilolane. Tamao-

Fleming oxidation and purification by silica gel chromatography gave 38 mg (72% overall yield) of **6d** as a white solid. ^{1}H NMR (500 MHz, CD_3OD) δ 7.32 – 7.09 (m, 5H), 4.95 – 4.82 (br, 3H), 3.61 (dd, *J* = 10.6, 6.2 Hz, 2H), 3.55 (dd, *J* = 10.6, 6.2 Hz, 2H), 2.55 – 2.41 (m, 1H), 2.10 – 1.97 (m, 1H), 1.97 – 1.80 (m, 4H),1.67 (d, *J* = 9.9 Hz, 2H), 1.58 – 1.41 (m, 4H). ^{13}C NMR (126 MHz, CD_3OD) δ 149.67, 130.17, 128.72, 127.75, 71.87, 66.34, 46.36, 46.01, 40.83, 39.43, 31.39. ESI-HR calcd for $C_{16}H_{24}NaO_3$ ($[M+Na]^+$) 287.1618, found 287.1614.

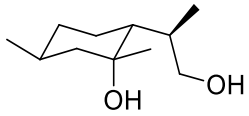

Diol 4t: Following the general procedure, (*1R,2R,5S*)-2-isopropyl-1,5-dimethylcyclohexanol (170 mg, 1.00 mmol) was converted to the corresponding diethyl(hydrido)silyl ether with $[Ir(cod)OMe]_2$ (0.20 mol %) as catalyst at room temperature for 14 h. The subsequent cyclization was conducted with RhCl(Xantphos) at 100 °C for 15 h to provide the intermediate oxasilolane. Tamao-Fleming oxidation and purification by silica gel chromatography gave 153 mg (82% overall yield) of **4t** as a colorless oil. ^{1}H NMR (500 MHz, $CDCl_3$) δ 4.92 (s, 2H), 3.42 (t, *J* = 10.8 Hz, 1H), 3.33 (dd, *J* = 10.9, 3.4 Hz, 1H), 2.39 – 2.29 (m, 1H), 1.87 – 1.76 (m, 2H), 1.65 (dt, *J* = 22.6, 7.3 Hz, 1H), 1.55 – 1.42 (m, 2H), 1.25 (s, 3H), 1.24 – 1.17 (m, 1H), 1.05 (t, *J* = 23.1Hz, 1H), 0.92 – 0.81 (m, 7H). ^{13}C NMR (126 MHz, $CDCl_3$) δ 71.26, 63.54, 51.62, 50.01, 35.50, 33.60, 29.09, 27.89, 22.30, 20.45, 18.34. ESI-HR calcd for $C_{11}H_{22}O_2Na$ ($[M+Na]^+$) 209.1512, found 209.1508.

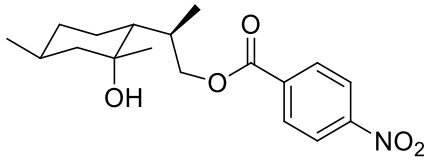

Protected diol 5t: A mixture of **4t** (150 mg, 0.600 mmol), 4-nitrobenzoyl chloride (134 mg, 0.720 mmol), NEt_3 (165 μL, 1.60 mmol), DMAP (3.7 mg, 0.030 mmol) in 5 mL of anhydrous CH_2Cl_2 was stirred at room temperature for 14 h. The crude reaction mixture was concentrated and directly purified by column chromatography to afford the product as a white solid (149 mg, 74%). Single crystal suitable for X-ray crystallography was obtained by slow diffusion of hexane to a solution of the product in EtOAc at room temperature. ^{1}H NMR (400 MHz, $CDCl_3$) δ 8.32 (d, *J* = 8.8 Hz, 2H), 8.24 (d, *J* = 8.9 Hz, 2H), 4.89 (dd, *J* = 10.8, 4.2 Hz, 1H), 4.09 (dd, *J* = 10.7, 9.3 Hz, 1H), 2.57 – 2.40 (m, 1H), 1.85 – 1.65 (m,

5H), 1.48 (ddd, *J* = 26.1, 13.0, 3.2 Hz, 1H), 1.35 (s, 3H), 1.31 – 1.20 (m, 2H), 1.14 (d, *J* = 6.9 Hz, 3H), 0.96 – 0.86 (m, 4H). ^{13}C NMR (101 MHz, $CDCl_3$) δ 164.94, 150.43, 135.91, 130.61, 123.53, 72.45, 69.25, 50.37, 50.24, 35.31, 31.46, 29.10, 28.04, 22.18, 21.60, 18.44. ESI-HR calcd for $C_{18}H_{25}NO_5$ $[M]^+$ 335.1733, found 335.1738.

Crystal data and structure refinement for 6d:

A colorless plate 0.050 x 0.040 x 0.020 mm in size was mounted on a Cryoloop with Paratone oil. Data were collected in a nitrogen gas stream at 100(2) K using phi and omega scans. Crystal-to-detector distance was 60 mm and exposure time was 10 seconds per frame using a scan width of 2.0°. Data collection was 98.5% complete to 67.000° in □. A total of 5741 reflections were collected covering the indices, -7<=*h*<=7, -8<=*k*<=8, -21<=*l*<=21. 5741 reflections were found to be symmetry independent, with an R_{int} of 0.0473. Indexing and unit cell refinement indicated a primitive, triclinic lattice. The space group was found to be P 1 (No. 1). The data were integrated using the Bruker SAINT software program and scaled using the TWINABS software program. Solution by iterative methods (SHELXT-2014) produced a complete heavy-atom phasing model consistent with the proposed structure. All non-hydrogen atoms were refined anisotropically by full-matrix least-squares (SHELXL-2014). All hydrogen atoms were placed using a riding model. Their positions were constrained relative to their parent atom using the appropriate HFIX command in SHELXL-2014. Absolute stereochemistry was unambiguously determined to be *R* at C4, C9, C22, and C27, and *S* at C1, C6, C19, and C24, respectively.

Empirical formula	$C_{18}H_{25}NO_5$	
Formula weight	335.39	
Temperature	100(2) K	
Wavelength	1.54178 Å	
Crystal system	Triclinic	
Space group	P 1	
Unit cell dimensions	a = 6.5555(3) Å	□= 88.767(2)°.
	b = 7.2872(3) Å	□= 87.077(2)°.
	c = 17.9836(7) Å	□ = 88.171(2)°.
Volume	857.37(6) Å^3	

Z	2
Density (calculated)	1.299 Mg/m^3
Absorption coefficient	0.776 mm^{-1}
F(000)	360
Crystal size	0.050 x 0.040 x 0.020 mm^3
Theta range for data collection	2.461 to 68.734°.
Index ranges	-7<=h<=7, -8<=k<=8, -21<=l<=21
Reflections collected	5741
Independent reflections	5741 [R(int) = 0.0473]
Completeness to theta = 67.000°	98.5 %
Absorption correction	Semi-empirical from equivalents
Max. and min. transmission	0.929 and 0.808
Refinement method	Full-matrix least-squares on F^2
Data / restraints / parameters	5741 / 3 / 442
Goodness-of-fit on F^2	1.011
Final R indices [I>2sigma(I)]	R1 = 0.0403, wR2 = 0.1077
R indices (all data)	R1 = 0.0464, wR2 = 0.1120
Absolute structure parameter	-0.13(11)
Extinction coefficient	n/a
Largest diff. peak and hole	0.212 and -0.168 $e.Å^{-3}$

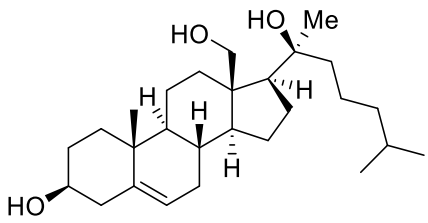

Triol 4u: Following the general procedure, compound **1v'** (103 mg, 0.200 mmol) was converted to the corresponding diethyl(hydrido)silyl ether with $[Ir(cod)OMe]_2$ (0.50 mol %) as catalyst at room temperature for 14 h. The subsequent cyclization was conducted with RhCl(Xantphos) at 100 °C for 15 h to provide the intermediate oxasilolane. Tamao-Fleming oxidation and purification by silica gel chromatography gave 38 mg (44% overall yield) of **4u** as a white solid. ^{1}H NMR (500 MHz, $CDCl_3$) δ 5.35 (d, *J* = 4.4 Hz, 1H), 3.69 (d, *J* = 11.7 Hz, 1H), 3.58 (d, *J* = 11.8 Hz, 1H), 3.56 – 3.49 (m, 1H), 2.84 (br, 3H), 2.59 (d, *J* = 12.6 Hz, 1H), 2.27 (dt, *J* = 22.9, 9.8 Hz, 2H), 1.99 (d, *J* = 9.0 Hz, 1H), 1.92 – 1.79 (m, 3H), 1.68 (dd, *J* = 27.5, 9.3 Hz, 2H), 1.62 – 1.45 (m, 9H), 1.39 (s, 3H), 1.33 – 1.24 (m, 4H), 1.15 (t, *J* = 13.3 Hz, 4H), 1.04 (s, 3H), 0.98 (d, *J* = 6.7 Hz, 1H), 0.89 (d, *J* = 6.5 Hz, 6H). ^{13}C NMR (126 MHz, $CDCl_3$) δ 140.96, 121.31, 74.83, 71.75, 58.96, 57.41, 56.29, 50.21, 47.00, 44.11, 42.23, 39.60, 37.24, 36.57, 34.46, 32.09, 31.88, 31.60, 27.91, 26.98, 23.43, 22.75, 22.60, 22.48, 22.32, 20.63, 19.48. ESI-HR calcd for $C_{27}H_{46}O_3Na$ ($[M+Na]^+$) 441.3339, found 441.3336.

Synthesis of materials and complexes for studies of the reaction mechanism

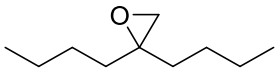

Synthesis of Dibutyl Oxirane

Trimethylsulfoxonium iodide (4.4 g, 20 mmol) was added to a 50 mL two necked round bottom flask fitted with a stir bar. The flask was sealed with two septa and purged with N_2. 15 mL DMSO from an Aldrich Sure/Seal bottle was added through a septum. The flask was placed under a positive pressure of N_2, and one septum was removed. A 60% dispersion of NaH in oil (800 mg, 20 mmol) was added portionwise to the solution with vigorous stirring. When no more H_2 evolution was observed, the septum was replaced. 5-Nonanone (2 mL, 11.6 mmol) was added through the septum. The solution was stirred for 18 h. The solution was diluted with Et_2O, washed with water, and washed with brine. The organic layer was dried with sodium sulfate, filtered, and concentrated under reduced

pressure. The resulting oil was purified by column chromatography (1:10, Et_2O to hexane) to yield 1.43 g (79% yield) of a colorless oil.

^{1}H NMR (400 MHz, Chloroform-*d*) δ 2.57 (s, 2H), 1.68 – 1.45 (m, 4H), 1.38 – 1.27 (m, 8H), 0.91 (t, 6H).

^{13}C NMR (101 MHz, $CDCl_3$) δ 59.72, 52.81, 34.09, 27.19, 23.01, 14.19.

HRMS (EI +) Calc for $C_{10}H_{20}O$ $[M]^+$ 156.1514 found 156.1516

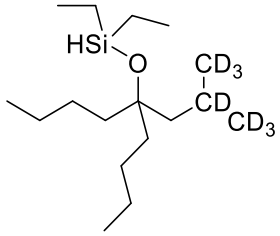

Synthesis of 2a-*d*$_7$

In an N_2 filled glovebox, Mg metal (242 mg, 9.96 mmol), I_2 (1 crystal), and 8 mL of Et_2O was added to a 25 mL round bottom flask containing a stir bar. In a separate flask, a solution of 1,2-dibromoethane (0.085 mL) in 2 mL of Et_2O was prepared. These solutions were removed from glovebox. Under a flow of nitrogen, the solution of 1,2-dibromoethane was added, by syringe, to the stirring suspension of Mg metal. Evolution of gas was observed. As gas evolution slowed, a solution of isopropylbromide-d_7 (0.80 mL, 8.5 mmol) in 4 mL of Et_2O was added dropwise to the activated Mg metal suspension. This solution was stirred for 2 h at room temperature, at which point little solid remained. CuI (1 g, 5 mmol) was added to a 50 mL round bottom flask fitted with a stir bar. This flask was evacuated and refilled with nitrogen, followed by 20 mL of THF. This suspension was stirred at -20 °C. The solution of Grignard reagent was canula transferred to the CuI suspension. A solution of dibutyloxirane (320 mg, 2.0 mmol) in 5 mL THF was added dropwise to the stirring solution of isopropylcuprate. The resulting solution was stirred for 1 h and then allowed to come to room temperature. The solution was diluted with Et_2O, washed with water, washed with brine, dried with sodium sulfate, filtered, and concentrated under reduced pressure. The resulting oil was purified by column chromatography (1:5, Et_2O to hexane) to yield a colorless oil, which contained unreacted epoxide starting material. This material was brought into a nitrogen filled glovebox and treated with 2 mL of a 4 M solution of [Ir(COD)(OMe)] followed by diethylsilane (0.1 mL, 0.8 mmol) at room temperature. Hydrogen evolution was observed. After 3 h, the volatiles were evaporated under reduced pressure and the resulting oil was purified by column chromatography (1:20, Et_2O to hexane) to yield 97 mg of **2a-*d*$_7$** (17%).

^{1}H NMR (600 MHz, Chloroform-*d*) δ 4.43 (p, *J* = 2.3 Hz, 1H), 1.46 – 1.42 (m, 4H), 1.38 – 1.22 (m, 10H), 0.99 (t, *J* = 7.9 Hz, 6H), 0.90 (t, *J* = 7.0 Hz, 6H), 0.66 (dq, *J* = 8.1, 2.1 Hz, 4H).

^{13}C NMR (151 MHz, $CDCl_3$) δ 74.65, 37.05, 34.11, 27.92, 22.98, 14.25, 6.91, 5.80.

Synthesis of (H)Si(Et)$_2$(OAd)

In a N_2-filled glovebox, 1-adamantyl alcohol (76 mg, 0.50 mmol) was weighed into a 4 mL vial, fitted with a stir bar. To this vial, 1 mL of a 6 mM solution of $[Ir(cod)OMe]_2$ in Et_2O was added, followed by Et_2SiH_2 (0.1 mL, 0.8 mmol). The vial was capped with a Teflon-lined screw cap, and the resulting solution was stirred in the glovebox at room temperature for 15 h. Hydrogen evolution was observed. Complete conversion to the corresponding diethyl(hydrido)silyl ether was determined by GC-MS. Solvent and excess silane were removed by placing the vial under high vacuum for 1 h.

^{1}H NMR (500 MHz, Benzene-d_6) δ 4.92 – 4.85 (m, 1H), 2.03 – 1.92 (m, 3H), 1.84 (d, *J* = 3.1 Hz, 6H), 1.48 (t, *J* = 3.1 Hz, 6H), 1.07 (t, *J* = 7.9 Hz, 6H), 0.68 (dq, *J* = 10.5, 4.8 Hz, 4H).

^{13}C NMR (126 MHz, $CDCl_3$) δ 71.19, 45.88, 36.49, 31.29, 7.49, 7.23.

Observations of the Soluble Precatalyst and Resting State

In an N_2-filled glovebox, 5-*iso*butylnonan-5-ol (25 mg) and Et_2SiH_2 (25 □L) were weighed in a 4 mL screw-capped vial. 0.25 mL of a 12 mM solution of $[Ir(cod)OMe]_2$ in Et_2O was then added. The vial was capped with a Teflon-lined screw cap, and the resulting solution was stirred in the glovebox at room temperature for 2 h, at which point GC analysis indicated full conversion to diethyl(hydrido)silyl ether. The volatile materials were evaporated by placing the reaction mixture directly under high vacuum for 0.5 h. The concentrated diethyl(hydrido)silyl ether was then sequentially treated with norbornene (30 mg, 0.3 mmol), RhCl(Xantphos) (7.2 mg, 0.010 mmol) and THF-d_8 (0.75 mL). This solution was a brick red suspension but was observed to form a clear solution after 10 m (ca.). This solution was transferred to a J-Young NMR tube and analyzed by ^{1}H and ^{31}P NMR spectroscopy. The J-Young tube was placed in a pre-heated aluminum block at 100 °C for 1 h. Upon heating the solution turned red. The solution was then cooled to room temperature, and was analyzed by ^{1}H and ^{31}P NMR spectroscopy.

Before Heating:

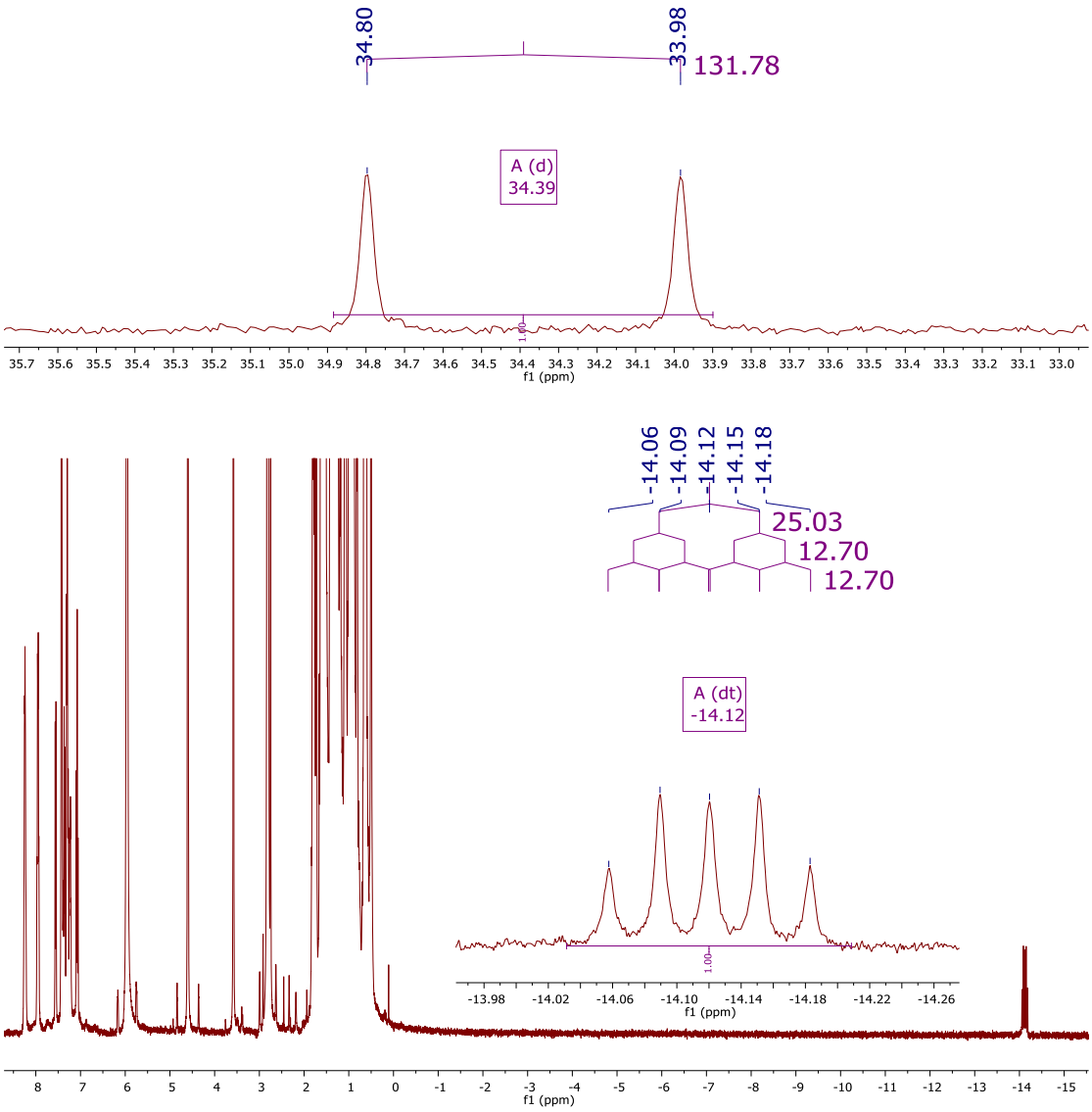
34.80
33.98
131.78
A (d)
34.39
1.00
35.7 35.6 35.5 35.4 35.3 35.2 35.1 35.0 34.9 34.8 34.7 34.6 34.5 34.4 34.3 34.2 34.1 34.0 33.9 33.8 33.7 33.6 33.5 33.4 33.3 33.2 33.1 33.0
f1 (ppm)
-14.06
-14.09
-14.12
-14.15
-14.18
25.03
12.70
12.70
A (dt)
-14.12
1.00
-13.98 -14.02 -14.06 -14.10 -14.14 -14.18 -14.22 -14.26
f1 (ppm)
8 7 6 5 4 3 2 1 0 -1 -2 -3 -4 -5 -6 -7 -8 -9 -10 -11 -12 -13 -14 -15
f1 (ppm)

After heating:

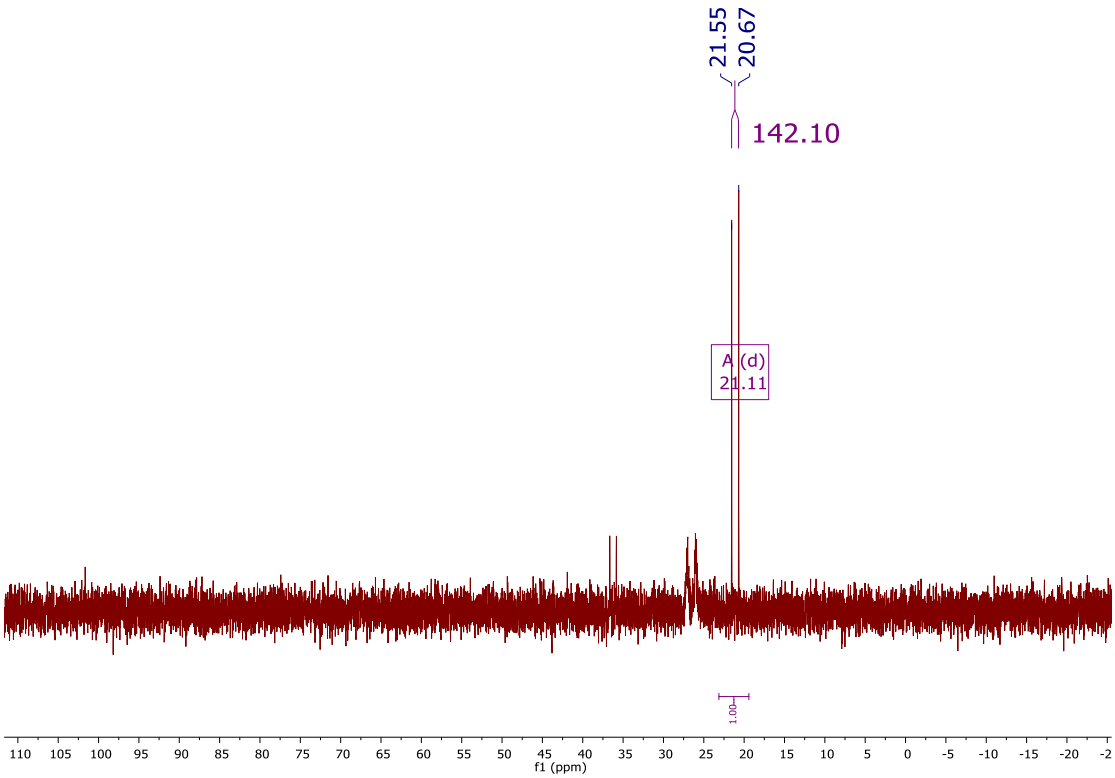

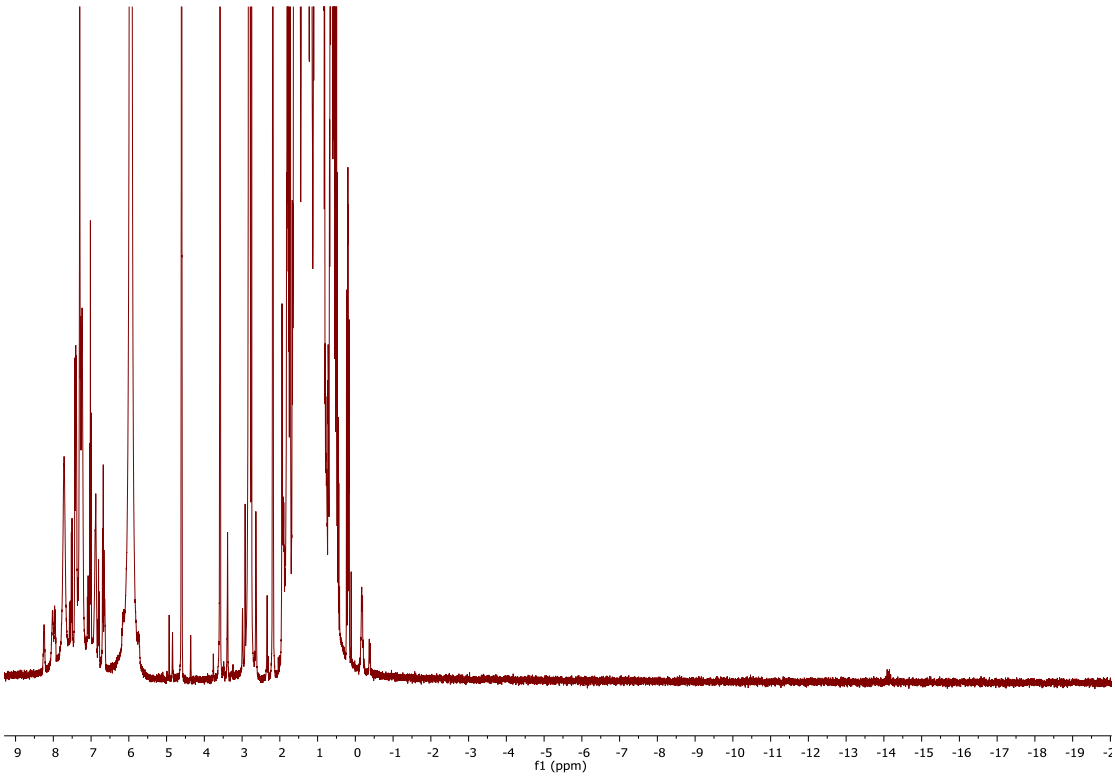

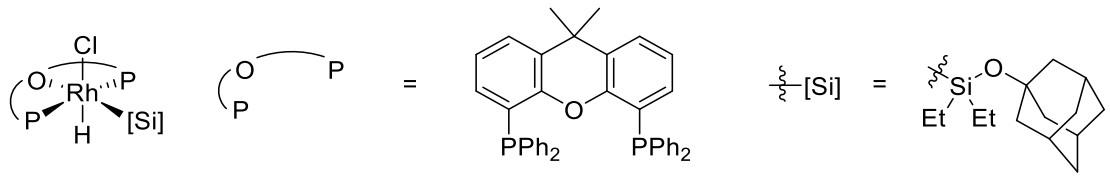

Synthesis of (Xantphos)Rh(Cl)(H)(SiEt$_2$OAd) (8)

In a N_2-filled glovebox, (Xantphos)Rh(Cl) (72 mg, 0.10 M) was weighed into a 20 mL vial. A stir bar was added. 5 mL of a 0.2 M solution of **2v** in THF was added. The resulting solution was stirred in the glovebox at room temperature for 24 h. Pentane was carefully added to form a separate phase above the solution and then allowed to diffuse into the solution over 2 d at -28 °C. A white precipitate formed which was filtered, washed with Et_2O and dried under vacuum yielding 42 mg (0.044 mmol, 44%) of white solid. The solid was dissolved in THF and crystallized by slow diffusion of pentane.

^{1}H NMR (600 MHz, Benzene-d_6) δ 8.35 (dq, J = 30.9, 5.6, Hz, 8H), 7.27 – 7.19 (m, 2H), 7.14 – 7.05 (m, 10H), 7.05 – 6.98 (m, 4H), 6.73 (t, J = 7.7 Hz, 2H), 1.91 (d, J = 4.2 Hz, 3H), 1.61 (apparent doublet, 6 H), 1.43 (s, 6H), 1.33 (s, 3H), 1.30 (t, J = 7.6 Hz, 6H), 0.95 (s, 3H), 0.93 (d, 7.6 Hz, 2H), 0.91 (d, 7.6 Hz, 2H), -13.49 (dt, J = 25.5, 14.0 Hz, 1H).

Observation of Rh hydride in THF-d_8: ^{1}H NMR (400 MHz, THF-d_8) δ -14.02 (dt, J = 25.3, 14.2 Hz, 1H).
^{13}C NMR (151 MHz, Benzene-d_6) δ 152.9 (t, J = 6.7 Hz), 135.0 (t, J = 5.8 Hz), 134.6 (t, J = 7.0 Hz), 133.5, 133.1 (t, J = 22.4 Hz), 132.0 (t, J = 2.6 Hz), 130.0, 129.6, 127.2, 123.9, 72.7, 45.0, 36.2, 34.7, 34.4, 31.0, 27.4, 17.5, 9.1.

^{31}P NMR (243 MHz, Benzene-d_6) δ 34.7 (d, J = 131.4 Hz).

Elemental analysis (%) calcd for $C_{58}H_{70}ClO_2P_2RhSi$ [M+pentane]: C 67.79, H 6.23, found: C 67.89, 6.27

IR (neat, cm–1) ν 3051, 2905, 2849, 2116, 1435, 1087, 692.

HRMS (ESI +) Calc for $C_{53}H_{58}O_2P_2RhSi$ $[M\text{-}Cl]^+$ 919.2736 found 919.2731

X-Ray structural data for Complex 8:

A yellow prism 0.050 x 0.040 x 0.040 mm in size was mounted on a Cryoloop with Paratone oil. Data were collected in a nitrogen gas stream at 100(2) K using phi and omega

scans. Crystal-to-detector distance was 60 mm and exposure time was 10 seconds per frame using a scan width of 2.0°. Data collection was 98.8% complete to 67.000° in □. A total of 69005 reflections were collected covering the indices, -13<=*h*<=10, -19<=*k*<=19, -32<=*l*<=32. 17750 reflections were found to be symmetry independent, with an R_{int} of 0.0913. Indexing and unit cell refinement indicated a primitive, triclinic lattice. The space group was found to be P -1 (No. 2). The data were integrated using the Bruker SAINT software program and scaled using the SADABS software program. Solution by iterative methods (SHELXT-2014) produced a complete heavy-atom phasing model consistent with the proposed structure. All non-hydrogen atoms were refined anisotropically by full-matrix least-squares (SHELXL-2014). All hydrogen atoms were placed using a riding model. Their positions were constrained relative to their parent atom using the appropriate HFIX command in SHELXL-2014.

Empirical formula	$C_{54}H_{59}Cl_2O_2P_2RhSi$	
Formula weight	1003.85	
Temperature	100(2) K	
Wavelength	1.54178 Å	
Crystal system	Triclinic	
Space group	P -1	
Unit cell dimensions	a = 11.5444(5) Å	□= 95.114(3)°.
	b = 16.0589(7) Å	□= 92.970(3)°.
	c = 26.8374(14) Å	□ = 90.036(3)°.
Volume	4948.9(4) $Å^3$	
Z	4	
Density (calculated)	1.347 Mg/m^3	
Absorption coefficient	4.931 mm^{-1}	
F(000)	2088	
Crystal size	0.050 x 0.040 x 0.040 mm^3	

Theta range for data collection	2.763 to 69.312°.
Index ranges	-13<=h<=10, -19<=k<=19, -32<=l<=32
Reflections collected	69005
Independent reflections	17750 [R(int) = 0.0913]
Completeness to theta = 67.000°	98.8 %
Absorption correction	Semi-empirical from equivalents
Max. and min. transmission	0.929 and 0.616
Refinement method	Full-matrix least-squares on F^2
Data / restraints / parameters	17750 / 12 / 1126
Goodness-of-fit on F^2	1.087
Final R indices [I>2sigma(I)]	R1 = 0.1059, wR2 = 0.2772
R indices (all data)	R1 = 0.1193, wR2 = 0.2935
Extinction coefficient	n/a
Largest diff. peak and hole	5.911 and -1.528 e.$Å^{-3}$

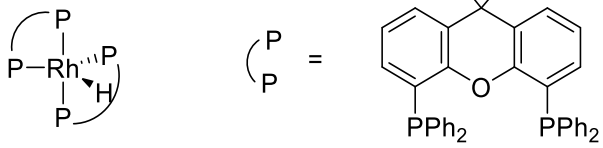

Synthesis of (Xantphos)$_2$Rh(H)

In a N_2-filled glovebox, (Xantphos)Rh(Cl) (14 mg, 0.020 mmol) and Xantphos (12 mg, 0.021 mmol) was weighed into a 4 mL vial. 1 mL of a 0.2 M solution of **2v** in THF was added. The resulting solution was kept in the glovebox at room temperature for 24 h. Red crystals, suitable for x-ray diffraction, formed in an otherwise colorless solution. The solvent was removed by pipette, and the remaining solids were washed with 2 mL of Et_2O and 2 mL of pentane and dried under vacuum yielding 18 mg (0.014 mmol, 73%) of red crystalline solids.

Elemental analysis (%) calcd for $C_{78}H_{65}O_2P_4Rh$: C 74.28, H 5.20, found: C 74.36, 5.31

IR (neat, cm^{-1}) ν 3058, 2973, 2156, 1584, 1431, 1398, 1221, 913, 743, 694

X-Ray structure data for Complex 9:
A yellow prism 0.050 x 0.030 x 0.030 mm in size was mounted on a Cryoloop with Paratone oil. Data were collected in a nitrogen gas stream at 100(2) K using phi and omega scans. Crystal-to-detector distance was 40 mm and exposure time was 10 seconds per frame using a scan width of 2.0°. Data collection was 98.1% complete to 25.000° in □. A total of 26276 reflections were collected covering the indices, -20<=*h*<=20, -20<=*k*<=21, -22<=*l*<=22. 5321 reflections were found to be symmetry independent, with an R_{int} of 0.0597. Indexing and unit cell refinement indicated a C-centered, monoclinic lattice. The space group was found to be C 2/c (No. 15). The data were integrated using the Bruker SAINT software program and scaled using the SADABS software program. Solution by iterative methods (SHELXT 2014) produced a complete heavy-atom phasing model consistent with the proposed structure. All non-hydrogen atoms were refined anisotropically by full-matrix least-squares (SHELXL-2016). All hydrogen atoms were placed using a riding model. Their positions were constrained relative to their parent atom using the appropriate HFIX command in SHELXL-2016.

Empirical formula	$C_{78}H_{65}O_2P_4Rh$
Formula weight	1260.18
Temperature/K	100.15
Crystal system	monoclinic
Space group	C2/c
a/Å	17.6304(6)
b/Å	18.1797(6)
c/Å	18.7127(6)
α/°	90
β/°	96.862(1)
γ/°	90
Volume/$Å^3$	5954.7(3)

Z	4
ρ_{calc}g/cm^3	1.4055
μ/mm^{-1}	0.445
F(000)	2610.1
Crystal size/mm^3	0.05 × 0.03 × 0.03
Radiation	Mo Kα (λ = 0.71073)
2Θ range for data collection/°	3.22 to 50.76
Index ranges	-20 ≤ h ≤ 20, -20 ≤ k ≤ 21, -22 ≤ l ≤ 22
Reflections collected	26276
Independent reflections	5321 [R_{int} = 0.0597, R_{sigma} = 0.0633]
Data/restraints/parameters	5321/0/386
Goodness-of-fit on F^2	1.034
Final R indexes [I>=2σ (I)]	R_1 = 0.0452, wR_2 = 0.0990
Final R indexes [all data]	R_1 = 0.0676, wR_2 = 0.1098
Largest diff. peak/hole / e Å^{-3}	1.39/-0.80

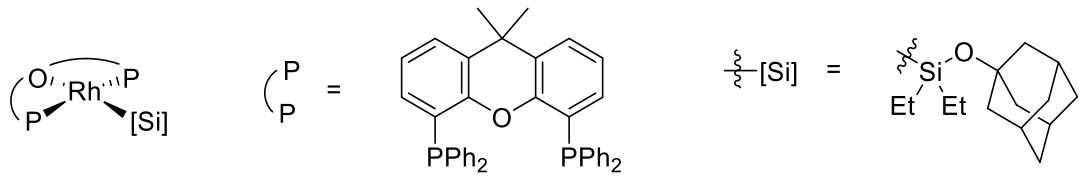

Synthesis of (Xantphos)Rh(SiEt$_2$OAd)

In a N_2-filled glovebox, (Xantphos)Rh(Cl)(H)(SiEt$_2$OAd) (10 mg, 0.01 mmol) was weighed into a 4 mL vial. A stir bar was added. LiHMDS (2 mg, 0.01 mmol) was weighed into a separate 4 mL vial. THF-d_8 (600 □L) was added to the LiHMDS. When the LiHMDS was fully dissolved, this solution was added to the vial containing complex **8**. After stirring at room temperature for 15 min, the solution was observed to turn red. This solution was transferred to a J-Young tube, and NMR analysis was performed directly on this mixture. Isolation was attempted by slow diffusion of pentane, leading to precipitation of the complex. NMR spectroscopy of the isolated red solid indicated the same material was present as in the crude reaction mixture but with additional impurities. Repeated attempts

at precipitation, crystallization and washing only produced more impurities and eventually eliminated any red products and gave an orange solid that produced no signal in the ^{31}P NMR spetrum.

^{1}H NMR (400 MHz, THF-d_8) δ 7.87 (qd, J = 5.3, 2.7 Hz, 8H), 7.57 (dd, J = 7.7, 1.6 Hz, 2H), 7.34 – 7.25 (m, 14H), 7.09 (t, J = 7.6 Hz, 2H), 1.73 (s, 6H), 1.65 (s, 6H), 1.36 (apparent doublet, J = 2.9 Hz, 6H), 1.33 (s, 3H), 0.81 (t, J = 7.7 Hz, 6H), 0.51 – 0.39 (m, 2H), 0.23 – 0.13 (m, 2H).

^{31}P NMR (162 MHz, THF-d_8) δ 32.6 (d, J = 193.4 Hz).

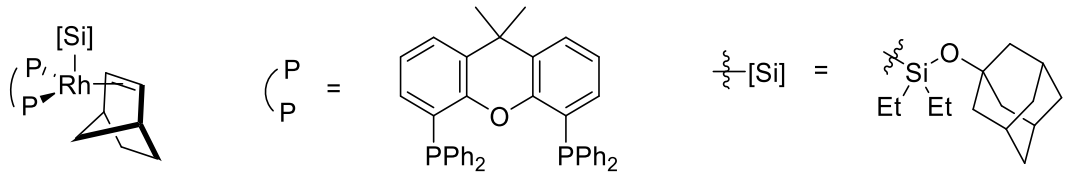

Synthesis of (Xantphos)Rh(SiEt$_2$OAd)(nbe)

In a N_2-filled glovebox, (Xantphos)Rh(Cl)(H)(SiEt$_2$OAd) (38 mg, 0.040 mmol) was weighed into a 4 mL vial. A stir bar was added. LiHMDS (34 mg, 0.20 mmol) and norbornene (4 mg, 0.04 mmol) were weighed into a separate 4 mL vial. C_6D_6 (600 □L) was added to the vial containing LiHMDS and norbornene. When the LiHMDS was dissolved, this solution was added to the vial containing complex **8**. After stirring at room temperature for 1 h, the solution was observed to turn red. This solution was transferred to a J-Young tube and NMR analyses showed that complex **8** was fully consumed. Inside of a N_2-filled glovebox, the solution was transferred to a 20 mL vial. The product was crystallized by slow diffusion of pentane at -30 °C. Reddish orange crystals formed after several days, along with a larger amount of orange powder. This powder was observed to decompose instantaneously upon removal of solvent, though the crystalline material could be removed from solvent without immediate decomposition. The powder was removed as a suspension in Et_2O, and the remaining crystals were washed with pentane. The resulting solids had a mass of 9.5 mg (24%). A few crystals were removed from the vial and dissolved in C_6D_6 (600 □L) for NMR analysis.

^{1}H NMR (500 MHz, Benzene-d_6) δ 8.03 (s, 8H), 7.22 – 7.16 (m, 2H), 7.08 (m, 12H), 6.93 (d, J = 7.6 Hz, 2H), 6.74 (t, J = 7.7 Hz, 2H), 2.62 (s, 2H), 2.03 (s, 2H), 1.94 (s, 3H), 1.74 (s, 6H), 1.47 (s, 6H), 1.46 – 1.33 (m, 2H), 1.23 – 0.98 (m, 14H), 0.98 – 0.88 (m, 2H), 0.85 (t, J = 7.1 Hz, 3H), 0.57 (t, J = 7.8 Hz, 1H).

^{31}P NMR (202 MHz, Benzene-d_6) δ 21.47 (d, J = 143.0 Hz).

X-Ray structural data for Complex 11:

A yellow blade 0.070 x 0.040 x 0.020 mm in size was mounted on a Cryoloop with Paratone oil. Data were collected in a nitrogen gas stream at 100(2) K using phi and omega scans. Crystal-to-detector distance was 40 mm and exposure time was 10 seconds per frame using a scan width of 0.5°. Data collection was 100.0% complete to 25.000° in □. A total of 127076 reflections were collected covering the indices, -22<=*h*<=22, -15<=*k*<=15, -30<=*l*<=30. 11400 reflections were found to be symmetry independent, with an R_{int} of 0.0545. Indexing and unit cell refinement indicated a primitive, monoclinic lattice. The space group was found to be P 21/c (No. 14). The data were integrated using the Bruker SAINT software program and scaled using the SADABS software program. Solution by iterative methods (SHELXT-2014) produced a complete heavy-atom phasing model consistent with the proposed structure. All non-hydrogen atoms were refined anisotropically by full-matrix least-squares (SHELXL-2016). All hydrogen atoms were placed using a riding model. Their positions were constrained relative to their parent atom using the appropriate HFIX command in SHELXL-2016.

Empirical formula	$C_{66}H_{73}O_2P_2RhSi$	
Formula weight	1091.18	
Temperature	100(2) K	
Wavelength	0.71073 Å	
Crystal system	Monoclinic	
Space group	P 21/c	
Unit cell dimensions	a = 18.4691(15) Å	□= 90°.
	b = 13.1762(10) Å	□= 95.478(4)°.
	c = 25.638(2) Å	□ = 90°.
Volume	6210.6(9) $Å^3$	
Z	4	
Density (calculated)	1.167 mg/m^3	
Absorption coefficient	0.386 mm^{-1}	

F(000)	2296
Crystal size	0.070 x 0.040 x 0.020 mm^3
Theta range for data collection	1.108 to 25.377°.
Index ranges	-22<=h<=22, -15<=k<=15, -30<=l<=30
Reflections collected	127076
Independent reflections	11400 [R(int) = 0.0545]
Completeness to theta = 25.000°	100.0 %
Absorption correction	Semi-empirical from equivalents
Max. and min. transmission	0.928 and 0.852
Refinement method	Full-matrix least-squares on F^2
Data / restraints / parameters	11400 / 0 / 653
Goodness-of-fit on F^2	1.045
Final R indices [I>2sigma(I)]	R1 = 0.0418, wR2 = 0.1018
R indices (all data)	R1 = 0.0531, wR2 = 0.1088
Extinction coefficient	n/a
Largest diff. peak and hole	0.915 and -0.523 e.$Å^{-3}$

Details of Kinetic Analyses

Test of Kinetic Competence

The silylation of **2a** was conducted in diglyme with a total volume of 0.40 mL. The concentrations of each reagent under the standard conditions for catalytic silylation were: 0.2 M silane, 0.4 M norbornene, and 8 mM catalyst. To determine the catalytic competence of each pre-catalyst, the reaction was conducted three times, with (Xantphos)Rh(Cl) as precatalyst, complex **8** as precatalyst, and complex **9** as precatalyst. The rate of the reaction was determined by the method of initial rates at 120 °C, monitored by GC analysis with dodecane as the internal standard. No product was observed when complex **9** was used as precatalyst for the silylation reaction.

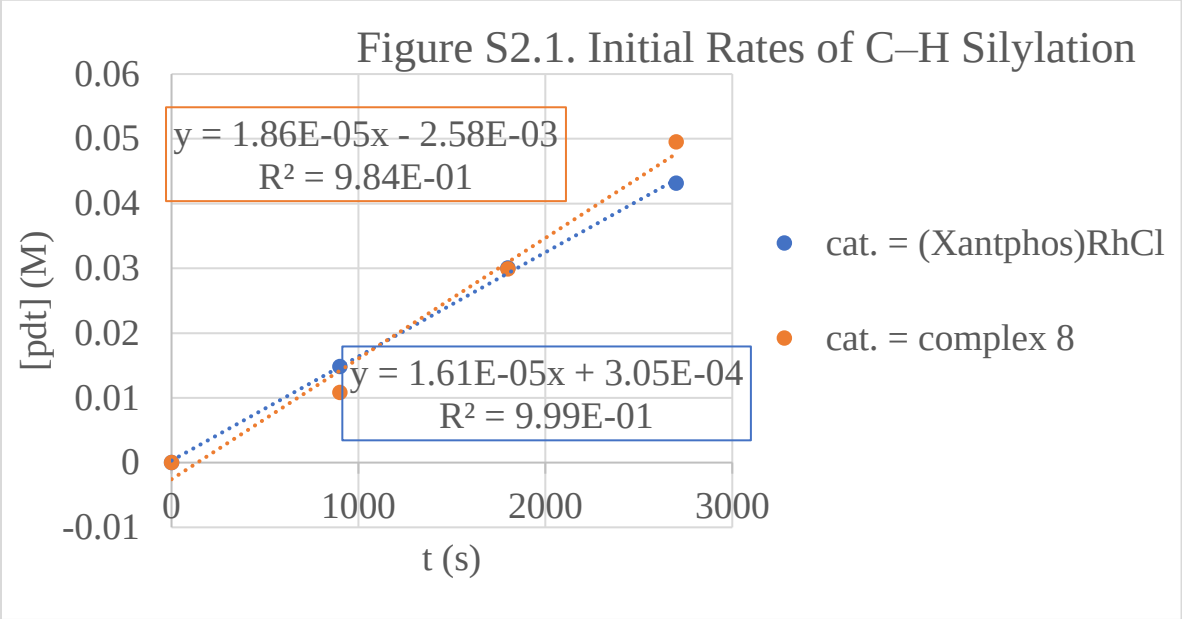

Determination of Experimental Rate Law

Silylation of **2a** was conducted in diglyme with a total volume of 0.40 mL. The concentrations of each reagent under the standard conditions for catalytic silylation were: 0.16 M silane, 0.4 M norbornene, 8 mM catalyst (**8**). To determine the rate dependence on one reagent, the concentration of that reagent was varied, while the concentration of the other reagents and the total volume (0.40 mL) were held constant. The concentration of the silane was varied between 0.04 and 0.32 M. The concentration of the catalyst (**8**) was varied between 2 and 16 mM. The concentration of norbornene was varied between 0.4 M and 3 M. The rate law of the reaction was determined by the method of initial rates at 120 °C monitored by GC analysis with dodecane as the internal standard.

Figure S2.2. Dependence of Rate of Silylation on [norbornene]

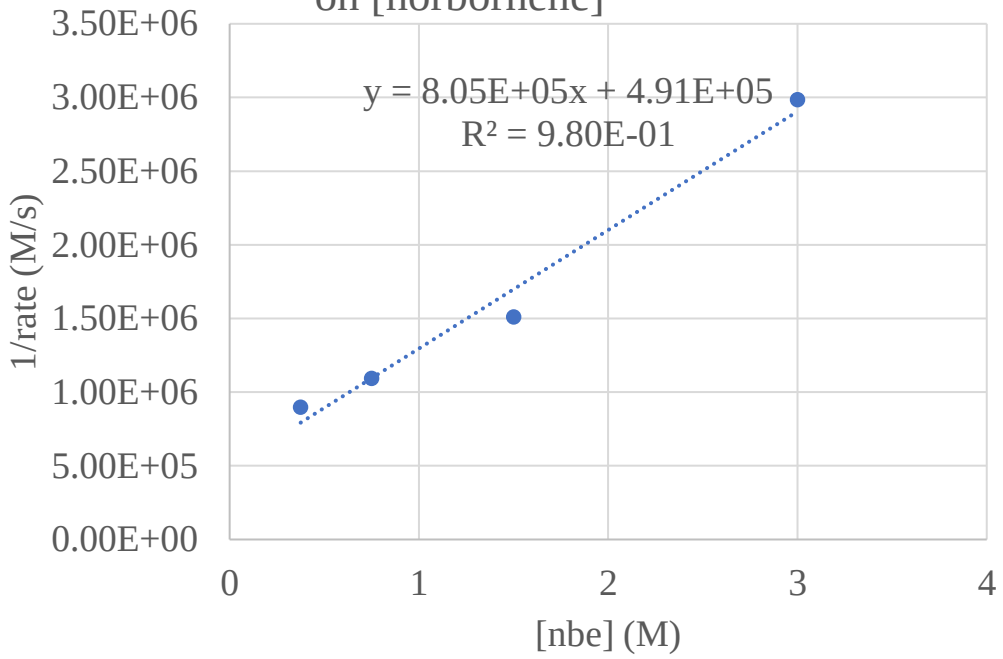

Figure S2.3. Dependence of Rate of Silylation on [complex 8]

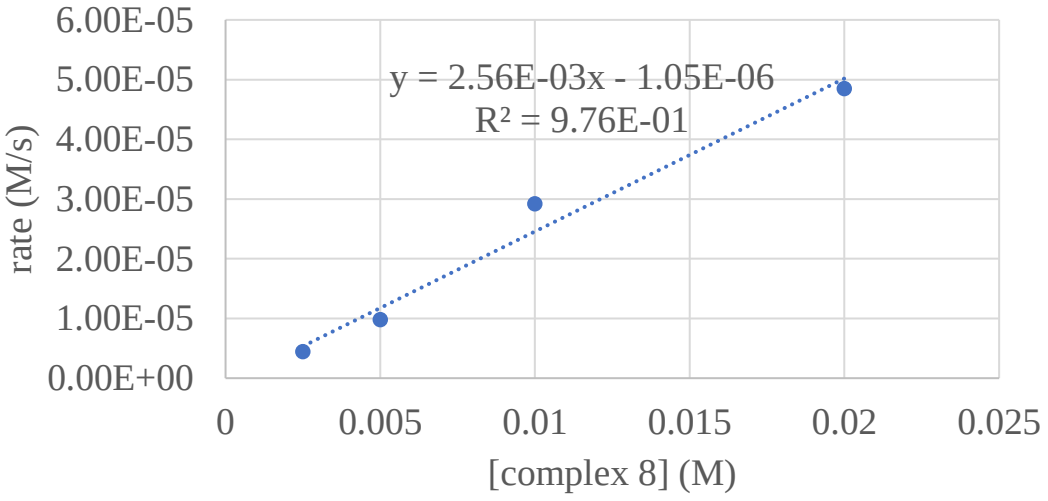

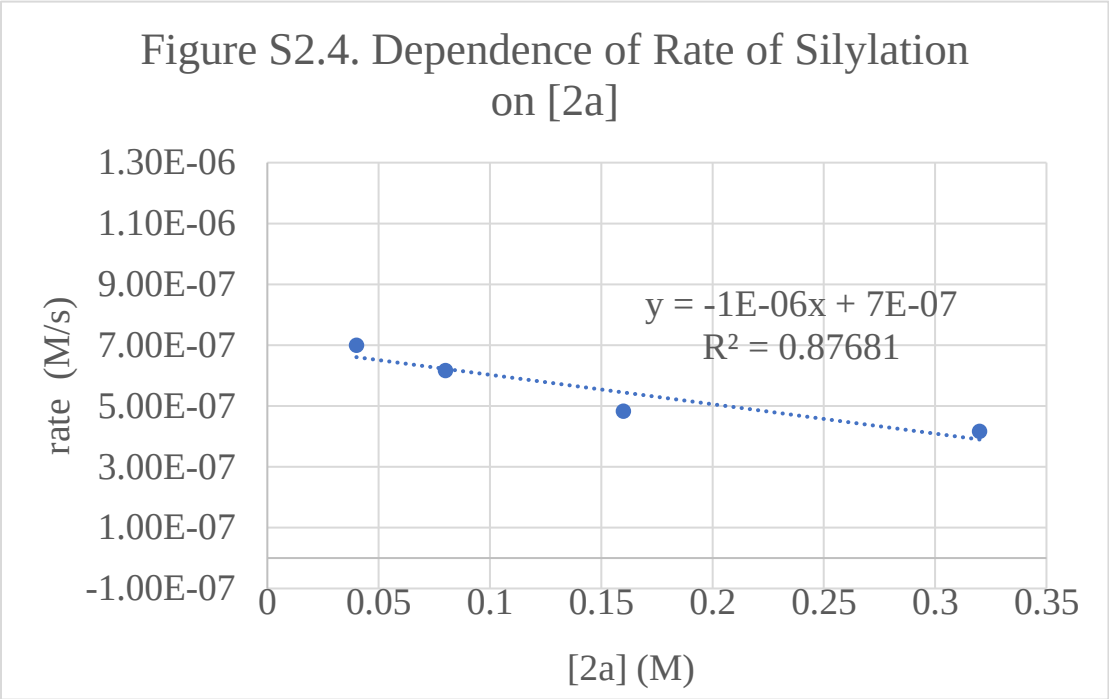

Determination of the Kinetic Isotope Effect

The silylation of **2a-*d*$_7$** was conducted in THF with a total volume of 0.40 mL. The concentrations of each reagent under the standard conditions were 0.2 M **2a-*d*$_7$**, 0.4 M norbornene and 8 mM catalyst. The silylation of **2a** was conducted under the same conditions. The initial rate of the reactions of **2a** and **2a-*d*$_7$** at 100 °C were monitored by GC analysis with dodecane as the internal standard. The kinetic isotope effect (k_H/k_D) was determined to be 4.6±0.5.

Figure S2.5. Difference in Rate of Silylation for 2a and 2a-d_7

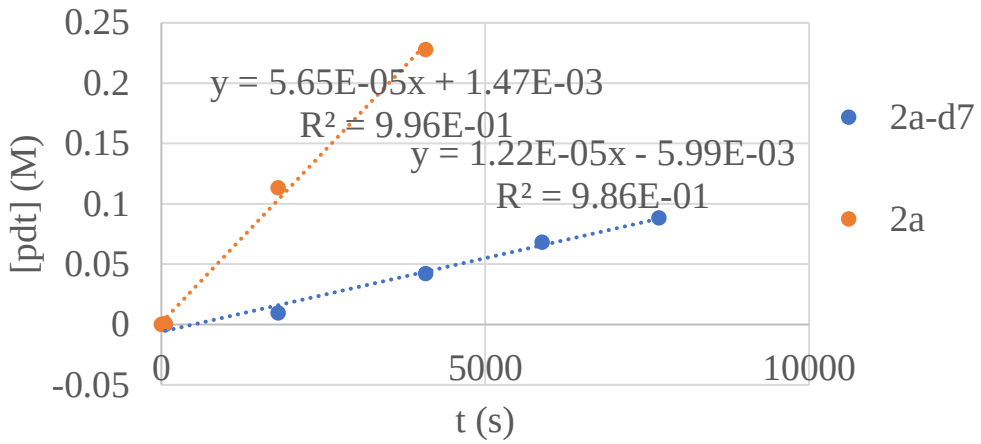

Procedures for Computational Study

DFT calculations were performed with the Gaussian 09 software package. B3LYP functionals (with gd3 dispersion correction), and LANL2DZ basis set for Rh and 6-31g(d,p) basis set for all other atoms was applied for geometry optimizations. The M06 functional, and LANL2TZ basis set for Rh and 6-31++g** basis set for all other atoms, and SMD THF solvent correction was applied to single point energy calculations. Thermal corrections from the geometry optimizations were added to the energies found in single point energy calculations to find values for Gibbs free energy. Single point energy calculations were not performed for geometry comparisons

2.5 References

Portions of this chapter were reprinted with permission from:

"Rhodium-Catalyzed Regioselective Silylation of Alkyl C–H Bonds for the Synthesis of 1,4-Diols" Karmel, C.; Li, B.; Hartwig, J. F., *J. Am. Chem. Soc.* **2018,** *140*, 1460.

(1) (a) Mkhalid, I. A. I.; Barnard, J. H.; Marder, T. B.; Murphy, J. M.; Hartwig, J. F. *Chem. Rev.* **2010**, *110*, 890. (b) Hartwig, J. F. *Acc. Chem. Res.* **2012**, *45*, 864.
(2) Cheng, C.; Hartwig, J. F. *Chem. Rev.* **2015**, *115*, 8946.
(3) selected early examples of C-H silylation (a) Gustavson, W. A.; Epstein, P. S.; Curtis, M. D. *Organometallics* **1982**, *1*, 884. (b) Sakakura, T.; Tokunaga, Y.; Sodeyama, T.; Tanaka, M. *Chem. Lett.* **1987**, 2375.
(4) selected examples of intramolecular silylation: (a) Tsukada, N.; Hartwig, J. F. *J. Am. Chem. Soc.* **2005**, *127*, 5022. (b) Furukawa, S.; Kobayashi, J.; Kawashima, T. *J. Am. Chem. Soc.* **2009**, *131*, 14192. (c) Ureshino, T.; Yoshida, T.; Kuninobu, Y.; Takai, K. *J. Am. Chem. Soc.* **2010**, *132*, 14324. (d) Simmons, E. M.; Hartwig, J. F. *J. Am. Chem. Soc.* **2010**, *132*, 17092. (e) Kuznetsov, A.; Gevorgyan, V. *Org. Lett.* **2012**, *14*, 914. (f) Kuznetsov, A.; Onishi, Y.; Inamoto, Y.; Gevorgyan, V. *Org. Lett.* **2013**, *15*, 2498. (g) Kuninobu, Y.; Yamauchi, K.; Tamura, N.; Seiki, T.; Takai, K. *Angew. Chem., Int. Ed.* **2013**, *52*, 1520. (h) Zhang, Q.-W.; An, K.; Liu, L.-C.; Yue, Y.; He, W. *Angew. Chem., Int. Ed.* **2015**, *54*, 6918. (i) Murai, M.; Matsumoto, K.; Takeuchi, Y. Takai, K. *Org. Lett.* **2015,** *17*, 3102. (j) Lee, T.; Wilson, T. W.; Berg, R.; Ryberg, P.; Hartwig, J. F. *J. Am. Chem. Soc.* **2015**, *137*, 6742. (k) Murai, M.; Takeshima, H.; Morita, H.; Kuninobu, Y.; Takai, K. *J. Org. Chem.* **2015,** *80*, 5407. (l) Ghavtadze, N.; Melkonyan, F. S.; Gulevich, A. V.; Huang, C.; Gevorgyan, V. *Nat. Chem.* **2014**, *6*, 122.
(5) selected examples of intermolecular sp^2 C-H silylation (a) Ishikawa, M.; Okazaki, S.; Naka, A.; Sakamoto, H. *Organometallics* **1992,** *11*, 4135. (b) Uchimaru, Y.; El Sayed, A. M. M.; Tanaka, M. *Organometallics* **1993**, *12*, 2065. (c) Ishikawa, M.; Naka, A.; Ohshita, J. *Organometallics* **1993**, *12*, 4987. (d) Ezbiansky, K.; Djurovich, P. I.; LaForest, M.; Sinning, D. J.; Zayes, R.; Berry, D. H. *Organometallics* **1998,** *17,* 1455. (e) Ishiyama, T.; Sato, K.; Nishio, Y.; Miyaura, N. *Angew. Chem., Int. Ed.* **2003**, *42*, 5346. (f) Ishiyama, T.; Sato, K.; Nishio, Y.; Saiki, T.; Miyaura, N. *Chem. Commun.* **2005**, 5065. (g) Sadow, A. D.; Tilley, T. D. *J. Am. Chem. Soc.* **2005**, *127*, 643. (h) Saiki, T.; Nishio, Y.; Ishiyama, T.; Miyaura, N. *Organometallics* **2006**, *25*, 6068. (i) Fukuyama, N.; Wada,

J.-i.; Watanabe, S.; Masuda, Y.; Murata, M. *Chem. Lett.* **2007**, *36*, 910. (j) Lu, B.; Falck, J. R. *Angew. Chem., Int. Ed.* **2008**, *47*, 7508. (k) Klare, H. F.; Oestreich, M.; Ito, J.-i.; Nishiyama, H.; Ohki, Y.; Tatsumi, K. *J. Am. Chem. Soc.* **2011**, *133*, 3312.
(6) Selected examples of directed sp^2 C-H silylation: (a) Williams, N. A.; Uchimaru, Y.; Tanaka, M. *J. Am. Chem. Soc., Chem. Commun.* **1995**, 1129. (b) Kakiuchi, F.; Matsumoto, M.; Sonoda, M.; Fukuyama, T.; Chatani, N.; Murai, S.; Furukawa, N.; Seki, Y. *Chem. Lett.* **2000**, 750. (c) Kakiuchi, F.; Igi, K.; Matsumoto, M.; Chatani, N.; Murai, S. *Chem. Lett.* **2001**, 422. (d) Kakiuchi, F.; Igi, K.; Matsumoto, M.; Hayamizu, T.; Chatani, N.; Murai, S. *Chem. Lett.* **2002**, 396. (e) Kakiuchi, F.; Matsumoto, M.; Tsuchiya, K.; Igi, K.; Hayamizu, T.; Chatani, N.; Murai, S. *J. Organomet. Chem.* **2003**, *686*, 134. (f) Tobisu, M.; Ano, Y.; Chatani, N. *Chem.-Asian J.* **2008**, *3*, 1585. (g) Ihara, H.; Suginome, M. *J. Am. Chem. Soc.* **2009**, *131*, 7502. (h) Oyamada, J.; Nishiura, M.; Hou, Z. *Angew. Chem., Int. Ed.* **2011**, *50*, 10720. (i) Sakurai, T.; Matsuoka, Y.; Hanataka, T.; Fukuyama, N.; Namikoshi, T.; Watanabe, S.; Murata, M. *Chem. Lett.* **2012**, *41*, 374. (j) Chen, C.; Guan, M.; Zhang, J.; Wen, Z.; Zhao, Y. *Org. Lett.* **2015**, *17*, 3646.
(7) Selected examples of directed sp^3 C-H silylation: (a) Kakiuchi, F.; Tsuchiya, K.; Matsumoto, M.; Mizushima, E.; Chatani, N. *J. Am. Chem. Soc.* **2004**, *126*, 12792. (b) Mita, T.; Michigami, K.; Sato, Y. *Org. Lett.* **2012**, *14*, 3462. (c) Mita, T.; Michigami, K.; Sato, Y. *Chem. Asian J.* **2013**, *8*, 2970. (d) Ihara, H.; Ueda, A.; Suginome, M. *Chem. Lett.* **2011**, *40*, 916.
(8) (a) Simmons, E. M.; Hartwig, J. F. *Nature* **2012**, *483*, 70. (b) Li, B.;
Driess, M.; Hartwig, J. F. *J. Am. Chem. Soc.* **2014**, *136*, 6586.
(9) (a) Frihed, T. G.; Heuckendorff, M.; Pedersen, C. M.; Bols, M. *Angew. Chem., Int. Ed.* **2012**, *51*, 12285. (b) Frihed, T. G.; Pedersen, C. M.; Bols,M. *Angew. Chem. Int. Ed.* **2014**, *53*, 13889.
(10) Hua, Y.; Jung, S.; Roh, J.; Jeon, J. *J. Org. Chem.* **2015**, *80*, 4661.
(11) (a) Čeković, Z. *Tetrahedron* **2003**, *59*, 8073. (b) Allen, J.; Boar, R. B.; McGhie, J. F.; Barton, D. H. R. *J. Chem. Soc., Perkin Trans. 1* **1973**, 2402. (c) Boar, R. B.; Copsey, D. B. J. *Chem. Soc., Perkin Trans. 1* **1979**, 563
(12) (a) Cheng, C.; Hartwig, J. F. *J. Am. Chem. Soc.* **2014**, 136, 12064. (b) Lee, T.; Hartwig, J. F. *J. Am. Chem. Soc.* **2017**, 139, 4879.
(13) Catalysts bound by ligands with wide bite angles have been used for specific types of hydroacylation reactions: (a) Moxham, G. L.; Randell-Sly, H. E.; Brayshaw, S. K.; Woodward, R. L.; Weller, A. S.; Willis, M. C. *Angew. Chem.* **2006**, *118*, 7780. (b) Chaplin, A. B.; Hooper, J. F.; Weller, A. S.; Willis, M. C. *J. Am. Chem. Soc.* **2012**, *134*, 4885.
(14) (a) Mita, T.; Hanagata, S.; Michigami, K.; Sato, Y. *Org. Lett.* **2017,** *19*, 5876; (b) Michigami, K.; Mita, T.; Sato, Y. *J. Am. Chem. Soc.* **2017,** *139*, 6094; (c) Cabrera-Pardo, J. R.; Trowbridge, A.; Nappi, M.; Ozaki, K.; Gaunt, M. J. *Angew. Chem. Int. Ed.* **2017,** *56*, 11958; (d) Probst, N.; Grelier, G.; Ghermani, N.; Gandon, V.; Alami, M.; Messaoudi, S. *Org. Lett.* **2017,** *19*, 5038.
(15) The nuclearity of this species is unknown, in part due to its lack of solubility. Although many L_2RhCl complexes are dimeric with bridging chlorides, the complex of the Xantphos analog with *i*Pr groups in place of Ph groups is monomeric with Xantphos coordinated in a tridentate fashion through two phosphorus and one oxygen atom.
(16) Stappenbeck, F.; Xiao, W.; Epperson, M.; Riley, M.; Priest, A.; Huang, D.; Nguyen, K.; Jung, M. E.; Thies, R. S.; Farouz, F. *Bioorg. Med. Chem. Lett.* **2012**, 22, 5893.
(17) Michaudel, Q.; Journot, G.; Regueiro-Ren, A.; Goswami, A.; Guo, Z.; Tully, T. P.; Zou, L.; Ramabhadran, R. O.; Houk, K. N.; Baran, P. S. *Angew. Chem. Int. Ed.* **2014**, *53*, 12091.
(18) For the synthesis of related Rh(III) silyl complexes, see: Esteruelas, M. A.; Oliván, M.; Vélez, A. *Inorg. Chem.* **2013**, *52*, 12108–12119.

(19) Prepared in a manner similar to that used to prepare (Xantphos-iPr)Rh(H): Haibach, M. C.; Wang, D. Y.; Emge, T. J.; Krogh-Jespersen, K.; Goldman, A. S. *Chem. Sci.* **2013**, *4*, 3683–3692.
(20) Esteruelas, M. A.; Oliván, M.; Vélez, A. *Inorg. Chem.* **2013**, *52*, 5339.
(21) Qadir, M.; Priestley, R. E.; Rising, T.; Gelbrich, T.; Coles, S. J.; Hursthouse, M. B.; Sheldrake, P. W.; Whittall, N.; Hii, K. K. *Tetrahedron Lett.* **2003**, *44*, 3675

Chapter 3

Iridium-Catalyzed Silylation of C-H bonds in Unactivated Arenes: A Sterically-Encumbered Phenanthroline Ligand Accelerates Catalysis

3.1 Introduction

The functionalization of C-H bonds in arenes and alkanes is becoming a valuable methodology for the synthesis of pharmaceutical drug candidates,[1] and the reactions of boranes and diboranes with arenes catalyzed by transition-metal complexes have proven particularly useful. These reactions occur at the most electron-poor C-H bond that is sterically accessible, and this regioselectivity is complementary to electrophilic aromatic substitutions, which generally occur at the most electron-rich position.[2] The products of these reactions are versatile synthetic intermediates that undergo further halogenation, cyanation, etherification, hydroxylation, amination, and trifluoromethylation,[3] as well as cross-coupling reactions to form carbon-carbon bonds that are widely employed in medicinal chemistry.[4]

Although the functionalizations of aryl C-H bonds with boron reagents are useful, several features of these reactions could limit broad utility. For example, the reagents can be expensive relative to the value of the products, some heteroarylboronates are unstable to protodeboronation, and the lengthy synthesis of diboron reagents can lead to large amounts of waste.[5] The functionalization of C-H bonds with silanes is an attractive alternative to the functionalization with boranes because many silanes are produced and consumed on a large scale,[6] silylarenes containing heteroatom substituents attached to silicon can be employed in a wide range of coupling reactions and oxidative transformations,[7] and the heteroarylsilanes are more stable than heteroarylboronates.[7d, 8] Several groups have reported silylations of the C-H bonds of arenes with trialkylsilanes, difluoroalkylsilanes, silatrane, or siloxysilanes catalyzed by complexes that are

similar to those that catalyze the borylation of C-H bonds. However, these reactions require large excess of the arene[9] or a directing group.[10]

Scheme 3.1 Functionalization of Aryl C-H bonds With Boron and Silicon Reagents

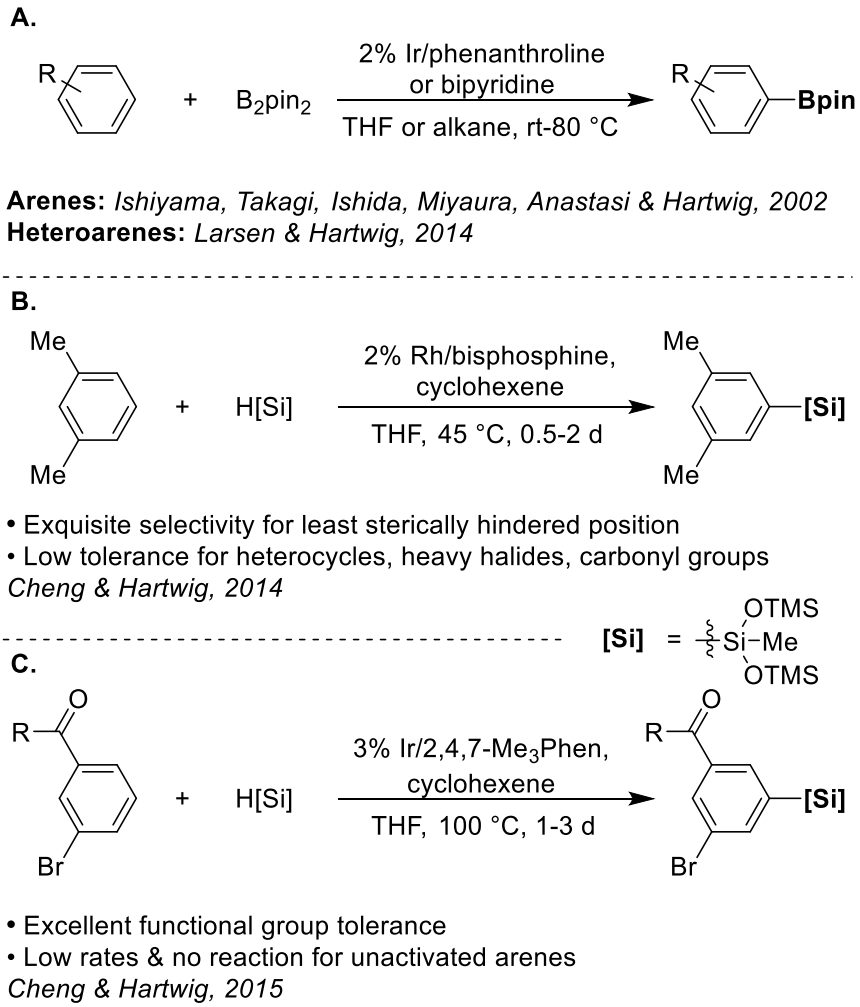

Our group has reported silylations of aryl C-H bonds with the arene as limiting reagent catalyzed by rhodium and iridium complexes with the silane $HSiMe(OTMS)_2$, which is available in bulk at low cost.[11] Due to the presence of two heteroatoms attached to the central silicon, the silylarenes produced from the functionalization of aryl and heteroaryl C-H bonds with this reagent undergo a wide variety of cross-coupling and functionalization reactions.[8] The silylations catalyzed by a rhodium-bisphosphine complex we reported functionalize arenes with high sterically-derived regioselectivity. However, a series of functional groups, including Lewis basic groups, such as nitriles, most basic heterocycles, and reducible groups, such as aryl iodides, aryl bromides, aryl esters, and ketones, did not undergo silylation (Scheme 3.1b).[12] In contrast, the silylations catalyzed by an iridium complex of 2,4,7-trimethyl phenanthroline occurred with exceptionally high functional-group tolerance. Yet, reactions catalyzed by this system required long times and required high temperatures to reach high conversion of starting material.

Furthermore, the reactions of electron-neutral arenes occurred in only modest yields, and the reactions of electron rich arenes formed little to no product (Scheme 3.1c).[13]

Here, we describe a new iridium catalyst and conditions for the silylation of arenes with hydrosilanes that together lead to reactions of electron-rich arenes and much faster reactions of heteroarenes and electron-poor arenes, along with experimental mechanistic studies that reveal the origin of this high reactivity. This catalyst contains 2,9-dimethylphenanthroline (2,9-Me_2phen) as ligand. The high activity of this catalyst is masked under standard conditions by its susceptibility to inhibition by the hydrogen byproduct. The high activity is evident from initial rates and becomes practical when the product inhibition is alleviated by removing the hydrogen from the system. Cleavage of the aryl C-H bond is reversible, and the higher rates, counterintuitively, appear to result from a more thermodynamically favorable oxidative addition of C-H bonds to the iridium complex of this hindered ligand than to complexes of ligands lacking substituents in the 2 and 9 positions. Applications to the synthesis of a series of intermediates to medicinally important compounds demonstrate the value of this new system.

3.2 Results & Discussion

3.2.1 Initial Rates and Reaction Development

To identify highly active catalysts for the silylation of aryl C-H bonds, including those of electron-rich arenes, we first measured the rates of the silylation of benzene in the presence of an iridium pre-catalyst and phenanthrolines possessing varied steric properties. The initial rate of the reaction of $HSiMe(OTMS)_2$ and benzene was determined by measuring the amount of silyl-arene produced at 80 °C with a 1:1.5 ratio of benzene to silane (Figure 3.1). The rates of reactions catalyzed by the combination of 1 mol % $[Ir(COD)(OMe]_2$ and 3 mol % of four phenanthroline ligands (**L1**-**L4**, Figure 3.1) containing methyl substituents in different quantities and positions were measured. The initial rates of the reactions catalyzed by the combination of iridium and a phenanthroline containing methyl groups in the 2 and the 9 positions (**L1** and **L4**) are higher than those of the reactions catalyzed by the combination of iridium and phenanthroline ligands lacking one or both of the methyl groups in the 2 and the 9 positions (**L2** and **L3**) (Figure 3.1). The silylation of aryl C-H bonds catalyzed by iridium-complexes of phenanthrolines bearing methyl groups in the 2 and the 9 positions were more than five times faster than those catalyzed by iridium complexes of the 2, 4, 7-substituted phenanthroline **L2** previously reported for the silylation of C-H bonds.

Despite the high initial rate of the silylation catalyzed by the combination of $[Ir(COD)(OMe]_2$ and 2,9-Me_2phen, the overall yield of this reaction was reported to be lower than that of the reaction catalyzed by complexes containing other ligands.[13] Indeed, when the reaction of benzene and silane catalyzed by iridium and this ligand approached 5% conversion, the rate began to decrease (Figure 3.1), and after 15% conversion, the amount of silylbenzene produced by the reaction conducted with 2-methyl ligand **L2** is greater than that produced by the catalyst containing 2,9-dimethyl ligands **L1** or **L4**. We hypothesized that inhibition of the catalyst by the hydrogen produced by the reaction could cause the observed decrease in rates during reactions catalyzed by complexes ligated by **L1** or **L4**.

To determine whether hydrogen inhibited the silylation reaction, we first measured the amount of silylbenzene formed in the presence of $[Ir(COD)(OMe]_2$ and **L1** with added dihydrogen. The rate at which silylbenzene is formed is ten times slower under an atmosphere of hydrogen than under an atmosphere of nitrogen (See SI). We examined whether a series of hydrogen acceptors

could prevent inhibition by hydrogen formed in the course of the reaction. The profile of the reaction of benzene and silane was the same in the presence or absence of cyclohexene or tetramethylethylene as hydrogen acceptors (Figure 3.2). Consistent with this observation, the ^{1}H NMR spectrum of the crude reaction catalyzed by iridium and 2,9-Me_2phen with cyclohexene as the hydrogen acceptor contained signals corresponding to less than 0.05 equivalents of cyclohexane, even though 16% of the starting material was converted to product. This result shows that the rate of the reduction of cyclohexene is much lower than the rate of the silylation of benzene. The conversion of silane in the reaction conducted with the strained alkene norbornene (nbe) was higher in less time than that in reactions conducted with other hydrogen acceptors, but the silylation of the alkene C-H bond of nbe to form vinylsilane was faster than silylation of the C-H bond of benzene, and a low yield of silylarene was observed. Thus, the complex formed by the combination of iridium and 2,9-Me_2phen and silane does not reduce unstrained internal alkenes with hydrogen at a rate that is commensurate with the rate of the silylation of benzene, and this complex leads to the silylation of the C-H bond of a strained alkene. For this reason, a different approach to removing hydrogen from the reaction was required to prevent the inhibition of the catalysts by hydrogen.

To test further the effect of the hydrogen byproduct, the reaction was run in a closed system, as is typically done for reactions on small scale, as well as a system containing a flow of nitrogen. The reaction of *o*-xylene and silane catalyzed by $[Ir(cod)(OMe)]_2$ and 2,9-Me_2Phen in a closed vial produced only the silylarene in only 18% yield. However, the same reaction conducted in a vessel equipped with a nitrogen inlet and gas outlet formed silylarene **4** in 77% yield within 20 h. It appears that the flow of nitrogen gas through the system prevents catalyst inhibition by removing hydrogen gas and allows reactions catalyzed by iridium complexes ligated by 2,9-Me_2Phen to reach high conversion.

Figure 3.1 Measurement of Rate of Silylation and Reaction Profile with Different Iridium Catalysts[a]

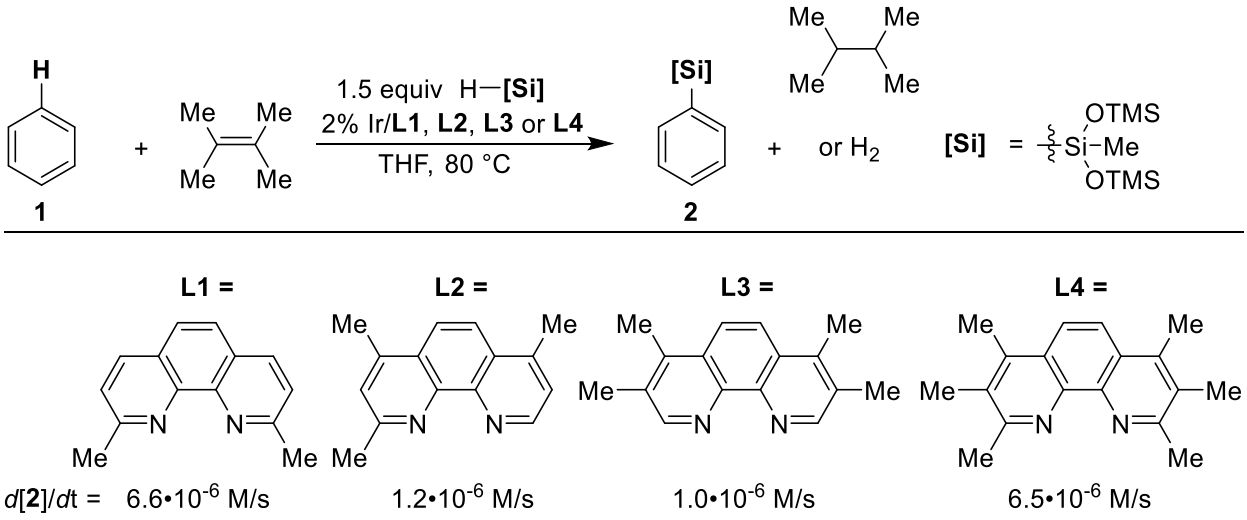

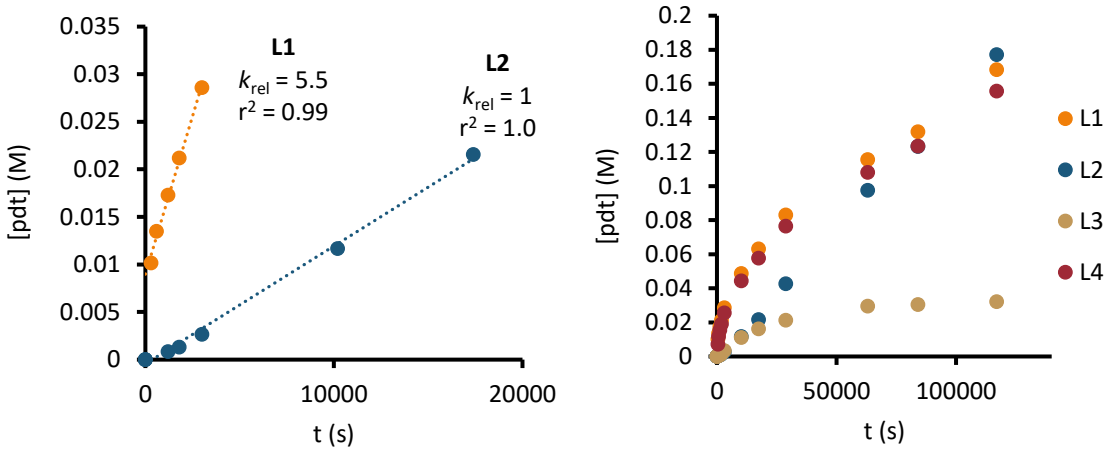

[a]Conditions: benzene (0.25 mmol), $HSiMe(OTMS)_2$ (1.5 equiv), tetramethylethylene (1.0 equiv), $[Ir(cod)(OMe)]_2$ (1.0 mol %), ligand (3.0 mol %), dodecane (1.0 equiv), THF (1 M). Silylarene concentration was determined by GC using *n*-dodecane as an internal standard.

Figure 3.2 Measurement of Rate of Silylation and Reaction Profile with a Series of Hydrogen Acceptors[a]

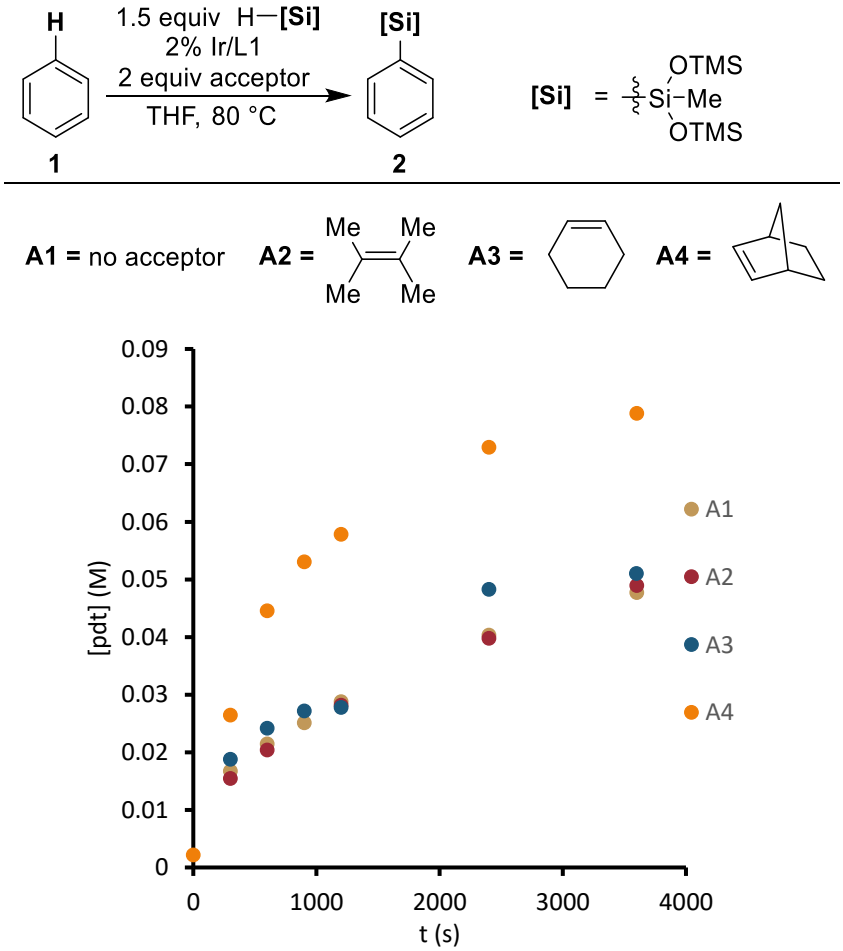

[a]Conditions: benzene (0.25 mmol), $HSiMe(OTMS)_2$ (1.5 equiv), hydrogen acceptor (1.0 equiv), $[Ir(cod)(OMe)]_2$ (1.0 mol %), 2,9-Me_2Phen (2.0 mol %), dodecane (1.0 equiv), THF (1 M). Silylarene concentration was determined by GC using *n*-dodecane as an internal standard.

3.2.2 Scope of the Silylation of Aryl C-H Bonds

Having identified a combination of ligand that generates a highly active catalyst and having gained evidence that the catalyst activity is inhibited by the hydrogen byproduct, we explored the scope of the reactions catalyzed by the complex of 2,9-dimethyl ligand **L1** under conditions in which hydrogen is removed by a flow of nitrogen. Most reactions were conducted in a Radley Carousel Reactor equipped with nitrogen inlet and outlets, heating block and cooling jacket. Under these conditions, electron-rich, electron-neutral, electron-poor and heteroaromatic silylarene products were obtained in high yields from reactions catalyzed by iridium complexes of **L1**. Silylarenes also were produced in high yield from reactions conducted in a simple round-bottom flask fitted with a reflux condenser and a nitrogen inlet and gas outlet.

The dramatic increase in rates of reactions catalyzed by the complex of 2,9-Me_2phen enabled the first iridium-catalyzed silylations of electron-rich arenes with the arene as limiting reagent. Arenes containing alkyl, methoxy and dimethylamino substituents were obtained in yields ranging from 66% to 94% (Table 3.1). The silylation of 1,3-dimethoxybenzene occurred with >10:1 selectivity for functionalization at the meta C-H bond over the ortho C-H bond. In all other cases, the sole C-H bond that reacted was distal to functional groups on the arene. To assess whether the influence of the steric properties of the C-H bonds on the selectivity of the silylation reaction was larger than the effect of the electronic properties of the arene and whether reactions would occur at particularly electron-rich C-H bonds, the reaction of 2,6-dimethylanisole was conducted. The C-H bond that is *para* to the electron-donating methoxy group in this arene is particularly electron rich, due to the presence of three substituents that are electron-donating to the

C-H bond at the sterically accessible 5-position. Despite the high electron density at this C-H bond, the reaction occurred exclusively to form the 5-silylarene **8** in a high 83% yield.

Table 3.1 C-H Silylation of Electron-Rich Arenes[a]

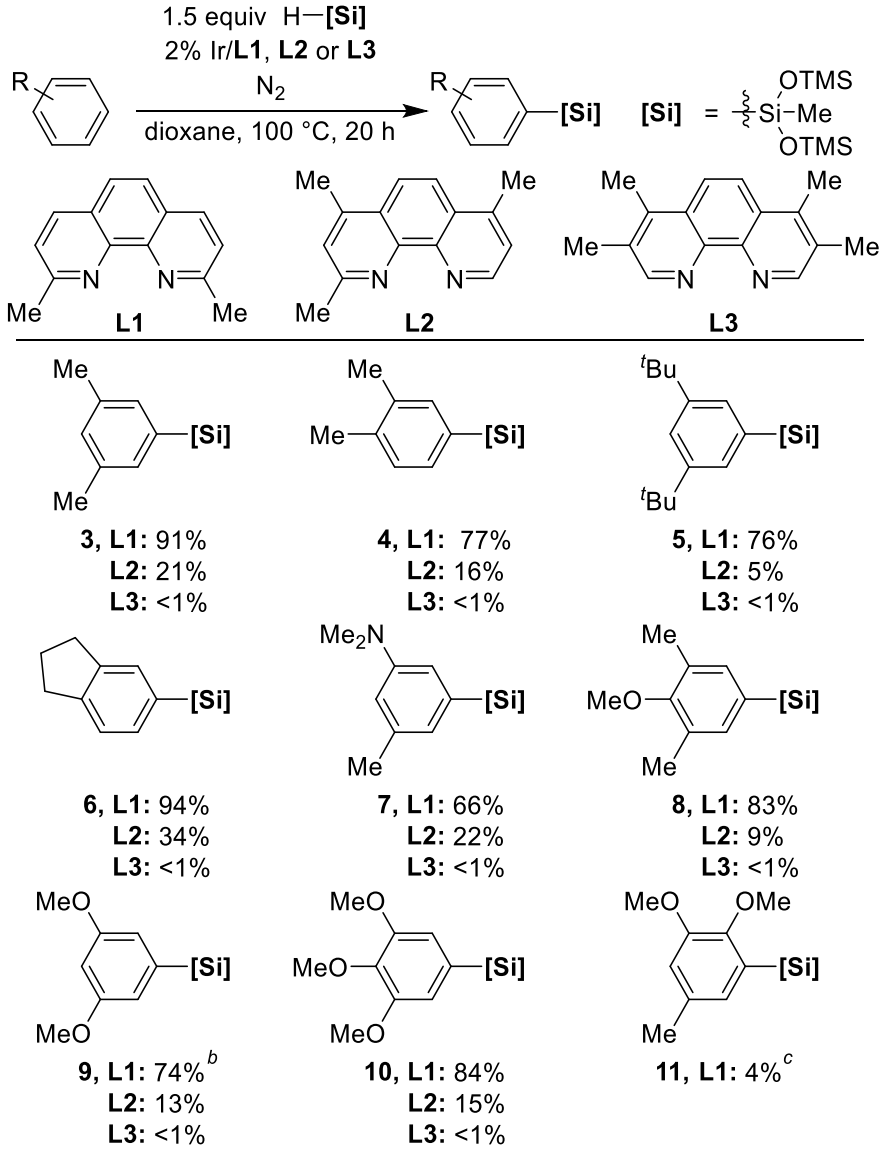

[a]Conditions for reactions with **L1**: Arene (0.5 mmol), $HSiMe(OTMS)_2$ (1.5 equiv), $[Ir(cod)(OMe)]_2$ (1 mol %), ligand (2 mol %), 1,4-dioxane (200 µL), 100 °C, under a stream of N_2, 20-24 h. Isolated yields reported. Conditions for reactions with **L2** and **L3**: Arene (0.5 mmol), $HSiMe(OTMS)_2$ (1.5 equiv), $[Ir(cod)(OMe)]_2$ (1 mol %), ligand (2 mol %), 1,4-dioxane (200 µL), 100 °C, under a stream of N_2, 20 h. Yield was determined by NMR spectroscopy relative to CH_2Br_2 internal standard. [b]Conducted at 80 °C. [c]Yield was determined by NMR spectroscopy relative to CH_2Br_2 internal standard.

To assess the effect of the ligand on the reactions of electron-rich arenes, we also conducted the silylations with the catalyst generated from 2,4,7-Me_3phen and 3,4,7,8-tetramethyl

phenanthroline. The reactions of electron-rich arenes conducted with 2,4,7-Me_3phen instead of 2,9-Me_2phen formed silylarenes in low yields, whether the reaction was conducted under a flow of nitrogen or in a closed system with alkene hydrogen acceptor. The yields from reactions of these arenes under a flow of nitrogen catalyzed by iridium and 2,4,7-Me_3phen (**L2**) ranged from 5% (**5**) to 34% (**6**). No electron-rich silylarene products were obtained from reactions catalyzed by iridium and Me_4phen (**L3**). These results demonstrate that previously reported systems for the iridium-catalyzed silylation of aryl C-H bonds would require unacceptably high catalyst loadings to produce reasonable yields of electron-rich silylarenes.

Electron-neutral and electron-poor arenes underwent C-H silylation in yields that ranged from 56% to 99% (Table 3.2). The reactions of these substrates occurred with high functional group tolerance in less than 20 h. Esters were tolerated; no products from reduction of this functionality were observed (**13**, **16** and **20**). Likewise, two representative benzonitriles underwent silylation in 84% (**15**) and 97% (**18**) yield without any detectable reduction of the cyano groups. These reactions occurred with >10:1 selectivity for functionalization at the meta C-H bond over the ortho C-H bond. Borylation of benzonitriles often occurs to give mixtures of products from reaction ortho and meta to the cyano group.[14] Silylarenes containing iodo, bromo or chloro substituents were obtained in high yield without hydrodehalogenation (substrates: **12**, **14**, **18**, **20-23**).

Table 3.2 C-H Silylation of Electron-Neutral Arenes (top) and Electron-Poor Arenes (bottom)[a]

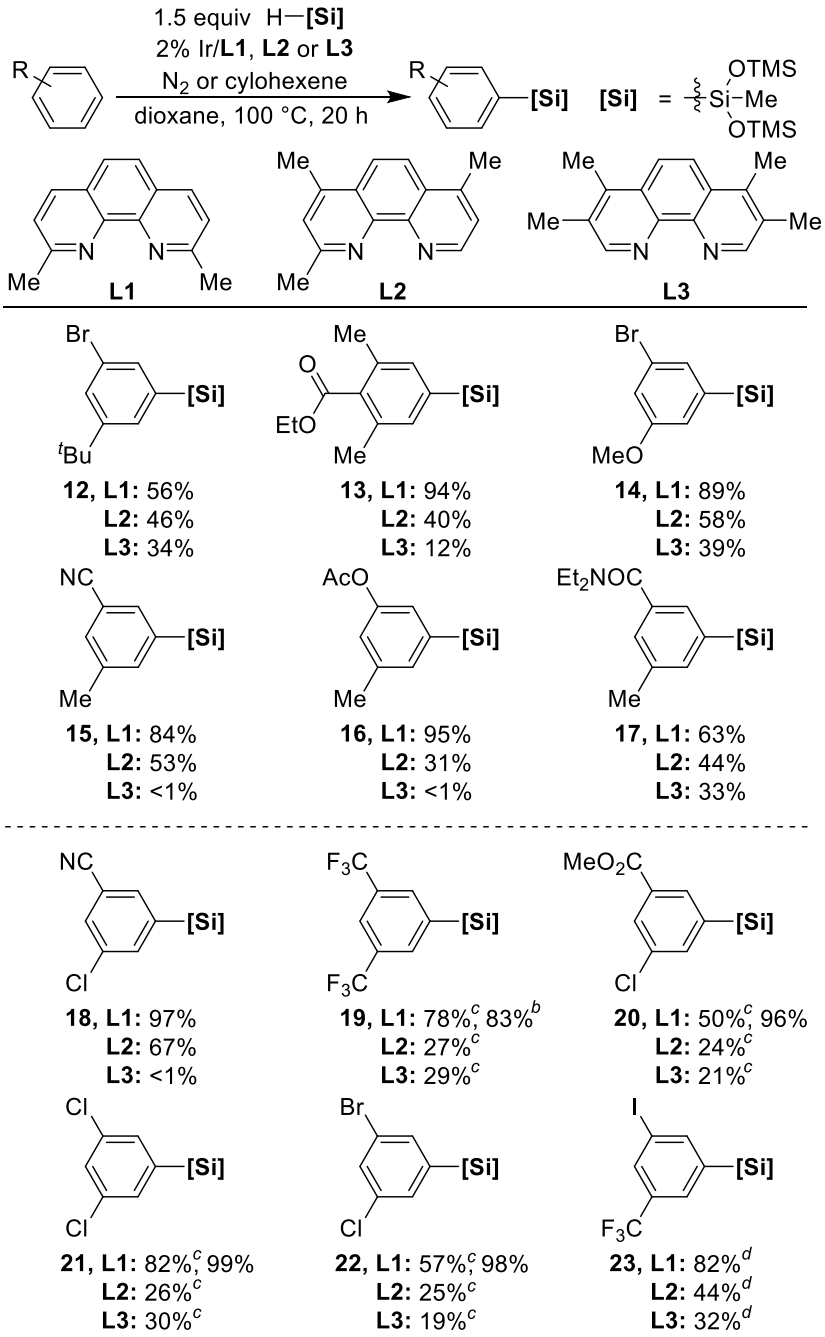

[a]Conditions for reactions with **L1**: Arene (0.5 mmol), $HSiMe(OTMS)_2$ (1.5 equiv), $[Ir(cod)(OMe)]_2$ (1 mol %), ligand (2 mol %), 1,4-dioxane (200 µL), 100 °C, under a stream of N_2, 6-24 h. Isolated yields reported. Conditions for reactions with **L2** and **L3**: Arene (0.1 mmol), $HSiMe(OTMS)_2$ (1.5 equiv), cyclohexene (1.5 equiv), $[Ir(cod)(OMe)]_2$ (1 mol %), ligand (2 mol %), THF (100 µL), 100 °C. Yield was determined by NMR spectroscopy relative to CH_2Br_2 internal standard. [b]Conducted at 80 °C. [c]Yield was determined by NMR spectroscopy relative to CH_2Br_2 internal standard. 0.2-0.25% $[Ir(cod)(OMe)]_2$, 18 h. [d]4% $[Ir(cod)(OMe)]_2$, 20 h.

The reactions catalyzed by complexes of the previously reported ligands (**L2** or **L3** with added hydrogen acceptor) form electron-neutral silylarene products in much lower yields under similar conditions. Most of these electron-neutral silylarenes (Table 3.2, top) were produced in acceptable yield in reactions catalyzed by iridium ligated by **L2**, but these reactions required days to reach high conversion. The conversion of electron-neutral arenes to the corresponding silylarenes catalyzed by the complex of **L2**, after 20 hours, ranged from low (**16**, 31%) to modest (**14**, 58%). In contrast, the conversion of electron-neutral arenes into the corresponding silylarenes was complete after 20 hours when catalyzed by the complex of **L1**.

Arenes in which all C-H bonds are *ortho* to a substituent were silylated, but the rates of these reactions were low. For example, the reaction of 3,4-dimethoxytoluene formed the silylarene resulting from C-H activation *ortho* to the methoxy group. However, only 4% yield of **11** was observed after 2 d, even with a higher catalyst loading of 4%.

In some cases, running the silylation reaction in a closed system with a hydrogen acceptor is more convenient than running the reaction under a flow of nitrogen. We hypothesized that the rates of the silylation of heteroarenes might be significantly faster than the rate of the competitive silylation of a norbornenyl C-H bond, allowing this alkene to be employed as hydrogen acceptor in a closed system. As shown in Table 3.3, both 5-membered and 6-membered ring heterocycles underwent silylation with norbornene as acceptor or in an open system in high yields under conditions that are milder than those for the silylation of aromatic substrates. As was observed for reactions of aryl halides, reactions of heteroaryl halides occurred without proto-dehalogenation. The reactions of heteroarenes also occurred with the same tolerance for carbonyl groups observed in the reactions of arenes. Furyl ketone **25** underwent silylation in 97% yield without any reduction of the carbonyl group. The silylation of thiophenes and furans occurred exclusively at the 2-position. Indole **24** underwent silylation with high selectivity for the 2-position over the 3-position (2-Si:3-Si = 17:1). 2,6-Dichloropyridine underwent silylation exclusively at the 4-position in 77% yield.

Table 3.3 C-H Silylation of Heteroarenes[a]

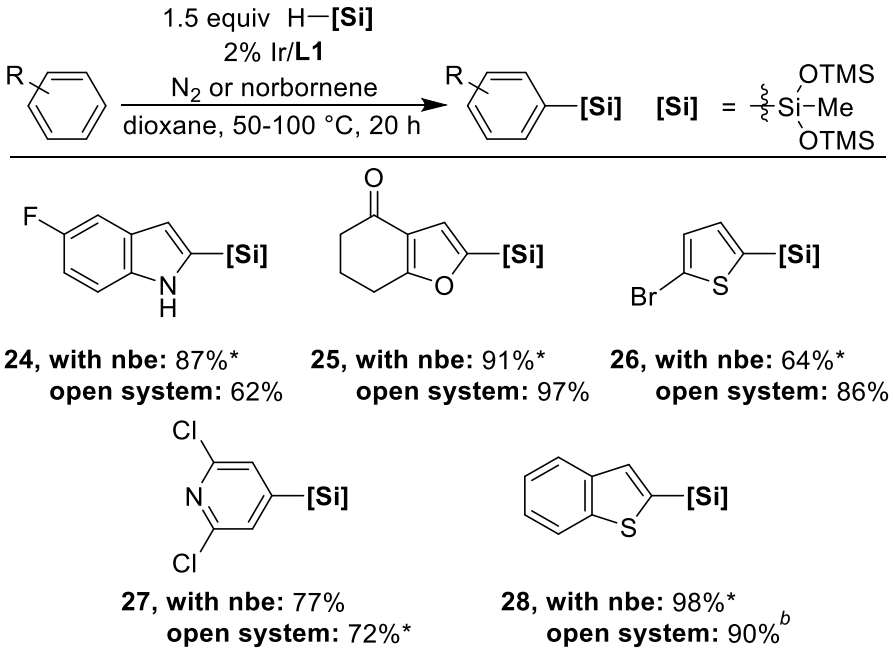

[a]Conditions with norbornene: Arene (0.25 mmol), $HSiMe(OTMS)_2$ (1.5 equiv), norbornene (1 equiv), $[Ir(cod)(OMe)]_2$ (1 mol %), ligand (2 mol %), THF (100 µL), 100 °C, 2 h. Isolated yields reported. Conditions with open system: Arene (0.5 mmol), $HSiMe(OTMS)_2$ (1.5 equiv), $[Ir(cod)(OMe)]_2$ (1 mol %), ligand (2 mol %), 1,4-dioxane (200 µL), 50-60 °C, under a stream of N_2, 20 h. Isolated yields reported. *Yield was determined by NMR spectroscopy relative to CH_2Br_2 internal standard.

Scheme 3.2 Reported Functionalizations of Silylarene Products

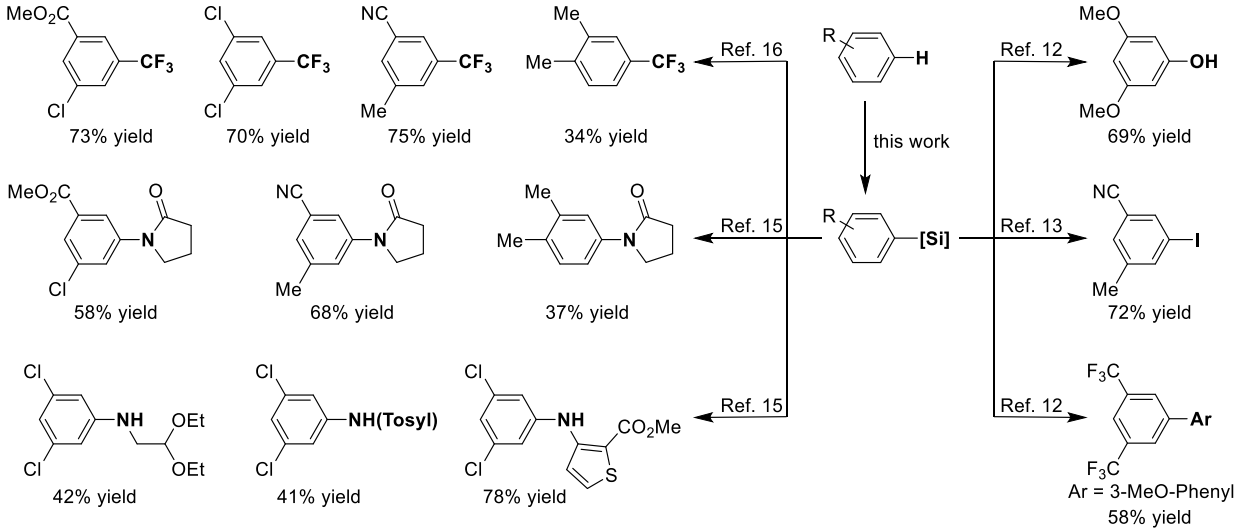

3.3 Functionalizations of Silylarenes

The transformations of the silyl group of these silylarenes into common functional groups is well documented and underscore the value of these silylation reactions (Scheme 3.2). Silylarene **21** has undergone cross-coupling reactions mediated by copper with a broad range of nitrogen nucleophiles including anilines, pyrroles, amides, sulfonamides and alkyl amines with yields of aniline products that range from 41% to 78%. The coupling of **4**, **15**, and **20** with amides has also been reported.[15] Tamao-Fleming oxidation of silylarene **9** has been reported to form 3,5-dimethoxyphenol in 69% yield.[12] Silylarene **15** also has been iodinated using ICl.[13] Silylarene **19** has been coupled with 3-iodoanisole in a reaction catalyzed by palladium to produce biaryl product in 58% yield.[12] Finally, **4**, **15**, **20**, and **21** have been converted into the corresponding trifluoromethyl arenes in 34% to 75% yield by reaction with (phenanthroline)$CuCF_3$ in the presence of fluoride activator.[16] Clearly, the silylarenes formed by the reactions reported here are versatile intermediates that can be transformed into aryl halides and phenols in good yields and coupled with haloarenes, amines, anilines and sources of trifluoromethyl groups in modest to good yields.[12-13, 15-16]

3.4 Synthesis of Pharmaceutical Intermediates

To demonstrate the applicability of the silylation of C-H bonds, we synthesized arenes and heteroarenes that are intermediates in synthesis of medicinally relevant molecules, as shown in Scheme 3.3. Doravirine is the active ingredient in Pifeltro and the combination tablet Delstrigo recently approved by the FDA for the treatment of HIV. 1,3,5-Substituted arenes **29** and **30** containing multiple ortho-para directing groups are intermediates in two different process-scale routes to doravirine.[17] Arenes with such substitution patterns are well suited to being prepared by the silylation of C-H bonds. A second medicinally relevant compound, Ozenoxacin, is an antibiotic discovered by Toyama Chemical Co., developed by Maruho Co,[18] and approved in Japan for the treatment of acne and skin infections. Heteroaryl bromide **31** is an intermediate in the synthesis of Ozenoxacin. Because electron-poor heteroarenes, such as **36**, do not undergo electrophilic aromatic bromination, C-H bond functionalization is well suited to the synthesis of this class of heteroarenes, *vide supra*. A third medicinally relevant compound, AR-C123196, was produced on multikilogram scale by AstraZeneca to furnish studies on its anti-inflammatory properties and as a treatment for asthma.[19] Hetero-biaryl **32** is an intermediate in the synthesis of AR-C123196 assembled by Pd-catalyzed coupling of a heteroaryl bromide and an arylboronic acid. The nucleophile and electrophile can be reversed when C-H bond silylation is used because the boronate for the coupling is generated from an aryl bromide. In contrast, the heteroaryl silane can

be used directly as nucleophile, whereas the corresponding heterarylboronic acid undergoes spontaneous proto-deboronation.

Scheme 3.3 Disconnections of Doravirine (top), Ozenoxacin (middle) and AR-C123196 (bottom)

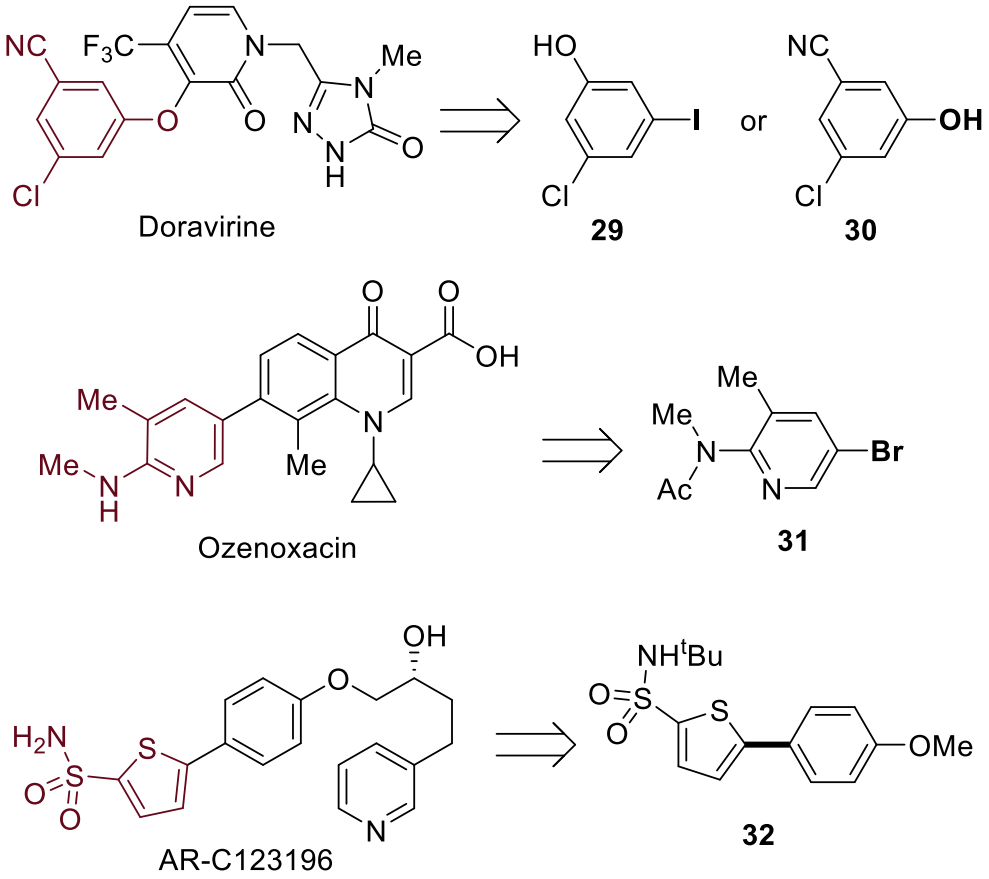

Three routes to related intermediates in the synthesis of doravirine are shown in Scheme 3.4. The first route, reported by Merck, starts from *m*-chloroiodobenzene and comprises the borylation of the C-H bond of the arene in the 5-position and oxidation to generate 1,3,5-chloroiodophenol. Aryl iodides are produced on a smaller scale than phenols, and the iodide in in this molecule is ultimately transformed into a nitrile. Thus, it might be preferable to start the synthesis from an arene that contains the nitrile or to install the iodide by C-H activation. However, the borylation of 3-chlorobenzonitrile generates a mixture of products, which result from monoborylation ortho and meta to the nitrile and from diborylation. An alternative synthesis by the borylation of a protected phenol, such as **34**, would form a single arylboronate, but iodination of arylboronic esters generally occurs in only modest yield.[20] In contrast, entry 7 of Table 3.2 above, shows that the silylation of 3-chlorobenzonitrile occurred with excellent selectivity for the meta position without formation of any product from disilylation. We found that silylarene **18** undergoes oxidation with hydrogen peroxide to generate phenol **30** in 55% yield from the arene over two steps. Alternatively, acyl-protected 3-chlorophenol, **34**, underwent silylation in high

yield. Iodination with ICl afforded iodoarene **35**, an acyl protected form on the intermediates in 89% isolated yield over two steps.

Scheme 3.4 Synthesis of Doravirine Intermediates[a]

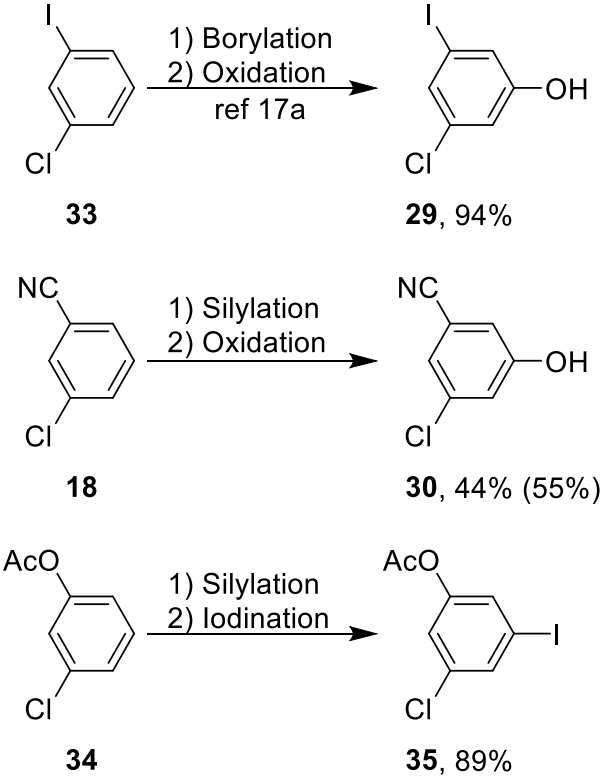

[a]Isolated yield is reported. Yield determined by ^{1}H NMR spectroscopy relative to CH_2Br_2 internal standard in parenthesis.

Heteroaryl bromide **31**, an intermediate in the synthesis of Ozenoxacin, was prepared in 68% yield by the combination of silylation of pyridine **36**, with the catalyst containing **L1**, followed by treatment with *N*-bromosuccinimide. (Scheme 3.5). Although direct bromination of **36** is challenging, the *ipso* bromination of the silylheteroarene occurs under mild conditions. Heterobiaryl **32**, an intermediate in AstraZeneca's anti-inflammatory for asthma AR-C123196, was prepared by silylation and coupling. Silylation of the thienyl sulfonamide **37** occurred in quantitative yield, and coupling of the resulting silylarene with 4-bromoanisole occurred in the presence of catalytic amounts of $Pd(P^tBu_3)_2$ to produce **32** in 82% yield. In contrast to the reported instability of 5-boryl analogues of **37**, the silylated heteroarene was stable to chromatography and storage on the bench top. These reaction sequences comprising silylation of a C-H bond and

functionalization at the C-Si bond demonstrate that the system we report here for the silylation of C-H bonds is useful for the synthesis of medicinally important compounds.

Scheme 3.5 Synthesis of Ozenoxacin Intermediate and AR-C123196 Intermediate[a]

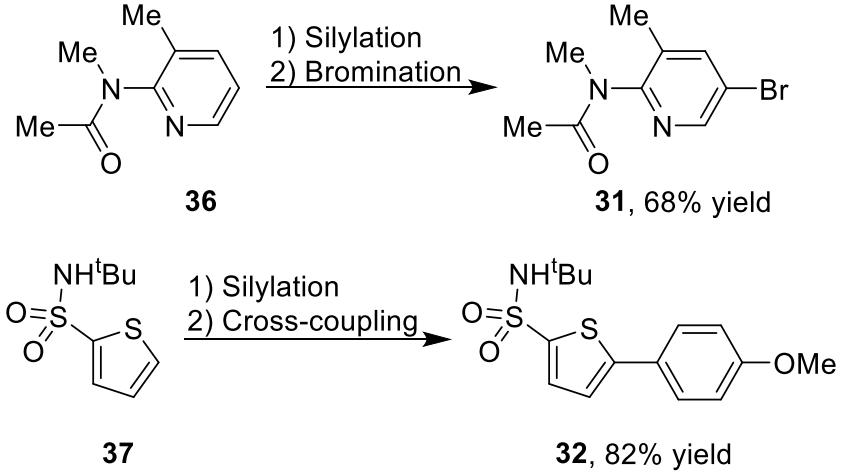

[a]Isolated yield is reported.

3.5 Mechanistic Studies

To gain information on the steps of the catalytic process influenced by the steric properties of the methyl-substituted phenanthrolines, we measured kinetic isotope effects for the silylation reactions of benzene and conducted studies on H/D exchange between the silane and benzene catalyzed by complexes of the series of phenanthrolines. To probe if C-H bond cleavage was rate-limiting, we first measured the kinetic isotope effect for reactions of benzene in separate vessels with catalysts containing 2,9-dimethyl, 2,4,7-trimethyl and 3,4,7,8-tetramethyl phenanthrolines (ligands **L1**, **L2**, and **L3**). The initial rates were determined by monitoring the silylarene product in the reactions catalyzed by the combination of $[Ir(COD)OMe]_2$ and ligand. As shown in Table 3.4, the kinetic isotope effects were 1.3, 1.6 and 2.0 for the silylation of benzene and deuterobenzene catalyzed by the combination of iridium and **L1**, **L2**, or **L3** respectively with silane is the limiting reagent. Similar kinetic isotope effects of 1.6 or 1.7 were measured for the silylation of benzene and deuterobenzene catalyzed by the combination of iridium and **L2**, or **L3** with arene

as the limiting reagent. These kinetic isotope effects are too small to be considered simple primary values and more likely indicate that cleavage of the C-H bond is fully or partially reversible.

Table 3.4 Kinetic Isotope Effects Determined from Independent Reactions[a]

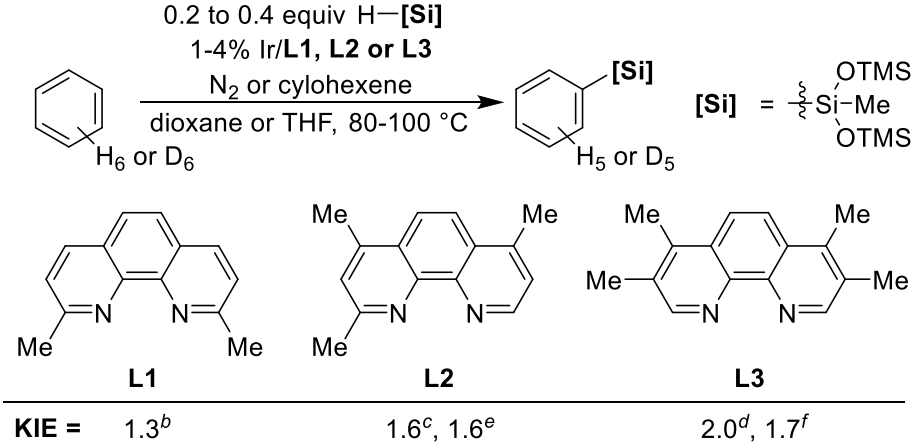

[a]Rates from reactions containing **L1** determined by GC-FID relative to dodecane internal standard. Rates from reactions containing **L2** and **L3** determined by ^{1}H NMR spectroscopy relative to dodecane internal standard. [b]Arene (7.5 equiv), $HSiMe(OTMS)_2$ (1 equiv). [c]Arene (5.6 equiv), $HSiMe(OTMS)_2$ (1 equiv). [d]Arene (17 equiv), $HSiMe(OTMS)_2$ (1 equiv). [e]Arene (1 equiv), $HSiMe(OTMS)_2$ (1.4 equiv), average of three experiments (KIE = 1.6±0.3). [f]Arene (1 equiv), $HSiMe(OTMS)_2$ (1.4 equiv).

To gain further information about the potential reversibility of the reaction, we studied H/D exchange between the Si-H bond of the silane and deuterated arene. These data are shown in Figure 3.3. H/D exchange between the silane and benzene-d_6 was evidenced by the growth of ^{1}H NMR signals of the arene. The rates at which the benzene-d_6 was transformed into benzene-d_5 under the catalytic reaction conditions with ligand **L1** and with ligand **L2** were measured. The incorporation of protons into deuterated benzene catalyzed by the combination of iridium and **L1** was nearly five times faster than that catalyzed by the combination of iridium and **L2**. These relative rates closely mirror the five-times greater rates for the silylation reaction catalyzed by the complex of **L1** than by the complex of **L2**.

Figure 3.3 Rate of Protiation of Deuterobenzene

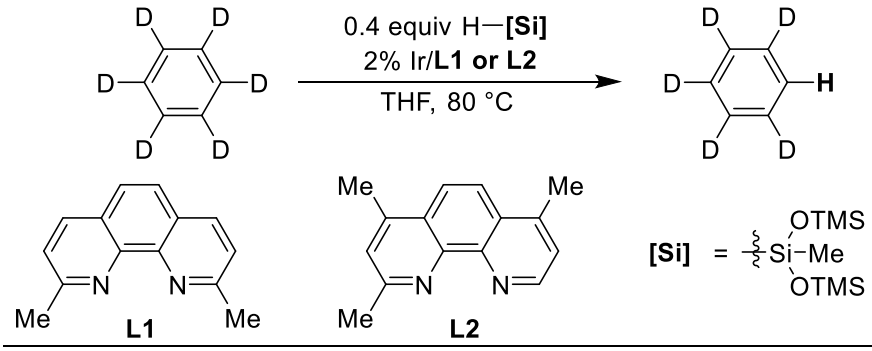

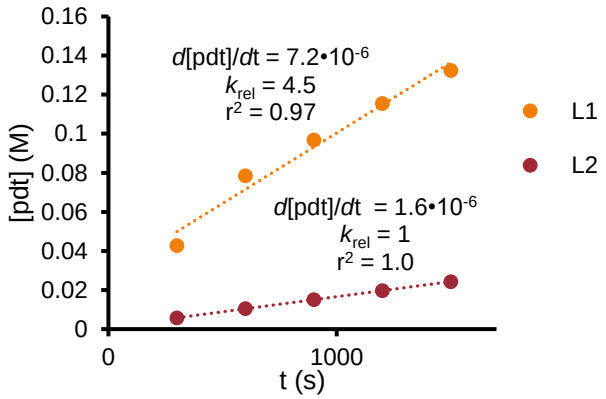

[a]Conditions: $HSiMe(OTMS)_2$ (0.4 mmol), $[Ir(cod)(OMe)]_2$ (1.0 mol %), ligand (2.0 mol %), dodecane (0.5 equiv), benzene-*d6* (100 µL), THF, 80 °C. Silylarene concentration was determined by ^1H NMR spectroscopy using *n*-dodecane as an internal standard.

The faster rate of the silylation catalyzed by the complex of **L1** versus that of the silylation catalyzed by the complex of **L2** could result from faster cleavage of the C-H bond, a more favorable equilibrium for cleavage of the C-H bond, or larger effect of the ligand on the formation of the C-Si bond than on the cleavage of the C-H bond. The small KIE value observed for reactions of benzene and the observation of H/D exchange between the silane and benzene imply that cleavage of the C-H bond in benzene is reversible. In this case, a difference in the equilibrium constant for cleavage of the C-H bond or a difference in the rate of formation of the C-Si bond could lead to the difference in rates of reaction catalyzed by complexes of **L1** and **L2.** The similarity between the difference in the rates of H/D exchange between the silane and benzene catalyzed by the two complexes and the difference in rates of the overall silylation of benzene catalyzed by the two complexes implies that the cleavage of the C-H bond is the step that leads to the difference in rates of reaction of the two catalysts. These conclusions can be shown in the reaction coordination diagram of Figure 3.4. In this diagram, the rate and equilibrium constant for

cleavage of the C-H bond in the arene is larger for the reaction of the complex of **L1** than of the complex of **L2**, as suggested by our mechanistic data.

Figure 3.4 Proposed Reaction Coordinate

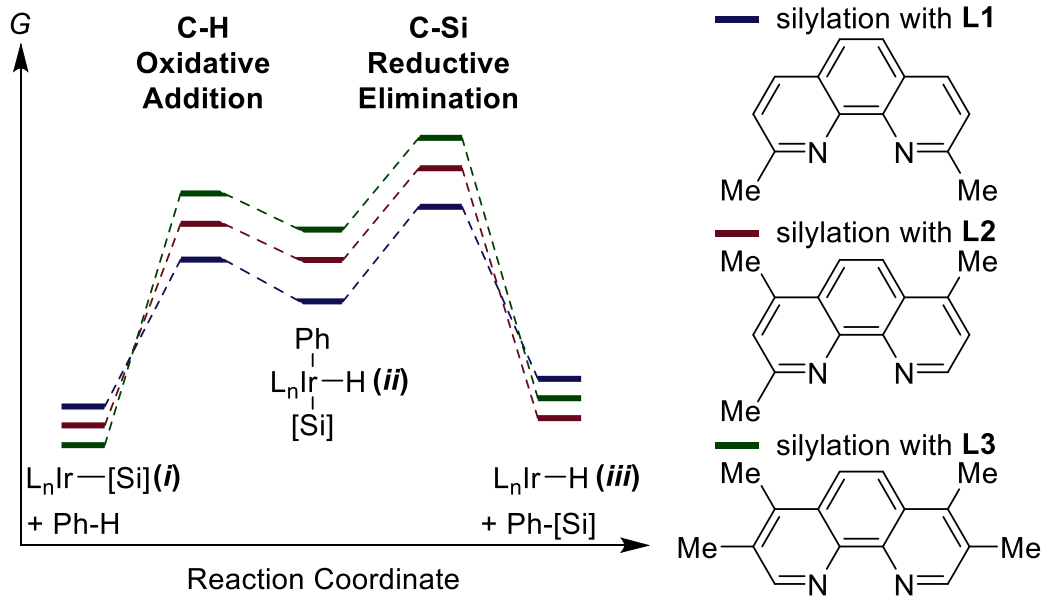

Faster and thermodynamically more favorable oxidative addition of a C-H bond to a more sterically hindered complex seems counterintuitive in a system that is unlikely to involve dissociation of the hindered ligand. We suggest that the seven-coordinate product from oxidative addition, counterintuitively, suffers less steric hindrance than the starting square pyramidal complex. As shown in Figure 3.5, seven coordinate complexes in a geometry like a capped trigonal prism likely contain fewer ligands in the plane of the substituted phenanthroline ligand. The five-coordinate square-based pyramidal geometry of a d^6 iridium-complex contains two ligands in the equatorial plane (shown as the plane of the page in Figure 3.5) in addition to the nitrogens of the phenanthroline, whereas the seven-coordinate complex contains just one additional ligand in the equatorial plane. This model implies that the destabilization of the resting state of the catalyst by the methyl groups of **L1** is greater than the destabilization of the intermediate following oxidative addition. This analysis is consistent with our assertion that the difference in energy between these

two species is responsible for the high rate of the silylation of aryl C-H bonds observed in reactions catalyzed by the iridium complexes containing the 2,9-dimethyl phenanthroline ligand.

Figure 3.5 Model for the Relief of Steric Upon Oxidative Addition of C-H Bonds

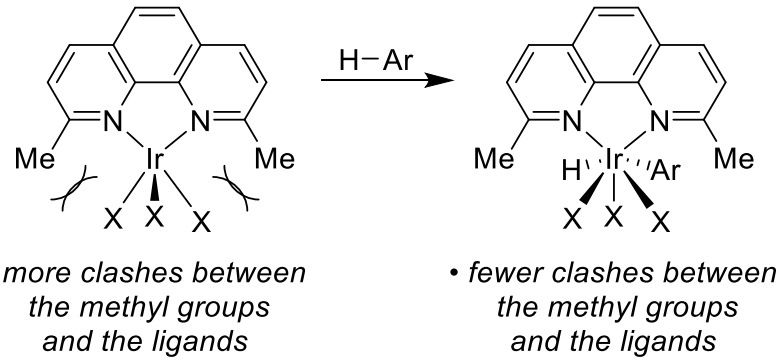

3.3 Conclusion

In summary, we report an iridium catalyst for the silylation of arenes with hydrosilanes revealed by measuring the difference between initial rates and overall conversion. These measurements distinguished between catalysts that react with low rates and those that react with high rates but are short-lived. By determining the origin of inhibition of a catalyst that reacts with high initial rates, we have developed the combination of a highly active catalyst and appropriate reaction conditions to achieve a large increase in scope of the silylation of arenes and large increase in rates for arenes that reacted with catalysts reported previously. The new system tolerates most common functional groups, and the reactions occur with high sterically derived regioselectivity. The products of these reactions can be transformed into many common functional groups, and the utility of this method was demonstrated by constructing intermediates in the syntheses of medicinally important molecules. This method significantly increases the utility of C-H silylation by allowing reactions to be conducted on convenient timescales under mild conditions and with inexpensive reagents.

Studies on isotopically labeled arenes showed that the cleavage of the C-H bond is reversible. The relative rates of H/D exchange catalyzed by complexes of 2,9-dimethylphenanthroline and 2,4,7-trimethylphenanthroline mirrored those of the initial rates of the silylation. These data imply that the difference in activity observed for reactions of arenes and silane with the two catalysts results from a difference in the equilibrium constant for addition of the arene to the two catalysts. More favorable oxidative addition of the arene to the complex of the more hindered ligand is counterintuitive, but likely results from the difference in geometry of a five-coordinate square-planar d^6 complex and a seven-coordinate intermediate that would contain fewer ligands in the plane of the phenanthroline ligand. Further experimental mechanistic studies to prepare potential intermediates and detailed computational studies on the reactivity of these intermediates to gain further insight into the mechanism and to create even more active catalysts are in progress.

3.4 Experimental

Materials and Methods

All silylation reactions were assembled in an N_2-filled glovebox using oven-dried glassware. $[Ir(cod)OMe]_2$ was obtained as a gift from Johnson Matthey and was used as received. 3,4,7,8-Tetramethyl-1,10-phenanthroline (Me_4phen, **L3**) was purchased from Aldrich and was used as received. 2,9-dimethyl-1,10-phenanthroline (**L1**) was purchased from Alfa Aesar and used as received. 2,4,7-trimethyl-1,10-phenanthroline (**L1**) and 2,3,4,7,8,9-hexamethyl-1,10-phenanthroline were synthesized by reported procedures.[13, 21] 1,1,1,3,5,5,5-heptamethyl-trisiloxane was purchased from TCI and was used as received. Norbornene (nbe) and cyclohexene were purchased from Aldrich and were used as received. Diethyl ether and tetrahydrofuran (THF) were degassed by purging with nitrogen and then dried with a solvent purification system containing activated alumina. All other solvents and reagents were used as received. Reaction temperatures above 23 °C refer to temperatures of an aluminum heating block, which were controlled by an electronic temperature modulator. NMR spectra were recorded on Bruker AV-300, AVQ-400, AVB-400, AV-500, DRX-500 and AV-600 instruments. Chemical shifts (δ) are reported in ppm relative to the residual solvent signal. Data from ^1H NMR spectra are reported as follows: chemical shift (multiplicity, coupling constants, number of hydrogens). Abbreviations are as follows: s (singlet), d (doublet), t (triplet), q (quartet), m (multiplet), br (broad). GC-MS data were obtained on an Agilent 6890-N GC system containing an Alltech EC-1 capillary column and an Agilent 5973 mass selective detector. High-resolution mass spectral data were obtained from the University of California, Berkeley Mass Spectrometry Laboratory.

General procedure for the synthesis of substrates

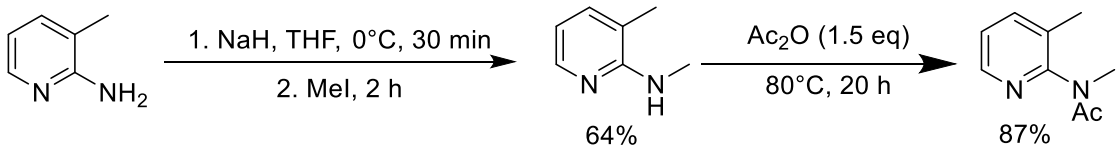

***N*,3-dimethylpyridin-2-amine:** 1.06 g (9.80 mmol) of 3-methyl-2-aminopyridine was added to an oven-dried three-necked round-bottom flask fitted with a magnetic stir-bar. The flask was sealed with three rubber septa, evacuated, and back-filled with N_2. One of the septa was fitted with a N_2 line, and 25 mL of dry THF were added via syringe. The flask was cooled to 0 ℃, and 0.330 g of NaH (13.8 mmol, 1.4 equiv) was added portionwise to the stirring solution. The solution was stirred at room temperature for 30 minutes before it was cooled to 0℃. MeI (600 μL) was then added dropwise via a syringe. The reaction was warmed to room temperature and stirred for 1 hour before quenching by 5 mL saturated NaCl solution and 5 mL of ethyl acetate. The organic layer was transferred to a separate flask, and the aqueous layer was extracted an additional three times with ethyl acetate. The combined organic layers were washed with brine, dried with Na_2SO_4, and concentrated. The residue was purified by flash column chromatography on silica (15 % ethyl acetate in hexanes) to give the title compound as a solid (772 mg, 6.32 mmol, 64% yield). ^{1}H NMR (600 MHz, chloroform-*d*) δ 7.98 (dt, *J* = 5.0, 2.3 Hz, 1H), 7.13 – 7.08 (m, 1H), 6.43 (dd, *J* = 7.2, 4.9 Hz, 1H), 4.23 (bs, 1H), 2.95 (d, *J* = 5.0 Hz, 3H), 1.97 (s, 3H). ^{13}C NMR (151 MHz, chloroform-*d*) δ 157.5, 145.3, 136.4, 116.6, 112.2, 28.6, 16.8. These NMR data matched those reported in the literature.[22]

***N*-methyl-*N*-(3-methylpyridin-2-yl)acetamide:** 420 μL of acetic anhydride (4.4 mmol) and 484 mg of N,3-dimehtylpyridin-2-amine (3.96 mmol) was added to a 20 mL vial equipped with a magnetic stir bar. The mixture was stirred at 80 ℃ for 20 hours. The vial was cooled to room temperature, and the mixture was neutralized with saturated aqueous $NaHCO_3$ and extracted with DCM three times. The combined organic layers were dried with Na_2SO_4 and concentrated. The residue was purified by flash column chromatography on basic alumina to give the title compound as a pale-yellow solid (570 mg, 3.47 mmol, 87% yield). Major rotamer: ^{1}H NMR (500 MHz, chloroform-*d*) δ 8.33 (dd, *J* = 4.8, 1.8 Hz, 1H), 7.62 (dd, *J* = 7.6, 1.8 Hz, 1H), 7.20 (dd, *J* = 7.6, 4.7 Hz, 1H), 3.14 (s, 3H), 2.22 (s, 3H), 1.72 (s, 3H). ^{13}C NMR (126 MHz, chloroform-*d*) δ 170.7, 155.6, 147.9, 140.8, 130.8, 124.2, 34.6, 22.4, 17.5. These NMR data matched those reported in the literature.[23]

Measurement of rate of silylation with a series of iridium catalysts

In an N_2-filled glovebox, $[Ir(cod)OMe]_2$ (6.6 mg, 0.010 mmol), 2,3-dimethyl-2-butene (84 mg, 1.0 mmol), benzene (78 mg, 1.0 mmol), dodecane (170 mg, 1.0 mmol), and 1,1,1,3,5,5,5-heptamethyl-trisiloxane (334 mg, 1.50 mmol) were weighed into a 4 mL vial. The solution was transferred to a 1 mL volumetric flask, the vial was washed with THF, and the washings were transferred to the flask. The solution was diluted to 1 mL total volume with THF, and the flask was capped and shaken. **L1** (2.1 mg, 0.01 mmol) **L2** (2.2 mg, 0.010 mmol), **L3** (2.4 mg, 0.010 mmol) or **L4** (2.6 mg, 0.010 mmol) were weighed into separate 4 mL vials. 200 μL (800 μL total) of stock solution was added to each of the four vials. The vials were capped and removed from the glovebox and placed in an aluminum block that had been preheated to 80 °C. At the specified times, the vials were removed from the heating block and brought into the glovebox. 5 μL of solution was removed from each vial and analyzed by GC-FID. The vials were then removed from the glovebox and placed in the preheated aluminum block. The rates of the reactions were determined by the method of initial rates with dodecane as the internal standard.

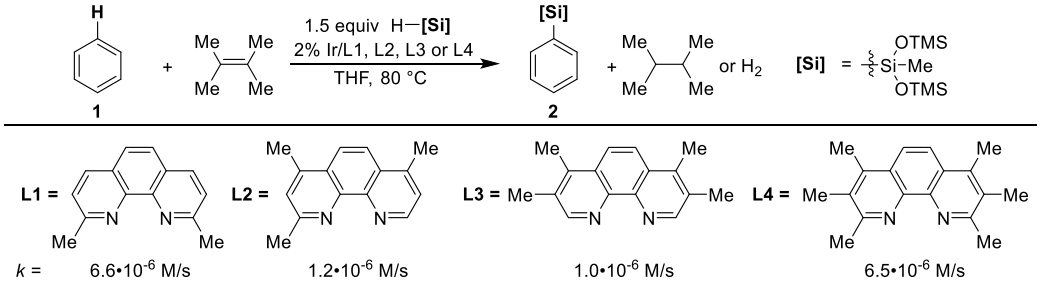

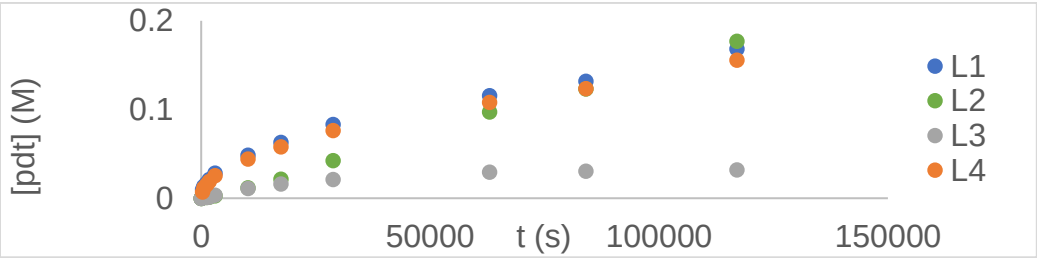

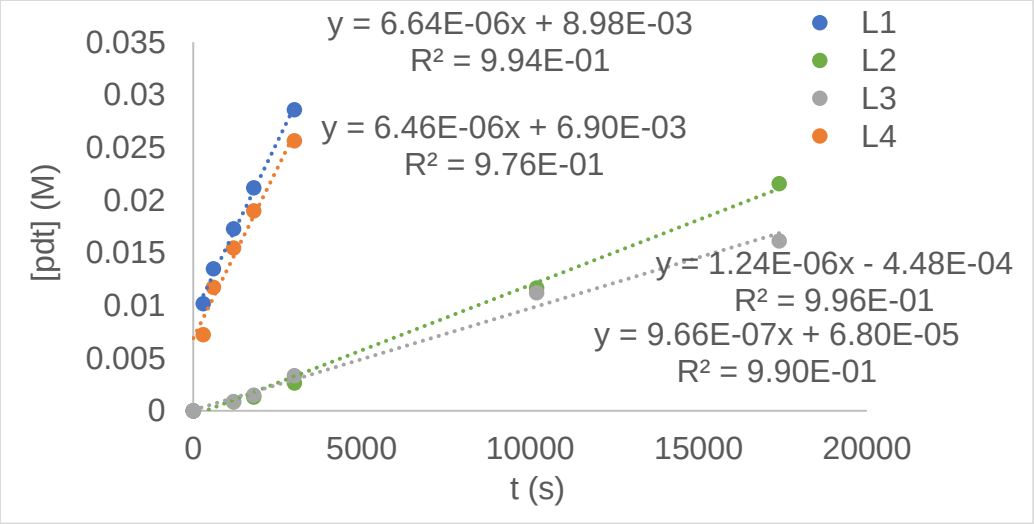

Measurement of rate of silylation under an atmosphere of hydrogen or nitrogen

In an N_2-filled glovebox, $[Ir(cod)OMe]_2$ (6.6 mg, 0.010 mmol), **L1** (4.2 mg, 0.020 mmol), benzene (78 mg, 1.0 mmol), dodecane (170 mg, 1.0 mmol), and 1,1,1,3,5,5,5-heptamethyl-trisiloxane (334 mg, 1.50 mmol) were weighed into a 4 mL vial. After 20 minutes, the solution was transferred to a 1 mL volumetric flask, the vial was washed with THF, and the washings were transferred to the flask. The solution was diluted to 1 mL total volume with THF, and the flask was capped and shaken. 0.45 mL of the solution was then transferred to separate J-Young NMR tubes twice. The tubes were then capped and removed from the glovebox. The solution in one of the two J-Young tubes was frozen in a bath of liquid nitrogen and the headspace of the tube was evacuated under high vacuum. The headspace was then refilled with hydrogen gas (1 atm). The J-Young NMR tubes were place in an aluminum block that had been preheated to 80 °C. The tubes were removed from the heating block at the specified times and analyzed by ^1H NMR spectroscopy. The rates of the reactions were determined by the method of initial rates, with dodecane as the internal standard.

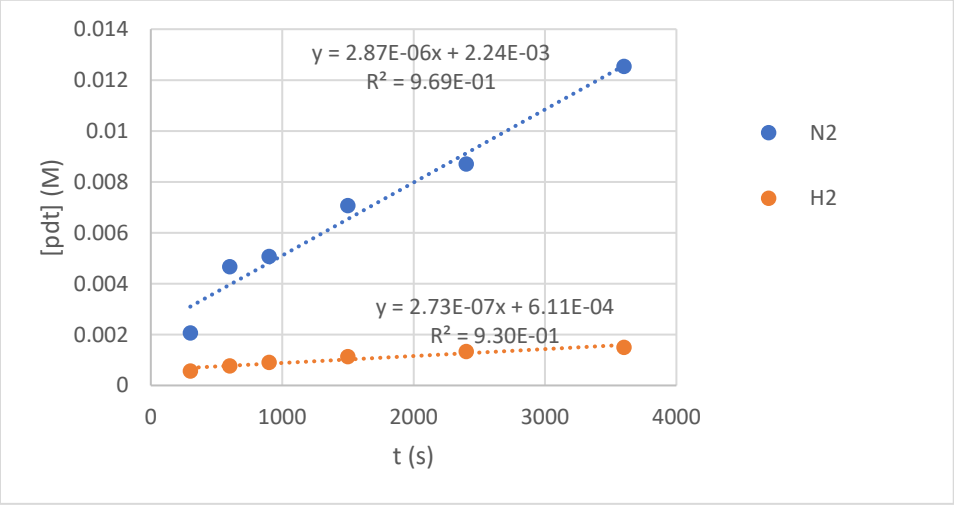

Measurement of rate of silylation with a series of hydrogen acceptors

In an N_2-filled glovebox, $[Ir(cod)OMe]_2$ (6.6 mg, 0.010 mmol), **L1** (4.2 mg, 0.020 mmol), benzene (78 mg, 1.0 mmol), dodecane (170 mg, 1.0 mmol), and 1,1,1,3,5,5,5-heptamethyltrisiloxane (334 mg, 1.50 mmol) were weighed into a 4 mL vial. After 20 minutes, the solution was transferred to a 1 mL volumetric flask, the vial was washed with THF, and the washings were transferred to the flask. The solution was diluted to 1 mL total volume with THF, and the flask was capped and shaken. THF (36 mg) 2,3-dimethyl-2-butene (42 mg, 0.50 mmol), cyclohexene (41 mg, 0.50 mmol), nbe (47 mg, 0.50 mmol) were weighed into separate 4 mL vials. 200 µL (800 µL total) of stock solution was added to each of the four vials. The vials were capped and removed from the glovebox and placed in an aluminum block that had been preheated to 80 °C. At the specified times, the vials were removed from the heating block and brought into the glovebox. 5 µL of solution was removed from each vial and analyzed by GC-FID. The vials were then removed from the glovebox and placed in the preheated aluminum block. The rates of the reactions were determined by the method of initial rates with dodecane as the internal standard.

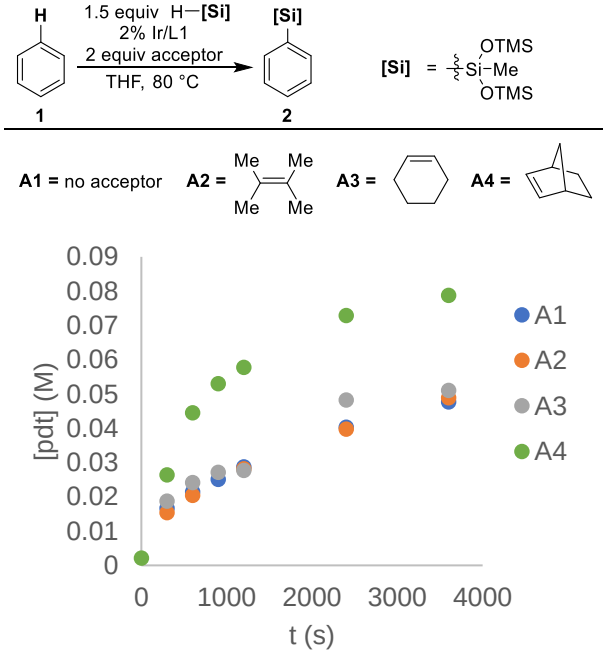

Procedure A for the Ir-catalyzed silylation of arenes:

In a N_2-filled glovebox, 0.5 mmol of the arene was weighed into a 4 mL vial. To a separate vial, $[Ir(cod)OMe]_2$ (3.3 mg, 5.0 μmol, 1.0 mol%), ligand (10 μmol, 2.0 mol%), 1,1,1,3,5,5,5-heptamethyl-trisiloxane (167 mg, 0.750 mmol, 1.50 equivalents) and dioxane (200 μL) were added. The vial was capped with a Teflon-lined screw cap and kept in the glovebox at room temperature for 20-30 minutes. The contents of the second vial were then added to the contents of the first vial. The combined solution was transferred to a set of reaction vessels in a Radley Carousel, and the vessels were sealed with the accompanying cap. The sealed vessel was removed from the glovebox and placed in a preheated Radley Carousel. The top aluminum block of the Radley Carousel was cooled with circulating ice water. A nitrogen line was affixed to the reaction vessel, and the reaction vessel was fitted with a rubber septum. The vessel was then fitted with a 21-gauge needle through the rubber septum. After the indicated length of time, the reaction vessel was removed from the Radley Carousel, and the reaction was quenched with ~1 mL of MeOH, and the crude solution was purified through silica-gel chromatography or a solution of dibromomethane in $CDCl_3$ was added as an internal standard and the yield was determined by ^1H NMR spectroscopy.

Procedure B for the Ir-catalyzed silylation of arenes:

In an N_2-filled glovebox, 0.1 mmol of the arene was weighed into a 4 mL vial. To a separate vial, $[Ir(cod)OMe]_2$ (0.7 mg, 1 μmol, 1 mol%), ligand (4 μmol, 4 mol%), 1,1,1,3,5,5,5-heptamethyl-trisiloxane (33 mg, 0.15 mmol, 1.5 equivalents), cyclohexene (12 mg, 0.15, 1.5 equivalents) and THF (100 μL) were added. The vial was capped with a Teflon-lined screw cap and kept in the glovebox at room temperature for 20-30 minutes. The contents of the second vial were then added to the contents of the first vial. The vial was capped with a Teflon-lined screw-cap, removed from the glovebox and placed in a pre-heated aluminum block. After the indicated amount of time, the vial was removed from the heating block and cooled. Subsequently, a solution of dibromomethane in $CDCl_3$ was added and the yield was determined by ^1H NMR spectroscopy.

Procedure C for the Ir-catalyzed silylation of arenes:

In an N_2-filled glovebox, 0.25 mmol of the arene was weighed into a 4 mL vial. To a separate vial, $[Ir(cod)OMe]_2$ (1.7 mg, 2.5 μmol, 1.0 mol%), 2,9-dimethyl-1,10-phenanthroline (1.0 mg, 5.0 μmol, 2.0 mol%), 1,1,1,3,5,5,5-heptamethyl-trisiloxane (85 mg, 0.38 mmol, 1.5 equivalents), nbe (24 mg, 0.25 mmol, 1.0 equivalent) and THF (100 μL) were added. The vial was capped with a Teflon-lined screw cap and kept in the glovebox at room temperature for 20-30 minutes. The contents of the second vial were then added to the contents of the first vial. The vial was capped with a Teflon-lined screw-cap, removed from the glovebox and placed in a pre-heated aluminum block. After the indicated amount of time, the vial was removed from the heating block and cooled. Subsequently, a solution of dibromomethane in $CDCl_3$ was added and the yield was determined by ^1H NMR spectroscopy.

Silylation of m-xylene

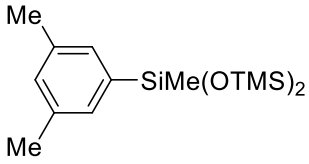

3

Procedure A was followed for the reaction of m-xylene (52 mg, 0.49 mmol). The reaction was conducted with ligand **L1** (2.1 mg, 10 μmol, 2.0 mol%) at 100 ℃ for 20 hours. The crude reaction mixture was purified by silica-gel chromatography to afford the product as a colorless liquid (145 mg, 91% yield). ^{1}H NMR (600 MHz, chloroform-*d*) δ 7.20 (d, *J* = 1.7 Hz, 2H), 7.06 – 7.05 (m, 1H), 2.36 (s, 6H), 0.30 (s, 3H), 0.16 (s, 18H). ^{13}C NMR (151 MHz, chloroform-*d*) δ 138.2, 136.7, 131.1, 131.0, 21.4, 1.9, 0.2. HRMS (EI), calculated for [$C_{15}H_{30}O_2Si_3$]: 326.1554, found: 326.1559.

Procedure A was followed for the reaction of m-xylene (53 mg, 0.50 mmol). The reaction was conducted with ligand **L2** (2.2 mg, 10 μmol, 2 mol%) at 100 ℃ for 20 hours. The NMR yield was determined to be 21% with dibromomethane internal standard.

Procedure A was followed for the reaction of m-xylene (53 mg, 0.50 mmol). The reaction was conducted with ligand **L3** (2.4 mg, 10 μmol, 2 mol%) at 100 ℃ for 20 hours. The NMR yield was determined to be <1% with dibromomethane internal standard.

Silylation of o-xylene

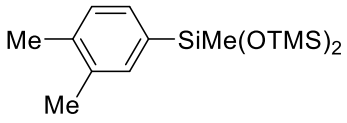

4

Procedure A was followed for the reaction of o-xylene (49 mg, 0.46 mmol). The reaction was conducted with ligand **L1** (2.1 mg, 10 μmol, 2.0 mol%) at 100 ℃ for 18 hours. The crude reaction mixture was purified by silica-gel chromatography to afford the product as a colorless liquid (116 mg, 77% yield). ^{1}H NMR (600 MHz, chloroform-*d*) δ 7.36 (s, 1H), 7.34 (d, *J* = 7.5 Hz, 1H), 7.17 (d, *J* = 7.3 Hz, 1H), 2.32 (s, 3H), 2.31 (s, 3H), 0.29 (s, 3H), 0.16 (s, 18H). ^{13}C NMR (151 MHz, chloroform-*d*) δ 137.9, 135.6, 135.5, 134.6, 130.9, 129.0, 19.8, 19.7, 1.9, 0.2. HRMS (EI), calculated for [$C_{15}H_{30}O_2Si_3$]: 326.1554, found: 326.1555.

Procedure A was followed for the reaction of o-xylene (53 mg, 0.50 mmol). The reaction was conducted with ligand **L2** (2.2 mg, 10 μmol, 2 mol%) at 100 ℃ for 20 hours. The NMR yield was determined to be 16% with dibromomethane internal standard.

Procedure A was followed for the reaction of o-xylene (53 mg, 0.50 mmol). The reaction was conducted with ligand **L3** (2.4 mg, 10 μmol, 2 mol%) at 100 ℃ for 20 hours. The NMR yield was determined to be <1% with dibromomethane internal standard.

Silylation of 1,3-^{t}Bu$_2$-benzene

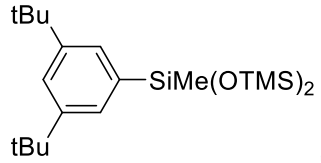

5

Procedure A was followed for the reaction of 1,3-^{t}Bu$_2$-benzene (119 mg, 0.63 mmol). The reaction was conducted with ligand **L1** (2.1 mg, 10 μmol, 2.0 mol%) at 100 °C for 20 hours. The crude reaction mixture was purified by silica-gel chromatography to afford the product as a colorless liquid (197 mg, 76% yield). ^{1}H NMR (500 MHz, chloroform-*d*) δ 7.50 (s, 1H), 7.48 (s, 2H), 1.39 (s, 18H), 0.32 (s, 3H), 0.17 (s, 18H). ^{13}C NMR (126 MHz, chloroform-*d*) δ 149.4, 137.3, 127.3, 123.5, 34.9, 31.6, 2.0, 0.40. HRMS (EI), calculated for [$C_{21}H_{42}O_2Si_3$]: 410.2493, found: 410.2491.

Procedure A was followed for the reaction of 1,3-^{t}Bu$_2$-benzene (94 mg, 0.49 mmol). The reaction was conducted with ligand **L2** (2.2 mg, 10 μmol, 2 mol%) at 100 °C for 20 hours. The NMR yield was determined to be 5% with dibromomethane internal standard.

Procedure A was followed for the reaction of 1,3-^{t}Bu$_2$-benzene (95 mg, 0.50 mmol). The reaction was conducted with ligand **L3** (2.4 mg, 10 μmol, 2 mol%) ligand at 100 °C for 20 hours. The NMR yield was determined to be <1% with dibromomethane internal standard.

Silylation of indane

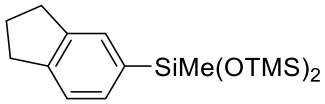

6

Procedure A was followed for the reaction of indane (58 mg, 0.49 mmol. The reaction was conducted with ligand **L1** (2.1 mg, 10 μmol, 2.0 mol%) at 100 °C for 22 hours. The crude reaction mixture was purified by silica-gel chromatography to afford the product as a colorless liquid (157 mg, 94% yield). ^{1}H NMR (500 MHz, chloroform-*d*) δ 7.53 (s, 1H), 7.45 (d, *J* = 7.4 Hz, 1H), 7.33 (d, *J* = 7.3 Hz, 1H), 3.02 (td, *J* = 7.4, 3.3 Hz, 4H), 2.16 (p, *J* = 7.4 Hz, 2H), 0.37 (s, 3H), 0.22 (s, 18H). ^{13}C NMR (126 MHz, chloroform-*d*) δ 145.7, 143.4, 135.9, 131.2, 129.3, 123.9, 33.0, 32.8, 25.2, 2.0, 0.40. HRMS (EI), calculated for [$C_{16}H_{30}O_2Si_3$]: 338.1554, found: 338.1555.

Procedure A was followed for the reaction of indane (60 mg, 0.51 mmol). The reaction was conducted with ligand **L2** (2.2 mg, 10 μmol, 2 mol%) at 100 °C for 20 hours. The NMR yield was determined to be 34% with dibromomethane internal standard.

Procedure A was followed for the reaction of indane (57 mg, 0.48 mmol). The reaction was conducted with ligand **L3** (2.4 mg, 10 μmol, 2 mol%) at 100 °C for 20 hours. The NMR yield was determined to be <1% with dibromomethane internal standard.

Silylation of N,N,3-trimethyl-benzene

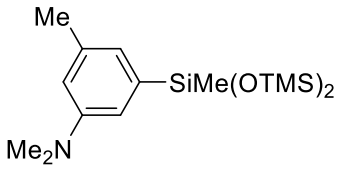

7

Procedure A was followed for the reaction of N,N,3-trimethyl-benzene (65 mg, 0.48 mmol). The reaction was conducted with ligand **L1** (2.1 mg, 10 μmol, 2.0 mol%) at 100 ℃ for 20 hours. The crude reaction mixture was purified by silica-gel chromatography to afford the product as a colorless liquid (131 mg, 66% yield). ^{1}H NMR (500 MHz, chloroform-*d*) δ 6.81 (s, 1H), 6.77 (s, 1H), 6.63 (s, 1H), 2.96 (s, 6H), 2.35 (s, 3H), 0.27 (s, 3H), 0.14 (s, 18H). ^{13}C NMR (126 MHz, chloroform-*d*) δ 150.0, 138.8, 137.8, 122.8, 114.9, 114.8, 40.8, 21.9, 2.0, 0.3. HRMS (ESI+), calculated for $[C_{16}H_{34}O_2NSi_3]^+$: 356.1897, found: 356.1893.

Procedure A was followed for the reaction of N,N,3-trimethyl-benzene (68 mg, 0.50 mmol). The reaction was conducted with ligand **L2** (2.2 mg, 10 μmol, 2 mol%) at 100 ℃ for 20 hours. The NMR yield was determined to be 22% with dibromomethane internal standard.

Procedure A was followed for the reaction of N,N,3-trimethyl-benzene (68 mg, 0.50 mmol). The reaction was conducted with ligand **L3** (2.4 mg, 10 μmol, 2 mol%) at 100 ℃ for 20 hours. The NMR yield was determined to be <1% with dibromomethane internal standard.

Silylation of 1-methoxy-2,6-dimethylbenzene

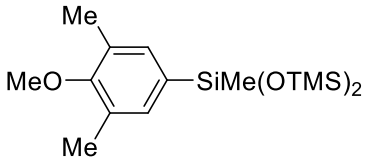

8

Procedure A was followed for the reaction of 1-methoxy-2,6-dimethylbenzene (66 mg, 0.48 mmol). The reaction was conducted with ligand **L1** (2.1 mg, 10 μmol, 2.0 mol%) at 100 ℃ for 20 hours. The crude reaction mixture was purified by silica-gel chromatography to afford the product as a colorless liquid (143 mg, 83% yield). ^{1}H NMR (600 MHz, chloroform-*d*) δ 7.20 (s, 2H), 3.74 (s, 3H), 2.30 (s, 6H), 0.25 (s, 3H), 0.13 (s, 18H). ^{13}C NMR (151 MHz, chloroform-*d*) δ 158.2, 134.1, 133.6, 129.8, 59.5, 16.1, 1.9, 0.2. HRMS (EI), calculated for $[C_{16}H_{32}O_3Si_3]$: 356.1659, found: 356.1662.

Procedure A was followed for the reaction of 1-methoxy-2,6-dimethylbenzene (68 mg, 0.50 mmol). The reaction was conducted with ligand **L2** (2.2 mg, 10 μmol, 2 mol%) ligand at 100 ℃ for 20 hours. The NMR yield was determined to be 9% with dibromomethane internal standard.

Procedure A was followed for the reaction of 1-methoxy-2,6-dimethylbenzene (69 mg, 0.51 mmol). The reaction was conducted with ligand **L3** (2.4 mg, 10 μmol, 2 mol%) at 100 ℃ for 20 hours. The NMR yield was determined to be <1% with dibromomethane internal standard.

Silylation of 1,3-dimethoxybenzene

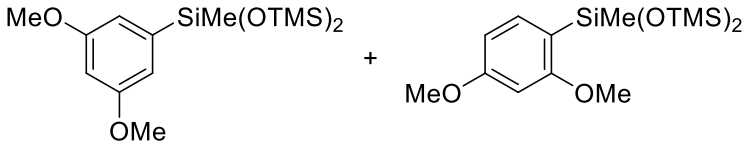

9

Procedure A was followed for the reaction of 1,3-dimethoxybenzene (69 mg, 0.50 mmol). The reaction was conducted with ligand **L1** (2.1 mg, 10 μmol, 2.0 mol%) at 80 ℃ for 24 hours. The crude reaction mixture was purified by silica-gel chromatography to afford the product as a colorless liquid (133 mg, 74% yield). Ratio of regioisomers (m:o) was determined by GC analysis to be 15:1. ^{1}H NMR (500 MHz, chloroform-*d*) δ 6.74 (d, *J* = 2.4 Hz, 2H), 6.52 (t, *J* = 2.4 Hz, 1H), 3.84 (s, 6H), 0.29 (s, 3H), 0.16 (s, 18H). ^{13}C NMR (126 MHz, chloroform-*d*) δ 160.3, 140.8, 110.6, 101.6, 55.2, 1.9, 0.0. HRMS (APCI-MS), calculated for [$C_{15}H_{30}O_4Si_3$]: 359.1530, found: 359.1526.

Procedure A was followed for the reaction of 1,3-dimethoxybenzene (69 mg, 0.50 mmol). The reaction was conducted with ligand **L2** (2.2 mg, 10 μmol, 2 mol%) at 100 ℃ for 20 hours. The NMR yield was determined to be 13% with dibromomethane internal standard.

Procedure A was followed for the reaction of 1,3-dimethoxybenzene (69 mg, 0.50 mmol). The reaction was conducted with ligand **L3** (2.4 mg, 10 μmol, 2 mol%) at 100 ℃ for 20 hours. The NMR yield was determined to be <1% with dibromomethane internal standard.

Silylation of 1,2,3-trimethoxybenzene

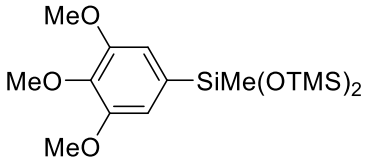

10

Procedure A was followed for the reaction of 1,2,3-trimethoxybenzene (96 mg, 0.57 mmol). The reaction was conducted with ligand **L1** (2.1 mg, 10 μmol, 2.0 mol%) at 100 ℃ for 22 hours. The crude reaction mixture was purified by silica-gel chromatography to afford the product as a colorless liquid (187 mg, 84% yield). ^{1}H NMR (400 MHz, chloroform-*d*) δ 6.76 (s, 2H), 3.88 (s, 6H), 3.86 (s, 3H), 0.26 (s, 3H), 0.13 (s, 18H). ^{13}C NMR (101 MHz, chloroform-*d*) δ 152.8, 133.6, 109.8, 60.8, 56.0, 1.9, 0.2. HRMS (ESI+), calculated for [$C_{16}H_{33}O_5Si_3$]$^{+}$: 389.1636, found: 389.1649.

Procedure A was followed for the reaction of 1,2,3-trimethoxybenzene (82 mg, 0.49 mmol). The reaction was conducted with ligand **L2** (2.2 mg, 10 μmol, 2 mol%) ligand at 100 ℃ for 20 hours. The NMR yield was determined to be 15% with dibromomethane internal standard.

Procedure A was followed for the reaction of 1,2,3-trimethoxybenzene (84 mg, 0.50 mmol). The reaction was conducted with ligand **L3** (2.4 mg, 10 μmol, 2 mol%) at 100 ℃ for 20 hours. The NMR yield was determined to be <1% with dibromomethane internal standard.

Silylation of 3,4-dimethoxy-toluene

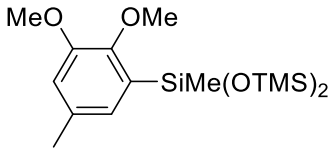

11

Procedure A was followed for the reaction of 1,2,3-trimethoxybenzene (38 mg, 0.25 mmol). The reaction was conducted with ligand **L1** (2.1 mg, 10 μmol, 4 mol%) at 100 ℃ for 24 hours. The NMR yield was determined to be 4% with dibromomethane internal standard.

Silylation of 1-bromo-3-tert-butylbenzene

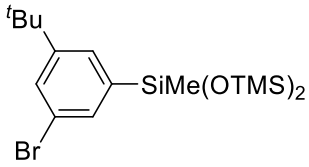

12

Procedure A was followed for the reaction of 1-bromo-3-tert-butylbenzene (106 mg, 0.50 mmol). The reaction was conducted with ligand **L1** (2.1 mg, 10 μmol, 2.0 mol%) at 100 ℃ for 20 hours. The crude reaction mixture was purified by silica-gel chromatography to afford the product as a colorless liquid (122 mg, 56% yield). ^{1}H NMR (400 MHz, chloroform-*d*) δ 7.54 (t, *J* = 1.9 Hz, 1H), 7.52 (dd, *J* = 1.9, 0.9 Hz, 1H), 7.48 (dd, *J* = 2.0, 0.9 Hz, 1H), 1.34 (s, 9H), 0.29 (s, 3H), 0.14 (s, 18H). ^{13}C NMR (101 MHz, chloroform-*d*) δ 152.7, 141.0, 133.1, 129.6, 128.6, 122.6, 34.9, 31.3, 1.9, 0.0. HRMS(EI), calculated for [$C_{17}H_{33}O_2Si_3Br$]: 432.0972, found: 432.0973.

Procedure B was followed for the reaction of 1-bromo-3-tert-butylbenzene (21 mg, 0.10 mmol). The reaction was conducted with ligand **L2** (1 mg, 4 μmol, 4 mol%) at 100 ℃ for 20 hours. The NMR yield was determined to be 46% with dibromomethane internal standard.

Procedure B was followed for the reaction of 1-bromo-3-tert-butylbenzene (21 mg, 0.10 mmol). The reaction was conducted with ligand **L3** (1 mg, 4 μmol, 4 mol%) at 100 ℃ for 20 hours. The NMR yield was determined to be 34% with dibromomethane internal standard.

Silylation of ethyl 2,6-dimethylbenzoate

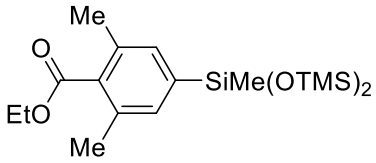

13

Procedure A was followed for the reaction of ethyl 2,6-dimethylbenzoate (88 mg, 0.49 mmol). The reaction was conducted with ligand **L1** (2.1 mg, 10 μmol, 2.0 mol%) at 100 ℃ for 20 hours. The crude reaction mixture was purified by silica-gel chromatography to afford the product as a colorless liquid (186 mg, 94% yield). ^{1}H NMR (400 MHz, chloroform-*d*) δ 7.21 (s, 2H), 4.41 (q, *J* = 7.1 Hz, 2H), 2.34 (s, 6H), 1.40 (t, *J* = 7.1 Hz, 3H), 0.25 (s, 3H), 0.13 (s, 18H). ^{13}C NMR (101 MHz, chloroform-*d*) δ 170.1, 139.9, 134.9, 133.6, 132.5, 60.9, 19.7, 14.3, 1.9, 0.1. HRMS (ESI+), calculated for [$C_{18}H_{34}O_4Si_3$]$^{+}$: 399.1843, found: 399.1855.

Procedure B was followed for the reaction of ethyl 2,6-dimethylbenzoate (18 mg, 0.10 mmol). The reaction was conducted with ligand **L2** (1 mg, 4 μmol, 4 mol%) at 100 ℃ for 20 hours. The NMR yield was determined to be 40% with dibromomethane internal standard.

Procedure B was followed for the reaction of ethyl 2,6-dimethylbenzoate (18 mg, 0.10 mmol). The reaction was conducted with ligand **L3** (1 mg, 4 μmol, 4 mol%) at 100 ℃ for 20 hours. The NMR yield was determined to be 12% with dibromomethane internal standard.

Silylation of 1-bromo-3-methoxybenzene

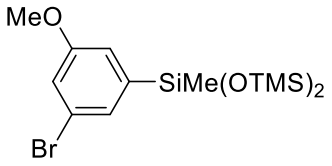

14

Procedure A was followed for the reaction of 1-bromo-3-methoxybenzene (93 mg, 0.50 mmol). The reaction was conducted with ligand **L1** (2.1 mg, 10 μmol, 2.0 mol%) at 100 ℃ for 20 hours. The crude reaction mixture was purified by silica-gel chromatography to afford the product as a colorless liquid (178 mg, 89% yield). ^{1}H NMR (600 MHz, chloroform-*d*) δ 7.22 (dd, *J* = 1.7, 0.8 Hz, 1H), 7.06 (dd, *J* = 2.5, 1.6 Hz, 1H), 7.02 – 6.98 (m, 1H), 3.80 (s, 3H), 0.26 (s, 3H), 0.12 (s, 18H). ^{13}C NMR (126 MHz, chloroform-*d*) δ 160.2, 142.7, 128.6, 123.3, 118.3, 117.9, 55.8, 2.3, 0.3. HRMS (EI), calculated for [$C_{14}H_{27}O_3Si_3Br$]: 406.0451, found: 406.0447.

Procedure B was followed for the reaction of 1-bromo-3-methoxybenzene (19 mg, 0.10 mmol). The reaction was conducted with ligand **L2** (1 mg, 4 μmol, 4 mol%) at 100 ℃ for 20 hours. The NMR yield was determined to be 58% with dibromomethane internal standard.

Procedure B was followed for the reaction of 1-bromo-3-methoxybenzene (19 mg, 0.10 mmol). The reaction was conducted with ligand **L3** (1 mg, 4 μmol, 4 mol%) at 100 ℃ for 20 hours. The NMR yield was determined to be 39% with dibromomethane internal standard.

Silylation of m-tolylnitrile

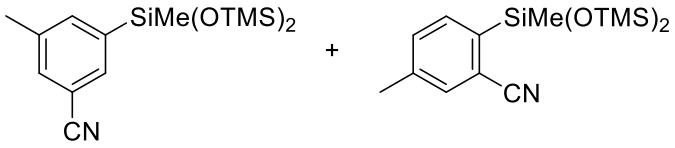

15

Procedure A was followed for the reaction of m-tolylnitrile (30 mg, 0.26 mmol). The reaction was conducted with ligand **L1** (1 mg, 5 μmol, 2.0 mol%) at 100 ℃ for 20 hours. The crude reaction mixture was purified by silica-gel chromatography to afford the product as a colorless liquid (73 mg, 84% yield). Ratio of regioisomers (m:o) was determined by GC analysis to be 11:1. ^{1}H NMR (500 MHz, chloroform-*d*) δ 7.61 (s, 1H), 7.55 (s, 1H), 7.46 (s, 1H), 2.39 (s, 3H), 0.27 (s, 3H), 0.12 (s, 18H). ^{13}C NMR (126 MHz, chloroform-*d*) δ 140.3, 138.2, 138.1, 134.0, 133.2, 119.4, 111.8, 21.2, 1.8, -0.1. HRMS (ESI+), calculated for [$C_{15}H_{28}NO_2Si_3$]$^{+}$: 338.1420, found: 338.1417.

Procedure B was followed for the reaction of m-tolylnitrile (12 mg, 0.10 mmol). The reaction was conducted with ligand **L2** (1 mg, 4 μmol, 4 mol%) at 100 ℃ for 20 hours. The NMR yield was determined to be 53% with dibromomethane internal standard.

Procedure B was followed for the reaction of m-tolylnitrile (12 mg, 0.10 mmol). The reaction was conducted with ligand **L3** (1 mg, 4 μmol, 4 mol%) at 100 ℃ for 20 hours. The NMR yield was determined to be <1% with dibromomethane internal standard.

Silylation of m-tolyl acetate

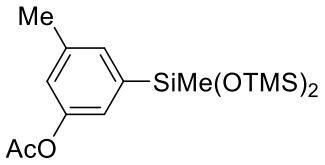

16

Procedure A was followed for the reaction of m-tolyl acetate (70 mg, 0.47 mmol). The reaction was conducted with ligand **L1** (2.1 mg, 10 μmol, 2.0 mol%) at 100 ℃ for 20 hours. The crude reaction mixture was purified by silica-gel chromatography to afford the product as a colorless liquid (164 mg, 95% yield). ^{1}H NMR (600 MHz, $CDCl_3$) δ 7.20 (s, 1H), 7.02 (s, 1H), 6.91(s, 1H), 2.36 (s, 3H), 2.30 (s, 3H), 0.25 (s, 3H), 0.11 (s, 18H). ^{13}C NMR (151 MHz, $CDCl_3$) δ 169.5, 150.2, 140.2, 138.7, 131.4, 123.2, 122.8, 21.1, 21.1, 2.0, 0.1. HRMS (ESI+) calculated for $[C_{16}H_{31}O_4Si_3]^+$: 371.1530, found: 371.1518.

Procedure B was followed for the reaction of m-tolyl acetate (15 mg, 0.10 mmol). The reaction was conducted with ligand **L2** (1 mg, 4 μmol, 4 mol%) at 100 ℃ for 20 hours. The NMR yield was determined to be 31% with dibromomethane internal standard.

Procedure B was followed for the reaction of m-tolyl acetate (15 mg, 0.10 mmol). The reaction was conducted with ligand **L3** (1 mg, 4 μmol, 4 mol%) at 100 ℃ for 20 hours. The NMR yield was determined to be <1% with dibromomethane internal standard.

Silylation of N,N-diethyl-3-methylbenzamide

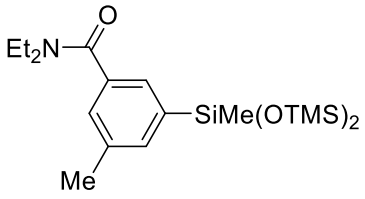

17

Procedure A was followed for the reaction of N,N-diethyl-3-methylbenzamide (93 mg, 0.49 mmol). The reaction was conducted with ligand **L1** (2.1 mg, 10 μmol, 2.0 mol%) at 100 ℃ for 20 hours. The crude reaction mixture was purified by silica-gel chromatography to afford the product as a colorless liquid (126 mg, 63% yield). ^{1}H NMR (500 MHz, chloroform-*d*) δ 7.36 – 7.33 (m, 1H), 7.30 (s, 1H), 7.19 (s, 1H), 3.53 (s, 2H), 3.22 (s, 2H), 2.35 (s, 3H), 1.27 – 1.18 (s, 3H), 1.09

(s, 3H), 0.24 (s, 3H), 0.09 (s, 18H). ^{13}C NMR (126 MHz, chloroform-*d*) δ 172.2, 139.0, 137.6, 136.9, 135.0, 128.5, 128.2, 43.6, 39.5, 21.8, 14.6, 13.3, 2.3, 0.4. HRMS (ESI+) calculated for $[C_{19}H_{38}O_3NSi_3]^+$: 412.2160, found: 412.2165.

Procedure B was followed for the reaction of N,N-diethyl-3-methylbenzamide (19 mg, 0.10 mmol). The reaction was conducted with ligand **L2** (1 mg, 4 μmol, 4 mol%) at 100 ℃ for 20 hours. The NMR yield was determined to be 44% with dibromomethane internal standard.

Procedure B was followed for the reaction of N,N-diethyl-3-methylbenzamide (19 mg, 0.10 mmol). The reaction was conducted with ligand **L3** (1 mg, 4 μmol, 4 mol%) at 100 ℃ for 20 hours. The NMR yield was determined to be 33% with dibromomethane internal standard.

Silylation of 3-chlorobenzonitrile

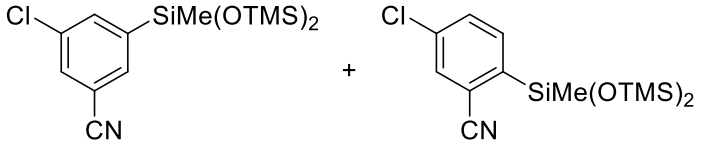

18

Procedure A was followed for the reaction of 3-chlorobenzonitrile (70 mg, 0.51 mmol). The reaction was conducted with ligand **L1** (2.1 mg, 10 μmol, 2.0 mol%) at 100 ℃ for 20 hours. The crude reaction mixture was purified by silica-gel chromatography to afford the product as a colorless liquid (177 mg, 97% yield). Ratio of regioisomers (m:o) is determined by GC analysis to be 19:1. ^{1}H NMR (500 MHz, chloroform-*d*) δ 7.70 – 7.68 (m, 1H), 7.67 – 7.66 (m, 1H), 7.62 (d, *J* = 2.0 Hz, 1H), 0.29 (s, 3H), 0.13 (s, 18H). ^{13}C NMR (126 MHz, chloroform-*d*) δ 143.0, 137.4, 134.8, 132.3, 117.8, 113.6, 1.8, -0.2. HRMS (EI), calculated for $[C_{13}H_{21}NO_2Si_3Cl]$ (M-CH_3): 342.0569, found: 342.0564.

Procedure B was followed for the reaction of 3-chlorobenzonitrile (14 mg, 0.10 mmol). The reaction was conducted with ligand **L2** (1 mg, 4 μmol, 4 mol%) at 100 ℃ for 20 hours. The NMR yield was determined to be 67% with dibromomethane internal standard.

Procedure B was followed for the reaction of 3-chlorobenzonitrile (14 mg, 0.10 mmol). The reaction was conducted with ligand **L3** (1 mg, 4 μmol, 4 mol%) at 100 ℃ for 20 hours. The NMR yield was determined to be <1% with dibromomethane internal standard.

Silylation of 1,3-bistrifluorobenzene

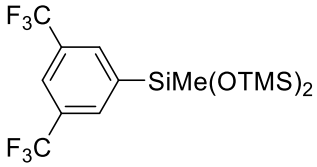

19

Procedure A was followed for the reaction of 1,3-bistrifluorobenzene (104 mg, 0.49 mmol). The reaction was conducted with ligand **L1** (2.1 mg, 10 μmol, 2.0 mol%) at 100 ℃ for 20 hours. The

crude reaction mixture was purified by silica-gel chromatography to afford the product as a colorless liquid (174 mg, 83% yield). ^{1}H NMR (400 MHz, chloroform-*d*) δ 7.97 (s, 2H), 7.88 (s, 1H), 0.33 (s, 3H), 0.14 (s, 18H). ^{13}C NMR (126 MHz, chloroform-*d*) 141.7, 133.1, 130.6 (d, *J* = 32.7 Hz), 123.6 (d, *J* = 272.5 Hz), 123.1 (p, *J* = 3.9 Hz), 1.7, 0.2. ^{19}F NMR (376 MHz, chloroform-*d*) δ -62.2. HRMS (EI), calculated for [$C_{14}H_{21}F_6O_2Si_3$]: 419.0754, found: 419.0762.

Procedure A was followed with modifications for the reaction of 1,3-bistrifluorobenzene (214 mg, 1.00 mmol). The reaction was conducted with [Ir(cod)OMe]$_2$ (0.8 mg, 1.3 μmol, 0.13 mol%) and ligand **L1** (1 mg, 5 μmol, 0.5 mol%) at 100 ℃ for 20 hours. The NMR yield was determined to be 78% with dibromomethane internal standard.

Procedure B was followed with modifications for the reaction of 1,3-bistrifluorobenzene (214 mg, 1.00 mmol). The reaction was conducted with [Ir(cod)OMe]$_2$ (0.8 mg, 1.3 μmol, 0.13 mol%) and ligand **L2** (1 mg, 5 μmol, 0.5 mol%) at 100 ℃ for 20 hours. The NMR yield was determined to be 27% with dibromomethane internal standard.

Procedure B was followed with modifications for the reaction of 1,3-bistrifluorobenzene (214 mg, 1.00 mmol). The reaction was conducted with [Ir(cod)OMe]$_2$ (0.8 mg, 1.3 μmol, 0.13 mol%) and ligand **L3** (1 mg, 5 μmol, 0.5 mol%) at 100 ℃ for 20 hours. The NMR yield was determined to be 29% with dibromomethane internal standard.

Silylation of methyl 3-chlorobenzoate

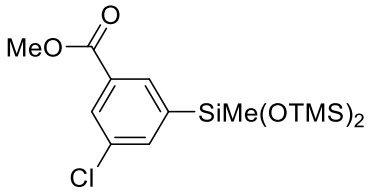

20

Procedure A was followed with modifications for the reaction of methyl 3-chlorobenzoate (52.5 mg, 0.308 mmol). The reaction was conducted with [Ir(cod)OMe]$_2$ (3.0 mg, 4.5 μmol, 1.5 mol%) and ligand **L1** (2.4 mg, 11 μmol, 3.6 mol%) at 100 ℃ for 6 hours. The crude reaction mixture was purified by silica-gel chromatography to afford the product as a colorless liquid (116 mg, 96% yield). ^{1}H NMR (600 MHz, $CDCl_3$) δ 8.10 (t, J=1.2Hz, 1H), 8.01 (t, J=1.93Hz, 1H), 7.66 (dd, J=2.81, 0.82Hz 1H), 3.93 (s, 3H), 0.29 (s, 3H), 0.13 (s, 18H). ^{13}C NMR (151 MHz, $CDCl_3$) δ 166.1, 141.5, 137.3, 134.2, 132.3, 131.1, 130.3, 52.3, 1.8, 0.2. HRMS (EI), calculated for [$C_{15}H_{27}ClO_4Si_3$]: 390.0906, found: 390.0902.

Procedure A was followed with modifications for the reaction of methyl 3-chlorobenzoate (171 mg, 1.00 mmol). The reaction was conducted with [Ir(cod)OMe]$_2$ (0.8 mg, 1.3 μmol, 0.09 mol%)

and ligand **L1** (1 mg, 5 μmol, 0.5 mol%) at 100 ℃ for 20 hours. The NMR yield was determined to be 50% with dibromomethane internal standard.

Procedure B was followed with modifications for the reaction of methyl 3-chlorobenzoate (171 mg, 1.00 mmol). The reaction was conducted with $[Ir(cod)OMe]_2$ (0.8 mg, 1.3 μmol, 0.09 mol%) and ligand **L2** (1 mg, 5 μmol, 0.5 mol%) at 100 ℃ for 20 hours. The NMR yield was determined to be 24% with dibromomethane internal standard.

Procedure B was followed with modifications for the reaction of methyl 3-chlorobenzoate (171 mg, 1.00 mmol). The reaction was conducted with $[Ir(cod)OMe]_2$ (0.8 mg, 1.3 μmol, 0.09 mol%) and ligand **L3** (1 mg, 5 μmol, 0.5 mol%) at 100 ℃ for 20 hours. The NMR yield was determined to be 21% with dibromomethane internal standard.

Silylation of 1,3-dichlorobenzene

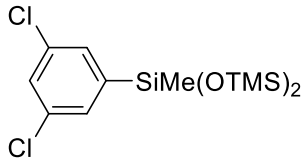

21

Procedure A was followed for the reaction of 1,3-dichlorobenzene (71 mg, 0.49 mmol). The reaction was conducted with ligand **L1** (2.1 mg, 10 μmol, 2.0 mol%) at 100 ℃ for 6 hours. The crude reaction mixture was purified by silica-gel chromatography to afford the product as a colorless liquid (176 mg, 99% yield). ^{1}H NMR (400 MHz, chloroform-*d*) δ 7.37 (s, 3H), 0.28 (s, 3H), 0.14 (s, 18H). ^{13}C NMR (101 MHz, chloroform-*d*) δ 142.9, 134.7, 131.2, 129.4, 1.8, -0.2. HRMS (EI), calculated for $[C_{13}H_{24}Cl_2O_2Si_3]$: 366.0461, found: 366.0455.

Procedure A was followed with modifications for the reaction of 1,3-dichlorobenzene (221 mg, 1.50 mmol). The reaction was conducted with $[Ir(cod)OMe]_2$ (0.8 mg, 1.3 μmol, 0.13 mol%) and ligand **L1** (1 mg, 5 μmol, 0.5 mol%) at 100 ℃ for 20 hours. The NMR yield was determined to be 82% with dibromomethane internal standard.

Procedure B was followed with modifications for the reaction of 1,3-dichlorobenzene (221 mg, 1.50 mmol). The reaction was conducted with $[Ir(cod)OMe]_2$ (0.8 mg, 1.3 μmol, 0.13 mol%) and ligand **L2** (1 mg, 5 μmol, 0.5 mol%) at 100 ℃ for 20 hours. The NMR yield was determined to be 26% with dibromomethane internal standard.

Procedure B was followed with modifications for the reaction of 1,3-dichlorobenzene (221 mg, 1.50 mmol). The reaction was conducted with $[Ir(cod)OMe]_2$ (0.8 mg, 1.3 μmol, 0.13 mol%) and ligand **L3** (1 mg, 5 μmol, 0.5 mol%) at 100 ℃ for 20 hours. The NMR yield was determined to be 30% with dibromomethane internal standard.

Silylation of 1-bromo-3-chlorobenzene

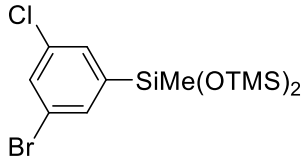

22

Procedure A was followed with modifications for the reaction of 1-bromo-3-chlorobenzene (182 mg, 0.95 mmol). The reaction was conducted with ligand **L1** (2.1 mg, 10 μmol, 1.0 mol%) at 100 ℃ for 24 hours. The crude reaction mixture was purified by silica-gel chromatography to afford the product as a colorless liquid (386 mg, 98% yield). ^{1}H NMR (600 MHz, chloroform-*d*) δ 7.53 (t, *J* = 2.0 Hz, 2H), 7.42-7.41 (m, 1H), 0.28 (s,3H), 0.14 (s, 18H). ^{13}C NMR (151 MHz, chloroform-*d*) δ 143.2, 134.8, 134.0, 132.1, 131.6, 122.8, 1.8, -0.2. HRMS (EI), calculated for [$C_{13}H_{24}O_2Si_3ClBr$]: 409.9956, found: 409.9952.

Procedure A was followed with modifications for the reaction of 1-bromo-3-chlorobenzene (191 mg, 1.00 mmol). The reaction was conducted with [Ir(cod)OMe]$_2$ (0.8 mg, 1.3 μmol, 0.13 mol%) and ligand **L1** (1 mg, 5 μmol, 0.5 mol%) at 100 ℃ for 20 hours. The NMR yield was determined to be 57% with dibromomethane internal standard.

Procedure B was followed with modifications for the reaction of 1-bromo-3-chlorobenzene (191 mg, 1.00 mmol). The reaction was conducted with [Ir(cod)OMe]$_2$ (1.3 μmol, 0.13 mol%) and ligand **L2** (1 mg, 5 μmol, 0.5 mol%) at 100 ℃ for 20 hours. The NMR yield was determined to be 25% with dibromomethane internal standard.

Procedure B was followed with modifications for the reaction of 1-bromo-3-chlorobenzene (191 mg, 1.00 mmol). The reaction was conducted with [Ir(cod)OMe]$_2$ (0.8 mg, 1.3 μmol, 0.13 mol%) and ligand **L3** (1 mg, 5 μmol, 0.5 mol%) at 100 ℃ for 20 hours. The NMR yield was determined to be 19% with dibromomethane internal standard.

Silylation of 1-iodo-3-(trifluoromethyl)benzene

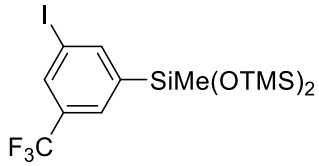

23

Procedure A was followed for the reaction of 1-iodo-3-(trifluoromethyl)benzene (132 mg, 0.48 mmol). The reaction was conducted with [Ir(cod)OMe]$_2$ (6.6 mg, 10 μmol, 2 mol%), and ligand **L1** (4.2 mg, 20 μmol, 4.0 mol%) at 100 ℃ for 21 hours. The crude reaction mixture was purified by silica-gel chromatography to afford the product as a colorless liquid (196 mg, 82% yield). ^{1}H NMR (500 MHz, chloroform-*d*) δ 8.04 (s, 1H), 7.96 (s, 1H), 7.75 (s, 1H), 0.30 (s, 3H), 0.14 (s, 18H). ^{13}C NMR (126 MHz, chloroform-*d*) δ 145.9 – 145.8 (m), 143.3, 135.2 (q, *J* = 3.8 Hz), 132.1 (q, *J* = 32.2 Hz), 129.2 (q, *J* = 3.7 Hz), 123.6 (d, *J* = 273.1 Hz), 94.8, 2.2, 0.2. ^{19}F NMR (376 MHz, chloroform-*d*) δ -66.9. HRMS (EI), calculated for [$C_{13}H_{21}O_2F_3Si_3I$] (M-CH_3): 476.9846, found: 476.9852.

Procedure B was followed with modifications for the reaction of 1-iodo-3-(trifluoromethyl)benzene (26 mg, 0.096 mmol). The reaction was conducted with ligand **L2** (1 mg, 4 μmol, 4 mol%) at 100 ℃ for 21 hours. The NMR yield was determined to be 44% with dibromomethane internal standard.

Procedure B was followed with modifications for the reaction of 1-iodo-3-(trifluoromethyl)benzene (26 mg, 0.096 mmol). The reaction was conducted with ligand **L3** (1 mg, 4 μmol, 4 mol%) at 100 ℃ for 21 hours. The NMR yield was determined to be 32% with dibromomethane internal standard.

Silylation of 5-fluoroindole

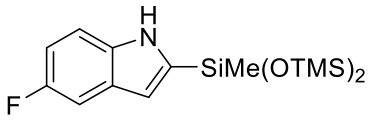

24

Procedure A was followed for the reaction of 5-fluoroindole (34 mg, 0.25 mmol). The reaction was conducted with ligand **L1** (1 mg, 5 μmol, 2 mol%) at 50 ℃ for 22 hours. The crude reaction mixture was purified by silica-gel chromatography to afford the product as a colorless liquid (58 mg, 62% yield). ^{1}H NMR (500 MHz, chloroform-*d*) δ 8.25 – 8.10 (m, 1H), 7.34 (dd, *J* = 8.9, 4.3 Hz, 1H), 7.30 (dd, *J* = 9.6, 2.5 Hz, 1H), 6.98 (td, *J* = 9.0, 2.5 Hz, 1H), 6.73 (dd, *J* = 2.1, 1.0 Hz, 1H), 0.38 (s, 3H), 0.17 (s, 18H). ^{13}C NMR (126 MHz, chloroform-*d*) δ 157.9 (d, *J* = 234.4 Hz), 138.4, 134.6, 128.9 (d, *J* = 10.0 Hz), 111.6 (d, *J* = 9.8 Hz), 111.4 (d, *J* = 4.9 Hz), 111.1 (d, *J* = 26.9 Hz), 105.4 (d, *J* = 23.2 Hz), 1.9, 0.7. ^{19}F NMR (376 MHz, chloroform-*d*) δ -129.2. HRMS (APCI-MS), calculated for [$C_{15}H_{26}FNO_2Si_3$]: 356.1334, found: 356.1341.

Procedure C was followed for the reaction of 5-fluoroindole (34 mg, 0.25 mmol), The reaction was conducted at 100 ℃ for 1 hours. The NMR yield was determined to be 87% with dibromomethane internal standard.

Silylation of 6,7-dihydrobenzofuran-4(5H)-one

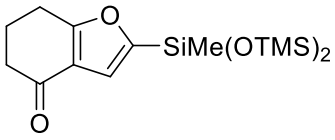

25

Procedure A was followed for the reaction of 6,7-dihydrobenzofuran-4(5H)-one (71 mg, 0.52 mmol). The reaction was conducted with 0.5 % [Ir(cod)OMe]$_2$ and ligand **L1** (1 mg, 5 μmol, 1 mol%) at 60 ℃ for 24 hours. The crude reaction mixture was purified by silica-gel chromatography to afford the product as a colorless liquid (180 mg, 97% yield). ^{1}H NMR (600 MHz, chloroform-*d*) δ 6.87 (s, 1H), 2.85 (t, *J* = 6.3 Hz, 2H), 2.44 (t, *J* = 6.3 Hz, 2H), 2.12 (p, *J* = 6.3 Hz, 2H), 0.22 (s, 3H), 0.06 (s, 18H). ^{13}C NMR (151 MHz, chloroform-*d*) δ 194.6, 170.6, 158.6, 121.0, 116.3, 37.7, 23.7, 22.6, 1.8, -0.2. HRMS (ESI+), calculated for [$C_{15}H_{29}BrO_2SSi_3$]$^{+}$: 357.1374, found: 357.1377.

Procedure C was followed for the reaction of 6,7-dihydrobenzofuran-4(5H)-one (34 mg, 0.25 mmol), The reaction was conducted at 100 ℃ for 1 hours. The NMR yield was determined to be 91% with dibromomethane internal standard.

Silylation of 2-bromothiophene

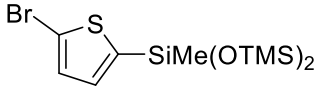

26

Procedure A was followed for the reaction of 2-bromothiophene (80 mg, 0.49 mmol). The reaction was conducted with ligand **L1** (2.1 mg, 10 μmol, 2.0 mol%) at 60 ℃ for 22 hours. The crude reaction mixture was purified by silica-gel chromatography to afford the product as a colorless liquid (162 mg, 86% yield). ^{1}H NMR (500 MHz, chloroform-*d*) δ 7.08 (d, *J* = 3.5 Hz, 1H), 7.03 (d, *J* = 3.5 Hz, 1H), 0.30 (s, 3H), 0.13 (s, 18H). ^{13}C NMR (126 MHz, chloroform-*d*) δ 141.3, 134.8, 131.0, 117.2, 1.8, 0.9. HRMS (EI), calculated for [$C_{11}H_{23}BrO_2Si_3S$]: 381.9910, found: 381.9908.

Procedure C was followed for the reaction of 2-bromothiophene (41 mg, 0.25 mmol), The reaction was conducted at 100 ℃ for 1 hours. The NMR yield was determined to be 64% with dibromomethane internal standard.

Silylation of 2,6-dichloro-pyridine

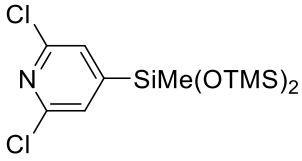

27

Procedure A was followed for the reaction of 2,6-dichloro-pyridine (74 mg, 0.50 mmol), The reaction was conducted with ligand **L1** (2.1 mg, 10 μmol, 2.0 mol%) at 100 ℃ for 2 hours. The NMR yield was determined to be 72% with dibromomethane internal standard.

Procedure C was followed for the reaction of 2-bromothiophene (37 mg, 0.25 mmol), The reaction was conducted at 100 ℃ for 2 hours. The crude reaction mixture was purified by silica-gel chromatography to afford the product as a colorless liquid (71 mg, 77% yield). ^{1}H NMR (600 MHz, chloroform-*d*) δ 7.32 (s, 2H), 0.29 (s, 3H), 0.14 (s, 18H). ^{13}C NMR (151 MHz, chloroform-*d*) δ 155.0, 150.1, 126.5, 1.7, -0.5. HRMS (ESI+), calculated for [$C_{12}H_{24}O_2Si_3NCl_2$]$^{+}$: 368.0492, found: 368.0485.

Silylation of benzothiophene

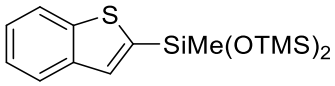

28

Procedure A was followed with modifications for benzothiophene (141 mg, 1.05 mmol). The reaction was conducted with 0.5 % [Ir(cod)OMe]$_2$ and ligand **L1** (2.1 mg, 10 μmol, 1.0 mol%). The reaction was conducted in an oven-dried 10 mL round-bottomed flask fitted with a reflux condenser. The top of the reflux condenser was fitted with a rubber septum before the flask was removed from the glovebox. The flask was place in an oil bath preheated to 60 ℃. A nitrogen line

and a 21-guage needle were affixed to the septum. After 22 hours, the reaction was cooled to room temperature and ~ 1 mL of MeOH was added to the reaction mixture. Volatile solvents and reagents were removed under reduced pressure, and the mixture was filtered through a plug of silica. Solvent was removed under reduced pressure, affording 335 mg of a colorless oil (90% yield). ^{1}H NMR (500 MHz, chloroform-*d*) δ 8.03 – 7.99 (m, 1H), 7.98 – 7.94 (m, 1H), 7.66 (s, 1H), 7.44 (tt, *J* = 7.2, 5.5 Hz, 2H), 0.54 (s, 3H), 0.31 (s, 18H). ^{13}C NMR (126 MHz, chloroform-*d*) δ 143.6, 141.0, 140.0, 131.5, 124.6, 124.1, 123.9, 122.4, 2.0, 1.1. HRMS (EI), calculated for [$C_{15}H_{26}O_2SSi_3$]: 354.0961, found: 354.0960.

Procedure C was followed for the reaction of benzothiophene (34 mg, 0.25 mmol), The reaction was conducted at 100 ℃ for 1 hours. The NMR yield was determined to be 98% with dibromomethane internal standard.

Synthesis of Pharmaceutical Intermediates
Silylation of 3-chlorophenyl acetate and iodination of the silylarene

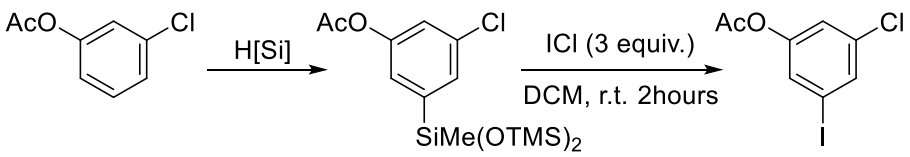

35a **35**

35a

Procedure A was followed for the reaction of 3-chlorophenyl acetate (170 mg, 1.00 mmol) The reaction was conducted with 1.5 % $[Ir(cod)OMe]_2$ and **L1** ligand (6.2 mg, 30 μmol, 3.0 mol%) at 100 ℃ for 24 hours. The crude reaction mixture was purified by silica-gel chromatography to afford the product as a colorless liquid (371 mg, 95% yield). ^{1}H NMR (400 MHz, chloroform-*d*) δ 7.35 (dd, *J* = 2.0, 0.8 Hz, 1H), 7.14 (t, *J* = 2.1 Hz, 1H), 7.12 (dd, *J* = 2.2, 0.8 Hz, 1H), 2.30 (s, 3H), 0.27 (s, 3H), 0.12 (s, 18H). ^{13}C NMR (101 MHz, chloroform-*d*) δ 169.0, 150.7, 142.3, 134.3, 130.5, 124.2, 123.1, 21.1, 1.8, -0.2. HRMS (EI), calculated for $[C_{15}H_{27}O_4Si_3Cl]$: 390.0906, found: 390.0911.

35

98 mg (0.25 mmol) of **35a** was added to a 4 mL vial fitted with a stir-bar followed by 2 mL of DCM. The solution was cooled in an ice bath and stirred. 0.25 mL of ICl solution (3M in DCM) was added dropwise to the stirring solution. After addition of ICl, the ice bath was removed, and the solution was warmed to room temperature. After 2 h, the volatile materials were evaporated under reduced pressure. The residue was purified by silica-gel chromatography (neat hexanes to 2% EtOAc in hexanes) to afford **29** (70 mg, 94%). ^{1}H NMR (400 MHz, chloroform-*d*) δ 7.74 – 7.53 (m, 1H), 7.42 (t, *J* = 1.7 Hz, 1H), 7.16 (d, *J* = 2.1 Hz, 1H), 2.33 (s, 3H). ^{13}C NMR (101 MHz, chloroform-*d*) δ 168.6, 151.1, 135.3, 134.7, 129.3, 122.1, 93.1, 21.0. HRMS (EI), calculated for $[C_8H_6O_2ClI]$: 295.9101, found: 295.9100.

Oxidation of the silylarene 18

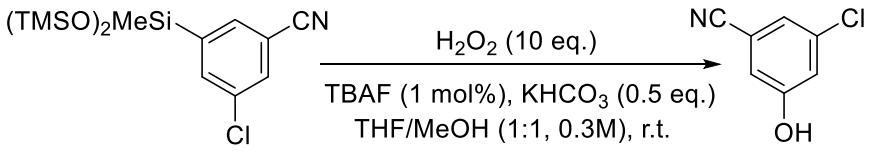

18 **30**

30

108 mg (0.30 mmol) of silylarene **18** and 15 mg of $KHCO_3$ (0.50 equiv, 0.15 mmol) was added to a 4 mL vial fitted with a stir-bar followed by 0.5 mL of THF and 0.5 mL of MeOH. 3μl of TBAF solution (1 mol%, 1 M in THF) and 125μl of aqueous H_2O_2 (10 equiv, 3 mmol, 50% by weight) was added to the 4 mL vial. The solution was stirred at room temperature for 20 hours. Volatiles were then removed under reduced pressure. The residue was neutralized with 1N HCl and extracted with EtOAc (5ml, 3 times). The combined organic phase was washed with brine, dried over Na_2SO_4, and concentrated. The NMR yield based on this crude material was determined to

be 57% with dibromomethane internal standard. The crude material was then purified by column chromatography (silica, 20% EtOAc in hexanes) to give **29** as a white solid (21 mg, 45% yield). ^{1}H NMR (500 MHz, Acetone-d_6) δ 9.64 (s, 1H), 7.34 (t, J = 1.6 Hz, 1H), 7.22 (t, J = 2.1 Hz, 1H), 7.19 (dd, J = 2.3, 1.3 Hz, 1H). ^{13}C NMR (126 MHz, Acetone-d_6) δ 159.2, 135.8, 123.1, 120.9, 117.9, 117.5, 114.7. These NMR data matched those reported in the literature.[24]

Silylation of *N*-methyl-*N*-(3-methylpyridin-2-yl)acetamide and bromination of the silylheteroarene

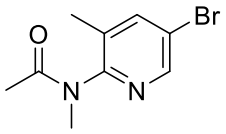

31

Procedure A was followed with modifications for *N*-methyl-*N*-(3-methylpyridin-2-yl)acetamide (42 mg, 0.26 mmol) The reaction was conducted with **L1** ligand (1 mg, 5 μmol, 2 mol%) at 100 °C for 20 hours. The volatile materials were evaporated under reduced pressure, and the residue was dissolved in 2 mL MeCN. 5 mg of NBS was added to the solution; the solution was stirred for 15 minutes and then filtered through a ~1-inch plug of silica. The filtrate was concentrated under reduced pressure. The residue was introduced to a nitrogen-filled glovebox and dissolved in 2 mL of dry MeCN. 63 mg of AgF and 50 mg of NBS to a separate 4 mL vial fitted with a stir-bar, followed by the MeCN solution. The resultant solution was capped with a Teflon-line screw-cap and stirred at room temperature for 3 hours. The solution was concentrated under reduced pressure and the residue was purified by silica-gel chromatography (1% Et_3N, 25% EtOAc, 75% hexanes) to afford the product as a white crystalline solid (42 mg, 67% yield). ^{1}H NMR (600 MHz, 325 K, chloroform-d) δ 8.43 (s, 1H), 7.79 (s, 1H), 3.17 (s, 3H), 2.26 (s, 3H), 1.78 (s, 3H). ^{13}C NMR (151 MHz, 325K, chloroform-d) δ 167.0, 154.1, 148.5, 142.5, 132.2, 119.9, 34.1, 21.9, 16.9. HRMS (ESI+), calculated for $[C_9H_{12}O_1N_2Br]^+$: 243.0128, found: 243.0128.

Silylation of *N*-*tert*-butyl-thiophene-2-sulphonamide

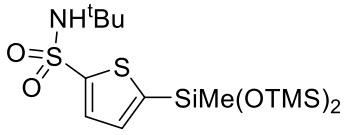

32a

Procedure C was followed for the reaction of *N*-*tert*-butyl-thiophene-2-sulphonamide (219 mg, 1.00 mmol). The reaction was conducted at 100 °C for 6 hours. The crude reaction mixture was purified by silica-gel chromatography to afford the product as a pale orange liquid (441 mg, 100% yield). ^{1}H NMR (400 MHz, Chloroform-d) δ 7.65 (d, J = 3.5 Hz, 1H), 7.19 (d, J = 3.5 Hz, 1H), 4.71 (s, 1H), 1.32 (s, 9H), 0.37 (s, 3H), 0.15 (s, 18H). ^{13}C NMR (101 MHz, $CDCl_3$) δ 149.0, 145.8, 133.4, 132.3, 54.9, 29.8, 1.6, 0.7. HRMS (ESI+), calculated for $[C_{15}H_{34}NO_4S_2Si]^+$: 440.1232, found: 440.1255.

Coupling of silylarene 32a with 4-bromo-anisole

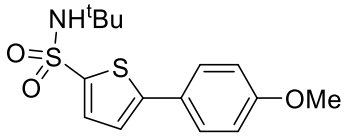

32

In an N_2-filled glovebox, silylarene **32a** (44 mg, 0.10 mmol), 4-bromoanisole (22 mg, 0.12 mmol), AgF (32 mg, 0.20 mmol), and Pd(^{t}Bu$_3$P)$_2$ (2.6 mg, 0.0050 mmol) were added to a 4 mL vial. A magnetic stir bar and 0.2 mL of THF were added to the vial, and the vial was capped. The vial was removed from the glovebox and placed in an aluminum block preheated to 65 °C. After 6 hours, the vial was removed from the heating block, and the contents of the vial were filtered through a pad of silica. The volatile materials were then evaporated under reduced pressure. The crude product was then dissolved in Et_2O, layered with hexanes, and recrystallized at −10 °C. After 20 h, the supernatant was removed, and the crystalline material was dried under high vacuum. ^{1}H NMR (300 MHz, Chloroform-*d*) δ 7.55 – 7.49 (m, 3H), 7.09 (d, *J* = 3.9 Hz, 1H), 6.93 (d, *J* = 8.8 Hz, 2H), 3.84 (s, 4H), 1.31 (s, 11H). ^{13}C NMR (151 MHz, $CDCl_3$) δ 160.4, 150.8, 142.0, 132.9, 127.7, 125.7, 121.6, 114.7, 55.6, 55.3, 30.1. HRMS (ESI+), calculated for $[C_{15}H_{20}NO_3S_2]^+$: 326.0879, found: 326.0888.

Determination of Kinetic Isotope Effect with a Series of Catalysts

a) Determination of Kinetic Isotope Effect with Catalyst Containing L1

In an N_2-filled glovebox, $[Ir(cod)OMe]_2$ (6.6 mg, 0.010 mmol), **L1** (4.2 mg, 0.020 mmol), dodecane (170 mg, 1.0 mmol), and 1,1,1,3,5,5,5-heptamethyl-trisiloxane (334 mg, 1.50 mmol) were weighed into a 4 mL vial. After 20 minutes, the solution was transferred to a 1 mL volumetric flask, the vial was washed with dioxane, and the washings were transferred to the flask. The solution was diluted to 1 mL total volume with dioxane, and the flask was capped and shaken. 200 µL (400 µL total) of stock solution was added to two separate Radley Carousel reaction vessels. 200 µL of benzene was added to one of the vessels and 200 µL of benzene-d_6 was added to the other. The vessels were capped. The capped vessel was removed from the glovebox and placed in a Radley Carousel that had been preheated to 80 °C. The rates of the reactions were determined by the method of initial rates, monitored by GC analysis with dodecane as the internal standard. The kinetic isotope effect (k_H/k_D) was determined to be 1.3.

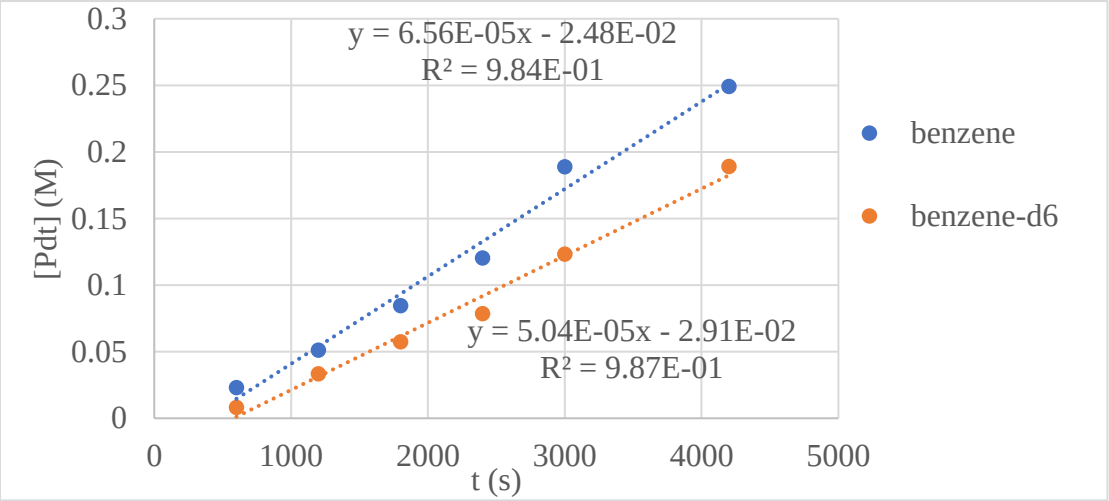

b) Determination of Kinetic Isotope Effect with Catalyst Containing L2 (Limiting Silane)

In an N_2-filled glovebox, $[Ir(cod)OMe]_2$ (6.6 mg, 0.010 mmol), **L2** (4.4 mg, 0.020 mmol), dodecane (85 mg, 0.50 mmol), 1,1,1,3,5,5,5-heptamethyl-trisiloxane (223 mg, 1.00 mmol), cyclohexene (82 mg, 1.0 mmol) and THF-d_8 (300 µL) were added to a 4 mL vial. After 20 minutes, the solution was transferred to a 1 mL volumetric flask, the vial was washed with THF, and the washings were transferred to the flask. The solution was diluted to 1 mL total volume with THF, and the flask was capped and shaken. 400 µL (800 µL total) of stock solution was added to two separate J-Young NMR tubes. 200 µL of benzene was added to one of the tubes, and 200 µL of benzene-d_6 was added to the other. The tubes were then capped and removed from the glovebox. The J-Young NMR tubes were placed in an aluminum block that had been preheated to 100 °C. The tubes were removed from the heating block at the specified times and analyzed by NMR. The rates of the reactions were determined by the method of initial rates, with dodecane as the internal standard. The kinetic isotope effect (k_H/k_D) was determined to be 1.6.

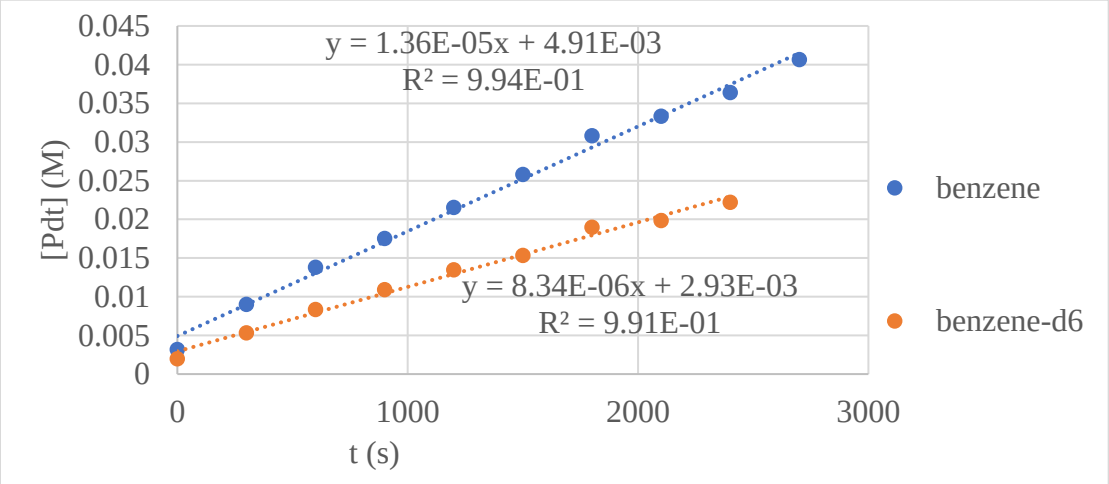

c) Determination of Kinetic Isotope Effect with Catalyst Containing L2 (Limiting Arene)

In an N_2-filled glovebox, $[Ir(cod)OMe]_2$ (6.6 mg, 0.010 mmol), **L2** (4.4 mg, 0.020 mmol), dodecane (85 mg, 0.50 mmol), 1,1,1,3,5,5,5-heptamethyl-trisiloxane (445 mg, 2.00 mmol), cyclohexene (82 mg, 1.0 mmol) and THF-d_8 (100 μL) were added to a 4 mL vial. After 20 minutes, the solution was transferred to a 1 mL volumetric flask, the vial was washed with THF-d_8, and the washings were transferred to the flask. The solution was diluted to 1 mL total volume with THF-d_8, and the flask was capped and shaken. 400 μL (800 μL total) of stock solution was added to two separate J-Young NMR tubes. 50 μL of benzene was added to one of the tubes, and 50 μL of benzene-d_6 was added to the other. The tubes were then capped and removed from the glovebox. The J-Young NMR tubes were placed in an aluminum block that had been preheated to 100 °C. The tubes were removed from the heating block at the specified times and analyzed by NMR. The rates of the reactions were determined by the method of initial rates, with dodecane as the internal standard. The experiment was repeated three times. The average rate of the silylation of benzene was $1.2 \cdot 10^{-5} \pm 0.1$ M/s. The average rate of the silylation of benzene was $7.6 \cdot 10^{-6} \pm 0.2$ M/s. The kinetic isotope effect determined from this data is 1.6±0.3.

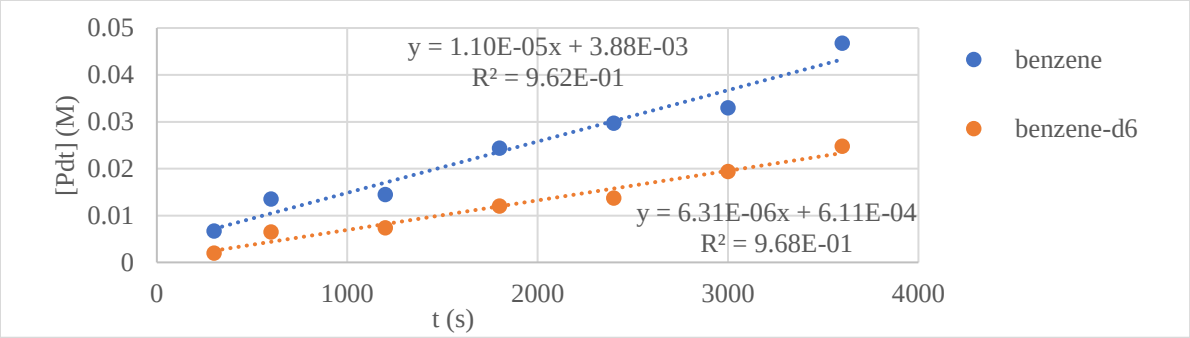

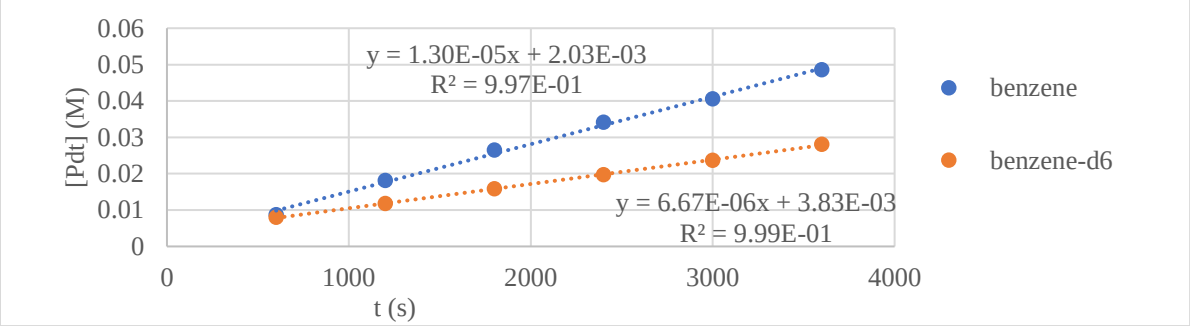

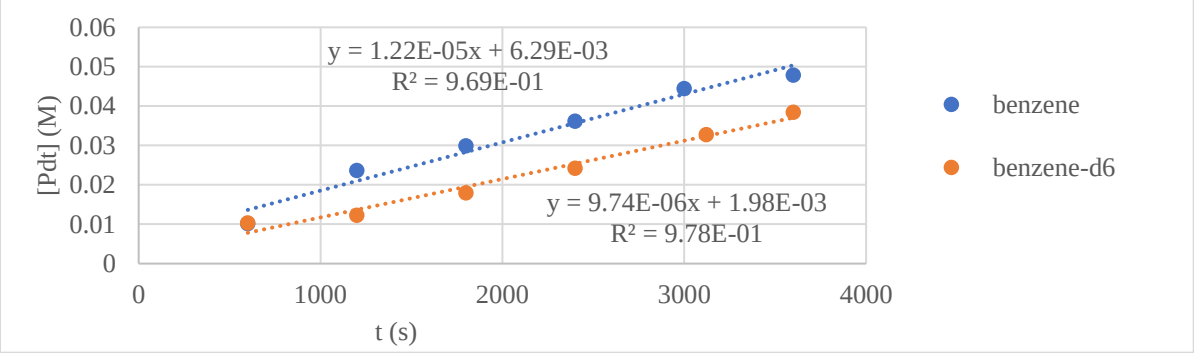

Determination of Kinetic Isotope Effect with Catalyst Containing L3 (Limiting Silane)

In an N_2-filled glovebox, $[Ir(cod)OMe]_2$ (13.3 mg, 0.0200 mmol), **L3** (9.4 mg, 0.040 mmol), dodecane (85 mg, 0.50 mmol), 1,1,1,3,5,5,5-heptamethyl-trisiloxane (223 mg, 1.00 mmol), and THF-d_8 (100 µL) were added to a 4 mL vial. After 20 minutes, 200 µL (400 µL total) of stock solution was added to two separate J-Young NMR tubes. 300 µL of benzene was added to one of the tubes and 300 µL of benzene-d_6 was added to the other. The tubes were then capped and removed from the glovebox. The J-Young NMR tubes were placed in an aluminum block that had been preheated to 100 °C. The tubes were removed from the heating block at the specified times and analyzed by NMR. The rates of the reactions were determined by the method of initial rates, with dodecane as the internal standard. The kinetic isotope effect (k_H/k_D) was determined to be 2.0.

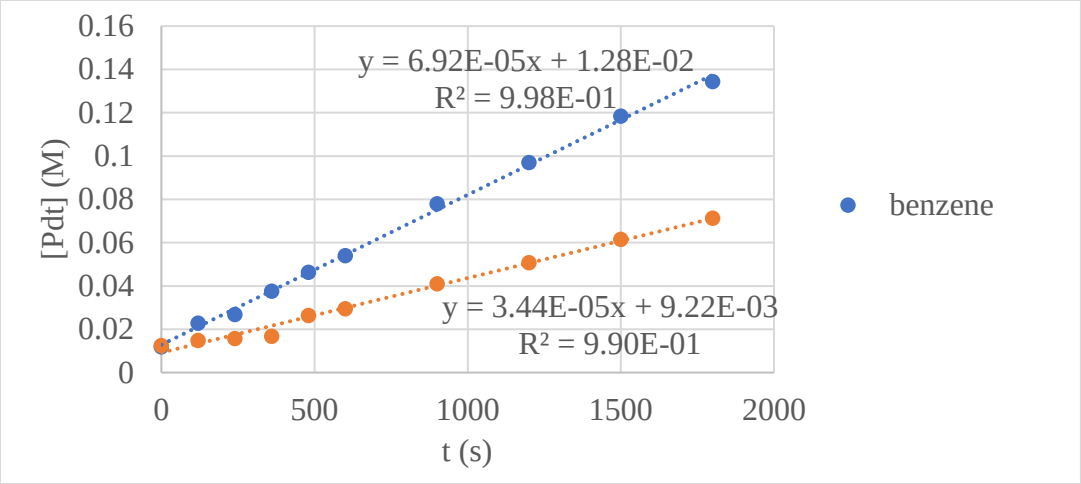
0.16
0.14
0.12
0.1
0.08
0.06
0.04
0.02
0
[Pdt] (M)
y = 6.92E-05x + 1.28E-02
R² = 9.98E-01
y = 3.44E-05x + 9.22E-03
R² = 9.90E-01
0
500
1000
1500
2000
t (s)
benzene

d) Determination of Kinetic Isotope Effect with Catalyst Containing L3 (Limiting Arene)

In an N_2-filled glovebox, $[Ir(cod)OMe]_2$ (6.6 mg, 0.010 mmol), **L3** (4.7 mg, 0.020 mmol), dodecane (85 mg, 0.50 mmol), 1,1,1,3,5,5,5-heptamethyl-trisiloxane (445 mg, 2.00 mmol), cyclohexene (82 mg, 1.0 mmol) and THF-d_8 (100 µL) were added to a 4 mL vial. After 20 minutes, the solution was transferred to a 1 mL volumetric flask, the vial was washed with THF-d_8, and the washings were transferred to the flask. The solution was diluted to 1 mL total volume with THF-d_8, and the flask was capped and shaken. 400 µL (800 µL total) of stock solution was added to two separate J-Young NMR tubes. 50 µL of benzene was added to one of the tubes, and 50 µL of benzene-d_6 was added to the other. The tubes were then capped and removed from the glovebox. The J-Young NMR tubes were placed in an aluminum block that had been preheated to 100 °C. The tubes were removed from the heating block at the specified times and analyzed by NMR. The rates of the reactions were determined by the method of initial rates, with dodecane as the internal standard. The kinetic isotope effect (k_H/k_D) was determined to be 1.7.

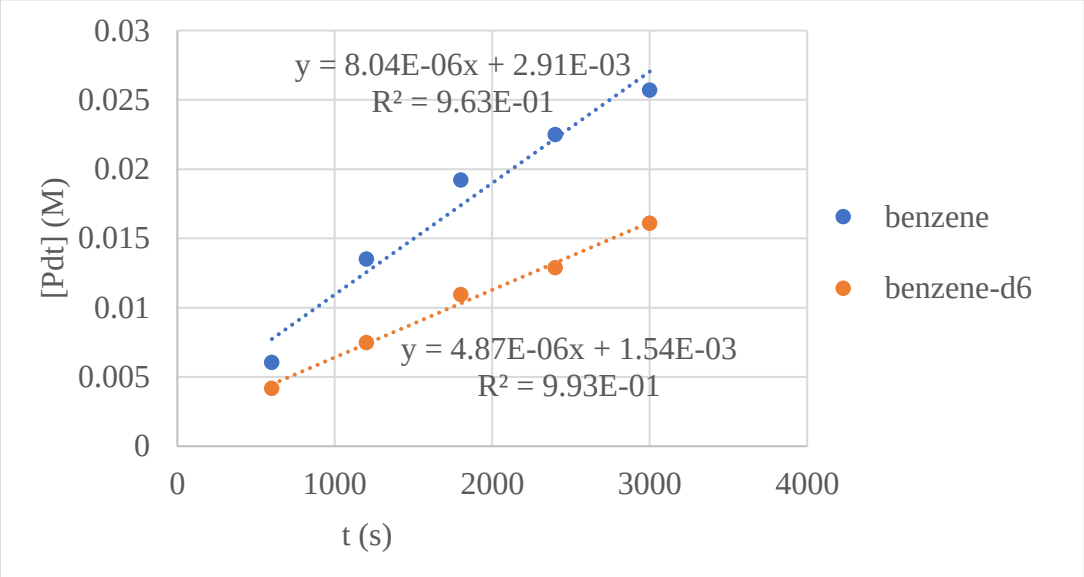

Rate of protiation of benzene-d_6

In an N_2-filled glovebox, $[Ir(cod)OMe]_2$ (6.6 mg, 0.01 mmol), dodecane (85 mg, 0.50 mmol), and 1,1,1,3,5,5,5-heptamethyl-trisiloxane (223 mg, 1.00 mmol) were added to a 4 mL vial. The solution was transferred to a 1 mL volumetric flask, the vial was washed with THF, and the washings were transferred to the flask. The solution was diluted to 1 mL total volume with THF, and the flask was capped and shaken. **L1** (2.1 mg, 0.01 mmol) and **L2** (2.2 mg, 0.01 mmol) were added to two separate vials. 400 µL (800 µL total) of stock solution was added to the two 4 mL vials containing the ligands. 100 µL of benzene-d_6 was added to each vial. The solution in each vial was then transferred to a separate J-Young NMR tube. The tubes were then capped and removed from the glovebox. The J-Young NMR tubes were place in an aluminum block that had been preheated to 80 °C. The tubes were removed from the heating block at the specified times and analyzed by ^{1}H NMR spectroscopy. The rates of the reactions were determined by the method of initial rates, with dodecane as the internal standard.

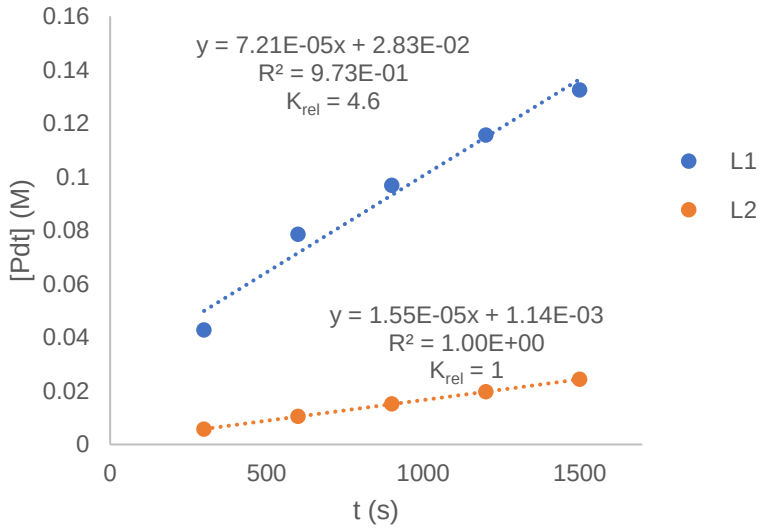

3.5 References

Portions of this chapter were reprinted with permission from:

"Iridium-Catalyzed Silylation of C–H Bonds in Unactivated Arenes: A Sterically Encumbered Phenanthroline Ligand Accelerates Catalysis" Karmel, C.; Chen, Z.; Hartwig, J. F., *J. Am. Chem. Soc.* **2019,** *141*, 7063.

1. (a) Godula, K.; Sames, D. C-H Bond Functionalization in Complex Organic Synthesis. *Science* **2006**, *312*, 67. (b) Newhouse, T.; Baran, P. S. If C–H Bonds Could Talk: Selective C–H Bond Oxidation. *Angew. Chem. Int. Ed.* **2011**, *50*, 3362. (c) Davies, H. M. L.; Du Bois, J.; Yu, J.-Q. C-H Functionalization in organic synthesis. *Chem. Soc. Rev.* **2011**, *40*, 1855. (d) Gutekunst, W. R.; Baran, P. S. C-H functionalization logic in total synthesis. *Chem. Soc. Rev.* **2011**, *40*, 1976. (e)

McMurray, L.; O'Hara, F.; Gaunt, M. J. Recent developments in natural product synthesis using metal-catalysed C–H bond functionalisation. *Chem. Soc. Rev.* **2011**, *40*, 1885. (f) Yamaguchi, J.; Yamaguchi, A. D.; Itami, K. C-H Bond Functionalization: Emerging Synthetic Tools for Natural Products and Pharmaceuticals. *Angew. Chem. Int. Ed.* **2012**, *51*, 8960. (g) White, M. C. Adding Aliphatic C–H Bond Oxidations to Synthesis. *Science* **2012**, *335*, 807. (h) Neufeldt, S. R.; Sanford, M. S. Controlling Site Selectivity in Palladium-Catalyzed C–H Bond Functionalization. *Acc. Chem. Res.* **2012**, *45*, 936. (i) Wencel-Delord, J.; Glorius, F. C-H bond activation enables the rapid construction and late-stage diversification of functional molecules. *Nat. Chem.* **2013**, *5*, 369. (j) Cernak, T.; Dykstra, K. D.; Tyagarajan, S.; Vachal, P.; Krska, S. W. The medicinal chemist's toolbox for late stage functionalization of drug-like molecules. *Chem. Soc. Rev.* **2016**, *45*, 546. (k) Wedi, P.; van Gemmeren, M. Arene-Limited Nondirected C−H Activation of Arenes. *Angew. Chem. Int. Ed.* **2018**, *57*, 13016.

2. (a) Mkhalid, I. A. I.; Barnard, J. H.; Marder, T. B.; Murphy, J. M.; Hartwig, J. F. C-H Activation for the Construction of C-B Bonds. *Chem. Rev.* **2010**, *110*, 890. (b) Hartwig, J. F. Borylation and Silylation of C-H Bonds: A Platform for Diverse C-H Bond Functionalizations. *Acc. Chem. Res.* **2012**, *45*, 864. (c) Hartwig, J. F. Evolution of C–H Bond Functionalization from Methane to Methodology. *J. Am. Chem. Soc.* **2016**, *138*, 2. (d) Hartwig, J. F.; Larsen, M. A. Undirected, Homogeneous C–H Bond Functionalization: Challenges and Opportunities. *ACS Cent. Sci.* **2016**, *2*, 281.

3. (a) Maleczka, R. E.; Shi, F.; Holmes, D.; Smith, M. R. I. C–H activation/borylation/oxidation: A one-pot unified route to meta-substituted phenols bearing ortho-/para-directing groups. *J. Am. Chem. Soc.* **2003**, *125*, 7792. (b) Miyaura, N., Metal-Catalyzed Cross-Coupling Reactions of Organoboron Compounds with Organic Halides. In *Metal-Catalyzed Cross-Coupling Reactions*, de Meijere, A.; Diederich, F., Eds. Wiley-VCH: Weinheim, 2004; Vol. 1, pp 41. (c) Tzschucke, C. C.; Murphy, J. M.; Hartwig, J. F. Arenes to anilines and aryl ethers by sequential iridium-catalyzed borylation and copper-catalyzed coupling. *Org. Lett.* **2007**, *9*, 761. (d) Murphy, J. M.; Liao, X.; Hartwig, J. F. Meta Halogenation of 1,3-Disubstituted Arenes via Iridium-Catalyzed Arene Borylation. *J. Am. Chem. Soc.* **2007**, *129*, 15434. (e) Liskey, C. W.; Liao, X.; Hartwig, J. F. Cyanation of Arenes via Iridium-Catalyzed Borylation. *J. Am. Chem. Soc.* **2010**, *132*, 11389. (f) Partridge, B. M.; Hartwig, J. F. Sterically Controlled Iodination of Arenes via Iridium-Catalyzed C–H Borylation. *Org. Lett.* **2012**, *15*, 140. (g) Robbins, D. W.; Hartwig, J. F. A C-H Borylation Approach to Suzuki-Miyaura Coupling of Typically Unstable 2-Heteroaryl and Polyfluorophenyl Boronates. *Org. Lett.* **2012**, *14*, 4266. (h) Litvinas, N. D.; Fier, P. S.; Hartwig, J. F. A General Strategy for the Perfluoroalkylation of Arenes and Arylbromides by Using Arylboronate Esters and (phen)CuRF. *Angew. Chem. Int. Ed.* **2012**, *51*, 536. (i) Robbins, D. W.; Hartwig, J. F. Sterically Controlled Alkylation of Arenes through Iridium-Catalyzed C–H Borylation. *Angew. Chem. Int. Ed.* **2013**, *52*, 933. (j) Fier, P. S.; Luo, J.; Hartwig, J. F. Copper-Mediated Fluorination of Arylboronate Esters. Identification of a Copper(III) Fluoride Complex. *J. Am. Chem. Soc.* **2013**, *135*, 2552.

4. Brown, D. G.; Boström, J. Analysis of Past and Present Synthetic Methodologies on Medicinal Chemistry: Where Have All the New Reactions Gone? *J. Med. Chem.* **2016**, *59*, 4443.

5. Brotherton, R. J.; McCloskey, A. L.; Boone, J. L.; Manasevit, H. M. The Preparation and Properties of Some Tetraalkoxydiborons. *J. Am. Chem. Soc.* **1960**, *82*, 6245.

6. Obligacion, J. V.; Chirik, P. J. Earth-abundant transition metal catalysts for alkene hydrosilylation and hydroboration. *Nat. Rev. Chem.* **2018**, *2*, 15.

7. (a) Bracegirdle, S.; Anderson, E. A. Arylsilane oxidation—new routes to hydroxylated aromatics. *Chem. Commun.* **2010**, *46*, 3454. (b) Nakao, Y.; Hiyama, T. Silicon-based cross-coupling reaction: an environmentally benign version. *Chem. Soc. Rev.* **2011**, *40*, 4893. (c) Rayment, E. J.; Summerhill, N.; Anderson, E. A. Synthesis of Phenols via Fluoride-free Oxidation of Arylsilanes and Arylmethoxysilanes. *J. Org. Chem.* **2012**, *77*, 7052. (d) Denmark, S. E.; Ambrosi, A. Why You Really Should Consider Using Palladium-Catalyzed Cross-Coupling of Silanols and Silanolates. *Org. Process Res. Dev.* **2015**, *19*, 982. (e) Rayment, E. J.; Mekareeya, A.; Summerhill, N.; Anderson, E. A. Mechanistic Study of Arylsilane Oxidation through ^{19}F NMR Spectroscopy. *J. Am. Chem. Soc.* **2017**, *139*, 6138.
8. Cheng, C.; Hartwig, J. F. Catalytic Silylation of Unactivated C–H Bonds. *Chem. Rev.* **2015**, *115*, 8946.
9. (a) Ezbiansky, K.; Djurovich, P. I.; Laforest, M.; Sinning, D. J.; Zayes, R.; Berry, D. H. Catalytic C-H Bond Functionalization - Synthesis of Arylsilanes By Dehydrogenative Transfer Coupling of Arenes and Triethylsilane. *Organometallics* **1998**, *17*, 1455. (b) Ishiyama, T.; Sato, K.; Nishio, Y.; Miyaura, N. Direct synthesis of aryl halosilanes through iridium(I)-catalyzed aromatic C-H silylation by disilanes. *Angew. Chem. Int. Ed.* **2003**, *42*, p 5346. (c) Tsukada, N.; Hartwig, J. F. Intermolecular and Intramolecular, Platinum-Catalyzed, Acceptorless Dehydrogenative Coupling of Hydrosilanes with Aryl and Aliphatic Methyl C-H Bonds. *J. Am. Chem. Soc.* **2005**, *127*, 5022. (d) Saiki, T.; Nishio, Y.; Ishiyama, T.; Miyaura, N. Improvements of Efficiency and Regioselectivity in the Iridium(I)-Catalyzed Aromatic C-H Silylation of Arenes with Fluorodisilanes. *Organometallics* **2006**, *25*, 6068. (e) Murata, M.; Fukuyama, N.; Wada, J.-i.; Watanabe, S.; Masuda, Y. Platinum-catalyzed Aromatic C-H Silylation of Arenes with 1,1,1,3,5,5,5-Heptamethyltrisiloxane. *Chem. Lett.* **2007**, *36*, 910. (f) Ishiyama, T.; Saiki, T.; Kishida, E.; Sasaki, I.; Ito, H.; Miyaura, N. Aromatic C–H silylation of arenes with 1-hydrosilatrane catalyzed by an iridium(i)/2,9-dimethylphenanthroline (dmphen) complex. *Org. Biomol. Chem.* **2013**, *11*, 8162.
10. (a) Kakiuchi, F.; Igi, K.; Matsumoto, M.; Chatani, N.; Murai, S. Ruthenium-catalyzed dehydrogenative silylation of aryloxazolines with hydrosilanes via C-H bond cleavage. *Chem. Lett.* **2001**, 422. (b) Tobisu, M.; Ano, Y.; Chatani, N. Rhodium-catalyzed silylation of aromatic carbon-hydrogen bonds in 2-arylpyridines with disilane. *Chem. Asian J.* **2008**, *3*, 1585. (c) Ihara, H.; Suginome, M. Easily Attachable and Detachable ortho-Directing Agent for Arylboronic Acids in Ruthenium-Catalyzed Aromatic C-H Silylation. *J. Am. Chem. Soc.* **2009**, *131*, 7502. (d) Choi, G.; Tsurugi, H.; Mashima, K. Hemilabile N-Xylyl-N′-methylperimidine Carbene Iridium Complexes as Catalysts for C–H Activation and Dehydrogenative Silylation: Dual Role of N-Xylyl Moiety for ortho-C–H Bond Activation and Reductive Bond Cleavage. *J. Am. Chem. Soc.* **2013**, *135*, 13149. (e) Kanyiva, K. S.; Kuninobu, Y.; Kanai, M. Palladium-Catalyzed Direct C–H Silylation and Germanylation of Benzamides and Carboxamides. *Org. Lett.* **2014**, *16*, 1968.
11. Hongliu Liao; Renyuan Peng; Rongmei Lu; Xiao, S. Method for synthesizing 1,1,1,3,5,5,5-heptamethyltrisiloxane by continuous catalysis of solid phase catalyst. CN101921287B, 2010-12-22, 2012.
12. Cheng, C.; Hartwig, J. F. Rhodium-Catalyzed Intermolecular C-H Silylation of Arenes with High Steric Regiocontrol. *Science* **2014**, *343*, 853.
13. Cheng, C.; Hartwig, J. F. Iridium-Catalyzed Silylation of Aryl C–H Bonds. *J. Am. Chem. Soc.* **2015**, *137*, 592.
14. (a) Chotana, G. A.; Rak, M. A.; Smith, M. I. Sterically Directed Functionalization of Aromatic C-H Bonds. Selective Borylation Ortho to Cyano Groups in Arenes and Heterocycles. *J. Am.*

Chem. Soc. **2005**, *127*, 10539. (b) Bisht, R.; Hoque, M. E.; Chattopadhyay, B. Amide Effects in C−H Activation: Noncovalent Interactions with L-Shaped Ligand for meta Borylation of Aromatic Amides. *Angew. Chem.* **2018**, *130*, 15988.
15. Morstein, J.; Kalkman, E. D.; Bold, C.; Cheng, C.; Hartwig, J. F. Copper-Mediated C–N Coupling of Arylsilanes with Nitrogen Nucleophiles. *Org. Lett.* **2016**, *18*, 5244.
16. Morstein, J.; Hou, H.; Cheng, C.; Hartwig, J. F. Trifluoromethylation of Arylsilanes with [(phen)CuCF3]. *Angew. Chem. Int. Ed.* **2016**, 8054.
17. (a) Campeau, L.-C.; Chen, Q.; Gauvreau, D.; Girardin, M.; Belyk, K.; Maligres, P.; Zhou, G.; Gu, C.; Zhang, W.; Tan, L.; O'Shea, P. D. A Robust Kilo-Scale Synthesis of Doravirine. *Org. Process Res. Dev.* **2016**, *20*, 1476. (b) Deeks, E. D. Doravirine: First Global Approval. *Drugs* **2018**, *78*, 1643.
18. Flick, A. C.; Ding, H. X.; Leverett, C. A.; Kyne, R. E.; Liu, K. K. C.; Fink, S. J.; O'Donnell, C. J. Synthetic Approaches to the New Drugs Approved During 2015. *J. Med. Chem.* **2017**, *60*, 6480.
19. Allsop, G. L.; Cole, A. J.; Giles, M. E.; Merifield, E.; Noble, A. J.; Pritchett, M. A.; Purdie, L. A.; Singleton, J. T. A Convergent Synthesis of AR-C123196 Utilising Reaction Between a Cyclic Carbonate and a Phenol for Aryl Alkyl Ether Formation. *Org. Process Res. Dev.* **2009**, *13*, 751.
20. Partridge, B. M.; Hartwig, J. F. Sterically Controlled Iodination of Arenes via Iridium-Catalyzed C-H Borylation. *Org. Lett.* **2013**, *15*, 140.
21. Lee, J. H.; Li, Z.; Osawa, A.; Kishi, Y. Extension of Pd-Mediated One-Pot Ketone Synthesis to Macrocyclization: Application to a New Convergent Synthesis of Eribulin. *J. Am. Chem. Soc.* **2016**, *138*, 16248.
22. Mita, T.; Michigami, K.; Sato, Y. Iridium- and Rhodium-Catalyzed Dehydrogenative Silylations of C(sp3)□H Bonds Adjacent to a Nitrogen Atom Using Hydrosilanes. **2013**, *8*, 2970.
23. Manley, P. J.; Bilodeau, M. T. A Mild Method for the Formation and in Situ Reaction of Imidoyl Chlorides: Conversion of Pyridine-1-oxides to 2-Aminopyridine Amides. *Org. Lett.* **2002**, *4*, 3127.
24. Davidson, J. P.; Sarma, K.; Fishlock, D.; Welch, M. H.; Sukhtankar, S.; Lee, G. M.; Martin, M.; Cooper, G. F. A Synthesis of 3,5-Disubstituted Phenols. *Org. Process Res. Dev.* **2010**, *14*, 477.

Chapter 4

Mechanism of the Iridium-Catalyzed Silylation of Aromatic C–H Bonds

4.1 Introduction

The iridium-catalyzed silylation of aromatic C–H bonds forms aryl silanes with high sterically derived regioselectivity and is conducted with silane reagents that are produced and consumed on large scales.[1] In many cases, the heteroaryl silane and aryl silane products are more stable than the corresponding aryl boronic esters and undergo related subsequent reactions, such as hydroxylation,[2] amination,[3] halogenation,[4] and arylation.[5] In addition, the silylation of aryl and heteroaryl C–H bonds often occurs with higher sterically derived selectivity than the iridium-catalyzed borylation of the same arenes.[4a, 6]

To facilitate access to silicon-containing organic compounds, our group and others have reported silylations of aryl[4b, 4c, 7] and alkyl C–H bonds,[8] with a range of silane reagents and a series of iridium catalysts.[4a, 4b, 7a, 7c, 7e-g, 9] Such efforts to develop new silylation reactions would be aided by a detailed understanding of the mechanism by which these reactions occur. Yet, little is known about the mechanism of these reactions or even the identity of the Ir complexes present during the reaction. This dearth of experimental mechanistic data has motivated several groups to conduct computational studies. Sunoj et. al. reported DFT calculations on the iridium-catalyzed intramolecular silylation of sp^3 C–H bonds that suggested that an Ir(I) silyl species containing a bidentate nitrogen ligand and an additional norbornene ligand can cleave C–H bonds and mediate C–Si bond formation with energetic barriers that are consistent with the observed rate of the reaction.[10] However, in later studies, the groups of Li[11] and Huang[12] calculated that an Ir(III) silyl complex is the resting state of the catalyst and that the difference in free energy between this complex and the transition state for oxidative addition of the C–H bond to the Ir(III) complex was smaller than the difference in free energy between the Ir(III) complex and the transition state for for oxidative addition of a C–H bond to a related Ir(I) complex. These contrasting computational results indicate the need for experimental mechanistic studies to determine the identity of the iridium complexes that lie on the catalytic cycle for the silylation of C–H bonds.

We recently reported a highly active catalyst for the silylation of aromatic C–H bonds that is formed from the combination of $[Ir(cod)(OMe)]_2$ and 2,9-Me_2-phenanthroline (2,9-Me_2-phen, **L1**) (Figure 4.1).[4b] Two unusual features of this reaction motivated further study of the mechanism. First, the catalyst containing a phenanthroline ligand bearing methyl groups in the 2- and 9-positions was much more active than the catalysts containing phenanthrolines lacking substituents in one or both of those positions. Second, the rate of the reaction is ten times faster under an atmosphere of nitrogen than under an atmosphere of hydrogen.[4b] Consequently, the reactions of these highly active catalysts were conducted in an open system to remove the hydrogen byproduct with a stream of nitrogen. Thus, we sought to understand the origin of the high sensitivity of the rate of the reaction to the hydrogen byproduct and to the substitution pattern on the phenanthroline ligand. We also sought to provide a foundation for the aforementioned computational data by

determining whether the iridium complex that mediates this reaction is an Ir(I) or Ir(III) complex and by identifying the number and type of silyl or hydride ligands bound to the iridium center.

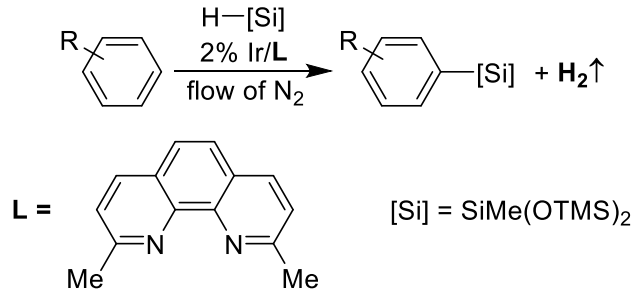

Which Ir complexes are intermediates in the reaction?

Why is the reaction slow in the presence of hydrogen?

What are the roles of substituents on phenanthroline?

Figure 4.1 Catalytic silylation of aromatic C–H bonds.

To this end, we conducted a study that included both experimental and computational investigations. We generated and determined the identity of the resting state of the iridium catalyst in solution, isolated derivatives of this complex, and measured kinetic isotope effects for the silylation of arenes with varying electronic properties. Computational data are consistent with the intermediates and rate-limiting step in the catalytic cycle that we observed experimentally and reveal principles that dictate the activity and selectivity of these iridium complexes that catalyze the silylation of aryl and heteroaryl C–H bonds.

4.2 Results & Discussion

4.2.1 Determination of the Resting State of the Catalyst

To determine the identity of the iridium complexes in the silylation of aromatic C–H bonds, we first subjected a mixture of $[Ir(cod)(OMe)]_2$, 2,9-Me_2phen, and excess heptamethyltrisiloxane to analysis by high resolution ESI-mass spectrometry. The resulting spectrum contained a peak

corresponding to the exact mass of a protonated iridium complex bearing 2,9-Me$_2$phen, two silyl ligands, and one hydride (complex **1**) (Scheme 4.1).

Scheme 4.1 Synthesis of Catalyst Resting State and Solid-State Structure of Complex 3

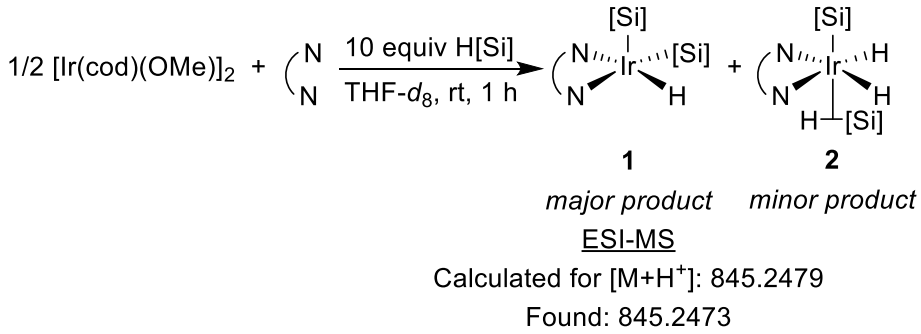

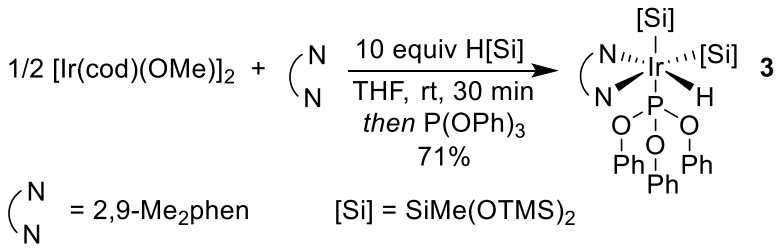

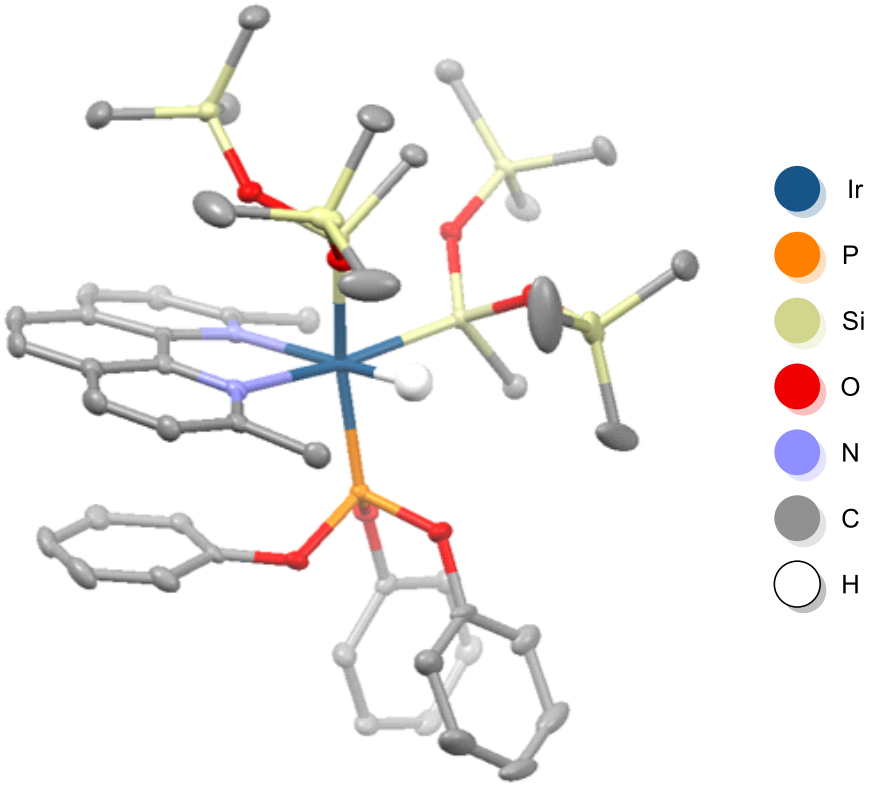

To assess the validity of the MS data, we acquired ^{1}H NMR spectra of the mixture of [Ir(cod)(OMe)]$_2$, 2,9-Me$_2$phen, and excess heptamethyltrisiloxane at room temperature and low temperatures. The ^{1}H NMR spectrum acquired at room temperature contains a set of four signals

corresponding to the phenanthroline ligand and a broad peak at –13 ppm that suggests the presence of a metal hydride. A large broad peak was also observed at 3.5 ppm that corresponds to the hydrogen attached to the silicon of free silane. This signal is located 1.2 ppm upfield of that for free silane (4.7 ppm), suggesting that the proton bound to silicon in the silane is exchanging with that in the hydride position of iridium.

The ^{1}H NMR spectrum acquired at –86 °C contains peaks that are different from those in the spectrum acquired at room temperature. The peak for the hydrogen of free silane was observed as a quartet at 4.6 ppm, corresponding to the chemical shift observed in the absence of any metal complex. The peak corresponding to the metal hydride was observed as a sharp singlet at -16 ppm. The ratio of the integrals of the peaks for the bound 2,9-Me$_2$phen and the hydride suggests that this complex contains only a single hydride ligand. Furthermore, a singlet at -0.5 ppm integrates to 36 hydrogens, indicating the presence of four TMS groups in the complex. These data imply that the resting state of the catalyst **1** contains a phenanthroline ligand, two silyl groups, and a hydride, and this conclusion matches that from mass spectrometry (Scheme 4.1). The ^{1}H NMR spectrum also contains a set of peaks corresponding to a smaller amount of a second complex (**2**), which is the major species observed when this solution is placed under an atmosphere of hydrogen gas. The identity of this complex will be discussed in detail below.

To convert the resting state of the catalyst to a 6-coordinate species that would be more stable to isolation than the putative five-coordinate resting state **1**, triphenylphosphite was added to the mixture of [Ir(cod)(OMe)]$_2$, 2,9-Me$_2$phen, and excess heptamethyltrisiloxane. The resulting phosphite complex **3** was isolated by column chromatography and characterized by NMR spectroscopy. The ^{1}H NMR spectrum of **3** contains eight distinct signals that correspond to the protons of 2,9-Me$_2$phen. The spectrum also contains six peaks in a 3:3:3:3:1:1 ratio between –1 and 1 ppm that correspond to the two inequivalent methyl groups on the two Ir-bound silyl groups and to two pairs of OTMS groups on the silyl groups, each of which are diastereotopic due to the stereogenic iridium center in the complex. A doublet (J = 14 Hz) at –20 ppm indicates that **3** contains a metal hydride and is consistent with coupling to the phosphorus of a phosphite ligand. The signal at –20 ppm is observed as a singlet in the in the ^{1}H{^{31}P} NMR spectrum, and the proton-coupled ^{31}P NMR spectrum contains a doublet at 103 ppm with the same coupling constant, confirming that the complex contains a hydride and a bound phosphine. The resonance in the ^{31}P NMR spectrum contains ^{29}Si satellites with a coupling constant ($J_{P–Si}$ = 303 Hz) that is larger than the typical range of one- or two-bond Si–P coupling constants ($^{1}J_{P–S}$ = 16-256 Hz, $^{2}J_{P–S}$ = 0-44 Hz).[13] We hypothesize that the coupling constant is large because the Si atom and the P atom of the phosphite are mutually *trans* across the Ir center.[14] Overall, these data demonstrate that the combination of [Ir(cod)(OMe)]$_2$, 2,9-Me$_2$phen, and excess heptamethyltrisiloxane forms an iridium complex that contains one phenanthroline ligand, two heptamethyltrisiloxyl ligands, and one hydride (Scheme 4.1).

The identity and connectivity of phosphite adduct **3** was further assessed by single-crystal x-ray diffraction. The solid-state structure of **3** consists of an octahedral Ir(III) center containing mutually *trans* silyl and phosphite ligands. An additional silyl group, and the hydride ligand, are located in the same plane as the phenanthroline ligand. The silyl groups are geared to minimize steric interactions. The two siloxy groups of the axial silyl group lie over the phenanthroline so that the methyl group points toward the other large silyl group. One of the trimethylsiloxy substituents on the equatorial silyl ligand lies in the equatorial plane of the complex and is close to the hydride ligand, while the other two substituents lie above and below the methyl group of the

2,9-Me_2phen. It is difficult to envision an orientation of the silyl groups that would allow three silyl groups, rather than two silyl groups and a hydride, to be present on iridium.

Lewis bases other than phosphites form similar iridium complexes that are less stable to isolation. Reaction of complex **1** with 4-dimethylaminopyridine (DMAP) yielded a six-coordinate complex **4** containing DMAP bound to iridium (Scheme 4.2). The ^{1}H NMR spectrum of this complex contains a pattern of signals that are similar to those of phosphite adduct **3**, including a signal corresponding to a metal hydride at -20 ppm that integrates to 1 proton. However, only one set of broad peaks was observed for the protons of DMAP when excess DMAP was present in solution, and the integration of these broad peaks corresponded to more than one equivalent of DMAP. This result suggests that free and bound DMAP undergo exchange on the NMR timescale.[15]

Scheme 4.2 Synthesis of Pyridine Adduct of Catalyst

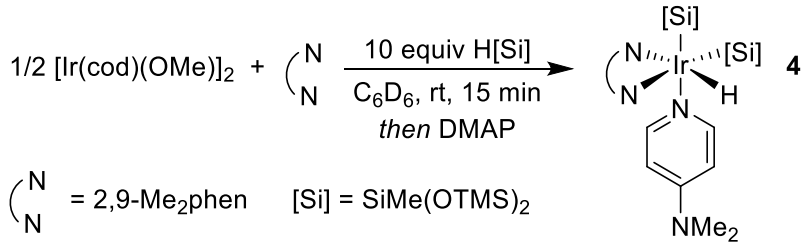

The rate of the silylation of arenes is ten times lower under an atmosphere of hydrogen than under nitrogen. To determine the mechanism by which hydrogen gas inhibits the silylation reaction, Complex **1** generated *in situ* was treated with one atmosphere of H_2.

The ^{1}H NMR spectrum of this solution at –86 °C contains peaks that are different from those in the spectrum acquired under nitrogen. Under nitrogen, a single hydride peak that integrates to one proton is observed at -16 ppm. Under hydrogen and at –86 °C, two sharp peaks corresponding to metal hydrides, which integrate to one and two protons, were observed at –2.7 ppm and at –18.4 ppm. The peak at –2.7 ppm contains satellites from coupling to ^{29}Si ($J_{H–Si}$ = 61 Hz). This coupling constant and the downfield chemical shift of this peak, relative to that of the other hydride, indicate that this resonance corresponds to the proton of a silane σ-complex.[16] Thus, we assign complex **2** as an iridium complex bearing a phenanthroline unit, two hydride ligands, a silyl ligand, and an Si–H-bound silane (Scheme 4.3). This complex is the second, minor species

formed from the combination of $[Ir(cod)(OMe)]_2$, 2,9-Me_2phen, and excess heptamethyltrisiloxane discussed earlier in this section.

Scheme 4.3 Synthesis of Iridium Dihydride Complexes

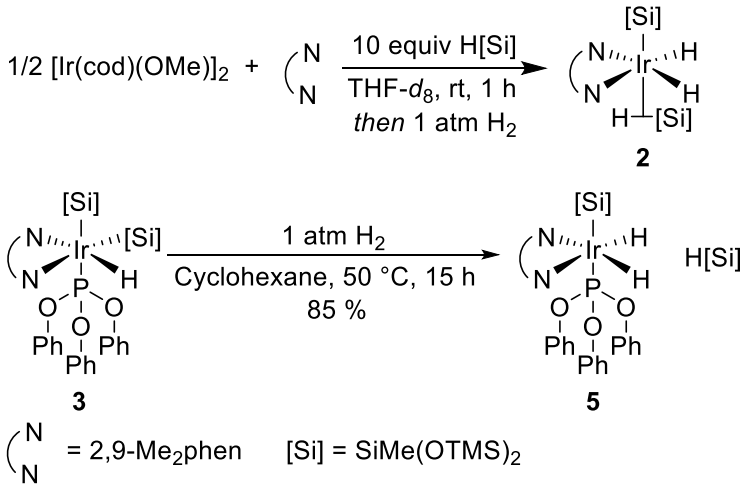

The formation of σ-silane complex **2** in the presence of hydrogen implies that the inhibition of the catalytic silylation reaction by hydrogen gas results from a difference in the resting state of the catalyst in the presence and absence of hydrogen. Complex **1** contains an open coordination site that binds the C–H bond of an arene, whereas complex **2** is coordinatively saturated and must dissociate silane or hydrogen to react with an arene.

To further assess the effect of hydrogen gas on the iridium complexes formed from silane phosphite adduct **3** was allowed to react with hydrogen gas (Scheme 4.3). The reaction of **3** with 1 atm of H_2 formed complex **5**, which contains two hydrides and one silyl group, in addition to the phosphite. This complex was characterized by ^{1}H, ^{13}C and ^{31}P NMR spectroscopy. The identity of **5** was clear from the doublet at –19 ppm in the ^{1}H NMR spectrum integrating to two hydrogens and the triplet at 108 ppm in the ^{31}P NMR spectrum.

4.2.2 Reactivity of Isolated Iridium Complex

To assess the relevance of the iridium complexes bearing phenanthroline, hydride, and silyl ligands to the silylation of C–H bonds phosphite-adduct **3** was allowed to react with a series of arenes. Reaction of **3** with 2-Cl-thiophene conducted in the presence of varied amounts of triphenyl phosphite showed that this reaction is inverse first order in the concentration of phosphite (see experimental section for details). These data indicate that **3** reacts with arenes after initial reversible dissociation of the phosphite ligand.

The reaction of phosphite-ligated disilyl hydride **3** with 3-Cl-thiophene produced a 2.8 to 1 ratio of the two isomeric thienyl silanes **6** and **7** from the silylation of the C–H bonds alpha to sulfur (Scheme 4.4). The catalytic reaction of heptamethyltrisiloxane with 3-Cl-thiophene in the presence of the combination of $[Ir(cod)(OMe)]_2$ and 2,9-Me_2phen also produced **6** and **7** in the ratio of 2.8 to 1. These identical ratios imply that the catalytic silylation occurs through the five-coordinate disilyl monohydride complex **1** formed by dissociation of phosphite and imply that the observed resting state **1** lies directly on the catalytic cycle.

Iridium complex **3** reacted with both electron-rich and electron-poor deuterated arenes to produce deutero-aryl silanes (Scheme 4.5). The reaction of *o*-xylene-d_4 with **3** produced deutero-

aryl silane **8** and iridium complex **5** that contains a mixture of hydride and deuteride ligands. At partial conversion of complex **3**, ^{1}H NMR spectroscopy indicated the lack of exchange of deuterium into the hydride position of **3**. This result implies that cleavage of the C–D bond of electron rich arene *o*-xylene-d_4 is effectively irreversible, due to faster formation of the Si-C bond from the aryliridium complex than reformation of the C-H bond.

Scheme 4.4 Reactions of **3** or Silane with Heteroarene

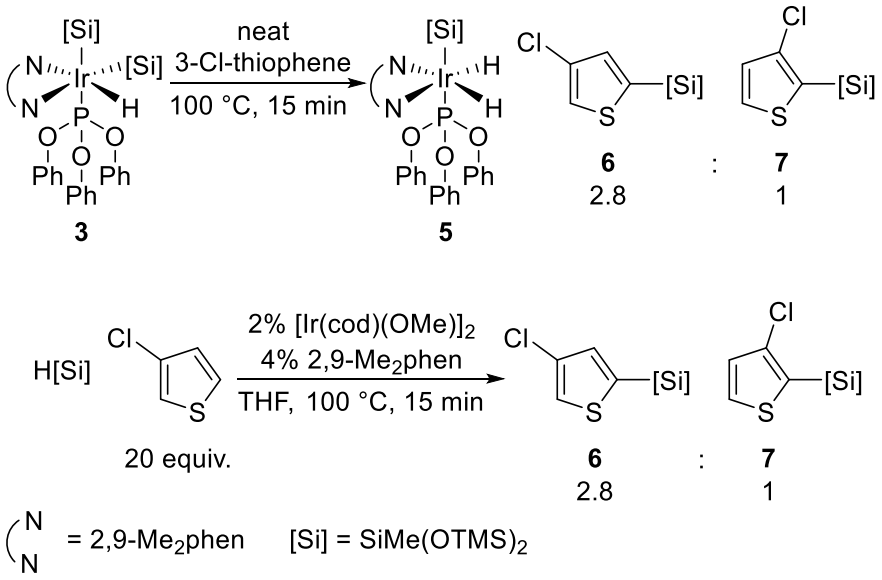

In contrast, the reaction of **3** with the electron poor deutero-arene *o*-Cl_2-benzene-d_4 led to exchange of deuterium into **3.** The reaction of **3** with *o*-Cl_2-benzene-d_4 produced deutero-aryl silane and complex **5** containing a mixture of hydride and deuteride ligands. However, at partial conversion of complex **3** to product, ^{1}H NMR spectroscopy indicated significant substitution of

deuterium from the arene for the hydride of **3**. These results indicate that the cleavage of the C–D bond of electron poor arene Cl_2-benzene-d_4 is reversible.

Scheme 4.5 Reactions of 3 with Deuterated Arenes

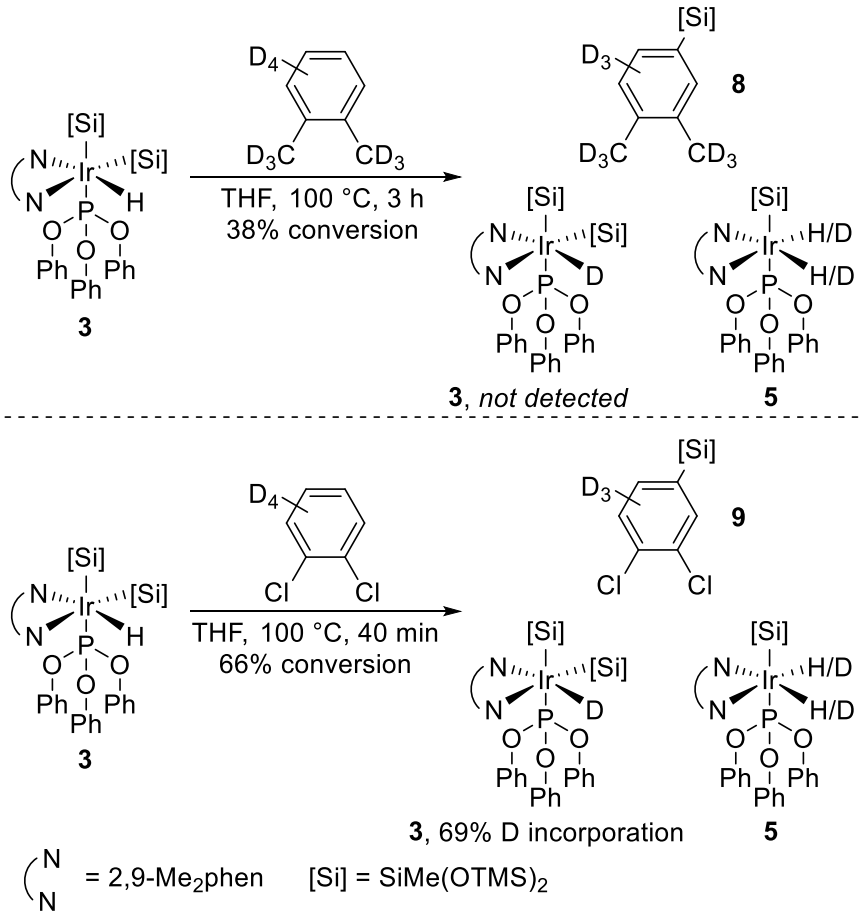

4.2.3 Kinetic Analysis of the Catalytic Process

The dependence of rate of the catalytic silylation reaction on the concentration of each reagent was measured to reveal the rate limiting step of the catalytic process. The reaction orders in silane, catalyst, and arene were determined by measuring initial rates of the silylation reaction at 60-100 °C with varied concentrations of each reagent. Reactions with concentrations of catalyst ranging from 1.25 mM to 10 mM showed that the reaction is first order in catalyst. Reactions with concentrations of silane varying from 0.5 M to 4 M showed that the reaction is zero order in silane (see experimental section for details).

The order in arene depended on the electronic character of the C–H bonds of the arene. The rates of reactions of silane with an electron-poor arene, methyl 3-CF_3-benzoate, and an electron rich arene 1,3-$(OMe)_2$-benzene were determined (see experimental section for details). Reactions conducted with concentrations of methyl 3-CF_3-benzoate varying from 0.25 M to 2 M were first order in the concentration of arene.

However, the order of the reaction in the electron-rich arene, 1,3-$(OMe)_2$-benzene, was not straightforward. The increase of rates of reactions conducted with concentrations of 1,3-$(OMe)_2$-benzene varying from 0.25 M to 2 M in an open system diminished as the concentration of 1,3-

$(OMe)_2$-benzene increased (Figure 4.2, top). We hypothesized that this saturation of the rate resulted from a change in resting state from five-coordinate **1** to a complex with arene bound at high concentrations of the arene. To test this hypothesis, we measured the rate of the same reaction in the presence of 0.2 equiv of 3,5-lutidine. We hypothesized that lutidine would bind iridium more tightly than an arene, prevent binding of the arene, and simplify the kinetic behavior. Indeed, reactions conducted with concentrations of 1,3-$(OMe)_2$-benzene varying from 0.25 M to 2 M in the presence of 3,5-lutidine were first order in 1,3-$(OMe)_2$-benzene (Figure 4.2, bottom). These results suggest that electron-rich arenes bind to the catalyst in the absence of strong Lewis bases.

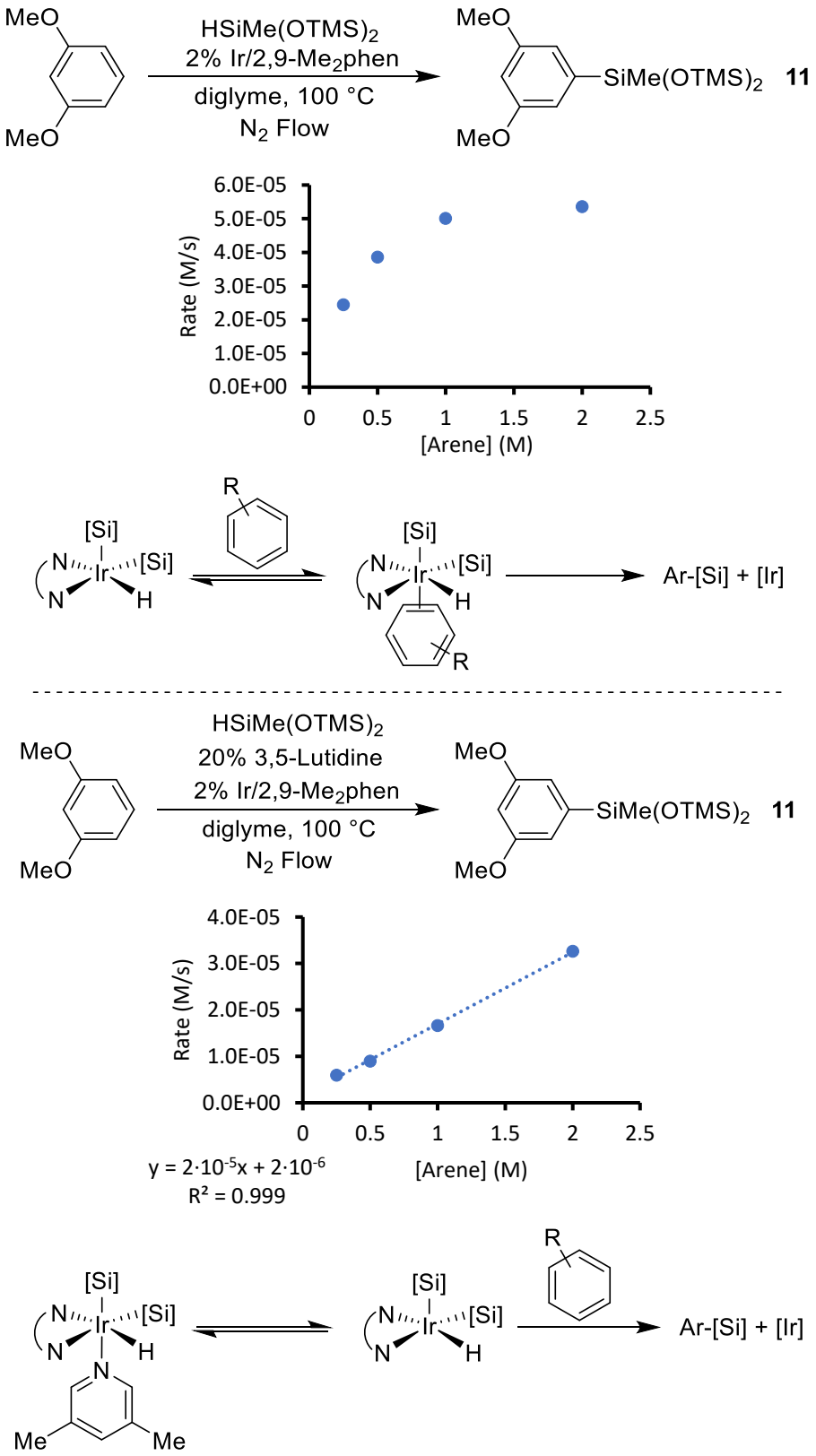

Figure 4.2 Dependence of Rate on Arene Concentration**.**

The kinetic isotope effect (KIE) of the catalytic process was measured for three electronically varied arenes to gain further information on the reversibility of the C–H bond cleavage (Figure 4.3). The rates of the reaction of the protio and deutero substrates were measured independently. A kinetic isotope effect of 3.2 was obtained from the rate of formation of silylarene from *o*-xylene and *o*-xylene-d_4 side by side ($7.3\cdot10^{-5}$ and $2.3\cdot10^{-5}$ M/s). This KIE is similar in magnitude to those measured for the borylation of protio and deutero *o*-Cl_2-benzene catalyzed by an Ir(III) boryl complex (KIE = 3.3).[17] Based on these data, C–H bond cleavage of the arene is irreversible and rate limiting for the silylation of electron-rich arenes. These data are consistent with the observed irreversibility of C–H bond cleavage of *o*-xylene-d_4 by complex **3** (*vide supra*).

The KIEs measured for reactions of electron-poor and electron-neutral arenes were different from that observed for *o*-xylene. The KIE for the analogous silylation of benzene and benzene-d_6 was reported previously to be 1.3.[4b] The KIE from the rate of formation of silylarene from *o*-Cl_2-benzene and *o*-Cl_2-benzene-d_4 side by side was 1.6 ($k_H = 6.3\cdot10^{-5}$, $k_D = 3.9\cdot10^{-5}$ M/s). These KIE values are smaller than that of the reaction of electron-rich *o*-xylene and do not suggest that the KIE is primary and resulting from rate-limiting C–H bond cleavage. Instead, these data are more consistent with reversible C–H bond cleavage during reactions of electron-poor or electron-neutral substrates. Such equilibrium isotope effects suggest that reductive elimination of the C–Si bond is rate-limiting for reactions of electron-poor and electron-neutral arenes.

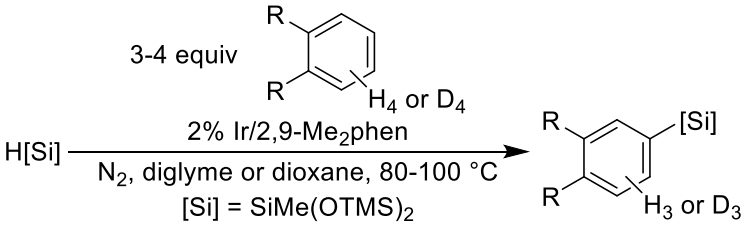

Independent Rates Kinetic Isotope Effect

R =	Cl	H	Me
KIE =	1.6	1.3[a]	3.2

Figure 4.3 Determination of kinetic isotope effects. [a]Ref 13

The low KIE values measured for the silylation of protiated and deuterated electron-neutral and electron-poor arenes indicate that the transition state for a step following cleavage of the C–H bond is the highest-energy transition state during the silylation of these arenes. This transition state could be the one for reductive elimination of the C–Si bond or for an isomerization of the Ir complex that results from addition of the C–H bond. Such an isomerization has been computed to occur during the borylation of benzylic methyl groups catalyzed by iridium complexes of phenanthroline ligands. On the basis of a modest, but positive ρ, value for the borylation of benzylic C–H bonds with different electronic character (ρ=2.1), that isomerization was concluded to be the rate-limiting step of the borylation of benzylic methyl groups.[18]

We considered that rate-limiting isomerization and rate-limiting reductive elimination could be distinguished by the effects of the electronic properties of the arene on the outcome of

the silylation reaction. If an isomerization of the Ir complex that results from addition of the C–H bond is the rate-limiting step, then the effect of the electronic properties of the arene on the silylation should be large because the starting material is a free arene and the transition-state for the rate-limiting step contains a metal-carbon bond. However, if reductive elimination is rate-limiting, then the effect of the electronic properties of the arene on the silylation should be smaller. The effect should be smaller because the amount of negative charge on the *ipso* carbon in the transition state for reductive elimination is less than that of the complex that immediately precedes reductive elimination.

A Hammett plot of the effect of the electronics of the arene on the rate of the silylation is shown in Figure 4.4. The ρ value for this plot is 1.3. This positive ρ value indicates the accumulation of negative charge on the *ipso* carbon in the transition state of the rate-limiting step of the reaction. The magnitude of this ρ value is inconsistent the values obtained from related borylation reactions that occur with rate-limiting cleavage of the C-H bond (ρ=3.3) or isomerization of the complex that results from oxidative addition (ρ=2.1).[18] Instead, the measured ρ value is most consistent with the silylation of electron-poor arenes occurring by reversible cleavage of the C–H bond followed by rate-limiting reductive elimination of the C–Si bond.

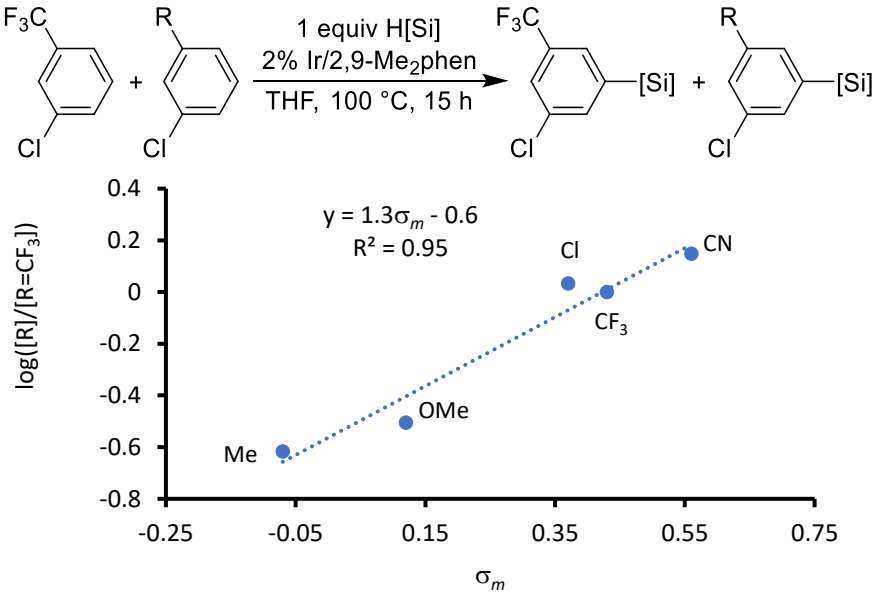

Figure 4.4 Hammett plot for silylation of arenes.

4.4 Proposed Catalytic Cycles

Based on the orders in arene, silane, catalyst, kinetic isotope effects, isolated adducts of the resting state, and iridium complexes observed in solution, we conclude that the iridium-catalyzed silylation of aromatic C–H bonds occurs by the catalytic cycle in Scheme 4.6. The silylation of electron-rich, electron-neutral, and electron-poor C–H bonds occurs by the same intermediate

iridium complexes, but reactions of these arenes differ in the rate-limiting step and the resting state of the catalyst.

Scheme 4.6 Proposed Catalytic Cycles for the Silylation of Electron-Rich or Electron-Poor Aromatic C–H Bonds

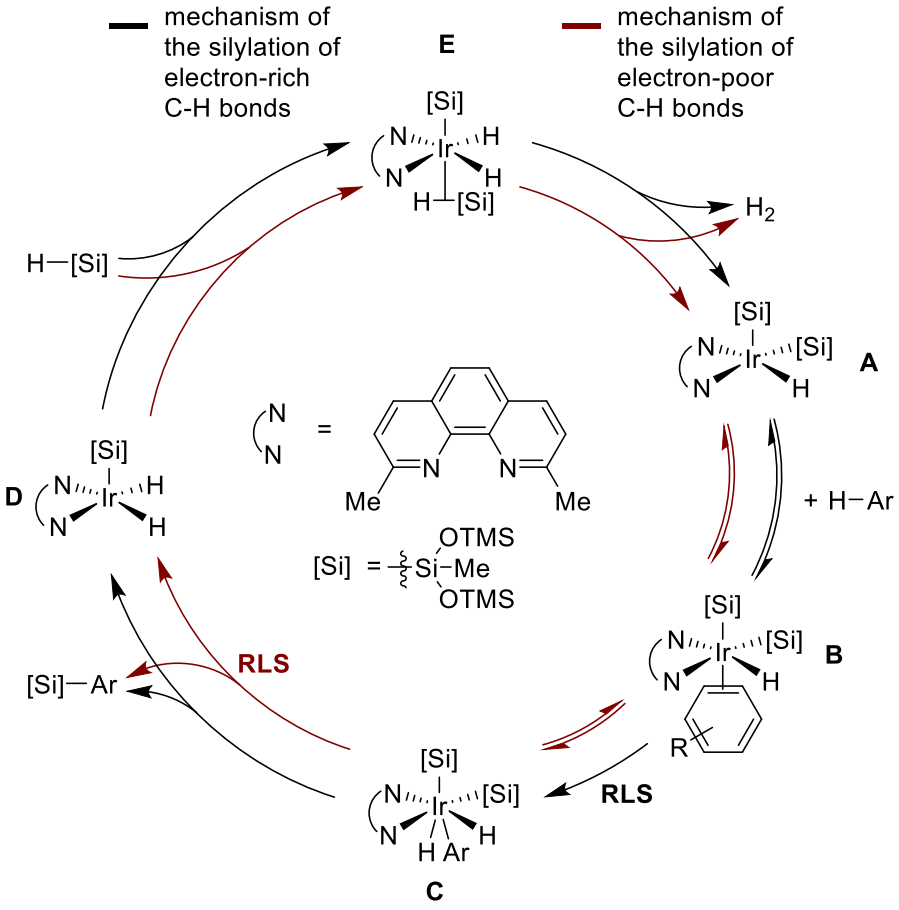

For reactions of electron-poor or electron-neutral arenes (Scheme 4.6, red), the resting state of the catalyst is the 5-coordinate iridium disilyl hydride complex (**A**). Complex **A** reversibly binds the arene to form complex **B**. Complex **B** undergoes reversible C–H bond cleavage to form an Ir(V) complex (**C**). Reductive elimination of the C–Si bond from **C** forms the aryl silane product and complex **D**. Complex **D** undergoes oxidative addition of the silane silane to produce complex **E**. For reactions conducted in an open system, complex **E** undergoes irreversible loss of H_2 to regenerate resting state **A**.

For reactions of electron-rich arenes (Scheme 4.6, black), the resting state of the catalyst is the coordinatively saturate arene-bound iridium disilyl hydride complex (**B**). Complex **B** undergoes irreversible and rate-limiting C–H bond cleavage to form complex **C**. Reductive elimination of a C–Si bond from **C** forms aryl silane product and complex **D**. Complex **D** undergoes oxidative addition of the silane and reductive elimination of H_2 to generate the

coordinatively unsaturated complex **A**. **A** binds arene to regenerate the resting state of the catalyst, **B**.

4.5 Origin of Selectivity

The silylation of *o*-Cl_2-benzene-d_4 provided information on the origin of the high selectivity for functionalization of the least sterically hindered C–H bond. During the silylation of *o*-Cl_2-benzene-d_4, the substitution of deuterium in the arene for hydrogen from the silane occurred sixty times faster than the silylation of the arene (Scheme 4.7). However, no incorporation of hydrogen is observed at the positions proximal to chlorine. These data demonstrate that the origin of high selectivity for the silylation of the least sterically hindered C–H bond in six-membered arenes is the high barrier to cleavage of the C–H bonds proximal to existing substituents.

This origin of selectivity contrasts with that we reported recently for the silylation of five-membered ring heteroarenes.[6] In our study of H/D exchange between the silane and these heteroarenes, the selectivity for H/D exchange at the least hindered C–H bond was lower than the selectivity for silylation at the least sterically hindered C–H bond. These data imply that the high selectivity for reactions of these less hindered substrates results from a slower rate for reductive elimination from a more hindered arylsilane than from a less hindered arylsilane.

Scheme 4.7 Observation of H/D Exchange Reaction

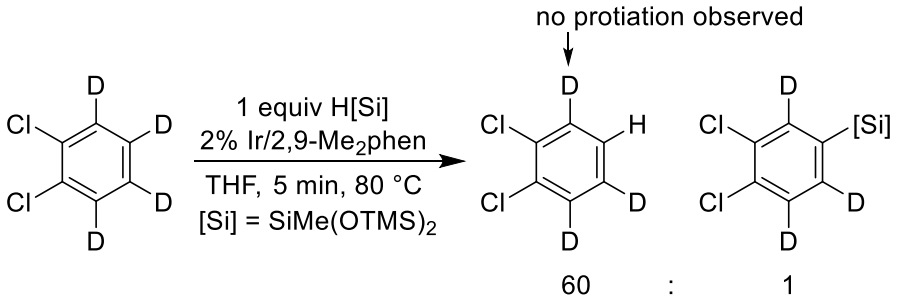

4.6 Computational Model of Reaction Mechanism

Experimental mechanistic studies enabled us to identify the iridium complexes that catalyze the silylation of aromatic C–H bonds and probe some of the elementary steps of the reaction. However, our experiments did not reveal why complexes containing two silyl ligands and one hydride ligand formed in the reaction, rather than complexes containing three silyl ligands. Our structural data from single-crystal X-ray diffraction of the disilyl hydride complex **3** began to show the severe steric hindrance that would be created by replacing the hydride with a third silyl group. The related iridium-catalyzed borylation reaction occurs by generation of triboryl compounds containing a phenanthroline or bipyridine ligand and reaction of this complex with arenes.[17] The similarities in conditions and catalysts for the silylation and borylation reactions alone make it unclear why iridium complexes that contain three silyl ligands do not form during the silylation reaction and react with arenes.

However, our experimental studies do not reveal why the silylation reaction is faster with catalysts containing more sterically encumbered ligands. Like the difference in number of main-group ligands on the metal, this trend is not observed for the borylation of aromatic C–H bonds. One might imagine that the sterically encumbered 2,9-Me_2phen could make low coordinate, Ir(I) silyl complexes thermodynamically accessible. We sought to use computational modelling to

assess the effect of the sterics of the phenanthroline ligand on which iridium species form and the rates with which they react with the C–H bonds of arenes.

To understand the importance of the identity of the ancillary ligands on the rate and outcome of the reaction, we modeled iridium silyl complexes ligated by 3,4,7,8-tetramethylphenanthroline (Me_4phen, **L2**) and by the sterically encumbered 2,9-Me_2phen. We chose to simplify our model of the silane from $SiMe(OTMS)_2$ to $SiMe(OMe)_2$ (henceforth abbreviated as "[Si]") to reduce the required computational time. Geometry optimizations of each structure were conducted with the Gaussian 09 software package, B3LYP functional (with gd3 dispersion correction), and LANL2DZ basis set for Ir and 6-31g(d,p) basis set for all other atoms. The energy of each geometry optimized structure was further refined with single-point energy calculations that were conducted with the PBE functional (with g2 dispersion correction) and LANL2TZ basis set for Ir and the 6-31++g** basis set for all other atoms, along with the SMD THF solvent correction. This combination of basis set and functional was identified as particularly accurate by Hopmann for reactions of complexes of iridium.[19]

To assess whether an Ir(I) silyl complex is a thermodynamically accessible intermediate in the catalytic cycle of this reaction, we modelled the thermodynamics of the addition of two molecules of silane to (L)Ir[Si] complexes (L = Me_4phen or 2,9-Me_2phen) to produce (L)Ir$[Si]_3$ complexes and one molecule of hydrogen (Figure 4.5). (**L2**)Ir[Si] and two molecules of silane was found to be 62 kcal/mol higher in energy than (**L2**)Ir$[Si]_3$ and hydrogen. Because the Me_4phen-Ir(I) species lies uphill of Ir(III)-silyl complexes in the presence of silane by such a large amount of energy, Ir(I) intermediates are unlikely to be part of the catalytic cycle.

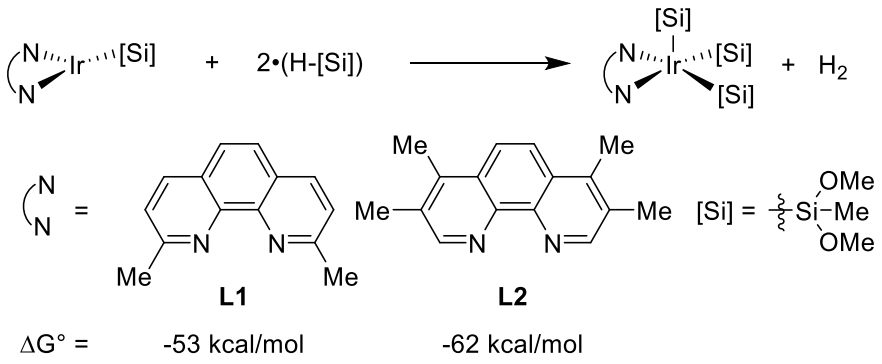

Figure 4.5 Computed energies for formation of Ir(III) complexes from Ir(I) complexes.

However, it is possible that the two methyl groups ortho to the nitrogen atoms in 2,9-Me_2phen would destabilize Ir(III) intermediates. Thus, we calculated the thermodynamics for the same equation with 2,9-Me_2phen as ligand. While less uphill, the reaction of (**L1**)Ir[Si] with two molecules of silane to form (**L1**)Ir$[Si]_3$ and H_2 remains exergonic by 53 kcal/mol. This result shows that the Ir(I) complex ligated by 2,9-Me_2phen remains too far uphill thermodynamically to be a plausible intermediate in the catalytic reaction.

We modeled six Ir(III) complexes that are potential intermediates in the silylation of aromatic C–H bonds: (ligand)Ir$[Si]_3$, (ligand)Ir$[Si]_2$H, and (ligand)Ir[Si]H_2 (Figures 4.6 and 4.7). Each complex was modelled with 2,9-Me_2phen (**L1**) or Me_4phen (**L2**) as ligand and was posed in a square pyramidal geometry with a silyl group in the axial position. This disposition of silyl and hydride ligands is based on the observed solid-state structure of complex **3**, most sterically accessible geometry, and strong trans influence of a silyl ligand.[20] For each combination of silyl

and hydride ligands, we also modelled the transition state for cleavage of the C–H bond of benzene to the iridium and the ground-state energy of the seven-coordinate Ir(V) complex that is the product of this reaction (Figures 4.9 and 4.10).

For iridium complexes ligated by Me_4phen, we found that the addition of silane to (**L2**)Ir[Si](H)$_2$ to form hydrogen and (**L2**)Ir[Si]$_2$(H) is exergonic by 9 kcal/mol (Figure 4.6). The addition of silane to (**L2**)Ir[Si]$_2$(H) to form hydrogen and (**L2**)Ir[Si]$_3$ is exergonic by a further 4 kcal/mol. These results predict that (**L2**)Ir[Si]$_3$ would be the resting state of a C–H silylation reaction catalyzed by the combination of iridium precatalyst and Me_4phen. This predicted resting state contains a different number of silyl and hydride ligands than the observed resting state of reactions catalyzed by iridium complexes containing the more sterically encumbered 2,9-Me_2phen ligand (complex **1**).[21]

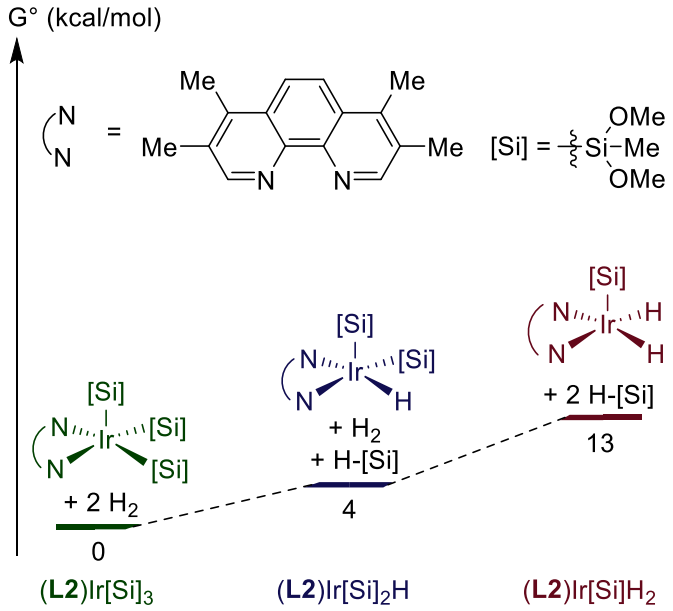

Figure 4.6 Computed energies of Ir(III) complexes of Me_4phen and silyl and hydride Ligands.

The thermodynamics of the ground-state iridium complexes ligated by 2,9-Me_2phen were much different from those of the complexes ligated by tmphen. For iridium complexes ligated by 2,9-Me_2phen, the addition of silane to (**L1**)Ir[Si](H)$_2$ to form hydrogen and (**L1**)Ir[Si]$_2$(H) was computed to be exergonic by only 3 kcal/mol (Figure 4.7). This value is 6 kcal/mol less favorable than that for the reaction of silane with (**L2**)Ir[Si](H)$_2$, in which the complex contains an unhindered ligand, Me_4phen. Moreover, the addition of silane to (**L1**)Ir[Si]$_2$(H) to form hydrogen and (**L1**)Ir[Si]$_3$ was computed to be endergonic by 3 kcal/mol. This value is 7 kcal/mol less favorable than that for the reaction of silane with (**L2**)Ir[Si](H)$_2$, in which the complex contains the unhindered ligand, Me_4phen and suggests that (**L2**)Ir[Si]$_2$(H), not the trisilyl analog will be the resting state of a C–H silylation reaction catalyzed by the combination of iridium precatalyst and

2,9-Me_2phen. This computational prediction is consistent with the experimentally observed observation of complexes **1** and **3** in the catalytic and stoichiometric reactions.

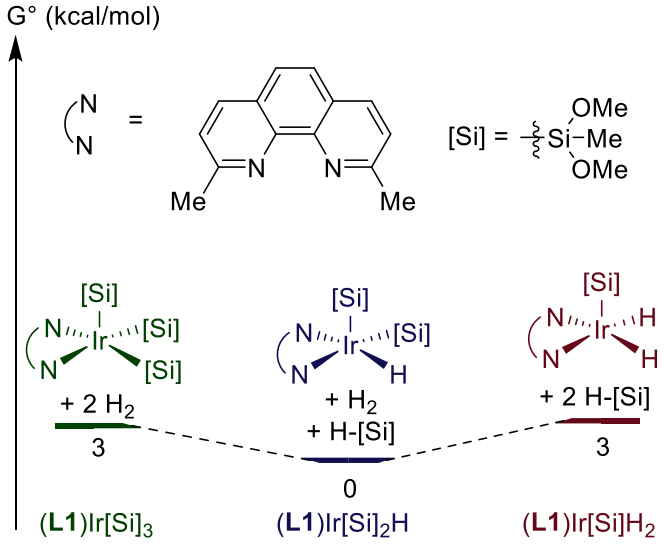

Figure 4.7 Computed energies of Ir(III) complexes of 2,9-Me_2phen and silyl and hydride ligands.

The geometry of (**L1**)Ir[Si]$_3$ is different from that of the other Ir(III) complexes we computed. For all complexes except (**L1**)Ir[Si]$_3$, the plane of the phenanthroline ligand lies in the same plane as the basal plane of the iridium complex. In contrast, for (**L1**)Ir[Si]$_3$, the phenanthroline ligand lies 64° out of the basal plane of the iridium complex (Si(1)-N(1)-C(3) = 116°), causing the methyl groups to lie further from the silyl substituents (Figure 4.8). For comparison, this distortion is 16° for (**L1**)Ir[Si]$_2$(H) and 7° for (**L2**)Ir[Si]$_3$. A comparison of the structures of (**L1**)Ir[Si]$_3$ to that of (**L1**)Ir[Si]$_2$(H) and (**L2**)Ir[Si]$_3$ shows that the distortions of the

ligand in (**L1**)Ir[Si]$_3$ reduce clashes between the methyl groups of the ligand and the silyl groups. This distortion hinders approach of the arene to the open coordination site of the iridium complex.

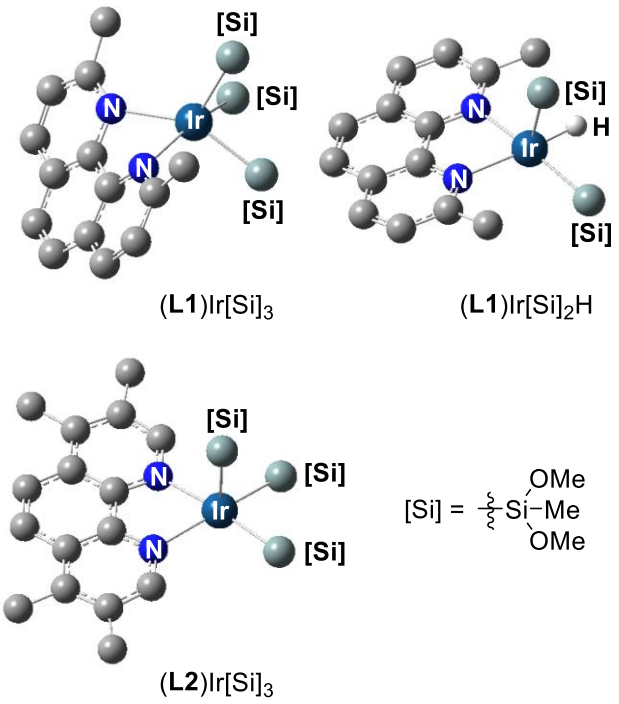

Figure 4.8 Computed structures of Ir(III) complexes. Silyl groups are truncated for visual clarity.

We also computed the transition state for cleavage of the C–H bond. This process is best described as an oxidative addition to form an iridium(V) complex containing a hydride and aryl unit. However, the addition to related boryl complexes occurs with association of the hydrogen of the C–H bond to the boryl group and addition of the silane occurs with partial association of the silane with the same hydrogen. This process resembles a σ-CAM mechanism, but the resulting Ir complex is better described as an Ir(V) complex than an Ir(III) silyl complex. More details on these relationships will be published elsewhere, but the Si–H bond order determined by NBO analysis in the transition state and product are 0.1 and 0.2. Previously, iridium complexes with bond orders of this magnitude between a hydride and silyl group have been assigned as iridium silyl complexes, rather than iridium silane complexes.[22] The computed bond order of classic Mn silane complexes were greater than 0.3.[23]

The barrier to oxidative addition of benzene to the Ir(III) silyl complexes depended on the number of silyl and hydride ligands. Addition to (**L2**)Ir[Si](H)$_2$ (**L2**= Me$_4$phen) was computed to be just 14 kcal/mol, that to oxidative addition to (**L2**)Ir[Si]$_2$(H) to be 18 kcal/mol and that to oxidative addition to (**L2**)Ir[Si]$_3$ to be 23 kcal/mol (Figure 4.9). Thus, each substitution of a small hydride ligand for a bulky silyl ligand led to a 4-5 kcal/mol increase in the barrier to C–H activation. These results show that a catalyst containing fewer silyl ligands and more hydride ligands cleaves C–H bonds with higher rates than a catalyst containing more silyl ligands and fewer hydride ligands.

The computed relative energies of the barriers to oxidative addition of the C–H bond of benzene to 2,9-Me$_2$phen-ligated iridium complexes were different than those to oxidative addition to Me$_4$phen-ligated complexes. The barrier to oxidative addition of the C–H bond of benzene was

computed to be 17 kcal/mol for both (**L1**)Ir[Si]$_2$(H) and (**L1**)Ir[Si](H)$_2$ (Figure 4.10). In contrast, we could not even locate a transition state geometry for the oxidative addition of the C–H bond of benzene to (**L1**)Ir[Si]$_3$; attempts to model this transition state showed that the open coordination site was too hindered to accommodate approach of benzene to the Ir center. These calculations corroborate our conclusion that the resting state of C–H silylation reactions catalyzed by the combination of iridium and 2,9-Me$_2$phen contains two silyl ligands and one hydride and that C–H bond cleavage occurs by oxidative addition to this species. These results also are consistent with the experimentally observed reactivity of isolated complex **3** with arenes and heteroarenes.

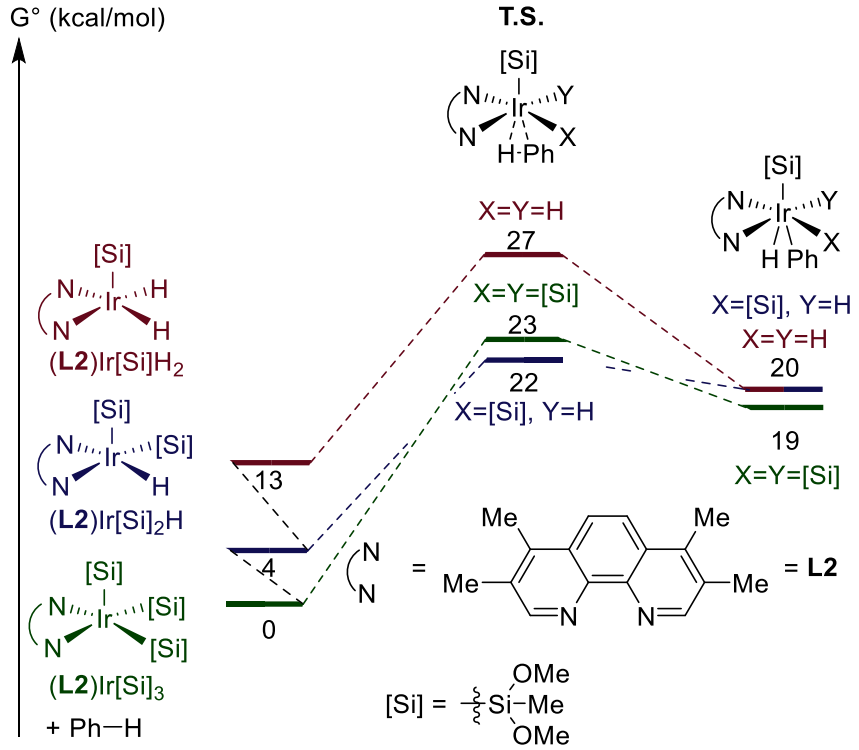

Figure 4.9 Computed energies of barriers to oxidative addition of benzene to Ir(III) complexes of Me$_4$phen.

The calculated free energy of activation for oxidative addition of the C–H bond of benzene to (**L1**)Ir[Si]$_2$(H) (17 kcal/mol) is lower than the experimental value of 27 kcal/mol for the catalytic process. However, this difference likely results from the difference in the silane used in the calculations. The silane used, HSiMe(OMe)$_2$, contains alkoxy substituents that are much smaller than the siloxy substituents in the heptamethyltrisiloxane used in the catalytic reaction. It is likely that the larger silyl groups present in the catalytic reaction would hinder the approach of the arene to the Ir center and increase the barrier to oxidative addition. Indeed, the calculated free energy of activation for oxidative addition of the C–H bond of benzene to complex **1** is 21 kcal/mol. While

lower than the experimental value, this calculated barrier is more consistent with the observed rates of the catalytic reaction.

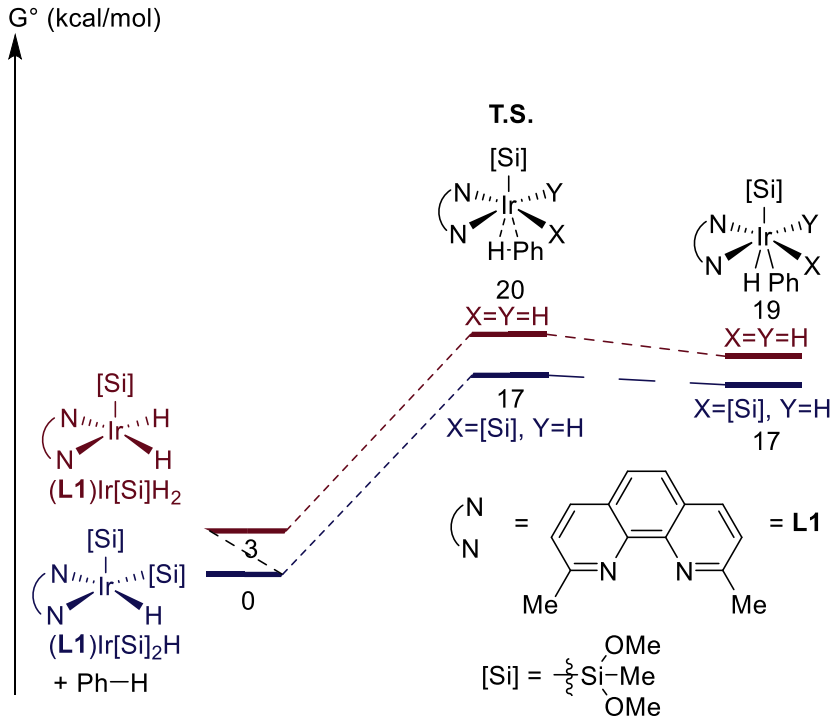

Figure 4.10 Computed energies of barriers to oxidative addition of benzene to Ir(III) complexes of 2,9-Me_2phen.

To understand the full catalytic cycle, we modelled other iridium complexes that are intermediates in the catalytic process, including the transition-state geometry for the carbon-silicon bond-forming reductive elimination and the Ir(V) complex that contains two silyl ligands and three hydride ligands. The barrier to reductive elimination of the phenylsilane derivative from (**L1**)Ir[Si]$_2$(H)$_2$(Ph) lies 17 kcal/mol higher in energy than the combination of (**L1**)Ir[Si]$_2$(H) and benzene (Figure 4.11, left). This barrier to reductive elimination to form the C-Si bond is almost identical to the barrier to oxidative addition of the C–H bond. The similarities in the barriers for oxidative addition of the C–H bond of benzene and reductive elimination of the C–Si bond of the phenylsilane derivative are consistent with the experimental observation that differences in the electronic properties of the arene can cause the oxidative addition of the C–H bond or the reductive elimination to be the step with the highest-energy transition state or "rate-limiting step."

The energies of the products of reductive elimination, (**L1**)Ir[Si](H)$_2$ and the phenylsilane derivative, are 7 kcal/mol higher than those of the starting molecules, (**L1**)Ir[Si]$_2$(H) and benzene. The energy of (**L1**)Ir[Si]$_2$(H)$_3$, and the phenylsilane derivative is 1 kcal/mol lower than the energy of (**L1**)Ir[Si]$_2$(H), silane and benzene. (**L1**)Ir[Si]$_2$(H)$_3$, which is similar to the observed iridium complex with one silyl, two hydride, and one silane ligands (complex **2**), is calculated to be 5 kcal/mol more stable than (**L1**)Ir[Si]$_2$(H) and H_2. The overall reaction of benzene with silane to form the phenylsilane derivate and H_2 is computed to be 4 kcal/mol uphill in free energy at standard state. These results suggest that the experimental observation that continuous removal of hydrogen from the reaction is necessary to obtain high rates and yields of aryl silane formation is due to the

unfavorable thermodynamics of the overall process and is manifested in the unfavorable regeneration of resting state complex **1** from hydrogen adduct **2** in a closed system.

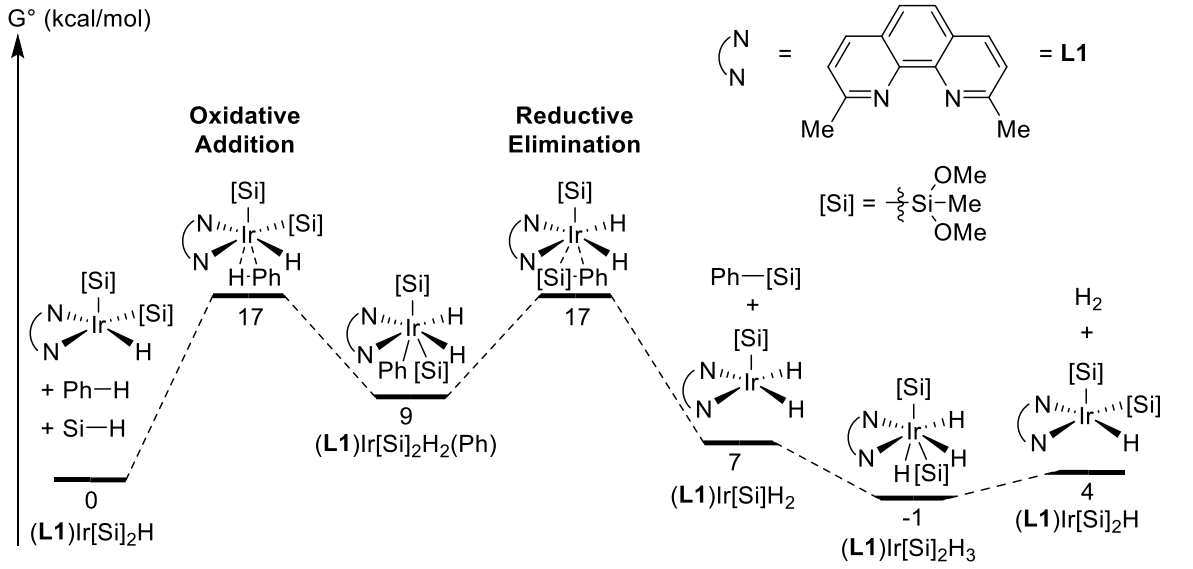

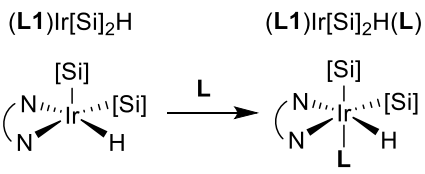

Ligand (**L**)	ΔG° (kcal/mol)
Pyridine	-9.2
1,3-$(OMe)_2$-Benzene	-3.5
Benzene	-1.0
Dioxane	-0.4
Diethyl Ether	+1.8

Figure 4.11 Computed energies for silylation of benzene and energies of binding of ligands to (**L1**)Ir[Si]$_2$H.

The potential catalyst resting states that were modelled are all five-coordinate iridium complexes with an open coordination site. Having identified the most stable combination of silyl and hydride ligands, we modelled complexes of (**L1**)Ir[Si]$_2$(H) with, 1,4-dioxane, Et$_2$O, benzene, 1,3-(OMe)$_2$-benzene, or pyridine as a sixth ligand. We found that the difference in the free energy of (**L1**)Ir[Si]$_2$(H)(**L**) and of the combination of (**L1**)Ir[Si]$_2$(H) and **L** was small for Et$_2$O, dioxane and benzene (Figure 4.11, bottom). However the free energy of (**L1**)Ir[Si]$_2$(H)(**L**) was significantly lower than that of (**L1**)Ir[Si]$_2$(H) and **L** for **L**=1,3-(OMe)$_2$-benzene and pyridine (-3.5 and -9.2 kcal/mol respectively). These results predict that electron-rich arenes and pyridines should be bound to iridium in the resting state of the catalyst, and this prediction is consistent with the observation of signals in the ^{1}H NMR spectrum of the solution of Ir, silane, 2,9-Me$_2$phen and the pyridine indicating that the pyridine binds to iridium and the saturation of the rates of the reactions of electron rich arene, 1,3-(OMe)$_2$-benzene as a function of the concentration of arene.

The computational model described here suggests that the rate of oxidative addition of aromatic C–H bonds is slower to iridium complexes that contain more bulky silyl ligands and fewer small hydride ligands than to complexes that contain fewer silyl ligands and more hydride ligands. The substituents ortho to nitrogen on the phenanthroline ligand prevent the formation of Ir complexes containing three silyl ligands that are the least reactive. This destabilization of the Ir complex containing three silyl ligands changes the resting state of the reaction from a trisilyl complex with the less hindered tmphen ligand to an iridium complex containing two silyl ligands and one hydride with the more hindered 2,9-Me$_2$phen ligand. This complex undergoes more rapid oxidative addition of C–H bonds than the corresponding iridium complex that contains three silyl groups.

4.3 Conclusion

At the outset of this study, no experimental data had been published on iridium complexes that are likely intermediates in the silylation of aromatic C–H bonds. Only computational studies were reported on the mechanism of the silylation of any type of C–H bond. Through the combination of high-resolution mass spectrometry, low-temperature NMR spectroscopy, and trapping experiments with several dative ligands, we showed that the resting state of the iridium catalyst to be (2,9-Me$_2$phen)Ir(SiMe(OTMS)$_2$)$_2$(H). By studying the reactions of deuterated arenes with an isolated iridium complex and silane in the catalytic reaction, we determined that C-H bond cleavage occurs to the five-coordinate, Ir(III) complex (2,9-Me$_2$phen)Ir(SiMe(OTMS)$_2$)$_2$(H). This C–H bond cleavage is the rate limiting step of the silylation of electron-rich arenes, and C–Si bond formation is the rate limiting step of the silylation of electron-neutral and electron-poor arenes. In addition, the combination of kinetic data and computational modelling revealed the propensity of electron-rich arenes to bind the catalyst. Finally, our computational model rationalizes the high rates observed for the silylation of arenes catalyzed by iridium complexes of sterically encumbered phenanthrolines. Steric clashes between the methyl groups on the phenanthroline and the silyl groups on Ir prevent the formation of the less reactive (**L1**)Ir[Si]$_3$ complexes and favor the formation of the more reactive (**L1**)Ir[Si]$_2$(H) complexes.

The mechanistic data described here provide a new model for understanding the silylation of C–H bonds. The knowledge that the catalyst contains an unsymmetrical disposition of silicon

and hydrogen ligands informs the design of ligands for new silylation reactions and lays the groundwork for a new generation of catalysts for the functionalization of C–H bonds that are currently being developed in our laboratory.

4.4 Experimental

Materials and Methods

All silylation reactions and syntheses of Ir complexes were assembled in an N_2-filled glovebox with oven-dried glassware unless otherwise noted. $[Ir(cod)OMe]_2$ was synthesized by following reported procedures.[24] 2,9-Dimethyl-1,10-phenanthroline (Me_2phen) was purchased from Alfa Aesar and was used as received. 1,1,1,3,5,5,5-Heptamethyl-trisiloxane was purchased from TCI and was used as received. All arenes, heteroarenes, triphenylphosphite, and hexamethyldisiloxane were purchased from Sigma-Aldrich and were degassed by purging with nitrogen. Diethyl ether, pentane, and tetrahydrofuran (THF) were degassed by purging with nitrogen and then dried with a solvent purification system containing activated alumina. Anhydrous degassed diglyme and dioxane were purchased from Sigma-Aldrich and used as received. Reaction temperatures above 23 °C refer to those of an aluminum heating block, which were controlled by an electronic temperature modulator. NMR spectra were recorded on Bruker AV-300, AVQ-400, AVB-400, AV-500, DRX-500 and AV-600 instruments. Chemical shifts (δ) are reported in ppm, relative to the residual solvent signal. Data from ^{1}H NMR spectra are reported as follows: chemical shift (multiplicity, coupling constants, number of hydrogens). Abbreviations are as follows: s (singlet), d (doublet), t (triplet), q (quartet), m (multiplet), br (broad). GC-MS data were obtained on an Agilent 6890-N GC system containing an Alltech EC-1 capillary column and an Agilent 5973 mass selective detector. High-resolution mass spectral data were obtained from the University of California, Berkeley Mass Spectrometry Laboratory. High resolution ESI-MS was acquired by Dr Zhongui Zhou. FT-IR data was collected on a Bruker VORTEX 80 FTIR spectrometer.

Observations of catalyst resting states

Observation of (2,9-Me$_2$phen)Ir(SiMe(OTMS)$_2$)$_2$H (1)

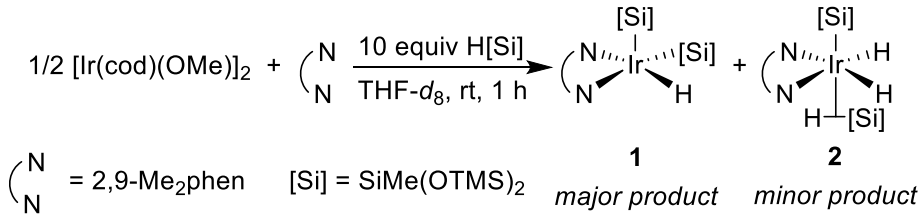

In an N$_2$-filled glovebox, [Ir(cod)(OMe)]$_2$ (13.3 mg, 0.0200 mmol), 2,9-Me$_2$phen (8.5 mg, 0.040 mmol), HSiMe(OTMS)$_2$ (0.1 mL), and THF-d_8 (0.4 mL) were added sequentially to a 4 mL vial. The vial was capped with a Teflon-lined screw cap, and the resulting solution was kept in the glovebox at room temperature for 1 h. This dark red solution was transferred to a J-Young NMR tube and analyzed by ^{1}H NMR spectroscopy at temperatures from -86 °C to room temperature. HRMS (ESI+), calculated for [$C_{28}H_{56}IrN_2O_4Si_6^+$]: 845.2479, found: 845.2473.

^{1}H NMR spectrum at room temperature:

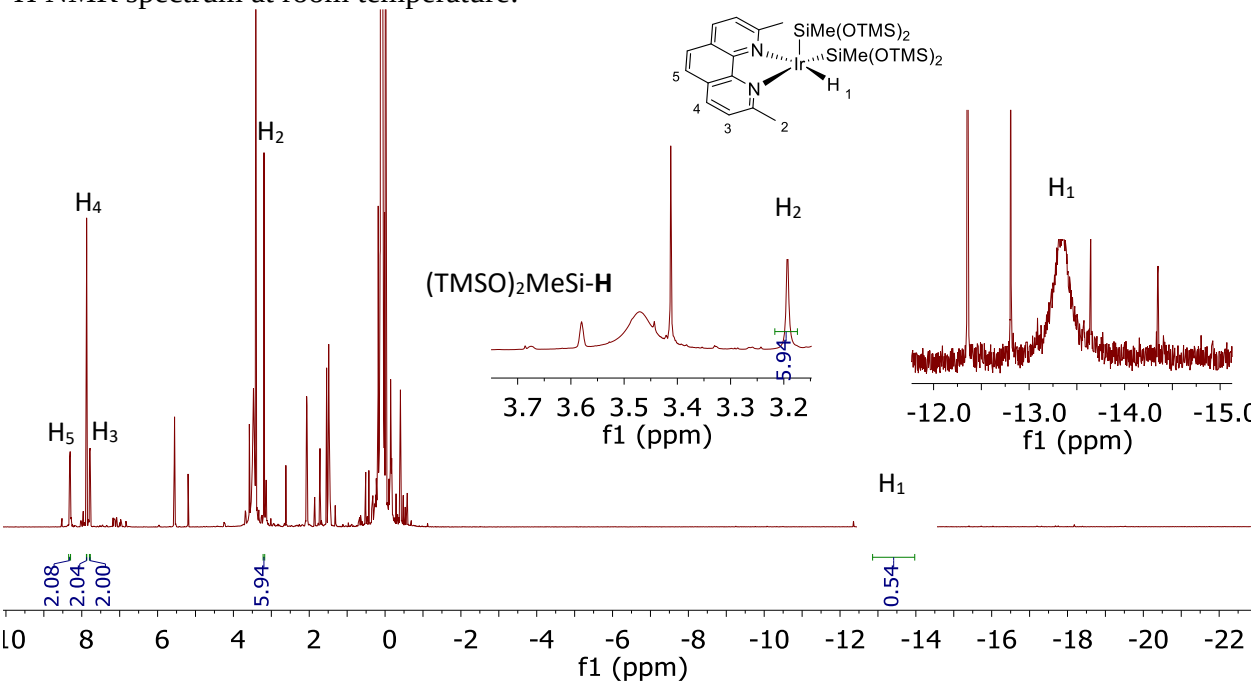

^{1}H NMR spectrum at -86 °C:

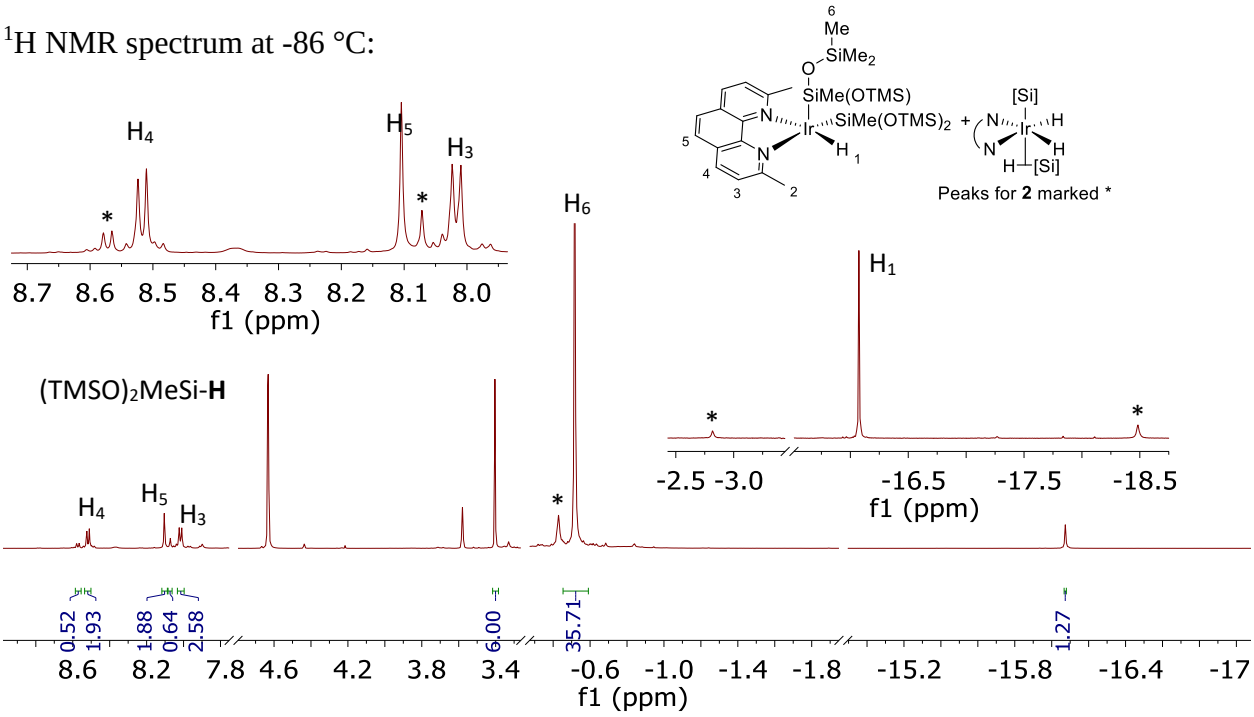

Note: The observation of equivalent protons for the silyl groups and for the two sides of the phenanthroline ligand indicate that the hydride and equatorial silyl group undergo rapid site exchange and that the two silyl groups also undergo rapid site exchange.

Observation of (2,9-Me$_2$phen)Ir(SiMe(OTMS)$_2$)$_2$H(HSiMe(OTMS)$_2$) (2)

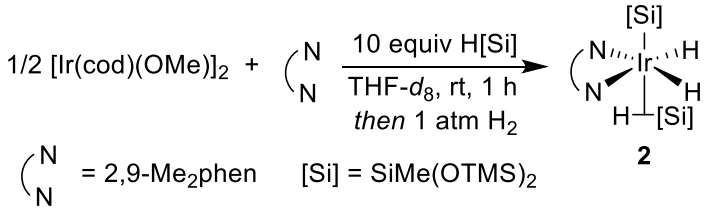

In an N_2-filled glovebox, [Ir(cod)(OMe)]$_2$ (13.3 mg, 0.0200 mmol), 2,9-Me$_2$phen (8.5 mg, 0.040 mmol), HSiMe(OTMS)$_2$ (0.1 mL), and THF-d_8 (0.4 mL) were added sequentially to a 4 mL vial. The vial was capped with a Teflon-lined screw cap, and the resulting solution was kept in the glovebox at room temperature for 1 h. This solution was transferred to a J-Young NMR tube, which was then removed from the glovebox. The J-Young NMR tube was connected to a Schlenk line. The solution was frozen by placing the NMR tube in a bath of liquid nitrogen, and the headspace of the J-Young tube was evacuated with high vacuum. The frozen solution was placed under static vacuum and allowed to thaw. The freeze-pump-thaw cycle was repeated once. The solution was frozen, and the headspace of the NMR tube was evacuated a third time. The headspace of the NMR tube was backfilled with 1 atm of H_2. The solution was allowed to thaw, and the NMR tube was inverted several times. On mixing, the color of the solution changed from dark red to dark yellow. The solution was analyzed by ^{1}H NMR spectroscopy at temperatures from -86 °C to room temperature.

^{1}H NMR spectrum at room temperature:

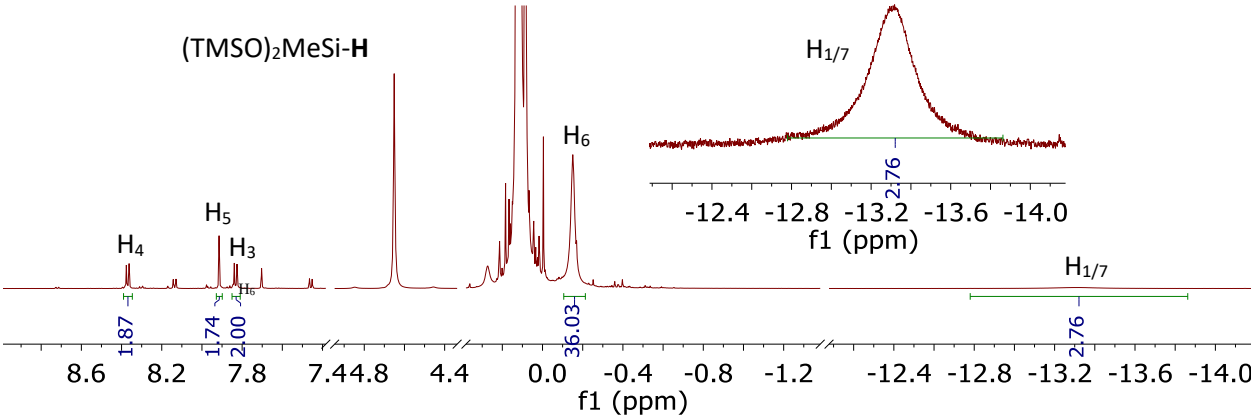

^{1}H NMR spectrum at -86 °C:

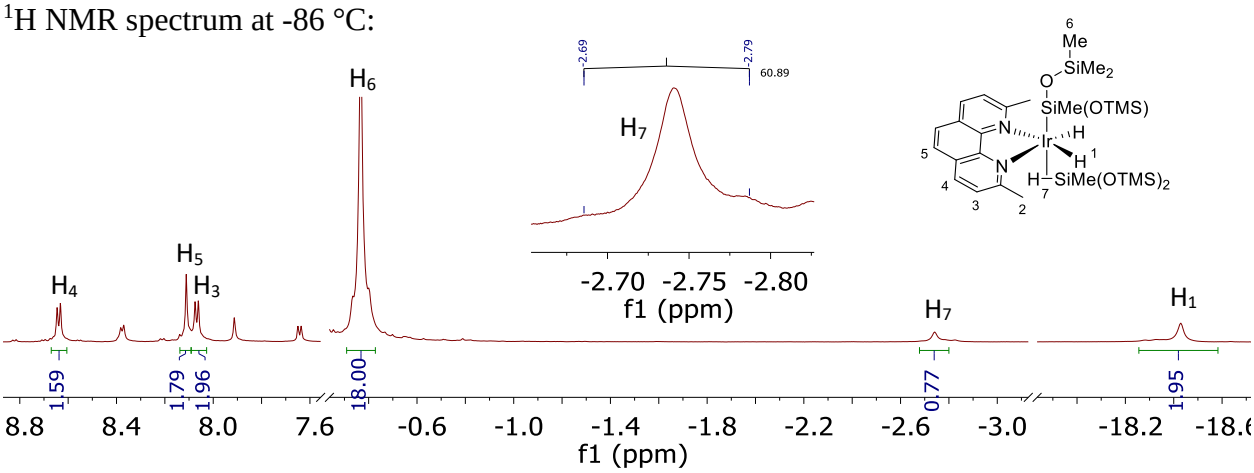

Observation of (2,9-Me$_2$phen)Ir(SiMe(OTMS)$_2$)$_2$H(DMAP) (4)

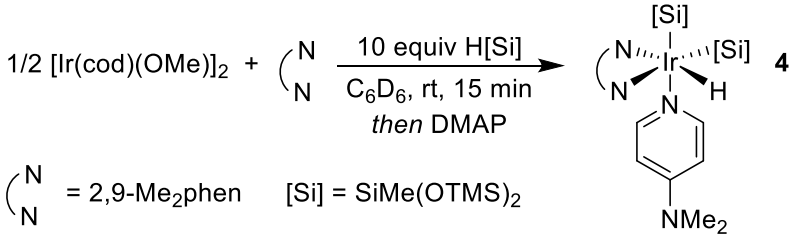

In an N_2-filled glovebox, [Ir(cod)(OMe)]$_2$ (13.3 mg, 0.0200 mmol), 2,9-Me$_2$phen (10 mg, 0.05 mmol), HSiMe(OTMS)$_2$ (0.2 mL), and C_6D_6 (0.4 mL) were added sequentially to a 4 mL vial. After 5 min, the dark red solution of Ir, ligand, and silane was added to a vial containing DMAP (20 mg, 0.2 mmol) and THF (10 µL). Upon mixing, the solution turned yellow. The vial was capped with a Teflon-lined screw cap, and the resulting solution was kept in the glovebox at room temperature for 15 min. The solution was transferred to a J-Young NMR tube and analyzed by ^{1}H NMR spectroscopy.

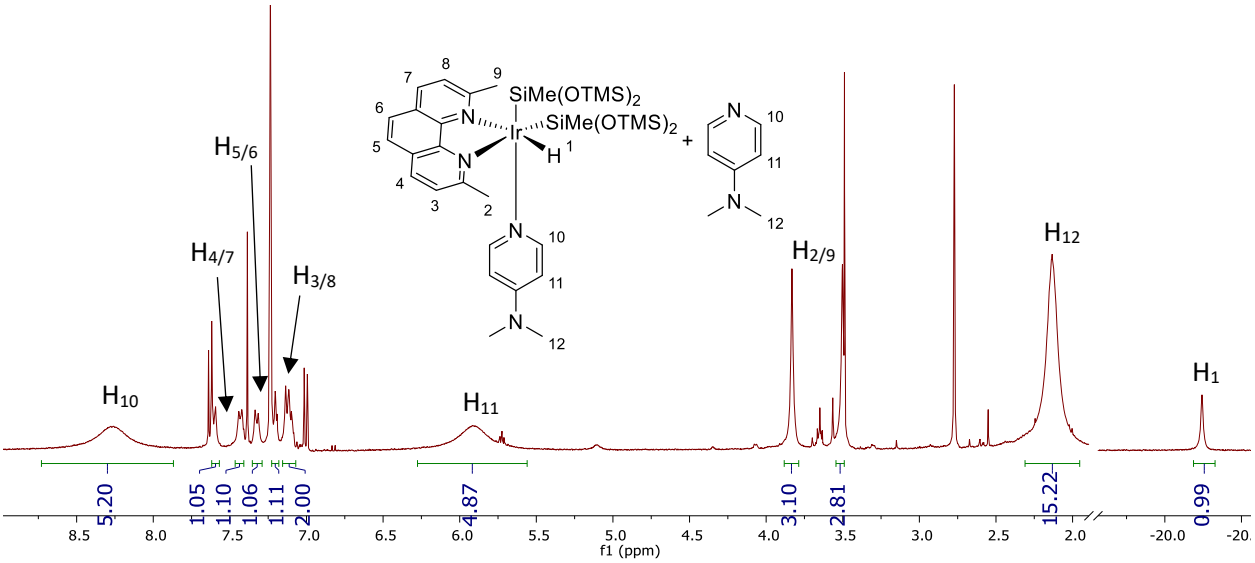

Observation of (2,9-Me$_2$phen)Ir(SiMe(OTMS)$_2$)$_2$H(3,5-lutidine)

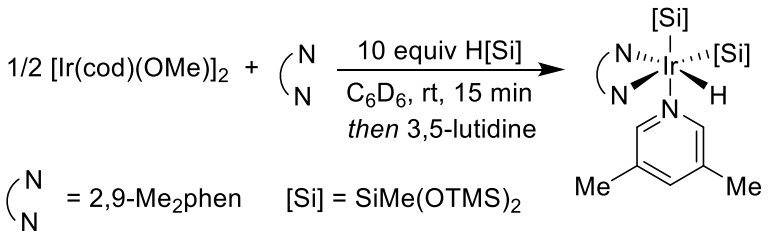

In an N_2-filled glovebox, [Ir(cod)(OMe)]$_2$ (13 mg, 0.020 mmol), 2,9-Me$_2$phen (11 mg, 0.050 mmol), HSiMe(OTMS)$_2$ (0.15 mL), and C_6D_6 (0.2 mL) were added sequentially to a 4 mL vial. After 5 min, 3,5-lutidine (0.15 mL) was added to the solution. The vial was capped with a Teflon-lined screw cap, and the resulting solution was kept in the glovebox at room temperature for 15 min. The solution was transferred to a J-Young NMR tube and analyzed by ^{1}H NMR spectroscopy.

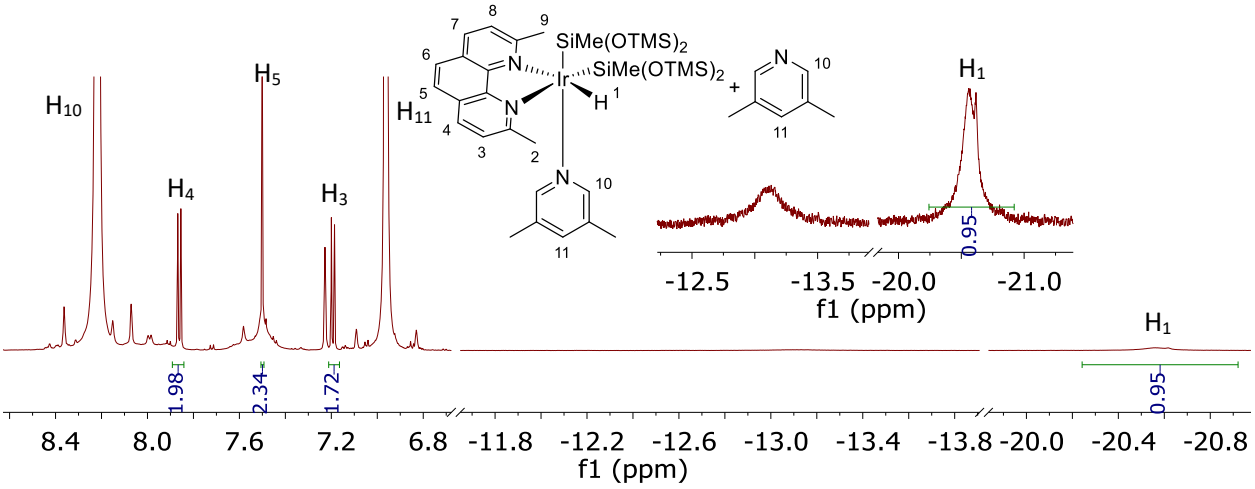

Observation of (3,4,7,8-Me$_4$phen)Ir(SiMe(OTMS)$_2$)$_2$H(P(OPh)$_3$)

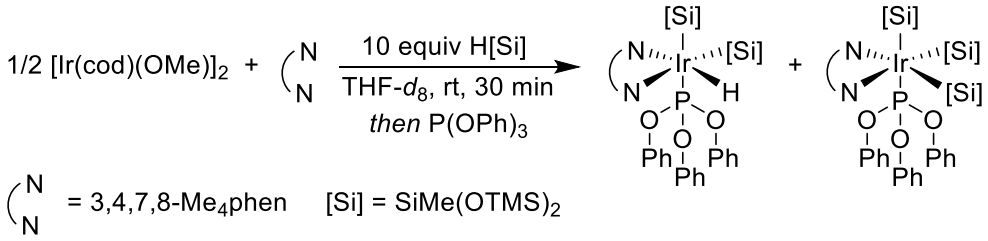

= 3,4,7,8-Me$_4$phen [Si] = SiMe(OTMS)$_2$

In an N_2-filled glovebox, [Ir(cod)(OMe)]$_2$ (13 mg, 0.020 mmol), 3,4,7,8-Me$_4$phenanthroline (11 mg, 0.047 mmol), HSiMe(OTMS)$_2$ (89 mg, 0.40 mmol), and THF-d_8 (0.5 mL) were added sequentially to a 4 mL mL vial. The vial was capped with a Teflon-lined screw cap, and the resulting solution was kept in the glovebox at room temperature for 30 min. Triphenyl phosphite (13 μL, 0.050 mmol) was added to the vial. The solution was transferred to a J-Young NMR tube and analyzed by ^{1}H and ^{31}P NMR spectroscopy.

^{1}H NMR:

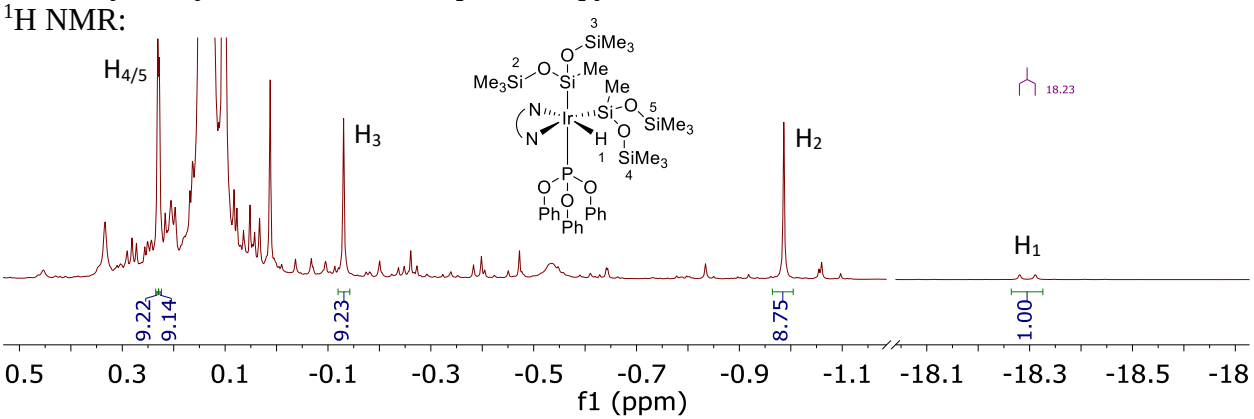

^{31}P NMR:

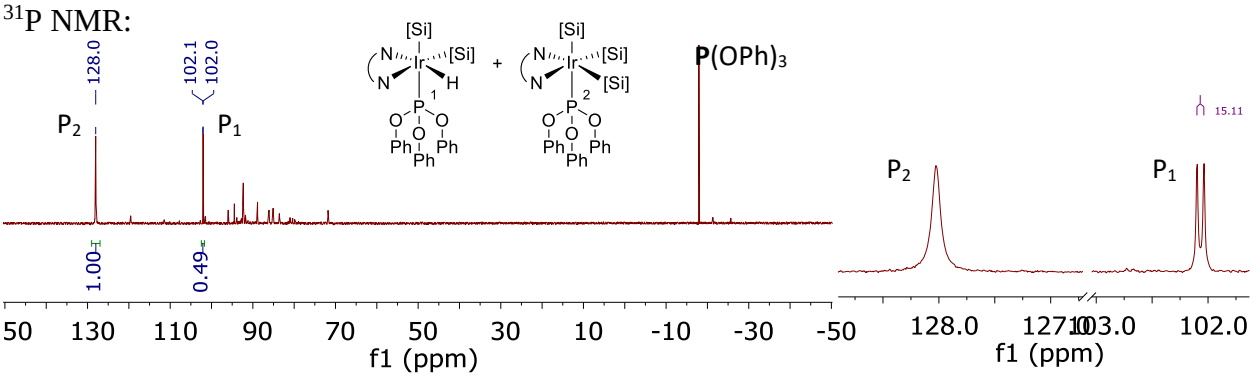

Synthesis of Ir Complexes

Synthesis of (2,9-Me$_2$phen)Ir(SiMe(OTMS)$_2$)$_2$H(P(OPh)$_3$) (3)

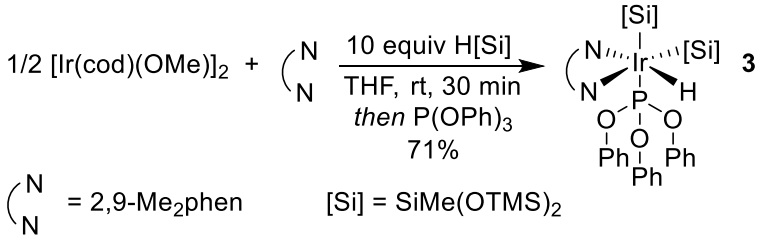

In an N_2-filled glovebox, $[Ir(cod)(OMe)]_2$ (133 mg, 0.200 mmol), 2,9-Me$_2$phen (105 mg, 0.505 mmol), $HSiMe(OTMS)_2$ (1 g, 0.4 mmol), and THF (4 mL) were added sequentially to a 20 mL mL vial. The vial was capped with a Teflon-lined screw cap, and the resulting dark red solution was kept in the glovebox at room temperature for 30 min. Triphenyl phosphite (155 mg, 0.500 mmol) was added to the vial and the color of the solution turned dark yellow. The vial was removed from the glovebox and the solvent was evaporated under reduced pressure. The crude product was purified by column chromatography (0-30% Et_2O/Hexanes) to yield a yellow oil which solidified under high vacuum yielding 330 mg (71%) of yellow solids.

^{1}H NMR (400 MHz, $CDCl_3$) δ 8.12 (d, *J* = 8.3 Hz, 1H), 7.89 (d, *J* = 8.2 Hz, 1H), 7.66 (d, *J* = 8.6 Hz, 1H), 7.63 (d, *J* = 8.3 Hz, 1H), 7.54 (d, *J* = 8.6 Hz, 1H), 7.41 (d, *J* = 8.2 Hz, 1H), 6.81 – 6.68 (m, 15H), 3.52 (s, 3H), 2.71 (s, 3H), 0.83 (s, 3H), 0.28 (s, 3H), 0.21 (s, 9H), 0.19 (s, 9H), -0.36 (s, 9H), -0.75 (s, 9H), -19.91 (d, *J* = 13.7 Hz, 1H).

^{13}C NMR (151 MHz, $CDCl_3$) δ 164.8, 161.7, 152.0 (d, *J* = 10.7 Hz), 150.4, 149.3, 135.0, 134.9, 129.6, 129.1, 128.9, 128.4, 125.4, 124.5, 124.3, 123.0, 120.5 (d, *J* = 4.2 Hz), 32.5, 32.4, 15.5 (d, *J* = 5.1 Hz), 13.3 (d, *J* = 29.5 Hz), 3.2, 3.0, 2.7, 2.1.

^{31}P{^{1}H} NMR (162 MHz, $CDCl_3$) δ 102.6.

^{31}P NMR (243 MHz, $CDCl_3$) δ 102.4 (d, *J* = 13.7 Hz).

^{29}Si NMR (119 MHz, $CDCl_3$) δ -1.0 (d, *J* = 4.8 Hz), -1.1 (d, *J* = 4.9 Hz), -2.0, -3.5, -4.0 (d, *J* = 302.6 Hz), -34.6 (d, *J* = 15.1 Hz).

Elemental analysis (%) calcd for $C_{46}H_{70}IrN_2O_7PSi_6$ [M]: C 47.85, H 6.11, N 2.43 found: C 48.56, H 6.53, N 2.09

IR (neat, cm–1) ν 3065, 2953, 2898, 2248, 1933, 1592, 687.

Crystals of complex **3** were obtained by adding 80 mg of complex **3** and 3 mL of pentane to a 4 mL vial. The vial was capped with a rubber septum. The vial was removed from the glovebox and fitted with a nitrogen line. The solution was cooled to -78 °C in a bath of $CO_{2(s)}$ and acetone. A bright yellow solid precipitated, and the mother liquor was removed with a syringe fitted with a needle. The solid was dissolved in 3 mL of pentane. The septum was punctured with a 21-gauge needle three times. The pentane evaporated overnight yielding crystals suitable for X-ray diffraction.

An orange block 0.15 x 0.07 x 0.04 mm in size was mounted on a Cryoloop with Paratone oil. Data were collected in a nitrogen gas stream at 100(2) K using omega scans. Crystal-to-detector distance was 33.00 mm and exposure time was 15.00 seconds per frame using a scan width of 0.5°. Data collection was 100% complete to 28.000° in θ. A total of 65730 reflections were collected covering the indices -16<=h<=16, -16<=k<=16, -25<=l<=25. 13464 reflections were found to be symmetry independent, with a R_{int} of 0.0640. Indexing and unit cell refinement indicated a

primitive, triclinic lattice. The space group was found to be P -1 (No. 2). The data were integrated using the CrysAlis^{Pro} 1.171.40.68a software program and scaled using the SCALE3 ABSPACK scaling algorithm. Solution by intrinsic phasing (SHELXT-2015) produced a heavy-atom phasing model consistent with the proposed structure. All non-hydrogen atoms were refined anisotropically by full-matrix least-squares (SHELXL-2014). All hydrogen atoms were placed using a riding model. Their positions were constrained relative to their parent atom using the appropriate HFIX command in SHELXL-2014.

Empirical formula	C_{46} H_{70} Ir N_2 O_7 P Si_6	
Formula weight	1154.75	
Temperature	100(2) K	
Wavelength	0.71073 Å	
Crystal system	Triclinic	
Space group	P -1	
Unit cell dimensions	a = 12.1998(2) Å	a= 76.7080(10)°.
	b = 12.3637(2) Å	b= 75.7050(10)°.
	c = 19.2246(2) Å	g = 81.4550(10)°.
Volume	2721.69(7) Å^3	
Z	2	
Density (calculated)	1.409 Mg/m^3	
Absorption coefficient	2.661 mm^{-1}	
F(000)	1184	
Crystal size	0.150 x 0.070 x 0.040 mm^3	
Theta range for data collection	2.861 to 28.282°.	
Index ranges	-16<=h<=16, -16<=k<=16, -25<=l<=25	
Reflections collected	65730	
Independent reflections	13464 [R(int) = 0.0640]	
Completeness to theta = 28.000°	99.6 %	
Absorption correction	Semi-empirical from equivalents	
Max. and min. transmission	1.00000 and 0.74549	
Refinement method	Full-matrix least-squares on F^2	
Data / restraints / parameters	13464 / 1 / 588	
Goodness-of-fit on F^2	1.023	
Final R indices [I>2sigma(I)]	R1 = 0.0271, wR2 = 0.0590	
R indices (all data)	R1 = 0.0343, wR2 = 0.0609	
Extinction coefficient	n/a	
Largest diff. peak and hole	1.463 and -0.934 e.Å^{-3}	

Synthesis of (2,9-Me$_2$phen)Ir(SiMe(OTMS)$_2$)H$_2$(P(OPh)$_3$) (5)

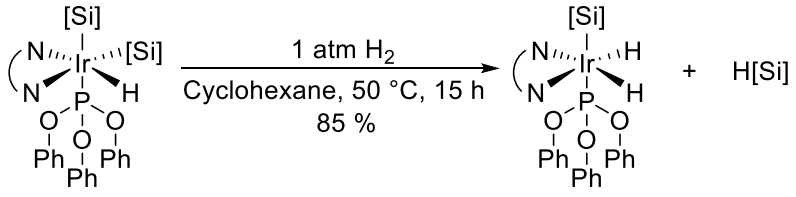

3 **5**

N N = 2,9-Me$_2$phen [Si] = SiMe(OTMS)$_2$

In an N_2-filled glovebox, complex **3** (22 mg, 0.019 mmol), and cyclohexane (1 mL) were added to a 4 mL vial. The vial was capped with a rubber septum, removed from the glovebox, and warmed to 50 °C. The solution was sparged with H_2 for 5 min. After a further 15 h, the solution was cooled to room temperature and the volatiles were removed under high vacuum, yielding a red oil (15 mg, 85%).

^{1}H NMR (600 MHz, $CDCl_3$) δ 8.01 (dd, *J* = 8.1, 1.8 Hz, 2H), 7.68 (s, 2H), 7.53 (d, *J* = 8.1 Hz, 2H), 6.91 (d, *J* = 8.0 Hz, 6H), 6.84 (t, *J* = 7.9 Hz, 6H), 6.75 (t, *J* = 7.3 Hz, 3H), 2.98 (s, 6H), -0.42 (s, 18H), -0.61 (s, 3H), -18.97 (d, *J* = 19.0 Hz, 2H).

^{13}C NMR (151 MHz, $CDCl_3$) δ 161.7 (d, *J* = 2.8 Hz), 152.6 (d, *J* = 4.7 Hz), 149.4, 133.6, 128.8, 128.6, 125.6, 123.3, 123.2, 121.2 (d, *J* = 5.0 Hz), 33.1, 12.5 (d, *J* = 28.9 Hz), 2.2.

^{31}P{^{1}H} NMR (162 MHz, THF-d_8) δ 108.4.

^{31}P NMR (162 MHz, THF-d_8) δ 108.4 (t, *J* = 17.7 Hz).

IR (neat, cm–1) ν 3062, 2954, 2180, 1934, 1590, 1487, 754.

Stoichiometric reactions of Ir complex 3
Reaction of 3 with 3-Cl-Thiophene

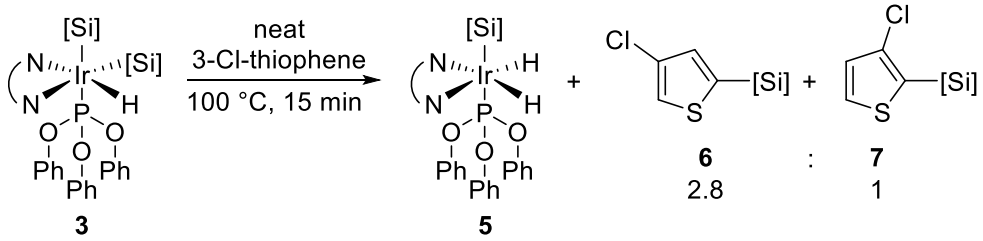

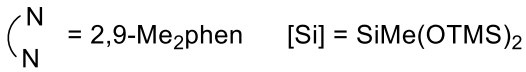

In an N_2-filled glovebox, complex **3** (5 mg, 0.004 mmol), and 3-Cl-thiophene (100 μL) were added to a 4 mL vial. The vial was capped with a Teflon-lined screw cap and removed from the glovebox. The vial was heated at 100 °C for 15 min and the vial was then brought into the glovebox. 400 μL of THF-d_8 was added to the vial, and the solution was transferred to a J-Young NMR. The combined yield of the silylated products was determined to be 81% and the ratio of products from silylation at the 2-position and at the 5-position was determined to be 2.8:1 by ^{1}H NMR spectroscopy.

Reaction of 3 with *o*-Cl_2-Benzene-d_4

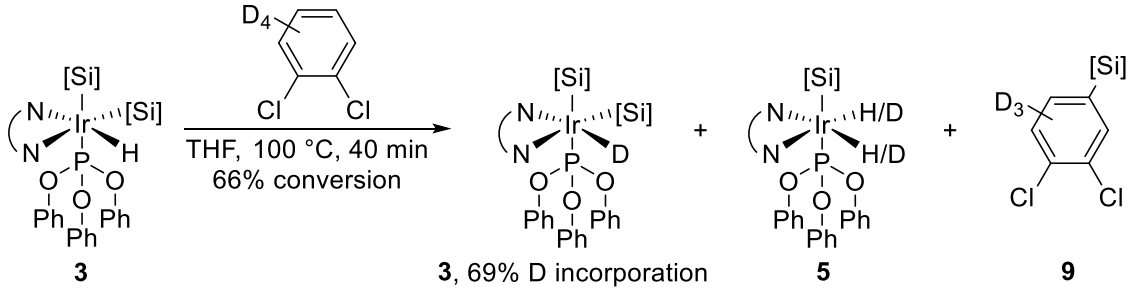

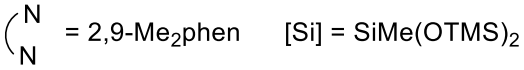

In an N_2-filled glovebox, complex **3** (6 mg, 0.005 mmol), dodecane (19 mg, 0.11 mmol), *o*-Cl_2-benzene-d_4 (0.25 mL), and THF (0.25 mL) were added to a 4 mL vial. The solution was transferred to a J-Young NMR tube and heated at 100 °C for 40 min. The conversion of **3** to products **5** and **9** was determined to be 66% by ^{1}H NMR spectroscopy. The yield of **5** was determined to be 41% by ^{1}H NMR spectroscopy with dodecane internal standard. The yield of **9** was determined to be 39% by ^{1}H NMR spectroscopy with dodecane internal standard. The incorporation of deuterium in place of the hydride of **3** was determined to be 69% by comparing the integrations of the signals for the hydride and phenanthroline ligands in the ^{1}H NMR spectrum.

Reaction of 3 with *o*-Xylene-d_{10}

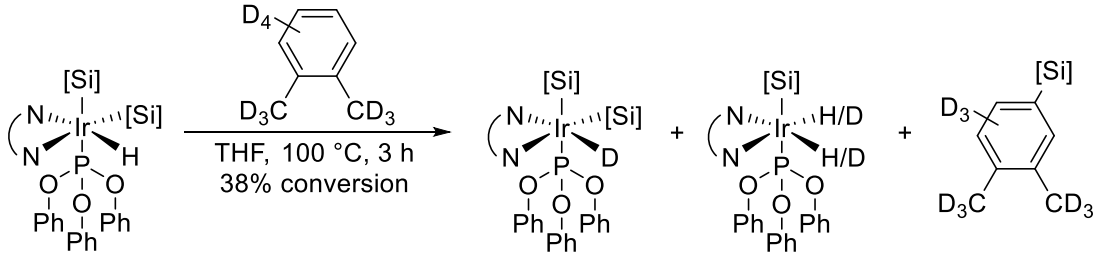

3 **3**, *not detected* **5** **8**

N = 2,9-Me_2phen [Si] = $SiMe(OTMS)_2$

In an N_2-filled glovebox, complex **3** (6 mg, 0.005 mmol), dodecane (19 mg, 0.11 mmol), *o*-xylene-d_4 (0.25 mL), and THF (0.25 mL) were added to a 4 mL vial. The solution was transferred to a J-Young NMR tube and heated at 100 °C for 3 h. The conversion of **3** to products **5** and **8** was determined to be 38% by ^{1}H NMR spectroscopy. The yield of **5** was determined to be 28% by ^{1}H NMR spectroscopy with dodecane internal standard. The yield of **8** was determined to be 18% by ^{1}H NMR spectroscopy with dodecane internal standard. The incorporation of deuterium in place of the hydride of **3** was determined to be 0% by comparing the integrations of the signals for the hydride and phenanthroline ligands in the ^{1}H NMR spectrum.

Details of Kinetic Analysis

Determination of Dependence of Rate of Silylation with 3 on Concentration of Phosphite

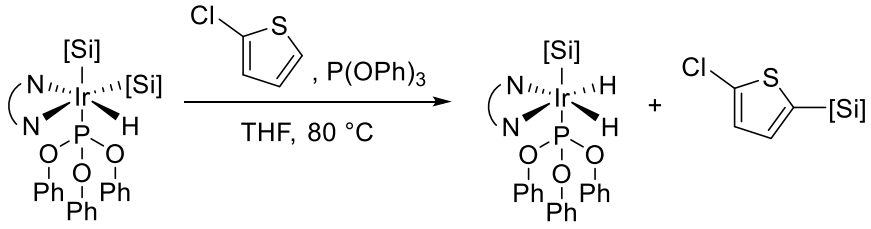

3 **5**

N = 2,9-Me_2phen [Si] = $SiMe(OTMS)_2$

The silylation of 2-Cl-thiophene was conducted in a 4:1 mixture of 2-Cl-thiophene and C_6D_6 with a total volume of 0.5 mL. The concentrations of complex **3** was 0.03 M. To determine the dependence of the rate of the reaction on the concentration of phosphite, the concentration of triphenyl phosphite was varied between 0 and 0.02 M. The dependence of the rate of the silylation on the concentration of phosphite was determined by the method of initial rates at 80 °C monitored by ^{1}H NMR spectroscopy with decane as the internal standard.

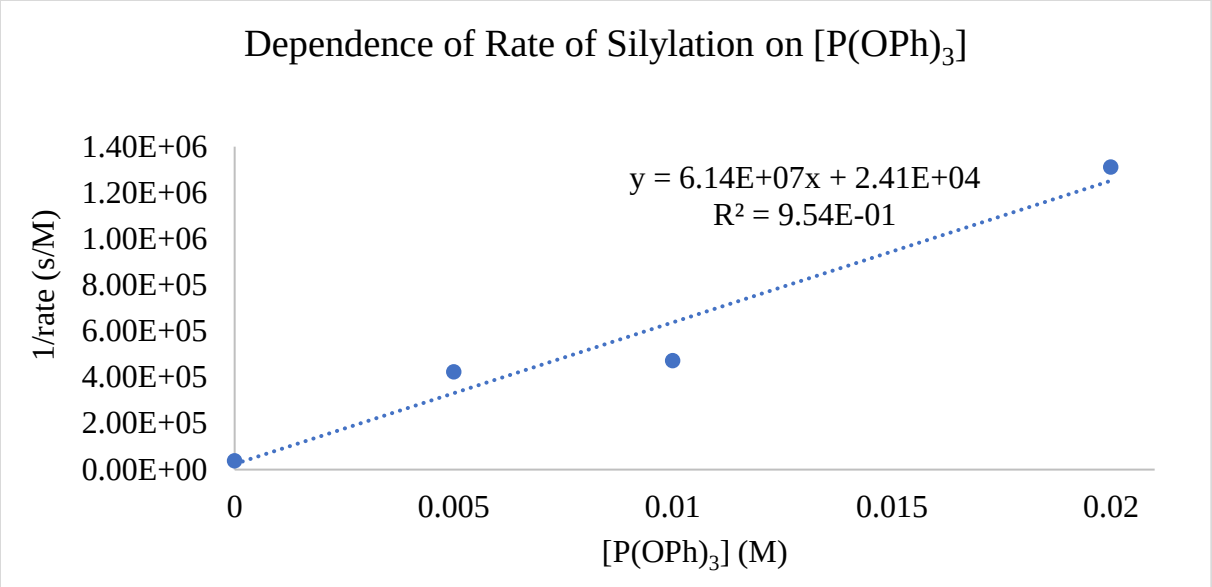

Determination of Experimental Rate Law of Catalytic Arene Silylation

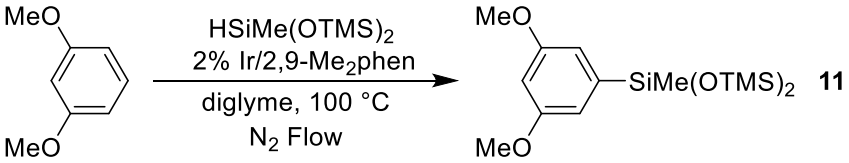

11

The silylation of 1,3-$(OMe)_2$-benzene was conducted in diglyme with a total volume of 0.4 mL. The concentrations of each reagent under the standard conditions were: 2 M 1,3-$(OMe)_2$-benzene, 0.5 M heptamethyltrisiloxane, 10 mM catalyst. To determine the dependence on one reagent, the concentration of that reagent was varied while the while the concentrations of the other reagents and the total volume were held constant. The concentration of 1,3-$(OMe)_2$-benzene was varied between 0.25 and 2 M. The concentration of heptamethyltrisiloxane was varied between 0.063 and 0.05 M. The concentration of catalyst was varied between 2.5 and 20 mM. The reactions were conducted in Radley carousel reaction vessels fitted with nitrogen inlet and gas outlet and placed in a preheated Radley carousel. The rate law of the reaction was determined by the method of initial rates at 100 °C monitored by GC analysis with dodecane as the internal standard.

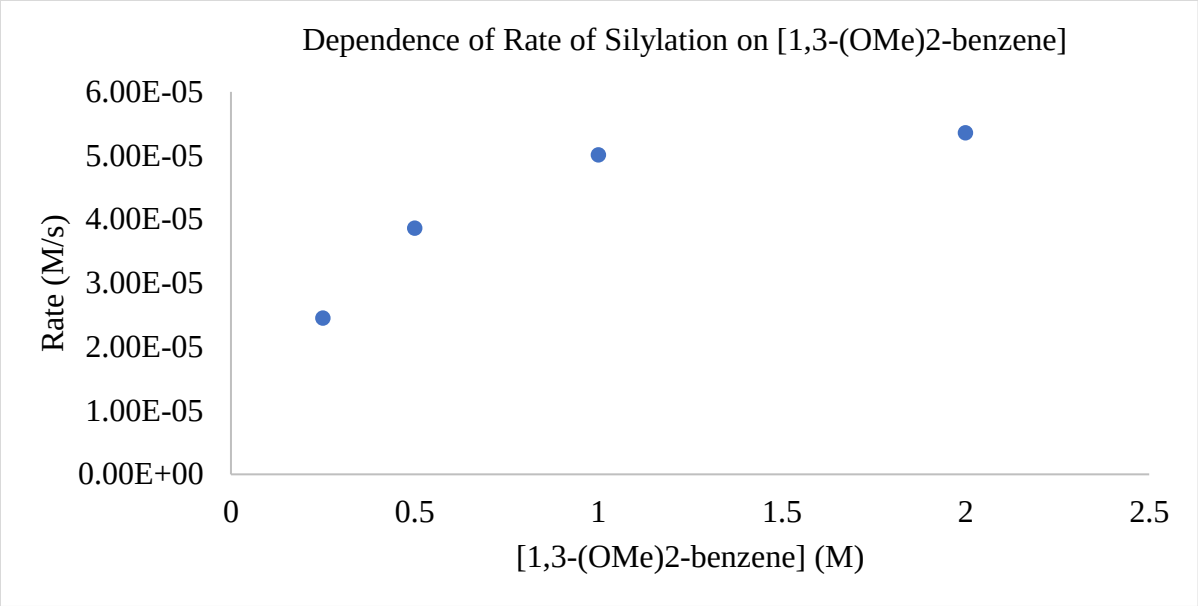
Dependence of Rate of Silylation on [1,3-(OMe)2-benzene]
6.00E-05
5.00E-05
4.00E-05
3.00E-05
2.00E-05
1.00E-05
0.00E+00
Rate (M/s)
0
0.5
1
1.5
2
2.5
[1,3-(OMe)2-benzene] (M)

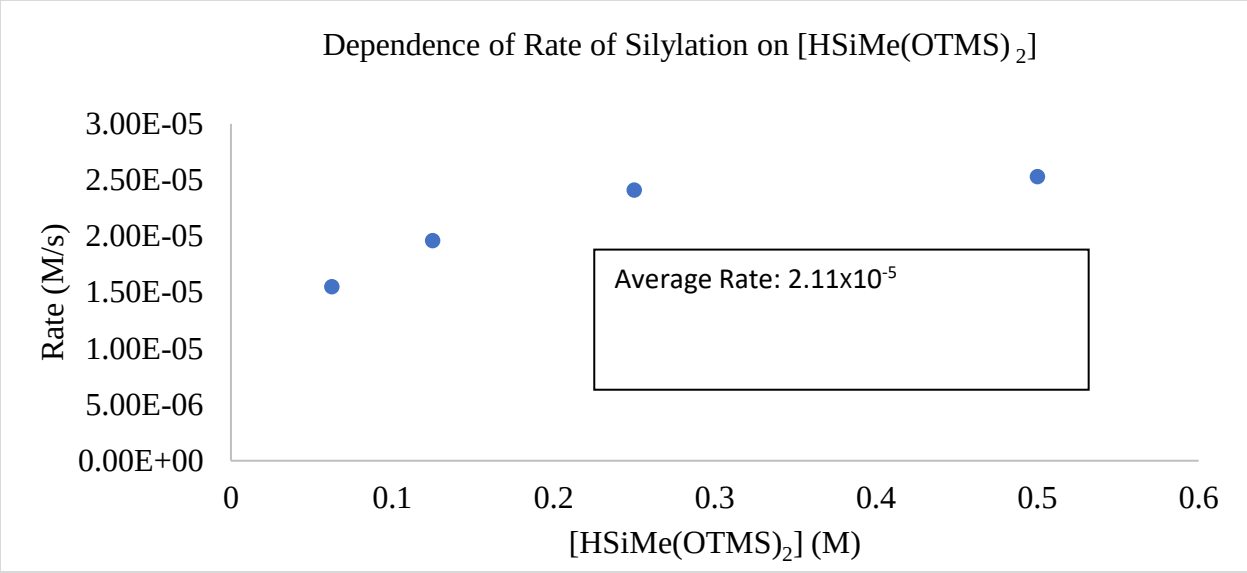
Dependence of Rate of Silylation on [HSiMe(OTMS)2]
3.00E-05
2.50E-05
2.00E-05
1.50E-05
1.00E-05
5.00E-06
0.00E+00
Rate (M/s)
Average Rate: 2.11x10-5
0
0.1
0.2
0.3
0.4
0.5
0.6
[HSiMe(OTMS)2] (M)

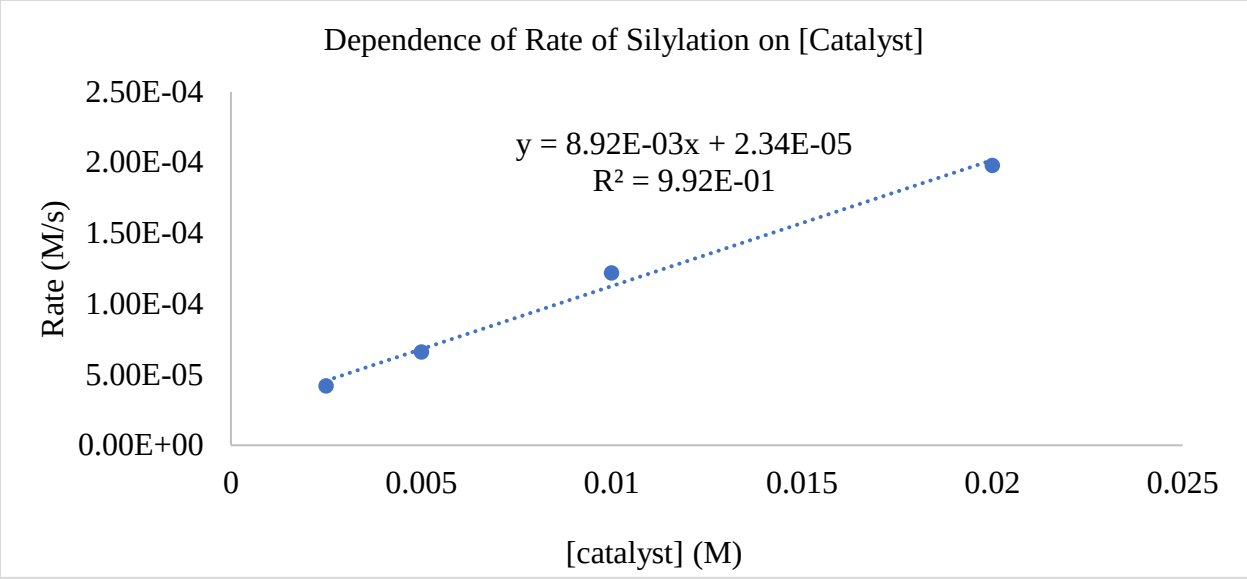

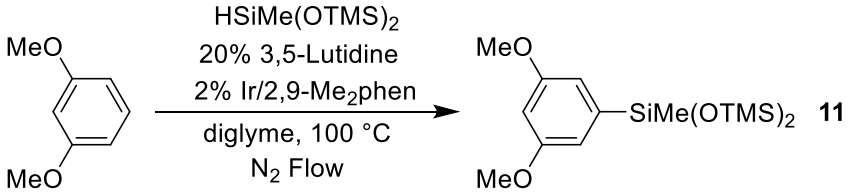

The silylation of 1,3-$(OMe)_2$-benzene was conducted in diglyme with a total volume of 0.4 mL. The concentrations of each reagent besides 1,3-$(OMe)_2$-benzene were: 0.1 M 3,5-lutidine, 0.5 M heptamethyltrisiloxane, 10 mM catalyst. The concentration of 1,3-$(OMe)_2$-benzene was varied between 0.25 and 2 M. The reactions were conducted in Radley carousel reaction vessels fitted with nitrogen inlet and gas outlet and placed in a preheated Radley carousel. The dependence of the rate of the reaction on the concentration of 1,3-$(OMe)_2$-benzene was determined by the method of initial rates at 100 °C monitored by GC analysis with dodecane as the internal standard.

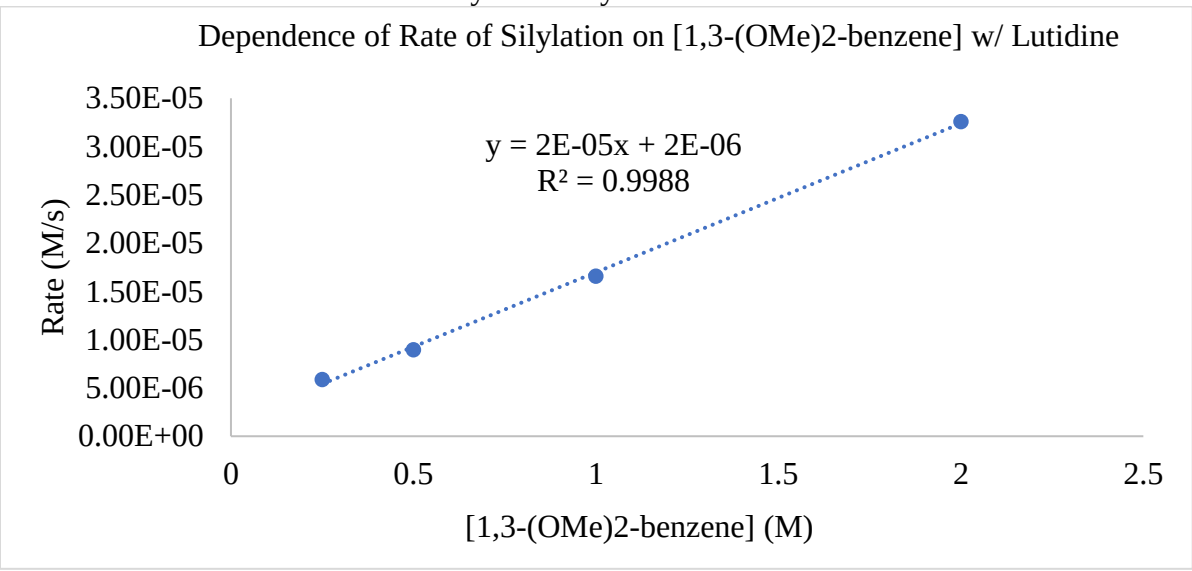

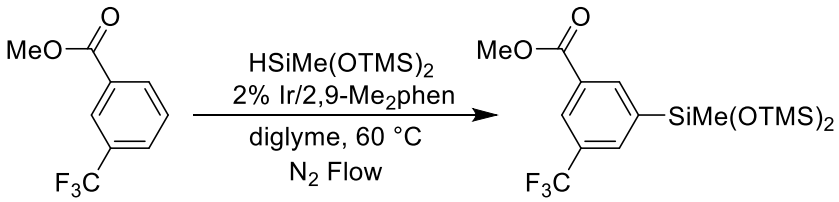

The silylation of methyl 3-CF_3-benzoate was conducted in diglyme with a total volume of 0.4 mL. The concentrations of each reagent besides methyl 3-CF_3-benzoate were: 0.5 M heptamethyltrisiloxane, 10 mM catalyst. The concentration of methyl 3-CF_3-benzoate was varied between 0.8 and 3.2 M. The reactions were conducted in Radley carousel reaction vessels fitted with nitrogen inlet and gas outlet and placed in a preheated Radley carousel. The dependence of the rate of the reaction on the concentration of methyl 3-CF_3-benzoate was determined by the method of initial rates at 60 °C monitored by GC analysis with dodecane as the internal standard.

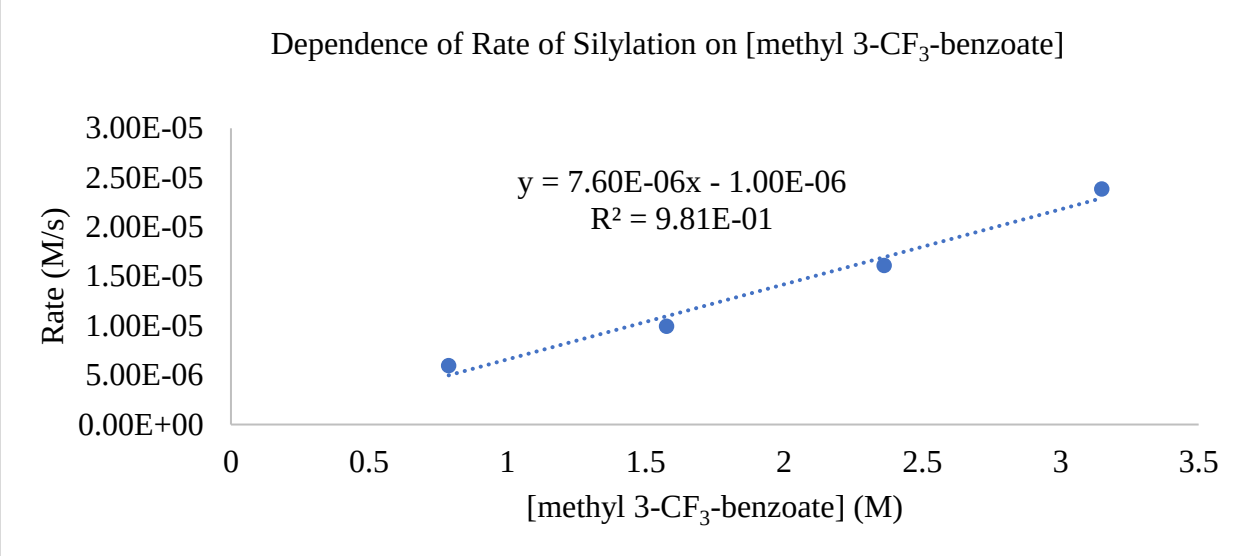

Determination of the Kinetic Isotope Effect with *o*-Cl_2-Benzene and *o*-Cl_2-Benzene-d_4

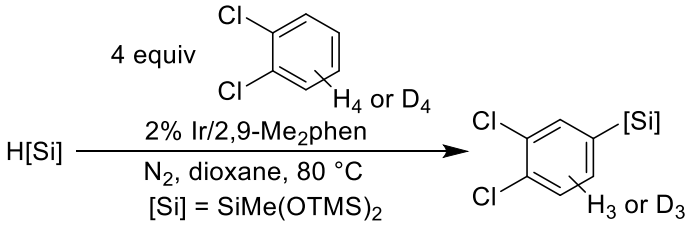

In an N_2-filled glovebox, $[Ir(cod)OMe]_2$ (6.6 mg, 0.010 mmol), 2,9-Me_2phen (4.2 mg, 0.020 mmol), dodecane (85 mg, 0.050 mmol), and heptamethyltrisiloxane (223, 1.00 mmol) were weighed into a 4 mL vial. After 20 minutes, the solution was transferred to a 1 mL volumetric flask, the vial was washed with dioxane, and the washings were transferred to the flask. The solution was diluted to 1 mL total volume with dioxane, and the flask was capped and shaken. 200 µL (400 µL total) of stock solution was added to two separate Radley Carousel reaction vessels. 100 µL (200 µL total) of dioxane was dispensed to each vessel. 200 µL of *o*-Cl_2-benzene was added to one of the vessels and 200 µL of *o*-Cl_2-benzene-d_4 was added to the other. The vessels were capped. The capped vessel was removed from the glovebox and placed in a Radley Carousel that had been preheated to 80 °C. The rates of the reactions were determined by the method of

initial rates, monitored by GC analysis with dodecane as the internal standard. The kinetic isotope effect (k_H/k_D) was determined to be 1.6.

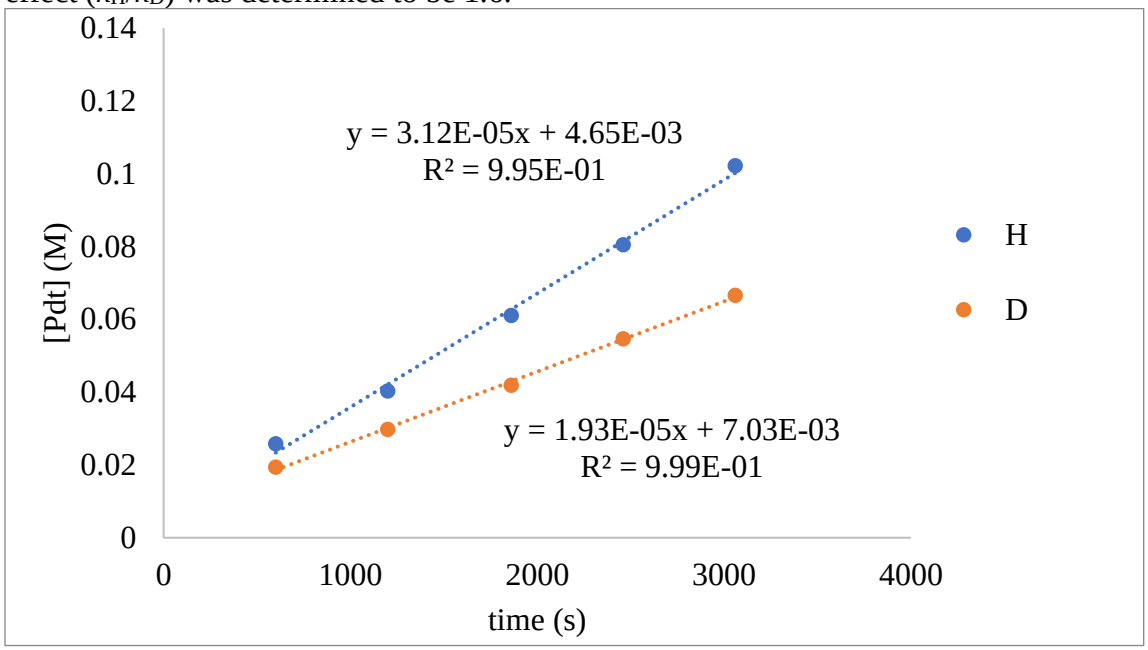

Determination of the Kinetic Isotope Effect with *o*-Xylene and *o*-Xylene-d_4

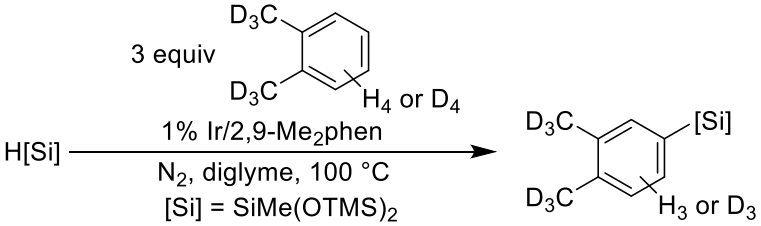

In an N_2-filled glovebox, $[Ir(cod)OMe]_2$ (3.3 mg, 0.0050 mmol), 2,9-Me_2phen (2.1 mg, 0.010), dodecane (85 mg, 0.5 mmol), and heptamethyltrisiloxane (223, 1.00 mmol) were weighed into a 4 mL vial. After 20 minutes, the solution was transferred to a 1 mL volumetric flask, the vial was washed with dioxane, and the washings were transferred to the flask. The solution was diluted to 1 mL total volume with dioxane, and the flask was capped and shaken. 250 µL (500 µL total) of stock solution was added to two separate Radley Carousel reaction vessels. 100 µL of *o*-xylene was added to one of the vessels and 100 µL of *o*-xylene-d_4 was added to the other. The vessels were capped. The capped vessel was removed from the glovebox and placed in a Radley Carousel that had been preheated to 100 °C. The rates of the reactions were determined by the method of initial rates, monitored by GC analysis with dodecane as the internal standard. The kinetic isotope effect (k_H/k_D) was determined to be 3.2.

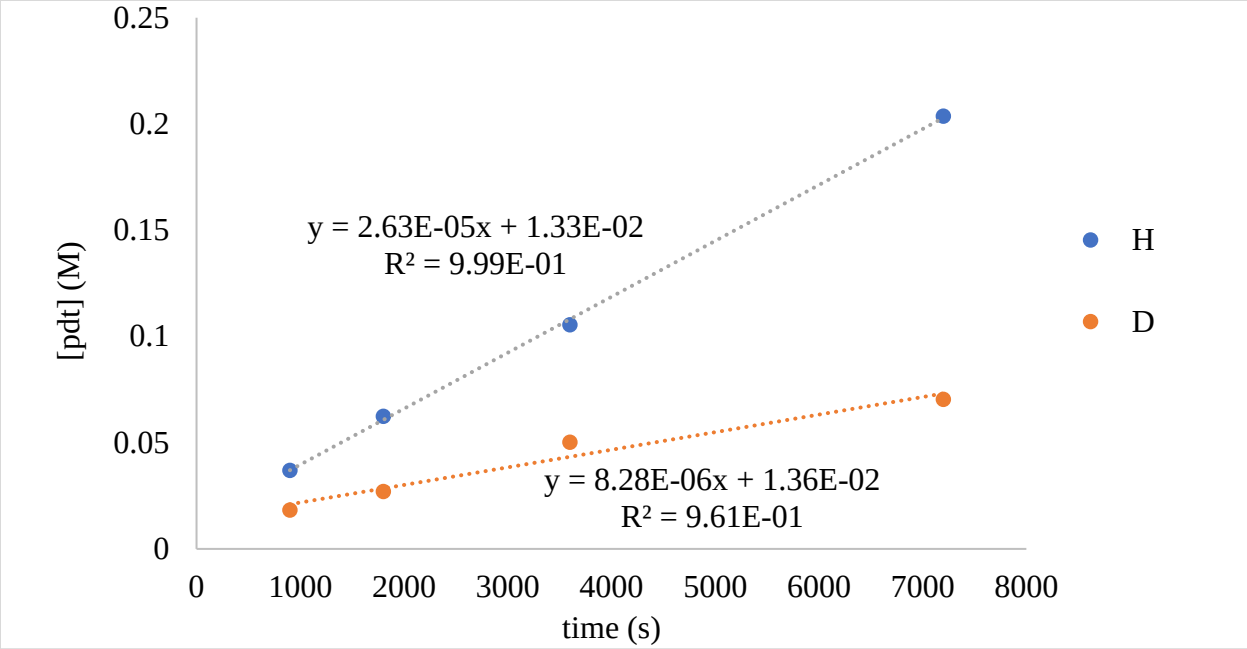
0.25
0.2
0.15
0.1
0.05
0
[pdt] (M)
y = 2.63E-05x + 1.33E-02
R² = 9.99E-01
y = 8.28E-06x + 1.36E-02
R² = 9.61E-01
H
D
0
1000
2000
3000
4000
5000
6000
7000
8000
time (s)

Catalytic Silylations of Arenes

Reaction of Silane with 3-Cl-thiophene

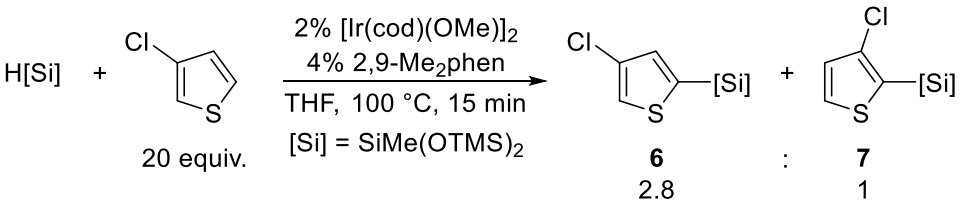

In an N_2-filled glovebox, $[Ir(cod)OMe]_2$ (1.3 mg, 0.0020 mmol), 2,9-Me_2phen (1 mg, 0.005 mmol), dodecane (38 mg, 0.2 mmol), 3-Cl-thiophene (238 mg, 2.00 mmol), heptamethyltrisiloxane (23 mg, 0.10 mmol) and THF (50 µL) were weighed into a 4 mL vial. The vial was capped with a Teflon-lined screw cap and removed from the glovebox. The vial was heated to 100 °C for 15 min. The vial was then allowed to cool to room temperature. The solution was diluted with 500 µL $CDCl_3$ and transferred to an NMR tube. The combined yields of silylated heteroarenes were determined to be 84% by ^{1}H NMR spectroscopy with dodecane internal standard. The ratio of silylarenes **6** and **7** was determined to be 2.8 to 1 by ^{1}H NMR spectroscopy.

Silylation of Chloroarenes for Construction of Hammett Plot

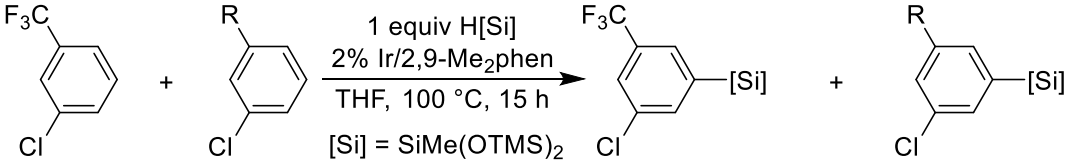

In an N_2-filled glovebox, $[Ir(cod)OMe]_2$ (1.3 mg, 0.0020), 2,9-Me_2phen (1 mg, 0.005), dodecane (19 mg, 0.10 mmol), 3-CF_3-chlorobenzene (18 mg, 0.10 mmol), heptamethyltrisiloxane (22 mg, 0.10 mmol), an arene (**A**-**E**, 0.10 mmol), and THF (200 µL) were weighed into a 4 mL vial. The vial was capped with a Teflon-lined screw cap and removed from the glovebox. The vial was heated to 100 °C for 15 h. The vial was then allowed to cool to room temperature. The solution was diluted with 300 µL of $CDCl_3$ and the ratio of silylated products was determined by ^{1}H NMR spectroscopy. The products were identified based on previously reported ^{1}H NMR spectra of the isolated compounds.[4a, 4b, 25] The σ_m values were drawn from the literature.[26]

Arene	R	σ_m	[Arene-Si]/[**D-Si**]
A	Me	-0.07	0.24
B	OMe	0.12	0.31
C	Cl	0.37	1.08
D	CF_3	0.43	1
E	CN	0.56	1.41

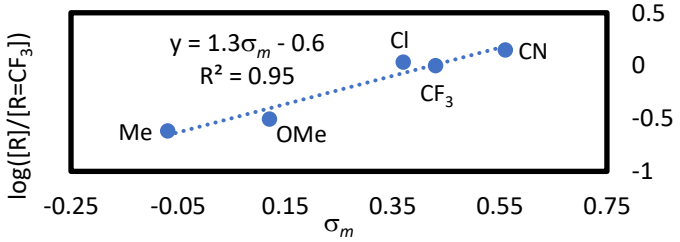

Reaction of Silane with *o*-Cl_2-Benzene-d_4

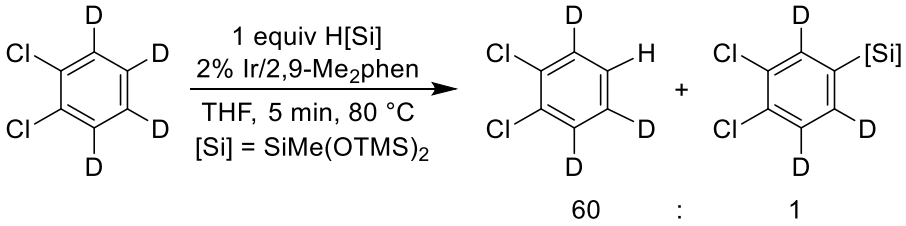

In an N_2-filled glovebox, $[Ir(cod)OMe]_2$ (1.7 mg, 0.0025 mmol), 2,9-Me_2phen (1.1 mg, 0.005 mmol), dodecane (24 mg, 0.13 mmol), *o*-Cl_2-benzene-d_4 (50 μL, 0.44 mmol), heptamethyltrisiloxane (56 mg, 0.25 mmol) and THF (50 μL) were weighed into a 4 mL vial. The solution was transferred to a J-Young NMR tube. The solution was analyzed by ^{1}H NMR spectroscopy. The solution was then heated to 80 °C for 5 min. The ratio of *o*-Cl_2-benzene-d_3 to *o*-Cl_2-silylbenzene-d_3 was determined to be 60:1 by ^{1}H NMR spectroscopy. The ^{1}H NMR spectrum of the solution acquired before heating contained small peaks corresponding to the 2-position and 3-position of *o*-Cl_2-benzene. The ^{1}H NMR spectrum of the solution acquired after heating contained a large peak corresponding to the 3-position of *o*-Cl_2-benzene but the signal corresponding to the 2-position was determined to be the same size as before heating by comparison to the internal standard, dodecane.

Procedures for Computational Study

DFT calculations were performed with the Gaussian 16 software package at the Molecular Graphics and Computation Facility at the University of California, Berkeley. B3LYP functionals (with gd3 dispersion correction), and LANL2DZ basis set (Ir) and 6-31g(d,p) basis set (all other atoms) was applied for geometry optimizations. The PBE functional (with gd2 dispersion correction and SMD, THF solvent correction), and LANL2TZ basis set (Ir) and 6-31++g** basis set (all other atoms) was applied to single point energy calculations.[19] Thermal corrections from the geometry optimizations were added to the energies found in single point energy calculations to find values for Gibbs free energy.

4.5 References

Portions of this chapter were reprinted with permission from:

"Mechanism of the Iridium-Catalyzed Silylation of Aromatic C–H Bonds" Karmel, C.; Hartwig, J. F., *J. Am. Chem. Soc.* **2020**.

1. (a) Hartwig, J. F. Borylation and Silylation of C–H Bonds: A Platform for Diverse C–H Bond Functionalizations. *Acc. Chem. Res.* **2012**, *45*, 864. (b) Cheng, C.; Hartwig, J. F. Catalytic Silylation of Unactivated C–H Bonds. *Chem. Rev.* **2015**, *115*, 8946. (c) Obligacion, J. V.; Chirik, P. J. Earth-abundant transition metal catalysts for alkene hydrosilylation and hydroboration. *Nat. Rev. Chem.* **2018**, *2*, 15.

2. (a) Bracegirdle, S.; Anderson, E. A. Arylsilane oxidation—new routes to hydroxylated aromatics. *Chem. Commun.* **2010**, *46*, 3454. (b) Rayment, E. J.; Summerhill, N.; Anderson, E. A. Synthesis of Phenols via Fluoride-free Oxidation of Arylsilanes and Arylmethoxysilanes. *J. Org. Chem.* **2012**, *77*, 7052. (c) Rayment, E. J.; Mekareeya, A.; Summerhill, N.; Anderson, E. A. Mechanistic Study of Arylsilane Oxidation through ^{19}F NMR Spectroscopy. *J. Am. Chem. Soc.* **2017**, *139*, 6138.
3. Morstein, J.; Kalkman, E. D.; Bold, C.; Cheng, C.; Hartwig, J. F. Copper-Mediated C–N Coupling of Arylsilanes with Nitrogen Nucleophiles. *Org. Lett.* **2016**, *18*, 5244.
4. (a) Cheng, C.; Hartwig, J. F. Iridium-Catalyzed Silylation of Aryl C–H Bonds. *J. Am. Chem. Soc.* **2015**, *137*, 592. (b) Karmel, C.; Chen, Z.; Hartwig, J. F. Iridium-Catalyzed Silylation of C–H Bonds in Unactivated Arenes: A Sterically Encumbered Phenanthroline Ligand Accelerates Catalysis. *J. Am. Chem. Soc.* **2019**, *141*, 7063. (c) Karmel, C.; Rubel, C. Z.; Kharitonova, E. V.; Hartwig, J. F. Iridium-Catalyzed Silylation of Five-Membered Heteroarenes: High Sterically Derived Selectivity from a Pyridyl-Imidazoline Ligand. *Angew. Chem. Int. Ed.* **2020**, *59*, 6074.
5. (a) Nakao, Y.; Hiyama, T. Silicon-based cross-coupling reaction: an environmentally benign version. *Chem. Soc. Rev.* **2011**, *40*, 4893. (b) Denmark, S. E.; Ambrosi, A. Why You Really Should Consider Using Palladium-Catalyzed Cross-Coupling of Silanols and Silanolates. *Org. Process Res. Dev.* **2015**, *19*, 982.
6. Karmel, C.; Rubel, C. Z.; Kharitonova, E. V.; Hartwig, J. F. Iridium-Catalyzed Silylation of Five-Membered Heteroarenes: High Sterically Derived Selectivity from a Pyridyl-Imidazoline Ligand. *Angew. Chem. Int. Ed.* **2020**, *59*, 2.
7. (a) Ishiyama, T.; Sato, K.; Nishio, Y.; Miyaura, N. Direct Synthesis of Aryl Halosilanes through Iridium(I)-Catalyzed Aromatic C–H Silylation by Disilanes. *Angew. Chem. Int. Ed.* **2003**, *42*, 5346. (b) Ishiyama, T.; Sato, K.; Nishio, Y.; Saiki, T.; Miyaura, N. Regioselective aromatic C-H silylation of five-membered heteroarenes with fluorodisilanes catalyzed by iridium(I) complexes. *Chem. Commun.* **2005**, 5065. (c) Saiki, T.; Nishio, Y.; Ishiyama, T.; Miyaura, N. Improvements of Efficiency and Regioselectivity in the Iridium(I)-Catalyzed Aromatic C-H Silylation of Arenes with Fluorodisilanes. *Organometallics* **2006**, *25*, 6068. (d) Simmons, E. M.; Hartwig, J. F. Iridium-Catalyzed Arene Ortho-Silylation by Formal Hydroxyl-Directed C–H Activation. *J. Am. Chem. Soc.* **2010**, *132*, 17092. (e) Ishiyama, T.; Saiki, T.; Kishida, E.; Sasaki, I.; Ito, H.; Miyaura, N. Aromatic C–H silylation of arenes with 1-hydrosilatrane catalyzed by an iridium(i)/2,9-dimethylphenanthroline (dmphen) complex. *Org. Biomol. Chem.* **2013**, *11*, 8162. (f) Choi, G.; Tsurugi, H.; Mashima, K. Hemilabile N-Xylyl-N′-methylperimidine Carbene Iridium Complexes as Catalysts for C–H Activation and Dehydrogenative Silylation: Dual Role of N-Xylyl Moiety for ortho-C–H Bond Activation and Reductive Bond Cleavage. *J. Am. Chem. Soc.* **2013**, *135*, 13149. (g) Su, B.; Zhou, T. G.; Li, X. W.; Shao, X. R.; Xu, P. L.; Wu, W. L.; Hartwig, J. F.; Shi, Z. J. A Chiral Nitrogen Ligand for Enantioselective, Iridium-Catalyzed Silylation of Aromatic C-H Bonds. *Angew. Chem. Int. Ed.* **2017**, *56*, 1092.
8. (a) Simmons, E. M.; Hartwig, J. F. Catalytic functionalization of unactivated primary C-H bonds directed by an alcohol. *Nature* **2012**, *483*, 70. (b) Frihed, T. G.; Heuckendorff, M.; Pedersen, C. M.; Bols, M. Easy Access to L-Mannosides and L-Galactosides by Using C–H Activation of the Corresponding 6-Deoxysugars. *Angew. Chem. Int. Ed.* **2012**, *51*, 12285. (c) Li, B. J.; Driess, M.; Hartwig, J. F. Iridium-Catalyzed Regioselective Silylation of Secondary Alkyl C-H Bonds for the Synthesis of 1,3-Diols. *J. Am. Chem. Soc.* **2014**, *136*, 6586. (d) Frihed, T. G.; Pedersen, C. M.; Bols, M. Synthesis of All Eight L-Glycopyranosyl Donors Using C–H Activation. *Angew. Chem. Int. Ed.* **2014**, *53*, 13889. (e) Hua, Y.; Jung, S.; Roh, J.; Jeon, J. Modular Approach to Reductive

Csp_2–H and Csp_3–H Silylation of Carboxylic Acid Derivatives through Single-Pot, Sequential Transition Metal Catalysis. *J. Org. Chem.* **2015**, *80*, 4661. (f) Manna, K.; Zhang, T.; Greene, F. X.; Lin, W. Bipyridine- and Phenanthroline-Based Metal–Organic Frameworks for Highly Efficient and Tandem Catalytic Organic Transformations via Directed C–H Activation. *J. Am. Chem. Soc.* **2015**, *137*, 2665. (g) Su, B.; Hartwig, J. F. Ir-Catalyzed Enantioselective, Intramolecular Silylation of Methyl C-H Bonds. *J. Am. Chem. Soc.* **2017**, *139*, 12137. (h) Su, B.; Lee, T.; Hartwig, J. F. Iridium-Catalyzed, β-Selective C(sp_3)–H Silylation of Aliphatic Amines To Form Silapyrrolidines and 1,2-Amino Alcohols. *J. Am. Chem. Soc.* **2018**, *140*, 18032. (i) Ma, X.; Kucera, R.; Goethe, O. F.; Murphy, S. K.; Herzon, S. B. Directed C–H Bond Oxidation of (+)-Pleuromutilin. *J. Org. Chem.* **2018**, *83*, 6843. (j) Bian, L.; Cao, S.; Cheng, L.; Nakazaki, A.; Nishikawa, T.; Qi, J. Semi-synthesis and Structure–Activity Relationship of Neuritogenic Oleanene Derivatives. *ChemMedChem* **2018**, *13*, 1972. (k) Bunescu, A.; Butcher, T. W.; Hartwig, J. F. Traceless Silylation of β-C(sp_3)–H Bonds of Alcohols via Perfluorinated Acetals. *J. Am. Chem. Soc.* **2018**, *140*, 1502. (l) Hung, K.; Condakes, M. L.; Novaes, L. F. T.; Harwood, S. J.; Morikawa, T.; Yang, Z.; Maimone, T. J. Development of a Terpene Feedstock-Based Oxidative Synthetic Approach to the Illicium Sesquiterpenes. *J. Am. Chem. Soc.* **2019**, *141*, 3083.

9. Simmons, E. M.; Hartwig, J. F. Iridium-Catalyzed Arene Ortho-Silylation by Formal Hydroxyl-Directed C-H Activation. *J. Am. Chem. Soc.* **2010**, *132*, 17092.

10. Parija, A.; Sunoj, R. B. Mechanism of Catalytic Functionalization of Primary C–H Bonds Using a Silylation Strategy. *Org. Lett.* **2013**, *15*, 4066.

11. Li, Z.; Xia, M.; Boyd, R. J. Theoretical study on the mechanism of iridium-catalyzed γ-functionalization of primary alkyl C–H bonds. *Can. J. Chem.* **2016**, *94*, 1028.

12. Zhang, M.; Liang, J.; Huang, G. Mechanism and Origins of Enantioselectivity of Iridium-Catalyzed Intramolecular Silylation of Unactivated C(sp_3)–H Bonds. *J. Org. Chem.* **2019**, *84*, 2372.

13. (a) Marsmann, H. In *^{29}Si-NMR Spectroscopic Results*, Berlin, Heidelberg, Springer Berlin Heidelberg: Berlin, Heidelberg, 1981; pp 65. (b) Smith, P. W.; Tilley, T. D. Base-Free Iron Hydrosilylene Complexes via an α-Hydride Migration that Induces Spin Pairing. *J. Am. Chem. Soc.* **2018**, *140*, 3880.

14. (a) Bertrand, R. D.; Ogilvie, F. B.; Verkade, J. G. Signs of phosphorus-phosphorus coupling constants in coordination compounds. *J. Am. Chem. Soc.* **1970**, *92*, 1908. (b) Brown, J. M.; Dayrit, F. M.; Lightowler, D. Interconversion of cis-and trans-dihydrides derived from chelate biphosphine iridium cations. *J. Chem. Soc., Chem. Commun.* **1983**, 414.

15. The reaction of excess 3,5-lutidine with complex 1 yielded a six-coordinate complex containing lutidine bound to iridium. However, the 1H NMR of the solution of 5 contains signals that are more similar in pattern to those of complex 1 than to those of the phosphite adduct 3. As in the 1H NMR spectra of 3 and DMAP-adduct 4, a signal corresponding to a metal hydride is present at -20 ppm, which integrates to 1 proton. These data indicate that exchange of the positions of the hydride and silyl ligands on this complex is much faster than that in DMAP adduct 4, due to the weaker binding constant of lutidine.

16. (a) Lipke, M. C.; Liberman-Martin, A. L.; Tilley, T. D. Electrophilic Activation of Silicon–Hydrogen Bonds in Catalytic Hydrosilations. *Angew. Chem. Int. Ed.* **2017**, *56*, 2260. (b) Lipke, M. C.; Poradowski, M.-N.; Raynaud, C.; Eisenstein, O.; Tilley, T. D. Catalytic Olefin Hydrosilations Mediated by Ruthenium η^3-H_2Si σ Complexes of Primary and Secondary Silanes. *ACS Catalysis* **2018**, *8*, 11513. (c) Handford, R. C.; Smith, P. W.; Tilley, T. D. Activations of all

Bonds to Silicon (Si–H, Si–C) in a Silane with Extrusion of [CoSiCo] Silicide Cores. *J. Am. Chem. Soc.* **2019**, *141*, 8769.
17. Boller, T. M.; Murphy, J. M.; Hapke, M.; Ishiyama, T.; Miyaura, N.; Hartwig, J. F. Mechanism of the Mild Functionalization of Arenes by Diboron Reagents Catalyzed by Iridium Complexes. Intermediacy and Chemistry of Bipyridine-Ligated Iridium Tris Boryl Complexes. *J. Am. Chem. Soc.* **2005**, *127*, 14263.
18. Larsen, M. A.; Wilson, C. V.; Hartwig, J. F. Iridium-Catalyzed Borylation of Primary Benzylic C-H Bonds without a Directing Group: Scope, Mechanism, and Origins of Selectivity. *J. Am. Chem. Soc.* **2015**, *137*, 8633.
19. Hopmann, K. H. How Accurate is DFT for Iridium-Mediated Chemistry? *Organometallics* **2016**, *35*, 3795.
20. Zhu, J.; Lin, Z.; Marder, T. B. Trans Influence of Boryl Ligands and Comparison with C, Si, and Sn Ligands. *Inorg. Chem.* **2005**, *44*, 9384.
21. When the crude mixture of [Ir(cod)(OMe)]2, L2, and excess heptamethyltrisiloxane was treated with triphenyl phos-phite, the 1H NMR spectrum indicated that multiple phe-nanthroline containing and phosphite containing products formed. A doublet at -18.3 ppm, and the presence of 4 singlets between 0.5 and -1 ppm indicated the formation of a complex similar to 3. In addition, the 31P NMR spectrum contained a doublet at 102 ppm with the same coupling constant at the hydride in the 1H NMR spectrum. However, the signal intensities indicated that the doublet at 102 ppm corresponded to a minor species. Instead, a singlet at 128 ppm corresponded to the major product. Although these data are far from conclusive, we hypothesize that, in the presence of unhindered ligand L2, both trisilyl and disilyl hydride complexes are formed. The reaction catalyzed by complexes of L2 occur with both low rates and low cata-lyst lifetime; thus, it is unclear whether the formation of trisilyl complexes leads to less active catalysts for the si-lylation of aromatic C–H bonds or to catalyst deactiva-tion.
22. Hamdaoui, M.; Ney, M.; Sarda, V.; Karmazin, L.; Bailly, C.; Sieffert, N.; Dohm, S.; Hansen, A.; Grimme, S.; Djukic, J.-P. Evidence of a Donor–Acceptor (Ir–H)→SiR_3 Interaction in a Trapped Ir(III) Silane Catalytic Intermediate. *Organometallics* **2016**, *35*, 2207.
23. McGrady, G. S.; Sirsch, P.; Chatterton, N. P.; Ostermann, A.; Gatti, C.; Altmannshofer, S.; Herz, V.; Eickerling, G.; Scherer, W. Nature of the Bonding in Metal-Silane σ-Complexes. *Inorg. Chem.* **2009**, *48*, 1588.
24. Dinuclear Methoxy, Cyclooctadiene, and Barrelene Complexes of Rhodium(I) and Iridium(I). In *Inorg. Synth.*, pp 126.
25. Cheng, C.; Hartwig, J. F. Rhodium-Catalyzed Intermolecular C-H Silylation of Arenes with High Steric Regiocontrol. *Science* **2014**, *343*, 853.
26. Hansch, C.; Leo, A.; Taft, R. W. A survey of Hammett substituent constants and resonance and field parameters. *Chem. Rev.* **1991**, *91*, 165.

Chapter 5

Iridium-Catalyzed Silylation of Five-Membered Heteroarenes: High Sterically Derived Selectivity from a Pyridyl-Imidazoline Ligand

5.1 Introduction

The application of C-H bond functionalization to synthetic chemistry requires the selective activation of a single C–H bond among multiple C–H bonds that possess different steric and electronic properties.[1, 2] A common strategy for controlling the selectivity of catalytic reactions that functionalize the C–H bonds of arenes is to incorporate a functional group on the arene that coordinates to a transition-metal catalyst and directs the reaction to C–H bonds that are ortho, meta or para to that functional group.[3]

Undirected functionalizations of the C–H bonds of arenes occur with selectivities that are determined by the steric and electronic properties of the various types of C–H bonds.[4] The most classical undirected functionalizations include uncatalyzed or Lewis-acid catalyzed electrophilic aromatic substitution (EAS) processes. In general, these reactions occur at the most electron-rich C–H bonds, and the steric properties of the groups impart a secondary influence on selectivity.[5]

In contrast, the silylations and borylations of the C–H bonds of arenes catalyzed by iridium complexes of bipyridine or phenanthroline ligands generally occur at the most sterically accessible and acidic C–H bonds.[6] The regioselectivity of these reactions is almost exclusively determined by the steric properties of the arene; these catalysts selectively functionalize C–H bonds that are distal to functional groups in preference to C-H bonds that are more acidic, but proximal to functional groups. Thus, symmetrical 1,2-disubstituted or unsymmetrical 1,3-disubstituted or 1,2,3-trisubstituted arenes undergo borylation at the C–H meta to the nearest substituent (Figure 5.1).

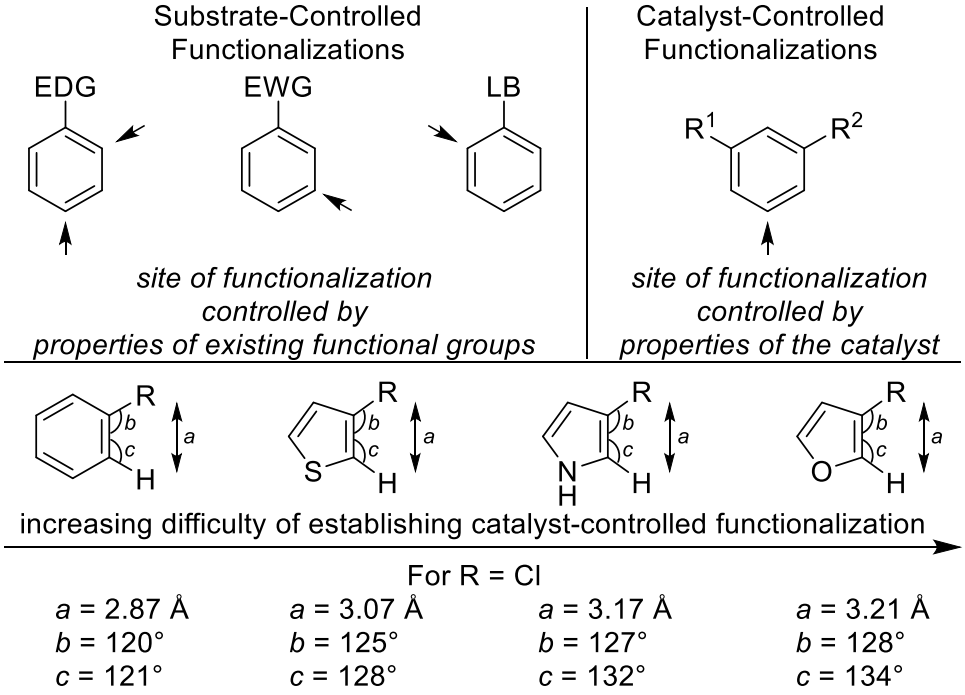

Figure 5.1 EDG = Electron donating functional group. EWG = electron withdrawing functional group LB = Lewis basic functional group.

The regioselectivity of the functionalization of heteroarenes is more complex than that of 6-membered rings because the more acute bond angles in 5-membered rings cause the distances between the substituents to be longer than those in 6-membered rings. This difference in distances between substituents in 5- and 6-membered rings makes the influence of steric properties on the selectivity of the functionalization of 5-membered heteroarenes less pronounced (Figure 5.1). Thus, catalytic functionalization of a single C–H bond in a five-membered ring heteroarene with high regioselectivity derived from steric effects is rare due to the distinct electronic properties of the positions of heteroarenes and the weaker steric influence in five-membered ring structures.

Consistent with this trend, the functionalization of these rings is limited by the poor selectivity of iridium-catalyzed borylation reaction, the low activity of catalysts for silylation reactions, and the requirement of special reagents for silylation. In particular, the current borylations of five-membered heteroarenes, in many cases, form isomers from the functionalization of sites ortho to small or medium-sized substitutents and product from diborylation,[7] even with the recently developed catalyst of Smith and Maleczka that contains a novel N-N ligand and with excess of thiophene.[8] Iridium-catalyzed silylations of these rings reported by Ishiyama and Miyaura with a phenanthroline bearing a large substituent in the 2-position occurred with several 3-substituted thiophenes and one furan with high sterically derived regioselectivity, but the low activity of this catalyst caused the reactions to require a large excess of heteroarene and high temperatures, and the tetrafluoro disilane used in this process is not commercially available and requires three steps to prepare.[9] Finally, neither the work of Ishiyama nor Smith describes the functionalization of heteroarenes containing multiple heteroatoms, even though these structures are among the most prevalent heteroarenes in medicinal and agrochemical chemistry.[10]

The identification of reactions that functionalize C-H bonds in five-membered-ring heteroarenes containing one or multiple heteroatoms regioselectively is important because these structural motifs are common in pharmaceuticals, electronic materials, agrochemicals, and natural products.[11] The regioselective silylation and borylation of heteroarenes would be particularly useful because silylarenes and aryl boronic esters undergo hydroxylation,[12] etherification,[13] amination,[14] cyanation,[15] halogenation,[16] and arylation,[17] and analogous derivatization of heteroarenes would provide an array of heteroarenes with substitution patterns that are derived from the catalytic system. The silylation of heteroarenes can be particularly valuable because the heteroarylsilanes are often more stable than the corresponding heteroarylboronates.[18]

We report silylations of five-membered heteroarenes catalyzed by an iridium complex that contains a pyridyl-imidazoline ligand, and also silylations catalyzed by a recently disclosed complex of 2,9-Me_2-phenanthroline (Me_2phen). We demonstrate that reactions with these catalysts produce high yields of products that are formed from functionalization of the most sterically accessible C–H bonds of five-membered heteroarenes under conditions in which borylation reactions produce mixtures of products. We also illustrate the versatility of the heteroarylsilanes by developing conditions for ipso substitution reactions to produce the corresponding five-membered-ring heteroarenes bearing halogen, aryl and perfluoroalkyl substituents.

5.2 Results & Discussion

5.2.1 Reaction Development

To achieve the undirected functionalization of five-membered heteroarenes with regioselectivity that is dictated by steric effects, we investigated reactions catalyzed by iridium complexes of a series of ligands that contain nitrogen donors. Two of the ligands, **L1** and **L2**, are based on pyridyl oxazoline structures, and two of the ligands, **L3** and **L4**, are based on pyridyl imidazoline structures. Ligand **L4** is new, and none of the ligands have been reported for the borylation or silylation of aromatic C–H bonds. We included pyridyl imidazoline structures in our study because the nitrogen atoms should be more electron donating than those in the pyridyl oxazoline structures, and substituents on the nitrogen in the imidazoline could influence the structures of these ligands.

To create a benchmark for our studies on the silylation of five-membered ring heteroarenes, we first measured the yield and selectivity of the borylation of 3-chlorothiophene that was catalyzed by the previously reported combination of $[Ir(COD)(OMe)]_2$ and 4,4'-di-tert-butylbipyridine (dtbpy).[19] Under standard conditions, the products from functionalization at positions both proximal and distal to the chlorine substituent formed, and the major product resulted from diborylation (Scheme 5.1). Similarly, the silylation of 3-chlorothiophene under the conditions recently reported by our group with 2,9-dimethylphenanthroline as ligand formed a mixture of products from silylation at both the 2 and 5-positions.

In contrast, the silylation of 3-chlorothiophene that was catalyzed by the combination of $[Ir(COD)(OMe)]_2$ and **L2** was selective for functionalization at the 5-position of the heteroarene. This regioselectivity was even higher when the reaction was catalyzed by $[Ir(COD)(OMe)]_2$ and the imidazoline ligand **L3** and was the highest when catalyzed by $[Ir(COD)(OMe)]_2$ and imidazoline ligand **L4**, which contains a 2,6-^{i}Pr-phenyl group on the imidazoline nitrogen. The silylation of 3-chlorothiophene, when catalyzed by iridium and **L3**, formed the product from functionalization at the 5-position in 74% yield, and the silylation of this thiophene, when catalyzed by iridium and **L4**, formed the product from functionalization at the 5-position in 90% yield with a 9:1 selectivity for this isomer over others and the product from di-functionalization.

Scheme 5.1 Effect of Ligand on Selectivity

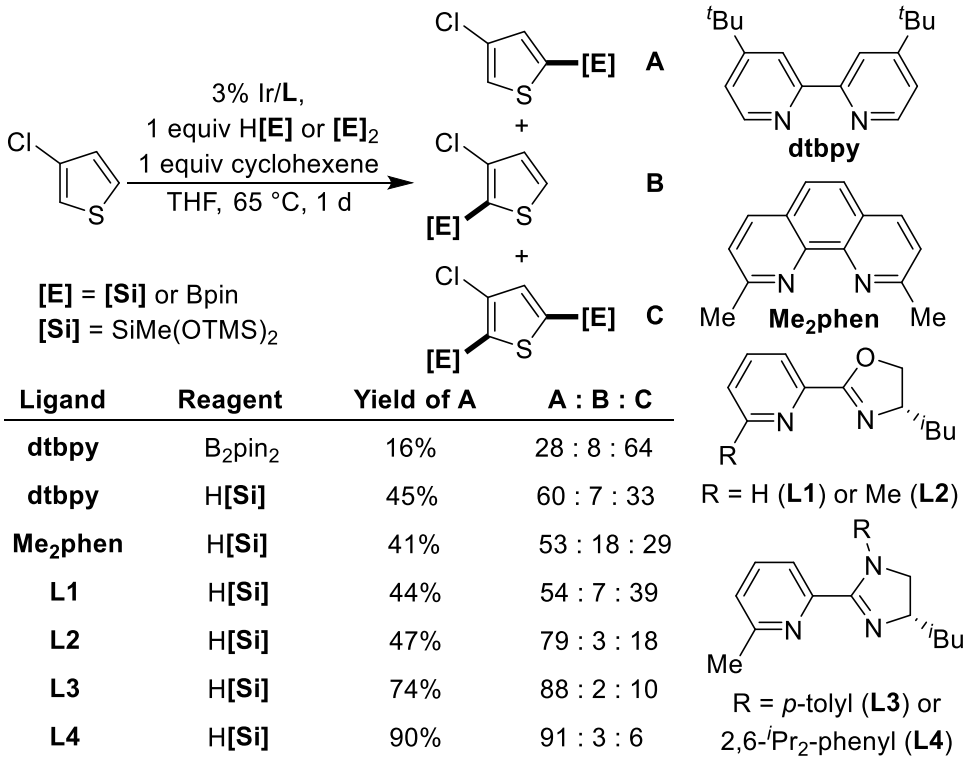

Ligand	Reagent	Yield of A	A : B : C
dtbpy	B_2pin_2	16%	28 : 8 : 64
dtbpy	H**[Si]**	45%	60 : 7 : 33
Me$_2$phen	H**[Si]**	41%	53 : 18 : 29
L1	H**[Si]**	44%	54 : 7 : 39
L2	H**[Si]**	47%	79 : 3 : 18
L3	H**[Si]**	74%	88 : 2 : 10
L4	H**[Si]**	90%	91 : 3 : 6

We note that this regioselectivity for silylation and chemoselectivity for monosilylation is obtained with limiting heteroarene. The regioselectivity is similar to that reported for the borylation or silylation of the same substrate, but our silylation reaction occurs with the thiophene as limiting reagent. The results on borylation or silylation were obtained with an excess of thiophene, and high selectivity for mono-borylation of such a thiophene with the heteroarene as limiting reagent has not been reported with any catalyst.[8-9]

5.2.2 Reaction Scope

Having identified a ligand that greatly increases the sensitivity of the iridium-catalyzed silylation of thiophenes to the steric environment of the C–H bonds, we studied the selectivity of this catalyst for the silylation of thiophenes that contain varied functional groups. We conducted silylation reactions with the catalyst that contains **L4** and cyclohexene as hydrogen acceptor, silylations with the catalyst that contains Me_2Phen and norbornene as hydrogen acceptor, and borylations with the catalyst that contains dtbpy (Scheme 5.2) without any hydrogen acceptor. These combinations of catalyst and acceptor for the silylations were used because the yields of silyl arenes from reactions conducted with the catalyst that contains Me_2Phen and cyclohexene were low, and only traces of silyl arenes were detected from reactions conducted with **L4** and norbornene.[19c] 5-Silyl-thiophenes that contain methyl, methoxy, phenyl, ester, boryl, bromide and iodide substituents in the 3-position were obtained with perfect selectivity for the monosilylation product, with perfect regioselectivity, and in yields ranging from 44% to 100% from reactions catalyzed by the combination of iridium and **L4**. The ethyl ester of **5** and the nitrile of **6** were tolerated; no products from reduction of these functional groups were observed. Thiophene **6**,

which contains a small cyano substituent, was converted to the corresponding silylarene with 85:12:3 selectivity for functionalization at the 5-position of 3-cyanothiophene to functionalization at the 2-position to di-silylation. Likewise, heteroarylsilanes that contain halogen substituents were obtained from the corresponding arenes (**7-9**) in moderate (3-iodo) to high (3-bromo and 3-chloro) yield and without proto-dehalogenation. The reactions of the larger of the three halides gave a single product; the reactions of the 3-chloro isomer gave 94:1 regioselectivity and 95:5 selectivity of monosilylation to disilylation.

Scheme 5.2 C-H Silylation of Thiophenes[a]

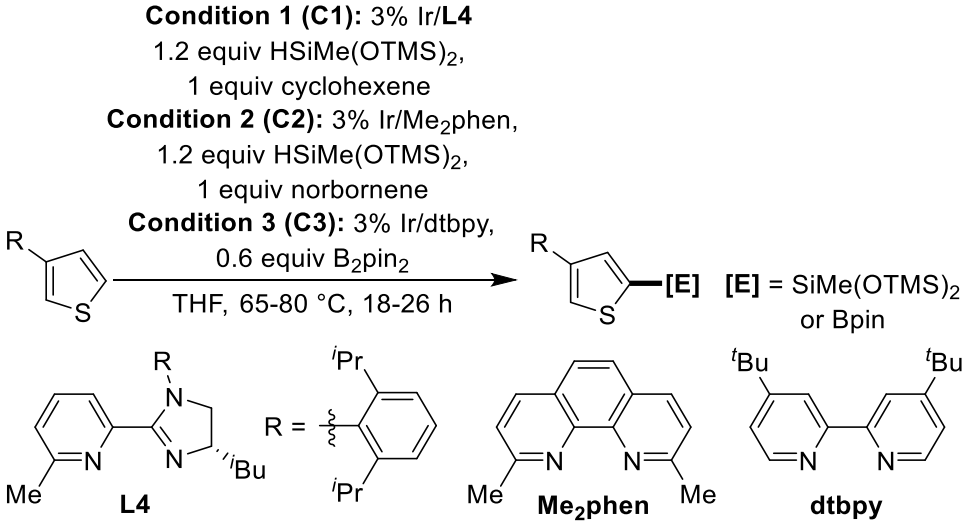

1, **C1**: 94%
C2: 40% (61:4:36)
C3: 33% (37:8:55)

2, **C1**: 90%
C2: 78% (94:0:6)
C3: 18% (39:30:30)

3, **C1**: 100%
C2: 26%
C3: 24%

4, **C1**: 85%
C2: 60%
C3: 13% (18:0:82)

5, **C1**: 100%
C2: 79%
C3: 84%

6, **C1**: 57% (85:12:3)
C2: 22% (26:28:46)
C3: 26% (30:31:39)

7, **C1**: 93% (94:1:5)
C2: 54% (60:10:30)
C3: 50% (52:16:32)

8, **C1**: 92%
C2: 30%
C3: 37% (60:12:28)

9, **C1**: 44%
C2: 42%
C3: 24% (90:0:10)

[a]Yields correspond to ^{1}H NMR yield of desired product (desired product : undesired, mono- : undesired, di-)

Results from the silylations catalyzed by the complex of Me_2Phen and the borylations catalyzed by the complex of dtbpy in Scheme 5.2 show the value of the silylation of the catalyst that contains **L4** for obtaining high regioselectivity. The silylation of thiophenes that contain smaller substituents occurred with low selectivity for functionalization at the 5-position (**1**, **6**, **7**) when catalyzed by the combination of iridium and Me_2phen. The borylations of these heteroarenes with iridium and dtbpy also produced mixtures of products. Silylations of thiophenes that contain larger phenyl, boryl, ester, bromide, and iodide substituents (**3**-**5**, **8**, **9**) and that were catalyzed by iridium and Me_2phen occurred with complete selectivity for functionalization at the 5-position of the heteroarene, but the yields were much lower than those catalyzed by iridium and **L4**. Likewise, borylation with dtbpy was highly selective for the 5-position of 3-phenylthiophene and ethyl 3-thiophenecarboxylate. However, the borylation of all the other thiophenes in Scheme 5.2 occurred with low selectivity for the 5-position. These results demonstrate that the catalyst formed from the combination of iridium and **L4** is more active and more selective for the functionalization of the least sterically hindered position of thiophenes than previously reported catalysts.

Scheme 5.3 C-H Silylation of Furans and Pyrroles[a]

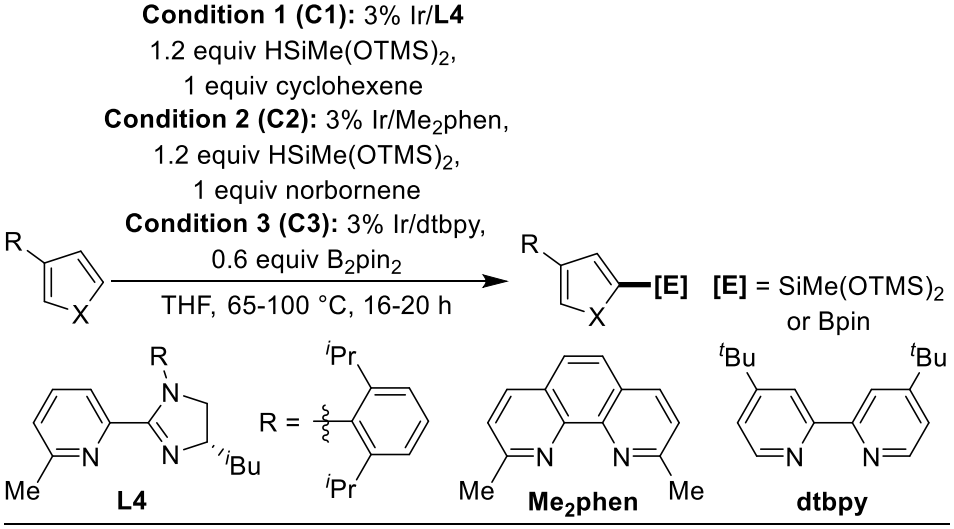

10, **C1**: 86% (82:14:4)[b]
C2: 30% (34:46:20)[b]
C3: 41% (55:8:37)[b]

11, **C1**: 100%
C2: 99%
C3: 87% (90:0:10)

12, **C1**: 100%
C2: 100%
C3: 18% (19:6:75)

13, **C1**: 83%
C2: 53% (78:0:22)
C3: 17% (34:4:62)

14, **C1**: 60%
C2: 43%
C3: 48% (64:36:0)

15, **C1**: 90%
C2: 48% (75:18:7)
C3: 64% (76:16:8)

[a]Yields correspond to ^{1}H NMR yield of desired product (desired product : undesired, mono- : undesired, di-). [b]4 °C, 5 d.

The analogous silylation and borylation reactions of furans and pyrroles are shown in Scheme 5.3 The silylations of 3-substituted furans and pyrroles catalyzed by iridium and imidazoline ligand **L4** occurred with perfect selectivity and in good yield (**11-15**, 60% to 100% yield). The silylation of 3-bromofuran (**10**) occurred with greater than 80% selectivity for the 5-position. In contrast, the silylation or borylation of 3-bromofuran under previously reported conditions led to the formation of large amounts of products from functionalization at the 2-position. In addition, the silylations of furans or pyrroles that contain esters at the 3-positions produced significant amounts of products from functionalization at the 2-position when the catalyst contained Me_2phen. The borylations of these nitrogen or oxygen-containing heterocycles occurred with universally poor selectivity for the least sterically hindered C–H bonds.

Five-membered ring heterocycles that contain multiple heteroatoms also underwent silylation in good yield and with high selectivity (Scheme 5.4). In these cases, the reactions occurred in the highest yields when catalyzed by $[Ir(COD)(OMe)]_2$ and Me_2phen. In all cases, the regioselectivity with which the silyl-azole products formed was high. The regioselectivity was dictated by steric effects with electronic effects influencing selectivity when potentially reactive C–H bonds were present in similar steric environments.

Three examples of the silylation of pyrazoles are provided in Scheme 5.4. The reactions of 1,3-dimethylpyrazole **16**, in which the two aromatic C–H bonds are in similar steric environments was completely selective for the 5-position, and this selectivity was consistent with the high preference for functionalization α to heteroatoms observed for the functionalization of thiophenes, furans and pyrroles. However, the silylation of pyrazoles that contain larger *tert*-butyl carbonate or tosyl substituents on nitrogen occurred distal to the nitrogen that bears that substituent. These results indicate that the silylation of pyrazoles occurs with a selectivity that is determined primarily by the steric environment of the C–H bonds, with electronic effects imparting a secondary influence.

Scheme 5.4 C-H Silylation of Azoles[a]

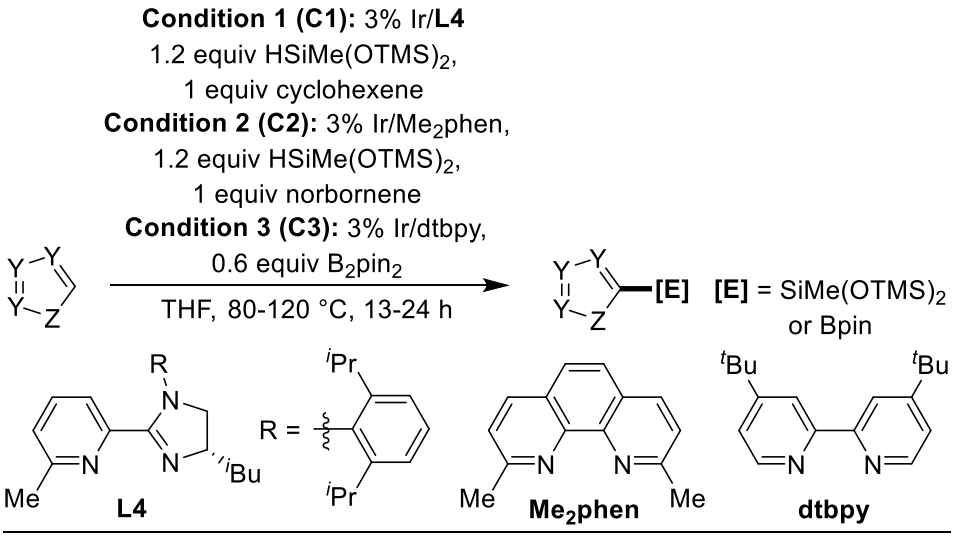

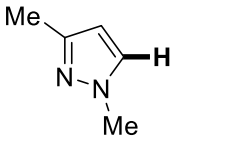

16, **C1**: 27%
C2: 38%, 99%[b]
C3: 37% [26%]

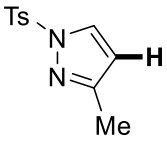

17, **C1**: 21%
C2: 70%
C3: 74% [72%]

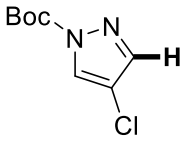

18, **C1**: 9%
C2: 85%
C3: 68% [20%]

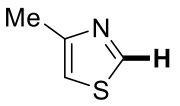

19, **C1**: trace product
C2: 75% (93:7:0)
C3: no product

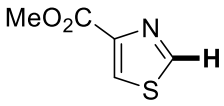

20, **C1**: trace product
C2: 72%
C3: no product

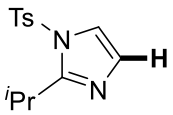

21, **C1**: 53%
C2: 82%
C3: 64% [no product]

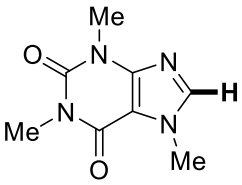

22, **C1**: trace product
C2: 68%
C3: 72% [no product]

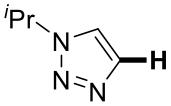

23, **C1**: 17%[b]
C2: 62%[b]
C3: 73% [no product]

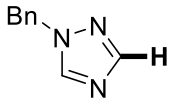

24, **C1**: 20%
C2: 30%, 87%[b]
C3: no product

[a]Yields correspond to ^{1}H NMR yield of desired product (desired product : undesired, mono- : undesired, di-), [yield after filtration through silica]. [b]5% Ir/L and 2 equiv. HSiMe(OTMS)$_2$.

The silylations of the thiazoles occurred at the position that is most sterically accessible. One might expect that the reaction would occur at the position more distal to the basic nitrogen because borylations of pyridines were shown previously not to form products from reaction at the position alpha to a basic nitrogen atom.[20] However, the silylation reaction formed a stable product

from reaction at the 2-position of 4-substituted thiazoles due to the steric congestion at the 5-position, even if the substituent at the 4-position was as small as a methyl group.

The silylations of heteorarenes containing multiple nitrogen atoms also formed stable products in good yield. The silylation of imidazole **21** containing substituents at the 1 and 2 positions gave a single product from reaction at the 4 position. The imidazole unit of caffeine gave a stable product from reaction at the only available aromatic C–H bond. Silylation of the 1,2,3- and 1,2,4-triazoles also occurred at the sterically more accessible of the two heteroaryl C–H bonds to form stable products albeit with 5 mol % catalyst.

The borylations of **16**, **18** and **21**-**23** occurred with high selectivity to form the products indicated in Scheme 5.4, but the borylated products were unstable. The borylations of **16**-**18**, **21**, and **22** gave the functionalized product in only 37-74% yields, and reactions of **19**, **20**, and **24** gave no borylated product, as determined by evaluating the crude reaction mixtures. Moreover, the amounts of borylated products from the reactions of **16** and **18** were lower after the reaction mixtures were filtered through silica, and no borylated products were present from reactions of **21**, **22** and **23** after the reaction mixtures were filtered through silica. Thus, consistent with prior literature, the products from the borylation of azoles are, in many cases, unstable to air and, in most cases, unstable to silica.[18, 20] In contrast, the products from the silylation of azoles **16-23** were isolated by silica gel chromatography, and the largest difference in yield of isolated silyl-azole products and yield determined from the crude reaction mixture was only 12%. The silyl-azole products are stable to air, moisture from solvents stored on the benchtop, and silica. The greater stability of silyl-azoles than of boryl-azoles renders the silylation of the C–H bonds of azoles particularly useful.

5.2.3 Functionalization of Heteroarylsilanes

To demonstrate the utility of C–H silylation to the preparation of functionalized heteroarenes, we assessed the ability to convert the silyl heteroarenes to heteroarenes that are functionalized with halogens or with aryl or trifluoromethyl groups (Scheme 5.5, right). In addition, we compared the products one would obtain from the combination of silylation and functionalization to those from more classical processes (Scheme 5.5, left). The silylation of ethyl 3-furan carboxylate, followed by functionalization with *N*-chlorosuccinimide in the presence of AgF formed ethyl 2-chloro-4-furancarboxylate **25** in 63% yield over two steps. In contrast, directed metalation of the related 3-furancarboxylate, followed by quenching with hexachloroethane, is known to produce 2-chloro-3-furancarboxylate.[21] The silylation of 3-chlorothiophene, followed by functionalization with *N*-bromosuccinimide and AgF, formed bromide 2-bromo-4-chlorothiophene **26** in 72% yield over two steps. In contrast, the direct bromination of 3-chlorothiophene with NBS has been reported to form 2-bromo-3-chlorothiophene.[22] Likewise, the sequential silylation and iodination of 3-methoxythiophene formed 2,4-functionalized product **27**, whereas direct iodination of the unfunctionalized arene is known to form the 2,3 functionalized product.[23] Heteroarylsilanes also undergo coupling reactions to form arylated products. The silylation of 3-methoxythiophene at the 5-position followed by Hiyama cross-coupling in the presence of a palladium catalyst furnished 5-arylated product **28** in 58% yield over 2 steps. Previous literature reported that the direct arylation of 3-

methoxythiophene, when catalyzed by rhodium or palladium complexes, leads to arylation with high selectivity for the 2-position,[24] although direct arylation of 3-methoxythiophene at the 5-position does occur with diaryliodonium salts in the presence of a Cu/Fe catalyst.[25] The 5-arylated product **29** formed in 67% yield over two steps by the sequential silylation and cross-coupling of ethyl 3-furancaryboxylate. In contrast, ethyl 3-furancarboxylate is known to undergo direct arylation at the 2-position in the presence of $Pd(PPh_3)_4$ as catalyst and undergoes arylation at the 5-position with a modest 3 to 1 selectivity in the presence of Pd/C.[26]

Scheme 5.5 Regio-Divergent Functionalization of Heteroarenes

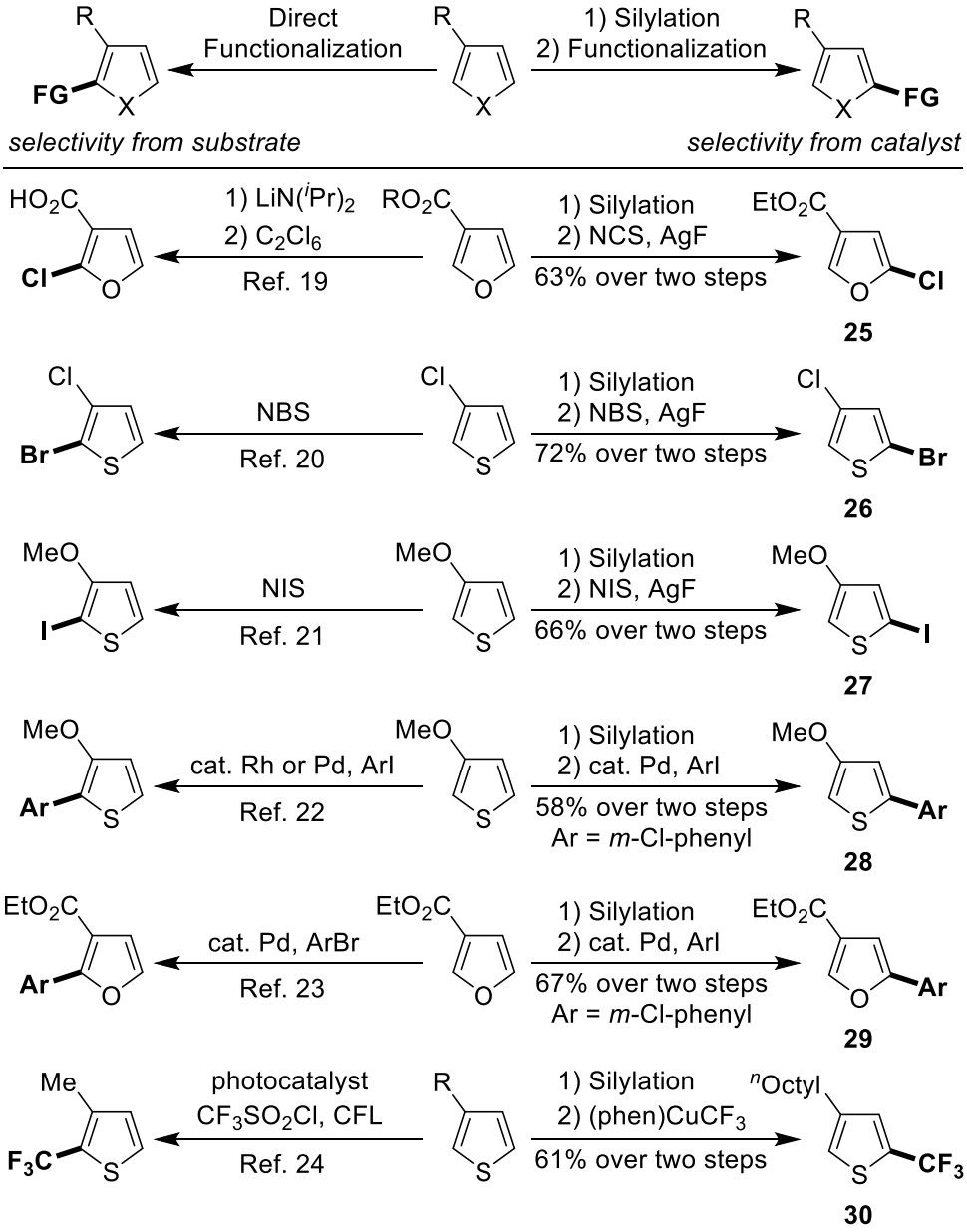

Finally, the silylation of 3-methylthiophene, followed by coupling $(phen)CuCF_3$ under an atmosphere of oxygen, formed the product from trifluoromethylation of the 5-position of the

thiophene. In contrast, the direct addition of trifluoromethyl radical is known to occur at the 2-position of 3-methylthiophene.[27] Due to the volatility of 2-trifluoromethyl-4-methylthiophene, this product, was characterized by the ^{19}F NMR of the crude reaction mixture. However, to form an isolable analog, the silylation of 3-octylthiophene and coupling of the silyl thiophene with a source of trifluoromethyl group was studied, and 2-trifluoromethyl-4-octylthiophene was formed by this process in 61% yield by NMR spectroscopy and 37% isolated yield. These results demonstrate that the silylations of heteroarenes with high sterically derived regioselectivity, followed by functionalizations of the resulting heteroarylsilanes, generate products that are distinct from those accessible from the direct functionalization of the same heteroarenes.

The silyl-azoles presented in Scheme 5.4 are more electron-deficient than the silyl-thiophenes and silyl-furans in Scheme 5.5. To determine whether silyl-azoles are nucleophilic enough to undergo transformations that are similar to those of other silyl-arenes and heteroarenes, we conducted a series of derivatizations of silyl pyrazole **31** (Scheme 5.6). The reaction of **31** with NCS in the presence of AgF formed chloropyrazole **32** in 52% yield. Similarly, the reaction of **31** with NBS formed bromopyrazole **33** in 81% yield. Silyl-pyrazole **31** also coupled with 3,5-$(MeO)_2$-phenyl triflate to form biaryl **34** in 70% yield when catalyzed by $Pd_2dba_3{\cdot}CHCl_3$ and BINAP. The identification of that catalyst system is discussed in greater detail below. In addition, **31** coupled with (phen)$CuCF_3$ under an atmosphere of oxygen to form 1-Ts-3-Me-4-CF_3-pyrazole (**35**) in 50% yield. These results demonstrate that the silylation of azoles, followed by the functionalization of the product, also can lead to products containing a diverse array of functional groups.

Scheme 5.6 Transformations of Silyl-Pyrazole

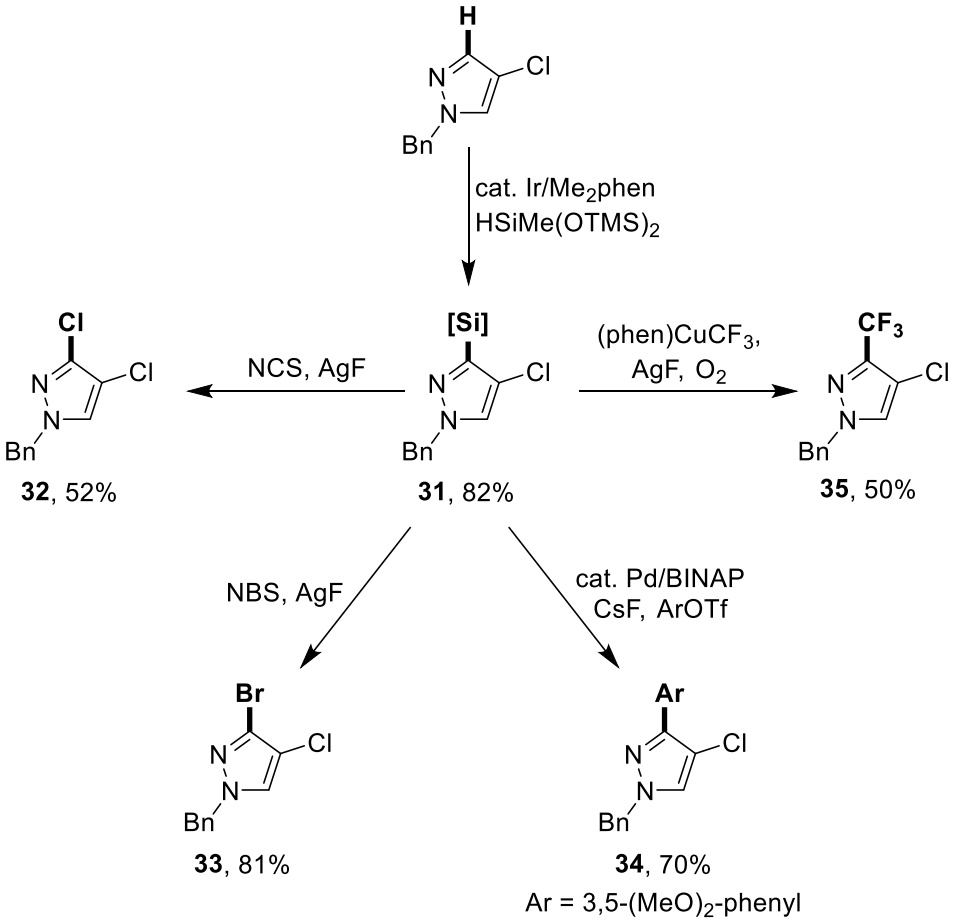

Suzuki couplings are widely used, in part, because the aryl boronic acid and ester reagents are stable to air and moisture and can be stored. However, as discussed, the boronic acids or esters of azoles are often unstable. Therefore, coupling of the more stable silyl derivatives of five-membered heteroarenes would be valuable. We found that the silyl-thiophenes and silyl-furans that result from the silylation of C–H bonds couple with aryl iodides in the presence of AgF and catalytic amounts of $Pd(P^tBu_3)_2$. However, under similar conditions, only 10% of the product from the reaction of the silyl thiazole 2-silyl-4-thiazolecarboxylate methyl ester formed from coupling the representative partner *m*-Cl-iodobenzene (Scheme 5.7). After conducting reactions with a series of fluoride additives and phosphine ligands, we found that a high yield of biaryl product (85%) was obtained from reactions with CsF as activator and the combination of $Pd_2dba_3{\cdot}CHCl_3$ and BINAP as catalyst. The 2-silyl-4-thiazolecarboxylate methyl ester also coupled with heteroaryl bromides catalyzed by the same system to form biaryls **37** and **38** in 76% and 50% yield. Although bithiazole **39** formed in a modest 22% yield from the same coupling of the silyl thiazole with 2-bromothiazole, this reaction has not been accomplished previously by Suzuki coupling of the analogous boronate, presumably due to the instability of this boronate. As noted in the previous paragraph, these conditions were also suitable for the coupling of the silyl-pyrazole **31** to form 3-aryl pyrazole **34**. Thus, the combination of CsF activator and BINAP-ligated

palladium is an effective system to catalyze the coupling of silylazoles with aryl halides under mild conditions.

Scheme 5.7 Hiyama Coupling of Silyl-Azoles[a]

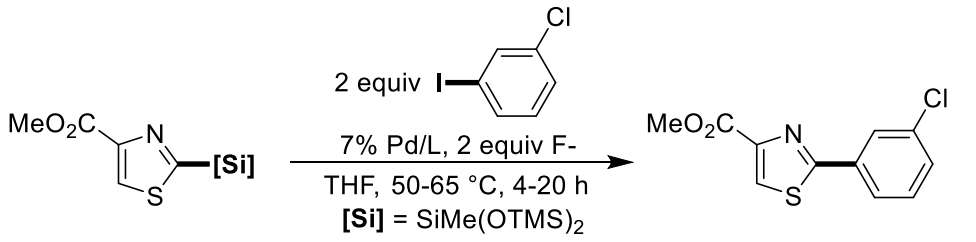

Pd Precatalyst	Ligand	F-	Temp.	Time	Yield[c]
$Pd(P^tBu_3)_2$	-	AgF	65 °C	20 h	10%
Pd_2dba_3•$CHCl_3$	$PAd_2{}^nBu$	AgF	65 °C	20 h	17%
Pd_2dba_3•$CHCl_3$	$PAd_2{}^nBu$	KHF_2	65 °C	20 h	50%
Pd_2dba_3•$CHCl_3$	$PAd_2{}^nBu$	TBAF•H_2O	65 °C	20 h	7%
Pd_2dba_3•$CHCl_3$	$PAd_2{}^nBu$	CsF	65 °C	20 h	83%
Pd-Xphos-G2	-	CsF	50 °C	20 h	54%
$(dppf)PdCl_2$	-	CsF	50 °C	20 h	54%
Pd_2dba_3•$CHCl_3$	$PAd_2{}^nBu$	CsF	50 °C	20 h	67%
Pd_2dba_3•$CHCl_3$[b]	BINAP	CsF	50 °C	20 h	83%
Pd_2dba_3•$CHCl_3$[b]	BINAP	CsF	50 °C	4 h	85%

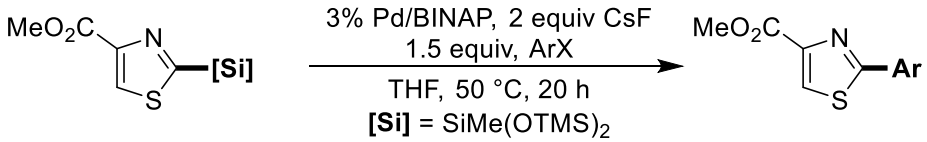

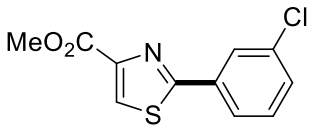

36, 63%
X = I

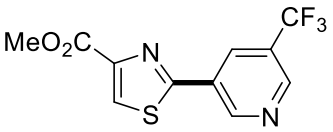

37, 76%
X = Br

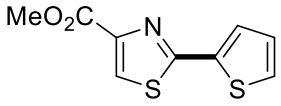

38, 40%, 50%[c]
X = Br

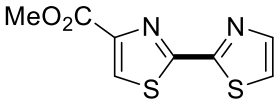

39, 22%
X = Br

[b]3% Pd/L. [c]Determined by ^1H NMR spectroscopy with dibromomethane internal standard.

5.2.4 Origin of Regioselectivity

To determine the elementary steps controlling the high selectivity for the silylation of unhindered C–H bonds of heteroarenes catalyzed by complexes of **L4**, we conducted studies on the reactions of deuterated silane with 3-chlorothiophene (**7**). The reactions of an excess of **7** with deuterated silane catalyzed by iridium and Me_2phen or L4 exchanged deuterium between the silane Si–D bond and the 2-positions and 5-positions of the heteroarene to form deuterated products **7c** and **7d**, respectively. This reaction occurred in concert with the formation of silylated products **7a** and **7b**. After 15 min at 65 °C, the amounts of deuterated products **7c** and **7d** were greater than the amounts of silylated products **7a** and **7b** by factors of about 2:1 and 6:1 for the catalysts containing ligands Me_2phen and **L4**, respectively. This incorporation of deuterium into the heteroarene reactant indicates that cleavage of the C–H bond is reversible.

The ratio of deuterated products was distinct from the ratio of silylated products. The reaction catalyzed by the complex of Me_2phen formed deuterated products **7c** and **7d** in a ratio of 1.5:1 but formed the silylated products **7a** and **7b** in a higher ratio of 2.9:1 (Scheme 5.8). The reaction catalyzed by a complex of **L4** formed the deuterated products **7c** and **7d** in a ratio of only 1.1:1 but formed the silylated products **7a** and **7b** in a high ratio of 14:1. Thus, the cleavage of C–H bonds by the catalyst that contains **L4** is less regioselective than that of the catalyst that contains Me_2phen, but the formation of silylated products by the catalyst that contains **L4** occurs with much greater regioselectivity than that of the catalyst that contains Me_2phen. These results demonstrate that the regioselectivity of these two catalysts for the silylation of C–H bonds does not reflect the propensity of the catalysts to cleave C–H bonds. Rather, the selectivity of the silylation reaction is controlled by the relative rates of formation of the carbon-silicon bond from 2- or 5-heteroaryliridium intermediates that are formed reversibly. These experimental results resemble the computations reported by Sakaki for the selectivity of the borylations of β over α C–H bonds in THF, as well as the experiments and computations our group reported previously on the origins of selectivity of Rh-catalyzed borylations and silylations of primary over secondary alkyl C–H bonds.[28]

Scheme 5.8 Reactions of Deuterated Silane with Excess Arene[a]

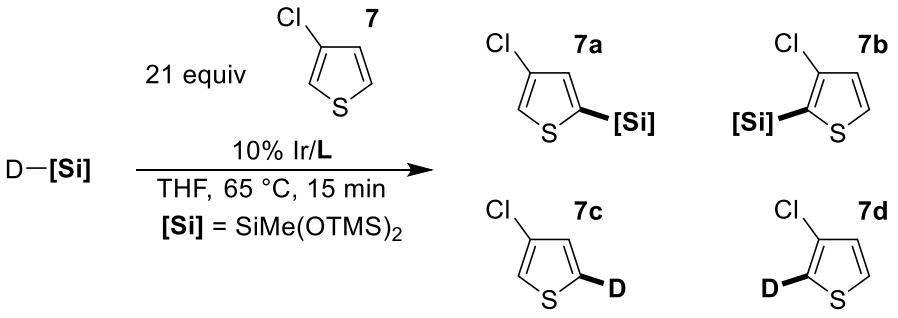

Ligand	7a	7b	7c	7d	7a : 7b	7c : 7d
Me_2phen	29%	10%	40%	27%	2.9 : 1	1.5 : 1
L4	11%	0.8%	32%	29%	14 : 1	1.1 : 1

5.3 Conclusion

In summary, we have developed a method for the silylation of heteroaromatic compounds with high sterically derived regioselectivity. In many cases, these high selectivities are achieved with a new pyridyl-imidazoline ligand **L4.** The selectivity of this silylation to form functionalized products from reaction at the least sterically hindered position of five-membered heteroarenes is much higher than that of previously reported borylations of these heteroarenes, and the products formed are much more stable than the analogous boronates. Moreover, functionalizations of the heteroarylsilanes form products with substitution patterns that are orthogonal to those that have been reported by traditional methods and other catalytic processes. Mechanistic studies showed that the rates of formation of the carbon-silicon bond from isomeric heteoraryliridium complexes influences the selectivities of the silylation reactions more than the rates of the cleavage of carbon-hydrogen bonds to form these complexes and that the selectivities from the reactions catalyzed by the combination of iridium and the pyridyl-imidazoline ligand **L4** result almost exclusively from the rates of formation of the carbon-silicon bond. Additional studies on the mechanism and origin of high selectivity of the silylation reaction with catalysts that contain imidazoline ligands are ongoing in our laboratory.

5.4 Experimental

Materials and Methods

All silylation reactions and substrate syntheses were assembled in an N_2-filled glovebox with oven-dried glassware unless otherwise noted. $[Ir(cod)OMe]_2$ was synthesized by following reported procedures.[29] 2,9-Dimethyl-1,10-phenanthroline (Me_2phen) was purchased from Alfa Aesar and was used as received. **L1**,[30] **L2**,[31] and **L3**[32] were synthesized through literature procedures. 4,4'-Ditertbutylbipyridine (dtbpy) was purchased from TCI. 1,1,1,3,5,5,5-Heptamethyl-trisiloxane was purchased from TCI and was used as received. **6**,[33] **12**,[34] **23**,[35] **24**,[36] 3-*n*octylthiophene,[37] and N-benzyl-4-Cl-pyrazole[38] were synthesized by following reported procedures. 1,1,1,3,5,5,5-Heptamethyl-3-*d*-trisiloxane was synthesized by a reported procedure.[39] Norbornene (nbe) and cyclohexene were purchased from Aldrich and were used as received. Diethyl ether and tetrahydrofuran (THF) were degassed by purging with nitrogen and then dried with a solvent purification system containing activated alumina. All other solvents and reagents were used as received, except for 3-iodothiophene, which was filtered through a plug of silica before use. Reaction temperatures above 23 °C refer to temperatures of an aluminum heating block, which were controlled by an electronic temperature modulator. NMR spectra were recorded on Bruker AV-300, AVQ-400, AVB-400, AV-500, DRX-500 and AV-600 instruments. Chemical shifts (δ) are reported in ppm relative to the residual solvent signal. Data from ^{1}H NMR spectra are reported as follows: chemical shift (multiplicity, coupling constants, number of hydrogens). Abbreviations are as follows: s (singlet), d (doublet), t (triplet), q (quartet), m (multiplet), br (broad). GC-MS data were obtained on an Agilent 6890-N GC system containing an Alltech EC-1 capillary column and an Agilent 5973 mass selective detector. High-resolution mass spectral data were obtained from the University of California, Berkeley Mass Spectrometry Laboratory. High resolution ESI-MS was acquired by Dr. Rita Nichiporuk and high resolution EI-MS was acquired by Dr Zhongui

Zhou. FT-IR data was collected on a Bruker VORTEX 80 FTIR spectrometer. Atom distances and bond angles in Figure 1 were calculated with the MolView web-based software.[40]

Procedures for the Synthesis of Substrates

***N*-Cyclohexylfuran-3-carboxamide (14)**

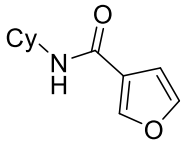

3-Furoic acid (10 mmol, 1.12 g, 1 equiv) was added to anhydrous DCM (0.1 M, 70 mL) in a 250 mL round-bottom flask. The flask was placed in an ice bath, and *N*-methylmorpholine (1.2 mL, 10.25 mmol, 1.025 equiv) was added dropwise while the solution was stirred. Then, isobutyl chloroformate (1.4 mL, 10 mmol, 1.0 equiv) was added, and the reaction mixture stirred for 30 min. Finally, cyclohexylamine (1.4 mL, 10 mmol, 1.0 equiv) was added dropwise, and the mixture stirred for 3.5 h at room temperature. The solution was extracted with saturated aqueous potassium carbonate, and the aqueous layers were back extracted with hexane. The combined organic layers were dried with sodium sulfate and concentrated under reduced pressure. The crude product was purified by silica gel chromatography (3% methanol in DCM) to afford 1.1 g (54% yield) of a white solid. ^{1}H NMR (400 MHz, $CDCl_3$) δ 7.90 (q, *J*= 1.1 Hz, 1H), 7.42 (t, *J*= 1.7 Hz, 1H), 6.58 (dd, *J*= 1.9, 0.9 Hz, 1H), 5.57 (br s, 1H), 3.97 – 3.88 (m, 1H), 2.02 -1.98 (m, 2H), 1.74 (dt, J = 13.9, 3.8 Hz, 2H), 1.64 (dt, J = 13.1,3.8 Hz, 1H) 1.46 - 1.35 (m, 2H), 1.24 - 1.13 (m, 3H). ^{13}C NMR (101 MHz, $CDCl_3$) δ 144.6, 143.7, 123.0, 108.3, 48.3, 33.3, 25.6, 25.0. HRMS (ESI+), calculated for [$C_{11}H_{16}O_2N$+]: 194.1176, found: 194.1177.

2-(Furan-3-yl)-4,4,5,5-tetramethyl-1,3,2-dioxaborolane (11)

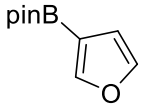

Furan-3-ylboronic acid (336 mg, 3 mmol, 1 equiv), pinacol (372 mg, 3.15 mmol, 1.05 equiv), and toluene (10 mL, 0.3 M) were added to a 20 mL vial fitted with a stir bar. The vial was capped with a Teflon-lined screw cap, and the solution was heated to 100 ºC for 24 h with stirring. The reaction was quenched with water and extracted with Et_2O. The combined organic layers were washed with brine, dried with sodium sulfate and concentrated under reduced pressure. The crude residue was purified by silica gel chromatography (10% ethyl acetate in hexanes) to afford 200 mg (34% yield) of a colorless oil. ^{1}H NMR (400 MHz, $CDCl_3$) δ 7.79 (s, 1H), 7.46 (s, 1H), 6.59 (s, 1H), 1.31 (s, 12H). These spectroscopic data match those reported in the literature.[41] The carbon bonded to boron was not observed via ^{13}C NMR spectroscopy due to broadening by the quadrupolar boron nucleus.

N-Boc-4-Cl-pyrazole (16)

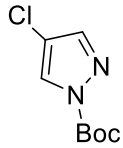

4-Cl-Pyrazole (205 mg, 2.00 mmol), Boc_2O (524 mg, 2.40 mmol, 1.20 equiv), 4-dimethylaminopyridine (24 mg, 0.20 mmol, 0.10 equiv), and acetonitrile (2 mL) were added to a 20 mL vial fitted with a stir bar. The vial was capped with a Teflon-lined screw cap, and the solution was stirred at room temperature for 16 h. The reaction was quenched with aqueous ammonium chloride and extracted with DCM. The combined organic layers were washed with brine, dried with sodium sulfate and concentrated under reduced pressure. The crude residue was purified by silica gel chromatography (25% ethyl acetate in hexanes) to afford 400 mg (99% yield) of a colorless oil. ^{1}H NMR (300 MHz, $CDCl_3$) δ 8.05 (d, *J* = 0.8 Hz, 1H), 7.64 (d, *J* = 0.8 Hz, 1H), 1.65 (s, 9H). These spectroscopic data match those reported in the literature.[42]

N-Ts-3-Me-pyrazole (17)

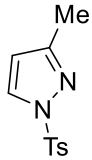

3-Me-Pyrazole (164 mg, 2.00 mmol), 4-toluenesulfonyl chloride (573 mg, 3.00 mmol, 1.50 equiv), diisopropylethylamine (700 μL, 4 mmol, 2 equiv), and DCM (10 mL) were added to a 20 mL vial fitted with a stir bar. The vial was capped with a Teflon-lined screw cap, and the solution was stirred at room temperature for 16 h. The solution was concentrated under reduced pressure. The crude residue was purified by silica gel chromatography (50-100% ethyl acetate in hexanes) to afford 280 mg (59% yield) of a white solid. ^{1}H NMR (500 MHz, $CDCl_3$) δ 7.93 (d, *J* = 2.8 Hz, 1H), 7.80 (d, *J* = 8.4 Hz, 2H), 7.24 (d, *J* = 8.4 Hz, 2H), 6.14 (d, *J* = 2.8 Hz, 1H), 2.33 (s, 3H), 2.19 (s, 3H). These spectroscopic data match those reported in the literature.[43]

N-Ts-2-Isopropyl-imidazole (21)

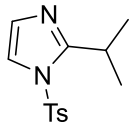

2-Isopropyl-Imidazole (220 mg, 2.0 mmol), 4-toluenesulfonyl chloride (573 mg, 3.00 mmol, 1.50 equiv), diisopropylethylamine (700 μL, 4 mmol, 2 equiv), and DCM (10 mL) were added to a 20 mL vial fitted with a stir bar. The vial was capped with a Teflon-lined screw cap, and the solution was stirred at room temperature for 16 h. The solution was concentrated under reduced pressure. The crude residue was purified by silica gel chromatography (50-100% ethyl acetate in hexanes) to afford 515 mg (97% yield) of a colorless oil. ^{1}H NMR (500 MHz, $CDCl_3$) δ 7.70 (d, *J* = 8.5 Hz, 2H), 7.34 (d, *J* = 1.7 Hz, 1H), 7.29 (d, *J* = 8.5 Hz, 2H), 6.90 (d, *J* = 1.7 Hz, 1H), 3.41 (hept, *J* = 6.8 Hz, 1H), 2.38 (s, 3H), 1.14 (d, *J* = 6.8 Hz, 6H). ^{13}C NMR (126 MHz, $CDCl_3$) δ 154.9, 145.9, 135.6, 130.3, 128.0, 127.1, 118.9, 27.3, 22.1, 21.7. HRMS (ESI+), calculated for [$C_{13}H_{17}N_2O_2S$+]: 265.1005, found: 265.1009.

Procedure for the synthesis of L4

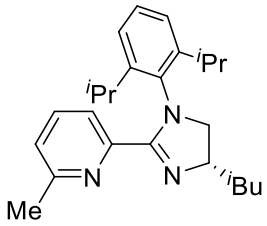

An oven dried, 3-neck, 250 mL round bottom flask was fitted with a stirbar, three rubber septa, and an N_2 line. The flask was evacuated with a high-vacuum and backfilled with nitrogen three times. 60 mL of dry DCM was added, and a third septum was placed on the flask. Under a positive pressure of N_2, a septum was removed, and 6-methylpyridine-2-carboxylic acid (6 mmol, 883 mg, 1 equiv) was added to the flask. The septum was replaced, and the solution was stirred and cooled in an ice bath. *N*-Methylmorpholine (6.6 mmol, 67 mg, 0.73 mL, 1.1 equiv) was then added dropwise via syringe, followed isobutylchloroformate (6.6 mmol, 900 mg, 0.86 mL, 1.1 equiv), also dropwise via syringe. The mixture was stirred at 0 ºC for 15 min. Then, (s)-(+)-leucinol (6.6 mmol. 770 mg, 0.84 mL, 1.1 equiv) was added dropwise via syringe. The ice bath was removed, and the solution was stirred for 5 h. Water was added to the solution. The resulting mixture was transferred to a separatory funnel and extracted with DCM three times. The combined organic layers were washed with brine, dried over sodium sulfate and filtered through a plug of cotton. Volatile materials were evaporated under reduced pressure, and the residue was transferred to a 20 mL vial fitted with a stirbar. The vial was placed in an N_2 filled glovebox. Dry, degassed toluene (12 ml) and PCl_5 (18 mmol, 3.7 g, 3.0 equiv) were added to the vial. The vial was sealed with a Teflon-lined screw cap, removed from the glovebox, placed in a 100 ºC preheated aluminum heating bock, and stirred for 4 h.

The reaction mixture was cooled and placed under high vacuum overnight. The vial was placed in an N_2 filled glovebox, and dry acetonitrile (6 mL, 1 M) was added. Then, dry triethylamine (18 mmol, 2.5 mL, 3.0 equiv) was added dropwise, while the vial was manually agitated. 2,6-Diisopropylaniline (7.2 mmol, 1.4 mL, 1.2 equiv) was added, and the vial was sealed with a Teflon-lined cap, removed from the glovebox, placed in a 100 ºC preheated aluminum heating block, and stirred for 16 h. After cooling, the product mixture was quenched with water and extracted with ethyl acetate. The organic layers were dried over magnesium sulfate and filtered through a plug of cotton. Solvent was removed under reduced pressure. The crude product was purified by silica-gel chromatography (40% to 90& EtOAc:hexanes with 1% Et_3N) to afford **L4** as a brown oil (1.4 g 61% yield). ^{1}H NMR (400 MHz, $CDCl_3$) δ 7.53 (d, *J* = 7.7 Hz, 1H), 7.41 (t, *J* = 7.7 Hz, 1H), 7.19 (t, *J* = 7.7 Hz, 1H), 7.04 (d, *J* = 7.7 Hz, 2H), 6.92 (d, *J* = 7.7 Hz, 1H), 4.38 (ddd, *J* = 10.8, 8.4, 5.9 Hz, 1H), 3.89 (t, *J* = 10.0 Hz, 2H), 2.14 (s, 3H), 1.94 – 1.80 (m, 2H), 1.20 (dd, *J* = 6.9, 2.9 Hz, 6H), 0.94 (dt, *J* = 44.0, 6.8 Hz, 12H). ^{13}C NMR (151 MHz, $CDCl_3$) δ 162.1, 157.4, 146.6, 146.3, 136.5, 128.1, 124.6, 123.9, 123.9, 122.2, 60.7, 46.3, 28.3, 25.1, 25.0, 23.7, 23.3, 23.2, 23.0, 22.6. HRMS (ESI+), calculated for [$C_{25}H_{36}N_3$+]: 378.2904, found: 378.2897.

Assessment of effect of ligands on silylations and borylation of a thiophene

Silylation of 3-chlorothiophene

In an N_2-filled glovebox, $[Ir(cod)OMe]_2$ (1.0 mg, 1.5 μmol, 1.5 mol%), ligand (3.0 μmol, 3.0 mol%), 1,1,1,3,5,5,5-heptamethyl-trisiloxane (2.4 mg, 0.10 mmol, 1 equiv), cyclohexene (8.2 mg, 0.1 mmol, 1 equiv), and THF (100 μL) were added to a 4 mL vial. To this mixture was added 3-chlorothiophene (12 mg, 0.1 mmol). The vial was capped with a Teflon-lined screw cap, and the sealed vial was removed from the glovebox and placed in a preheated aluminum heating block. After 24 h, the vial was removed from the heating block, and 5 μL of dibromomethane was added as an internal standard. The selectivity of the silylation reaction and the yield were determined by ^{1}H NMR spectroscopy.

Borylation of 3-chlorothiophene

In an N_2-filled glovebox, $[Ir(cod)OMe]_2$ (1.0 mg, 1.5 μmol, 1.5 mol%), dtbpy (1.1 mg, 3 μmol, 3.0 mol%), B_2pin_2 (13 mg, 0.050 mmol, 0.50 equiv), and THF (45 μL) were added to a 4 mL vial. After 15 min, 3-chlorothiophene (12 mg, 0.10 mmol) was added to the vial. The vial was capped with a Teflon-lined screw cap, and the sealed vial was removed from the glovebox and placed in a preheated aluminum heating block. After 24 h, the vial was removed from the heating block, and 5 μL of dibromomethane was added as an internal standard. The selectivity of the borylation reaction and the yield were determined by ^{1}H NMR spectroscopy.

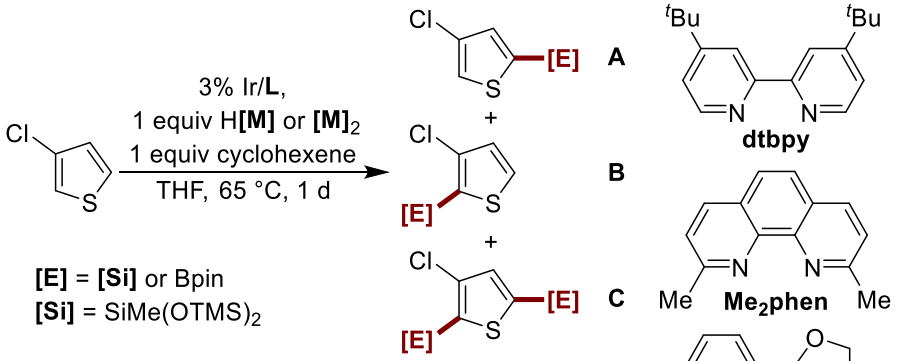

Ligand	Reagent	Yield of A	A : B : C
dtbpy	B_2pin_2	16%	28 : 8 : 64
dtbpy	H**[Si]**	45%	60 : 7 : 33
Me$_2$phen	H**[Si]**	41%	53 : 18 : 29
L1	H**[Si]**	44%	54 : 7 : 39
L2	H**[Si]**	47%	79 : 3 : 18
L3	H**[Si]**	74%	88 : 2 : 10
L4	H**[Si]**	90%	91 : 3 : 6

General Procedures for the Ir-catalyzed Silylations and Borylations of Arenes

Procedure A for the Ir-catalyzed silylation of heteroarenes:
In an N_2-filled glovebox, $[Ir(cod)OMe]_2$ (2.5 mg, 3.8 μmol, 1.5 mol%), **L4** (3.0 mg, 7.5 μmol, 3.0 mol%), 1,1,1,3,5,5,5-heptamethyl-trisiloxane (67 mg, 0.30 mmol, 1.2 equiv), cyclohexene (20 mg, 0.25 mmol, 1 equiv), and THF (100 μL) were added to a 4 mL vial. After 15-30 min, substrate (0.25 mmol) was added. The vial was capped with a Teflon-lined screw cap, and the vial was removed from the glovebox and placed in a preheated aluminum heating block at the indicated temperature. After the indicated length of time, the vial was removed from the heating block, and dibromomethane was added as an internal standard. The yield and selectivity were determined by ^1H NMR spectroscopy.

Procedure B for the Ir-catalyzed silylation of heteroarenes
In an N_2-filled glovebox, $[Ir(cod)OMe]_2$ (2.5 mg, 3.8 μmol, 1.5 mol%), 2,9-dimethyl-1,10-phenanthroline (1.6 mg, 7.5 μmol, 3.0 mol%), 1,1,1,3,5,5,5-heptamethyl-trisiloxane (67 mg, 0.30 mmol, 1.2 equiv), norbornene (24 mg, 0.25 mmol, 1 equiv), and THF (100 μL) were added to a 4 mL vial. After 15-30 min, substrate (0.25 mmol) was added. The vial was capped with a Teflon-lined screw cap, and the vial was removed from the glovebox and placed in a preheated aluminum heating block at the indicated temperature. After the indicated length of time, the vial was removed from the heating block, and dibromomethane was added as an internal standard. The yield and selectivity were determined by ^1H NMR spectroscopy.

Procedure C for the Ir-catalyzed borylation of heteroarenes
In an N_2-filled glovebox, $[Ir(cod)OMe]_2$ (2.5 mg, 3.8 μmol, 1.5 mol%), 4,4′-di-*tert*-butyl-2,2′-dipyridyl (2.0 mg, 7.5 μmol, 3.0 mol%), bis(pinacolato)diboron (38 mg, 0.15 mmol, 0.6 equiv), and THF (100 μL) were added to a 4 mL vial. After 15-30 min, substrate (0.25 mmol) was added. The vial was capped with a Teflon-lined screw cap, and the vial was removed from the glovebox and placed in a preheated aluminum heating block at the indicated temperature. After the indicated length of time, the vial was removed from the heating block, and dibromomethane was added as an internal standard. The yield and selectivity were determined by ^1H NMR spectroscopy.

Silylation and borylation reactions of heteroarenes

Silylation of 3-methoxythiophene (1)

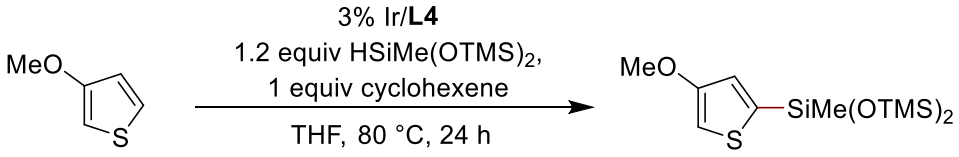

1 **1A**

Procedure A was followed for the reaction of 3-methoxythiophene (114 mg, 1.00 mmol) at 65 ℃ for 25 h. The yield of **1A** determined by ^{1}H NMR spectroscopy with dibromomethane internal standard was 94%. The crude reaction mixture was purified by silica-gel chromatography to afford the product as a pale red oil (292 mg, 87% yield). ^{1}H NMR (600 MHz, $CDCl_3$) δ 6.90 (d, *J* = 1.2 Hz, 1H), 6.5 (d, *J* = 1.2 Hz, 1H), 3.81 (s, 3H), 0.28 (s, 3H), 0.12 (s, 18H). ^{13}C NMR (151 MHz, $CDCl_3$) δ 159.8, 137.7, 125.9, 102.3, 57.6, 1.7, 0.8. HRMS (EI), calculated for [$C_{12}H_{26}O_3SSi_3$]: 334.0910, found: 334.0907.

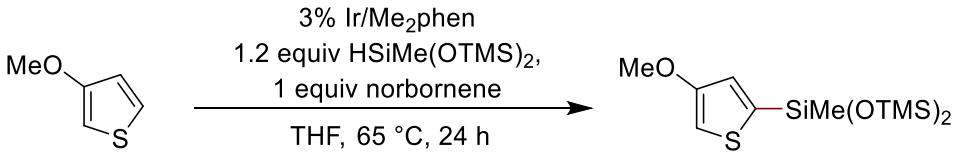

1 **1A**

Procedure B was followed for the reaction of 3-methoxythiophene (29 mg, 0.25 mmol) at 65 ºC for 24 h. The yield of **1A** determined by ^{1}H NMR spectroscopy with dibromomethane internal standard was 40%. The ratio of products from silylation of **1** at the 5-position to that from silylation at the 2-position to that from di-silylation was determined to be 61:4:36 by ^{1}H NMR spectroscopy.

Borylation of 3-methoxythiophene (1)

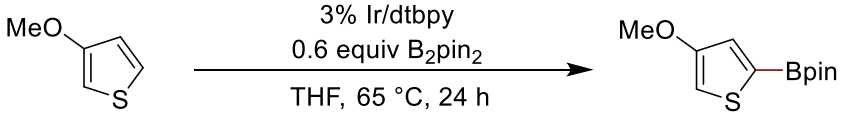

1 **1B**

Procedure C was followed for the reaction of 3-methoxythiophene (29 mg, 0.25 mmol) at 65 ºC for 24 h. The yield of **1B** determined by ^{1}H NMR spectroscopy with dibromomethane internal standard was 33%. The ratio of products from borylation of **1** at the 5-position, borylation at the 2-position and di-borylation was determined to be 37:8:55 by ^{1}H NMR spectroscopy.

Silylation of 3-methylthiophene (2)

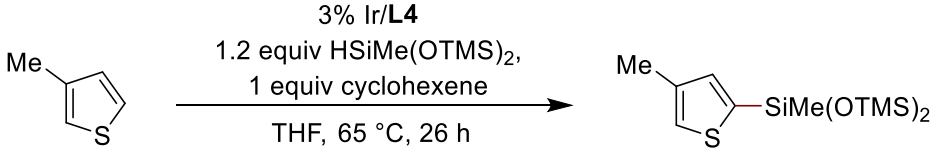

2 **2A**

Procedure A was followed for the reaction of 3-methylthiophene (23 mg, 0.25 mmol) at 65 ℃ for 26 h. The yield of **2A** determined by ^{1}H NMR spectroscopy with dibromomethane internal standard was 90%. The crude reaction mixture was purified by silica-gel chromatography to afford the product as a colorless liquid (71 mg, 89% yield). ^{1}H NMR (500 MHz, $CDCl_3$) δ 7.14 (s, 1H), 7.08 (s, 1H), 2.30 (s, 3H), 0.31 (s, 3H), 0.12 (s, 18H). ^{13}C NMR (101 MHz, $CDCl_3$) δ 138.6, 138.2, 136.9, 126.2, 15.1, 1.9, 1.2. HRMS (EI), calculated for [$C_{12}H_{26}O_2SSi_3$]: 318.0961, found: 318.0962.

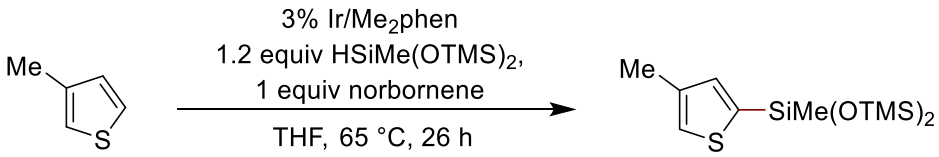

2 **2A**

Procedure B was followed for the reaction of 3-methylthiophene (23 mg, 0.25 mmol) at 65 ℃ for 26 h. The yield of **2A** determined by ^{1}H NMR spectroscopy with dibromomethane internal standard was 78%. The ratio of products from silylation of **2** at the 5-position, silylation at the 2-position and di-silylation was determined to be 94:0:6 by ^{1}H NMR spectroscopy.

Borylation of 3-metylthiophene (2)

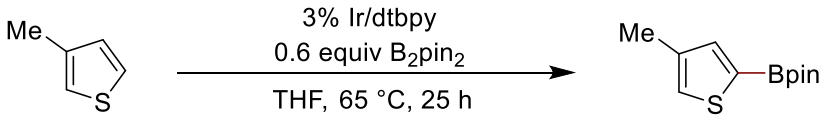

2 **2B**

Procedure C was followed for the reaction of 3-methylthiophene (23 mg, 0.25 mmol) at 65 ºC for 25 h. The yield of **2B** determined by ^{1}H NMR spectroscopy with dibromomethane internal standard was 18% with dibromomethane internal standard. The ratio of products from borylation of **2** at the 5-position, borylation at the 2-position and di-borylation was determined to be 39:30:30 by ^{1}H NMR spectroscopy.

Silylation of 3-phenylthiophene (3)

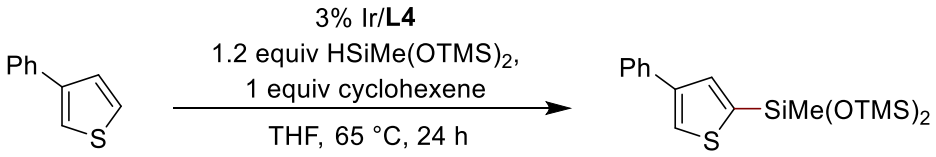

3 **3A**

Procedure A was followed for the reaction of 3-phenylthiophene (40 mg, 0.25 mmol) at 65 ℃ for 24 h. The yield of **3A** determined by ^{1}H NMR spectroscopy with dibromomethane internal standard was 100%. The crude reaction mixture was purified via silica-gel chromatography to afford the product as a colorless liquid (83 mg, 88% yield). ^{1}H NMR (500 MHz, $CDCl_3$) δ 7.67 (d, *J* = 1.3 Hz, 1H), 7.60 (dd, *J* = 8.3, 1.4 Hz, 2H), 7.54 (d, *J* = 1.3 Hz, 1H), 7.40 (t, *J* = 7.7 Hz, 2H), 7.31 – 7.27 (m, 1H), 0.35 (s, 3H), 0.14 (s, 18H). ^{13}C NMR (126 MHz, $CDCl_3$) δ 143.65, 139.61, 136.10, 133.78, 128.92, 127.16, 126.73, 125.97, 1.99, 1.24. HRMS (EI), calculated for [$C_{17}H_{28}O_2SSi_3$]: 380.1118, found: 380.1115.

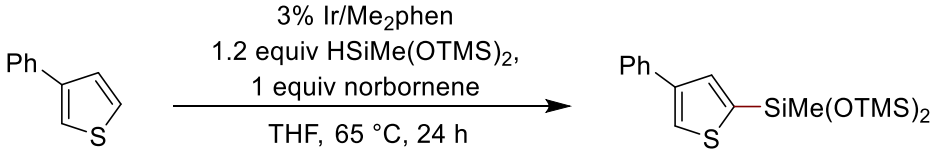

3 **3A**

Procedure B was followed for the reaction of 3-phenylthiophene (40 mg, 0.25 mmol) at 65 ℃ for 24 h. The yield of **2A** determined by ^{1}H NMR spectroscopy with dibromomethane internal standard was 26%.

Borylation of 3-phenylthiophene (3)

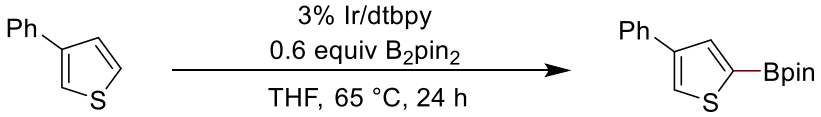

3 **3B**

Procedure C was followed for the reaction of 3-phenylthiophene (40 mg, 0.25 mmol) at 65 ℃ for 24 h. The yield of **3B** determined by ^{1}H NMR spectroscopy with dibromomethane internal standard was 24%.

Silylation of 3-Bpinthiophene (4)

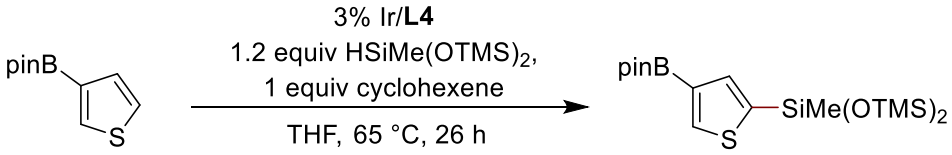

4 **4A**

Procedure A was followed for the reaction of 3-Bpin-thiophene (53 mg, 0.25 mmol) at 65 ℃ for 26 h. The yield of **4A** determined by ^{1}H NMR spectroscopy with dibromomethane internal standard was 85%. The crude reaction mixture was purified by silica-gel chromatography to afford the product as a pale brown oil (110 mg, 99% yield). ^{1}H NMR (600 MHz, $CDCl_3$) δ 8.13 (s, 1H), 7.58 (s, 1H), 1.34 (s, 12H), 0.32 (s, 3H), 0.11 (s, 18H). ^{13}C NMR (151 MHz, $CDCl_3$) δ 141.6, 139.8, 138.5, 83.5, 24.8, 1.8, 1.0. The carbon bonded to boron was not observed via ^{13}C NMR spectroscopy due to broadening by the quadrupolar boron nucleus. HRMS (EI), calculated for [$C_{17}H_{35}O_4SSi_3$]: 430.1657, found: 430.1656.

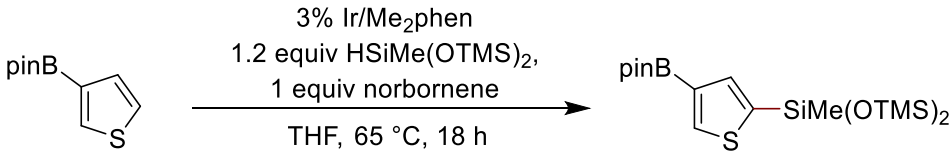

4 **4A**

Procedure B was followed for the reaction of 3-Bpin-thiophene (12 mg, 0.1 mmol) at 65 ℃ for 18 h. The yield of **4A** determined by ^{1}H NMR spectroscopy with dibromomethane internal standard was 60%.

Borylation of 3-Bpin-thiophene (4)

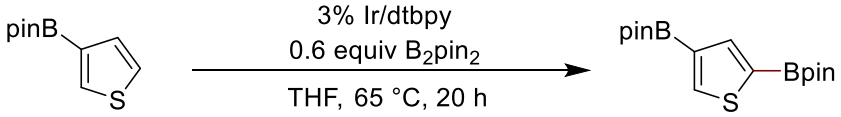

4 **4B**

Procedure C was followed for the reaction of 3-Bpin-thiophene (12 mg, 0.1 mmol) at 65 ℃ for 20 h. The yield of **4B** determined by ^{1}H NMR spectroscopy with dibromomethane internal standard was 13%. The ratio of products from borylation of **4** at the 5-position, borylation at the 2-position, and di-borylation was determined to be 18:0:82 by ^{1}H NMR spectroscopy.

Silylation of ethyl 3-thiophenecarboxylate (5)

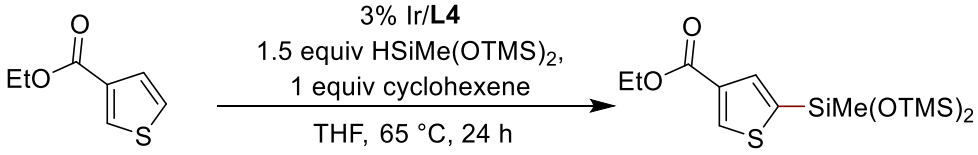

5 **5A**

Procedure B was followed for the reaction of ethyl 3-thiophenecarboxylate (78 mg, 0.5 mmol) with $[Ir(cod)OMe]_2$ (3.3 mg, 5 μmol, 1.0 mol%), **L6** (3.8 mg, 10 μmol, 2.0 mol%), 1,1,1,3,5,5,5-heptamethyl-trisiloxane (167 mg, 0.75 mmol, 1.5 equiv), cyclohexene (41 mg, 0.5 mmol, 1 equiv), and THF (100 μL) at 65 ℃ for 24 h. The yield of **5A** determined by ^{1}H NMR spectroscopy with dibromomethane internal standard was 100%. The crude mixture was purified by silica-gel chromatography to afford the product as an orange oil (150 mg, 81% yield). ^{1}H NMR (400 MHz, $CDCl_3$) δ 8.28 (d, *J* = 0.9 Hz, 1H), 7.67 (d, *J* = 0.9 Hz, 1H), 4.33 (q, *J* = 7.1 Hz, 2H), 1.37 (t, *J* = 7.1 Hz, 3H), 0.32 (s, 3H), 0.12 (s, 18H). ^{13}C NMR (101 MHz, $CDCl_3$) δ 163.0, 139.7, 137.4, 135.2, 135.0, 60.6, 14.4, 1.8, 0.9. HRMS (EI), calculated for $[C_{14}H_{28}O_4SSi_3]$: 376.1016, found: 376.1016. IR (neat, cm^{-1}) ν 2958, 1720, 1520, 1379, 1253, 1214, 1050, 1011, 936, 866

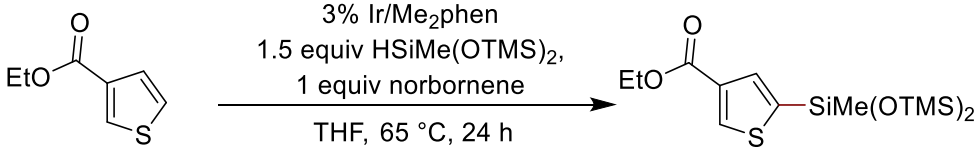

5 **5A**

Procedure B was followed for the reaction of ethyl 3-thiophenecarboxylate (39 mg, 0.25 mmol) at 65 ℃ for 24 h. The yield of **5A** determined by ^{1}H NMR spectroscopy with dibromomethane internal standard was 79%.

Borylation of ethyl 3-thiophenecarboxylate (5)

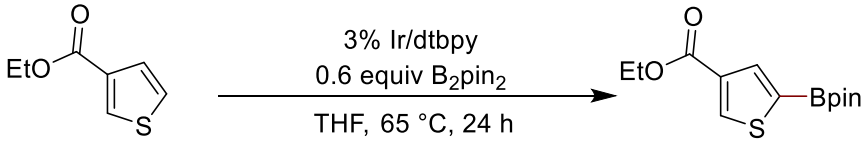

5 **5B**

Procedure C was followed for the reaction of ethyl 3-thiophenecarboxylate (39 mg, 0.25 mmol) at 65 ℃ for 24 h. The yield of **5B** determined by ^{1}H NMR spectroscopy with dibromomethane internal standard was 84%.

Silylation of 3-cyanothiophene (6)

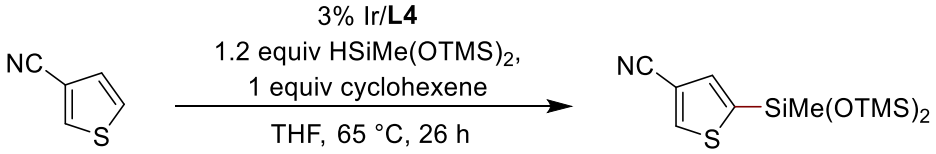

6 **6A**

Procedure A was followed for the reaction of 3-cyanophene (27 mg, 0.25 mmol) at 65 ℃ for 26 h. The yield of **6A** determined by ^{1}H NMR spectroscopy with dibromomethane internal standard was 57%. The ratio of products from silylation of **6** at the 5-position, silylation at the 2-position and di-silylation was determined to be 85:12:3 by ^{1}H NMR spectroscopy. The crude reaction mixture was purified by silica-gel chromatography to afford the product as a pink oil (55 mg, 67% yield). ^{1}H NMR (400 MHz, $CDCl_3$) δ 8.12 (d, *J* = 0.9 Hz, 1H), 7.41 (d, *J* = 0.9 Hz, 1H), 0.32 (s, 3H), 0.12 (s, 18H). ^{13}C NMR (126 MHz, $CDCl_3$) δ 141.5, 139.7, 135.4, 115.2, 111.6, 1.6, 0.8. HRMS (EI), calculated for [$C_{12}H_{23}NO_2SSi_3$]: 329.0757, found: 329.0745. IR (neat, cm^{-1}) ν 2230, 1635, 1461, 1268, 1036, 928, 841, 777, 756

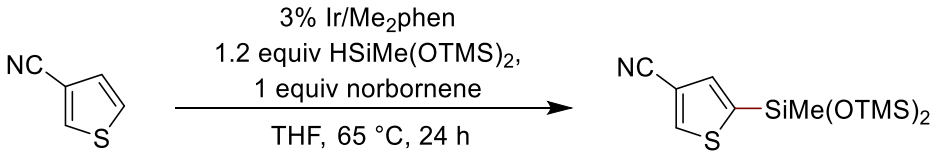

6 **6A**

Procedure B was followed for the reaction of 3-cyanothiophene (27 mg, 0.25 mmol) at 65 ℃ for 24 h. The yield of **6A** determined by ^{1}H NMR spectroscopy with dibromomethane internal standard was 22%. The ratio of products from silylation of **6** at the 5-position, silylation at the 2-position and di-silylation was determined to be 26:28:46 by ^{1}H NMR spectroscopy.

Borylation of 3-cyanothiophene (6)

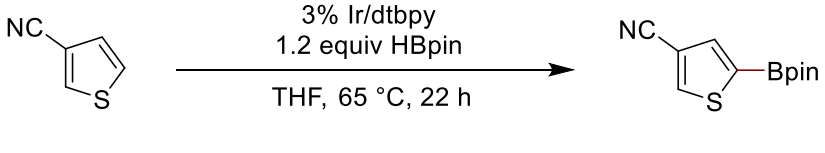

6 **6B**

Procedure C was followed for the reaction of 3-cyanothiophene (11 mg, 0.10 mmol) and HBpin (15 mg, 0.12 mmol) at 65 ℃ for 22 h. The yield of **6B** determined by ^{1}H NMR spectroscopy with dibromomethane internal standard was 29%. The ratio of products from borylation of **6** at the 5-position, borylation at the 2-position and di-borylation was determined to be 30:31:39 by ^{1}H NMR spectroscopy.

Silylation of 3-chlorothiophene (7)

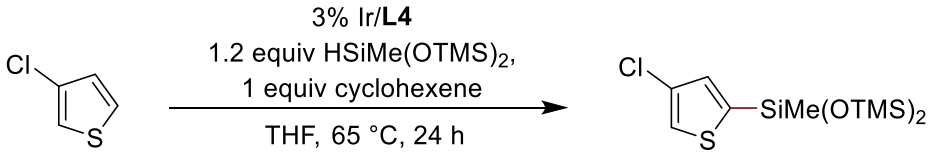

7 **7A**

Procedure A was followed for the reaction of 3-chlorothiophene (30 mg, 0.25 mmol) at 65 ℃ for 24 h. The yield of **7A** determined by ^{1}H NMR spectroscopy with dibromomethane internal standard was 93%. The ratio of products from silylation of **7** at the 5-position, 2-position and di-silylation was determined to be 94:1:5 by ^{1}H NMR spectroscopy. The crude reaction mixture was purified by silica-gel chromatography to afford the product as a clear liquid (82 mg, 97% yield). ^{1}H NMR (600 MHz, $CDCl_3$) δ 7.32 (s, 1H), 7.08 (s, 1H), 0.30 (s, 3H), 0.12 (s, 18H). ^{13}C NMR (101 MHz, $CDCl_3$) δ 139.7, 134.3, 126.3, 125.0, 1.8, 0.9. HRMS (EI), calculated for [$C_{11}H_{23}O_2SSi_3$]: 338.0415, found: 338.0416.

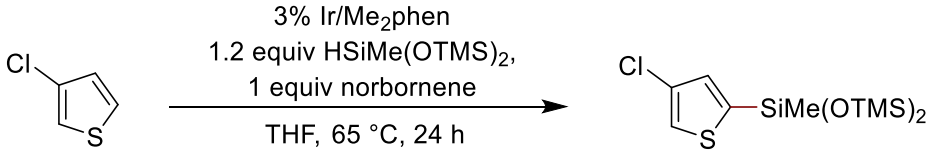

7 **7A**

Procedure B was followed for the reaction of 3-chlorothiophene (30 mg, 0.25 mmol) at 65 ºC for 24 h. The yield of **7A** determined by ^{1}H NMR spectroscopy with dibromomethane internal standard was 54%. The ratio of products from silylation of **7** at the 5-position, silylation at the 2-position and di-silylation was determined to be 60:10:30 by ^{1}H NMR spectroscopy.

Borylation of 3-chlorothiophene (7)

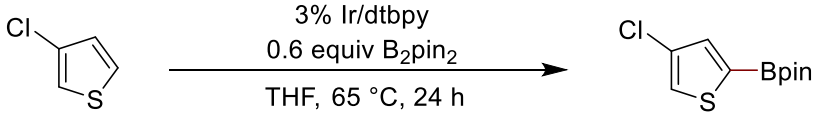

7 **7B**

Procedure C was followed for the reaction of 3-chlorothiophene (30 mg, 0.25 mmol) at 65 ºC for 24 h. The yield of **7B** determined by ^{1}H NMR spectroscopy with dibromomethane internal standard was 50%. The ratio of products from borylation of **7** at the 5-position, borylation at the 2-position and di-borylation was determined to be 52:16:32 by ^{1}H NMR spectroscopy.

Silylation of 3-bromothiophene (8)

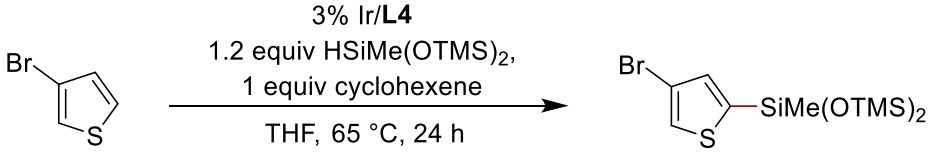

8 **8A**

Procedure A was followed for the reaction of 3-bromophene (49 mg, 0.30 mmol) at 65 ℃ for 24 h. The yield of **8A** determined by ^{1}H NMR spectroscopy with dibromomethane internal standard

was 92%. The crude reaction mixture was purified by silica-gel chromatography to afford the product as a clear liquid (110 mg, 96% yield). ^{1}H NMR (600 MHz, $CDCl_3$) δ 7.43 (s, 1H), 7.14 (s, 1H), 0.30 (s, 3H), 0.12 (s, 18H). ^{13}C NMR (151 MHz, $CDCl_3$) δ 140.2, 136.6, 127.7, 110.8, 1.7, 0.8. HRMS (EI), calculated for [$C_{11}H_{23}BrO_2SSi_3$]: 381.9901, found: 381.9903.

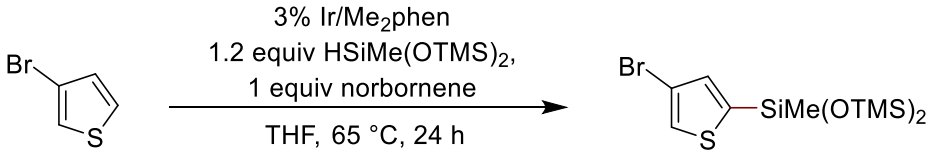

8 **8A**

Procedure B was followed for the reaction of 3-bromothiophene (56 mg, 0.34 mmol) at 65 ℃ for 24 h. The yield of **8A** determined by ^{1}H NMR spectroscopy with dibromomethane internal standard was 30%.

Borylation of 3-bromothiophene (8)

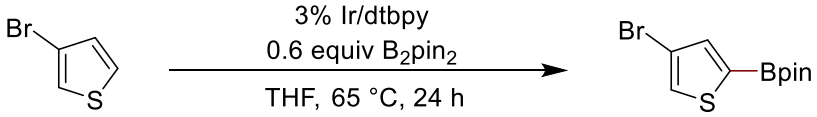

8 **8B**

Procedure C was followed for the reaction of 3-bromothiophene (41 mg, 0.25 mmol) at 65 ºC for 24 h. The yield of **8B** determined by ^{1}H NMR spectroscopy with dibromomethane internal standard was 37%. The ratio of products from borylation of **8** at the 5-position, borylation at the 2-position and di-borylation was determined to be 60:12:28 by ^{1}H NMR spectroscopy.

Silylation of 3-iodothiophene (9)

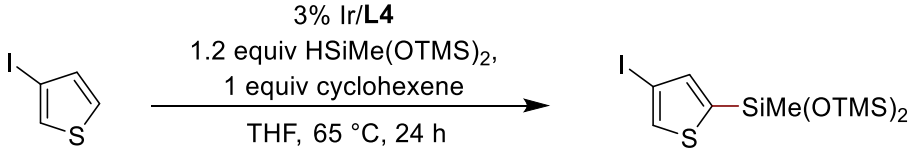

9 **9A**

Procedure A was followed for the reaction of 3-bromophene (53 mg, 0.25 mmol) at 65 ℃ for 24 h. The yield of **9A** determined by ^{1}H NMR spectroscopy with dibromomethane internal standard was 44%.

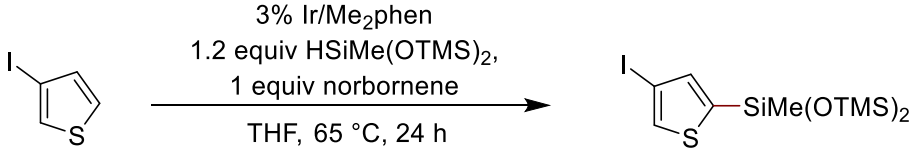

9 **9A**

Procedure B was followed for the reaction of 3-iodothiophene (53 mg, 0.25 mmol) at 65 ℃ for 24 h. The yield of **9A** determined by ^{1}H NMR spectroscopy with dibromomethane internal standard was 42%. The crude reaction mixture was purified by silica-gel chromatography to afford the

product as a colorless oil (52 mg, 48% yield). ^{1}H NMR (400 MHz, $CDCl_3$) δ 7.6 (s, 1H), 7.23 (s, 1H), 0.32 (s, 3H), 0.13 (s, 18H). ^{13}C NMR (101 MHz, $CDCl_3$) δ 141.6, 141.0, 133.6, 78.4, 1.8, 0.9. HRMS (EI), calculated for [$C_{11}H_{23}IO_2SSi_3$]: 429.9771, found: 381.9770.

Borylation of 3-iodothiophene (9)

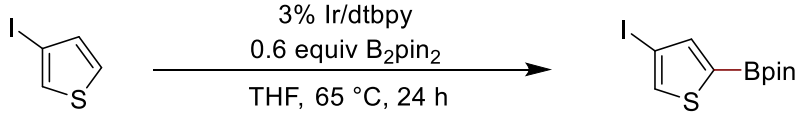

9 **9B**

Procedure C was followed for the reaction of 3-iodoothiophene (53 mg, 0.25 mmol) at 65 ºC for 24 h. The yield of **9B** determined by ^{1}H NMR spectroscopy with dibromomethane internal standard was 24%. The ratio of products from borylation of **9** at the 5-position, borylation at the 2-position and di-borylation was determined to be 90:0:10 by ^{1}H NMR spectroscopy.

Silylation of 3-bromofuran

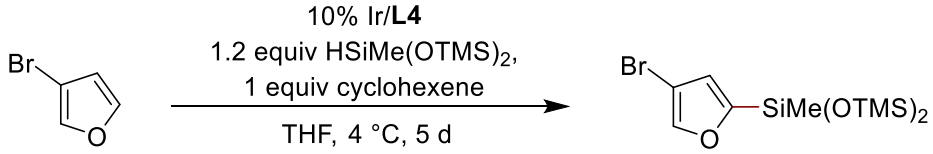

10 **10A**

Procedure A was followed for the reaction of 3-bromofuran (37 mg, 0.25 mmol) with $[Ir(cod)OMe]_2$ (8.2 mg, 13 μmol, 5.0 mol%), **L4** (8.0 mg, 25 μmol, 10 mol%), 1,1,1,3,5,5,5-heptamethyl-trisiloxane (67 mg, 0.30 mmol, 1.2 equiv) at 4 ºC for five days. The yield of **10A** determined by ^{1}H NMR spectroscopy with dibromomethane internal standard was 86%. The ratio of products from silylation of **10** at the 5-position, silylation at the 2-position and di-silylation was determined to be 82:14:4 by ^{1}H NMR spectroscopy. The crude reaction mixture was purified by silica-gel chromatography to afford the mixture of silylated products as a pale brown oil (89 mg, 97% yield). ^{1}H NMR (300 MHz, $CDCl_3$) δ 7.59 (d, J = 0.6 Hz, 1H), 6.66 (d, J = 0.6 Hz, 1H), 0.26 (s, 3H), 0.11 (s, 18H). ^{13}C NMR (101 MHz, $CDCl_3$) δ 160.3, 145.0, 123.4, 99.9, 2.2, 0.3. HRMS (EI), calculated for [$C_{11}H_{23}BrO_3Si_3$]: 366.0138, found: 366.0131.

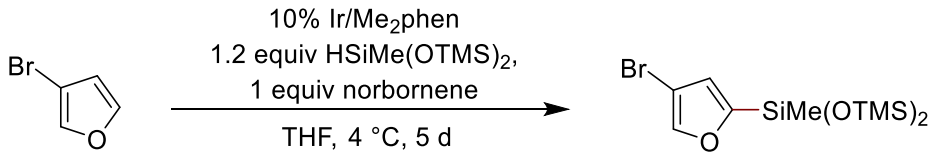

10 **10A**

Procedure B was followed for the reaction of 3-bromofuran (37 mg, 0.25 mmol) with $[Ir(cod)OMe]_2$ (8.2 mg, 12.5 μmol, 5 mol%), neocuproine (5.2 mg, 25 μmol, 10 mol%), 1,1,1,3,5,5,5-heptamethyl-trisiloxane (67 mg, 0.30 mmol, 1.2 equiv) at 4 ºC for five days. The yield of **10A** determined by ^{1}H NMR spectroscopy with dibromomethane internal standard was 22%. The ratio of products from silylation of **10** at the 5-position, silylation at the 2-position and di-silylation was determined to be 34:46:20 by ^{1}H NMR spectroscopy.

Borylation of 3-bromofuran (10)

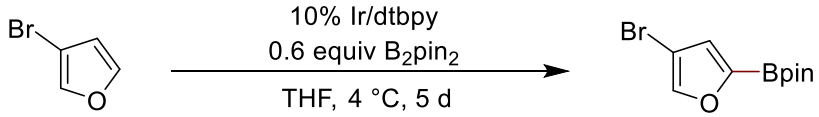

10 **10B**

Procedure C was followed for the reaction of 3-bromofuran (37 mg, 0.25 mmol) with $[Ir(cod)OMe]_2$ (8.2 mg, 12.5 μmol, 5 mol%), dtbpy (6.6 mg, 25 μmol, 10 mol%) at 4 ºC for five days. The yield of **10B** determined by ^{1}H NMR spectroscopy with dibromomethane internal standard was 41%. The ratio of products from borylation of **10** at the 5-position, borylation at the 2-position and di-borylation was determined to be 55:8:37 by ^{1}H NMR spectroscopy.

Silylation of 2-(furan-3-yl)-4,4,5,5-tetramethyl-1,3,2-dioxaborolane (11)

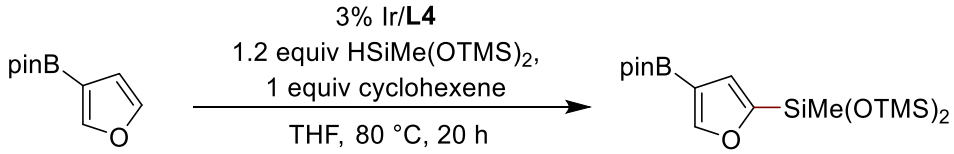

11 **11A**

Procedure A was followed for the reaction of 2-(furan-3-yl)-4,4,5,5-tetramethyl-1,3,2-dioxaborolane (49 mg, 0.25 mmol) at 80 ℃ for 20 h. The yield of **11A** determined by ^{1}H NMR spectroscopy with dibromomethane internal standard was 100%. The crude reaction mixture was purified by silica-gel chromatography to afford the product as a pale brown oil (102 mg, 98% yield). ^{1}H NMR (400 MHz, $CDCl_3$) δ 7.94 (s, 1H), 6.87 (s, 1H), 1.32 (s, 12H), 0.25 (s, 3H), 0.08 (s, 18H). ^{13}C NMR (151 MHz, $CDCl_3$) δ 158.6, 155.0, 124.0, 83.6, 25.0, 1.9, 0.1. The carbon bonded to boron was not observed via ^{13}C NMR spectroscopy due to broadening by the quadrupolar boron nucleus. [$C_{17}H_{35}BO_5Si_3$]: 414.1885, found: 414.1883.

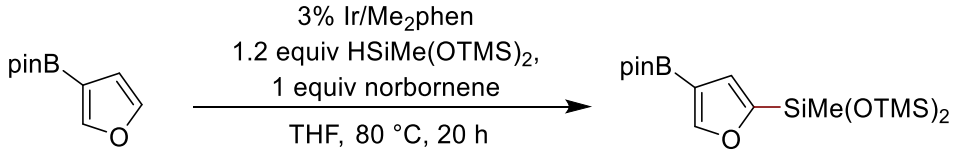

11 **11A**

Procedure B was followed for the reaction of 2-(furan-3-yl)-4,4,5,5-tetramethyl-1,3,2-dioxaborolane (49 mg, 0.25 mmol) at 80 ºC for 20 h. The yield of **11A** determined by ^{1}H NMR spectroscopy with dibromomethane internal standard was 99%.

Borylation of 2-(furan-3-yl)-4,4,5,5-tetramethyl-1,3,2-dioxaborolane (11)

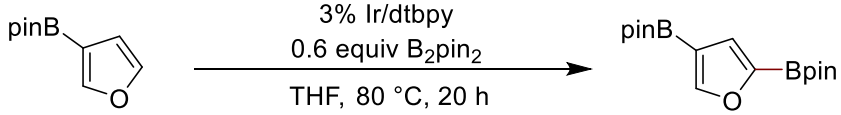

11 **11B**

Procedure C was followed for the reaction of 2-(furan-3-yl)-4,4,5,5-tetramethyl-1,3,2-dioxaborolane (48.5 mg, 0.25 mmol) at 80 ºC for 20 h. The yield of **11B** determined by ^{1}H NMR spectroscopy with dibromomethane internal standard was 87%. The ratio of products from borylation of **11** at the 5-position, borylation at the 2-position and di-borylation was determined to be 90:0:10 by ^{1}H NMR spectroscopy.

Silylation of 3-phenylfuran (12)

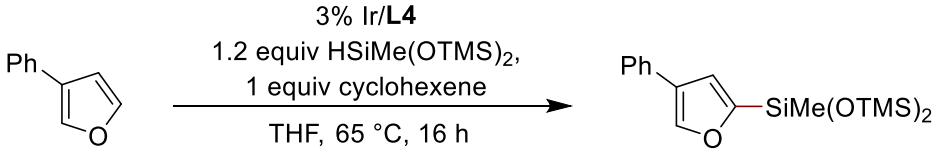

12 **12A**

Procedure A was followed for the reaction of 3-phenylfuran (38 mg, 0.25 mmol) at 65 ℃ for 16 h. The yield of **12A** determined by ^{1}H NMR spectroscopy with dibromomethane internal standard was 100%. The crude reaction mixture was purified by silica-gel chromatography to afford the product as a pale brown oil (96 mg, 100% yield). ^{1}H NMR (600 MHz, $CDCl_3$) δ 7.90 (d, *J* = 0.6 Hz, 1H), 7.52 – 7.48 (m, 2H), 7.37 (t, *J* = 7.8 Hz, 2H), 7.25 (t, *J* = 7.5 Hz, 1H), 6.96 (d, *J* = 0.6 Hz, 1H), 0.31 (s, 3H), 0.13 (s, 18H). ^{13}C NMR (151 MHz, $CDCl_3$) δ 159.6, 142.5, 132.8, 128.9, 126.9, 126.4, 126.1, 119.1, 1.9, 0.1. [$C_{17}H_{28}O_3Si_3$]: 364.1346, found: 364.1351.

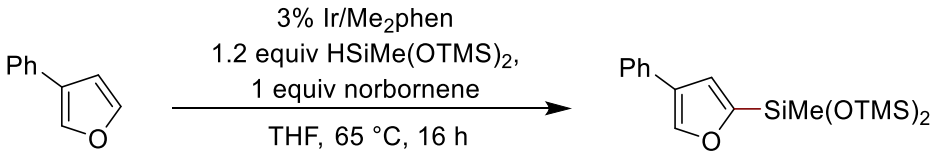

12 **12A**

Procedure B was followed for the reaction of 3-phenylfuran (36 mg, 0.25 mmol) at 65 ºC for 16 h. The yield of **12A** determined by ^{1}H NMR spectroscopy with dibromomethane internal standard was 100%.

Borylation of 3-phenylfuran (12)

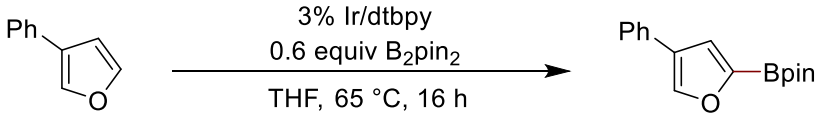

12 **12B**

Procedure C was followed for the reaction of 3-phenylfuran (36 mg, 0.25 mmol) at 65 ºC for 16 h. The yield of **12B** determined by ^{1}H NMR spectroscopy with dibromomethane internal standard was 18%. The ratio of products from borylation of **12** at the 5-position, borylation at the 2-position and di-borylation was determined to be 19:6:75 by ^{1}H NMR spectroscopy.

Silylation of ethyl 3-furancarboxylate (13)

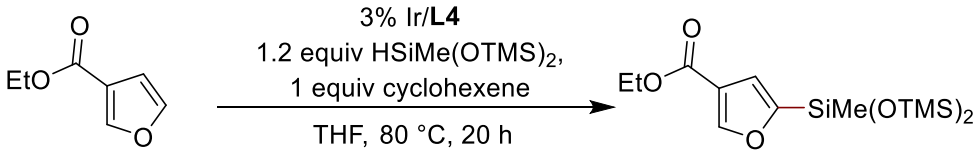

13 **13A**

Procedure A was followed for the reaction of ethyl 3-furancarboxylate (35 mg, 0.25 mmol) at 80 ℃ for 20 h. The yield of **13A** determined by ^{1}H NMR spectroscopy with dibromomethane internal standard was 83%. The crude reaction mixture was purified by silica-gel chromatography to afford the product as a pale brown oil (55 mg, 61% yield). ^{1}H NMR (400 MHz, $CDCl_3$) δ 8.16 (s, 1H), 6.96 (s, 1H), 4.30 (q, *J* = 7.1 Hz, 2H), 1.34 (t, *J* = 7.1 Hz, 3H), 0.27 (s, 3H), 0.10 (s, 18H). ^{13}C NMR (151 MHz, $CDCl_3$) δ 163.4, 160.0, 151.1, 119.6, 119.3, 60.3, 14.3, 1.9, -0.3. [$C_{14}H_{28}O_5Si_3$]: 360.1245, found: 360.1241.

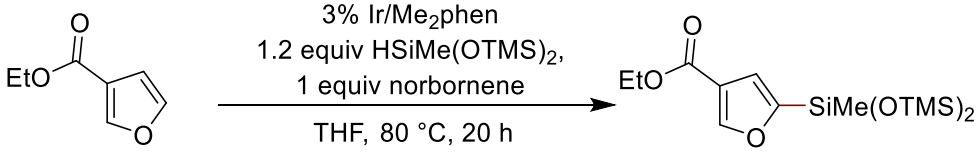

13 **13A**

Procedure B was followed for the reaction of ethyl 3-furancarboxylate (35 mg, 0.25 mmol) at 80 ºC for 20 h. The yield of **13A** determined by ^{1}H NMR spectroscopy with dibromomethane internal standard was 53%. The ratio of products from silylation of **13** at the 5-position, silylation at the 2-position and di-silylation was determined to be 78:0:22 by ^{1}H NMR spectroscopy.

Borylation of ethyl 3-furancarboxylate (13)

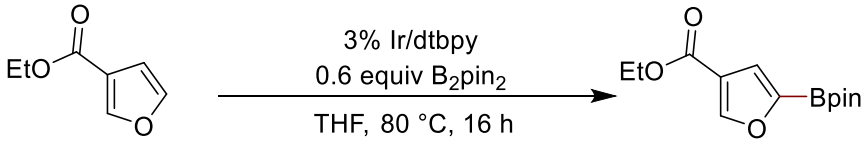

13 **13B**

Procedure C was followed for the reaction of ethyl 3-furancarboxylate (35 mg, 0.25 mmol) at 80 ºC for 20 h. The yield of **13B** determined by ^{1}H NMR spectroscopy with dibromomethane internal standard was 17%. The ratio of products from borylation of **13** at the 5-position, borylation at the 2-position and di-borylation was determined to be 34:4:62 by ^{1}H NMR spectroscopy.

Silylation of N-cyclohexylfuran-3-carboxamide (14)

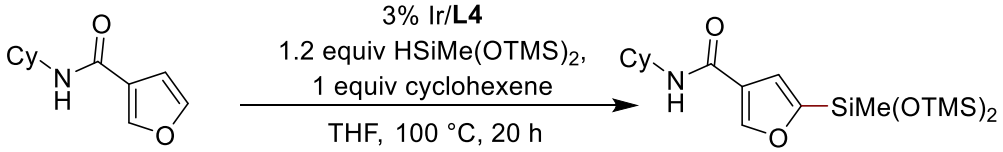

14 **14A**

Procedure A was followed for the reaction of N-cyclohexylfuran-3-carboxamide (48 mg, 0.25 mmol) at 100 ℃ for 20 h. The yield of **14A** determined by ^{1}H NMR spectroscopy with dibromomethane internal standard was 43%. The crude reaction mixture was purified by silica-gel chromatography to afford the product as a pale brown oil (30 mg, 29% yield). ^{1}H NMR (600 MHz, $CDCl_3$) δ 8.05 (s, 1H), 6.79 (s, 1H), 5.59 (s, 1H), 3.92 (ddp, *J* = 11.7, 8.1, 4.0 Hz, 1H), 2.00 (dd, *J* = 12.4, 3.4 Hz, 2H), 1.74 (dt, *J* = 13.6, 3.5 Hz, 2H), 1.64 (dt, *J* = 13.0, 3.7 Hz, 1H), 1.46 – 1.35 (m, 2H), 1.19 (m, 3H), 0.27 (s, 3H), 0.10 (s, 18H). ^{13}C NMR (151 MHz, $CDCl_3$) δ 162.1, 160.1, 148.3, 122.9, 118.1, 48.4, 33.5, 25.7, 25.1, 1.8, 0.0. HRMS (ESI+), calculated for [$C_{18}H_{36}NO_4Si_3$]: 414.1947, found: 414.1945

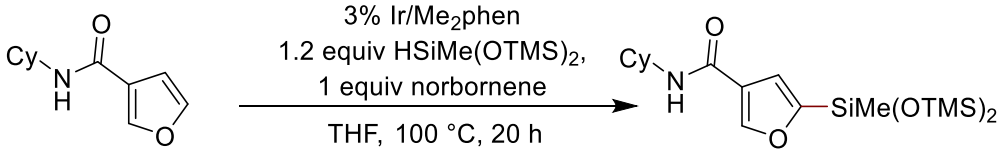

14 **14A**

Procedure B was followed for the reaction of N-cyclohexylfuran-3-carboxamide (48 mg, 0.25 mmol) at 100 ºC for 20 h. The yield of **14A** determined by ^{1}H NMR spectroscopy with dibromomethane internal standard was 43%.

Borylation of N-cyclohexylfuran-3-carboxamide (14)

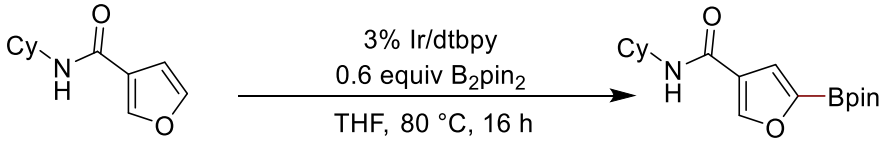

14 **14B**

Procedure C was followed for the reaction of N-cyclohexylfuran-3-carboxamide (48mg, 0.25 mmol) at 80 ºC for 16 h. The yield of **14B** determined by ^{1}H NMR spectroscopy with dibromomethane internal standard was 48%. The ratio of products from borylation of **14** at the 5-position, borylation at the 2-position and di-borylation was determined to be 64:36:0 by ^{1}H NMR spectroscopy.

Silylation of methyl 3-pyrrolecarboxylate (15)

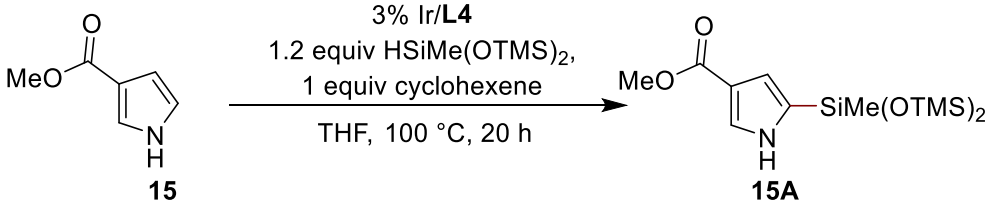

15 **15A**

Procedure A was followed for the reaction of methyl 1H-pyrrole-3-carboxylate (31 mg, 0.25 mmol) at 100 ℃ for 20 h. The yield of **15A** determined by ^{1}H NMR spectroscopy with dibromomethane internal standard was 90%. The crude reaction mixture was purified by silica-gel chromatography to afford the product as a pale brown crystalline solid. (57 mg, 66 % yield). ^{1}H NMR (600 MHz, $CDCl_3$) δ 8.58 (s, 1H), 7.54 (dd, *J* = 3.0, 1.3 Hz, 1H), 6.85 (dd, *J* = 2.6, 1.3 Hz, 1H), 3.81 (s, 3H), 0.27 (s, 3H), 0.10 (s, 18H). ^{13}C NMR (151 MHz, $CDCl_3$) δ 165.4, 130.9, 126.3,

118.6, 117.1, 51.0, 1.7, 0.5. HRMS (EI), calculated for [$C_{13}H_{27}NO_4Si_3$]: 345.1248, found: 345.1244.

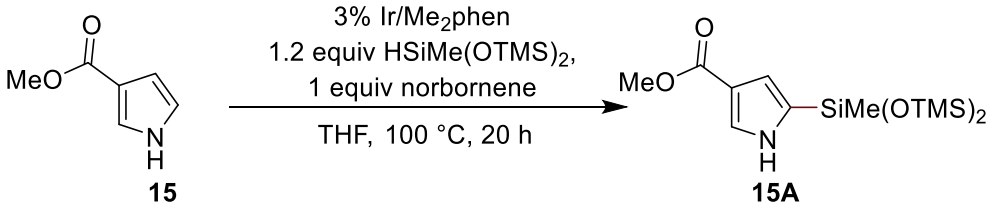

15 **15A**

Procedure B was followed for the reaction of methyl 3-pyrrolecarboxylate (31 mg, 0.25 mmol) at 100 ºC for 20 h. The yield of **15A** determined by ^{1}H NMR spectroscopy with dibromomethane internal standard was 48%. The ratio of products from silylation of **15** at the 5-position, silylation at the 2-position and di-silylation was determined to be 75:18:7 by ^{1}H NMR spectroscopy.

Borylation of methyl 3-pyrrolecarboxylate (15)

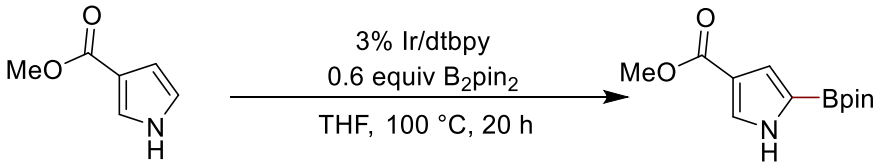

15 **15B**

Procedure C was followed for the reaction of methyl 3-pyrrolecarboxylate (31 mg, 0.25 mmol) at 100 ºC for 20 h. The yield of **15B** determined by ^{1}H NMR spectroscopy with dibromomethane internal standard was 64%. The ratio of products from borylation of **15** at the 5-position, borylation at the 2-position and di-borylation was determined to be 76:16:8 by ^{1}H NMR spectroscopy.

Silylation of 1,3-Me$_2$-pyrazole (16)

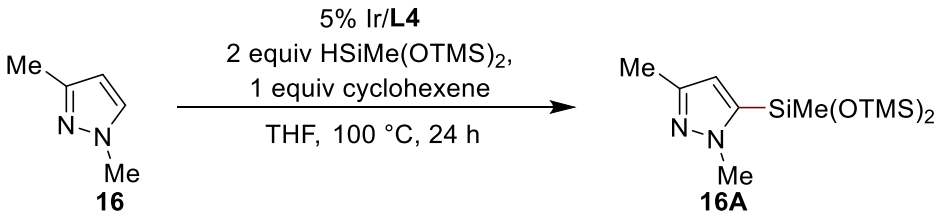

16 **16A**

Procedure A was followed for the reaction of 1,3-Me$_2$-Pyrazole (24 mg, 0.25 mmol) with 1,1,1,3,5,5,5-heptamethyl-trisiloxane (84 mg, 0.38 mmol) at 80 ℃ for 24 h. The yield of **16A** determined by ^{1}H NMR spectroscopy with dibromomethane internal standard was 27%.

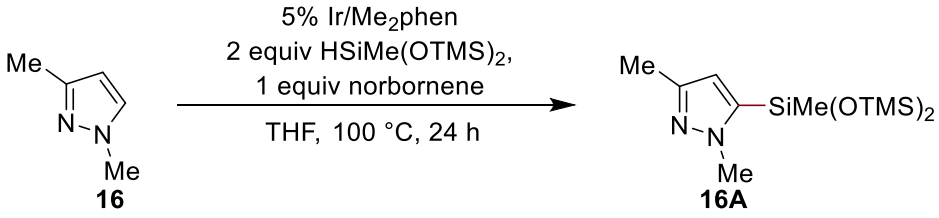

16 **16A**

Procedure B was followed for the reaction of 1,3-Me$_2$-Pyrazole (10 mg, 0.10 mmol) with 1,1,1,3,5,5,5-heptamethyl-trisiloxane (45 mg, 0.20 mmol), norbornene (10 mg, 0.10 mmol), [Ir(cod)(OMe)]$_2$ (1.7 mg, 0.0025 mmol), neocuproine (1.1 mg, 0.005 mmol), and THF (50 µL) at 100 ºC for 24 h. The yield of **16A** determined by ^{1}H NMR spectroscopy with dibromomethane

internal standard was 99%. The crude reaction mixture was purified by silica-gel chromatography to afford the product as a colorless oil (30 mg, 95% yield). ^{1}H NMR (500 MHz, $CDCl_3$) δ 6.12 (s, 1H), 3.89 (s, 3H), 2.25 (s, 3H), 0.29 (s, 3H), 0.10 (s, 18H). ^{13}C NMR (126 MHz, $CDCl_3$) δ 147.4, 142.2, 114.1, 39.2, 13.1, 1.9, 0.8. HRMS (ESI+), calculated for [$C_{12}H_{29}N_2O_2Si_3^+$]: 317.1531, found: 317.1530

Borylation of 1,3-Me_2-pyrazole (16)

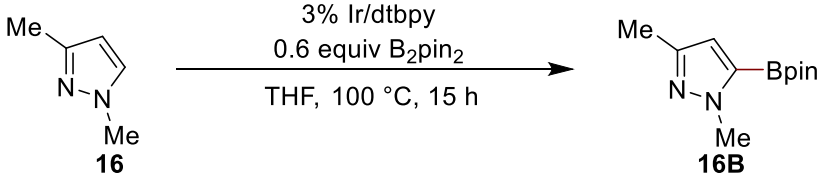

16 **16B**

Procedure C was followed for the reaction of 1,3-Me_2-pyrazole (10 mg, 0.10 mmol) at 100 ºC for 15 h. The yield of **16B** determined by ^{1}H NMR spectroscopy with dibromomethane internal standard was 37%. The crude material was filtered through a pad of silica which was washed with EtOAc. The ^{1}H NMR yield of **16B** in the filtrate was determined to be 26% with dibromomethane internal standard.

Silylation of 1-Ts-3-Me-pyrazole (17)

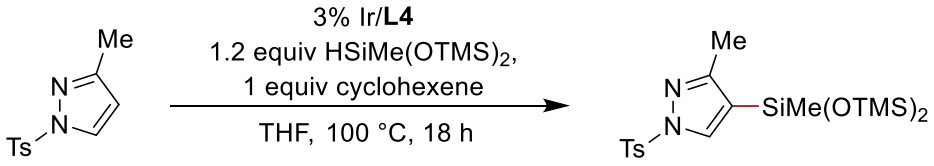

17 **17A**

Procedure A was followed for the reaction of 1-Ts-3-Me-Pyrazole (24 mg, 0.10 mmol) at 100 ℃ for 18 h. The yield of **17A** determined by ^{1}H NMR spectroscopy with dibromomethane internal standard was 21%.

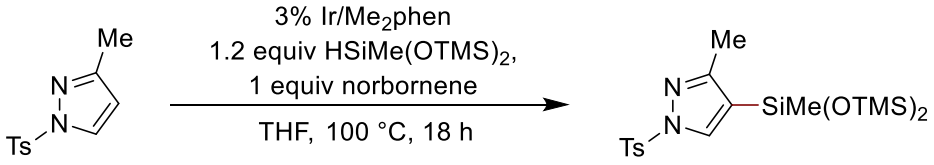

17 **17A**

Procedure B was followed for the reaction of 1-Ts-3-Me-Pyrazole (59 mg, 0.25 mmol) at 100 ºC for 18 h. The yield of **17A** determined by ^{1}H NMR spectroscopy with dibromomethane internal standard was 70%. The crude reaction mixture was purified by silica-gel chromatography to afford the product as a white solid (75 mg, 66% yield). ^{1}H NMR (500 MHz, $CDCl_3$) δ 7.91 (s, 1H), 7.86 (d, J = 8.1 Hz, 2H), 7.31 (d, J = 8.1 Hz, 2H), 2.41 (s, 3H), 2.27 (s, 3H), 0.23 (s, 3H), 0.08 (s, 18H). ^{13}C NMR (126 MHz, $CDCl_3$) δ 159.1, 145.6, 137.6, 134.6, 130.0, 128.1, 117.7, 21.8, 14.9, 1.9, 1.2. HRMS (ESI+), calculated for [$C_{18}H_{33}N_2O_4SSi_3^+$]: 457.1463, found: 457.1460

Borylation of 1-Ts-3-Me-pyrazole (17)

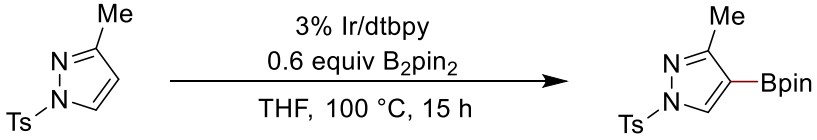

17 **17B**

Procedure C was followed for the reaction of 1-Ts-3-Me-pyrazole (24 mg, 0.10 mmol) at 100 ºC for 15 h. The yield of **17B** determined by ^{1}H NMR spectroscopy with dibromomethane internal standard was 74%. The crude material was filtered through a pad of silica which was washed with EtOAc. The ^{1}H NMR yield of **17B** in the filtrate was determined to be 72% with dibromomethane internal standard.

Silylation of 1-Boc-4-Cl-pyrazole (18)

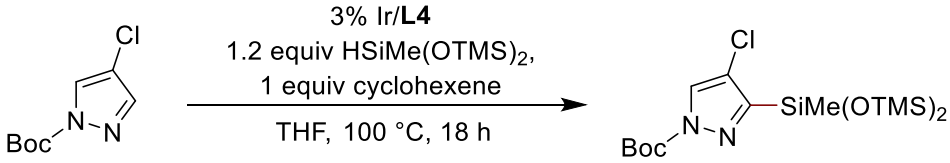

18 **18A**

Procedure A was followed for the reaction of 1-Boc-4-Cl-pyrazole (20 mg, 0.10 mmol) at 100 ℃ for 18 h. The yield of **18A** determined by ^{1}H NMR spectroscopy with dibromomethane internal standard was 9%.

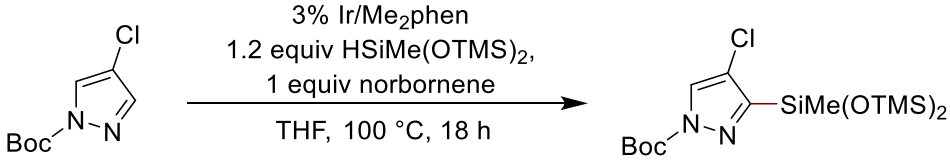

18 **18A**

Procedure B was followed for the reaction of 1-Boc-4-Cl-pyrazole (49 mg, 0.25 mmol) at 100 ºC for 18 h. The yield of **18A** determined by ^{1}H NMR spectroscopy with dibromomethane internal standard was 85%. The crude reaction mixture was purified by silica-gel chromatography to afford the product as a colorless oil (82 mg, 78% yield). ^{1}H NMR (400 MHz, $CDCl_3$) δ 8.00 (s, 1H), 1.62 (s, 9H), 0.36 (s, 3H), 0.12 (s, 18H). ^{13}C NMR (126 MHz, $CDCl_3$) δ 154.7, 147.2, 128.0, 119.0, 85.7, 28.0, 1.9, 0.4. HRMS (ESI+), calculated for [$C_{15}H_{32}ClN_2O_4Si_3^+$]: 423.1353, found: 423.1359

Borylation of 1-Boc-4-Cl-pyrazole (18)

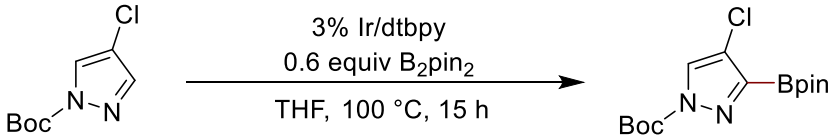

18 **18B**

Procedure C was followed for the reaction of 1-Boc-4-Cl-pyrazole (20 mg, 0.10 mmol) at 100 ºC for 15 h. The yield of **18B** determined by ^{1}H NMR spectroscopy with dibromomethane internal standard was 68%. The crude material was filtered through a pad of silica which was washed with

EtOAc. The ^{1}H NMR yield of **18B** in the filtrate was determined to be 20% with dibromomethane internal standard.

Silylation of 4-Me-thiazole (19)

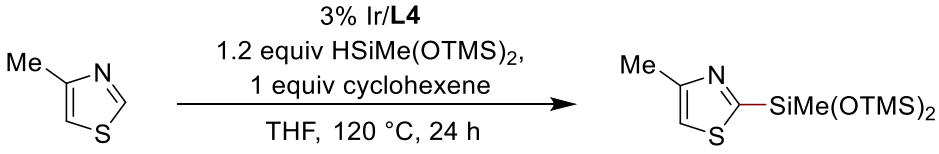

19 **19A**

Procedure A was followed for the reaction of 4-Me-thiazole (25 mg, 0.25 mmol) at 120 ℃ for 24 h. Only traces of **19A** could be detected by ^{1}H NMR spectroscopy.

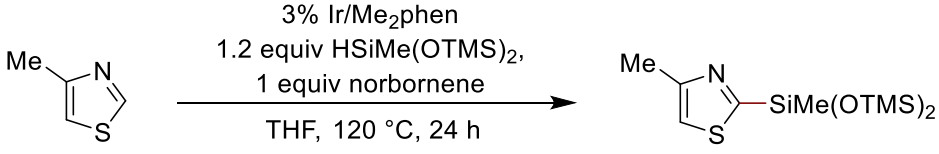

19 **19A**

Procedure B was followed for the reaction of 4-Me-thiazole (25 mg, 0.25 mmol) at 120 ℃ for 24 h. The yield of **19A** determined by ^{1}H NMR spectroscopy with dibromomethane internal standard was 75%. The ratio of products from silylation of **19** at the 2-position, 5-position and di-silylation was determined to be 93:7:0 by ^{1}H NMR spectroscopy. The crude reaction mixture was purified by silica-gel chromatography to afford a 13:1 mixture of the two isomeric products as a pale brown oil (63 mg, 80% yield). ^{1}H NMR (500 MHz, $CDCl_3$) δ 7.03 (q, *J* = 0.9 Hz, 1H), 2.54 (d, *J* = 0.9 Hz, 3H), 0.40 (s, 3H), 0.12 (s, 18H). ^{13}C NMR (126 MHz, $CDCl_3$) δ 171.2, 156.1, 116.3, 17.0, 1.8, 0.0. HRMS (EI), calculated for [$C_{11}H_{25}NO_2SSi_3$]: 319.0914, found: 319.0908

Borylation of 4-Me-thiazole (19)

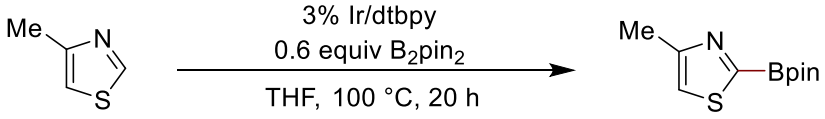

19 **19B**

Procedure C was followed for the reaction of 4-Me-thiazole (25 mg, 0.25 mmol) at 120 ºC for 24 h. No borylated product was observed by ^{1}H NMR spectroscopy.

Silylation of 4-thiazolecarboxylate methyl ester (20)

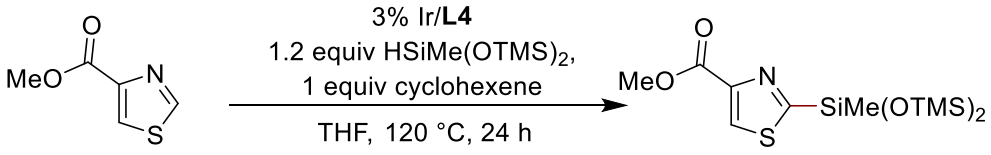

20 **20A**

Procedure A was followed for the reaction of 4-thiazolecarboxylate methyl ester (14 mg, 0.10 mmol) at 120 ℃ for 24 h. Only traces of **20A** could be detected by ^{1}H NMR spectroscopy.

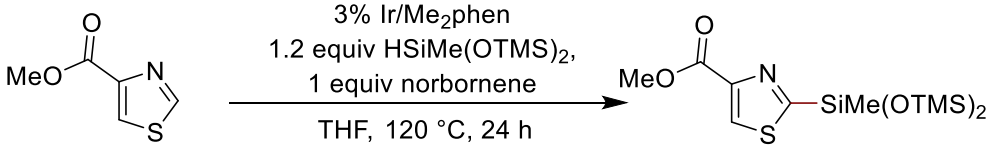

20 **20A**

Procedure B was followed for the reaction of 4-thiazolecarboxylate methyl ester (37 mg, 0.25 mmol) at 120 ℃ for 24 h. The yield of **20A** determined by ^{1}H NMR spectroscopy with dibromomethane internal standard was 72%. The crude reaction mixture was purified by silica-gel chromatography to afford the product as a pale brown oil (65 mg, 71% yield). ^{1}H NMR (500 MHz, $CDCl_3$) δ 8.35 (s, 1H), 3.96 (s, 3H), 0.45 (s, 3H), 0.12 (s, 18H). ^{13}C NMR (126 MHz, $CDCl_3$) δ 173.7, 162.4, 150.4, 130.4, 52.5, 1.9, -0.2. HRMS (EI), calculated for [$C_{12}H_{25}NO_4SSi_3$]: 362.0734, found: 362.0730

Borylation of 4-thiazolecarboxylate methyl ester (20)

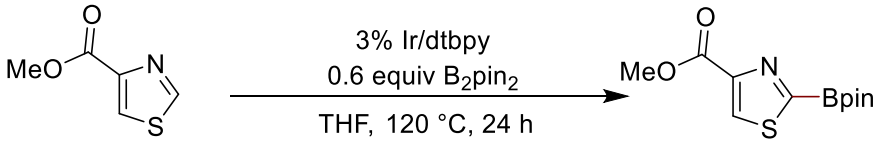

20 **20B**

Procedure C was followed for the reaction of 4-thiazolecarboxylate methyl ester (37 mg, 0.26 mmol) at 120 ºC for 24 h. No borylated product was observed by ^{1}H NMR spectroscopy.

Silylation of 1-Ts-2-^{i}Pr-imidazole (21)

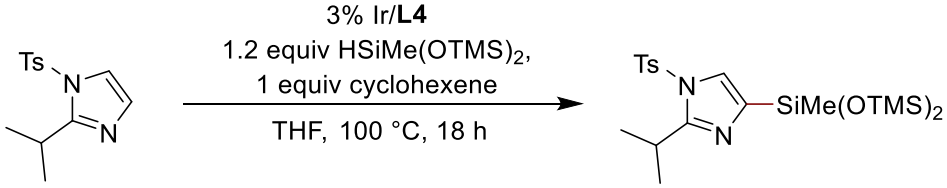

21 **21A**

Procedure A was followed for the reaction of 1-Ts-2-^{i}Pr-Imidazole (26 mg, 0.10 mmol) at 100 ℃ for 18 h. The yield of **21A** determined by ^{1}H NMR spectroscopy with dibromomethane internal standard was 53%.

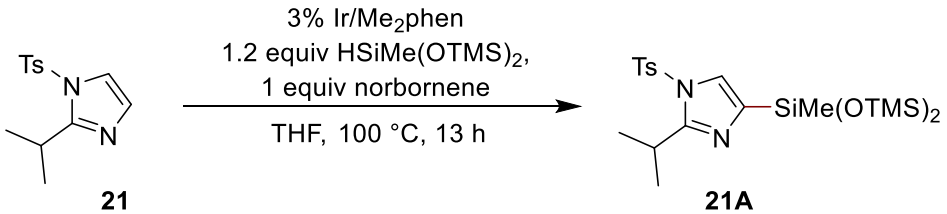

21 **21A**

Procedure B was followed for the reaction of 1-Ts-2-^{i}Pr-Imidazole (66 mg, 0.25 mmol) at 100 ºC for 13 h. The yield of **21A** determined by ^{1}H NMR spectroscopy with dibromomethane internal standard was 82%. The crude reaction mixture was purified by silica-gel chromatography to afford the product as a colorless oil (85 mg, 70% yield). ^{1}H NMR (500 MHz, $CDCl_3$) δ 7.71 (d, *J* = 8.0 Hz, 2H), 7.43 (s, 1H), 7.32 (d, *J* = 8.0 Hz, 2H), 3.38 (h, *J* = 6.8 Hz, 1H), 2.43 (s, 3H), 1.16 (d, *J* =

6.8 Hz, 6H), 0.25 (s, 3H), 0.08 (s, 18H). ^{13}C NMR (126 MHz, $CDCl_3$) δ 155.7, 145.7, 139.1, 136.1, 130.3, 127.2, 126.1, 27.5, 22.2, 21.8, 1.9, 0.2. HRMS (ESI+), calculated for [$C_{20}H_{37}N_2O_4SSi_3^+$]: 485.1776, found: 485.1777

Borylation of 1-Ts-2-*i*Pr-imidazole (21)

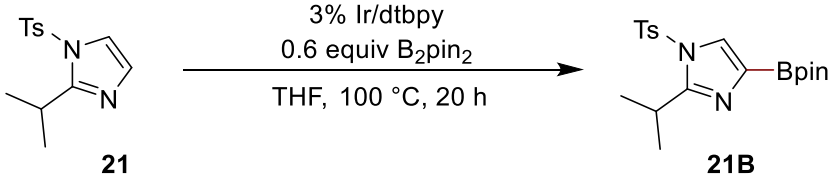

21 **21B**

Procedure C was followed for the reaction of 1-Ts-2-*i*Pr-imidazole (26 mg, 0.10 mmol) at 100 ºC for 20 h. The yield of **21B** determined by ^{1}H NMR spectroscopy with dibromomethane internal standard was 64%. The crude material was filtered through a pad of silica which was washed with EtOAc. The ^{1}H NMR spectrum of a sample of the filtrate contained no borylated products.

Silylation of caffeine (22)

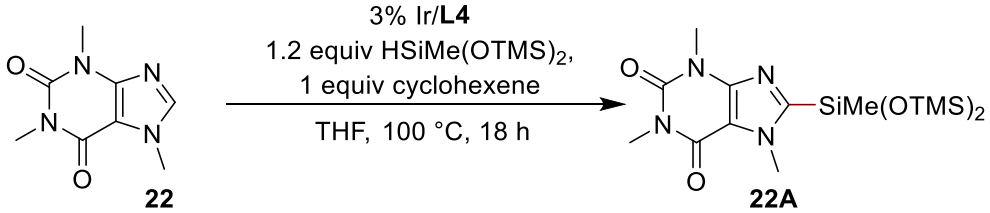

22 **22A**

Procedure A was followed for the reaction of caffeine (19 mg, 0.10 mmol) at 100 ℃ for 18 h. Only traces of **22A** could be detected by ^{1}H NMR spectroscopy.

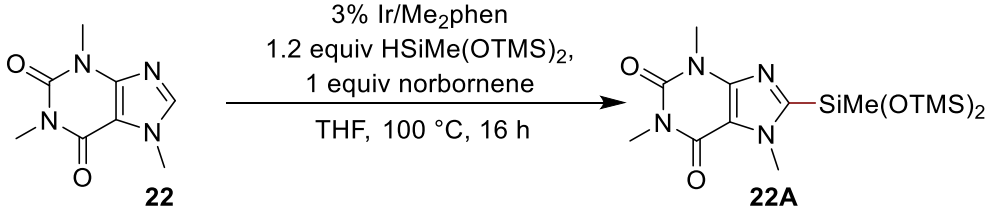

22 **22A**

Procedure B was followed for the reaction of caffeine (49 mg, 0.25 mmol) at 100 ºC for 16 h. The yield of **22A** determined by ^{1}H NMR spectroscopy with dibromomethane internal standard was 68%. The crude reaction mixture was purified by silica-gel chromatography to afford the product as a white solid (67 mg, 65% yield). ^{1}H NMR (500 MHz, $CDCl_3$) δ 4.04 (s, 3H), 3.55 (s, 3H), 3.36 (s, 3H), 0.41 (s, 3H), 0.11 (s, 18H). ^{13}C NMR (126 MHz, $CDCl_3$) δ 155.9, 155.5, 152.0, 149.0, 109.3, 33.8, 29.8, 28.0, 1.8, 0.3. HRMS (ESI+), calculated for [$C_{15}H_{31}N_4O_4Si_3^+$]: 415.1648, found: 415.1652

Borylation of caffeine (22)

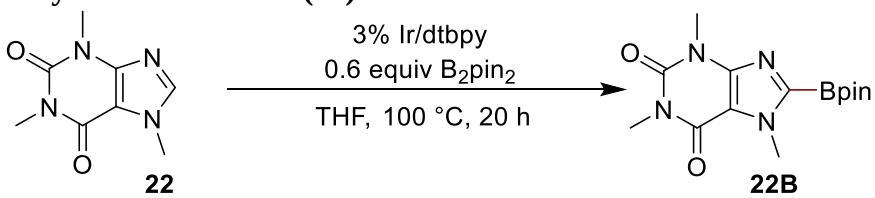

22 **22B**

Procedure C was followed for the reaction of caffeine (19 mg, 0.10 mmol) at 100 ºC for 20 h. The yield of **22B** determined by ^{1}H NMR spectroscopy with dibromomethane internal standard was

72%. The crude material was filtered through a pad of silica which was washed with EtOAc. The ^{1}H NMR spectrum of a sample of the filtrate contained no borylated products.

Silylation of 1-^{i}Pr-1,2,3-triazole (23)

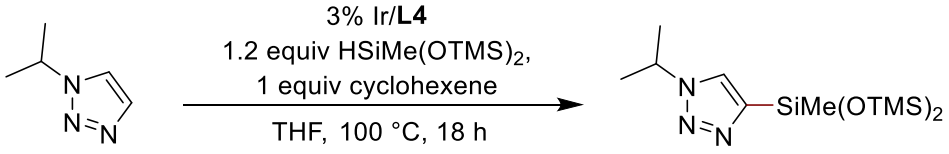

23 **23A**

Procedure A was followed for the reaction of 1-^{i}Pr-1,2,3-Triazole (11 mg, 0.10 mmol) at 100 ℃ for 18 h. The yield of **23A** determined by ^{1}H NMR spectroscopy with dibromomethane internal standard was 17%.

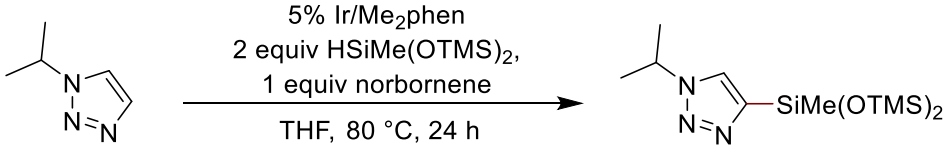

23 **23A**

Procedure B was followed for the reaction of 1-^{i}Pr-1,2,3-Triazole (28 mg, 0.25 mmol) with 1,1,1,3,5,5,5-heptamethyl-trisiloxane (111 mg, 0.50 mmol), norbornene (24 mg, 0.25 mmol), $[Ir(cod)(OMe)]_2$ (4.1 mg, 0.0063 mmol) and neocuproine (2.6 mg, 0.013 mmol) at 80 ºC for 24 h. The yield of **23A** determined by ^{1}H NMR spectroscopy with dibromomethane internal standard was 62%. The crude reaction mixture was purified by silica-gel chromatography to afford the product as a colorless oil (46 mg, 55% yield). ^{1}H NMR (500 MHz, $CDCl_3$) δ 7.51 (s, 1H), 4.85 (hept, J = 6.7 Hz, 1H), 1.57 (d, J = 6.7 Hz, 6H), 0.34 (s, 3H), 0.10 (s, 18H). ^{13}C NMR (126 MHz, $CDCl_3$) δ 145.0, 126.6, 52.4, 23.3, 1.9, 0.7. HRMS (ESI+), calculated for $[C_{12}H_{30}N_3O_2Si_3^+]$: 332.1640, found: 332.1637

Borylation of 1-^{i}Pr-1,2,3-triazole (23)

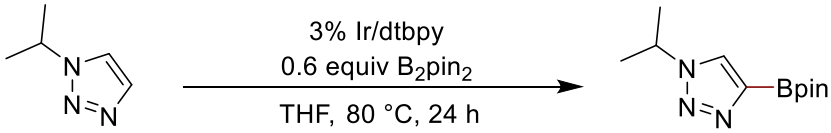

23 **23B**

Procedure C was followed for the reaction of 1-^{i}Pr-1,2,3-Triazole (11 mg, 0.10 mmol) at 80 ºC for 24 h. The yield of **23B** determined by ^{1}H NMR spectroscopy with dibromomethane internal standard was 73%. The crude material was filtered through a pad of silica which was washed with EtOAc. No borylated product was observed by ^{1}H NMR spectroscopy.

Silylation of 1-Bn-1,2,4-triazole (24)

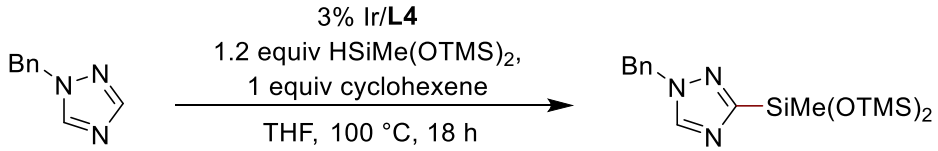

24 **24A**

Procedure A was followed for the reaction of 1-Bn-1,2,4-Triazole (16 mg, 0.10 mmol) at 100 ℃ for 18 h. The yield of **24A** determined by ^{1}H NMR spectroscopy with dibromomethane internal standard was 20%.

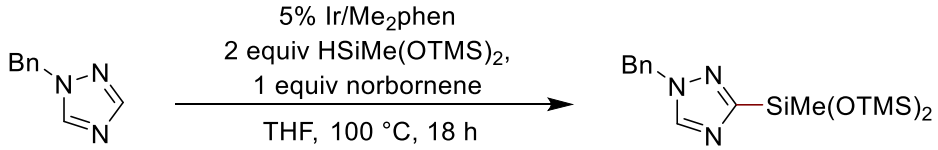

24 **24A**

Procedure B was followed for the reaction of 1-Bn-1,2,4-Triazole (16 mg, 0.10 mmol) with 1,1,1,3,5,5,5-heptamethyl-trisiloxane (45 mg, 0.20 mmol), norbornene (10 mg, 0.10 mmol), $[Ir(cod)(OMe)]_2$ (1.7 mg, 0.0025 mmol), neocuproine (1.1 mg, 0.005 mmol), and THF (50 μL) at 100 ºC for 18 h. The yield of **24A** determined by ^{1}H NMR spectroscopy with dibromomethane internal standard was 87%. The crude reaction mixture was purified by chromatography with neutral alumina treated with Et_3N to afford the product as a colorless oil (25 mg, 66% yield). ^{1}H NMR (300 MHz, $CDCl_3$) δ 8.00 (s, 1H), 7.37 – 7.27 (m, 3H), 7.16 (d, *J* = 5.6 Hz, 2H), 5.53 (s, 2H), 0.48 (s, 3H), 0.08 (s, 18H). ^{13}C NMR (101 MHz, C_6D_6) δ 156.2, 152.5, 137.4, 128.8, 127.9, 127.4, 53.4, 1.7, 0.7. HRMS (ESI+), calculated for $[C_{16}H_{30}N_3O_2Si_3^+]$: 380.1640, found: 380.1637

Borylation of 1-Bn-1,2,4-triazole

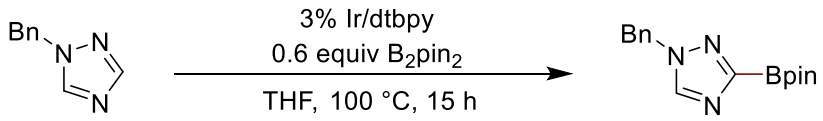

24 **24B**

Procedure C was followed for the reaction of 1-Bn-1,2,4-triazole (16 mg, 0.10 mmol) at 100 ºC for 15 h. No borylated product was observed by ^{1}H NMR spectroscopy.

Silylation of 3-octylthiophene

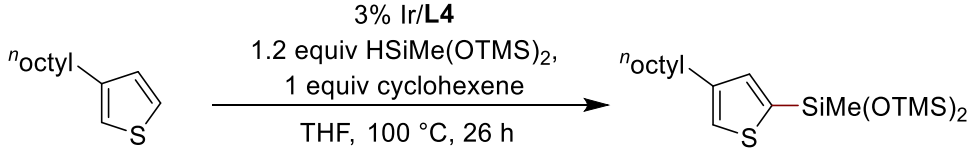

40

Procedure A was followed for the reaction of 3-octylthiophene (49 mg, 0.25 mmol) at 100 ℃ for 25 h. The yield of **40** determined by ^{1}H NMR spectroscopy with dibromomethane internal standard was 100%. The crude reaction mixture was purified by silica-gel chromatography to afford the product as a colorless liquid (101 mg, 97% yield). ^{1}H NMR (500 MHz, $CDCl_3$) δ 7.16 (d, *J* = 1.1

Hz, 1H), 7.13 (d, *J* = 1.1 Hz, 1H), 2.66 (t, *J* = 7.7 Hz, 2H), 1.65 (p, *J* = 7.4 Hz, 2H), 1.44 – 1.23 (m, 10H), 0.91 (t, *J* = 6.9 Hz, 3H), 0.33 (s, 3H), 0.15 (s, 18H). ^{13}C NMR (126 MHz, $CDCl_3$) δ 144.5, 138.1, 136.1, 125.6, 32.1, 30.9, 30.1, 29.6, 29.5, 29.5, 22.9, 14.3, 2.0, 1.2. HRMS (EI), calculated for [$C_{11}H_{23}O_2SSi_3$]: 416.2057, found: 416.2057

Silylation of N-benzyl-4-chloropyrazole

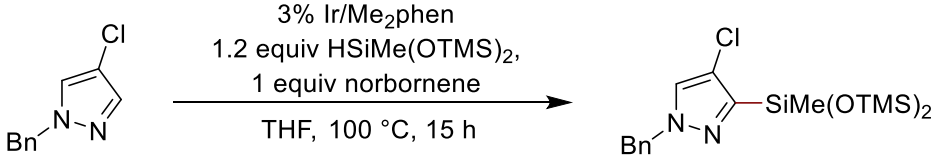

31

In an N_2-filled glovebox, [Ir(cod)OMe]$_2$ (17 mg, 25 μmol, 2.5 mol%), 2,9-dimethyl-1,10-phenanthroline (11 mg, 50 μmol, 5 mol%), 1,1,1,3,5,5,5-heptamethyl-trisiloxane (445 mg, 2.00 mmol, 2.00 equiv), and THF (200 μL) were added to a 4 mL vial. After 5 min, N-benzyl-4-chloropyrazole (193 mg, 1.00 mmol) was added. The solution was transferred to a Radley Carousel glass tube, which was sealed with the accompanying PTFE cap. The glass tube was removed from the glovebox and place in the preheated Radley Carousel. The bottom aluminum block was heated to 100 ℃ and the top aluminum block was cooled with circulating ice water. An N_2 line was attached to the gas inlet of the cap, and the rubber seal was replaced with a rubber septum pierced with a 21-guage needle. After 15 h, the tube was removed from the Carousel and the contents were purified by silica-gel chromatography to afford **35** as a colorless liquid (340 mg, 82% yield). ^{1}H NMR (600 MHz, $CDCl_3$) δ 7.36 – 7.31 (m, 3H), 7.30 (s, 1H), 7.24 – 7.20 (m, 2H), 5.28 (s, 2H), 0.37 (s, 3H), 0.12 (s, 18H). ^{13}C NMR (151 MHz, $CDCl_3$) δ 148.6, 136.3, 128.9, 128.3, 128.0, 127.2, 116.6, 56.7, 1.9, 0.7. HRMS (ESI+), calculated for [$C_{17}H_{30}O_2N_2ClSi_3^+$]: 413.1298, found: 413.1296.

Evaluation of hiyama coupling conditions

In an N_2 filled glovebox, Pd precursor (2.5 μmol), **20A** (13 mg, 0.035 mmol), *m*-iodochlorobenzene (18 mg, 0.075 mmol), and fluoride (0.10 mmol) were weighed into a 4 mL vial fitted with a stir bar and dissolved in 0.1 mL of THF. The vial was capped with a Teflon-lined screw cap and removed from the glovebox. The solution was stirred at the indicated temperature. After the indicated amount of time had elapsed, the yield was determined by ^{1}H NMR spectroscopy with dibromomethane internal standard.

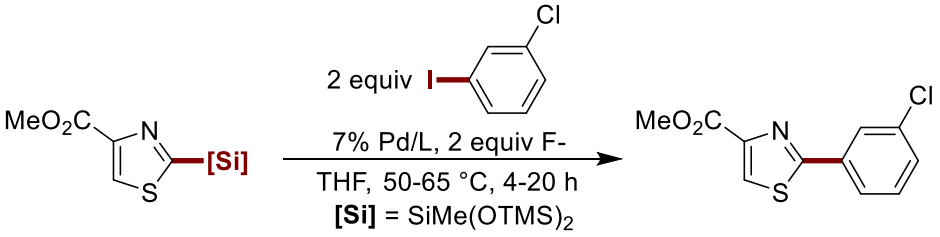

Pd Precatalyst	Ligand	Fluoride Source	Temperature	Time	Yield
$Pd(P^tBu_3)_2$	-	AgF	65 °C	20 h	10%
Pd_2dba_3•$CHCl_3$	$PAd_2{}^nBu$[a]	AgF	65 °C	20 h	17%
Pd_2dba_3•$CHCl_3$	$PAd_2{}^nBu$	KHF_2	65 °C	20 h	50%
Pd_2dba_3•$CHCl_3$	$PAd_2{}^nBu$	TBAF•H_2O	65 °C	20 h	7%
Pd_2dba_3•$CHCl_3$	$PAd_2{}^nBu$	TASF	65 °C	20 h	17%
Pd_2dba_3•$CHCl_3$	$PAd_2{}^nBu$	TBAT	65 °C	20 h	25%
Pd_2dba_3•$CHCl_3$	$PAd_2{}^nBu$	CsF	65 °C	20 h	83%
Pd_2dba_3•$CHCl_3$	$PAd_2{}^nBu$ (7%)	CsF	65 °C	20 h	60%
Pd_2dba_3•$CHCl_3$	$PAd_2{}^nBu$	CsF	65 °C	4 h	43%
$PdCl_2$	$PAd_2{}^nBu$	CsF	65 °C	20 h	39%
$Pd(OAc)_2$	$PAd_2{}^nBu$	CsF	65 °C	20 h	44%
$[Pd(cinnamyl)Cl]_2$	$PAd_2{}^nBu$	CsF	65 °C	20 h	83%
Pd-Xphos-G2	-	CsF	65 °C	20 h	67%
Pd-Ruphos-G2	-	CsF	65 °C	20 h	37%
Peppsi-SiPr	-	CsF	65 °C	20 h	13%
$(dppf)PdCl_2$	-	CsF	65 °C	20 h	71%
Pd_2dba_3•$CHCl_3$	APhos	CsF	65 °C	20 h	56%
Pd_2dba_3•$CHCl_3$	PCy_3	CsF	65 °C	20 h	43%
Pd_2dba_3•$CHCl_3$	Segphos	CsF	65 °C	20 h	69%
Pd_2dba_3•$CHCl_3$	BINAP	CsF	65 °C	20 h	77%
Pd-Xphos-G2	-	CsF	50 °C	20 h	54%
$(dppf)PdCl_2$	-	CsF	50 °C	20 h	54%
Pd_2dba_3•$CHCl_3$	$PAd_2{}^nBu$	CsF	50 °C	20 h	67%
Pd_2dba_3•$CHCl_3$[b]	BINAP	CsF	50 °C	20 h	83%
Pd_2dba_3•$CHCl_3$[b]	BINAP	CsF	50 °C	4 h	85%

[a]Unless otherwise stated, reactions with $PAd_2{}^nBu$ contained 14% of this ligand.
[b]3% Pd/L

Functionalization of silyl-heteroarenes

Synthesis of 25 by chlorination of silylarene 13A

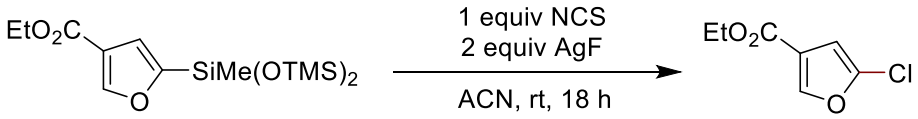

13A **25**

36 mg (0.10 mmol) of **13A**, 13 mg (0.10 mmol) of *N*-chlorosuccinimide, and 25 mg (0.20 mmol) of AgF were added to a 4 mL vial fitted with a sir-bar and dissolved in 1 mL of MeCN. The vial was capped with a Teflon-lined screw cap, and the solution was stirred at room temperature for 18 h. The solution was filtered through a pad of silica, which was then washed with Et_2O. The combined solution was concentrated under reduced pressure. The remaining residue was purified by silica-gel chromatography (20:80 Et_2O:hexanes) to afford the product as a colorless oil (13 mg, 74%). ^1H NMR (700 MHz, $CDCl_3$) δ 7.86 (s, 1H), 6.52 (s, 1H), 4.30 (q, *J* = 7.1 Hz, 2H), 1.34 (t, *J* = 7.1 Hz, 3H). ^{13}C NMR (176 MHz, $CDCl_3$) δ 162.0, 146.3, 138.2, 121.6, 106.2, 60.8, 14.2. MS (EI), calculated for [$C_7H_7ClO_3$]: 174.0084, found: 174.0082.

Synthesis of 26 by bromination of silylarene 7A

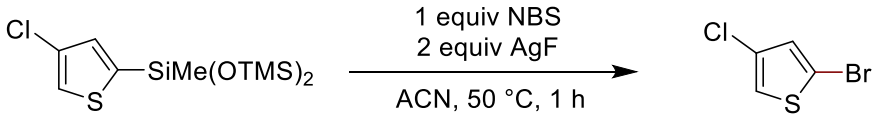

7A **26**

34 mg (0.10 mmol) of **7A**, 20 mg (0.10 mmol) of *N*-bromosuccinimide and 25 mg (0.20 mmol) of AgF were added to a 4 mL vial fitted with a sir-bar and dissolved in 1 mL of MeCN. The vial was capped with a Teflon-lined screw cap, and the solution was stirred at 50 ºC for 1 h. The solution was filtered through a pad of silica, which was washed with Et_2O. The yield based on this crude material determined by ^1H NMR spectroscopy with dibromomethane internal standard was 79%. The combined solution was concentrated under reduced pressure. The residue was purified by silica-gel chromatography (20:80 Et_2O:hexanes) to afford the product as a colorless oil (11 mg, 56%). ^1H NMR (400 MHz, $CDCl_3$) δ 7.03 (d, *J* = 1.7 Hz, 1H), 6.94 (d, *J* = 1.6 Hz, 1H). ^{13}C NMR (101 MHz, $CDCl_3$) δ 129.7, 125.0, 121.3, 112.4. HRMS (EI), calculated for [C_4H_2BrClS]: 195.8749, found:195.8752.

Synthesis of 27 by iodination of silylarene 1A

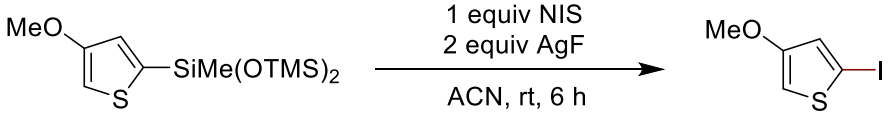

1A **27**

34 mg (0.10 mmol) of **1A** and 25 mg (0.20 mmol) of AgF were added to a 4 mL vial fitted with a sir-bar and dissolved in 0.5 mL of MeCN. 23 mg (0.10 mmol) of *N*-iodosuccinimide (NIS) was added to a separate vial and dissolved in 0.5 mL of MeCN. The solution of NIS was added dropwise to the solution of **1A**. The vial was capped with a Teflon-lined screw cap, and the combined solution was stirred at room temperature for 6 h. The solution was filtered through a pad

of silica, which was washed with Et_2O. The yield based on this crude material determined by ^1H NMR spectroscopy with dibromomethane internal standard was 70%. This solution was concentrated under reduced pressure. The remaining residue was purified by silica-gel chromatography (10:90 EtOAc:hexanes) to afford the product as a colorless oil (6 mg, 25%). ^1H NMR (400 MHz, $CDCl_3$) δ 6.89 (d, *J* = 1.8 Hz, 1H), 6.26 (d, *J* = 1.8 Hz, 1H), 3.77 (s, 3H). ^{13}C NMR (101 MHz, $CDCl_3$) δ 184.4, 158.8, 129.0, 102.9, 57.5. HRMS (EI), calculated for [C_5H_5IOS]: 239.9106, found: 239.9105. These spectroscopic data match those reported in the literature.[44]

Synthesis of 28 by Pd-catalyzed coupling of silylarene 1A

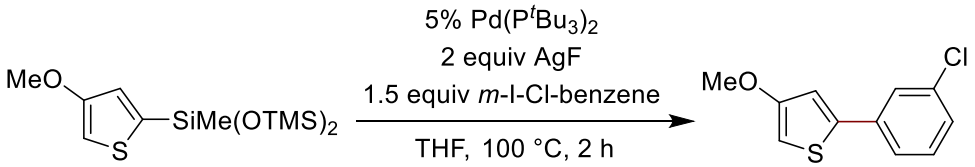

1A **28**

In an N_2 filled glovebox, Pd(P^{t}Bu$_3$)$_2$ (2.6 mg, 0.0050 mmol), **1A** (34 mg, 0.10 mmol), *m*-iodochlorobenzene (36 mg, 0.15 mmol), and AgF (25 mg, 0.20 mmol) were weighed into a 4 mL vial fitted with a stir bar and dissolved in 0.2 mL of THF. The vial was capped with a Teflon-lined screw cap and removed from the glovebox. The solution was stirred at 100 ºC for 2 h. The solution was filtered through a pad of silica, which was washed with Et_2O. The filtrate was concentrated under reduced pressure. The remaining residue was purified by silica gel chromatography (5:95 Et_2O:hexanes) to afford the product as a white solid (17 mg, 76%). ^1H NMR (500 MHz, $CDCl_3$) δ 7.54 (t, *J* = 1.7 Hz, 1H), 7.43 (dt, *J* = 7.7, 1.7 Hz, 1H), 7.29 (t, *J* = 7.7 Hz, 1H), 7.24 (m, 1H), 6.98 (d, *J* = 1.7 Hz, 1H), 6.24 (d, *J* = 1.7 Hz, 1H), 3.83 (s, 3H). ^{13}C NMR (126 MHz, $CDCl_3$) δ 158.9, 141.3, 136.2, 134.9, 130.2, 127.8, 125.6, 123.7, 116.2, 97.2, 57.4. HRMS (EI), calculated for [$C_{11}H_9ClOS$]: 224.0063, found: 224.0067.

Synthesis of 29 by Pd-catalyzed coupling of silylarene 13A

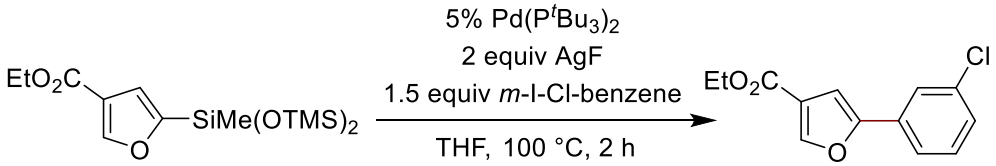

13A **29**

In an N_2 filled glovebox, Pd(P^{t}Bu$_3$)$_2$ (2.6 mg, 0.005 mmol), **13A** (36 mg, 0.10 mmol), *m*-iodochlorobenzene (36 mg, 0.15 mmol), and AgF (25 mg, 0.20 mmol) were weighed into a 4 mL vial fitted with a stir bar and dissolved in 0.2 mL of THF. The vial was capped with a Teflon-lined screw cap and removed from the glovebox. The solution was stirred at 100 ºC for 2 h. The solution was filtered through a pad of silica, which was washed with Et_2O. The filtrate was concentrated under reduced pressure. The yield based on this crude material determined by ^1H NMR spectroscopy with dibromomethane internal standard was 81. The crude material was purified by silica gel chromatography (20:80 Et_2O:hexanes) to afford the product as a white solid (17 mg, 68%). ^1H NMR (500 MHz, $CDCl_3$) δ 8.03 (d, *J* = 0.8 Hz, 1H), 7.67 (t, *J* = 1.9 Hz, 1H), 7.54 (dt, *J* = 7.8, 1.2 Hz, 1H), 7.33 (t, *J* = 7.8 Hz, 1H), 7.31 – 7.25 (m, 1H), 7.00 (d, *J* = 0.8 Hz, 1H), 4.33 (q,

J = 7.1 Hz, 2H), 1.37 (t, *J* = 7.1 Hz, 3H). ^{13}C NMR (126 MHz, $CDCl_3$) δ 163.1, 153.8, 147.3, 135.0, 131.7, 130.3, 128.3, 124.2, 122.2, 121.6, 105.8, 60.8, 14.5. HRMS (EI), calculated for [$C_{13}H_{11}ClO_3$]: 250.0397, found: 250.0397.

Synthesis of 30 by trifluoromethylation of silylarene 40

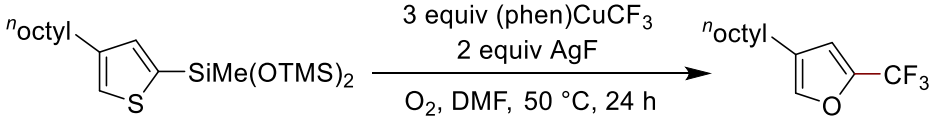

40 **30**

In an N_2 filled glovebox, (phen)$CuCF_3$ (94 mg, 0.30 mmol), **40** (42 mg, 0.10 mmol) and AgF (25 mg, 0.20 mmol) were weighed into a 4 mL vial fitted with a stir bar and dissolved in 1 mL of DMF. The vial was capped with a screw cap fitted with a rubber septum and removed from the glovebox. The solution was sparged with O_2 gas and stirred at 50 ºC for 24 h. The solution was diluted with 5 mL of Et_2O, washed twice with aqueous ammonium chloride, and dried with sodium sulfate. The crude material was then filtered through a pad of silica, which was then washed with Et_2O. The filtrate was concentrated under reduced pressure. The ^{19}F NMR yield based on this crude material was determined to be 63% with fluorobenzene internal standard. The crude material was purified by preparative thin-layer chromatography (pentane) to afford the product as a colorless oil (10 mg, 38%). ^{1}H NMR (400 MHz, $CDCl_3$) δ 7.27 (s, 1H), 7.07 (s, 1H), 2.60 (t, *J* = 7.7 Hz, 2H), 1.66 – 1.54 (p, *J* = 7.4 Hz, 2H), 1.26 (m, 10H), 0.88 (t, *J* = 6.6 Hz, 3H). ^{13}C NMR (126 MHz, $CDCl_3$) δ 143.5, 131.0, 129.8, 123.6, 121.7, 32.0, 30.5, 30.4, 29.5, 29.4, 29.3, 22.8, 14.2. ^{19}F NMR (376 MHz, $CDCl_3$) δ -54.5. HRMS (EI), calculated for [$C_{13}H_{11}ClO_3$]: 264.1160, found: 264.1161.

Synthesis of 32 by chlorination of silylarene 31

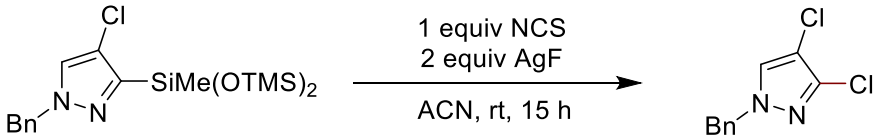

31 **32**

In an N_2 filled glovebox, 41 mg (0.10 mmol) of **31**, 14 mg (0.11 mmol) of *N*-chlorosuccinimide, and 25 mg (0.20 mmol) of AgF were added to a 4 mL vial fitted with a sir-bar and dissolved in 1 mL of dry MeCN. The vial was capped with a Teflon-lined screw cap and removed from the glovebox. The solution was stirred at room temperature for 15 h. The solution was filtered through a pad of silica, which was then washed with Et_2O. The combined solution was concentrated under reduced pressure. The remaining residue was purified by silica-gel to afford the product as a white solid (12 mg, 53%). ^{1}H NMR ($CDCl_3$ MHz, $CDCl_3$) δ 7.40 – 7.34 (m, 3H), 7.30 (s, 1H), 7.25 (d, *J* = 6.5 Hz, 2H), 5.19 (s, 2H). ^{13}C NMR (151 MHz, $CDCl_3$) δ 137.5, 135.0, 129.2, 128.9, 128.8, 128.3, 108.8, 57.5. HRMS (EI), calculated for [$C_{10}H_8N_2Cl_2$]: 226.0065, found: 226.0062.

Synthesis of 33 by bromination of silylarene 31

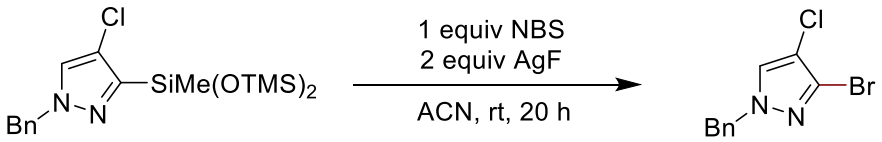

31 **33**

In an N_2 filled glovebox, 41 mg (0.10 mmol) of **31**, 20 mg (0.11 mmol) of *N*-bromosuccinimide, and 25 mg (0.20 mmol) of AgF were added to a 4 mL vial fitted with a sir-bar and dissolved in 1 mL of dry MeCN. The vial was capped with a Teflon-lined screw cap and removed from the glovebox. The solution was stirred at room temperature for 20 h. The solution was filtered through a pad of silica, which was then washed with Et_2O. The combined solution was concentrated under reduced pressure. The remaining residue was purified by silica-gel to afford the product as a pale-yellow oil (22 mg, 81%). ^{1}H NMR (500 MHz, $CDCl_3$) δ 7.41 – 7.33 (m, 3H), 7.27 (s, 1H), 7.25 (d, *J* = 8.0 Hz, 2H), 5.22 (s, 2H). ^{13}C NMR (126 MHz, $CDCl_3$) δ 135.0, 129.2, 128.9, 128.7, 128.3, 125.6, 111.9, 57.6. HRMS (EI), calculated for [$C_{10}H_8N_2ClBr$]: 269.9559, found: 269.9554.

Synthesis of 34 by Pd-catalyzed coupling of silylarene 31

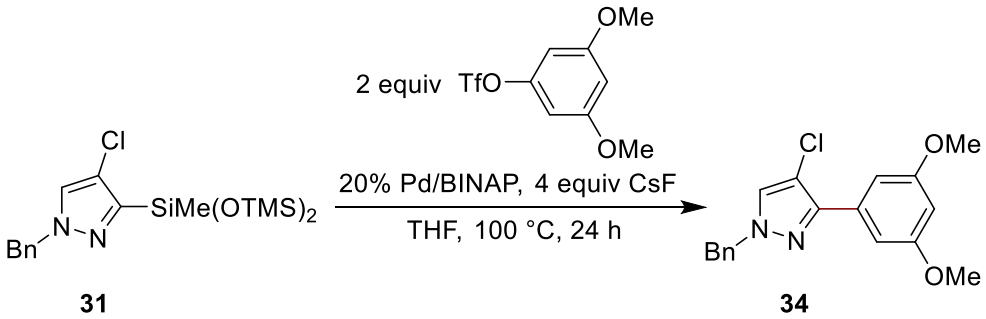

31 **34**

In an N_2 filled glovebox, $Pd_2dba_3 \bullet CHCl_3$ (10 mg, 10 μmol), rac-BINAP (13 mg, 20 μmol), **31** (41 mg, 0.10 mmol), 3,5-$(MeO)_2$-phenyl triflate (60 mg, 0.20 mmol), and cesium fluoride (60 mg, 0.40 mmol) were weighed into a 4 mL vial fitted with a stir bar and dissolved in 0.2 mL of THF. The vial was capped with a Teflon-lined screw cap and removed from the glovebox. The solution was stirred at 50 ºC for 14 h. The crude material was purified by silica gel chromatography to afford the product as a pale-yellow oil (23 mg, 70%). ^{1}H NMR (600 MHz, $CDCl_3$) δ 7.43 – 7.32 (m, 4H), 7.28 (d, *J* = 8.4 Hz, 2H), 7.12 (d, *J* = 2.3 Hz, 2H), 6.49 (t, *J* = 2.3 Hz, 1H), 5.29 (s, 2H), 3.85 (s, 6H). ^{13}C NMR (151 MHz, $CDCl_3$) δ 160.9, 146.8, 135.7, 133.6, 129.1, 128.5, 128.1, 108.4, 107.2, 105.4, 100.8, 57.0, 55.6. HRMS (ESI+), calculated for [$C_{18}H_{18}O_2N_2Cl^+$]: 329.1051, found: 329.1052.

Synthesis of 35 by trifluoromethylation of silylarene 31

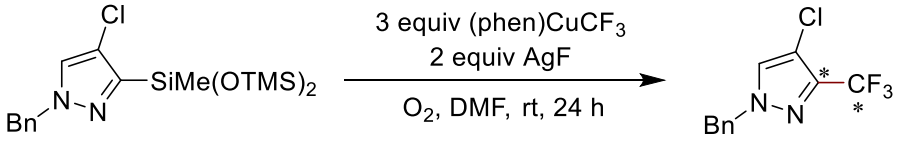

31 **35**

In an N_2 filled glovebox, (phen)$CuCF_3$ (94 mg, 0.30 mmol), **31** (41 mg, 0.10 mmol) and AgF (25 mg, 0.20 mmol) were weighed into a 4 mL vial fitted with a stir bar and dissolved in 1 mL of DMF. The vial was capped with a screw cap fitted with a rubber septum and removed from the glovebox. The solution was sparged with O_2 gas and then stirred at room temperature for 24 h.

The solution was diluted with 5 mL of Et_2O, washed twice with aqueous ammonium chloride, and dried with sodium sulfate. The crude material was then filtered through a pad of silica, which was then washed with Et_2O. The filtrate was concentrated under reduced pressure. The ^{19}F NMR yield based on this crude material was determined to be 63% with fluorobenzene internal standard. The crude material was purified by silica-gel chromatography to afford the product as a colorless oil (13 mg, 50%). ^1H NMR (600 MHz, Acetone-d_6) δ 8.13 (s, 1H), 7.43 – 7.34 (m, 5H), 5.46 (s, 2H). ^{13}C-{^1H} NMR (151 MHz, Acetone) δ 135.75, 131.05, 128.81, 128.36, 128.06, 121.80, 56.80. ^{13}C NMR-{^{19}F} (151 MHz, Acetone) δ 137.53, 120.91. ^{19}F NMR (565 MHz, Acetone) δ -62.38. The carbons marked with "*" could not be observed in the ^{13}C-{^1H} NMR spectrum due to coupling to fluorine. Those carbons were observed in the ^{13}C NMR-{^{19}F} spectrum. HRMS (EI), calculated for [$C_{10}H_8N_2ClBr$]: 260.0328, found: 260.0326.

Synthesis of 36 by Pd-catalyzed coupling of silylarene 20A

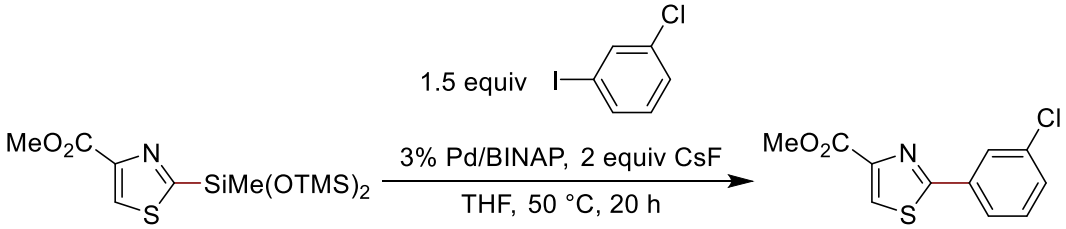

20A **36**

In an N_2 filled glovebox, $Pd_2dba_3 \bullet CHCl_3$ (1.6 mg, 1.5 μmol), rac-BINAP (1.9 mg, 3.0 μmol), **20A** (36 mg, 0.10 mmol), *m*-iodochlorobenzene (35 mg, 0.15 mmol), and cesium fluoride (30 mg, 0.20 mmol) were weighed into a 4 mL vial fitted with a stir bar and dissolved in 0.2 mL of THF. The vial was capped with a Teflon-lined screw cap and removed from the glovebox. The solution was stirred at 50 ºC for 20 h. The yield based on this crude material determined by ^1H NMR spectroscopy with dibromomethane internal standard was 63%. The crude material was purified by silica gel chromatography to afford the product as a white solid (16 mg, 63%). ^1H NMR (300 MHz, $CDCl_3$) δ 8.20 (s, 1H), 8.02 (t, J =1.7 Hz, 1H), 7.86 (dt, J = 7.2, 1.7 Hz, 1H), 7.42 (m, 2H), 3.98 (s, 3H). ^{13}C NMR (126 MHz, $CDCl_3$) δ 167.4, 161.9, 148.0, 135.3, 134.4, 130.8, 130.4, 127.9, 127.0, 125.2, 52.7. HRMS (ESI+), calculated for [$C_{11}H_9O_2N_1Cl_1S_1^+$]: 254.0037, found: 254.0039.

Synthesis of 37 by Pd-catalyzed coupling of silylarene 20A

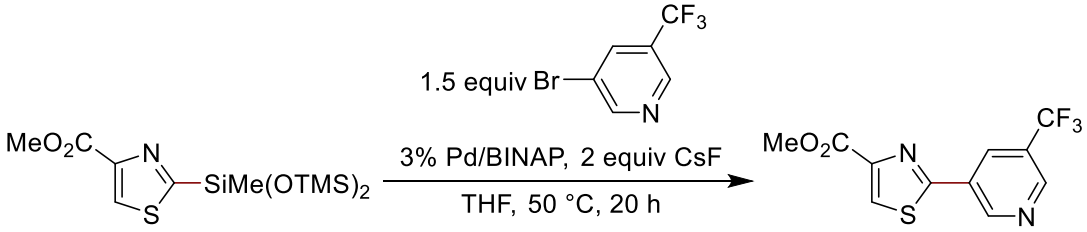

20A **37**

In an N_2 filled glovebox, $Pd_2dba_3 \bullet CHCl_3$ (1.6 mg, 1.5 μmol), rac-BINAP (1.9 mg, 3.0 μmol), **20A** (36 mg, 0.10 mmol), 3-Bromo-5-(trifluoromethyl)pyridine (34 mg, 0.15 mmol), and cesium fluoride (30 mg, 0.20 mmol) were weighed into a 4 mL vial fitted with a stir bar and dissolved in 0.2 mL of THF. The vial was capped with a Teflon-lined screw cap and removed from the glovebox. The solution was stirred at 50 ºC for 20 h. The yield based on this crude determined by ^1H NMR spectroscopy with dibromomethane internal standard was 77%. The crude material was

purified by silica gel chromatography to afford the product as a white solid (22 mg, 76%). ^{1}H NMR (300 MHz, $CDCl_3$) δ 9.35 (d, *J* = 2.0 Hz, 1H), 8.96 (d, *J* = 1.3 Hz, 1H), 8.59 (t, *J* = 1.8 Hz, 1H), 8.31 (s, 1H), 4.01 (s, 3H). ^{13}C NMR (126 MHz, $CDCl_3$) δ 163.7, 151.6, 150.9, 148.7, 148.1, 131.4, 129.0, 128.7, 127.2, 124.3, 52.9. ^{19}F NMR (470 MHz, $CDCl_3$) δ -62.5. HRMS (ESI+), calculated for [$C_{11}H_8O_2N_2F_3S_1^+$]: 289.0253, found: 289.0254.

Synthesis of 38 by Pd-catalyzed coupling of silylarene 20A

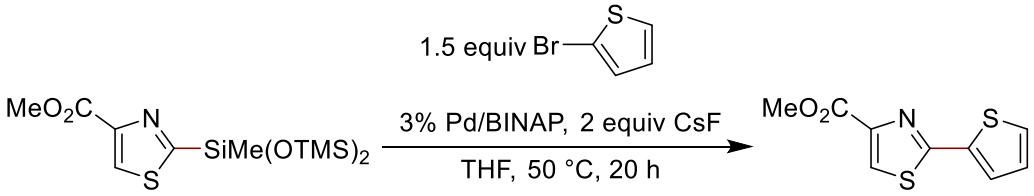

20A **38**

In an N_2 filled glovebox, $Pd_2dba_3 \bullet CHCl_3$ (1.6 mg, 1.5 μmol), rac-BINAP (1.9 mg, 3.0 μmol), **20A** (36 mg, 0.10 mmol), 2-bromothiophene (25 mg, 0.15 mmol), and cesium fluoride (30 mg, 0.20 mmol) were weighed into a 4 mL vial fitted with a stir bar and dissolved in 0.2 mL of THF. The vial was capped with a Teflon-lined screw cap and removed from the glovebox. The solution was stirred at 50 ºC for 20 h. The yield based on this crude material determined by ^{1}H NMR spectroscopy with dibromomethane internal standard was 50%. The crude material was purified by silica gel chromatography to afford the product as a white solid (9 mg, 40%). ^{1}H NMR (600 MHz, $CDCl_3$) δ 8.10 (s, 1H), 7.59 (dd, *J* = 3.7, 1.2 Hz, 1H), 7.45 (dd, *J* = 5.1, 1.1 Hz, 1H), 7.09 (dd, *J* = 5.0, 3.7 Hz, 1H), 3.96 (s, 3H). ^{13}C NMR (151 MHz, $CDCl_3$) δ 162.7, 161.9, 147.5, 136.4, 128.9, 128.1, 127.9, 126.8, 52.7. HRMS (ESI+), calculated for [$C_9H_8O_2N_1S_2^+$]: 225.9991, found: 225.9993.

Synthesis of 39 by Pd-catalyzed coupling of silylarene 20A

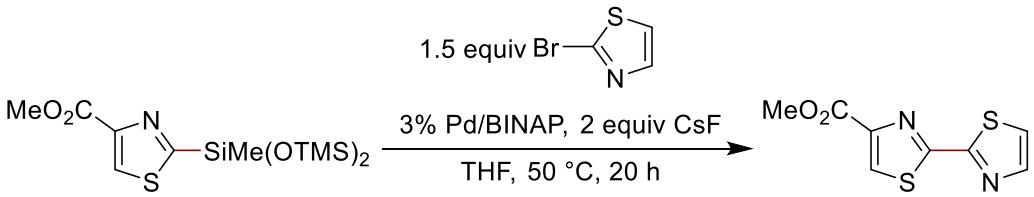

20A **39**

In an N_2 filled glovebox, $Pd_2dba_3 \bullet CHCl_3$ (1.6 mg, 1.5 μmol), rac-BINAP (1.9 mg, 3.0 μmol), **20A** (36 mg, 0.10 mmol), 2-bromothiazole (24.6 mg, 0.15 mmol), and cesium fluoride (30 mg, 0.20 mmol) were weighed into a 4 mL vial fitted with a stir bar and dissolved in 0.2 mL of THF. The vial was capped with a Teflon-lined screw cap and removed from the glovebox. The solution was stirred at 50 ºC for 20 h. The yield based on this crude material determined by ^{1}H NMR spectroscopy with dibromomethane internal standard was 25%. The crude material was purified by silica gel chromatography to afford the product as a pale-yellow oil (5 mg, 22%). ^{1}H NMR (600 MHz, $CDCl_3$) δ 8.25 (s, 1H), 7.92 (d, *J* = 3.1 Hz, 1H), 7.51 (d, *J* = 3.1 Hz, 1H), 3.99 (s, 3H). ^{13}C NMR (151 MHz, $CDCl_3$) δ 162.4, 161.6, 160.6, 147.9, 144.2, 129.2, 122.2, 52.8. HRMS (ESI+), calculated for [$C_8H_6O_2N_2Na_1S_2^+$]: 248.9763, found: 248.9763.

Reactions of a thiophene with deuterated silane

In an N_2-filled glovebox, $[Ir(cod)OMe]_2$ (1.7 mg, 2.5 μmol, 5.0 mol%), ligand (5.0 μmol, 10 mol%), 1,1,1,3,5,5,5-heptamethyl-3-*d*-trisiloxane (11 mg, 0.050 mmol), dodecane (43 mg, 0.25 mmol, 5.0 equiv), THF-d_8 (100 μL) and THF (300 μL) were added to a 4 mL vial. After 10 minutes, 3-chlorothiophene (100 μL, 1.10 mmol, 21 equiv) was added to the vial. The solution was then transferred to an oven-dried NMR tube and the tube was capped and removed from the glovebox and placed in an aluminum heating block that had been preheated to 65 ºC. After 15 min, the tube was removed from the heating block. The selectivity and yield of the silylation reaction were determined by ^{1}H NMR spectroscopy. The selectivity and yield of the deuteration reaction were determined by ^{2}H NMR spectroscopy.

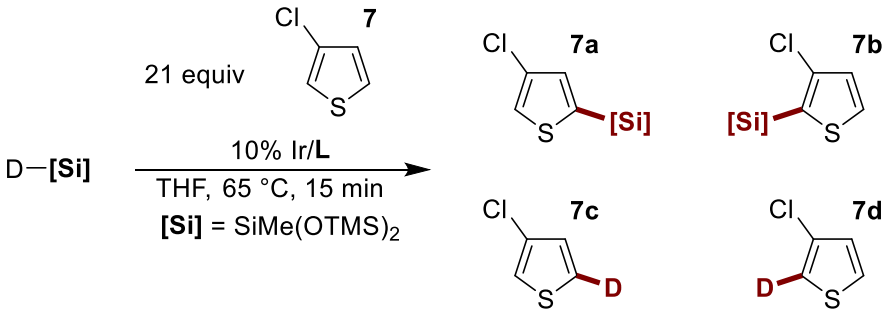

Ligand	7a	7b	7c	7d	7a : 7b	7c : 7d
Me_2phen	29%	10%	40%	27%	2.9 : 1	1.5 : 1
L4	11%	0.8%	32%	29%	14 : 1	1.1 : 1

5.5 References

Portions of this chapter were reprinted with permission from:

"Iridium-Catalyzed Silylation of Five-Membered Heteroarenes: High Sterically Derived Selectivity from a Pyridyl-Imidazoline Ligand" Karmel, C.; Rubel, C. Z.; Kharitonova, E. V.; Hartwig, J. F., *Angew. Chem. Int. Ed.* **2020,** *59,* 6074.

1. (a) Godula, K.; Sames, D. C-H Bond Functionalization in Complex Organic Synthesis. *Science* **2006**, *312*, 67. (b) Davies, H. M. L.; Du Bois, J.; Yu, J. Q. C-H Functionalization in organic synthesis. *Chem. Soc. Rev.* **2011**, *40*, 1855. (c) Gutekunst, W. R.; Baran, P. S. C-H functionalization logic in total synthesis. *Chem. Soc. Rev.* **2011**, *40*, 1976. (d) McMurray, L.; O'Hara, F.; Gaunt, M. J. Recent developments in natural product synthesis using metal-catalysed C–H bond functionalisation. *Chem. Soc. Rev.* **2011**, *40*, 1885. (e) Yamaguchi, J.; Yamaguchi, A. D.; Itami, K. C-H Bond Functionalization: Emerging Synthetic Tools for Natural Products and Pharmaceuticals. *Angew. Chem. Int. Ed.* **2012**, *51*, 8960. (f) White, M. C. Adding Aliphatic C–H Bond Oxidations to Synthesis. *Science* **2012**, *335*, 807. (g) Wencel-Delord, J.; Glorius, F. C-H bond activation enables the rapid construction and late-stage diversification of functional molecules. *Nat. Chem.* **2013**, *5*, 369. (h) Hartwig, J. F. Evolution of C–H Bond Functionalization from Methane to Methodology. *J. Am. Chem. Soc.* **2016**, *138*, 2.

2. (a) Neufeldt, S. R.; Sanford, M. S. Controlling Site Selectivity in Palladium-Catalyzed C–H Bond Functionalization. *Acc. Chem. Res.* **2012**, *45*, 936. (b) Hartwig, J. F. Catalyst-Controlled Site-Selective Bond Activation. *Acc. Chem. Res.* **2017**, *50*, 549.

3. (a) Lyons, T. W.; Sanford, M. S. Palladium-Catalyzed Ligand-Directed C–H Functionalization Reactions. *Chem. Rev.* **2010**, *110*, 1147. (b) Wang, X.; Leow, D.; Yu, J.-Q. Pd(II)-Catalyzed para-Selective C–H Arylation of Monosubstituted Arenes. *J. Am. Chem. Soc.* **2011**, *133*, 13864. (c) Engle, K. M.; Mei, T.-S.; Wasa, M.; Yu, J.-Q. Weak Coordination as a Powerful Means for Developing Broadly Useful C–H Functionalization Reactions. *Acc. Chem. Res.* **2012**, *45*, 788. (d) Leow, D.; Li, G.; Mei, T. S.; Yu, J. Q. Activation of remote meta-C-H bonds assisted by an end-on template. *Nature* **2012**, *486*, 518. (e) Dai, H.-X.; Li, G.; Zhang, X.-G.; Stepan, A. F.; Yu, J.-Q. Pd(II)-Catalyzed ortho- or meta-C–H Olefination of Phenol Derivatives. *J. Am. Chem. Soc.* **2013**, *135*, 7567. (f) Wan, L.; Dastbaravardeh, N.; Li, G.; Yu, J.-Q. Cross-Coupling of Remote meta-C–H Bonds Directed by a U-Shaped Template. *J. Am. Chem. Soc.* **2013**, *135*, 18056. (g) Ros, A.; Fernandez, R.; Lassaletta, J. M. Functional group directed C-H borylation. *Chem. Soc. Rev.* **2014**, *43*, 3229. (h) Wang, P.; Farmer, M. E.; Huo, X.; Jain, P.; Shen, P.-X.; Ishoey, M.; Bradner, J. E.; Wisniewski, S. R.; Eastgate, M. D.; Yu, J.-Q. Ligand-Promoted Meta-C–H Arylation of Anilines, Phenols, and Heterocycles. *J. Am. Chem. Soc.* **2016**, *138*, 9269. (i) Li, M.; Shang, M.; Xu, H.; Wang, X.; Dai, H.-X.; Yu, J.-Q. Remote Para-C–H Acetoxylation of Electron-Deficient Arenes. *Org. Lett.* **2019**, *21*, 540.

4. (a) Hartwig, J. F.; Larsen, M. A. Undirected, Homogeneous C–H Bond Functionalization: Challenges and Opportunities. *ACS Cent. Sci.* **2016**, *2*, 281. (b) Wedi, P.; van Gemmeren, M. Arene-Limited Nondirected C−H Activation of Arenes. *Angew. Chem. Int. Ed.* **2018**, *57*, 13016.

5. (a) Olah, G. A. Aromatic substitution. XXVIII. Mechanism of electrophilic aromatic substitutions. *Acc. Chem. Res.* **1971**, *4*, 240. (b) Boursalian, G. B.; Ham, W. S.; Mazzotti, A. R.; Ritter, T. Charge-transfer-directed radical substitution enables para-selective C–H functionalization. *Nat Chem* **2016**, *8*, 810.

6. (a) Mkhalid, I. A. I.; Barnard, J. H.; Marder, T. B.; Murphy, J. M.; Hartwig, J. F. C-H Activation for the Construction of C-B Bonds. *Chem. Rev.* **2010**, *110*, 890. (b) Hartwig, J. F. Regioselectivity of the borylation of alkanes and arenes. *Chem. Soc. Rev.* **2011**, *40*, 1992. (c) Hartwig, J. F. Borylation and Silylation of C–H Bonds: A Platform for Diverse C–H Bond Functionalizations. *Acc. Chem. Res.* **2012**, *45*, 864. (d) Cheng, C.; Hartwig, J. F. Catalytic Silylation of Unactivated C–H Bonds. *Chem. Rev.* **2015**, *115*, 8946.
7. (a) Chotana, G. A.; Kallepalli, V. A.; Maleczka, R. E. J.; Smith, M. R. I. Iridium-Catalyzed Borylation of Thiophenes: Versatile, Synthetic Elaboration Founded on Selective C-H Funtionalization. *Tetrahedron* **2008**, *64*, p 6103. (b) Cheng, C.; Hartwig, J. F. Iridium-Catalyzed Silylation of Aryl C–H Bonds. *J. Am. Chem. Soc.* **2015**, *137*, 592.
8. Miller, S. L.; Chotana, G. A.; Fritz, J. A.; Chattopadhyay, B.; Maleczka, R. E.; Smith, M. R. C–H Borylation Catalysts that Distinguish Between Similarly Sized Substituents Like Fluorine and Hydrogen. *Org. Lett.* **2019**, *21*, 6388.
9. Ishiyama, T.; Sato, K.; Nishio, Y.; Saiki, T.; Miyaura, N. Regioselective aromatic C-H silylation of five-membered heteroarenes with fluorodisilanes catalyzed by iridium(I) complexes. *Chem. Commun.* **2005**, 5065.
10. (a) Krämer, W., *Modern crop protection compounds*. Wiley-VCH: 2012. (b) Taylor, R. D.; MacCoss, M.; Lawson, A. D. G. Rings in Drugs. *J. Med. Chem.* **2014**, *57*, 5845.
11. Welsch, M. E.; Snyder, S. A.; Stockwell, B. R. Privileged scaffolds for library design and drug discovery. *Curr. Opin. Chem. Biol.* **2010**, *14*, 347.
12. (a) Maleczka, R. E.; Shi, F.; Holmes, D.; Smith, M. R. I. C–H activation/borylation/oxidation: A one-pot unified route to meta-substituted phenols bearing ortho-/para-directing groups. *J. Am. Chem. Soc.* **2003**, *125*, 7792. (b) Bracegirdle, S.; Anderson, E. A. Arylsilane oxidation—new routes to hydroxylated aromatics. *Chem. Commun.* **2010**, *46*, 3454. (c) Rayment, E. J.; Summerhill, N.; Anderson, E. A. Synthesis of Phenols via Fluoride-free Oxidation of Arylsilanes and Arylmethoxysilanes. *J. Org. Chem.* **2012**, *77*, 7052. (d) Rayment, E. J.; Mekareeya, A.; Summerhill, N.; Anderson, E. A. Mechanistic Study of Arylsilane Oxidation through ^{19}F NMR Spectroscopy. *J. Am. Chem. Soc.* **2017**, *139*, 6138.
13. Tzschucke, C. C.; Murphy, J. M.; Hartwig, J. F. Arenes to anilines and aryl ethers by sequential iridium-catalyzed borylation and copper-catalyzed coupling. *Org. Lett.* **2007**, *9*, 761.
14. (a) Qiao, J. X.; Lam, P. Y. S. Copper-promoted carbon-heteroatom bond cross-coupling with boronic acids and derivatives. *Synthesis* , **2011**, 829. (b) Morstein, J.; Kalkman, E. D.; Bold, C.; Cheng, C.; Hartwig, J. F. Copper-Mediated C–N Coupling of Arylsilanes with Nitrogen Nucleophiles. *Org. Lett.* **2016**, *18*, 5244.
15. Liskey, C. W.; Liao, X.; Hartwig, J. F. Cyanation of Arenes via Iridium-Catalyzed Borylation. *J. Am. Chem. Soc.* **2010**, *132*, 11389.
16. (a) Murphy, J. M.; Liao, X.; Hartwig, J. F. Meta Halogenation of 1,3-Disubstituted Arenes via Iridium-Catalyzed Arene Borylation. *J. Am. Chem. Soc.* **2007**, *129*, 15434. (b) Partridge, B. M.; Hartwig, J. F. Sterically Controlled Iodination of Arenes via Iridium-Catalyzed C-H Borylation. *Org. Lett.* **2013**, *15*, 140.
17. (a) Miyaura, N., Metal-Catalyzed Cross-Coupling Reactions of Organoboron Compounds with Organic Halides. In *Metal-Catalyzed Cross-Coupling Reactions*, Wiley-VCH Verlag GmbH: 2008; pp 41. (b) Nakao, Y.; Hiyama, T. Silicon-based cross-coupling reaction: an environmentally benign version. *Chem. Soc. Rev.* **2011**, *40*, 4893. (c) Robbins, D. W.; Hartwig, J. F. A C-H Borylation Approach to Suzuki-Miyaura Coupling of Typically Unstable 2-Heteroaryl and Polyfluorophenyl Boronates. *Org. Lett.* **2012**, *14*, 4266. (d) Denmark, S. E.; Ambrosi, A. Why

You Really Should Consider Using Palladium-Catalyzed Cross-Coupling of Silanols and Silanolates. *Org. Process Res. Dev.* **2015**, *19*, 982. (e) Brown, D. G.; Boström, J. Analysis of Past and Present Synthetic Methodologies on Medicinal Chemistry: Where Have All the New Reactions Gone? *J. Med. Chem.* **2016**, *59*, 4443.
18. (a) Denmark, S. E.; Regen, C. S. Palladium-Catalyzed Cross-Coupling Reactions of Organosilanols and Their Salts: Practical Alternatives to Boron- and Tin-Based Methods. *Acc. Chem. Res.* **2008**, *41*, 1486. (b) Lennox, A. J.; Lloyd-Jones, G. C. Selection of boron reagents for Suzuki–Miyaura coupling. *Chem. Soc. Rev.* **2014**, *43*, 412. (c) Cox, P. A.; Leach, A. G.; Campbell, A. D.; Lloyd-Jones, G. C. Protodeboronation of Heteroaromatic, Vinyl, and Cyclopropyl Boronic Acids: pH–Rate Profiles, Autocatalysis, and Disproportionation. *J. Am. Chem. Soc.* **2016**, *138*, 9145.
19. (a) Ishiyama, T.; Takagi, J.; Ishida, K.; Miyaura, N.; Anastasi, N.; Hartwig, J. F. Mild iridium-catalyzed borylation of arenes. High turnover numbers, room temperature reactions, and isolation of a potential intermediate. *J. Am. Chem. Soc.* **2002**, *124*, 390. (b) Ishiyama, T.; Takagi, J.; Yonekawa, Y.; Hartwig, J. F.; Miyaura, N. Iridium-catalyzed direct borylation of five-membered heteroarenes by bis(pinacolato)diboron: Regioselective, stoichiometric, and room temperature reactions. *Adv. Synth. Catal.* **2003**, *345*, 1103. (c) Karmel, C.; Chen, Z.; Hartwig, J. F. Iridium-Catalyzed Silylation of C–H Bonds in Unactivated Arenes: A Sterically Encumbered Phenanthroline Ligand Accelerates Catalysis. *J. Am. Chem. Soc.* **2019**, *141*, 7063.
20. Larsen, M. A.; Hartwig, J. F. Iridium-Catalyzed C-H Borylation of Heteroarenes: Scope, Regioselectivity, Application to Late-Stage Functionalization, and Mechanism. *J. Am. Chem. Soc.* **2014**, *136*, 4287.
21. Schnute, M. E.; Brideau, R. J.; Collier, S. A.; Cudahy, M. M.; Hopkins, T. A.; Knechtel, M. L.; Oien, N. L.; Sackett, R. S.; Scott, A.; Stephan, M. L. Synthesis of 4-oxo-4, 7-dihydrofuro [2, 3-b] pyridine-5-carboxamides with broad-spectrum human herpesvirus polymerase inhibition. *Bioorg. Med. Chem. Lett.* **2008**, *18*, 3856.
22. Mader, M. M.; Shih, C.; Considine, E.; De Dios, A.; Grossman, C. S.; Hipskind, P. A.; Lin, H.-S.; Lobb, K. L.; Lopez, B.; Lopez, J. E. Acyl sulfonamide anti-proliferatives. Part 2: Activity of heterocyclic sulfonamide derivatives. *Bioorg. Med. Chem. Lett.* **2005**, *15*, 617.
23. Grolleau, J.; Frère, P.; Gohier, F. Clean and Efficient Iodination of Thiophene Derivatives. *Synthesis* **2015**, *47*, 3901.
24. (a) Yanagisawa, S.; Sudo, T.; Noyori, R.; Itami, K. Direct C-H arylation of (hetero)arenes with aryl iodides via rhodium catalysis. *J. Am. Chem. Soc.* **2006**, *128*, 11748. (b) Borghese, A.; Geldhof, G.; Antoine, L. Direct C–H arylation of 3-methoxythiophene catalyzed by Pd. Application to a more efficient synthesis of π-alkoxy-oligothiophene derivatives. *Tetrahedron Lett.* **2006**, *47*, 9249.
25. Vásquez-Céspedes, S.; Chepiga, K. M.; Möller, N.; Schäfer, A. H.; Glorius, F. Direct C–H Arylation of Heteroarenes with Copper Impregnated on Magnetite as a Reusable Catalyst: Evidence for CuO Nanoparticle Catalysis in Solution. *ACS Catalysis* **2016**, *6*, 5954.
26. Glover, B.; Harvey, K. A.; Liu, B.; Sharp, M. J.; Tymoschenko, M. F. Regioselective Palladium-Catalyzed Arylation of 3-Carboalkoxy Furan and Thiophene. *Org. Lett.* **2003**, *5*, 301.
27. Nagib, D. A.; MacMillan, D. W. C. Trifluoromethylation of arenes and heteroarenes by means of photoredox catalysis. *Nature* **2011**, *480*, 224.
28. (a) Wei, C. S.; Jiménez-Hoyos, C. A.; Videa, M. F.; Hartwig, J. F.; Hall, M. B. Origins of the Selectivity for Borylation of Primary over Secondary C–H Bonds Catalyzed by Cp*-Rhodium Complexes. *J. Am. Chem. Soc.* **2010**, *132*, 3078. (b) Karmel, C.; Li, B.; Hartwig, J. F. Rhodium-

Catalyzed Regioselective Silylation of Alkyl C–H Bonds for the Synthesis of 1,4-Diols. *J. Am. Chem. Soc.* **2018**, *140*, 1460. (c) Zhong, R.-L.; Sakaki, S. sp3 C–H Borylation Catalyzed by Iridium(III) Triboryl Complex: Comprehensive Theoretical Study of Reactivity, Regioselectivity, and Prediction of Excellent Ligand. *J. Am. Chem. Soc.* **2019**, *141*, 9854.
29. Dinuclear Methoxy, Cyclooctadiene, and Barrelene Complexes of Rhodium(I) and Iridium(I). In *Inorg. Synth.*, pp 126.
30. Malkov, A. V.; Stewart-Liddon, A. J. P.; McGeoch, G. D.; Ramírez-López, P.; Kočovský, P. Catalyst development for organocatalytic hydrosilylation of aromatic ketones and ketimines. *Org. Biomol. Chem.* **2012**, *10*, 4864.
31. Wen, H.; Wang, K.; Zhang, Y.; Liu, G.; Huang, Z. Cobalt-Catalyzed Regio- and Enantioselective Markovnikov 1,2-Hydrosilylation of Conjugated Dienes. *ACS Catalysis* **2019**, *9*, 1612.
32. Su, B.; Lee, T.; Hartwig, J. F. Iridium-Catalyzed, β-Selective C(sp_3)–H Silylation of Aliphatic Amines To Form Silapyrrolidines and 1,2-Amino Alcohols. *J. Am. Chem. Soc.* **2018**, *140*, 18032.
33. Nicolas, M.; Fabre, B.; Marchand, G.; Simonet, J. New Boronic-Acid- and Boronate-Substituted Aromatic Compounds as Precursors of Fluoride-Responsive Conjugated Polymer Films. *Eur. J. Org. Chem.* **2000**, *2000*, 1703.
34. Kondolff, I.; Doucet, H.; Santelli, M. Suzuki Coupling Reactions of Heteroarylboronic Acids with Aryl Halides and Arylboronic Acids with Heteroaryl Bromides Using a Tetraphosphine/Palladium Catalyst. *Synlett* **2005**, *2005*, 2057.
35. Korenm, A. O. Acid-mediated regioselective alkylation of 1,2,3-triazole. *J. Heterocycl. Chem.* **2002**, *39*, 1111.
36. Jamal, Z.; Teo, Y.-C. Regioselective copper-diamine-catalyzed C–H arylation of 1,2,4-triazole ring with aryl bromides. *RSC Advances* **2016**, *6*, 75449.
37. Pandolfi, F.; Rocco, D.; Mattiello, L. Synthesis and characterization of new D–π-A and A–π-D–π-A type oligothiophene derivatives. *Org. Biomol. Chem.* **2019**, *17*, 3018.
38. Park, N. H.; Senter, T. J.; Buchwald, S. L. Rapid Synthesis of Aryl Fluorides in Continuous Flow through the Balz–Schiemann Reaction. *Angew. Chem. Int. Ed.* **2016**, *55*, 11907.
39. Cheng, C.; Hartwig, J. F. Mechanism of the Rhodium-Catalyzed Silylation of Arene C–H Bonds. *J. Am. Chem. Soc.* **2014**, *136*, 12064.
40. Bergwerf, H. MolView: an attempt to get the cloud into chemistry classrooms.
41. Renata, H.; Zhou, Q.; Dünstl, G.; Felding, J.; Merchant, R. R.; Yeh, C.-H.; Baran, P. S. Development of a Concise Synthesis of Ouabagenin and Hydroxylated Corticosteroid Analogues. *J. Am. Chem. Soc.* **2015**, *137*, 1330.
42. Samanta, R. C.; Yamamoto, H. Selective Halogenation Using an Aniline Catalyst. *Chem. Eur. J.* **2015**, *21*, 11976.
43. Li, N.; Li, B.; Chen, S. Base-Promoted Ecofriendly Synthesis of Trisubstituted Pyrazoles from α,β-Alkynyl N-Tosylhydrazones under Metal- and Solvent-Free Conditions. *Synlett* **2016**, *27*, 1597.
44. Takagi, K.; Kawai, J.; Kouchi, R. Termination reaction of living poly(3-hexylthiophene) using thiophene Grignard reagents: Substituent effect on the functionalization. *Polymer* **2017**, *117*, 354.